

# Sheffield Hallam University

*Detection of environmental pollution (radionuclides and heavy metals) using microorganisms.*

AL-SHANAWA, Maytham.

Available from the Sheffield Hallam University Research Archive (SHURA) at:

<http://shura.shu.ac.uk/19261/>

## A Sheffield Hallam University thesis

This thesis is protected by copyright which belongs to the author.

The content must not be changed in any way or sold commercially in any format or medium without the formal permission of the author.

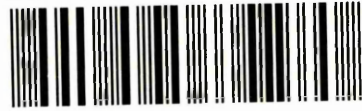
When referring to this work, full bibliographic details including the author, title, awarding institution and date of the thesis must be given.

Please visit <http://shura.shu.ac.uk/19261/> and <http://shura.shu.ac.uk/information.html> for further details about copyright and re-use permissions.

Learning and Information Services  
Adsetts Centre, City Campus  
Sheffield S1 1WD

28080

102 056 921 2



Sheffield Hallam University  
Learning and Information Services  
Adsetts Centre, City Campus  
Sheffield S1 1WD

**REFERENCE**

ProQuest Number: 10694141

All rights reserved

INFORMATION TO ALL USERS

The quality of this reproduction is dependent upon the quality of the copy submitted.

In the unlikely event that the author did not send a complete manuscript and there are missing pages, these will be noted. Also, if material had to be removed, a note will indicate the deletion.



ProQuest 10694141

Published by ProQuest LLC (2017). Copyright of the Dissertation is held by the Author.

All rights reserved.

This work is protected against unauthorized copying under Title 17, United States Code  
Microform Edition © ProQuest LLC.

ProQuest LLC.  
789 East Eisenhower Parkway  
P.O. Box 1346  
Ann Arbor, MI 48106 – 1346

**DETECTION of ENVIRONMENTAL POLLUTION  
(RADIONUCLIDES and HEAVY METALS) USING  
MICROORGANISMS**

**MAYTHAM AL-SHANAWA**

**A thesis submitted in partial fulfilment of the requirements of  
Sheffield Hallam University  
For the degree of Doctor of Philosophy**

**April 2015**



# DEDICATION

To my parents,

My father, Abdala Al-Shanawa

The soul of my affectionate mother

To my family

My beloved wife, Rukaiah Al-Ammar

My dear daughters

Aya Al-Shanawa, Noralhuda Al-Shanawa, Sara Al-Shanawa and Fatima Al-Shanawa

To my brothers and sisters

To my friends and everyone who has supported me during my study

## ABSTRACT

Radionuclide and heavy metal pollutants are a major concern for the environment nowadays as thousands of waste sites around the world pose a serious threat to all living organisms and humans in particular. In order to find an effective technique for the detection of these pollutants and their disposal, great efforts have been made. This is one of the most important reasons and motivation for research in this important field. In the present work bacteria cells were used as a sensitive material in biosensor for the detection of gamma radiation and heavy metals (cadmium chloride and nickel chloride) dissolved in water. The main aim of this project is to develop novel sensing technologies for the detection of environmental pollution; the project utilized two types of bacteria samples, *E. coli* and *D. radiodurans*, for this task.

The biomass (bacteria density or concentration) was firstly characterised by the optical techniques, including fluorescence microscopy, fluorescence spectroscopy, optical density  $OD_{600}$  and UV-visible spectroscopy and was evaluated or estimated according to or attributed to the time of exposure to gamma radiation, which are emitted from  $CO^{57}$  radiation source. From the exponentially decaying response it was shown that the *E. coli* bacteria (*DH5 $\alpha$*  strain, belong gram-negative bacteria) are very sensitive to gamma radiation and the time constant is around 40 hours, that it can be relied upon in determining the low level of radiation. While, *D. radiodurans* (R1 Anderson strain, which belongs to gram positive bacteria) appeared to be much less affected by gamma radiation and showed even smaller increase in the bacteria counts at low radiation doses followed by rather moderate decay at intermediate and high doses; the time constant is around 240 hours. A series of DC and AC electrical measurements were carried out on the same bacteria samples. As a first step, a correlation between DC and AC electrical conductivity and capacitance with bacteria concentration in solution was established. The study of the effect of  $\gamma$ -radiation on DC and AC electrical characteristics of bacteria revealed a possibility of pattern recognition of the above inhibition factors. The electrical results showed some match or consistency with the optical results.

The optical and electrical techniques were also used to study the effect of heavy metals, mainly  $NiCl_2$  and  $CdCl_2$  on bacteria samples. The relations between the optical and electrical properties with metals concentration were established. The electrical characteristics showed clear sequences according to metals concentration. Pattern recognition seems very interesting and proved to provide a simple method to calculate the environmental contamination levels.

The equivalent circuit was investigated and their results were compared with the experimental results; significant match to some extent between the practical and theoretical results was established.

## ACKNOWLEDGEMENTS

First of all, I would like to express my sincere thanks to my director of studies, Professor Alexei Nabok for his excellent supervision, guidance and support during the study period, and for his discussion and interpretation of various aspects of science, experimental procedures and the results analysis.

My special appreciations and thanks go to my supervisors, Dr. Abbas Hashim for his advice, encouragement, assistance and help. Professor Tom Smith of BMRC, Sheffield Hallam University for his advice, help, discussion and suggestion and Dr. Sue Forder of MERI, Sheffield Hallam University for her advice, help, directing and suggestion.

My thanks also go to the Department of Physics, Faculty of Science, University of Basra and to the Iraqi Ministry of Higher Education for their financial support of my PhD study.

I would like to express my special thanks to my mother soul, and my father Abdala Al-Shanawa for their continuity love, encouragement. My special thanks and love go to my lovely wife Rukaiah and my daughters Aya, Noralhuda, Sara and Fatima. Many thanks must go to my brothers and sisters: Magedha, Deeha, Ammal, Enass, Allaa and my brother soul Murtada. In addition, I would like to thanks my cousins Sabah and Kamel for their support, help and encouragement.

My sincere thanks must go to Dr. Jim Yong (BMRC), for his help with fluorescence microscope measurements. I must also thanks Dr. Aseel Hassan (MERI) for his advice and encouragement. Many thanks are also due to Dr. Malcolm (BMRC) for his essential help and discussion with bacteria preparation and culture. In addition, I would like to thanks Dr. Tim(BMRC),for his help and advice with microbiology laboratory and bacteria samples preparation.

My appreciation and gratitude for Professor Doug Cleaver (Head of Postgraduate Research) of MERI, Sheffield Hallam University, for his advice, suggestion and encouragement. Many thanks must go to MERI reception staff for the help and assistance. I would also like to thank all technical staff of Sheffield Hallam University workshop, especially Mr. Ian Broome for preparing the cell for the electrical measurements.

I would like to take this opportunity to thank all my colleagues for their help, good humour and advice during the past four years: Haitham, Khalid, Merriam, Harbi, Mohamed, Hikmeet, Buraq, Yaqoob, Abdul Hafiz, Haken and Selvan.

## LIST OF PUBLICATIONS

### Journal Publications

1. Maytham Al-Shanawa, A. Nabok, A. Hashim, T. Smith and S. Forder, (2013), Detection of ionization radiation effect using microorganism (Escherichia Coli), Sensors & Transducers journal, Vol. 149, pp. 179-186.
2. Maytham Al-Shanawa, A. Nabok, A. Hashim, T. Smith and S. Forder, (2013), Detection of  $\gamma$ -radiation and heavy metals using electrochemical bacterial-based sensor, IOP Publishing, Journal of Physics, Conference Series 450.
3. Maytham Al-Shanawa, A. Nabok, A. Hashim, T. Smith and S. Forder, (2014), Optical Study of the Effect of Gamma Radiation and Heavy Metals on Microorganisms (Bacteria), BioNanoSci. Journal (Springer), Vol. 4, pp. 180-188.
4. Maytham Al-Shanawa, A. Nabok, A. Hashim, T. Smith and S. Forder, Analysis of environmental pollutants using electrical characteristics of bacteria liquid samples, Biosensors and Bioelectronics, (in process of submission).

### Conference Publication

1. Maytham Al-Shanawa, A. Nabok, A. Hashim, T. Smith and S. Forder, Detection of Radiation and Environmental Pollutions Using Microorganisms (poster), 21 May2011, MERIstudent day, (MERI), Sheffield Hallam University, Sheffield, UK.
2. Maytham Al-Shanawa, 12th European Conference on Organized Films, ECOF 12 conference, 17-20 July, 2011, Sheffield Hallam University, Sheffield, UK. (Organiser committee, attended the all sessions).
3. Maytham Al-Shanawa, A. Nabok, A. Hashim, T. Smith and S. Forder, Detection the Radiation Pollutions Effect Using Microorganisms, 23Dec. 2011, BMRC & MERI Poster Evening, Sheffield Hallam University, Sheffield UK.
4. Maytham Al-Shanawa, A. Nabok, A. Hashim, T. Smith and S. Forder, Detection The Radiation Pollutions Effect Using Microorganisms, 11th European Conference on Optical Chemical Sensors and Biosensors, EUROPTRODE XI, 1-4 April, 2012, Barcelona, Spain.
5. Maytham Al-Shanawa, A. Nabok, A. Hashim, T. Smith and S. Forder, Environmental Pollution Detection Using Microorganism Sensing Technique, 15-16

June 2012, MERI student symposium (presentation), (MERI), Sheffield Hallam University, Sheffield, UK.

6. Maytham Al-Shanawa, A. Nabok, A. Hashim, T. Smith, M.R.Rahman, O.N. Oliveira J., J. Coatrini and M.L. Morales, The study of Electrical Properties of Bacteria using Bio-cell Sensor, 14th International conference on organized molecular films, ICOMF 14 (LB 14), 10-13 July, 2012, Paris, France.
7. Maytham Al-Shanawa, A. Nabok, A. Hashim, T. Smith and S. Forder, Bacteria-Based Sensors for Detection of Gamma Radiation and Heavy Metals, 19Dec 2012, BMRC & MERI Winter Poster Event, Sheffield Hallam University, Sheffield UK.
8. Maytham Al-Shanawa, A. Nabok, A. Hashim, T. Smith and S. Forder, The study of electrical properties of bacteria using bio-cell sensor, 13th European Conference on Organised Films (ECOF13) 8-12 July 2013, Ireland, UK.
9. Maytham Al-Shanawa, A. Nabok, A. Hashim, T. Smith and S. Forder, Detection of  $\gamma$ -radiation and heavy metals using electrochemical bacterial-based sensor, Institute of Physics, Sensors & their Applications XVII, 16-18 September, 2013, Dubrovnik, Croatia.
10. Maytham Al-Shanawa, A. Nabok, A. Hashim, T. Smith, Detection of gamma radiation and heavy metals using optical & electrical characteristics of liquid samples containing microorganisms, 17Dec. 2013. BMRC & MERI Poster Evening, Sheffield Hallam University, Sheffield, UK.
11. Maytham Al-Shanawa, A. Nabok, A. Hashim, T. Smith, Environmental Pollution (Radiodnuclides & Heavy Metals) Detection Using Microorganisms, will hold at 11 Dec. 2014. (BMRC & MERI) Poster Winter Evening, Sheffield Hallam University, Sheffield, UK.

## LIST OF ABBREVIATION

E. coli	Escherichia Coli Bacteria
D. radiodurans	Dienococcus Radiodurans Bacteria
OD <sub>600</sub>	Optical Density at 600nm
UV	Ultra Violate
CO <sup>57</sup>	Cobl-57 (source of radiation)
HD5 $\alpha$	Strain of E. coli Bacteria
DC	Direct Current
AC	Alternative Current
DNA	Deoxyribonucleic Acid (DNA) is a molecule that encodes the Genetic
PH	Measure of the Acidity of an aqueous solution
G-M	Geiger Molar Detector
ANN	Artificial Neural Networks
PCA	Principal Component Analysis
D	Absorbed Dose
Gy	Unit of Absorbed Dose
RBE	Relative Biological Effectiveness (measure of damage by radiation)
QF	Quality Factor (RBE of particular type of radiation)
DE	Biologically Equivalent Dose
SNTD	Sold Stat Nuclear Detector
ROS	Reactive Oxygen Species
dsDNA	double Strain DNA
D <sub>50</sub>	Bacteria Population Halved (reduce the bacteria population to half)
96hLC50	Test of Lethal Toxicity Effect after 96 hours
Ni-NPs	Nickel Non-particles
CFU	Colony Forming Unit

## CONTINENT

<b>DEDICATION</b>	<b>I</b>
<b>ABSTRACT</b>	<b>II</b>
<b>ACKNOWLEDGEMENTS</b>	<b>III</b>
<b>LIST OF PUBLICATIONS</b>	<b>V</b>
<b>LIST OF ABBREVIATIONS</b>	<b>VII</b>
<b>CONTINENT</b>	<b>VIII</b>
<b>LIST OF FIGURES</b>	<b>XIII</b>
<b>LIST OF TABLES</b>	<b>XVIII</b>
<b>CHAPTER 1</b>	<b>1</b>
INTRODUCTION	1
1. The Environment	1
1.1. Environmental Pollution	1
1.1.1. Radioactive Pollution	3
1.1.2. Heavy Metal Pollution	5
1.2. Detection of Pollution	8
1.3. Aims and Objectives	10
References	11
<b>CHAPTER 2</b>	<b>14</b>
Radiation and its Sources	14
2.1. Ionizing Radiation	14
2.1.1. Gamma Rays	14
2.1.2. Interaction of Gamma Rays with Matter	17
2.1.3. Absorption of Gamma Rays	19
2.2. Beta particles ( $\beta^-$ )	19
2.2.1. Interaction of Beta Particles	20

2.3. Alpha Particle ( $\alpha$ )	20
2.3.1. Interaction of Alpha Particles	21
2.4. Neutron Radiation	21
2.5. Units of Exposure and Absorbed Dose	23
2.6. Detection of Radionuclide Pollution	25
2.6.1. Radiation Detection	25
2.6.1.1. Gas Counters	25
2.6.1.2. Scintillation Counters	26
2.6.1.3. Semiconductor Detectors	26
2.7. Effect of Radiation on Living Organisms	27
2.8. Effect of Radiation on Microorganisms	32
References	37
<b>CHAPTER 3</b>	<b>42</b>
Heavy Metals	42
3.1. Heavy Metals Distribution in Environment	42
3.2. Heavy Metals Impact on Environment	44
3.2.1. Cadmium (Cd) and its sources	46
3.2.2. Nickel (Ni) and its Sources	48
3.3. Effects of Heavy Metals on Living Organisms	49
3.4. Detection of Heavy Metals	55
References	57
<b>CHAPTER 4</b>	<b>61</b>
Sensing Material	61

4.1. Bacteria	61
4.1.1. Bacteria Cell Wall	63
4.1.2. Growth of Bacteria	65
4.2. Escherichia Coli	65
4.3. Deinococcus Radiodurans	66
References	68
<b>CHAPTER 5</b>	<b>71</b>
Optical Methodology	71
5.1. Fluorescence Microscopy	71
5.2. Spectrophotometer Technique (Optical Density (OD <sub>600</sub> ))	75
5.3. Fluorescence Spectroscopy	77
5.4. UV-visible Absorption Spectrometer	81
References	84
<b>CHAPTER 6</b>	<b>85</b>
Electrical Methodology	85
6.1. Bio-Electrochemical Systems (BESs)	85
6.2. DC Elements	87
6.2.1. (I-V) Voltammetry	87
6.2.2. Electrochemical Cell Sensors	89
6.2.3. DC Electrometer (KEITHLEY)	91
2.2.4. Resistance Meter	92
6.3. AC Elements (Properties)	92
6.3.1 Electrical Conductivity	92
6.3.2. Electrical Capacitance	93

6.3.3. Electrical Impedance	94
6.3.4. AC Electrometer	95
6.4. Equivalent circuit	98
Reference	101
<b>CHAPTER 7</b>	<b>104</b>
Optical Study of the Effect of Gamma Radiation on Bacteria	104
7.1. Sample Preparation	104
7.1.1. E. coli Bacteria Growth	104
7.1.2. D. radiodurans Bacteria Growth	105
7.2. Irradiation of Samples	105
7.3. Optical Study of Effect of Gamma Radiation on E. coli	106
7.4. Optical Study of Effect of Gamma Radiation on D. radiodurans	119
7.5. Comparison of Optical Data for E. coli and D. radiodurans	127
Reference	132
<b>CHAPTER 8</b>	<b>133</b>
Electrical Study of Bacteria: the Effect of Gamma Radiation	133
8.1. Samples Tested by Electrical Techniques	133
8.2. Samples Preparation and Measurements	133
8.3. DC Electrical Measurements of Bacteria	134
8.4. AC Electrical Measurements of Bacteria	145
8.5. Data Analysis in Term of Equivalent Circuit	156
Reference	163

<b>CHAPTER 9</b>	<b>165</b>
Optical Study of the Effect of Heavy Metals on Bacteria	165
9.1. Optical Study of the Effect of Cadmium Chloride (CdCl <sub>2</sub> )	165
9.2. Optical Study of the Effect of Nickel Chloride (NiCl <sub>2</sub> )	172
Reference	181
<b>CHAPTER 10</b>	<b>183</b>
Electrical Study of the Effect of Heavy Metals on Bacteria	183
10.1. Samples for Electrical Tests	183
10.2. Electrical Study of the Effect of Cadmium Chloride (CdCl <sub>2</sub> ) on Bacteria	184
10.2.1. DC Electrical Measurements of Bacteria and CdCl <sub>2</sub>	184
10.2.2. AC Electrical Measurements of Bacteria and CdCl <sub>2</sub>	190
10.3. Electrical Study of the Effect of Nickel Chloride (NiCl <sub>2</sub> ) on Bacteria	200
10.3.1. DC Electrical Measurements of Bacteria and NiCl <sub>2</sub>	201
10.3.2. AC Electrical Measurements of Bacteria and NiCl <sub>2</sub>	207
10.4. Equivalent Circuit Results	217
References	236
<b>CHAPTER 11</b>	<b>237</b>
Conclusion and future work	237
11.1. Thesis conclusion	237
11.2. Suggestion for future work	240
<b>APPENDIXES</b>	<b>241</b>
APPENDIXES A	242
APPENDIXES B	246
APPENDIXES C	249
APPENDIXES D	253

## LIST OF FIGURES

Figure. 2.1. The scheme of decay of $^{60}\text{Co}$ to $^{60}\text{Ni}$	16
Figure. 2.2. The decay scheme of $^{57}\text{Co}$	16
Figure. 2.3. Interaction of gamma rays with matter	17
Figure. 2.4. Action of ionization radiation on cells	30
Figure. 2.5. Physical, biochemical and biological responses to radiation	31
Figure. 2.6. Survival curves for radiation resistant bacteria (D. Radiodurans)	33
Figure. 2.7. Survival curves of bacteria vs. Gamma radiation	36
Figure. 2.8. Number of surviving bacteria vs. X-ray dose	37
Figure 3.1. Biomass of E. coli bacteria vs. Pb and Ni	51
Figure 4.1. Structure of a typical Gram-positive bacteria cell	64
Figure 4.2. E. coli bacteria cells shape	66
Figure 4.3. D. radiodurans bacteria cells shape	68
Figure 5.1. Schematic of a fluorescence microscope	72
Figure 5.2. Fluorescence microscope instrument (Olympus-BX61)	73
Figure 5.3. Monitoring E. coli growth using OD <sub>600</sub> technique	76
Figure 5.4. Image of OD <sub>600</sub> spectrophotometer instrument (6715, JENWAY)	77
Figure 5.5. Fluoresce of single electron state by optical	78
Figure 5.6. Excitation of electron correspond to the amplitude of the excitation spectrum	79
Figure 5.7. Image of fluorescence spectroscopy instrument (Varian Cary Eclipse)	80
Figure 5.8. Electromagnetic spectrum (Wavelength Scale)	81
Figure 5.9. Relationship between light absorption and liquid concentration	82
Figure 5.10. Simple diagram of a UV-visible spectrophotometer diagram	83
Figure 5.11. Spectrometer instrument (UV-visible carry eclipse (Varian))	83
Figure 6.1. Three-electrode electrochemical cell set-up	90
Figure 6.2. High resistance meter model 6517a (electrometer high resistance) "Keithley"	92
Figure 6.3. Brief description of each key on the HP 4284A's front panel	95
Figure 6.4. Two electrodes cell design for DC/AC electric measurements	96
Figure 6.5. The equivalent circuit used for electrical analysis	98
Figure 6.6. The measure and circuit for AC properties	99
Figure 7.1. Irradiator system scheme used to irradiate bacteria sample	106

Figure 7.2. Fluorescence microscopy images of E. coli bacteria samples after 1 hour exposure to gamma radiation	107
Figure 7.3. Fluorescence microscopy images of E. coli bacteria samples 480 hours exposure to gamma radiation	108
Figure 7.4. Relation between L/D (live/dead) bacteria ratio and exposure time to Gamma radiation (fluorescence microscopy results)	110
Figure 7.5. Relation between ratios L/D (live/dead) of E. coli bacteria not exposed to Gamma radiation and time (fluorescence microscopy results)	111
Figure 7.6. Pattern recognition of ratios (live/dead) of E. coli bacteria with and without Gamma Ray Vs. time (fluorescence microscopy results)	111
Figure 7.7. Relation between the $((L/D)_a/(L/D)_b)$ ratio of live over dead bacteria after exposure to radiation against time of exposure (fluorescence microscopy results)	112
Figure 7.8. Optical densities ratio $((OD_{600})_a/(OD_{600})_b)$ for E. coli bacteria versus time exposure to gamma radiation dose	113
Figure 7.9. Absorption spectrum of E. coli bacteria sample and clear broth (LB-broth)	114
Figure 7.10. Fluorescence spectra of a liquid broth medium no-exposed and exposed to gamma radiation	115
Figure 7.11. Fluorescence spectra (light scatter) of two E. coli bacteria samples exposed to Gamma radiation for 24h (48000 mSv)	116
Figure 7.12. Fluorescence spectra (light scatter) of two E. coli bacteria samples exposed to Gamma radiation for 48h (96000 mSv)	116
Figure 7.13. Fluorescence spectra of E. coli samples in LB broth exposed to gamma radiation for 48 hours	117
Figure 7.14. Effect of gamma radiation on 2nd order diffraction peak for E. coli	118
Figure 7.15. Intensity for E. coli samples of different growth time (G. T)	118
Figure 7.16. Correlation between peak intensity and absorption optical density of E. coli bacteria	119
Figure 7.17. Fluorescence microscopy images for D. Radiodurans bacteria samples after 24 hours exposure to gamma radiation	120
Figure 7.18. Fluorescence microscopy image for D. Radiodurans bacteria samples after 240 hours exposure to gamma radiation	120
Figure 7.19. The pattern recognition of the ratios (live/dead) of D. radiodurans bacteria was exposed (red) and Gamma Ray vs. time (fluorescence microscopy results)	122

Figure 7.20. Relation between $((L/D)_a / (L/D)_b)$ ratio of live/dead <i>D. radiodurans</i> bacteria after exposure to radiation against the time of exposure (fluorescence microscopy results)	122
Figure 7.21. Optical density ratio for <i>D. radiodurans</i> bacteria versus time exposure to gamma radiation	123
Figure 7.22. Absorption spectrum of <i>D. radiodurans</i> bacteria sample and clear broth (OXOID-CM3 broth)	124
Figure 7.23. Fluorescence spectra of liquid broth medium exposed to gamma radiation for 120 hours	125
Figure 7.24. Fluorescence spectra (light scatter) of two <i>D. radiodurans</i> bacteria samples exposed to gamma radiation for 120h (240000 mSv)	126
Figure 7.25. The effect of gamma radiation on 2nd order diffraction peak for <i>D. radiodurans</i> exposed to radiation	127
Figure 7.26. Dependence of L/D bacteria ratio for both <i>E. coli</i> and <i>D. radiodurans</i> bacteria on time of exposure to gamma rays (fluorescence microscopy results)	128
Figure 7.27. Dependence of normalized absorbance values for both <i>E. coli</i> and <i>D. radiodurans</i> bacteria on time of exposure to gamma ray ( $OD_{600}$ results)	128
Figure 7.28. The effect of gamma rays on the 2nd order diffraction peak for <i>E. coli</i> and <i>D. radiodurans</i> bacteria	129
Figure 7.29. Comparison of relative responses of three optical methods to radiation for <i>E.coli</i> and <i>D. radiodurans</i> bacteria	131
Figure 8.1. Current and Voltage characteristics recorded on LB broth and <i>E. coli</i> samples of different dilutions	135
Figure 8.2. Values of anodic and cathodic current at ( $\pm 0.5V$ ) for different concentration of <i>E. coli</i> bacteria	135
Figure 8.3. DC conductance from cathode current at $-0.5V$ versus bacteria concentration of <i>E. coli</i>	136
Figure 8.4. Typical DC I-V characteristics of <i>E. coli</i> samples of different concentrations of optical density ( $OD_{600}$ )	137
Figure 8.5. I-V characteristics of <i>E. coli</i> samples for different time exposure to gamma radiation	137
Figure 8.6. I-V characteristics of <i>E. coli</i> samples not exposed to gamma ray	138
Figure 8.7.Ic (cathode current) at ( $-0.5$ Volte): <i>E. coli</i> samples for different time exposure to gamma radiation dose	139

Figure 8.8. ( $I_c$ -gamma / $I_c$ ) cathode current ratio at (-0.5 Volte): E. coli samples for different time exposure to gamma radiation	140
Figure 8.9.Ia anodic current at 0.5 V: E. coli samples for different time exposure to gamma radiation dose	140
Figure 8.10. Typical DC I-V characteristics of D. radiodurans samples of different concentrations measured of optical density (OD600)	141
Figure 8.11. I-V characteristics of D. radiodurans samples with different time exposures to gamma rays	142
Figure 8.12. Change in current at cathode electrode of D. radiodurans in (-0.5V) for different exposure times	143
Figure 8.13. Current at cathode electrode ratio	143
Figure 8.14. Comparison of relative responses of DC characteristic for E. coli and D. radiodurans bacteria	144
Figures 8.15.I <sub>a</sub> anodic current at 0.5 V: D. radiodurans samples for different time exposures to gamma radiation	144
Figure 8.16. Typical AC-Gp characteristics of E. coli samples of different concentrations measured of optical density (OD600)	145
Figure 8.17. Spectra of Cp for E. coli bacteria samples of different concentrations in optical density units	146
Figure 8.18. Spectra of Cp for E. coli bacteria samples of different concentrations presented in optical density units	146
Figure 8.19. Change in the AC conductance of E. coli bacteria as a function of time	147
Figure 8.20. AC conductance ratio of E. coli bacteria after exposure to	148
Figure 8.21. AC capacitance of E. coli samples by time exposure to gamma radiation	148
Figure 8.22. AC capacitance of E. coli samples not exposed to gamma radiation for different time	149
Figure 8.23. Change in the AC capacitance of E. coli bacteria as function of exposure time	149
Figure 8.24. AC capacitance ratio of E. coli bacteria after exposure to radiation	150
Figure 8.25. Typical AC-Gp characteristics of D. radiodurans samples of different concentrations	151
Figure 8.26. AC conductance of D. radiodurans samples for varied exposure to gamma radiation	151

Figure 8.27. Change in AC conductance of <i>D. radiodurans</i> bacteria as function of time exposure	152
Figure 8.28. AC conductance ratio for <i>D. radiodurans</i> bacteria exposed to radiation	152
Figure 8.29. Typical AC capacitance characteristics of <i>D. radiodurans</i> samples of different concentrations	153
Figure 8.30. Typical AC $C_p$ characteristics of <i>D. radiodurans</i> samples of different concentrations of optical density (OD600)	153
Figure 8.31. Change in AC conductance of <i>D. radiodurans</i> bacteria as function of time exposure	154
Figure 8.32. AC capacitance ratio for bacteria exposed to radiation to capacitance of bacteria samples not exposed to radiation	154
Figure 8.33. Comparison of relative responses of AC characteristic of conductance for <i>E. coli</i> and <i>D. radiodurans</i> bacteria	155
Figure 8.34. Comparison of relative responses of AC characteristic for capacitance $C_p$ methods to radiation for <i>E. coli</i> and <i>D. radiodurans</i> bacteria	155
Figure 8.35. Changes of bulk resistance ( $R_b$ ) at high frequency for <i>E. coli</i> bacteria vs. gamma radiation	157
Figure 8.36. Normalised curve for ratio of surface and bulk resistance of <i>E. coli</i> bacteria exposed to gamma radiation	157
Figure 8.37. Changes in surface resistance ( $R_s$ ) of <i>E. coli</i> bacteria samples exposed to gamma radiation	158
Figure 8.38. Curve for surface resistance of <i>E. coli</i> bacteria samples exposed to gamma radiation	158
Figure 8.39. Changes in surface resistance ( $R_s$ ) of <i>D. radiodurans</i> bacteria samples exposed to gamma radiation	159
Figure 8.40. Curve for surface resistance of <i>D. radiodurans</i> bacteria samples exposed to gamma radiation	159
Figure 8.41. Comparison of curves of surface resistance ( $K_s$ ) for <i>E. coli</i> and <i>D. radiodurans</i> bacteria as function of exposure time	160
Figure 8.42. Changes of double layer capacitance ( $C_s$ ) of <i>E. coli</i> bacteria samples exposed to gamma radiation	161
Figure 8.43. Curve for double layer capacitance ( $C_s$ ) of <i>E. coli</i> bacteria samples exposed to gamma radiation	161
Figure 8.44. Changes of double layer capacitance ( $C_s$ ) of <i>D. radiodurans</i> bacteria samples exposed to gamma radiation	162

Figure 8.45. Curve for double layer capacitance (Cs) of <i>D. radiodurans</i> bacteria samples exposed to gamma radiation	162
Figure 8.46. Comparison of curves of double layer capacitance (Cs) for <i>E. coli</i> bacteria and <i>D. radiodurans</i> bacteria as a function of exposure time	163
Figure 9.1. Fluorescence microscopy images of <i>E. coli</i> bacteria samples and CdCl <sub>2</sub> , after 24 hours	166
Figure 9.2. Effect of CdCl <sub>2</sub> on the L/D ratio of <i>E. coli</i> for different time incubations	166
Figure 9.3. Ratio (L/D) <sub>m</sub> of <i>E. coli</i> after adding salt against ratio (L/D) <sub>0</sub> of <i>E. coli</i> 72 hours	167
Figure 9.4. Fluorescence microscopy images of <i>D. radiodurans</i> bacteria sample and CdCl <sub>2</sub> after 550 hours	168
Figure 9.5. Ratio (L/D) <sub>m</sub> of <i>D. radiodurans</i> after adding salt for 72 hours exposure	168
Figure 9.6. Dependence of (L/D) <sub>m</sub> / (L/D) <sub>0</sub> bacteria ratio for both <i>E. coli</i> and <i>D. radiodurans</i> bacteria in CdCl <sub>2</sub> (fluorescence microscopy results)	169
Figure 9.7. The Optical Density test: optical densities OD <sub>600</sub> for <i>E. coli</i> bacteria versus CdCl <sub>2</sub> concentration	170
Figure 9.8. Optical densities for <i>D. radiodurans</i> bacteria versus time exposure to CdCl <sub>2</sub>	170
Figure 9.9. Fluorescence spectra (light scatter) of <i>E. coli</i> bacteria samples in CdCl <sub>2</sub> for 24 hours	171
Figure 9.10. Fluorescence spectra (light scatter) of <i>D. radiodurans</i> bacteria samples in CdCl <sub>2</sub> for 24 hours	171
Figure 9.11. Effect of CdCl <sub>2</sub> on 2-nd order diffraction peak for <i>E. coli</i> and <i>D. radiodurans</i> bacteria	172
Figure 9.12. Fluorescence microscopy images of <i>E. coli</i> bacteria sample for 72 hour	174
Figure 9.13. Effect of NiCl <sub>2</sub> on (L/D) ratio of <i>E. coli</i> for different time incubations	174
Figure 9.14. Ratio (L/D) <sub>m</sub> of <i>E. coli</i> after adding salt against ratio (L/D) <sub>0</sub> of <i>E. coli</i>	175
Figure 9.15. Fluorescence microscopy images of <i>D. radiodurans</i> bacteria sample in NiCl <sub>2</sub>	176
Figure 9.16. Effect of NiCl <sub>2</sub> on L/D ratio of <i>D. radiodurans</i> for different time incubations	176
Figure 9.17. Ratio (L/D) <sub>m</sub> of <i>D. radiodurans</i> after adding NiCl <sub>2</sub> against ratio (L/D) <sub>0</sub> of <i>D. radiodurans</i> after 240 hours	177
Figure 9.18. Dependence of (L/D) <sub>m</sub> / (L/D) <sub>0</sub> bacteria ratio for both <i>E. coli</i> and <i>D. radiodurans</i> bacteria for 240 hours in NiCl <sub>2</sub>	177

Figure 9.19. Fluorescence spectra (light scatter) of <i>E. coli</i> bacteria samples in $\text{NiCl}_2$ for after 72 hours	178
Figure 9.20. Fluorescence spectra (light scatter) of <i>D. radiodurans</i> bacteria samples in $\text{NiCl}_2$ after 72 hours	179
Figure 9.21. Effect of $\text{NiCl}_2$ on 2-nd order diffraction peak for <i>E. coli</i> and <i>D. radiodurans</i> bacteria	180
Figure 9.22. Effect of $\text{NiCl}_2$ on 2-nd order diffraction peak for <i>E. coli</i> and <i>D. radiodurans</i> bacteria after 240 hours	180
Figure 9.23. Comparisons of relative changes in (L/D) ratio, for <i>E. coli</i> and <i>D. radiodurans</i> bacteria in $\text{CdCl}_2$	181
Figure 10.1. I-V characteristics of <i>E. coli</i> samples for different concentration of $\text{CdCl}_2$ after 72 hours	185
Figure 10.2. I-V characteristics for $\text{CdCl}_2$ in LB broth	185
Figure 10.3. $I_c$ <i>E. coli</i> in $\text{CdCl}_2$ over $I_c$ $\text{CdCl}_2$ in LB broth	186
Figure 10.4. $I_c$ <i>E. coli</i> in $\text{CdCl}_2$ over $I_c$ of <i>E. coli</i> in LB broth at -0.5V after 72 hours	186
Figure 10.5. Relative change of cathodic current $I_c$ for <i>E. coli</i> in different concentration of $\text{CdCl}_2$ after 72 hours	187
Figure 10.6. $I_c$ <i>D. radiodurans</i> in $\text{CdCl}_2$ over $I_c$ $\text{CdCl}_2$	188
Figure 10.7. $I_c$ <i>D. radiodurans</i> in $\text{CdCl}_2$ over $I_c$ of <i>D. radiodurans</i> after 72 hours	188
Figure 10.8. Relative change $I_c$ for <i>D. radiodurans</i> in different concentration of $\text{CdCl}_2$ for $I_c$ of $\text{CdCl}_2$ after 72 hours	189
Figure 10.9. Comparison of relative responses of $I_c$ to $\text{CdCl}_2$ for <i>E. coli</i> and <i>D. radiodurans</i> bacteria	189
Figure 10.10. Comparison of relative responses of $I_c$ for <i>E. coli</i> and <i>D. radiodurans</i> bacteria in $\text{CdCl}_2$ to $I_c$ of bacteria	190
Figure 10.11. Comparison of relative responses of $I_c$ methods to $\text{CdCl}_2$ for both types of bacteria	190
Figure 10.12. Typical AC-Gp of <i>E. coli</i> for different concentrations of $\text{CdCl}_2$	191
Figure 10.13. Typical AC-Cp of <i>E. coli</i> samples for different concentrations of $\text{CdCl}_2$	191
Figure 10.14. Typical AC-Gp of LB broth for different concentrations of $\text{CdCl}_2$	192
Figure 10.15. Typical AC-Cp of different concentrations of $\text{CdCl}_2$ in LB broth	192
Figure 10.16. AC conductance ratio of <i>E. coli</i> bacteria in $\text{CdCl}_2$ after 72 hours over AC conductance for bacteria samples not exposed	193

Figure 10.17. AC capacitance ratio of E. coli bacteria in CdCl <sub>2</sub> after 72 hours over AC capacitance	193
Figure 10.18. Comparison of relative responses of conductance (AC-Gp) for E. coli and D. radiodurans bacteria in CdCl <sub>2</sub> to conductance (AC-Gp) of bacteria after 72 hours	194
Figure 10.19. Comparison of relative responses of capacitance (AC-Cp) for E. coli and D. radiodurans bacteria in CdCl <sub>2</sub> to capacitance (AC-Cp) of bacteria after 72 hours	195
Figure 10.20. Comparison of relative responses of conductance (AC-Gp) for E. coli in CdCl <sub>2</sub> to conductance (AC-Gp) of CdCl <sub>2</sub>	195
Figure 10.21. AC conductance ratio of E. coli bacteria in CdCl <sub>2</sub> after 72 hours over the conductance for CdCl <sub>2</sub>	196
Figure 10.22. Comparison of relative responses of capacitance (AC-Cp) for E. coli in CdCl <sub>2</sub> and capacitance (AC-Gp) of CdCl <sub>2</sub>	196
Figure 10.23. AC capacitance ratio of E. coli in CdCl <sub>2</sub> after 72 hours over the capacitance for CdCl <sub>2</sub>	197
Figure 10.24. Comparison of relative responses of conductance (AC-Gp) for D. radiodurans bacteria in CdCl <sub>2</sub> to conductance (AC-Gp) of CdCl <sub>2</sub>	197
Figure 10.25. AC conductance ratios of D. radiodurans in CdCl <sub>2</sub> after 72 hours over conductance for CdCl <sub>2</sub>	198
Figure 10.26. Comparison of relative responses of capacitance (AC-Gp) for D. radiodurans in CdCl <sub>2</sub> to capacitance (AC-Gp) of CdCl <sub>2</sub>	198
Figure 10.27. AC capacitance ratios of D. radiodurans in CdCl <sub>2</sub> after 72 hours over capacitance for CdCl <sub>2</sub>	199
Figure 10.28. Comparison of relative responses of conductance (AC-Gp) for E. coli and D. radiodurans in CdCl <sub>2</sub> to conductance (AC-Gp) of CdCl <sub>2</sub> after 72 hours	199
Figure 10.29. Comparison of relative responses of capacitance (AC-Cp) for E. coli and D. radiodurans in CdCl <sub>2</sub> to capacitance (AC-Cp) of CdCl <sub>2</sub> after 72 hours	200
Figure 10.30. I-V characteristics of E. coli in NiCl <sub>2</sub> after 72 hours	201
Figure 10.31. I-V characteristics of NiCl <sub>2</sub> with LB broth	202
Figure 10.32. I <sub>c</sub> of E. coli and NiCl <sub>2</sub> characteristics for different concentrations of NiCl <sub>2</sub>	202
Figure 10.33. I <sub>c</sub> of E. coli in NiCl <sub>2</sub> over I <sub>c</sub> NiCl <sub>2</sub> different concentrations of NiCl <sub>2</sub>	203
Figure 10.34. I <sub>c</sub> of E. coli in NiCl <sub>2</sub> over I <sub>c</sub> of E. coli for different concentration of NiCl <sub>2</sub> after 72 hours	203
Figure 10.35. Relative change of I <sub>c</sub> for E. coli in NiCl <sub>2</sub> for I <sub>c</sub> of NiCl <sub>2</sub> over I <sub>c</sub> of E. coli after 72 hours	204

Figure 10.36. $I_c$ of <i>D. radiodurans</i> in $NiCl_2$ and $I_c$ for $NiCl_2$ with OXOID broth	205
Figure 10.37. $I_c$ of <i>D. radiodurans</i> in $NiCl_2$ and $I_c$ for <i>E. coli</i> in $NiCl_2$ for different concentrations of $NiCl_2$	205
Figure 10.38. Ratio of $I_c$ of <i>D. radiodurans</i> in $NiCl_2$ over $I_c$ of <i>D. radiodurans</i> and $I_c$ of <i>E. coli</i> in $NiCl_2$ over $I_c$ of <i>E. coli</i>	206
Figure 10.39. Relative change of $I_c$ of <i>D. radiodurans</i> in $NiCl_2$ for $I_c$ of $NiCl_2$ over $I_c$ of <i>D. radiodurans</i> after 72 hours	206
Figure 10.40. Comparison of relative responses of $I_c$ of $NiCl_2$ for bacteria	207
Figure 10.41. Typical AC-Gp conductance characteristics of <i>E. coli</i> in $NiCl_2$	208
Figure 10.42. Typical AC-Gp conductance characteristics of LB broth in $NiCl_2$	208
Figure 10.43. Comparison of relative responses of AC-Gp for <i>E. coli</i> in $NiCl_2$	209
Figure 10.44. Comparison of relative responses of conductance (AC-Gp) for <i>E. coli</i> bacteria and $NiCl_2$ after 72 hours	209
Figure 10.45. AC conductance ratios of <i>E. coli</i> in $NiCl_2$ after 72 hours, against AC conductance for <i>E. coli</i>	210
Figure 10.46. Comparison of relative responses of conductance Gp of <i>D. radiodurans</i> in $NiCl_2$ and conductance Gp of $NiCl_2$ after 72 hours	210
Figure 10.47. Comparison of relative response of conductance Gp for <i>E. coli</i> and <i>D. radiodurans</i> bacteria in $NiCl_2$ over Gp of $NiCl_2$ after 72 hours	211
Figure 10.48. Comparison of relative response of conductance Gp for <i>E. coli</i> and <i>D. radiodurans</i> bacteria in $NiCl_2$ over Gp of bacteria after 72 hours	211
Figure 10.49. AC capacitance of $NiCl_2$ in LB broth	212
Figure 10.50. AC capacitance of <i>E. coli</i> in $NiCl_2$ after 72 hours	212
Figure 10.51. AC capacitance of <i>E. coli</i> in $NiCl_2$ and capacitance of $NiCl_2$ after 72 hours	213
Figure 10.52. AC capacitance ratios of <i>E. coli</i> in $NiCl_2$ over AC capacitance for $NiCl_2$	213
Figure 10.53. AC capacitance ratios of <i>E. coli</i> in $NiCl_2$ over AC capacitance for <i>E. coli</i>	214
Figure 10.54. AC capacitance of <i>D. radiodurans</i> in $NiCl_2$ and for $NiCl_2$ in OXOID broth	215
Figure 10.55. AC capacitance ratios of <i>D. radiodurans</i> in $NiCl_2$ over AC capacitance of OXOID broth in $NiCl_2$	215
Figure 10.56. AC capacitance ratios of <i>D. radiodurans</i> in $NiCl_2$ over AC capacitance for <i>D. radiodurans</i>	216

Figure 10.57. Comparison of relative response of capacitance $C_p$ for <i>E. coli</i> and <i>D. radiodurans</i> in $NiCl_2$ over $G_p$ capacitance of $NiCl_2$	216
Figure 10.58. Comparison of relative response of capacitance $C_p$ for <i>E. coli</i> and <i>D. radiodurans</i> bacteria in $NiCl_2$ over $C_p$ capacitance of <i>E. coli</i> and <i>D. radiodurans</i>	217
Figure 10.59. Changes in surface resistance ( $R_s$ ) of <i>E. coli</i> bacteria samples after being added $CdCl_2$ after 72 hours exposure	218
Figure 10.60. Changes in surface resistance ( $R_s$ ) of <i>E. coli</i> bacteria samples after being added $CdCl_2$ and for $CdCl_2$ with LB broth	218
Figure 10.61. Normalised curve for ratio of surface resistance of <i>E. coli</i> bacteria in $CdCl_2$ to surface resistance of $CdCl_2$ with LB broth	219
Figure 10.62. Relative changes curve for ratio of surface resistance of <i>E. coli</i> bacteria in $CdCl_2$ to surface resistance of $CdCl_2$ with LB broth	219
Figure 10.63. Changes in surface resistance ( $R_s$ ) of <i>D. radiodurans</i> bacteria after being added $CdCl_2$ and for $CdCl_2$ with OXOID broth	220
Figure 10.64. Normalised curve for ratio of surface resistance of <i>D. radiodurans</i> bacteria in $CdCl_2$ to surface resistance of $CdCl_2$ with OXOID broth	220
Figure 10.65. Relative changes curve for ratio of surface resistance of <i>D. radiodurans</i> bacteria in $CdCl_2$ to surface resistance of $CdCl_2$ with OXOID broth	221
Figure 10.66. Comparison curves for surface resistance substantial ( $K_{b-Sub}$ ) between <i>E. coli</i> and <i>D. radiodurans</i> bacteria response to $CdCl_2$	221
Figure 10.67. Changes in surface capacitance ( $C_s$ ) of <i>E. coli</i> bacteria samples after being added $CdCl_2$ and for $CdCl_2$ with LB broth	222
Figure 10.68. Normalised curve for ratio of surface capacitance of <i>E. coli</i> bacteria in $CdCl_2$ to surface capacitance of $CdCl_2$ with LB broth after 72 hours	222
Figure 10.69. Relative changes curve for ratio of surface capacitance of <i>E. coli</i> bacteria in $CdCl_2$ to surface capacitance of $CdCl_2$ with LB broth	223
Figure 10.70. Changes in surface capacitance ( $C_s$ ) of <i>D. radiodurans</i> bacteria samples after being added $CdCl_2$ and for $CdCl_2$ with OXOID broth	223
Figure 10.71. Normalised curve for ratio of surface capacitance of <i>D. radiodurans</i> bacteria in $CdCl_2$ to surface capacitance of $CdCl_2$ with LB broth	224
Figure 10.72. Relative changes curve for ratio of surface capacitance of <i>D. radiodurans</i> bacteria in $CdCl_2$ to surface capacitance of $CdCl_2$ with OXOID broth	224
Figure 10.73. Relative changes curve comprised for surface capacitance of <i>E. coli</i> and <i>D. radiodurans</i> bacteria in $CdCl_2$ after 72 hours	225

Figure 10.74. Changes in surface resistance ( $R_s$ ) of <i>E. coli</i> bacteria after being added $NiCl_2$ and for $NiCl_2$ with LB broth	226
Figure 10.75. Normalised curve for ratio of surface resistance of <i>E. coli</i> bacteria in $NiCl_2$ to surface resistance of $NiCl_2$ with LB broth	226
Figure 10.76. Relative changes curve for ratio of surface resistance of <i>E. coli</i> bacteria in $NiCl_2$ to surface resistance of $NiCl_2$ with LB broth over surface resistance of <i>E. coli</i>	227
Figure 10.77. Changes in surface resistance ( $R_s$ ) of <i>D. radiodurans</i> bacteria after being added $NiCl_2$ and for $NiCl_2$ with OXOID broth	227
Figure 10.78. Normalised curve for ratio of surface resistance of <i>D. radiodurans</i> bacteria in $NiCl_2$ to surface resistance of $NiCl_2$ with OXOID broth	228
Figure 10.79. Relative changes curve for ratio of surface resistance of <i>D. radiodurans</i> bacteria in $NiCl_2$ to surface resistance of $NiCl_2$ with OXOID broth	228
Figure 10.80. Comparison curves of normalised surface resistance ( $K_s$ ) for <i>E. coli</i> (black) and <i>D. radiodurans</i> (blue) in $NiCl_2$	229
Figure 10.81. Comparison curves of relative changes for surface resistance ( $K_{s-sub}$ ) for <i>E. coli</i> (black) and <i>D. radiodurans</i> (blue) in $NiCl_2$	229
Figure 10.82. Changes in surface capacitance ( $C_s$ ) of <i>E. coli</i> bacteria samples after being added $NiCl_2$ and for $NiCl_2$ with LB broth	230
Figure 10.83. Normalised curve for ratio of surface capacitance of <i>E. coli</i> bacteria in $NiCl_2$ to surface capacitance of $NiCl_2$	230
Figure 10.84. Relative changes curve for ratio of surface capacitance of <i>E. coli</i> bacteria in $NiCl_2$ to surface capacitance of $NiCl_2$ with LB broth	231
Figure 10.85. Normalised curve for ratio of surface capacitance of <i>D. radiodurans</i> bacteria in $NiCl_2$ to surface capacitance of $NiCl_2$ with OXOID broth	231
Figure 10.86. Relative changes curve for ratio of surface capacitance of <i>D. radiodurans</i> bacteria in $NiCl_2$ to surface capacitance of $NiCl_2$ with OXOID broth	232
Figure 10.87. Comparison curves of normalised surface capacitance ( $C_s$ ) for <i>E. coli</i> (blue) and <i>D. radiodurans</i> (black) in $NiCl_2$	232
Figure 10.88. Comparison curves of relative changes in surface capacitance ( $F_{s-sub}$ ) for <i>E. coli</i> (red) and <i>D. radiodurans</i> (black) in $NiCl_2$	233
Figure 10.89. Comparison curves of normalised surface resistances ( $K_{Normalised}$ ) for <i>E. coli</i> and <i>D. radiodurans</i> bacteria in ( $NiCl_2$ & $CdCl_2$ )	233
Figure 10.90. Comparison curves of relative changes surface resistances ( $K_{sub}$ ) for <i>E. coli</i> and <i>D. radiodurans</i> bacteria in ( $NiCl_2$ & $CdCl_2$ )	234

Figure 10.91. Comparison curves of normalised surface capacitance ( $F_s$ ) for E. coli and D. radiodurans bacteria in ( $NiCl_2$ & $CdCl_2$ )	234
Figure 10.92. Comparison curves of relative changes surface capacitance ( $F_s$ ) for E. coli and D. radiodurans bacteria in ( $NiCl_2$ & $CdCl_2$ )	235
Figure 10.93. Comparisons of relative changes in ( $I_{c-Sub}$ ) for E. coli and D. radiodurans bacteria in response to exposure to gamma radiation, $CdCl_2$ or $NiCl_2$	235
Figure 10.94. Comparisons of relative changes in $(AC-Gp)_{Sub}$ for E. coli and D. radiodurans bacteria in response to exposure to gamma radiation, $CdCl_2$ or $NiCl_2$	236

## Appendixes

### Appendix A

Figure A1. Fluorescence microscopy images of E. coli bacteria samples before (a) and after (b) 2 hours exposure to gamma radiation	242
Figure A2. Fluorescence microscopy images of E. coli bacteria samples before (a) and after (b) 480 hours exposure to gamma radiation	242
Figure A3. Fluorescence microscopy image for D. Radiodurans bacteria samples (a) before and (b) after 360 hours exposure to gamma radiation	143
Figure A4. Relation between (live/dead) D. radiodurans bacteria and exposure time to Gamma radiation (fluorescence microscopy results)	243
Figure A5. Relation between ratios (live/dead) of D. radiodurans bacteria exposed to Gamma Ray and time (fluorescence microscopy results)	244
Figure A6. Fluorescence spectra of D. radiodurans samples in nutrient broth exposed to gamma ray for 120 hours	244
Figure A7. Fluorescence spectra (light scatter) of two D. radiodurans bacteria samples exposed to gamma radiation for 600h 1200000 mSv	245

### Appendix B

Figure B1. I-V characteristics of D. radiodurans samples not exposed to $\gamma$ -ray	246
Figure B2. Conductance $G_p$ of E. coli samples for different time exposure to gamma radiation	246
Figure B3. Conductance $G_p$ of E. coli samples not exposed to gamma radiation for different time	247
Figure B4. AC conductance of D. radiodurans samples not exposed to gamma radiation	247

Figure B5. AC capacitance of <i>D. radiodurans</i> samples for varied exposure to gamma radiation	248
Figure B6. AC capacitance of <i>D. radiodurans</i> samples not exposed to gamma radiation	248
<b>Appendix C</b>	
Figure C1. Effect of CdCl <sub>2</sub> on L/D ratio of <i>D. radiodurans</i> for different incubation times	249
Figure C2. Ratio (L/D) <sub>m</sub> of <i>D. radiodurans</i> after adding salt over ratio (L/D) <sub>0</sub> of <i>D. radiodurans</i> after 72 hours	249
Figure C3. Effect of CdCl <sub>2</sub> on second order diffraction peak for <i>E. coli</i> bacteria	250
Figure C4. Effect of CdCl <sub>2</sub> on 2-nd order diffraction peak for <i>D. radiodurans</i>	250
Figure C5. Optical densities OD <sub>600</sub> for <i>E. coli</i> bacteria in NiCl <sub>2</sub>	251
Figure C6. Optical densities OD <sub>600</sub> for <i>D. radiodurans</i> bacteria in NiCl <sub>2</sub> for time exposure	251
Figure C7. Effect of NiCl <sub>2</sub> on second order diffraction peak for <i>E. coli</i>	252
Figure C8. Effect of NiCl <sub>2</sub> on second order diffraction peak for <i>D. radiodurans</i>	252
<b>Appendix D</b>	
Figure D1. I-V characteristics of <i>D. radiodurans</i> samples for different concentrations of CdCl <sub>2</sub> , after 72 hours	253
Figure D2. I-V characteristics for different concentrations of CdCl <sub>2</sub> with OXOID broth	253
Figure D3. Typical AC-Gp of <i>D. radiodurans</i> samples for different concentrations of CdCl <sub>2</sub>	254
Figure D4. Typical AC-Cp of <i>D. radiodurans</i> samples for different concentrations of CdCl <sub>2</sub>	254
Figure D5. Typical AC-Gp of OXOID broth for different concentrations of CdCl <sub>2</sub>	255
Figure D6. Typical AC-Gp of different concentrations of CdCl <sub>2</sub> with OXOID broth	255
Figure D7. AC conductance ratio of <i>D. radiodurans</i> bacteria in CdCl <sub>2</sub> after 72 hours over conductance for samples not exposed	256
Figure D8. AC capacitance ratios of <i>D. radiodurans</i> bacteria in CdCl <sub>2</sub> after 72 hours over the AC capacitance for samples not exposed	256

Figure D9. I-V characteristics of <i>D. radiodurans</i> in NiCl <sub>2</sub> after 72 hours	257
Figure D10. I-V characteristics for NiCl <sub>2</sub> in OXOID broth	257
Figure D11. I <sub>c</sub> of <i>D. radiodurans</i> in NiCl <sub>2</sub> over I <sub>c</sub> NiCl <sub>2</sub>	258
Figure D12. I <sub>c</sub> of <i>D. radiodurans</i> in NiCl <sub>2</sub> over I <sub>c</sub> of <i>D. radiodurans</i>	258
Figure D13. Typical AC-Gp of <i>D. radiodurans</i> in NiCl <sub>2</sub> after 72 hours	259
Figure D14. Typical AC-Gp conductance of OXOID broth in NiCl <sub>2</sub>	259
Figure D15. AC conductance ratios of <i>D. radiodurans</i> in NiCl <sub>2</sub> over AC conductance for NiCl <sub>2</sub>	260
Figure D16. AC conductance ratios of <i>D. radiodurans</i> in NiCl <sub>2</sub> over the AC conductance for <i>D. radiodurans</i>	260
Figure D17. AC capacitance of <i>D. radiodurans</i> in NiCl <sub>2</sub>	261
Figure D18. AC capacitance of NiCl <sub>2</sub> in OXOID broth	261
Figure D19. Changes in surface capacitance (C <sub>s</sub> ) of <i>D. radiodurans</i> bacteria after being added NiCl <sub>2</sub> and for NiCl <sub>2</sub> with OXOID broth	262

## LIST OF TABLES

Table. 2.1. Typical RBE values for different kinds of radiation	24
Table 7.1. Parameters of (Co <sup>57</sup> ) radiation source used for exposure of bacteria samples	105
Table 7.2. Summary of fluorescence microscopy measurements of effect of Gamma radiation on E. coli bacteria	109
Table 7.3. Summary of fluorescence microscopy measurements of effect of Gamma radiation on D. radiodurans bacteria	121

# CHAPTER 1

## Introduction

The problems in the detection of environmental pollution are outlined in this chapter. Two important types of environmental pollution, i.e. radionuclide and heavy metals, were discussed, as well as the existing methods of their detection. The concept of the proposed sensor, based on microorganisms (bacteria) and the associated fundamental study of optical and electrical properties of bacteria samples were outlined. The chapter concludes by giving a clear statement and brief description of the aims and objectives of this work.

### 1. The Environment

The environment includes the human and natural world and its surroundings, which consist of the atmosphere, hydrosphere and lithosphere. Human beings are very dependent on the environment. The atmosphere provides us with the air we breathe, the hydrosphere provides the water we drink, and the soil of the lithosphere provides us with the food that we eat. In addition, the environment provides us with raw materials to fulfil our other needs: the construction of housing; the production of consumer goods, etc. In a view of these important functions, it is imperative that we maintain the environment in a state that is as sustainable as possible. Fouling the environment by the products of our industrial society (called pollution) may have many harmful consequences, the damage to human health being of greatest concern.

#### 1.1. Environmental Pollution

Environmental pollution has become a considerable problem threatening the life of people, animals and other living species. Thousands of waste sites around the world contain different pollutants and toxins, particularly heavy metals and radioactive elements. These sites pose a serious threat to all living organisms, and humans in particular[1]. Environmental pollution can be defined as any discharge of material or energy into water, land and air, or can be due to introduction of contaminants into the natural environment that causes adverse changes, or may cause acute (short-term) or chronic (long-term) detriments to the Earth's ecological balance, or that lowers the quality of life. Pollutants may cause primary damage, with direct identifiable impacts on the environment, or secondary damage, in the form of minor perturbations in the

delicate balance of the biological food web that are detectable only over long time periods [2].

Until relatively recently in humanity history, where pollution has existed, it has been primarily a local problem. The industrialization of society and the explosion of the human population have changed the ecological system dramatically. The random discharge of untreated industrial and domestic waste into waterways; the release of thousands of tons of particulates and airborne gases into the atmosphere; the "throwaway" attitude toward solid waste; and the use of newly developed chemicals without considering potential consequences, have resulted in major environmental disasters, including the formation of smog and the pollution of large areas of the sea. Technology has begun to solve some pollution problems and public awareness of the extent of pollution will eventually force governments to undertake more effective environmental planning and adopt more effective anti-pollution measures.

Water pollution is the introduction into fresh or seawater of chemical, physical, or biological materials that degrade the quality of the water and affect the organisms living in it. This process ranges from the simple addition of dissolved or suspended solids to the discharge of the most insidious and persistent toxic pollutants, such as pesticides and heavy metals, as well as other non-degradable bio-accumulative chemicals [3].

Rapid urbanization and rapid population increases have produced sewage problems because treatment facilities have not kept pace with needs. Untreated and partially treated sewage from municipal wastewater systems and septic tanks in un-seeded areas contribute significant quantities of nutrients, suspended solids, dissolved solids, oil, metals (arsenic, mercury, chromium, lead, iron, and manganese), and biodegradable organic carbon to the water environment. An excess of dissolved solids make the water undesirable for drinking and for crop irrigation. Although essential to the aquatic habitat, nutrients such as nitrogen and phosphorus may also cause over-fertilization and accelerate the natural ageing process of lakes. This acceleration in turn produces an overgrowth of aquatic vegetation, massive algal blooms, and an overall shift in the biological community from low productivity with many diverse species to high productivity with large numbers of a few species of a less desirable nature. Bacterial action oxidizes biodegradable organic carbon and consumes dissolved oxygen in the water. In extreme cases where the organic-carbon loading is high, oxygen consumption may lead to oxygen depression causing disruption in the life of aquatic organisms.

Non-conventional pollutants include dissolved and particulate forms of metals, both toxic and nontoxic, and degradable and persistent organic carbon compounds discharged into water as a by-product of industry or as an integral part of marketable products. Thousands of untested chemicals are routinely discharged into waterways. In addition, coal strip mining releases acid waste that damages the surroundings. Non-conventional pollutants vary from biologically inert materials, such as clay and iron residues, to the most toxic and insidious materials [4]. The latter group may produce damage ranging from acute biological effects (complete sterilization of stretches of waterways) to chronic sub-lethal effects that may go undetected for years. The chronic low-level pollutants are proving to be the most difficult to correct and abate because of their ubiquitous nature and chemical stability. There are many types of environmental pollution, but this research will focus on radioactive and heavy metal pollution, and mostly on the development of new methods of their detection.

### **1.1.1. Radioactive Pollution**

The most dangerous type of pollution is radioactive contamination that results from the detonation of nuclear devices and other nuclear fallout. Nuclear fallout typically occurs from leaks from nuclear power plants, and from conventional weapons using depleted uranium. Nuclear explosion create radioactive dust and ash, consisting of materials either directly vaporized by a nuclear blast or charged by exposure, a highly dangerous radioactive contamination. It can lead to contamination of the environment and has a devastating effect on ecosystems years after the initial exposure. Other sources of radiation include spent fuel from nuclear plants, and by-products of mining operations and experimental research laboratories.

Radioactive contaminants are typically unstable radionuclide (or radioisotopes), some of them naturally occurring in the environment, such as Potassium-40 ( $^{40}\text{K}$ ) and Radium-226, while others, such as Strontium-90 ( $^{90}\text{Sr}$ ) and Technetium-99 ( $^{99}\text{Tc}$ ), appear as a result of human activities[5]. The presence of several natural radionuclide such as Tritium ( $^3\text{H}$ ) and particularly Uranium-238 ( $^{238}\text{U}$ ) has been substantially enhanced in the last 5-6 decades due to various nuclear projects of either military or civil origin.

A radionuclide is an atom with an unstable nucleus, which undergoes the nuclear reaction, called radioactive decay and releases energy as ionizing radiation, i.e. emits

gamma rays and/or subatomic particles [2]. The radiation is constantly present in the natural environment and called background radiation. It can be caused by numerous sources, including the following: Cosmic rays, the effect of which strongly depends on the state of stratosphere (e.g. “ozone holes” have recently appeared);

- (i) Radon gas, released from the Earth's crust into the atmosphere and then attaching to airborne dust and other particulate (granular, powder) materials, that human beings might ingest and inhale;
- (ii) Radionuclide's, present in natural minerals, stones and therefore in building materials;
- (iii) Mineral hot springs, containing mostly Radium 226 and small amounts of other radio-isotopes which are rather useful and used by people as spas [6];
- (iv) Artificial sources of background radiation used in radiological imaging and radiation therapy cannot be excluded from this list.

The level of natural background radiation varies, depending on location, and in some areas it is significantly higher than average [7]. However, such levels of radiation do not seem to have caused ill effects on the residents of the area and even possibly has made them slightly more radio resistant [8]. In addition, it has been reported that residents have healthier and longer lives. The knowledge of background radiation at relatively low levels is important; however, the focus of this project is on high levels of radiation caused by human activities [7].

The radiation risk level depends on several factors, namely the type of radioactive isotopes, the radiation intensity, and exposure period. The time of exposure also has a crucial effect on living cells. In contrast to the high radiation doses which cause direct damage to living cells and therefore almost immediate death, the effect of low levels of radiation (particularly with long time exposure) cause changes in DNA structure and result in different types of cancer (the cell multiplies uncontrollably) and/or genetic transformations (genetic mutation). Public concern over the release of radiation into the environment greatly increased following the disclosure of possible harmful effects to the public from nuclear weapons testing. The environmental effects of exposure to high-levels of ionizing radiation have been extensively documented through post-war studies on individuals who were exposed to nuclear radiation in Japan [8], but latent maladies of radiation poisoning have been recorded from 10 to 30 years after exposure.

The effects of exposure to low-level radiation are not yet fully known. A major concern of this type of exposure is the potential for genetic damage. Radioactive nuclear waste cannot be treated by conventional chemical methods and must be stored in heavily shielded containers in areas remote from biological habitats. The safest of storage sites currently used are impervious deep caves or abandoned salt mines. Most radioactive waste, however, has a half-life of hundreds to thousands of years, and to date no storage method has been found that is infallible.

### **1.1.2. Heavy Metal Pollution**

Heavy metal pollution is a problem associated with areas of intensive industry. However, roadways and automobiles are now considered as one of the largest sources of heavy metal pollution. Zinc, copper, and lead are three of the most common heavy metals released from road travel, accounting for at least 90 of the total metals in road runoff. Lead concentrations, however, have been decreasing consistently since leaded gasoline was discontinued. Smaller amounts of many other metals, such as nickel and cadmium, are also found in road runoff and exhaust [9].

Cadmium levels in the environment vary widely. As stated above, cadmium emissions into the environment are normally transported continually between the three main environmental compartments, air, water and soils. Three distinct categories may be recognised with respect to cadmium in air concentrations: cadmium in ambient air; cadmium air levels in occupational exposure situations; and cadmium in the air from the smoking of tobacco. Cadmium in ambient air represents, by far, the majority of total airborne cadmium. Inputs from all three categories may affect human cadmium intake and human health, but the levels and the transfer mechanisms to humans are substantially different for the three. Whereas cadmium from occupational environments and cadmium from cigarette smoke are transferred directly to humans, cadmium in ambient air is generally deposited onto waters or soils, then eventually transferred to plants and animals, and finally enter the human body through the food chain.

Ambient air cadmium concentrations have generally been estimated to range from 0.1 to 5 ng/m<sup>3</sup> in rural areas, from 2 to 15 ng/m<sup>3</sup> in urban areas, and from 15 to 150 ng/m<sup>3</sup> in industrialised areas, although some much lower values have been noted in extremely remote areas and some much higher values have been recorded in the past near uncontrolled industrial sources [10]. There are generally little or no differences noted in

cadmium levels between indoor and outdoor air in non-smoking environments. Smoking, however, may substantially affect indoor ambient air cadmium concentrations.

Cadmium air concentrations may be elevated in certain industrial settings, but these exposures are closely controlled today by national occupational exposure standards. Historically, average exposure levels and regulatory permissible exposure limits have decreased markedly in the past 40 years, in recognition of the importance of cadmium inhalation to human health and with the significant improvements in air pollution control technology over that period. Occupational exposure standards which were formerly set at 100 to 200  $\mu\text{g}/\text{m}^3$  are now specified at 2 to 50  $\mu\text{g}/\text{m}^3$ , along with the requirement to maintain biological indicators, such as cadmium-in-blood and cadmium-in-urine, below certain levels, in order to assure no adverse human health effects from cadmium occupational exposure [10]. The average cadmium content in the world's oceans has variously been reported as low as 5-20 ng/L [11], and as high from 20 to 100 ng/L [10]. Higher levels have been noted around certain coastal areas and variations of cadmium concentration with the ocean depth, presumably due to patterns of nutrient concentrations, have also been measured. Even greater variations are quoted for the cadmium contents of rainwater, fresh water, and surface water in urban and industrialised areas. Levels from 10 ng/L to 4000 ng/L have been quoted in the literature, depending on specific location and whether or not total cadmium or dissolved cadmium is measured. Cadmium is a natural, usually minor constituent of surface and groundwater. It may exist in water as the hydrated ion, as inorganic complexes such as carbonates, hydroxides, chlorides or sulphates, or as organic complexes with humic acids.

Nickel is a natural element of the earth's crust; therefore, small amounts are found in food, water, soil, and air [12]. Food is the major source of nickel exposure, with an average intake for adults estimated to be approximately 100 to 300 micrograms per day ( $\mu\text{g}/\text{d}$ ) [13]. Nickel is released into the air by power plants and trash incinerators. It will then settle to the ground or come down after reactions with raindrops. It usually takes a long time for nickel to be removed from air. Nickel can also end up in surface water when it is a part of wastewater streams. The larger part of all nickel compounds that are released to the environment will adsorb to sediment or soil particles and become immobile as a result. In acidic ground however, nickel is bound to become more mobile and it will often rinse out to the groundwater. The effect of nickel is mainly upon

organisms rather than humans. High nickel concentrations on sandy soils can clearly damage plants and high nickel concentrations in surface water can diminish the growth rates of algae. Microorganisms can also suffer from growth decline due to the presence of nickel, but they usually develop resistance to nickel after a while, and for animals, nickel is essential foodstuff, in small amounts. However, nickel is not only favourable as an essential element it can also be dangerous when the maximum tolerable amounts are exceeded. This can cause various kinds of cancer on different sites within the bodies of animals, mainly those that live near refineries. Nickel is not known to accumulate in plants or animals, and as a result, it does not penetrate into the food chain.

Zinc and Copper pollution contribution to the environment are from urbanization and automobiles. Brakes release copper, while tire wear releases Zinc. Motor oil also tends to accumulate metals, as it encounters surrounding parts as the engine runs, so oil leaks become another pathway by which metals enter the environment.

On the road surface, most heavy metals become bound to the surfaces of road dust or other particulates. During precipitation, the bound metals will either become soluble (dissolved) or be swept off the roadway with the dust. In either case, the metals enter the soil or are channelled into a storm drain. Whether in the soil or aquatic environment, metals can be transported by several processes. These processes are governed by the chemical nature of metals, soil and sediment particles, and the pH of the surrounding environment. Heavy metals are cations, meaning they carry a positive charge. Zinc and Copper, for instance, both carry a 2+ charge. Soil particles and loose dust also carry charges. Most clay minerals have a net negative charge. Soil organic matter tends to have a variety of charged sites on their surfaces, some positive and some negative. The negative charges of these various soil particles tend to attract and bind metal cations, preventing them from becoming soluble, and dissolved in water. The soluble form of metals is thought to be more dangerous because it is easily transported and more readily available to plants and animals. By contrast, soil bound metals tend to stay in place [14]. Metal behaviour in the aquatic environment (streams, lakes and rivers) is surprisingly similar to that in water environment. Streambed sediments exhibit the same binding characteristics found in the normal soil environment. As a result, many heavy metals tend to be sequestered at the bottom of water bodies. Some of these metals will dissolve. The aquatic environment is more susceptible to the harmful effects of heavy metal pollution because aquatic organisms are in close and prolonged contact with the soluble

metals. Ph tends to be a major variable in the whole process, being a measure of the concentration of hydrogen ions ( $H^+$ ) dissolved in water.  $H^+$  is the ion that causes acidity; however, it is also a cation, and as such is attracted to the negative charges of the soil and sediment particles. In acidic conditions, there are enough  $H^+$  ions to occupy many of the negatively charged surfaces of clay and organic matter [15]. Little room is left to bind metals, and as a result, more metals remain in the soluble phase. The effects of pH are even more pronounced in Washington because of the problem of acid rain. Acid rainfall can cause a large increase in acidity and a corresponding increase in heavy metals becoming soluble. The detection of heavy metals is within the scope of this PhD project.

## **1.2. Detection of Pollution**

To tackle the problem of environmental pollution, we need, first, to have reliable methods of detection and identification of pollutants. After pollutions have been identified and their levels measured, adequate remediation procedure can be deployed. In the course of the last 40-50 years, a large number of analytical methods for the detection of radiation and chemical contaminations have been developed [16]. For example, different types of penetrative radiation ( $\alpha$ ,  $\beta$ ,  $\gamma$ , or neutron) can be detected using physical methods, such as solid state nuclear detectors, G-M detectors, gas proportional chambers and gamma-ray spectroscopy [17]. Powerful analytical of chromatography can identify any chemical contamination in very low concentrations down to the part per billion (ppb) range. However, very often these methods are expensive, require the use of high-tech equipment, specialized laboratories, and well-trained personnel, and thus cannot be used for in-field trials. Nowadays, the demand for inexpensive, portable, easy-to-use sensor devices, which can be used even by non-specialists in field conditions, is growing.

Another aspect of sensor development is their specificity to particular types of pollutant. Identification of chemical pollutants is possible by using highly specific detectors. Advances of organic chemistry and biochemistry allow the development of specific receptors for every possible chemical compound. However, such an approach has been very expensive and ineffective. Novel types of smart sensors capable of both the identification and concentration evaluation of a large number of chemicals are presently in great demand [18]. Different types of multi-sensors or sensor-arrays combined with powerful data acquisition systems, such as artificial neural networks (ANN) or principal

component analysis (PCA), were developed in the last decade and resulted in advanced analytical instrument is called electronic nose. Despite all the advantages of such modern sensing systems, they are still quite expensive and, unfortunately no reliable. Cost-effectiveness is the main issue.

The use of natural systems for sensing, such as microorganisms or bacteria, can be advantageous. It is known that microorganisms (bacteria) can be badly affected by radiation and some chemical pollutants [19]. Such negative effects depend on the radiation level and concentration of pollutants: the damage ranges from partial loss of functionality at low doses (concentrations) up to the “death” of bacteria at high doses (concentrations). Therefore, the monitoring of the bacteria count in natural water resources could serve as a simple method of detecting contaminants. In the simplest scenario, the low bacteria count in a particular water sample can give an indication (warning) of the presence of some type of contaminants of either radioactive or toxic nature; then more detailed laboratory analysis can be undertaken on this particular sample. The concept of bacterial sensors can be developed further with the use of several types of bacteria affected differently by different types of pollutions alongside modern data acquisition software (ANN or PCA). Such advanced bacterial sensors can solve a complex problem of simultaneous identification and evaluation of different pollutants including radioactive and toxic ones. At the same time, microorganisms can be utilized for the remediation of pollution.

This work focuses on the development of simple and cost effective methods for monitoring environmental pollutants, particularly radionuclides and heavy metals, these being common contaminants of water resources [20,21]. It is known that microorganisms such as bacteria are very sensitive to  $\gamma$ -radiation produced by radionuclide's, as well as to heavy metals [22,23]. The use of microorganisms for assessments of general toxicity of aqueous environment has been reported previously [24]. Identification of the types of pollutants in the environment and the evaluation of their concentration is a much more difficult task, being impossible to solve using a single sensor. However, the sensor array approaches [25] utilising several types of bacteria which are inhibited differently by different types of pollutants, could solve the above problem.

Two types of bacteria were selected for this work, namely *Escherichia coli* (*E. coli*) and *Dinococcus radiodurans* (*D. radiodurans*). *E. coli* being quite sensitive to gamma radiation could be suitable for monitoring radionuclide's contamination at a low level.

While its resistance knows *D. radiodurans* to gamma radiation, it can be used for detection of intermediate and high levels of radioactive pollution [26]. In the meantime, these bacteria samples will be tested under treatment with heavy metals. In order to acquire the fundamental knowledge and understand the mechanism of inhibition of bacteria by different pollutants, the correlation between the bacteria concentration and optical and electrical properties of liquid bacteria samples must be established [27, 28]. For this purpose, several optical methods, including fluorescent microscopy and spectroscopy, and UV-vis absorption spectroscopy will be used in this work, along with electrical (electrochemical) AC and DC measurements, in order to study the effect of gamma radiation and heavy metals, namely  $\text{Cd}^{2+}$  and  $\text{Ni}^{2+}$ , on the above bacteria. Electrochemical measurements are considered promising for the development of simple bacteria-based sensors for the detection of gamma radiation and heavy metals. Our work is a logical continuation of previous research and a development into electrochemical cell-based sensors suitable for detection of different analytes [29]. The use of two (or more) types of bacteria may lead to the development of sensor arrays utilizing the principles of pattern recognition of inhibition factors.

### **1.3. Aims and Objectives**

The main aim of this project is the development of novel sensing technologies for the detection of environmental pollution. The project utilizes two types of bacteria samples (*E. coli* and *D. radiodurans*) for the study of their optical and electrical properties under effects of gamma radiation and heavy metals. One of the main reasons of using bacteria is their versatility in detecting different pollutants; another reason is the cost-effectiveness of bacterial sensors. Potentially, this work may lead to the development of novel, inexpensive, low power, and portable sensors for early detection of radionuclide and heavy metals.

These aims can be achieved through the following objectives:

1. To utilize several optical techniques, such as fluorescence microscopy, UV-visible absorption and fluorescence spectrometry for the detection of gamma radiation and heavy metals.
2. To utilize AC and DC electrical measurements for detection of gamma radiation and heavy metals.

3. To establish a correlation between optical and electrical properties and bacteria concentration.
4. To study the effect of gamma radiation and  $\text{Cd}^{2+}$  and  $\text{Ni}^{2+}$  ions on optical and electrical properties of bacteria.
5. To develop a sensor prototype for detection of radionuclide and heavy metals.

#### **References:**

1. Michael J Daly, (2000), Engineering radiation-resistant bacteria for environmental biotechnology, Elsevier Science Ltd, Current Opinion in Biotechnology, Vol. 11, pp. 280-285.
2. Spengler, John D. and Sexton, Ken (1983), Indoor Air Pollution: A Public Health Perspective" Science (New Series), Vol. 221 (4605), pp. 9-17.
3. John S. Gray, Farrukh B. Mirza, (1979), A possible method for the detection of pollution-induced disturbance on marine benthic communities, ELSELVER, Volume 10, Issue 5, pp. 142-146.
4. Chaychian M., Al-Sheikhly M., Silverman J. and McLaughlin W.L. (1998), The mechanism of removal of heavy metals from water by ionizing radiation. Radiat. Phys. Chem., Vol. 53, pp. 145-150.
5. Hassan Brim, Sara C. McFarlan, James K. Fredrickson, Kenneth W. Minton, Min Zhai, Lawrence P. Wackett, and Michael J. Daly, (2000), Engineering Deinococcus radiodurans for metal remediation in radioactive mixed waste environments, Nature Biotechnology, Vol. 18, pp. 85-90.
6. Hong, Sungmin et al. (1996), History of Ancient Copper Smelting Pollution During Roman and Medieval Times Recorded in Greenland Ice, Science (New Series) Vol. 272 (5259), pp. 246-249.
7. Mustonen R, Christensen T, Strandén E, Ehdwall H, Hansen H, Suolanen V, Vieno T, (1992), Natural Radiation, A perspective to radiation risk factors of nuclear energy production, The Environment, , Vol. 114, pp. 99-112.
8. Sato K, (1986), Current and future possibilities of radiation sterilization in Japan, International Journal of Radiation Applications and Instrumentation. Part A. Applied Radiation and Isotopes, Vol. 37, pp. 66-67.

9. Walter I, Martínez F, Cala, V, (2006), Heavy metal speciation and phytotoxic effects of three representative sewage sludges for agricultural uses, *Environmental Pollution*, February Vol. 139, pp. 507-514.
10. Carl-Gustaf Elindert, Monica Nordberge, Brita Palm, (1990), Is Cadmium Released from Metallothionein in Rejected Human Kidneys, *Biology of Metals*, Vol. 2, Issue 4, pp 219-222.
11. Gomes N. C. M, Landi, L, Smalla K, Nannipieri P, Brookes P. C, Renella G, (2010), Effects of Cd-and Zn-Enriched Sewage Sludge on Soil Bacterial and Fungal Communities, *Ecotoxicology and Environmental Safety*, ISSN 0147-6513, Vol. 73, Issue 6, pp. 1255-1263.
12. Agency for Toxic Substances and Disease Registry (ATSDR). (1997), Toxicological Profile for Nickel (Update). Public Health Service, U.S. Department of Health and Human Services, Atlanta, GA.
13. U.S. Environmental Protection Agency. (1986), Health Assessment Document for Nickel. EPA/600/8-83/012F. National Center for Environmental Assessment, Office of Research and Development, Washington, DC.
14. Tom Dauwe, Ellen Janssens, Rianne Pinxten, Marcel Eens, (2005), The reproductive success and quality of blue tits in a heavy metal pollution gradient, *Environmental Pollution*, Vol. 136, Issue 2, pp. 243-251.
15. Begemann, M, Gudeman, C. Pfaff, J. Saykally, R. (1983), Detection of the Hydronium Ion ( $H_3O^+$ ) by High-Resolution Infrared Spectroscopy. *Physical Review Letters* Vol. 51 (7), pp. 554–557.
16. Patricia Miretzky, Andrea Saralegui, Alicia Fernández Cirelli. (2006), Simultaneous heavy metal removal mechanism by dead macrophytes. *Radiat. Chemosphere*, Vol. 62, pp. 247–254.
17. Szentmiklósi, L; Belgya, T; Molnár, G L; Révay, Zs, (2007), Time resolved gamma-ray spectrometry, *Journal of Radioanalytical and Nuclear Chemistry*, ISSN 0236-5731, Vol. 271, Issue 2, pp. 439 – 445.
18. Yoshiaki Sakurai, Ho-Sup Jung, Toshinori Shimanouchi, Takao Inoguchi, Eiichi Morita, Ryoichi Kuboi, Kazuki Natsukawa, (2002), Novel array-type gas sensors using conducting polymers, and their performance for gas identification, *Sensors and Actuators B: Chemical*, Vol. 83, Issues 1-3, pp. 270-275.

19. Gao GuanJun, Fan Lu, Lu HuiMing and Hua YueJin, (2008), Engineering Deinococcus radiodurans into biosensor to monitor radioactivity and genotoxicity in environment, Chinese Science Bulletin, Vol. (53), pp. 1675-1681.
20. D. G Jones, (2001), Development and application of marine gamma-ray measurements, Journal of Environmental Radioactivity, Volume 53, Issue 3, pp. 313-333.
21. Adam K, Wanekava Wilfred Chen and Ashok Mulchandain, (2008), Recent biosensing developments in environmental security, Journal of Environmental Monitoring, Issue 6, pp. 703-712.
22. Kira S. Makarova, L. Aravind, Yuril. Wolf, Roman L. Tatusoy, Kenneth W. Minton, Eugene V. Koonin and Michael J. Daly,(2001), Genome of the Extremely Radiation-Resistant Bacterium Deinococcus radiodurans Viewed from the perspective of comparative Genomics, MicrobiolMolBiolRev; Vol. 65 (1), pp. 44-79.
23. Chua H, Yu P. H. F, Sin S. N, Cheung M. W. L, Sublethal Effects of Heavy Metals on Activated Sludge Microorganisms (1999),Elsevier (Chemosphere). Vol 39, Issue 15, pp. 2681-2692.
24. Starodub N.F, Katzev A. M, Levkovetzl. A, 2003, Biosensor Based on the Photoluminescent Bacteria and its Use for Express Control of Water Contamination by Some Surface Active Substances, Boston Transducers: Digest of Technical Papers 1- 2, pp. 1197-1200.
25. Alexei Nabok, (2005), Organic and Inorganic Nanostructures, Ch.7, Chemical and Biosensor, pp. 205-251.
26. Michael J Daly, Engineering radiation-resistant bacteria for environmental biotechnology, (2000), Current Opinion in Biotechnology, Vol. 11, Issue 3, pp. 280-285.
27. Al-Shanawa M, Nabok A, Hashim A, Smith T, (2013), Detection of ionization radiation effect using microorganism (Escherichia Coli), Sensors & Transducers journal, Vol. 149, pp. 179-186.
28. Al-Shanawa M, Nabok A, Hashim A, Smith T and Forder S, (2013), Detection of  $\gamma$ -radiation and heavy metals using electrochemical bacterial-based sensor, IOP Publishing, Journal of Physics, Conference Series 450.
29. Yufera A., Canete D., Daza P. (2011), SENSORDEVICES, The International Conference on SensorDevice Technologies and Application Technologies and Application, pp. 143-146.

## CHAPTER 2

### Radiation and its Sources

Radiation occurs naturally in the environment; therefore, radionuclides of naturally present in air, water, soil, sediments, wood, rocks, building materials, and food. Natural radiation exists everywhere around the Earth in different levels. This means radiation can be found all around us. Our natural environment, the food we eat, the water we drink, and the air we breathe may contain or be affected by some radioactive materials. This chapter describes the types of radiation and its sources.

#### 2.1. Ionizing Radiation

Three main sources of radiation can be identified. Firstly, radiation in the soils and rocks, which is mostly due to Potassium-40 and elements from U-238 and Th-232 series; then the radiation that comes from space, called cosmic rays or cosmogonist[1]; and finally there is human-made radiation, i.e. that created by humans that would not exist naturally, or substances emitting more radiation than normal. The four major types of radiation are:

- Gamma ( $\gamma$ ) radiation - high-energy electromagnetic waves;
- Beta ( $\beta$ ) radiation - emission of electrons or positrons;
- Alfa ( $\alpha$ ) radiation - emission of Helium nucleus ( $He_2^4$ );
- Neutron radiation - emission of high or low energy neutrons;

Ionizing electromagnetic radiation consists of photons that have sufficient energy to knock an electron out of an atom or molecule, thus forming an ion. The energy of such photons usually lies above the ultraviolet (UV) and X-ray ranges, in an area called the  $\gamma$ -ray region of the electromagnetic spectrum. Alpha ( $\alpha$ ) and beta ( $\beta$ ) particles as well as neutrons are emitted during certain radioactive reactions. The energy of 1 to 35 eV is needed to ionize atoms or molecules, while  $\alpha$  and  $\beta$  particles,  $\gamma$ -rays, and neutrons emitted during nuclear reactions often have energies of several MeV. Therefore, a single  $\alpha$ - particle,  $\beta$ - particle,  $\gamma$ -quantum, or neutron can ionize thousands of atoms (molecules) [2].

##### 2.1.1. Gamma Rays

A gamma ray is a packet of high-energy electromagnetic waves (or photons). Gamma photons are the most energetic in the electromagnetic spectrum, emitting from the nucleus of some unstable (radioactive) nucleus. Gamma photons have no rest mass and

no electrical charge, they are pure electromagnetic energy. High energy gamma photons travel at the speed of light in vacuum and can cover hundreds of meters in the air before dispersing their energy, They can easily pass through different types of materials, including human tissue, so both external and internal exposure to gamma rays have to be considered. Gamma rays can travel much farther than alpha or beta particles and have enough energy to pass entirely through the human body, potentially exposing all internal organs. High-energy gamma radiation, having a very small cross-section of interaction, passes through the human body practically without interacting with tissue. In contrast, alpha and beta particles having much larger mass and thus their larger interaction cross-section cause much more damage inside the body. Actually, Gamma rays do not directly ionize atoms in the tissue; instead, they cause secondary emission of electrons, which are essentially the same as beta particles  $\beta^-$ . These energized  $\beta^-$  particles then interact (ionise) the tissue, the same way as alpha or beta particles do. The speed of gamma photons ( $C$ ) is independent of their wavelength, frequency, and energy, and it is the same as that of all other types of electromagnetic radiation ( $C=3.10^8$  m/sec in vacuum). Their wavelength ( $\lambda$ ), frequency ( $\nu$ ) and energy ( $E$ ) are correlated by the following equations [3]:

$$\lambda = \frac{C}{\nu} , \quad E = h\nu \quad (2.1)$$

Gamma radiation can be produced by other forms of radiation, such as alpha or beta, through the secondary nuclear reactions (decays). The mechanism involves a nucleus emitting  $\alpha$  or  $\beta$  particles, and the daughter nucleus can also be in an excited state. It can then move to a lower energy state by emitting a gamma ray, in a similar way to when the electrons in an atom relax to a lower energy state and emit X-rays. Emission of gamma rays from an excited nuclear state typically requires only  $10^{-12}$  seconds, followed by another radioactive decay that produces other radioactive particles. For example,  $^{60}\text{Co}$  decays to an excited  $^{60}\text{Ni}$  by beta decay. Then the  $^{60}\text{Ni}$  drops down to the ground state by emitting two gamma rays in sequence (1.17 MeV then 1.33 MeV), as shown in Figure 2.1.

Another example is the alpha decay of  $^{241}\text{Am}$  to form  $^{237}\text{Np}$ , which is accompanied by gamma emission. In some cases, e.g.  $^{60}\text{Co}/^{60}\text{Ni}$ , the gamma emission spectrum for a daughter nucleus is quite simple, while in other cases, e.g.  $^{241}\text{Am}/^{237}\text{Np}$  or  $^{192}\text{Ir}/^{192}\text{Pt}$ , the

gamma emission spectrum is complicated, being associated with a series of nuclear energy levels [1].

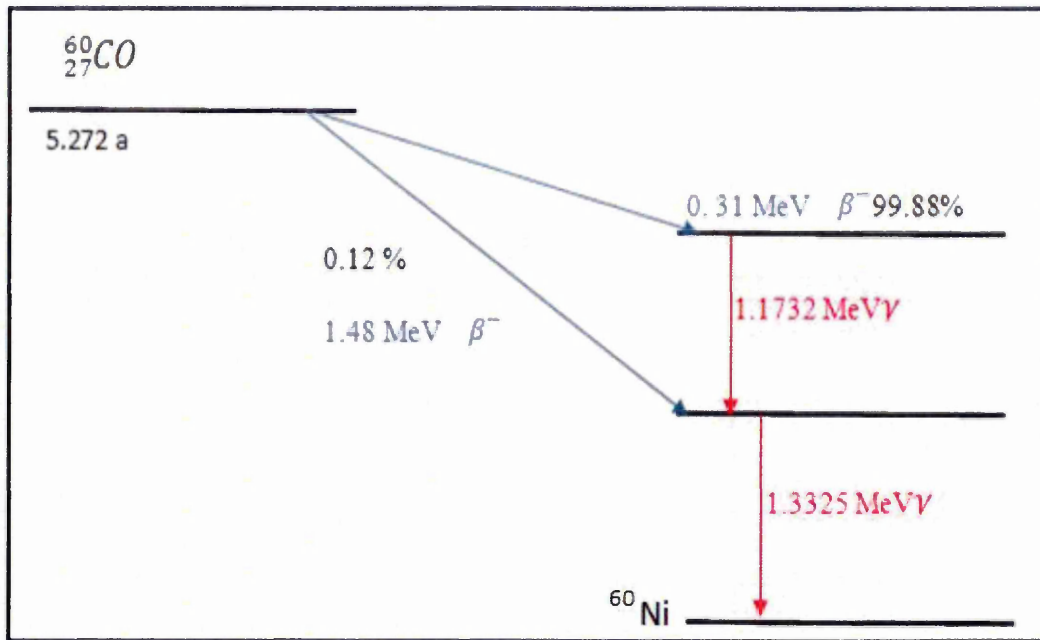


Figure 2.1. The scheme of decay of  $^{60}\text{Co}$  to  $^{60}\text{Ni}$  [1]

The fact that an alpha spectrum can have a series of different peaks with different energies supports the idea that several nuclear energy levels are possible. In addition, there is another process of gamma radiation emission called the Electron-Capture (EC) process, when an atomic electron captured by the nucleus is followed by conversion of a proton into a neutron, as illustrated by  $^{57}\text{Co}$  decay in Figure 2.2 [4].

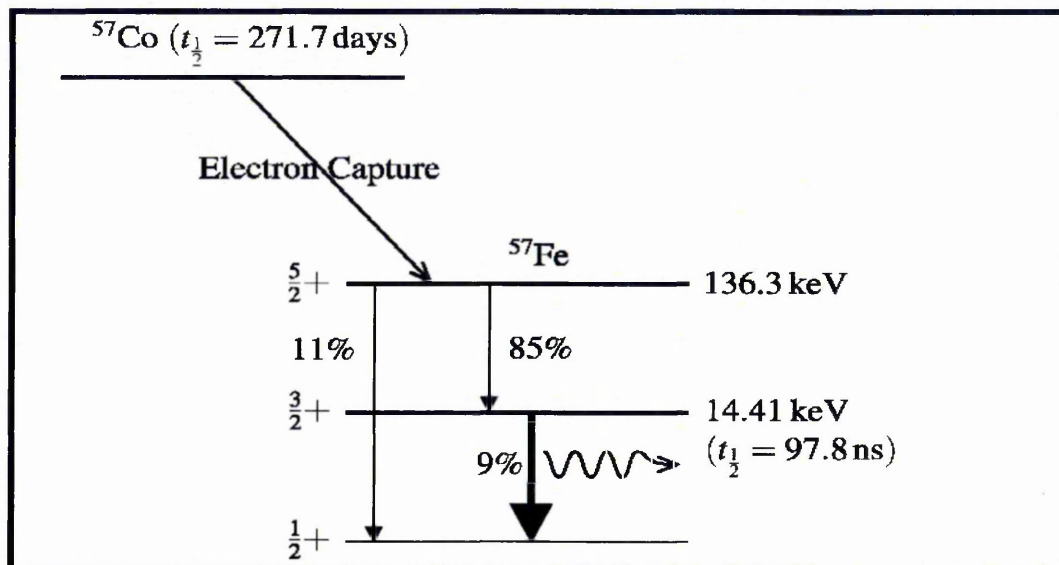


Figure 2.2. The decay scheme of  $^{57}\text{Co}$  [4]

### 2.1.2. Interaction of Gamma Rays with Matter

Several types of interaction between gamma photons and the atoms of the absorbing material are known. The degree of probability for each type depends on a number of variables, mainly on gamma photon energy and the atomic number ( $Z$ ) of the absorbing material. The interaction may occur between the incoming photon and either the orbital electrons or nucleus, or the electrostatic field of the nucleus; and the collision could be either elastic or inelastic [5]. There are three main types of interactions between gamma photons and the matter:

**A. Photoelectric effect:** The incident photons interact with a bound electron causing the emission of the electron from its shell with energy  $E_e$  given by the equation:

$$E_e = h\nu - E_b \quad (2.2)$$

Where  $h\nu$  is the incident photon energy and  $E_b$  is the binding energy. After a short time, another electron can fill the vacated place with the emission of characteristic radiation; see Figure 2.3 (A) [6].

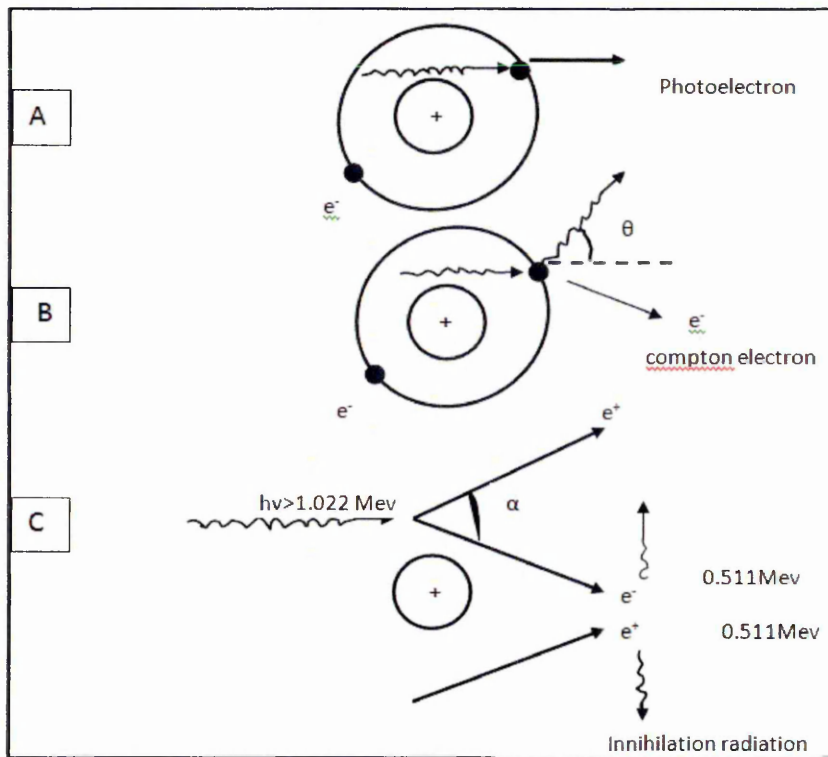


Figure. 2.3. Interaction of gamma rays with matter [5]: (A) Photoelectric effect; (B) Compton scattering; (C) electron-positron pair production.

**B. Compton Scattering:** The incident gamma photon collides with an orbital electron, without disappearing, Figure 2.3 (B). It is simply deflecting (scattered) from the path at an angle  $\theta$ , and after the collision it has a longer wavelength and therefore lower frequency and energy than the incident photon. The energy lost by the photon is imparted to the electron, which is usually one of the outermost orbits; the electron (Compton electron) is emitted from the atom with a certain amount of kinetic energy and thus with the ability to produce secondary ion pairs, taking into account the law of conservation of energy and momentum, the relationship between the energies of incident and scattered photons [5].

$$E_{\gamma'} = E_{\gamma} / [1 + (\frac{E_{\gamma}}{m_0 c^2} (1 - \cos\theta))] \quad (2.3)$$

Where  $E_{\gamma'}$  is the energy of scattered photon,  $E_{\gamma}$  is the energy of incident photon,  $m_0$  is the rest mass of the electron,  $c$  is the speed of light and  $\theta$  is the angle of deflection.

**C. Pair Production (Electron and Positron):** The rest mass of an electron is 0.511 MeV, and at photon energies in excess of 1.022 MeV, electron-positron pair production occurs, as a striking example of Einstein's principle of the equivalence of mass and energy ( $E=mc^2$ ). In the strong electric field surrounding the nucleus the photon disappears, being converted into an electron and a positron (which has the same mass as an electron but a positive charge) thus conserving the charge. Any photon energy in excess of 1.022 MeV is shared between the two particles as kinetic energy (see Fig. 2.5 C). Thus,

$$h\nu = 1.022 \text{ MeV} + T_{e^-} + T_{e^+} \quad (2.4)$$

Where  $T_{e^-}$  is the kinetic energy of the electron,  $T_{e^+}$  kinetic energy of the positron, this seemingly extraordinary effect obeys the law of conservation of charge, energy, mass and momentum, as well as the more sophisticated laws of quantum mechanics. The positron surrounded by a sea of electrons, when traversing through the absorber, is in considerable danger of annihilation; and after being slowed down by interactions similar to those of energetic electron, a positron eventually collides with an electron in the absorber, and the pair is annihilated [6].

### 2.1.3. Absorption of Gamma Rays

The energy of the incident photons will determine which of the three processes, i.e. photoelectric effect, Compton scattering or electron-positron pair production, plays the dominant role in their absorption. It has been found that ionizing electrons are produced during the interactions of X-rays and  $\gamma$ -rays with matter; without these interactions the photons would travel straight through matter at the speed of light. The depth of penetration of a photon in a material depends on the energy of the photon, the density of the material, and the atomic number ( $Z$ ) of the atoms of the material. Because of the complex and random interactions with matter, the beam of incident gamma photons gets progressively weaker in its intensity as it passes through it; the beam becomes attenuated, following Beer's law describing the absorption of  $\gamma$ - rays:

$$\Delta I = -\mu I \Delta X \quad (2.5)$$

Where  $\Delta I$  is the change in beam intensity,  $\Delta x$  is the thickness of material traversed. Integrating this equation gives:

$$I = I_0 e^{-\mu x} \quad (2.6)$$

Where  $I_0$  is the initial beam intensity,  $I$  is the beam intensity at thickness ( $x$ ). The parameter  $\mu$ , called the linear attenuation coefficient [7], depends on the mechanism of interaction and includes all three components: photoelectric effect, Compton scattering, and electron-positron pair production.

$$\mu = \tau \text{ (photoelectric)} + \sigma \text{ (Compton)} + \kappa \text{ (pair)}$$

### 2.2. Beta Particles ( $\beta^-$ )

Henri Becquerel was credited with the discovery of beta particles  $\beta^-$ . In 1900, he showed that they were identical to electrons, which had recently been discovered by Joseph John Thompson. Beta particles are subatomic particles ejected from the nucleus of some radioactive atoms, equivalent to electrons. The difference is that beta particles originate in the nucleus and electrons originate outside the nucleus. Beta particles have an electrical charge of (-1). Beta particles have a mass of 549 millionth of one atomic mass unit, which is about 1/2000 of the mass of a proton or neutron. The speed of individual beta particles depends on how much energy they have [8]. While atoms that

are radioactive emit beta particles, beta particles themselves are not radioactive. It is their energy, in the form of speed, which causes harm to living cells. When transferred, this energy can break chemical bonds and form ions [6]. Direct exposure to beta particles is a relatively small hazard; it may cause skin to redden or even burn. The beta-emission from inhaled or ingested substances, however, is the greatest concern. Beta particles released directly into living tissue can cause damage at the molecular level, which can disrupt cell function. Because beta particles are much smaller and have less charge than alpha particles, they generally travel further into tissues. As a result, the cellular damage is more dispersed [8]. Beta particles do not exist in the unstable nucleus before emission, they are produced as a result of sub-nuclear transformation, whereby a neutron changes to a proton ( $\beta^-$  particle is emitted) thus:



Alternatively, a proton changes to a neutron (a  $\beta^+$  particle is emitted):



Whereas a neutrons outside a nucleus undergoes negative beta decay and transforms into proton with a half-decay time ( $t_{1/2}$ =12 min. 16 sec.), much lighter protons cannot be transformed into a neutron except within a nucleus [9].

### 2.2.1. Interaction of Beta Particles

When beta particles travel through an absorbing material, they gradually dissipate their energy by interacting with the atoms of the absorber. If their energy dissipates completely within the absorber, we can say that they are fully absorbed. Evidently, absorption must be a function of beta-particle energy, as well as of absorber thickness and density [5].

The absorption of beta particles in matter is the consequence of their energy dissipation, which is caused by various types of interactions between the particles and atoms of the absorbing material.

### 2.3. Alpha-Particles ( $\alpha$ )

An alpha particle consists of two protons and two neutrons bound together into a particle identical to a helium nucleus. They are generally produced in the process of

alpha decay, but may also be made by other means. The symbol for the alpha particle is  $\alpha$  or  $\alpha^{2+}$ . Because they are identical to the helium nuclei, they are also sometimes written as  $He^{2+}$  or  ${}^4_2He^{2+}$ , indicating a Helium ion with a +2 charge (missing its two electrons). If the ion gains electrons from its environment, the alpha particle can be written as a normal (electrically neutral) Helium atom. The most well-known source of alpha particles is alpha decay of large atoms heavier than 106 units of atomic weight [10]. When an atom emits an alpha particle, the atom's mass number decreases by four, due to the loss of the four nucleons in the alpha particle, so the atomic number of the atom goes down by exactly two, because of the loss of two protons – the atom becomes a new element. All of the larger radioactive nuclei, such as Uranium, Thorium, Actinium, and Radium commonly emit alpha-particles. Unlike other types of decay, alpha decay must have a minimum-size atomic nucleus that can support it [11]. The smallest nuclei that have to date been found to be capable of alpha emission are the lightest nuclides of Tellurium (element 52), with a mass numbers between 106 and 110. The process of alpha-emission sometimes leaves the nucleus in an excited state, with the emission of a gamma ray required in order to remove the excess energy.

### **2.3.1. Interaction of Alpha Particles**

Electrostatic attraction between positively charged alpha particles and single negatively charged orbital electrons causes both the ionization and excitation events. When a positively charged alpha particle moves through the matter, it attracts many orbital electrons, leaving a wake of ion pairs. When the speed is slow enough, the alpha particle may capture electrons to produce elemental helium. A double positive charge and low velocity (due to the large mass) causes alpha particles to lose their energy over a relatively short distance [12]: for example, for the most energetic alpha particles it is in the range of 4 centimetres. A sheet of paper or a protective layer of dead skin can easily stop alpha particles. As alpha particles disperse their energy over a very short distance, they cause the most damage when the alpha-emitter is digested or inhaled, and thus appear in close proximity to living cells, so that alpha particles are an internal hazard.

### **2.4. Neutron Radiation**

Neutron radiation is a kind of ionizing radiation that consists of free neutrons. As a result of nuclear fission, free neutrons are released from atoms, and these free neutrons react with the nuclei of other atoms to form new isotopes which may produce radiation.

Neutrons may be emitted from nuclear fusion or nuclear fission, or from other types of nuclear reactions, such as radioactive decay or reactions with highly energetic particles, either coming as cosmic rays or created in particle accelerators. Large neutron sources are rare, and are usually limited to large-sized installations, like nuclear reactors or particle accelerators. Neutron radiation was discovered through observing a Beryllium nucleus reacting with an alpha particle, thus transforming into a Carbon nucleus and emitting a neutron ( $\text{Be} + \alpha \rightarrow \text{C} + \text{n}$ ).

The combination of an alpha particle emitter and an isotope with a large ( $\alpha, \text{n}$ ) nuclear reaction probability is still a common neutron source. Neutron radiation is often called indirectly ionizing radiation. It does not ionize atoms in the same way that charged particles such as protons and electrons do (exciting an electron), because neutrons have no charge. However, neutron interactions are largely ionizing, for example, when neutron absorption results in gamma emission and the gamma ray (photon) subsequently removes an electron from an atom, or a nucleus recoiling from a neutron interaction is ionized and causes more traditional subsequent ionization in other atoms. Because neutrons are uncharged, they are more penetrating than alpha radiation or beta radiation. In some cases, they are more penetrating than gamma radiation, which are impeded in materials of high atomic number. In materials of low atomic number, such as Hydrogen, a low energy gamma ray may be more penetrating than a high-energy neutron.

The neutrons in reactors are generally categorized as slow (thermal) neutrons or fast neutrons, depending on their energy. Thermal neutrons are similar to a gas in thermodynamic equilibrium but are easily captured by atomic nuclei and are the primary means by which elements undergo atomic transmutation. Neutron diffraction or elastic neutron scattering is the application of neutron scattering to the determination of the atomic and/or magnetic structure of a material [13]. A sample to be examined is placed in a beam of thermal or cold neutrons to obtain a diffraction pattern that provides information on the structure of the material. The technique is similar to X-ray diffraction but due to their different scattering properties, neutrons and X-rays provide complementary information.

## 2.5. Units of Exposure and Absorbed Dose

Exposure is a measure of ionization produced in air by X- rays or gamma rays passing through a mass ( $m$ ) of dry air at standard temperature 0 °C and pressure of 1 atm. When passing through the air, the beam produces positive ions whose total charge is  $q$ . Exposure is defined as the total charge per unit mass of air.

$$\text{Exposure } (X) = q/m$$

The SI unit for exposure is Coulombs per kilogram (C/kg). However, the first radiation unit to be defined was the Roentgen (R), with  $q$  expressed in Coulombs and  $m$  in kilograms (kg). The exposure in Roentgen is given by

$$X(R) = 2.5 * 10^{-4} q/m$$

Thus, when X-rays or  $\gamma$ -rays produce an exposure of one Roentgen, a positive charge of  $2.5 \times 10^{-4} \text{C}$  is produced in 1kg of dry air [14], and one roentgen equal:-

$$1\text{R} = 2.5 * 10^{-4} \text{C/Kg}$$

For biological purposes, the absorbed dose is a more suitable quantity, because it is the energy absorbed from radiation per unit mass of absorbing material.

$$\text{Absorbed dose} = (\text{Energy absorbed}) / (\text{Mass of absorbing material}) \quad (2.9)$$

The SI unit of absorbed dose is Gray (Gy), which is a unit of energy divided by a unit of mass:  $\text{Gy} = \text{J/kg}$ . Equation (2.9) is applicable to all types of radiation and absorbing media. Another unit often used for absorbed dose is rad (rd), an acronym for 'radiation absorbed dose'. The rad and Gray are related by  $1\text{rad} = 0.01\text{Gray}$  [15].

Rad is the amount of energy, which the human body absorbs. However, equal doses of different types of radiation may not have the same effects on the body; for instance, a dose of alpha particles is more damaging than the same dose of gamma rays or beta particles [16]. To compare the damage caused by different types of radiation, relative biological effectiveness (RBE) is used, also called the quality factor (QF). The relative biological effectiveness of particular type of radiation compares the dose of that radiation needed to produce a certain biological effect, to the X- rays needed to produce the same biological effect [5].

$$\text{RBE} = \left[ \frac{\text{the dose that produces a certain (reference) biological effect}}{\text{the dose of X-rays radiation that produces same biological effect}} \right] \quad (2-10)$$

The RBE depends on the ionizing radiation and its energy, as well as the type of tissue being irradiated.

Type of radiation	RBE
200-keV X-rays	1
$\gamma$ - rays	1
$\beta^-$ particles (electrons)	1-2
Protons	10
$\alpha$ - particles	10-20
slow neutrons	2
fast neutrons	10

Table. 2.1. Typical RBE values for different kinds of radiation [15]

The RBE is often used in connection with the absorbed dose to reflect the character of damage produced by radiation. The product of the absorbed dose in rad and RBE is the biologically equivalent dose (DE).

Biologically equivalent dose (in rem) = Absorbed dose in (rad) \* RBE

$$\text{DE} = \text{D} * \text{RBE} \quad (2-11)$$

The unit for the biologically equivalent dose is the rem [16]. The rem is the unit of radiation which accounts for the different effects of different types of radiation [16]. In order to calculate the equivalent dose in rem, the absorbed dose must be established. If the unit of the absorbed dose (D) is Gray, then the unit of DE is Sievert, or if the unit of the absorbed dose (D) is rad, then the unit of DE is rem [16].

where: 1 Sievert = 100 rem.

## **2.6. Detection of Radionuclide Pollution**

To tackle the problem of environmental pollution, the reliable methods of detection and identification of pollutants must be research. In the last 40-50 years, a large number of analytical methods for the detection of radioactive contamination have been developed [17]. For example, different types of penetrative radiation ( $\alpha$ ,  $\beta$ ,  $\gamma$ , or neutron) can be detected using physical methods, such as solid-state nuclear track detector (SNTD's), G-M detector, gas proportional chamber and gamma-ray spectroscopy [18]. A review of methods used in radiation detection is provided in this section.

### **2.6.1. Radiation Detection**

Detection of radiation is possible during the interaction of radiation with matter, because photons, electron-ion pairs, or electron-hole pairs can be produced. Gas counters (ionization chambers, proportional counters, and Geiger counters), cloud chambers, bubble chambers, and spark counters are all based on the principle of ionisation of matter by radiation [19]. In scintillation counters, radiation-induced excitation produces photons, and in semiconducting counters, radiation produces electron-hole pairs. The number of ions, photons, or electron-hole pairs depends on the fraction of the energy of the radiation expended in the sensitive volume, on the properties of the material, and sometimes on the nature of the radiation. Different types of devices were used for the detection of radiation.

#### **2.6.1.1. Gas Counters**

Geiger from Rutherford's laboratory developed gas counters for the detection of radiation in 1908. These counters became practical for the measurement of radiation shortly thereafter, even though scintillates were for a long time in use for this purpose. The original Geiger counter consists of a glass cylinder (containing idle or rare gas), an outer cylindrical electrode and an inner wire electrode, with a potential difference applied between them. Geiger found that radiation causes the ionisation of gas and therefore an electric current between electrodes, which was detectable with an electrometer of "moderate sensibility" [20]. The amount of charge (current) depends on the amount of radiation energy penetrating the gas tube.

### **2.6.1.2. Scintillation Counters**

When the radiation interacts with certain materials flashes of light can be seen, the phenomenon called ‘scintillation’. Detection of these flashes either by the naked eye or with the help of optical instrumentation was one of the oldest methods of radiation detection. Rutherford used a ZnS scintillating screen, and employed this method to count the scattered alpha particles in the historic alpha-scattering experiment [21]. This method is tedious and very crude and was soon replaced by gas counters, where the counting is done electronically and additional information about the energy of radiation can be obtained if needed. In 1944, Curran and Baker started using a photomultiplier in scintillating chambers, and later Kallman replaced ZnS crystals with naphthalene. These two changes revolutionized scintillation detection, making it possible to electronically detect, record, and analyze pulses produced by radiation.

### **2.6.1.3. Semiconductor Detectors**

The operation of a semiconductor detector is analogous to the operation of an ionization chamber. In contrast to ionization chambers, where the incident radiation produces positive ions and electrons, in semiconductor counters radiation produces electrons and holes, contributing to the electric current. One major difference, of course, is that only 3.5eV is required to produce an electron-hole pair in semiconductor detectors, while 30eV is needed for the ionization of gas. The lower energy increases the number of electron-hole pairs per MeV of radiation and thus increases the sensitivity of radiation detection [22]. However, very often these methods require the use of much equipment assistance in laboratories and well-trained personnel, and thus cannot be used, for example, in the water environment. Thus, the use of natural systems for sensing, such as microorganisms or bacteria, can be advantageous. It is known that microorganisms (bacteria) might be badly affected by radiation and some of the chemical pollutants [23]. Such negative effects depend on the radiation level and concentration of pollutants: the damage could range from partial loss of functionality at low doses (concentrations) up to the “death” of bacteria at high doses (concentrations). Therefore, the monitoring of bacteria counts in natural water resources could serve as a simple method for preliminary detection (or screening) of pollutants. In a simple scenario, a low bacteria count in a particular water sample can give an indication (warning) of the presence of some type of contaminant of either a radioactive or toxic nature. Then further and more

detailed laboratory analysis can be undertaken on this particular sample. The concept of bacterial sensors can be developed further with the use of several types of bacteria affected differently by different types of pollutions. Such advanced bacterial sensors can solve the complex problem of simultaneous identification and evaluation of different pollutants, including radioactive and toxic ones. For this task, the effect of radiation on organisms was studied.

## **2.7. Effect of Radiation on Living Organisms**

The effect of radiation on living organisms, including humans, appears mostly at cell level, since ionizing radiation can potentially affect the normal operation of cells. The biological effect of radiation lies in the ionization of atoms and molecules in the tissue. Ionizing radiation absorbed by human tissue has sufficient energy for ionization of atoms; this may subsequently lead to breaking chemical bonds and thus molecules. This is a basic model for understanding radiation damage. For a deeper understanding of the effect of ionizing radiation on cells, one needs to consider damage to critical parts of the cell [24], such as chromosomes that contain genetic information and instructions required for the cell to function, as well as to make copies of it for reproduction purposes. On the other hand, the cells have very effective repair mechanisms, which operate permanently and repair cellular damage - including chromosome damage.

Ionization may form chemically active substances that in some cases alter the structure of the cells. These alterations may be similar to those changes that occur naturally in the cell and may have no negative effect. Some ionizing events produce substances (such as amino acids or enzymes) not normally found in the cell [25]. These can lead to a breakdown of the cell structure and its components. Cells can repair the damage if it is limited. Even damage to chromosomes is usually repairable; thousands of chromosome aberrations occur constantly in our bodies and the majority are repaired spontaneously. If a damaged cell needs to perform a function but does not have sufficient time to repair itself, it will be either unable to perform the repair function or perform the repair function incorrectly (incompletely). This could be damaging to other cells. These altered cells may become unable to reproduce themselves or may reproduce at an uncontrolled rate. Such cells can be the underlying causes of cancers. If a cell is broadly damaged by radiation, or damaged in such a way that the reproduction is affected, the cell may die. Radiation damage to cells may depend on the sensitivity of these cells to

radiation. Not all cells are equally sensitive to radiation damage. In general, cells that divide rapidly and/or are relatively non-specialized tend to show effects at lower doses of radiation than those which divide less rapidly and are more specialized. Examples of such radiation sensitive cells are those involved in the production of blood. This system (called the hematopoietic system) is the most sensitive biological indicator of radiation exposure.

Potential biological effects depend on how high the radiation dose is and how fast it is received. Radiation doses can be grouped into two categories: *acute* and *chronic*. An acute radiation dose is defined as a large dose (10 rad or greater to the whole body) delivered during a short period (about a few days at most). If the dose is large enough, the negative effects may appear within a short period (hours, days, or weeks). Acute doses can cause a pattern of clearly identifiable symptoms (syndromes). These conditions are referred to as Acute Radiation Syndrome. Symptoms of radiation sickness are apparent following the acute doses of more than 100 rad. acute doses of more than 450 rad may result in a statistical expectation of 50% of the exposed population to die within 60 days, without medical attention. As in most illnesses, the specific symptoms, the therapy that a doctor might prescribe, and the prospects for recovery vary from one person to another and are generally dependent on the age and general health of the individual. The syndrome of bone marrow (blood-forming organ) which normally appears at doses higher than 100 rad is characterized by damage to cells that divide at the most rapid pace (such as bone marrow, the spleen, and lymphatic tissue). Symptoms include internal bleeding, fatigue, bacterial infections, and fever.

Central nervous system syndrome at doses higher than 5000 rad is associated with the damage of nerve cells that are not reproducible. Symptoms include loss of coordination, confusion, coma, convulsions, shock, etc [26]. Scientists now have evidence that deaths under such conditions are not caused by actual radiation damage to the nervous system, but rather from complications caused by internal bleeding and a build-up of brain fluid pressure. Other effects from an acute dose include 200 to 300 rad to the skin can result in the reddening of the skin. Similar to mild sunburn, and may result in hair loss due to damage to hair follicles; 600 rad to the ovaries or testicles can result in permanent sterility; and 50 rad to the thyroid gland can result in non-cancerous tumours. The effects caused by acute doses are called deterministic. Broadly speaking, this means that the severity of the effect can be determined by the dose received. Deterministic effects

usually have some threshold level below which the effect will probably not occur, but above which the effect is expected. When the dose is above the threshold the severity of the effect increases as the dose increases.

Humans and other organisms are continuously exposed to ionizing radiation from natural background sources in the environment, including cosmic radiation and Rn-222, alongside K-40 and C-14. This unavoidable exposure is not without consequences, as ionizing radiation exposure has been known to deliver a variety of injuries to DNA. Unfortunately, natural background is not the only source of ionizing radiation to which organisms are exposed. Numerous sites around the world have been contaminated with radionuclide, because of anthropogenic activity [27]. Human exposure can be minimized by limiting access to contaminated areas, but this is generally not feasible for other species, and resulting exposures can be significantly higher than those from natural background sources. In general, radiation exposure may be internal or external. Internal exposure comes from eating or drinking contaminated food or water, or from breathing contaminated air. A radioactive substance can also enter the body through cuts in the skin. Alpha and beta radiations contribute to internal exposure. External exposure can come from beta, gamma and X-ray; both internal and external radiation exposure can directly harm cells. When the body is exposed to radiation, the following events on the cell-level may occur [16]:

- 1) Radiation may pass through the cell without detectable damage.
- 2) It may damage the cell, but the cell may be able to repair the damage before producing new cells.
- 3) It may damage the cell in such a way that damage is passed on when new cells are formed.
- 4) It may kill the cell.

If the radiation passes through the cell without causing damage or the cell repairs itself successfully (number 1 and 2 above), there is no lasting damage or health effect. If the damage is passed on when new cells are formed (number 3 above), there may be a delayed health effect, such as genetic effects. When radiation kills a cell, there will be an acute (immediate) health effect if the dose is high and many cells die. Death may occur within days or weeks from the moment of exposure to radiation. Ionizing radiation acting on living system can result in biological endpoints, including tissue injury, carcinogenesis and death. The initial step in this interaction of radiation with

biological material is the deposition of energy into atoms and molecules that results in ionization and excitation. Small quantities of energy from radiation exposure result from the non-uniform deposition of energy and through biochemical processes that amplify damage [28]. There are two actions of ionization radiation on cell. Firstly, the direct action, when a molecule is ionized and/or excited by the incident of radiation, as has already been stated, the extra portion of energy of the ionizing particle is used to remove an electron from a molecule, as shown in Figure 2.4A. The remaining energy excites the molecule and can actually break molecules into smaller units that are identical because many larger molecules are composed of a chain of smaller molecules bonded together chemically. It appears that damage occurs at the same bond.

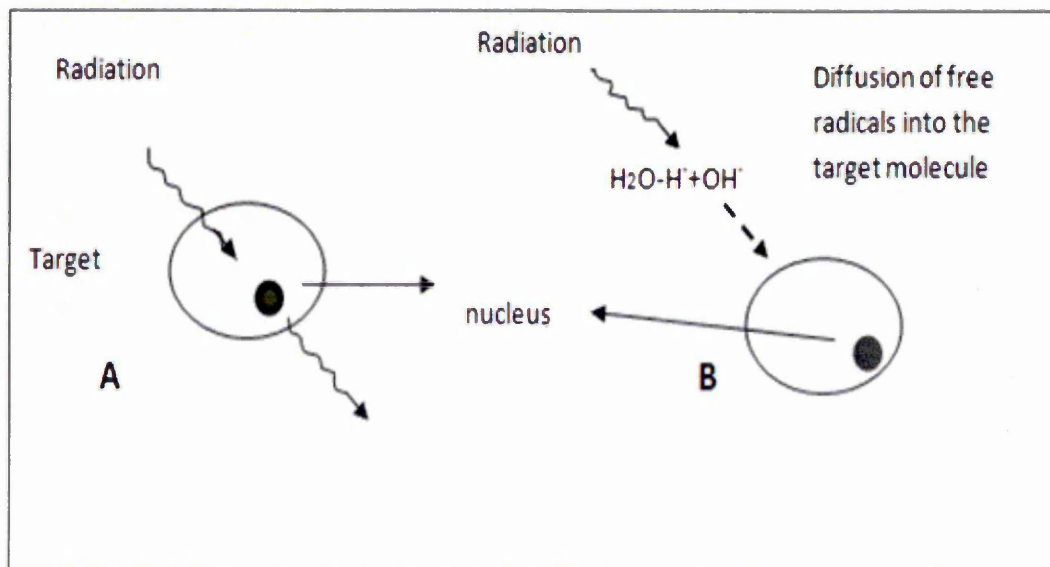


Figure. 2.4. Action of ionization radiation on cells [29]: (A) direct action, and (B) indirect action

Direct action occurs within milliseconds of irradiation. This type of action causes a number of physical events that bring about the death of the cell [28].

The radiation risk level depends on several factors, namely the type of radioactive isotopes, the radiation intensity and exposure period. Living organisms are affected differently by high or low levels of radiation sources, while the period of exposure also has a crucial effect on living cells. The effect of a low level of radiation (particularly with long time exposure) causes changes in DNA structure, which can result in different types of cancer and/or genetic transformations, called indirect action, see Figure 2.5.

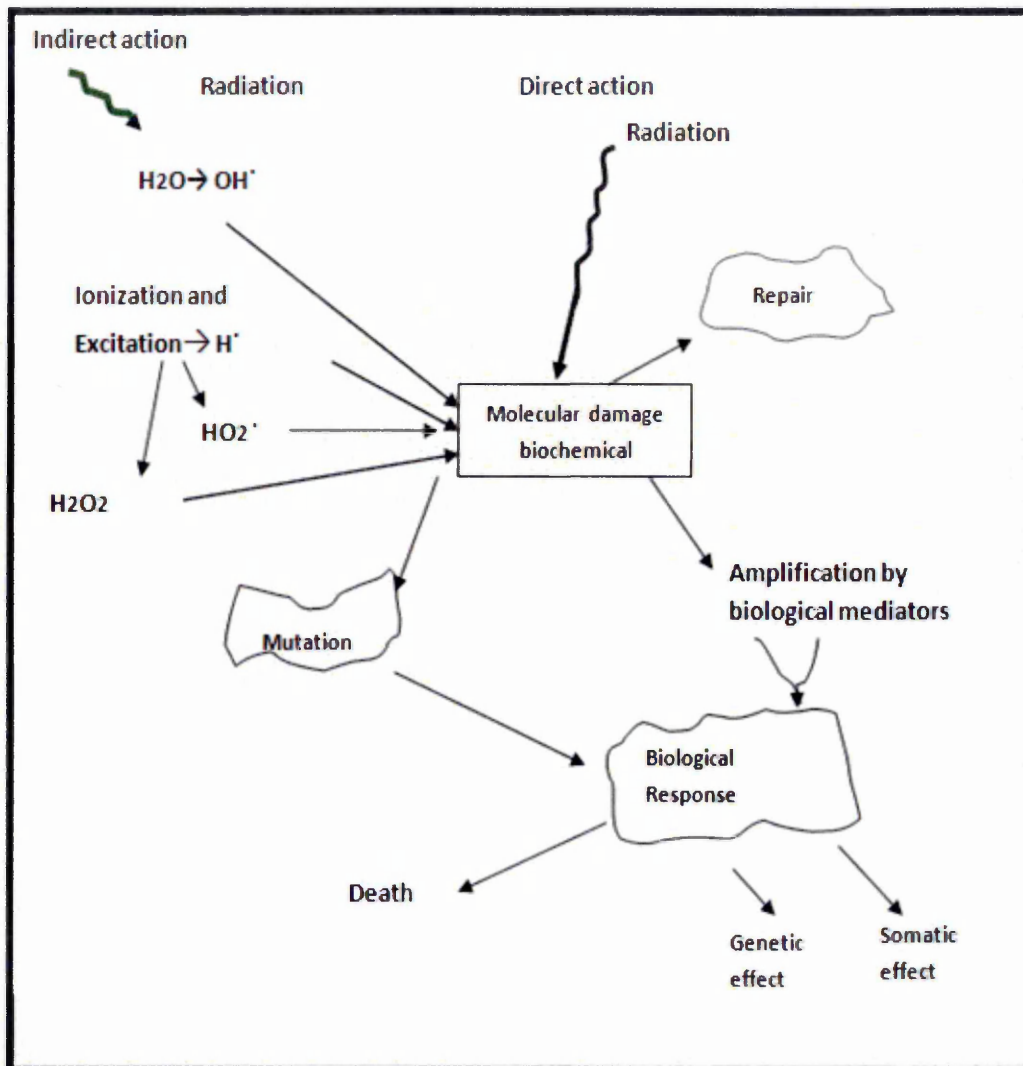


Figure. 2.5. Physical, biochemical and biological responses to radiation [30]

Free radicals result from radiation exposure; these are electrically neutral, having an unpaired electron in their outer orbits [6]. Free radicals are formed by radiation when an atom is left with one of its outer orbital electrons unpaired with respect to spin. Free radicals are usually very reactive since they have a great tendency to pair the odd electron with a similar one in another free radical or to eliminate the odd electron by an electron transfer reaction. Free radicals can therefore be electron acceptors (oxidizing species) or electron donors (reducing species) [31,6].

The simplest free radical is the hydrogen atom, which contains one proton and one electron. The most important radicals that may be involved in disease processes are species that may be derived from molecular oxygen, and certain oxides of nitrogen, especially nitric oxide. An unpaired electron can be associated with almost any atom,

but oxygen and carbon-centred free radicals are of the greatest biological relevance. Sources of radicals are alcohol, cigarette smoking, stress, strain, anger, air pollution, and solar radiation [32]. Radiation produces excitation, and thus ionizations at random, so that in a complex system such as a living organism those molecules that are most abundant are most likely to become ionized. It follows that, when living material, which is 70-90% water, is irradiated, the water molecules will take up most of the absorbed energy [33].

The effects of radiation doses on organisms differ; radiation resistance is the property of organisms that are capable of living in environments with very high levels of ionizing radiation [34]. Radiation resistance is surprisingly high in many organisms, contrary to previously held views [35]. For example, the study of the environment, animals and plants around the Chernobyl disaster area has revealed the unexpected survival of many species, despite high radiation levels. A Brazilian study in the hills in the state of Minas Gerais, which has high natural radiation levels from uranium deposits, has also shown many radio-resistant insects, worms and plants [36]. Radiation can also help some plants to become more adapted to their environment by increasing the growth rate of the seeds, helping them to germinate faster.

## **2.8. Effect of Radiation on Microorganisms**

Anderson, and his co-workers [37], first reported the isolation of a highly radiation-resistant microorganism. These were found in both irradiated and non-irradiated ground-meat samples from an Oregon packing plant, and pure culture studies indicated that the organism was a non-spore-forming, pink-pigmented coccus, occurring principally in tetrads with a cell diameter of 1  $\mu\text{m}$ . Subsequent studies resulted in the isolation of the organism from numerous meat and poultry samples procured from various sections of Oregon. It has not however, been isolated from numerous irradiated and non-irradiated fish and shellfish samples obtained from north-western Pacific waters and examined in laboratories.

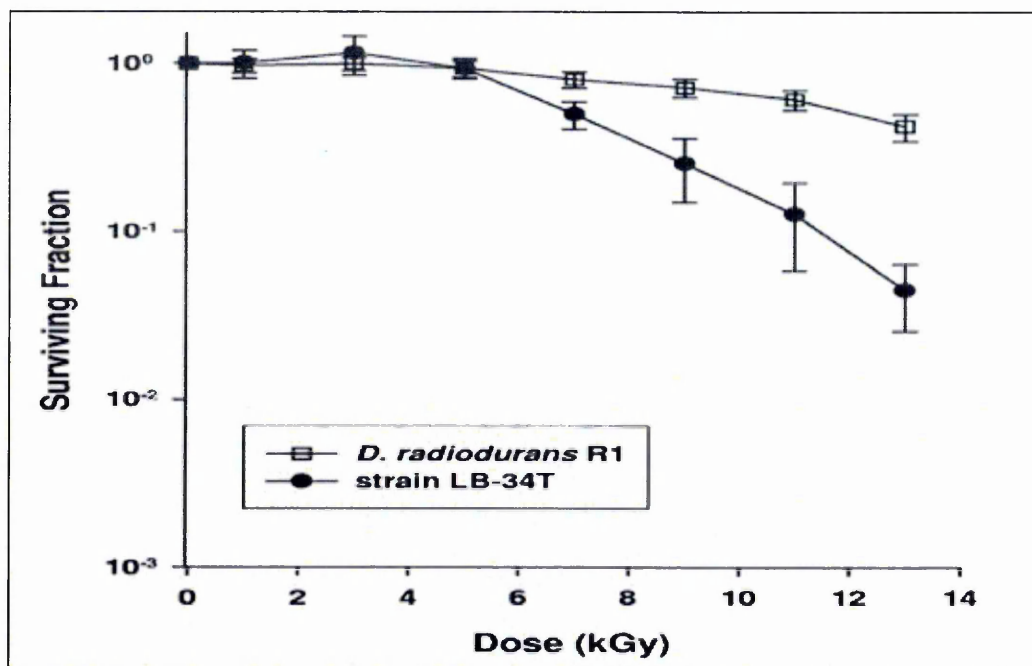


Figure. 2.6. Survival curves for (radiation resistant bacteria) *D. radiodurans* strains R1 and LB-34T [38]

Radio-resistance maybe induced by exposure to small doses of ionizing radiation. Several studies have documented this effect in yeast, bacteria, protozoa, algae, plants, insects, as well as in vitro mammalian and human cells and in animals[38]. Several cellular radioprotection mechanisms may be involved, such as alterations in the levels of some cytoplasm and nuclear protein, and increased gene expression, DNA repair and other processes. Many organisms have been found to possess a self-repair mechanism that can be activated by exposure to radiation in some cases. Figure 2.6 shows two strains of one type of bacteria have the ability to resist radiation.

The main effects of radiation are cytotoxic and mutagenic ones, which are principally the result of DNA damage caused during the period of irradiation. This might not always be the case, since environmental organisms, such as *Shewanella oneidensis* (MR-1), which encode relatively complex DNA repair systems, are killed at radiation doses that cause relatively little DNA damage [39].

The survival percentage of *Escherichia coli*, *Deinococcus radiodurans* and *S. oneidensis* due to the effect of ionizing radiation has been studied [40]. Results show that 90% of *S. oneidensis* cells do not survive 70 Gy Gamma-ray radiations, 10% of *D. radiodurans* cells survive 12,000 Gy, and 10% of *E. coli* survives 700 Gy. Moreover, *S. oneidensis* bacteria die after exposure to radiation and desiccate for only one day, whereas similarly treated *D. Radiodurans* can survive for months.

When the generation of reactive oxygen species (ROS) (superoxide, hydrogen peroxide and hydroxyl radicals) produced by irradiation or metabolism exceed the capacity of endogenous scavengers to neutralize them, cells in this case become more vulnerable to damage, due to the influence of oxidative stress. In general, most of the resistant bacteria reported are Gram-positive and the most sensitive are Gram-negative [41]. However, there are several reported exceptions to this paradigm. Gram-negative Cyanobacteria *Chroococci diopsis* is extremely radiation and desiccation resistant [42]. It has recently been reported that the differences in resistance to radiation and desiccation for different bacteria mirror their intracellular (Mn/Fe) concentration ratios, where very high, moderate and very low (Mn/Fe) ratios correlate with very high, moderate and very low resistances, respectively [40]. *D. radiodurans* (Mn/Fe ratio: 0.24) accumulates 150 times more Mn than *S. oneidensis* (Mn/Fe ratio: 0.0005) and is sensitized to ionizing radiation when Mn(II) is restricted, and *S. oneidensis* accumulates 3.3 times more Fe than *D. radiodurans*. In the case of *S. oneidensis* exposed to doses of 70 Gy, Fe (II)-dependent oxidative stress produced during recovery might lead to additional DNA, RNA, and the lipid and protein damage. The researchers found that *Deinococcus radiodurans* and other radiation resistant bacteria accumulate exceptionally high intracellular manganese and low iron levels [43]. In comparison, the dissimilarity metal-reducing bacterium *Shewanella oneidensis* accumulates Fe but not Mn and is extremely sensitive to radiation. So they have proposed that for Fe-rich, Mn-poor cells killed at radiation doses which cause very little DNA damage, cell death might be induced by the release of Fe(II) from proteins during irradiation, leading to additional cellular damage by Fe(II)-dependent oxidative stress. In contrast, Mn (II) ions concentrated in *D. radiodurans* might serve as antioxidants that reinforce enzymatic systems that defend against oxidative stress during recovery. They extend their hypothesis here to include consideration of respiration, tricarboxylic acid cycle activity, peptide transport and metal reduction, which, together with Mn (II) transport, represent potential new targets to control recovery from radiation injury.

*Deinococcus radiodurans* has contributed significantly to our understanding of the molecular genetics of radiation-resistance [44]. The DNA damage resistance of *D. radiodurans* has been shown to be due to highly efficient DNA repair. It has been shown that, following exposure to a dose of 10 kGy of ionizing radiation, *D. radiodurans* sustains about 100 double strand breaks per chromosome [45], which are repaired

without lethality, mutagenesis or rearrangement, whereas most other micro-organisms cannot survive and mend only two to three double strand breaks per chromosome.

*Deinococcus radiodurans*, as mentioned, is a Gram-positive bacterium well known for its ability to survive extreme doses of ionizing radiation. Though *Deinococcus radiodurans* is highly resistant to a broad spectrum of DNA damaging agents, it can recover from particularly high doses of ionizing radiation, which is known for producing dsDNA breaks. Since high doses of radiation lead to 150-200 dsDNA breaks per chromosome in *Deinococcus radiodurans*, radio-resistance is largely due to highly proficient mechanisms of DNA repair [46]. By contrast, *Escherichia coli* can survive only a few dsDNA breaks at a time. *Deinococcus radiodurans* has a typical prokaryotic repertoire of DNA repair enzymes, though nearly one third of its genes encode proteins of unknown functions that are not seen in other organisms [47]. The bacterium *Deinococcus radiodurans* is known for its resistance to extremely high doses of ionizing radiation and for its ability to reconstruct a functional genome from hundreds of radiation-induced chromosomal fragments. Recently, extreme ionizing radiation resistance had also been generated by directed development of an apparently radiation-sensitive bacterial species, *Escherichia coli* [48].

Radioresistant organisms are not only found among the bacteria but also among the Archaea, which represent the third kingdom of life. They present a set of particular features that differentiate them from the bacteria and eukaryotes. Moreover, Archaea are often isolated from extreme environments where they live under severe conditions of temperature, pressure, pH, salts or toxic compounds that are lethal for the large majority of living organisms. Thus, Archaea offer the opportunity to understand how cells are able to cope with such harsh conditions. The ability of microorganisms to resist ionizing radiation are clearly delineated in Figure 2.7.

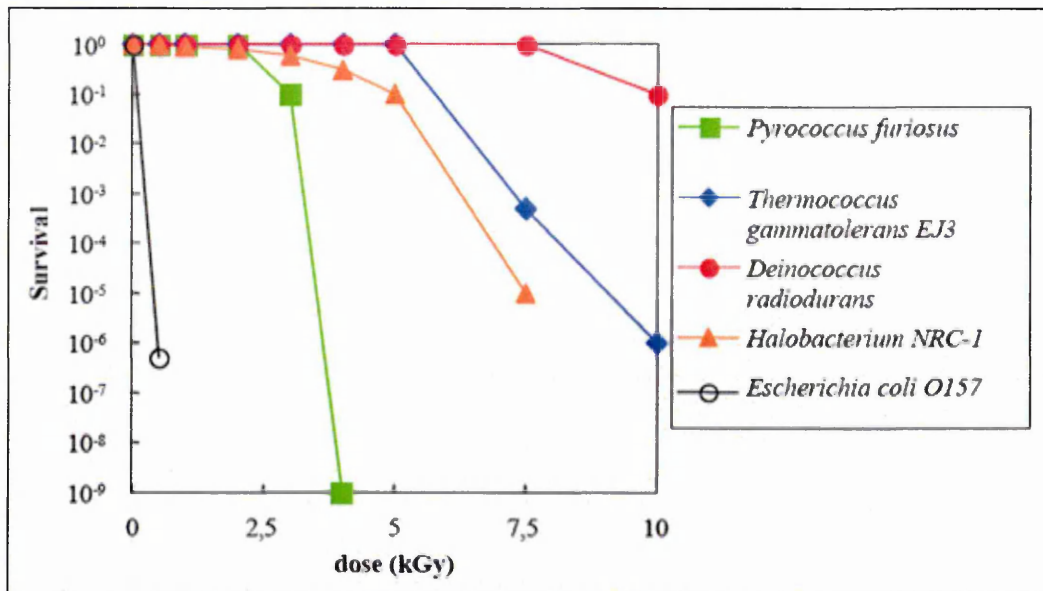


Figure. 2.7. Survival curves for *Pyrococcus furiosus*, *T. Gamma tolerance*, *D. Radiodurans*, *Halobacterium*, and *E. coli*, following exposure to  $\gamma$  radiation [49]

Obviously, *Escherichia coli* is more sensitive to radiation from other bacteria species included in this study because it has been classified as Gram-negative, in contrast, *D. radiodurans*, which shows extremely resistance to radiation.

The use of bacteria as a biosensor to monitor radioactivity and toxic heavy metals in the environment has recently been reported [50]. It found that the *E. coli* bacteria were able to survive at low levels of radiation. An *E. coli* bacterium has been employed as a biosensor to detect environmental genotoxicity. Much high resistance to radioactivity was established for *D. Radiodurans* bacteria, which has the ability to survive high radiation doses of around (15kGy) [17]. These bacteria were utilized for the treatment of mixed waste containing heavy metals (mercury), radionuclide's, such as U-235, and solvents (toluene) [51]. This research explained the mechanism for the transformation of toxic heavy metal salts to less toxic and less soluble compounds, using bacteria.

Some bacteria are capable of treating and detoxifying metallic pollutants, but they are very sensitive to radiation. In contrast to those, *D. Radiodurans* bacteria are extremely resistant to radiation [44]. These bacteria are able to repair DNA damage caused by exposure to ionized radiation. A comparative study of the effect of X-ray radiation on different types of bacteria revealed that *D. Radiodurans* bacteria is radiation resistant; the population of *D. Radiodurans* was halved ( $D_{50}$  level) after exposure to 200 kGy for 24 hours as shown in Figure 3.3 [51]. At the same time,  $D_{50}$  level for *R. Erythropolis* appeared at the intensity of radiation of 100 kGy. The other two bacteria studied P.

Syringae and *E. coli*, showed  $D_{50}$  after exposure to 20 kGy and 10 kGy, respectively. The total death of *E. coli* was observed after exposure to 150 kGy [51].

The research shows that *D. Radiodurans* are also capable of absorbing UV radiation [52]. A multi-layered film of bacteria deposited on carbon tape was capable of 20 % reduction of UV radiation. This ability can be enhanced when the bacteria grow in agar medium containing glucose and nitrates [53]. One of the most important parameters in this treatment technique is atmospheric temperature.

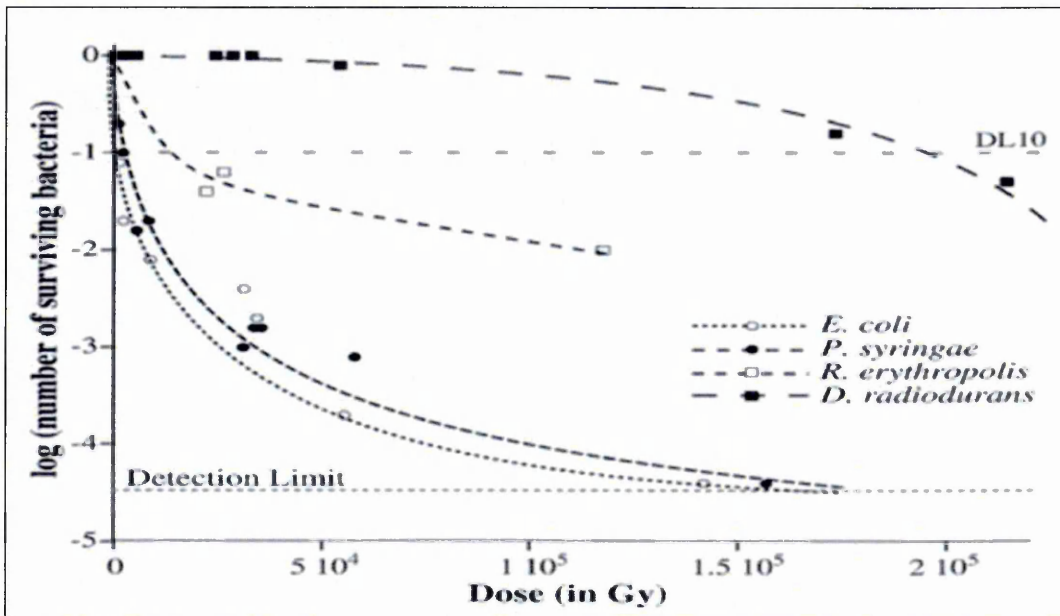


Figure. 2.8. Number of surviving bacteria (*E. coli*, *P. Syringae*, *R. Erythropolis* and *D. Radiodurans*) vs. X-ray dose in Gy units [51]

#### References:

1. Michael F. L Annunziata, (1988), Handbook radioactivity analysis, Academic Press.
2. Cutnell Johnson; (1994), Physics; 3<sup>rd</sup> edition; p(374).
3. Krane; (1987), Introductory nuclear physics; New York –Wiley.
4. Debertin K., Helmer R. G.(2001), Gamma and X-Ray Spectrometry with Semiconductor Detectors, Elsevier Science, B.
5. Victor Arena; (1971), Ionizing radiation and life; The C.V. Mosby Company.
6. Coggle J. E.(1983), Biological effect of radiation; 2nd edition; Taylor and Francis Lid, London.
7. Kmoll G. G. (1989), Radiation detection and measurement; 2<sup>nd</sup>edition ; John Wiley and Sons.

8. [www.epa.gov/radiation/understand/beta.htm](http://www.epa.gov/radiation/understand/beta.htm).(2013), Radiation and Radioactivity, U.S. Environmental Protection Agency.
9. Arthur Beiser, ( 2003), Concept of modern physics; 6th edition; McGraw Hill.
10. Krane, Kenneth S. (1988). Introductory Nuclear Physics. John Wiley & Sons. pp. 246-269. ISBN 0-471-80553-X.
11. Darling, David. (2010), Alpha particle, Encyclopedia of Science. Archived from the original on December. Retrieved 2010-12-07.
12. Rutherford E. and Royds T. (1908) "Spectrum of the radium emanation," Philosophical Magazine, Series 6, vol. 16, pp. 313-317.
13. Clifford Shull, (1995), Early development of neutron scattering. Rev. Mod. Phys. Vol. 67,pp.753-757.
14. Cember H.(1985), Introduction to health physics; New York, program on press; 2<sup>nd</sup> edition.
15. Cutnell Johnson, (1994), Physics; 3<sup>rd</sup> edition; p(374).
16. [www.wa.doh.gov/radiation/hhin.htm](http://www.wa.doh.gov/radiation/hhin.htm). Radiation Protection, Washington State Department of Health
17. Hassan Brim, Sara C. McFarlan, James K. Fredrickson, Kenneth W. Minton, Min Zhai, Lawrence P. Wackett, and Michael J. Daly,(2000), Engineering *Deinococcus radiodurans* for metal remediation in radioactive mixed waste environments, Nature Biotechnology, Vol. 18, pp. 85-90.
18. Chen Y, Sharma-Shivappa R, Keshwani D and Chen C. (2007), Potential of agricultural residues and hay for bioethanol production. Applied Biochemistry and Biotechnology, Vol. 142(3), pp. 276-290.
19. Rahman, K. S. M. et al. (2002), Bioremediation of gasoline contaminated soil by a bacterial consortium amended with poultry litter, coir pith and rhamnolipid bio surfactant, Bioresource Technology, Vol. 81 (1), pp.25-32.
20. Michael F, Annunziata L, (1988), Handbook radioactivity analysis, Academic Press.
21. Debertin K., Helmer R. G.(2001), Gamma and X-Ray Spectrometry with Semiconductor Detectors, Elsevier Science, B.
22. Taylor, J.R.; Zafiratos, C.D.; Dubson, M.A. (2004), Modern Physics for Scientists and Engineers (2nd ed.), Prentice Hall. pp. 9–136.
23. Chen KF, Kao CM, Chen CW, Surampalli RY, Lee MS, (2010), Control of petroleum-hydrocarbon contaminated groundwater by intrinsic and enhanced bioremediation. Environ Sci. (China), Vol. 22(6), pp. 864-871.

24. Karl Z. Morgan,(1975), Reducing Medical Exposure to Ionizing Radiation', American Industrial Hygiene Association Journal, pp. 361-362.
25. Venkateswaran A., McFarlan S.C., Ghosal D., Minton, K.W., Vasilenko A., Makarova K., Wackett L.P., Daly M.J.(2000), Physiologic determinants of radiation resistance in *Deinococcus radiodurans*, Appl. & Environ. Microbiology, Vol. 66, pp. 2620-2626.
26. Bertell R, (1981), Ionizing Radiation Exposure and Human Species Survival', Canadian Environmental Health Review, Vol 25, No. 2. pp. 21-25
27. Stavrev P, Stavreva N, Niemierko A, and GoiteinM, (2001), Generalization of a model of tissue response to radiation based on the idea of functional subunits and binomial statistics, Phys. Med. Biol. Vol. 46, pp. 10-15.
28. Walden TL, and Farzaneh N K, (1990), Biochemistry of ionizing radiation, New York Raven press.
29. Early P. J., Mohammed Abdel Razzak and Sodee D. B.(1979), Text book of nuclear medicine technology, pp. 144.
30. Walden TL. J, (1989), Low level of ionizing Radiation, Text book military medicine, publications office he surgeon general, Vol. 2, pp. 171-178.
31. Gillham B. , Despo K. P, and Thomas J. H, (2000), Biochemical basis of medicine, pp. 343-346.
32. Halliwell B. and Gutteridge J.M.C.(1999), Free radicals in biology and medicine, 3rd edition Oxford, University press.
33. Mitchell J.M., Russo A.,Kuppusny P. and Krishna M.C. (2000), Radiation radicals and images, Ann NY Acad Sci. 899, p. 221-225.
34. Joiner M. C, (1994), Induced Radioresistance: An Overview and Historical Perspective". International Journal of Radiation Biology, Vol. 65 (1), pp. 79-84.
35. Cordeiro A. R, Marques, E. K, Veiga-Neto, A. J. (1973), Radioresistance of a natural population of *Drosophila Williston* living in a radioactive environment. Mutation research, Vol.19 (3), pp. 325-329.
36. Anderson A, W.,Nordan H. C, Cain R. F, Parrish G,& Duggan D, (1956), Studies on a radio-resistant *Micrococcus*. I. Isolation, morphology, cultural characteristics, and resistance to gamma radiation. Food Techno, Vol. 10, pp. 575-577.
37. Brooks, B. W. & Murray, R. G. E. (1981), Nomenclature for *Micrococcus radiodurans* and other radiation-resistant cocci: *Deinococcaceae* fam. nov. and

- Deinococcus gen. nov, including five species. *Int. J Syst. Bacteriol*, Vol. 31, pp. 353–360.
38. Xiaoyun Qiu, Michael J. Daly, Alexander Vasilenko, Marina V. Omelchenko Elena K. Gaidamakova, Liyou Wu, Jizhong Zhou, George W. Sundin, and James M. Tiedje, (2006), Transcriptome Analysis Applied to Survival of *Shewanella oneidensis* MR-1 Exposed to Ionizing Radiation, *J Bacteriol*. Vol. 188(3), pp. 1199-1204.
39. D Ghosal, M. V. Omelchenko, E K Gaidamakova, V. Y. Matrosova, A. Vasilenko, A. Venkateswaran, M. Zhai, H. M. Kostandarithes, H. Brim, K. S. Makarova, L. P. Wackett, J. K. Fredrickson, M. J. Daly, (2005), How radiation kills cells: survival of *Deinococcus radiodurans* and *Shewanella oneidensis* under oxidative stress. *FEMS Microbiology Reviews*, Vol. 29, Issue: 2, pp. 361-375.
40. Robert W. Phillips, Juergen Wiegel, Christopher J. Berry, Carl Fliermans, Aaron D. Peacock, David C. White and, Lawrence J. Shimkets, (2002), *Kineococcus radiotolerans* sp. nov., a radiation-resistant, gram-positive bacterium *IJSEM*, vol. 52 no. 3, pp. 933-938.
41. Daniela Billi, E. Imre Friedmann, Richard F. Helm, and Malcolm Potts, (2001), Gene Transfer to the Desiccation-Tolerant Cyanobacterium *Chroococcidiopsis*, *J Bacteriol.*, Vol. 183(7), pp. 2298-2305.
42. Daly M. J, Gaidamakova E. K., Matrosova V. Y., Vasilenko A., Zhai M, (2004), Accumulation of Mn(II) in *Deinococcus radiodurans* facilitates gamma-radiation resistance. *Science Epub*, Vol. 5(306), pp. 1025-1033.
43. Kenneth W. Minton, (1996), Repair of ionizing-radiation damage in the radiation resistant bacterium *Deinococcus radiodurans* *Mutation Research*, Vol. (363), pp. 1-7.
44. John R. Battista, Ashlee M. Earl and Mie-Jung Park, (1999), Why is *Deinococcus radiodurans* so resistant to ionizing radiation *trends in microbiology*, Vol. 7, pp. 362-365.
45. Rakhi Rajan, Charles E Bell, (2004), Crystal structure of RecA from *Deinococcus radiodurans*: insights into the structural basis of extreme radioresistance, *Journal of Molecular Biology*, Vol. 344, Issue(4), pp. 951-963.
46. Kira S. Makarova, L. Aravind, Yuri I. Wolf, Roman L. Tatusov, Kenneth W. Minton, Eugene V. Koonin, and Michael J. Daly, (2001), Genome of the Extremely Radiation-Resistant Bacterium *Deinococcus radiodurans* Viewed from the Perspective of Comparative Genomics, *Microbiol Mol Biol Rev.*, Vol. 65(1), pp. 44-79.

47. F Confalonieri and S Sommer, (2011), Bacterial and archaeal resistance to ionizing radiation, *Phys. Journal, Conf. Ser.* 261012005.
48. Yvan Zivanovic, Jean Armengaud, Arnaud Lagorce, Christophe Leplat, Philippe Guérin, Murielle Dutertre, Véronique Anthouard, Patrick Forterre, Patrick Wincker, and Fabrice Confalonieri, (2009), Genome analysis and genome-wide proteomics of *Thermococcus gamma* tolerance, the most radioresistant organism known amongst the Archaea, *Genome Biol.*, Vol. 10(6): R70.
49. Ernest C. Pollard and Anna Tilberg, (1972), Action of Ionizing Radiation on Sensitive Strains of *Escherichia coli* B, *Biophys J.*, Vol. 12(2), pp. 133–156.
50. Gao Guanjun, Fan Lu, Lu HuiMing, and Hua Yue Jin, (2008), Engineering *Deinococcus radiodurans* into biosensor to monitor radioactivity and genotoxicity in environment” *Chinese Science Bulletin*, Vol. (53), pp. 1675-1681.
51. Phil M. Oger, I. Daniel, A. Simionovici, A. Picard, (2008), Micro-X-ray absorption near edge structure as a suitable probe monitor live organisms; *Spectrochimica Acta, Part B*, Vol. 63, pp. 512-517.
52. Howard I. Adler and Alice A. Hardigree, (1964), Analysis of a Gene Controlling Cell Division AND Sensitivity to Radiation in *Escherichia Coli* *Journal of Bacteriology*, Vol. 87, pp. 720-726.
53. Nriagu J.O. and Pacyna J.F.(1988), Quantitative Assessment of Worldwide Contamination of Air, Water, and Soils by Trace Metals. *Nature*, Vol. 333, pp. 134-139.

## CHAPTER 3

### Heavy Metals

Heavy metals are a member of a loosely defined subset of elements that exhibit metallic properties. It mainly includes the transition metals, some metalloids, lanthanides, and actinides. Many different definitions have been proposed, some based on density, some on atomic number or atomic weight, and some on chemical properties or toxicity. There is an alternative term “toxic metal”, for which no consensus of an exact definition exists either. As discussed, depending on context, heavy metals can include elements lighter than carbon and can exclude some of the heaviest metals. Heavy metals occur naturally in ecosystems, with large variations in concentration [1]. In modern times, anthropogenic sources of heavy metals, i.e. pollution, have been introduced to ecosystems. Waste-derived fuels are especially prone to containing heavy metals, so they are a concern in consideration of fuel waste. This chapter will discuss the distribution of heavy metals in the environment; their impact on the environment; methods for detection of heavy metals; and the effect of heavy metals on living organisms and bacteria in particular.

#### 3.1. Heavy Metals Distribution in Environment

The total concentration of trace metals and metalloid in the environment, their chemical forms, mobility and availability to the food chain, provide the basis for a range of problems in crops, animals and human health. Some 15 elements present in rocks and soil, normally in very small quantities, is essential for plant and/or animal nutrition. Boron, Copper, Iron, Manganese, Molybdenum, Silicon, Vanadium and Zinc are required by plants; Copper, Cobalt, Iodine, Iron, Manganese, Molybdenum, Selenium and Zinc by animals. The roles of Arsenic, Fluorine, Nickel, Silicon, Tin and Vanadium have also been established in recent years in animal nutrition. In large concentrations, many of the trace elements/metals may be toxic to plants/or animals, or may affect the quality of foodstuffs for human consumption. These potentially toxic elements include Arsenic, Boron, Cadmium, Fluorine, Lead, Mercury, Molybdenum, Nickel, Selenium and Zinc. Most trace metals in the environment are spread over a wide range. The main sources are parent materials from which the soil is derived. However, man-effected inputs may add to, and at times exceed, those from natural geological sources. The main

sources of metal contaminants in the environment are mining and smelting activities; other industrial emissions and effluents; urban development; vehicle emissions; dumped waste materials; contaminated dust and rainfall; sewage sludge; pig slurry (because it is one of the main sources of animal manure, which is transported as nutrient particles into soil and water or as organic effluent); composted town refuse; fertilizers; soil ameliorants and pesticides [2]. The soil is a primary supplier of trace metals to the soil-plant-animal system and the soil-food stuff-water-human system. In these systems, the metals metalloids do not, of course, occur in isolation, and a number of synergistic and antagonistic interactions are recognized at both deficiency and excess concentrations. These interactions sometimes involve major elements, as well as trace metals, which can be illustrated by the effect of calcium ions on specific adsorption of cadmium on to root surfaces and the copper-molybdenum-sulphur interrelationship in ruminant nutrition.

Sources of metals in soils may be from natural geological materials or from human activities [3]. The normal abundance of an element in earth material is commonly referred to by the geochemist as background [4]. The earth's crust is made up of 95% igneous rocks and 5% sedimentary rocks; of the latter about 80% are shale, 15% sandstones and 5% limestone [5]. The more biologically important trace metals, including copper, cobalt, manganese and zinc, occur mainly in the more easily weathered constituents of igneous rock, such as augite, hornblende and olivine [4]. Shale, on the other hand, may be of inorganic or organic origin, and usually contains larger amounts of trace metals [5]. It is seen that black shale, is enriched with copper, lead, zinc, molybdenum and mercury. Detailed studies on cadmium in British black shale showed a wide range of concentrations in those examined up to 219ppm [6]. On the other hand, potentially toxic amounts of trace metals in soils may be derived from naturally occurring metals-rich source rocks. Nickel-rich soil derived from ultra-basic rocks containing ferromagnesian minerals in part of Scotland may lead, under poor drainage conditions, to nickel toxicity in cereal and other crops [5]. Of particular significance to agriculture in Britain is the observation that excess molybdenum in soil and pastures can give rise to molybdenosis or molybdenum-induced copper deficiency in cattle. Heavy metals, as environmental contaminants of terrestrial ecosystems, is not a recent phenomenon. They are ubiquitous in trace concentrations in soils and vegetation, and in fact, plants and animals as micronutrients require many. In addition, naturally

occurring surface mineralization can produce metals concentrations in soil and vegetation that are as high, or higher, than those found around man made sources. The man made sources of metal contamination of terrestrial environments are mainly associated with certain industrial activities. There are seven major categories of sources of metals contamination of the environment.

1. Natural sources, such as surface mineralization, volcanic out gassings, spontaneous combustions or forest fires.
2. The use of metals containing agricultural sprays or soil amendments.
3. Emissions from large industrial sources, such as metal smelters and refineries.
4. The disposal of wastes from mines or mills.
5. Emissions from municipal utilities, such as coal or oil fired electricity generating stations or municipal incinerators.
6. Emissions from moving sources, principally automobiles.
7. Other relatively minor sources of contamination, such as smaller scale industries that process metals.

### **3.2. Heavy Metals Impact on Environment**

All living species have some impact on the environment, in some cases a profound one. The influence of life chemistry and other aspects of chemistry on the environment, the production of free Oxygen by photosynthesis, has changed the nature of the Earth's surface much more radically than anything humans are likely to do through global nuclear war. This natural evolution has, however, taken place very slowly, whereas the accelerating progress of technology risks producing changes at a much greater rate. The present chapter will discuss of the effect of Cadmium and the Nickel on the environmental [7].

Heavy metals pollution, is an emotive term, meaning different things, a reasonable general definition might be "too much of something in the wrong place" [8]. This can include entirely natural substances. For example, one of the most serious pollutants in many countries is sewage mostly human excreta which contaminates rivers with pathogenic bacteria and depletes them of dissolved oxygen.

Elements used intensively may have some potential for disturbing the natural environment. Ones with compounds that are non-volatile and insoluble in water are less likely to cause problems. Other factors include the toxicity of an element, and the chemical forms in which it is used: compounds of a different kind from those, which appear in nature, are more likely to be toxic or otherwise harmful.

General source of pollution is the processing and use of metals. Those from groups are quite heavily used in proportion to their abundance, and are toxic to varying degrees. These elements may be released into the environment in soluble form, during mining and other processing operations and into the atmosphere as dusts. As with carbon, the use of one element may mobilise others. Pollution by very toxic Cadmium can arise during the extraction of Zinc, as the two elements are often found in association.

Agriculture accounts for a high proportion of the usage of some elements, nitrogen and phosphorus especially. The intensive use of fertilisers and pesticides can give rise to many problems, especially as these compounds are spread deliberately in the environment. Excess fertiliser can contaminate water supplies, but changes in agricultural practice also have other consequences. A recent rise in the atmospheric concentration of some trace gases, such as the “greenhouse gases”, Methane ( $\text{CH}_4$ ) and Nitrous Oxide ( $\text{N}_2\text{O}$ ), may appear as a result of increased fertilisation. Biomass burning, especially of tropical rain forest, is another source of atmospheric perturbations.

Toxic metals are metals that form poisonous soluble compounds and have no biological role, i.e. are not essential minerals, or are in the wrong form. Often heavy metals are thought of as synonymous, but lighter metals also have toxicity, such as beryllium, and not all heavy metals are particularly toxic, and some are essential, such as iron. The definition may also include trace elements, when considered in abnormally high, toxic doses. A difference is that there is no beneficial dose for a toxic metal without a biological role. Toxic metals sometimes imitate the action of an essential element in the body, interfering with the metabolic process to cause illness. Many metals, particularly heavy metals are toxic, but some heavy metals are essential, and some, such as bismuth, have a low toxicity. Most often, the definition includes at least cadmium, lead, mercury and the radioactive metals. Metalloids (arsenic, polonium) may be included in the definition. Radioactive metals have both radiological toxicity and chemical toxicity. Metals in an oxidation state abnormal to the body may also become toxic: chromium is

an essential trace element but is a carcinogen. In addition, toxic metals can accumulate in the body and in the food chain. Therefore, a common characteristic of toxic metals is the chronic nature of their toxicity. This is particularly notable with radioactive heavy metals such as thorium, which imitates calcium to the point of being incorporated into human bone, although similar health implications are found in lead or mercury poisoning. This study researches the effect of Cadmium Chloride and Nickel Chloride (Toxic Heavy Metals) on living bacteria, in order to utilize bacteria response as detection indicators of heavy metals.

### **3.2.1. Cadmium (Cd) and Their Sources**

A relatively uncommon element in the natural environment, Cadmium is a strongly chalcophilic metals, found predominantly in combination with sulphur. The mineral greenockite, CdS, is rare, and most cadmium is found in low concentrations in Zinc ores, and obtained as a by-product of their processing. The element is used as an anti-corrosion coating for metals, and in batteries, but most anthropogenic cadmium in the environment comes not from these applications but from the mining and processing of Zinc and other chalcophilic metals. Cadmium is not believed to be essential for life, and it is very toxic. It is strongly scavenged by marine organisms, which accounts for its much lower concentrations in surface waters, where life is common, than in the deep ocean. Abnormally high concentrations can be found in rivers and coastal estuaries near mining and industrial centres, and in soils. Much of this pollution arises from airborne dust, although direct leaching from waste deposits also occurs. The particularly high levels of contamination found in some sewage sludge pose a serious problem of disposal [9].

Most cadmium in humans come from food, average daily consumption being around 35µg per day, of which about 2µg is absorbed. Tobacco also contains cadmium, and heavy smokers probably receive about the same amount again. Intake of the element stimulates the production of metallothionein in the liver. This enzyme contains an unusually high production of sulphur-containing cysteine residues, which bind Cd<sup>2+</sup> and forms a complex containing up to seven metal atoms per molecule. The complex is then transported to the kidneys, which therefore concentrate a significant amount of the body content of cadmium. This process is designed as a defence against cadmium and other heavy metals, and the toxic effect presumably arises from its incomplete take-up

metallothionein, especially when excessive doses are received. Cadmium competes with several essential metals, including zinc, and copper, and interferes with their metabolism. Symptoms of poisoning include damage to the function of lungs and kidneys, and a softening of the bones leading to intense pain in the joints [9].

The most common compound is Cadmium Chloride is a white crystalline compound of cadmium and chlorine, with the formula  $\text{CdCl}_2$ . A hygroscopic solid is highly soluble in water and slightly soluble in alcohol. Although it is considered ionic, it has considerable covalent character to its bonding. The crystal structure of cadmium chloride, [10] composed of two-dimensional layers of ions, is a reference for describing other crystal structures. Also known are  $\text{CdCl}_2 \cdot \text{H}_2\text{O}$  and  $\text{CdCl}_2 \cdot 5\text{H}_2\text{O}$  [11].

Cadmium chloride dissolves well in water and other polar solvents. In water, its high solubility is due in part to formation of complex ions such as  $[\text{CdCl}_4]^{2-}$  [12]. Cadmium Chloride forms crystals with rhombohedral symmetry; it has a very similar crystal structure to Cadmium iodide  $\text{CdI}_2$  but  $\text{CdCl}_2$  chloride ions are arranged in a CCP lattice [12]. Anhydrous cadmium chloride can be prepared by the following reaction of hydrogen chloride gas on heated cadmium metal.



Hydrochloric acid may be used to make hydrated  $\text{CdCl}_2$  from the metal, or from cadmium oxide or cadmium carbonate. Cadmium (Cd) is extremely toxic and provokes adverse effects on the biota in general and particularly on fish [10]. Cd is used in electroplating, pigments and plastic production and this has produced a sharp increase in the contamination of air, water and soil. Exposure of juveniles and adults of freshwater fishes to water-borne sub-lethal Cd may lead to many stress symptoms, such as the disruption of ion and water balance, changes in respiratory function associated with structural damage of the gills, nephrotoxicity, alterations in haematological and biochemical parameters, adverse effects of growth and reproduction, neurological and behavioural [13]. Therefore, it is interesting to see how the Cadmium Chloride affects microorganisms. One research result shown decrease in the oxygen consumption because of ion-regulatory and acid-base disturbances [14]. Oxygen consumption, therefore, could serve as a biomarker in metal toxicity studies in fish and other aquatic animals, such as the effects of exposure to cadmium chloride at three sub-lethal

concentrations of 0.636, 0.063 and 0.006 mg/ml on the oxygen consumption rate of *Esomus-danricus*. Differences in oxygen consumption of up to 14 days were not significant at 0.006 mg/l, which is 1/1000th of the 96hLC50 value of cadmium chloride for *E. danricus* [15]. However, significant differences could be observed on day 21, indicating that long-term exposure could produce toxic effects even at extremely low concentrations of cadmium chloride. At higher concentrations of 0.063 and 0.636 mg/l cadmium chloride (1/10th and 1/100th of 96hLC50 values, respectively) significant reductions in oxygen consumption rates could be observed after 7 days of exposure. The lethal concentration of  $\text{CdCl}_2$  for human is over 0.5 ppm per hour [16]. Metal toxicants produce a change in the respiration rate of fish, which is mostly a decline in the oxygen consumption rates, although, in few studies, elements like Fe and Cu increases oxygen so far as consumption is concerned [16], while selenate decreases it that slightly and increases it at lower concentrations. It is probable that Cu, Fe or Se, that are essential trace elements, have a stimulatory effect on oxygen consumption rates at low concentrations, although the process is reversed at higher, xenobiotic levels. On the contrary, Cd, being a non-essential element brought about progressive decline in oxygen consumption at all the three concentrations, results in the differences from control they found to be significant after longer exposure, even at the lowest level of 0.006 mg/ml.

### **3.2.2. Nickel (Ni) and its Sources**

Nickel is probably among the seven most abundant elements on Earth overall, making up about 10 per cent of the core. A strong siderophile, it is much less abundant in the crust. It occurs as both sulphide and oxide minerals. One major source is pentlandite of cobalt. Weathering of sulphide ores liberates the  $\text{Ni}^{2+}$  ion, which is similar in size to  $\text{Mg}^{2+}$ , and can be found in magnesium-containing minerals, especially silicates. Nickel is therefore relatively abundant in high basic rocks, and in serpentine soils derived from them by weathering [17]. The silicate mineral garnierite also forms an important source. Nickel is an important component of many ferrous and non-ferrous alloys, and is used for electroplating. Normal environmental concentrations of nickel are low, but large amounts can be found in some naturally derived serpentine soils, and surrounding mining and smelting areas, such as the major nickel producing site at Sudbury, Ontario. Nickel is an essential trace element, although its role in mammals (including humans) is

very limited, and may be confined to its presence in a single metalloid enzyme, urea's, which catalyses the decomposition of urea,  $(\text{NH}_2)_2\text{CO}$ , to ammonia. It is more important in many anaerobic bacteria, which derive their energy supply by metabolising dihydrogen,  $\text{H}_2$ , and liberating methane,  $\text{CH}_4$ .

Nickel is a toxic element. Many plant species cannot grow on contaminated soils, although there are especially tolerant species, some of which can accumulate high concentrations. In humans, nickel-containing dust has been recognised as a cause of occupational cancers, including lung cancer [18]. The metal is sometimes used in jewellery, such as earrings, and can cause dermatitis, it appears that some people are especially sensitive, or can become sensitised by prolonged contact with the element. The volatile compound nickel tetra carbonyl,  $\text{Ni}(\text{CO})_4$ , which is used in the extraction of the element by the Mond process, is especially poisonous [19].

Nickel (II) chloride (or just nickel chloride), is the chemical compound  $\text{NiCl}_2$ , the anhydrous salt is yellow, but the more familiar hydrate  $\text{NiCl}_2 \cdot 6\text{H}_2\text{O}$  is green. A dihydrate is also known. In general nickel(II) chloride, in various forms, is the most important source of nickel for chemical synthesis. Nickel salts are carcinogenic. They are also deliquescent, absorbing moisture from the air to form a solution.

$\text{NiCl}_2$  adopts the  $\text{CdCl}_2$  structure [20]. In this pattern, each  $\text{Ni}^{2+}$  centre is coordinated to six Cl- centres, and each chloride is bonded to three Ni(II) centres. In  $\text{NiCl}_2$ , the Ni-Cl bonds have "ionic character". Yellow  $\text{NiBr}_2$  and black  $\text{NiI}_2$  adopt similar structures, but with a different packing of the halides, adopting the  $\text{CdI}_2$  design. Note that only four of the six water molecules in the formula are bound to the nickel, and the remaining two are water of crystallisation. Many nickel(II) compounds are paramagnetic, due to the presence of two unpaired electrons on each metal centre. Square planar nickel complexes are, however, diamagnetic. In addition, Nickel(II) chloride solutions are acidic, with a pH of around 4 due to the hydrolysis of the  $\text{Ni}^{2+}$  ion.

### **3.3. Effects of Heavy Metals on Living Organisms**

Heavy metals are toxic and non-biodegradable pollutants released into the environment by industrial, mining and agricultural activities [21]. Heavy metals have a density of  $6.0 \text{ g/cm}^3$  or more (much higher than the average particle density of soils which is  $2.65$

g/cm<sup>3</sup>) and occur naturally in rocks but concentrations are frequently elevated, because of contamination. The most important heavy metals with regard to potential hazards and occurrence in contaminated soils are arsenic (As), cadmium (Cd), chromium (Cr), mercury (Hg), lead (Pb), nickel (Ni) and zinc (Zn).

Arsenic (As), which is known as a poison and a carcinogen, has an average concentration in the soil of 5 to 6 mg/kg, which is related to its rock type and industrial activity [22].

Cadmium's (Cd) toxicity has been linked to reproductive problem because it affects sperm and reduces birth weight. It is a potential carcinogen and seems to be a causal factor in cardiovascular diseases and hypertension [23,24].

Chromium (Cr) is required for carbohydrate and lipid metabolism and the utilization of amino acids. Its biological function is also closely associated with that of insulin and most Cr-stimulated reactions depend on insulin [24].

Lead (Pb) is known to be toxic. It is a widespread contaminant in soils. Lead poisoning is one of the most prevalent public health problems in many parts of the world. It was the first metal to be linked with failures in reproduction [24]. It can cross the placenta easily, and also affects the brain, causing hyperactivity.

Mercury (Hg) is toxic even at low concentrations to a wide range of organisms, including humans. The organic form of mercury can be particularly toxic.

Nickel (Ni) occurs in the environment only at very low levels. Foodstuffs have a low natural content of nickel but high amounts can occur in food crops grown in polluted soils. Uptake of high quantities of nickel can cause cancer, respiratory failure, birth defects, allergies, and heart failure [25]. Recent research showed the ability of microorganism to survive in the presence of different types of heavy metals in a wide range of concentrations. Figure 3.1 shows the survival rate of E. coli bacteria in the presence of Pb and Ni contamination. It was also shown recently that E. coli bacteria are able to reduce the heavy metals concentration levels in the environmental samples studied [25].

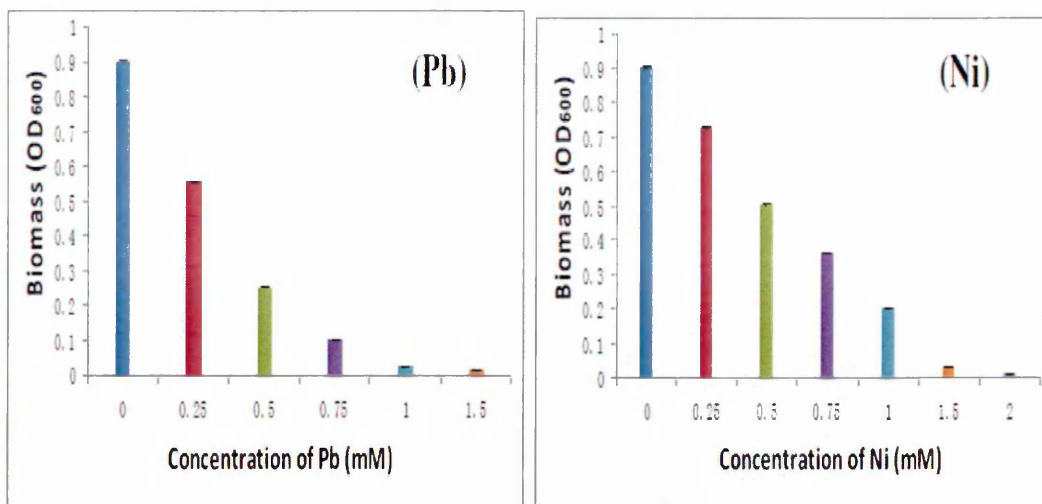


Figure 3.1. Biomass of *E. coli* bacteria vs concentration of heavy metals Pb and Ni [25]

The number of live cells was counted, and their percentage calculated in each case. In the control sample, where no dose of Ni NPs was given, the number of live bacteria was  $8.3 \times 10^7$ /ml. With 21  $\mu$ M concentration of Ni NPs, 34% of the bacterial in the control was alive as the concentration increased to 29  $\mu$ M, while the live cells decreased to 14% and with further increase of NPs concentration, i.e., 29  $\mu$ M only a small portion of *E. coli*, i.e., 0.084%, which is very small, as compared to the measured CFU in the control sample which was alive. The nickel nanoparticles were embedded in the cell membranes and destructed the bacterial cell membrane [29,30]. The small size of nanoparticles increased the membrane penetrability and caused uncontrolled mass transfer through the membranes, nickel nanoparticles permeation into the cells, which leads to the interaction of Ni-NPs with cells causing cell death. The presence of carboxylic group in excessive numbers makes the surface of bacteria negative upon dissociation at biological PH. The electrostatic forces cause the adhesion of nanoparticles to bacteria because of the presence of opposite charges on the bacteria and nanoparticles. Nanoparticles have a large surface to volume ratio and hence increased surface area, which increases their toxic effects against bacteria [31]. Nickel nanoparticles were found to be highly toxic for *E. coli*. High NP concentration was found to have highest toxicity to the bacteria.

Furthermore, in studying cadmium sensitivity of *Bradyrhizobium-japonicum*, and using a mineral medium, it was shown that a significant amount of the added cadmium bonded to uncharacterized medium components. Cadmium Chloride ( $\text{Cd}^{2+}$ ) causes a

sharp concentration reduction in the number of bacteria. The number of total aerobic, total anaerobic, gram-positive and gram-negative bacteria was reduced when cadmium was applied at doses of 23 and 30 mg kg<sup>-1</sup>, while at 37 mg kg<sup>-1</sup> or higher doses; no colony growth was observed for most of the species [32]. The number of viable bacteria was reduced to 2 \* 10<sup>3</sup>, 8 \* 10<sup>2</sup>, 3 \* 10<sup>3</sup> and 9 \* 10<sup>2</sup> CFU per mL for *B. cereus*, *Clostridium* spp., and *Lactobacillus* spp., respectively, due to the toxic effect of 30 mg kg<sup>-1</sup> cadmium, no viable colony could be detected at 37 mg kg<sup>-1</sup> or higher concentrations of cadmium except for *E. coli*, with some colonies growing when cadmium was administered at the dose of 37 mg kg<sup>-1</sup> [32]. Consequently, it appears that MICs determined with a traditional approach cannot be related to actual metal concentrations in the habitat from which the bacteria were isolated. In spite of these limits, the technique of MICs remains a valid approach to evaluate the action of heavy metals on the microbial activity in polluted habitats, such as agricultural soils, sludge-amended soils, marine sediments and municipal refuse.

On the other hand, the possibility of using metal resistant bacteria as bio-indicators of polluted environment has been shown to be a sensitive and reliable tool in detecting the sub-lethal toxicity of these polluting compounds. A combination of bioassays (fish, algae, bacteria) is increasingly recommended in the framework of integrated ecotoxicological approaches, in order to gain a better insight into the potential dangers associated with the disposal of complex industrial effluent in the environment. The tolerance of soil bacteria to heavy metals has been investigated as an indicator of potential toxicity of metals to other forms of life [33]. As mentioned, many heavy metals are toxic, non-biodegradable pollutants released into the environment by industrial, mining and agricultural activities [34]. The conventional treatments used to remove heavy metals from wastewater are precipitation, coagulation, reduction and membrane processes, ion exchange and adsorption. However, the application of such processes is often restricted because of technical and/or economic constraints. For example, precipitation processes cannot guarantee the metal concentration limits required by regulatory standards and produce waste, which is difficult to treat. On the other hand, ion exchange and adsorption processes are very effective, but require expensive adsorbent materials and difficult plant management [35]. Thus, the search for a new economical and effective heavy metal adsorbent focuses on biomaterials such as bacterial and algal biomass [36]. The advantages of bio-sorption lie in both its good

performance in metal removal, often comparable with their commercial competitors (ion exchangers), and cost-effectiveness, making use of algae and raw materials of fermentation and agricultural processes [37]. This aspect can play an important role in improving a zero-waste economic policy, especially in the case of the re-use of biomass coming from food, pharmaceutical and wastewater treatments.

Another bio-sorption advantage is the selectivity shown by some biomasses towards heavy metal even in the presence of high concentrations of other ions, such as alkaline and alkaline-earth metals. When a proper immobilisation or combination technique is adopted, it is also possible to regenerate the biomasses and re-use them. Bio-sorption of heavy metals is affected by many experimental factors, such as pH, ionic strength, biomass concentration, temperature and the presence of different metallic ions in the solution. The variability of these factors in real wastewaters makes it necessary to know how they influence the bio-sorption performance. Because of these possible, multiple interactions the comprehension of the bio-sorption phenomenon is very complex and requires a study of both the solution chemistry of metal ions (depending on pH, anions and/or ligands in solution) and the mechanisms of metal uptake (ion exchange, complication, micro-precipitation, etc.) [38]. An accurate knowledge of bio-sorption mechanisms and their main influencing factors allows optimisation of the operating conditions both in uptake and regeneration phases [39].

The understanding of the bio-sorption phenomenon by using a cultivated biomass of *Sphaerotilus-natans* (Gram-negative bacteria) gives good performance in heavy metal removal [40]. This microorganism is often present in domestic wastewater treatment plants and produces the undesirable bulking phenomenon reducing the settling capacity of the active sludge [41]. The effect of pH and biomass concentration has been studied [40]. The acidic and ion exchange properties of the biomass were determined in order to study the nature and capacity of the bio-sorbent. The potentiometric titration of the lyophilised biomass was performed by adding first a known amount of HCl to a cellular suspension and then NaOH as titrant. The pH of the cellular suspension they were measured after any titrant addition by using a pH-meter. The ionic content of the biomass was determined: a known amount of biomass (1 g) was washed four times with HCl 0.1 M (100 ml) and the washing water was analysed to determine the alkaline and alkaline earth metal content [41]. In previous studies the experimental tests were performed under different operating conditions: pH (levels: 3, 4, 5 and 6) and biomass

concentration (levels: 0.5, 1.0 and 2 g/l) were investigated as factors. Two different heavy metals, copper (II) and cadmium (II) ( $\text{CuCl}_2$  and  $\text{CdCl}_2$ , respectively), were tested for bio-sorption on *S. natans*. As mentioned, bacteria are the most abundant and versatile of microorganisms and constitute a significant fraction of the entire living terrestrial biomass of  $\sim 10^{18}$ g [42]. Some microorganisms were found to accumulate metallic elements with high capacity [43]. Some marine microorganisms enriched Pb and Cd by the factors of  $1.7 \times 10^5$  and  $1.0 \times 10^5$  respectively, relative to the aqueous solute concentration of these elements in ocean waters [42]. Bacteria were used as bio-sorbents because of their small size, their ubiquity, their ability to grow under controlled conditions, and their resilience to a wide range of environmental situations. Bacteria species such as *Bacillus*, *Pseudomonas*, *Streptomyces*, *Escherichia*, *Micrococcus*, etc. have been tested for their uptake of metals or organics. Metal uptake capacity is not necessarily to reach maximum values in the application. Some uptake values were experimental uptakes, and the Langmuir model predicted some. Bacteria either may possess the capacity for bio-sorption of many elements or, alternatively, depending on the species, may be element specific.

As the bio-sorption process involves mainly cell surface sequestration, the modification of a cell wall can greatly alter the binding of metal ions. A number of methods have been employed for microbial cell wall modification, in order to enhance the metal-binding capacity of biomass and to elucidate the mechanism of bio-sorption. The physical treatments include heating/boiling, freezing/thawing, drying and lyophilisation. The various chemical treatments used for biomass modification include washing the biomass with detergents, cross-linking with organic solvents, and acid treatment. The pre-treatments can modify the surface characteristics/groups, either by removing or masking the groups or by exposing more metal binding sites [44]. Now various pre-treatment methods are reported to deal with the cells of bacteria. Physical methods include vacuum and freeze-drying, boiling or heating, autoclaving, and mechanical disruption. Chemical methods include treatment with various organic and inorganic compounds, such as acid and caustic, methanol, formaldehyde, etc. Some methods are found to improve metal bio-sorption to some extent. Acid treatment of fungal organisms has been shown to increase the metal uptake capacity significantly, whereas acid treatment of biomass almost has no influence on metal [45]. Due to the important role of the cell wall for metal bio-sorption by non-viable cells, metal bio-sorption may be

enhanced by heat or chemical sterilization or by crushing. Thus, degraded cells would offer a larger available surface area and expose the intracellular components and more surface binding sites because of the destruction of the cell membranes [46]. The bio-sorption of cadmium and lead ions from synthetic aqueous solutions using yeast biomass was investigated [47]. The waste baker's yeast cells were treated by caustic, ethanol and heat methods, and the highest metal uptake capacity for  $\text{Cd}^{2+}$  and  $\text{Pb}^{2+}$  were obtained by ethanol treated yeast cells. However it gave the different results on pre-treatment [48]. The equilibrium uptake capacity of lead (in  $\text{mg Pb}^{2+} \text{ g}^{-1}$ ) decreased in the order: original cell (260) > 5 time as autoclaved cell for 15 min (150) > grinded cell after drying (100) > autoclaved cell for 5 min (30). After all of that has been reviewed above, the use of bacteria for detection and scavenging of heavy metals is a promising direction of research, which has been researched and discovered in the current PhD project.

### **3.4. Detection of Heavy Metals**

Heavy metals are defined as those metals with densities greater than  $5 \text{ g cm}^{-3}$ . Heavy metals are commonly referred to as trace metals; many trace metals are highly toxic to humans (e.g. Hg, Pb, Cd, Ni, As, Sn) and other living organisms, and their presence in surface waters at above background concentrations is undesirable [49]. There are many techniques used for detection of heavy metals, for example.

**Atomic Absorption Spectroscopy (AAS)** is a spectra-analytical procedure for the quantitative determination of chemical elements employing the absorption of light by free atoms in a gaseous state. In analytical chemistry, the technique is used for determining the concentration of a particular element (analyte) in a sample to be analysed. AAS can be used to determine over 70 different elements in solution or directly in solid samples employed in pharmacology, biophysics and toxicology research. Atomic absorption spectrometry was first used as an analytical technique, and the underlying principles were established in the second half of the 19th century. The modern form of AAS was largely developed during the 1950s. The technique makes use of absorption spectrometry to assess the concentration of an analyte in a sample. It requires standards with known analyte content to establish the relation between the measured absorbance and the analyte concentration [49]. In short, the electrons of the atoms in the atomizer can be promoted to higher orbital (excited state) for a short period

of time (nanoseconds) by absorbing a defined quantity of energy (radiation of a given wavelength). This amount of energy, i.e., wavelength, is specific to a particular electron transition in a particular element. In general, each wavelength corresponds to only one element, and the width of an absorption line is only of the order of a few picometers (pm), which gives the technique its elemental selectivity. The radiation flux without a sample and with a sample in the atomizer is measured using a detector, and the ratio between the two values (the absorbance) is converted to analyte concentration or mass using the Beer-Lambert Law [50].

**Inductively Coupled Plasma Mass Spectrometry (ICP-MS)** is a type of mass spectrometry which is capable of detecting metals and several non-metals at concentrations as low as one part in  $10^{12}$  (parts per trillion). Inductively Coupled Plasma-Mass Spectrometry (ICP-MS) is a very sensitive analytical technique with a high linear dynamic range (ultra-trace to main components). It is capable of analysing all elements from Li to U and can be applied to solutions, solids and gasses. ICP-MS sampled material is transferred by an argon flow into inductively coupled plasma in which an effective temperature of 7000 K results in atomisation and ionisation of the material. Subsequently, the ions are extracted into a mass spectrometer, with which the elemental composition of the material is determined [51]. This is achieved by ionizing the sample with inductively coupled plasma and then using a mass spectrometer to separate and quantify those ions. Compared to atomic absorption techniques, ICP-MS has greater speed, precision, and sensitivity. However, analysis by ICP-MS is also more susceptible to trace contaminants from glassware and reagents. In addition, the presence of some ions can interfere with the detection of other ions. Another reliable technique is Chromatography.

**Chromatography** is a physical method of separation that distributes components to separate between two phases, one stationary phase and the other mobile phase moving in a definite direction. Chromatography is the collective term for a set of laboratory techniques for the separation of mixtures. The mixture is dissolved in a fluid, the mobile phase, which carries it through a structure holding another material called the stationary phase. The various constituents of the mixture travel at different speeds, causing them to separate. The separation is based on differential partitioning between the mobile and stationary phases. A subtle difference in a compound's partition coefficient results in differential retention on the stationary phase and thus changes the separation.

Chromatography may be preparative or analytical. The purpose of preparative chromatography is to separate the components of a mixture for more advanced use (and is thus a form of purification) [52]. Analytical chromatography is done normally with smaller amounts of material and is for measuring the relative proportions of analytes in a mixture. The two are not mutually exclusive. In this project the bio-cell sensor that included the microorganisms (bacteria) was employed for detection of heavy metals, which is considered to be a cheap (cost effective), simple (easy to use), powerless (portable) and sensitive technique.

### **References:**

1. John H. Duffus, (2002), Heavy metals, a meaningless term, IUPAC Technical Report, Pure and Applied Chemistry, Vol. (74), pp. 793-807.
2. LeppN. W, (1981), Metals in the Environment, Vol. (2), Liverpool, UK.
3. Hawkes, H, E. and J. S. Webb, (1962), Geochemistry in mineral exploration, New York, Evanston, (415).
4. Cannon, H. L. and B. M. Anderson, (1979), the geochemistry involvement with pollution problems, Environmental Geochemistry in Health and Disease, Geological Society of America, Boulder, Colorado.
5. Mitchell, R. L. (1964), Trace element in soils, Chemistry of the Soil, 2nd Ed, New York, pp. 320-68.
6. Holmes, R. (1975), the regional distribution of cadmium in England and Wales, Ph.D. Thesis, University of London.
7. IUPAC, (1989), Nomenclature of inorganic chemistry, Butterworth's, London.
8. Lenihan, J. (1988), the crumbs of creation: trace elements in history, medicine, industry, crime, and folklore, Adam Hilger, Bristol.
9. CoxP. A, (1995), the elements on earth, inorganic Chemistry in the Environment, New York.
10. Suchisita Das, Abhik Gupta, (2011), Effects of cadmium chloride on oxygen consumption and gill morphology of Indian flying barb, J. Environ. Biol. (33), pp. 1057-1061.
11. Lide, David R. (1998), Handbook of Chemistry and Physics (87 ed.), Boca Raton, FL: CRC Press, pp. 4-67.
12. GreenwoodN. N, EarnshawA, (1997), Chemistry of the Elements, 2nd ed., Butterworth-Heinemann, Oxford, UK.

13. Espina, S., A. Salibian, C. Rosas, A. Sanchez and G. Alcaraz: (1995), Acute physiological responses of grass carp *Ctenopharyngodon idella* fingerlings to sublethal concentrations of cadmium. *Acta. Toxicol. Argent*, (3), pp. 8-10.
14. Van Aardt, W.J. and J. Booysen, (2004), Water hardness and the effects of Cd on oxygen consumption, plasma chlorides and bioaccumulation *Tilapia sparrmanii*. *Water*, (30), pp. 57-64.
15. Das S. and GuptaA, (2010), acute toxicity studies on Indian flying barb, *Esomus danricus* (Hamilton-Buchanan), in relation to exposure of heavy metals, cadmium and copper. *J. Environmental Res, Dei*, (4), pp. 705-712.
16. James, R, K. Sampath and D.S. Edward: (2003), Copper toxicity on growth and reproductive potential in an ornamental fish, *Xiphophorus helleri*. *Asian Fisheries Sci.*, (16), pp. 317-326.
17. Lars Stixrude, Evgeny Wasserman and Ronald Cohen, (1997), Composition and temperature of Earth's inner core. *Journal of Geophysical Research (American Geophysical Union)*, 102 (B11): pp. 24729-24740.
18. Kasprzak; Sunderman Jr, F. W.; Salnikow, K. (2003), Nickel carcinogenesis, *Mutation research* 533, (1-2): pp. 67-97.
19. Mond, L.; Langer, C.; Quincke, F. (1890), Action of Carbon Monoxide on Nickel. *Journal of the Chemical Society, Transactions* (57): pp. 749-753.
20. Wells, A. F. (1984), *Structural Inorganic Chemistry*, Oxford Press, Oxford, United Kingdom,.
21. J Byrne Brower, R.L Ryan, M Pazirandeh, (1997), Comparison of ion exchange resins and biosorbents for the removal of heavy metals from plating factory wastewater *Environ. Sci. Technol.*, (31) pp. 2910-2914.
22. MajetiNarasimhaVara Prasad. (2004), Heavy metal stress in plants: from biomolecules to ecosystems., pp. 462.
23. Oliver, M. A. (1997), Soil and human health: a review. *European Journal of Soil Science*, Vol. 48, pp. 573-592.
24. XuehuiXie, Jin Fu, Huiping Wang and Jianshe Liu, (2010), Heavy metal resistance by two bacteria strains isolated from a copper mine tailing in China, *African Journal of Biotechnology*, Vol. 9(26), pp. 4056-4066.
25. Abramowitz M, Davidson MW, (2007), *Introduction to Microscopy, Molecular Expressions*, Retrieved, pp. 08-22.

26. Hassen A, Saidi N & Cherif M, Boudabous A, (1998), resistance of environmental Bacteria to heavy metals, *Bioresource Technology* (64), pp. 07-15.
27. Liu, J., Zheng, B., Aposhian, H. V., Zhou, Y., Chen, M. L., Zhang, A., & Waalkes, M. P. (2002), Chronic arsenic poisoning from burning high-arsenic-containing coal in Guizhou, China. *Environ Health Perspect*, Vol. 110(2), pp. 119-122.
28. Shamaila S, Wali H, Sharif R, Nazir J, Zafar N, Rafique M S, (2013), Antibacterial effects of laser ablated Ni nanoparticles, *applied physics letters*, (103).
29. Sondi I and Salopek-Sondi B, (2004), *Colloid Interface Sci.* 275, pp. 177-182.
30. Morones J. R, Elechiguerra J. L, Camacho A., Holt K., Kouri J. B., Ramirez J. T., and Yacaman M. J., (2005), *Nanotechnology* (16), pp. 2346-2353.
31. Baker C, Pradhan A, Pakstis L, Pochan D. J, and Shah S. I, (2005), *Nanosci. Nanotechnol.* (5), 244.
32. Fazeli M, Hassanzadeh P and Alaei S, (2011), Cadmium chloride exhibits a profound toxic effect on bacterial microflora of the mice gastrointestinal tract, *Human and Experimental Toxicology*, 30(2), pp. 152–159.
33. Ken E Gillera, Ernst Witterb, Steve P Mcgrathc, Toxicity of heavy metals to microorganisms and microbial processes in agricultural soils: a review, *Soil Biology and Biochemistry*, Volume 30, Issues 10–11, (1998), pp. 1389–1414.
34. Byrne Brower J, Ryan R. L, Pazirandeh M, (1997), Comparison of ion exchange resins and biosorbents for the removal of heavy metals from plating factory wastewater, *inviron.Sci. Technol.* (31), pp. 2910-2914.
35. Beccari M, Di Pinto A. C, Marani D, Santori M, Tiravanti G, (1986), I metalli nelle acque: origine, distribuzione, metodidi rimozione, CNR, Istituto di ricerca sulle acque, Quaderni, (71), Roma.
36. Volesky B, Holan Z.R, (1995), Biosorption of heavy metals, *Biotechnol. Prog.* (11) pp. 235-250.
37. Volesky B, (1999), Biosorption for the next century, in: R. Amils, A. Ballester (Eds), *Biohydrometallurgy and Environment Toward the Mining of the 21st Century, Part B*, pp. 161-170.
38. Veglio F, Beolchini F, (1997), Removal of metals by biosorption: a review, *hydrometallurgy* (44), pp. 301-316.

39. Pagnanelli F, Petrangeli Papini M, Trifoni M, Toro L, Veglio F, (2000), Biosorption of metal ions on *Arthrobacter* sp. biomass characterization and biosorption modeling, *Environ. Sci Technol.* (34), pp. 2773-2778.
40. Esposito A., F. Pagnanelli, A. Lodi, C. Solisio, F. Veglio, (2001), Biosorption of heavy metals by *Sphaerotilus natans*, an equilibrium study at different pH and biomass concentrations, *Hydrometallurgy*, Vol. 60, pp. 129–141.
41. Solisio C, Lodi A, Converti A, Del Borghi M, (2000), The effect of acid pre-treatment on the biosorption of Chromium (III) by *Sphaerotilus natans* from industrial wastewater, *Water Res.* 34 (12), pp. 3171-3178.
42. Mann H. (1990), Removal and recovery of heavy metals by biosorption. In: Volesky B, editor. *Biosorption of heavy metals*, Boca Raton: CRC press; pp. 93-137.
43. Vijayaraghavan K, Yun YS. (2008), Bacterial biosorbents and biosorption. *Biotechnol Adv.* 26: pp. 266–291.
44. Vieira R H S F, Volesky B. *Biosorption: (2000), a solution to pollution*, *Int. Microbiol.* 3: pp. 17–24.
45. Kapoor A, Viraraghavan T, Cullimore DR. (1999), Removal of heavy metals using the fungus *Aspergillus niger*. *Bioresour Technol.* 70: pp. 95-104.
46. Errasquin EL, Vazquez C. (2003), Tolerance and uptake of heavy metals by *Trichoderma atroviride* isolated from sludge. *Chemosphere*; 50: pp. 137-143.
47. Goksungur Y, Uren S, Guvenc U. (2005), Biosorption of cadmium and lead ions by ethanol treated waste baker's yeast biomass. *Bioresour Technol.* 96: pp. 103-109.
48. Suh J. H, Kim D. S, (2000), Effects of Hg<sup>2+</sup> and cell conditions on Pb<sup>2+</sup> accumulation by *Saccharomyces cerevisiae*. *Bioprocess Eng.* 23. pp. 327-329.
49. McCarthy G.J, (2012), Walsh, Alan-Biographical entry, *Encyclopedia of Australian Science*, Retrieved.
50. Welz B, Sperling M, (1999), *Atomic Absorption Spectrometry*, Wiley-VCH, Weinheim, Germany, ISBN 3-527-28571-7.
51. Koninklijke Philips, (2008), *Inductively Coupled Plasma-Mass Spectrometry (ICP-MS)*, Electronics N.V.
52. International Union of Pure and Applied chemistry IUPAC Recommendations (1993), nomenclature for Chromatography.

## CHAPTER 4

### Sensing Material

This study utilised microorganisms (Bacteria) as a sensor material for detection of the environmental pollution, which is achieved through studying the optical and electrical properties of these microorganisms, which includes monitoring live bacteria numbers after expose to the pollutants.

#### 4.1. Bacteria

Bacteria comprise a large domain of prokaryotic microorganisms. Typically, a few micrometres in length, bacteria have a wide range of shapes, ranging from spheres to rods and spirals [1]. They were among the first life forms to appear on Earth, and are present in most habitats on the planet, including soil, acidic hot springs, radioactive waste, water, and deep in the Earth's shell, as well as in organic matter and the live bodies of plants and animals, providing outstanding examples of mutualism in the digestive tracts of humans [2].

There are typically 40 million bacterial cells in a gram of soil and a million bacterial cells in a millilitre of fresh water. In all, there are thousands of nonillions of bacteria on Earth [3], forming a biomass that exceeds that of all plants and animals. Bacteria are vital in recycling nutrients, with many steps in nutrient cycles depending on these organisms, such as the fixation of nitrogen from the atmosphere and putrefaction [4]. In biological communities surrounding hydrothermal vents and cold seeps, bacteria provides the nutrients needed to sustain life by converting dissolved compounds such as hydrogen sulphide and methane. Most bacteria have not been characterised, and only about half of the phyla of bacteria have species that can be grown in the laboratory.

Bacteria display a wide diversity of shapes and sizes, called morphologies. Bacterial cells are about one tenth the sizes of eukaryotic cells and are typically 0.5-5.0 micrometres in length. However, a few species are up to half a millimetre long and are visible to the unaided eye [5], for example, *E. fishelsoni* reaches 0.7 mm [6]. Among the smallest bacteria are members of the genus *Mycoplasma*, which measure only 0.3 micrometres, as small as the largest viruses. Some bacteria may be even smaller.

Most bacterial species are either spherical, called cocci or rod-shaped, called bacilli. The bacterial cell are surrounded by a lipid membrane, or cell membrane, which encloses the contents of the cell and acts as a barrier to hold nutrients, proteins and other essential components of the cytoplasm within the cell. As they are prokaryotes, bacteria do not tend to have membrane-bound organelles in their cytoplasm and thus contains few large intracellular structures. They consequently lack a true nucleus, mitochondria, chloroplasts and other organelles present in eukaryotic cells, such as the Golgi apparatus and endoplasmic reticulum [7]. Bacteria were once seen as simple bags of cytoplasm, but elements such as prokaryotic cytoskeleton [8], and the localization of proteins to specific locations within the cytoplasm have been found to show levels of complexity. These sub-cellular compartments have been called "bacterial hyper structures". Micro-compartments such as carboxysomes supply a further level of organization, which are compartments within bacteria that are surrounded by polyhedral protein shells, rather than by lipid membranes. These "polyhedral organelles" restrict and compartmentalize bacterial metabolism, a function performed by the membrane-bound organelles in eukaryotes.

Many important biochemical reactions, such as energy generation, occur by concentration gradients across membranes. The general lack of internal membranes in bacteria means reactions such as electron transport occur across the cell membrane between the cytoplasm and the periplasmic space. However, in many photosynthetic bacteria the plasma membrane is highly folded and fills most of the cell with layers of light-gathering membrane. These light-gathering complexes may even form lipid-enclosed structures called chlorosomes in green sulphur bacteria [9]. Other proteins import nutrients across the cell membrane, or expel undesired molecules from the cytoplasm.

Most bacteria do not have a membrane-bound nucleus, and their genetic material is typically a single circular chromosome located in the cytoplasm in an irregularly-shaped body, called the nucleoid. The nucleoid contains the chromosome, with associated proteins and RNA. The order Planctomycetes are an exception to the general absence of internal membranes in bacteria because they have a double membrane around their nucleoids and contain other membrane-bound cellular structures. Like all living organisms, bacteria contain ribosome's for the production of proteins, but the structure of the bacterial ribosome is different from those of eukaryotes and Archaea. Some

bacteria produce intracellular nutrient storage granules, such as glycogen, polyphosphate, sulfur or polyhydroxy alkanoates. These granules enable bacteria to store compounds for later use [10]. Certain bacterial species, such as the photosynthetic Cyanobacteria, produce internal gas vesicles, which they use to regulate their buoyancy, allowing them to move up or down into water layers with different light intensities and nutrient levels.

#### **4.1.1. Bacteria Cell Wall**

In most bacteria a tough outer layer, the cell wall, protects the delicate protoplast from mechanical damage and osmotic lysis; it also determines a cell's shape. Additionally, the cell wall acts as a molecular sieve, a permeability barrier that excludes various molecules. It also plays an active role in regulating the transport of ions and molecules. The cell walls of different species may differ greatly in thickness, structure and composition. There are broadly speaking two different types of cell wall in bacteria, whether a given cell has one or the other type of wall can generally be determined by the cells reaction to certain dyes, these two types called Gram-positive and Gram-negative. The names originate from the reaction of cells to the Gram stain (red stain), a test long-employed for the classification of bacterial species. Gram-positive bacteria (are a class of bacteria that take up the crystal violet stain used in the gram staining method of bacterial differentiation), which possess a thick cell wall (about 30-100 nm) and it generally has a simple, uniform appearance under the electron microscope. Some 40-80% of the wall is made of a tough, complex polymer, peptidoglycan. Essentially, peptidoglycan consists of linear heteropoly saccharide chains and teichoic acids. In contrast, Gram-negative bacteria (are a class of bacteria that do not retain the crystal violet stain (stained red) used in the Gram staining method of bacterial differentiation), which it have a relatively thin cell wall (20-30 nm) with a distinctly layered appearance under the electron microscope. The inner layer nearest the cytoplasmic membrane is widely believed to consist of a few layers of peptidoglycan (15 nm thick) surrounded by a second lipid membrane, containing lipopolysaccharides and lipoproteins. Most bacteria have the Gram-negative cell wall, and only the Firmicutes and Actino bacteria (which are known as the low G+C and high G+C Gram-positive bacteria, respectively) have the alternative Gram-positive arrangement [11]. These differences in structure can produce differences in antibiotic susceptibility. Therefore, the lipid membrane reaction for gram stain helped the researcher to

distinguish between the bacteria. The simple structure of a bacteria cell is shown in Figure 4.1.

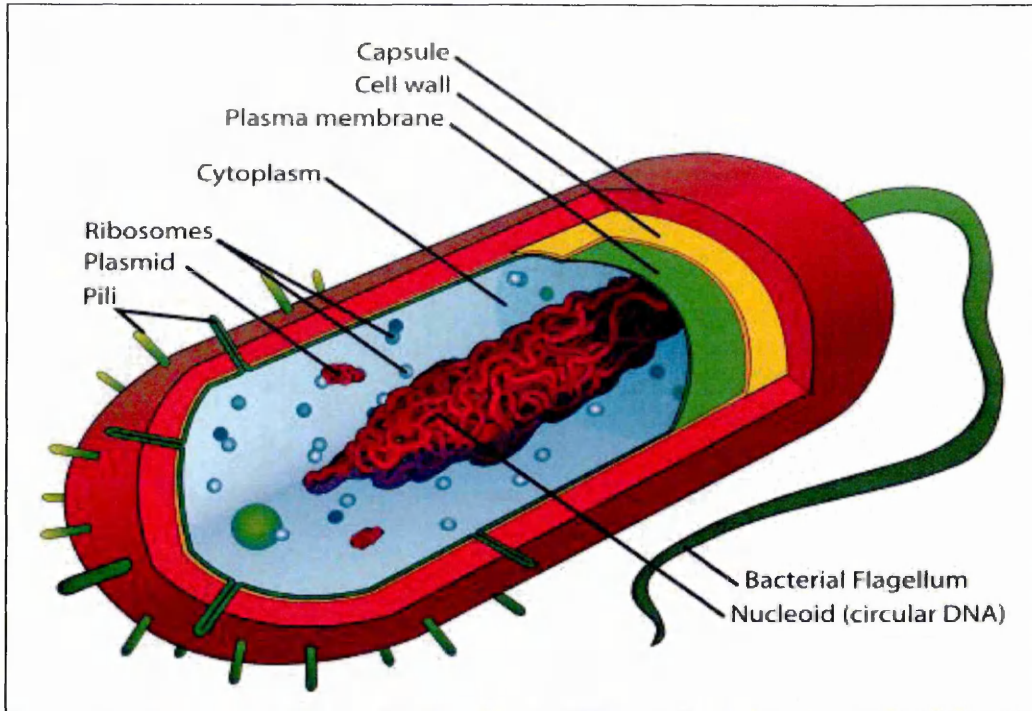


Figure 4.1. Structure and contents of a typical Gram-positive bacteria cell [12]

The lipid membrane is a thin polar membrane consisting of two layers of lipid molecules. These membranes are flat sheets that form a continuous barrier around cells. The cell membrane of almost all living organisms and many viruses are covered by a lipid, as are the membranes surrounding the cell nucleus and other sub-cellular structures. The lipid layer is the barrier that keeps ions, proteins and other molecules where they were needed and prevents them from diffusing into areas where they should not be. Lipid layers are ideally suited to this role because, even though they are only a few nanometres in width, they are impermeable to most water-soluble (hydrophilic) molecules. Layers are particularly impermeable to ions, which allow cells to regulate salt concentrations and pH by pumping ions across their membranes using proteins called ion pumps. In many bacteria there are fine, hair like proteinaceous filaments extending from the cell surface; these filaments can be divided into three main types: flagella, fimbriae and pili.

Pili (singular: pilus) are elongated or hair-like proteinaceous structures which project from a cell's surface; they are found specifically on those Gram-negative cells which have the ability to transfer DNA to other cells by conjugation, a process in which the

pili themselves play an essential role. The various types of pili differ in size and shape: for example, some are long, thin and flexible, while others are short, rigid and nail-like, the type of pilus correlates with the physical condition under which conjugation can take place.

#### **4.1.2. Growth of Bacteria**

Growth in a bacteria cell involves a coordinated increase in the mass of its constituent parts; it is not simply an increase in total mass, since this could be due, for example, to the accumulation of a storage compound within the cell. Usually, growth leads to the division of a cell into two similar or identical cells. Thus, growth and reproduction are closely linked in bacteria, and the term growth is generally used to cover both processes. Bacteria grow only if their environment is suitable; if it's not optimal, growth may occur at a lower rate or not at all or the bacteria may die, depending on species and condition. Essential requirements for growth include, (i) a supply of suitable nutrient; (ii) a source of energy; (iii) water; (iv) an appropriate temperature; (v) an appropriate PH; (vi) appropriate levels (or the absence) of oxygen.

Consider the growth of bacteria on a solid medium of one common type of solid medium widely used in bacteriological laboratories, which is a jelly like substance (an agar gel) containing nutrients and other ingredients. Suppose that a single bacterial cell is placed on the surface of such a medium and given everything necessary for growth and division. The cell grows, division continues, the progeny of the original cell eventually reach such immense numbers that they form a compact heap of the cells that is usually visible to the naked eye; this mass of cells is called a colony. In addition, either bacteria can move freely through a liquid medium by diffusion or, in motile species, by active movement; thus, as cells grow and divide, the progeny are commonly dispersed throughout the medium. Usually, as the concentration of cells increases, the medium becomes increasingly turbid (cloudy), so that each bacterial species needs specific medium and particular environmental conditions for pure growth. This study utilized two kinds of bacteria to scan a wide range of environmental pollution.

#### **4.2. Escherichia Coli**

Commonly abbreviated E. coli is a Gram-negative, rod-shaped bacterium commonly found in the lower intestine of warm-blooded organisms (endotherms). Most E. coli

strains are harmless, but some can cause serious food poisoning in humans, and are occasionally responsible for product recalls due to food contamination [13]. The harmless strains are part of the normal flora of the gut, and can benefit their hosts by producing vitamin K2, and by preventing the establishment of pathogenic bacteria within the intestine.

This work aims for the development of novel sensing technologies for detection of radionuclide's and heavy metals using microorganisms (Bacteria). *Escherichia coli* (*E. coli*), belonging to the gram-negative bacteria, was selected for this task; also, it is facultative anaerobic, rod prokaryotic. As mentioned in previous sections, there are hundreds of different strains of *E. coli*: some are harmless; others cause serious illness. A non-pathogenic strain of *E. coli* (DH5 $\alpha$ ) normally present in the intestinal tract in humans and animals was used in this study. Figure 4.2 shows the *E. coli* bacteria cells and their colonies.

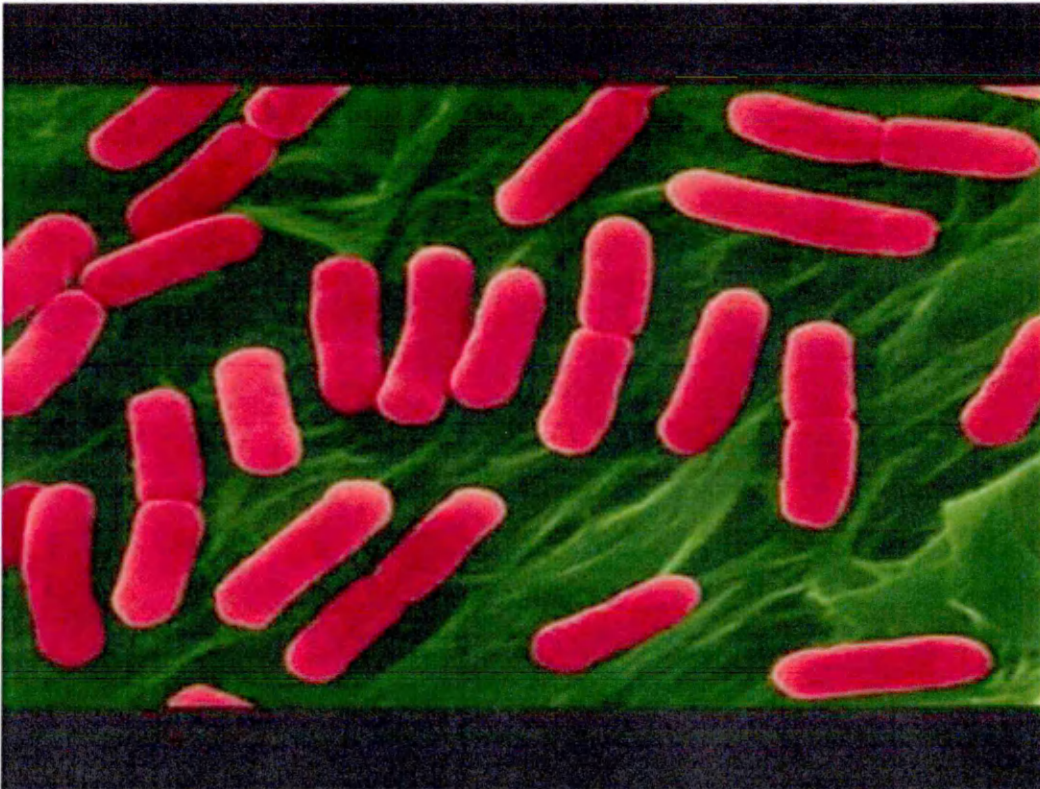


Figure 4.2. *E. coli* bacteria cells (Gram-Negative) [14]

#### 4.3. *Deinococcus Radiodurans*

Arthur W. Anderson at the Oregon Agricultural Experiment Station in Corvallis discovered *Deinococcus Radiodurans* (*D. radiodurans*) in 1956 [15]. Experiments were

being performed to determine if canned food could be sterilized using high doses of gamma radiation. A tin of meat was exposed to a dose of radiation that was thought to kill all known forms of life, but the meat subsequently spoiled, and *D. radiodurans* was isolated.

*Deinococcus radiodurans* has a unique quality in which it can repair both single and double-stranded DNA. When a mutation is apparent to the cell, it brings it into a compartmental ring-like structure where the DNA is repaired, and then it has able to fuse the nucleolus from the outside of the compartment with the damaged DNA. *D. radiodurans* is a rather large, spherical bacterium, with a diameter of 1.5 to 3.5  $\mu\text{m}$ . Four cells normally stick together, forming a tetrad. The bacteria are easily cultured and do not appear to cause disease. Colonies are smooth, convex, and pink to red in colour [16]. The cells stain Gram-positive, although its cell envelope is unusual and is reminiscent of the cell walls of Gram-negative bacteria, it does not form endospores and is non-motile. It is an obligate aerobic chemo-organo-heterotroph, i.e., it uses oxygen to derive energy from organic compounds in its environment. It is often found in habitats rich in organic materials, such as soil, feces, meat, or sewage, but has also been isolated from dried foods, room dust, medical instruments and textiles. It is extremely resistant to ionizing radiation, ultraviolet light, desiccation, and oxidizing and electrophilic agents. The name *Deinococcus radiodurans* derives from the Ancient Greek (deinos) and (kokkos), meaning "terrible grain/berry" and the Latin radius and durare, meaning "radiation surviving". The species was formerly called *Micrococcus radiodurans*. As a consequence of its hardiness, it has been nicknamed Conan the Bacterium [17]. *D. radiodurans* (Anderson R1 strain) was utilised in this work, Figure 4.3 showing the *D. radiodurans* bacteria cell's shape.



Figure 4.3. Gram-positive *D. radiodurans* bacteria cells [18]

#### References:

1. Rybicki E. P. (1990), the classification of organisms at the edge of life, or problems with virus systematic, *S Afr J Sci* (86): pp. 182-186.
2. Fredrickson J. K., Zachara J. M., Balkwill D. L., et al. (2004), Geomicrobiology of high-level nuclear waste-contaminated vadose sediments at the Hanford site, Washington state, *Applied and Environmental Microbiology* 70 (7): pp. 4230-4241.
3. Whitman W. B., Coleman D. C., Wiebe WJ. (1998), Prokaryotes: the unseen majority, *Proceedings of the National Academy of Sciences of the United States of America* 95 (12): pp. 6578-6583.
4. Rappé M. S., Giovannoni S. J. (2003), the uncultured microbial majority, *Annual Review of Microbiology* (57): pp. 369-394.
5. Robertson J., Gomersall M., Gill P. (1975), *Mycoplasma hominis*: growth, reproduction, and isolation of small viable cells, *J. Bacteriol.* 124(2): pp. 1007-1018.

6. Velimirov, B. (2001), Nanobacteria, Ultramicro bacteria and Starvation Forms: A Search for the Smallest Metabolizing Bacterium, *Microbes and Environments* 16 (2): pp. 67-77.
7. Kaiser D. (2004), Signaling in myxobacteria. *Annu Rev Microbiol* (58): pp. 75-98.
8. Shih Y. L., Rothfield L. (2006), the bacterial cytoskeleton. *Microbiology and Molecular Biology Reviews* 70 (3): pp. 729–754.
9. Harold F. M., (1972), Conservation and transformation of energy by bacterial membranes, *Bacteriological Reviews* 36 (2): pp. 172–230.
10. Kadouri D., Jurkevitch E., Okon Y., Castro-Sowinski S. (2005), Ecological and agricultural significance of bacterial polyhydroxyalkanoates. *Critical Reviews in Microbiology* 31 (2): pp. 55–67.
11. Engelhardt H., Peters J., (1998), Structural research on surface layers: a focus on stability, surface layer homology domains, and surface layer-cell wall interactions, *J StructBiol* 124 (2–3): pp. 276-302.
12. Ryter A., (1988), Contribution of new cryomethods to a better knowledge of bacterial anatomy, *Ann. Inst. Pasteur Microbiol.* 139 (1): pp. 33-44.
13. Hudault S., Guignot J., Servin A. L., (2001), *Escherichia coli* strains colonizing the gastrointestinal tract protect germ-free mice against *Salmonella typhimurium* infection, *Gut* 49 (1): pp. 47-55.
14. [http://www.ciriscience.org/ph\\_122-E.\\_coli\\_Copyright\\_Dennis\\_Kunkel\\_Microscopy](http://www.ciriscience.org/ph_122-E._coli_Copyright_Dennis_Kunkel_Microscopy)
15. Anderson A. W, Nordan H. C, Cain R. F, Parrish G, Duggan D, (1956), Studies on a radio-resistant micrococcus, Isolation, morphology, cultural characteristics, and resistance to gamma radiation, *Food Technol.* 10 (1): pp. 575-577.
16. Makarova, K. S., L. Aravind, Y. I. Wolf, R. L. Tatusov, K. W. Minton, E. V. Koonin, M. J. Daly, (2001), Genome of the extremely radiation-resistant bacterium *Deinococcus radiodurans* viewed from the perspective of comparative genomics, *Microbiology and molecular biology reviews* : MMBR 65 (1): pp. 44-79.

17. Huyghe, Patrick, (1998), Conan the Bacterium, the Sciences (New York Academy of Sciences): pp. 16-19.
18. Michael Daly, (2006), D. radiodurans acquired in the laboratory, Uniformed Services University, Bethesda, MD, USA.

## CHAPTER 5

### Optical Methodology

Several optical experimental techniques, such as fluorescence microscopy, fluorescence spectroscopy, UV-visible absorption spectroscopy and spectrophotometry (optical density ( $OD_{600}$ )) were utilised in this project for counting living bacteria and thus for studying the effect of environmental pollution (gamma radiation and heavy metals) on bacteria count. In order to identify the pollution level, the above optical characteristics were measured before and after exposure of bacteria to either radiation or heavy metals. This chapter includes a general description of the optical techniques and general illustrations for optical instruments used in this work.

#### 5.1. Fluorescence Microscopy

Optical microscopy is a powerful technique commonly used for studying morphology of different materials, including organic films and biological objects. Limitations in resolution of optical microscopy, due to diffraction limits and aberrations of optical elements, do not allow objects to be observed at the sub-micron scale. Alternative modern microscopic techniques, such as electron microscopy and scanning probe microscopy, offer much better resolution, down to nanometres. However, they could be invasive (due to the use of high vacuum or direct contact (for nano-probes) and thus not suitable for biological objects in particular. In this respect, a non-invasive optical microscopy is advantageous for studying biological objects. Recent advances of optical microscopy, such as near field optical microscopy, managed to overcome the diffraction limit. The use of modern image-processing software can also enhance the performance of optical instrumentation, such as IFM. Another problem in optical microscopy is the lack of contrast of some objects, such as organic and biological thin films. This problem can be solved by using polarised light, such as in dark-field microscopy or staining the material with light absorbing or fluorescent dyes [1]. The fluorescence microscope refers to any microscope that uses fluorescence to generate an image, whether it is a more simple set up, like an epifluorescence microscope, or a more complicated design, such as a confocal microscope, which uses optical sectioning to get better resolution of the fluorescent image.

The principle of fluorescence microscopy is that the specimen is illuminated with the light of a specific wavelength (or wavelengths) absorbed by fluorophores, causing them to emit light of longer wavelengths (i.e. of a different colour than the absorbed light). The illumination light is separated from the much weaker emitted fluorescence through the use of a spectral emission filter. Typical components of a fluorescence microscope are: a light source, such as xenon arc lamp, or mercury-vapour lamp, high-power LEDs and lasers (in more advanced instruments), the excitation filter, the dichroic mirror (or dichroic beam splitter), and the emission filter (see Figure 5.1). The filters and the dichroic elements are chosen to match the spectral excitation and emission characteristics of the fluorophore used to label the specimen [2]. In this manner, the distribution of a single fluorophore (colour) is imaged at a time. Multi-colour images of several types of fluorophores must be composed by combining several single-colour images [2].

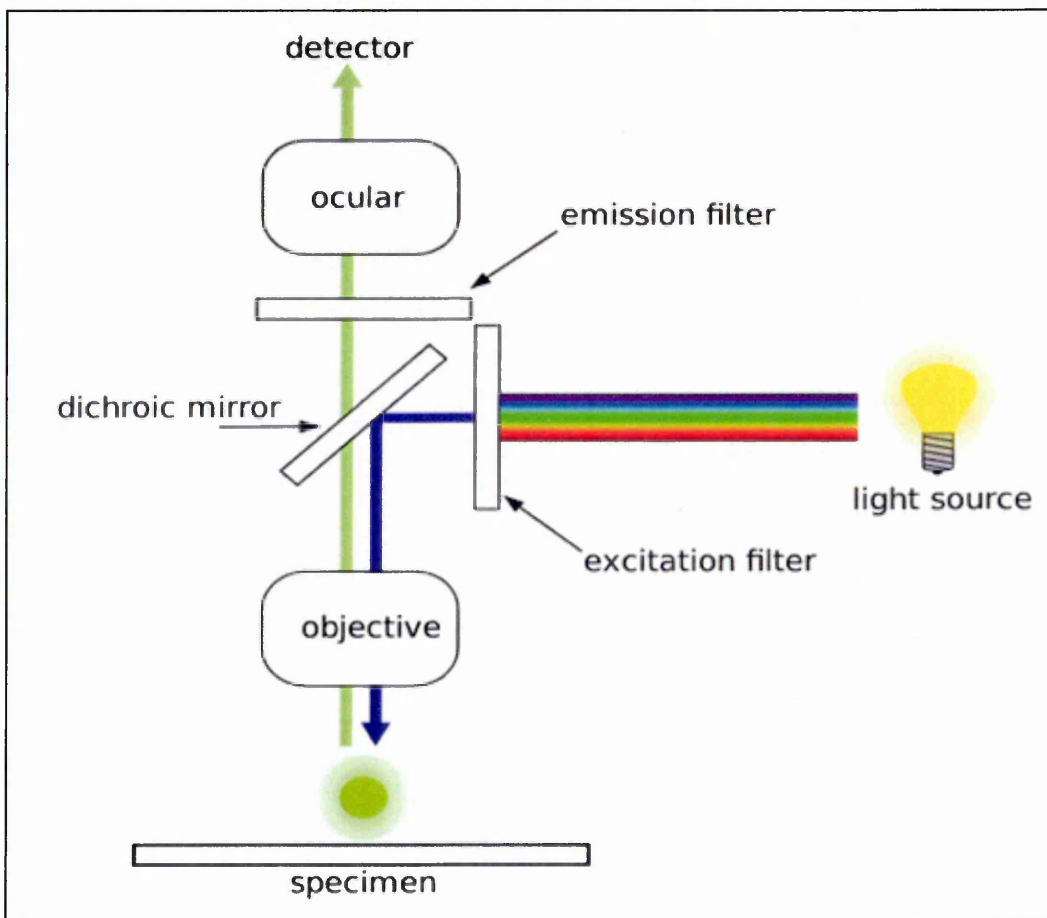


Fig.5.1. Schematic of a fluorescence microscope

Olympus (BX61), an upright fluorescence microscope with the fluorescent filter cube turret above the objective lenses, coupled with a digital camera, was used in this project (Figure 5.2).

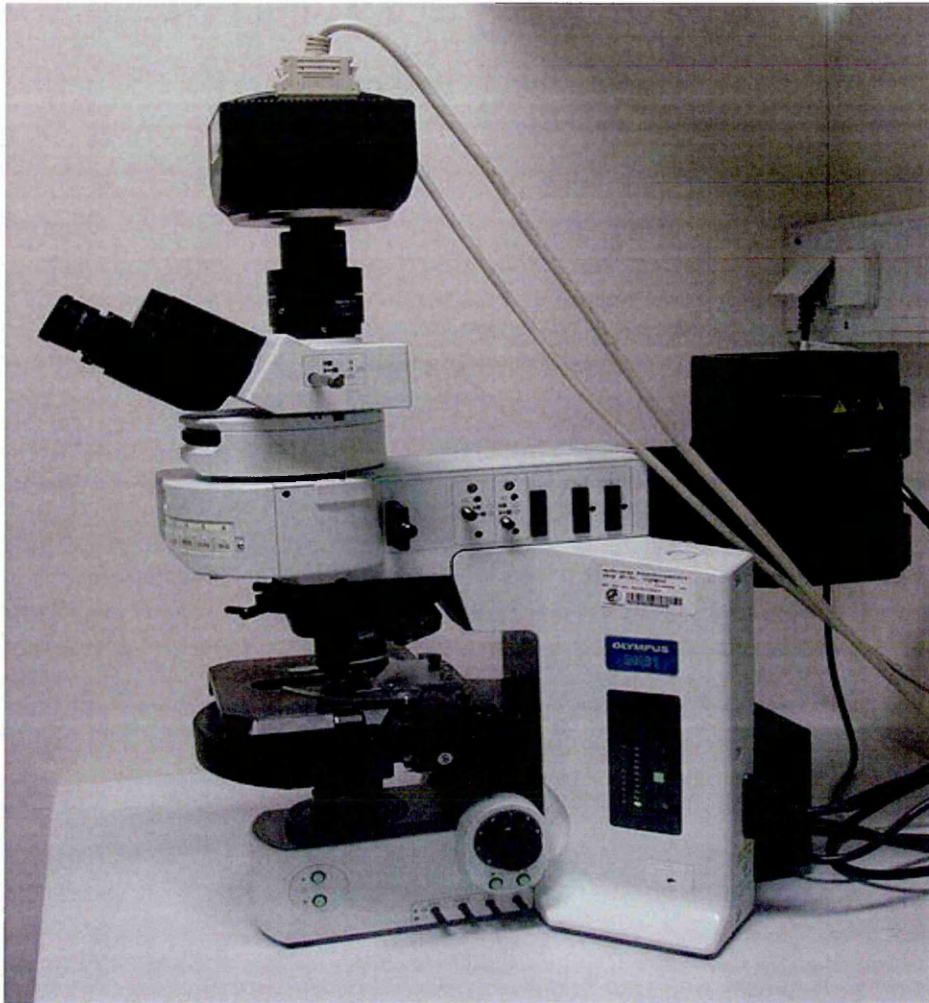


Fig.5.2. Fluorescence microscope instrument (Olympus-BX61) [2]

The biological cells are typical examples of non-contrast objects, and the most common way to increase it is to stain the cell culture with selective dyes (BacLight™ Bacterial Viability Kit, for microscopy and quantitative assays) [3]. Such staining must be carefully selected, in order to highlight some particular features of the cell culture, but not to affect bacteria functioning (in other words, the dye should not be toxic). Therefore, the fluorescence dyes used in this study is a BacLight bacterial viability kit, utilizing a mixture of the SYTO 9 green fluorescence nucleic acid stain and the red fluorescence nucleic acid stain, Propidium iodide. These stains differ both in their spectral characteristics and in their ability to penetrate healthy bacterial cells. The BacLight bacteria viability kits can easily distinguish live and dead bacteria in a short

time: bacteria with intact cell membranes stain fluorescence green (live cell), whereas bacteria with damaged membranes stain fluorescence red (dead cell) [4]. The background remains virtually non-fluorescent. The ratio of (excitation/emission) wavelength is about (480/500 nm) for the SYTO9 stain which shows a green spot, and (490/635 nm) for propidium iodide enabling to see the red spots, which refer to the dead cells.

Several staining protocols have been developed for flow cytometric analysis of bacterial viability. One promising method is dual staining with the LIVE/DEAD BacLight bacterial viability kit. In this procedure, cells are treated with two different DNA-binding dyes (SYTO9 and PI), and viability is estimated according to the proportion of bound stain. SYTO9 diffuses through the intact cell membrane and binds cellular DNA, while PI binds DNA of damaged cells only. This dual-staining method allows effective separation between viable and dead cells, which is far more difficult to achieve with single staining.

Propidium iodide (or PI) is an intercalating agent and a fluorescent molecule with a molecular mass of 668.4 Da that can be used to stain cells. When PI is bound to nucleic acids, the fluorescence excitation maximum is 535 nm and the emission maximum is 617 nm. Excitation energy can be supplied with a xenon or mercury-arc lamp or with the 488 lines of an argon-ion laser. Propidium iodide is used as a DNA stain for both flow cytometry, to evaluate cell viability or DNA content in cell cycle analysis, and microscopy, in order to visualise the nucleus and other DNA containing organelles [5]. It can be used to differentiate necrotic, apoptotic and normal cells. Propidium Iodide is the most commonly used dye to quantitatively assess DNA content.

A typical use of propidium iodide in plant biology is to stain the cell wall red fluorescent. This red fluorescent background is useful for determining the sub-localization of a gene, expressed as a green fluorescent protein fusion. In addition, propidium iodide is used as a stain in animal cells, for example, in *Apodemus sylvaticus*, more commonly known as the “wood mouse”, can be used to indicate the location of the nuclear region by emitting its characteristic red fluorescence. SYTO 9 green fluorescence nucleic acid stain does not penetrate living cells, and so was used to assess the integrity of the plasma membranes of bacteria. SYTO 9 green nucleic acid stain is an unsymmetrical cyanine dye with three positive charges which is completely excluded

from live eukaryotic and prokaryotic cells. Binding of SYTOX 9 green stain to nucleic acids resulted in more than 500-fold enhancement in fluorescence emission (absorption and emission maxima at 502 and 523 nm, respectively), rendering bacteria with compromised plasma membranes brightly fluorescent green. The 488-nm line of the argon ion laser readily excites the SYTO 9 green stain.

## 5.2. Spectrophotometer Technique (Optical Density ( $OD_{600}$ ))

Spectrophotometer techniques were used to measure the concentration of solutes in a solution by measuring the amount of light that is absorbed (or scattered) by the solutes. Spectrophotometer is an optical instrument for measurements of the absorption or transmission properties of a material as a function of wavelength. Typically it operates in wide spectral ranges covering the visible, near ultraviolet and near infrared [6]. Important features of spectrophotometers are spectral bandwidth and linear range of absorption or reflectance measurement.

A spectrophotometer is commonly used for the measurements of transmittance or absorbed light in solutions. However, they can also be designed to measure the scatter on any of the listed light ranges that usually cover around 200nm-2500nm, using different controls and calibrations.

The optical density (OD) value represents the amount of light that is absorbed by the cell culture at 600 nm. ( $OD_{600}$ ) is commonly used to determine the density of suspension of lives cells [7]. A linear relationship exists between the cells number (density of cells) and the absorption percentage (Abs %) for  $OD_{600}$ . It is understood from the fact that the real ( $OD_{600}$ ) readings refer to the light scattering by suspension of live bacteria cells, and thus linearly dependent on cell density. The concept of an OD device is based on the principle of light scattering. When measuring light-scattering, it is important to consider the wavelength of light used, so that the light absorption is minimal for most bacterial cultures. A wavelength of around 600 nm is a good choice. As a result, the measured translation in such samples is due to light-scattering [7].

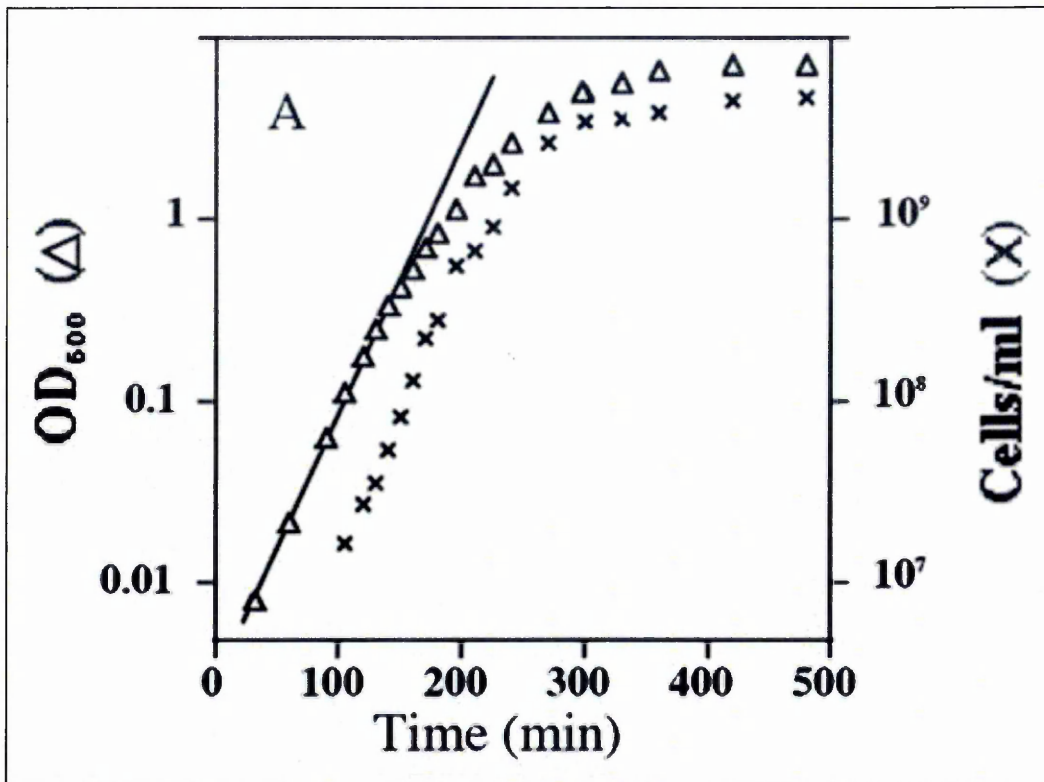


Figure 5.3. Monitoring *E. coli* growth using OD<sub>600</sub> (Δ) and actual cell concentration count (X) [9]

In order to present the outcome of OD<sub>600</sub> measurements in concentration units (cell/ml), the calibration has to be performed using an independent technique, such as optical microscopy [9] (See results in Figure 5.3). The feature Single Wavelength allows simple absorbance (Abs) or transmission (T %) measurements at a single wavelength, defined by the user [7]. The resulting window shows the amount of light passed through a sample relative to a reference. In this study, the optical density (OD<sub>600</sub>) was studied and plotted as a function of exposure to pollution levels.

The OD value represents the amount of light that is absorbed by the sample. However, that value is affected by the intensity of the light beam in the spectrometer and the spectrometer instrument design. This means that similar samples will give completely different OD values in different instruments, due to the different light sources, beam geometry, or even in the same spectrometer over time, as the beam intensity reduces the age of the light source. Therefore, to prevent the problem, the standard (reference) sample must be used in each practical experiment. Figure 5.4 gives an image of OD<sub>600</sub> spectrophotometer instrument used in this work (6715, JENWAY).



Figure 5.4. Image of OD<sub>600</sub> spectrophotometer instrument (6715, JENWAY)

Measuring optical density (OD<sub>600</sub>) using a spectrophotometer is often problematic, if the physics behind the method is not fully understood. For example, the relationship between biomass concentration and OD is more difficult to interpret because larger cells absorb and scatter more light. Furthermore, the relationship between OD and biomass concentration is not linear; it only approximates to linearity at low optical density (OD<sub>600</sub>).

### 5.3. Fluorescence Spectroscopy

In addition to fluorescence microscopy and spectrophotometry (OD<sub>600</sub>) described earlier in (5.1, 5.2) it will be useful to study the fluorescence spectra of bacteria cultures in pure form. The fluorescence spectroscopy technique enables researchers to study in detail electron transitions in molecules and molecular assemblies, including complex bio-molecular assemblies. Fluorescence spectroscopy (fluorometry or spectrofluorometry) is a type of electromagnetic spectroscopy that analyses fluorescence from a sample. It involves using a beam of light, usually ultraviolet light, that excites the electrons in molecules of certain compounds and causes them to emit light: typically, but not necessarily, this is visible light. The phenomenon of fluorescence is the result of a three-stage process that occurs in certain molecules, called fluorophores. Figure 5.5 illustrates the simple electronic-state diagram of the fluorescence process [10].

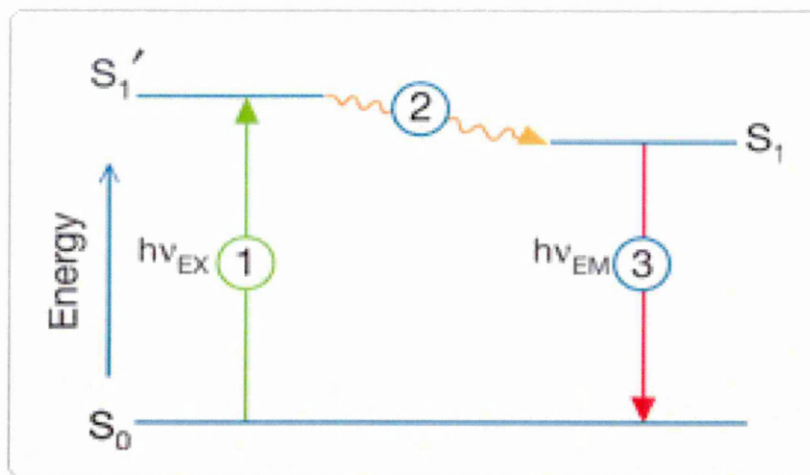


Figure 5.5. The scheme of electron transitions in fluorescence [10]

In the first stage, the photon of energy  $h\nu_{EX}$  (excitation energy) is supplied by an external source, such as an incandescent lamp or a laser, and absorbed by the fluorophore, creating an excited electron from ground state ( $S_0$ ) to singlet state ( $S_1'$ ). The second stage, i.e. the excited state, exists for a finite time (typically 1-10 nanoseconds). During this time, the fluorophore undergoes conformational changes and is subject to a multitude of possible interactions with its molecular environment [11]. These processes have two important consequences: (i) the energy of  $S_1'$  is partially dissipated, yielding a relaxed singlet excited state ( $S_1$ ) from which fluorescence emission originates; and (ii) not all the molecules initially excited by absorption (Stage 1) return to the ground state ( $S_0$ ). In the third stage, a photon of energy  $h\nu_{EM}$  (emission energy) is emitted, returning the fluorophore to its ground state ( $S_0$ ). Due to energy dissipation during the excited-state lifetime, the energy of this emission photon is lower than  $h\nu_{EX}$ , and has a longer wavelength than the excitation photon. The difference in energy or wavelength represented by  $(h\nu_{EX} - h\nu_{EM})$  is called the Stokes' shift. The emission intensity is proportional to the amplitude of the fluorescence excitation spectrum at the excitation wavelength, as clearly seen in Figure 5.6.

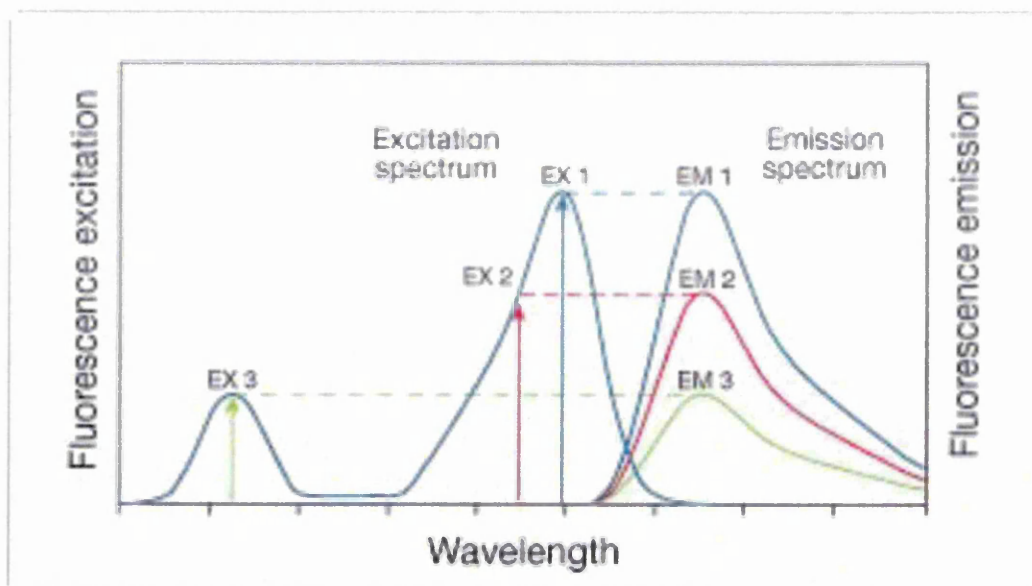


Figure 5.6. Excitation of electron at three different excitation wavelengths EX1, EX2, EX3: the fluorescence emission intensity EM1, EM2, EM3 [11]

In general, fluorescence spectra can be recorded in two possible ways: (i) emission spectra based on recording fluorescence spectra, emitted by a sample under monochromatic (fixed wavelength) excitation; and (ii) excitation spectra, when the intensity of the fluorescence at a fixed wavelength was recorded while varying the wavelength of the excitation light. An emission map can be measured by recording the emission spectra resulting from a range of excitation wavelengths and combining these together [10]. This is a semi-three-dimensional surface data set: emission intensity as a function of excitation and emission wavelengths, and is typically depicted as a contour map.

The spectrofluorometer is an instrument that takes advantage of fluorescent properties of some compounds in order to provide information regarding their concentration and chemical environment in a sample. A certain excitation wavelength is selected, and the emission is observed either at a single wavelength or a scan is performed to record the intensity versus wavelength, also called an emission spectra. Generally, spectrofluorometers use high intensity light sources to bombard a sample with as many photons as possible. This allows for the maximum number of molecules to be in an excited state at any one point in time. The light is either passed through a filter, selecting a fixed wavelength, or monochromatic, which allows the selection of a wavelength of interest to use as the exciting light. The emission is collected at 90 degrees to the exciting light.

The emission too is passed either through a filter or through a monochromator before being detected.

The instrumentation for fluorescence spectroscopy is well developed. In modern spectroscopic instruments, the “white light” decomposes into a spectrum using diffraction gratings. Typically, a spectroscopic fluorescence-metre, such as Cary Eclipse (Varian), is equipped with a single diffraction grating, which yields additional (parasitic) spectral lines corresponding to higher orders of diffraction. For example, during recording the emission spectra using the excitation of 300nm, a very intense line of 300nm is not included in the scanning range, but a sharp line at 600nm corresponding to a 2-nd order of diffraction always appears in the spectrum (3-rd and higher orders having much smaller intensities are usually not seen). Usually, such 2-nd order diffraction peaks are ignored in fluorescence spectroscopy and often filtered out from the spectra. However, in the case of opaque suspensions, these parasitic lines are enhanced by light scattering and therefore could be useful in the current study of bacteria cultures. Figure 5.7 shows the fluorescence spectroscopy instrument used in this work.

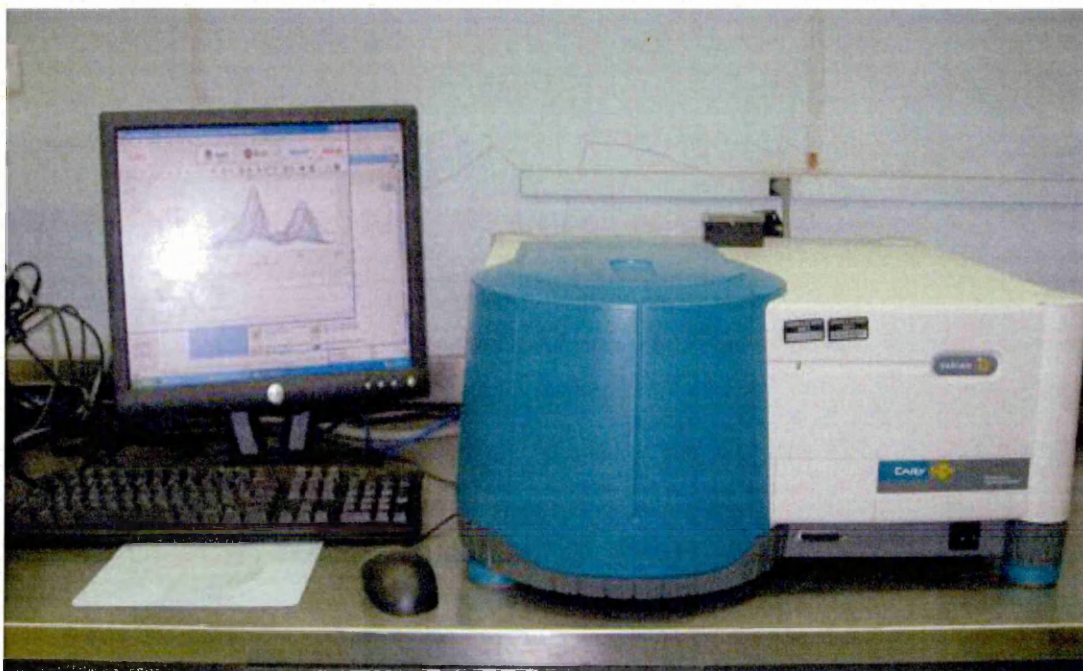


Figure 5.7. Image of fluorescence spectroscopy instrument (Varian Cary Eclipse)

## 5.4. UV-visible Absorption Spectrometer

Light (and therefore energy) is absorbed by a specific part of a molecule, called the chromophore. Different molecules absorb light at different wavelengths: Figure 5.8 shows the electromagnetic spectrum expanded in the region of UV, visible and infrared light.

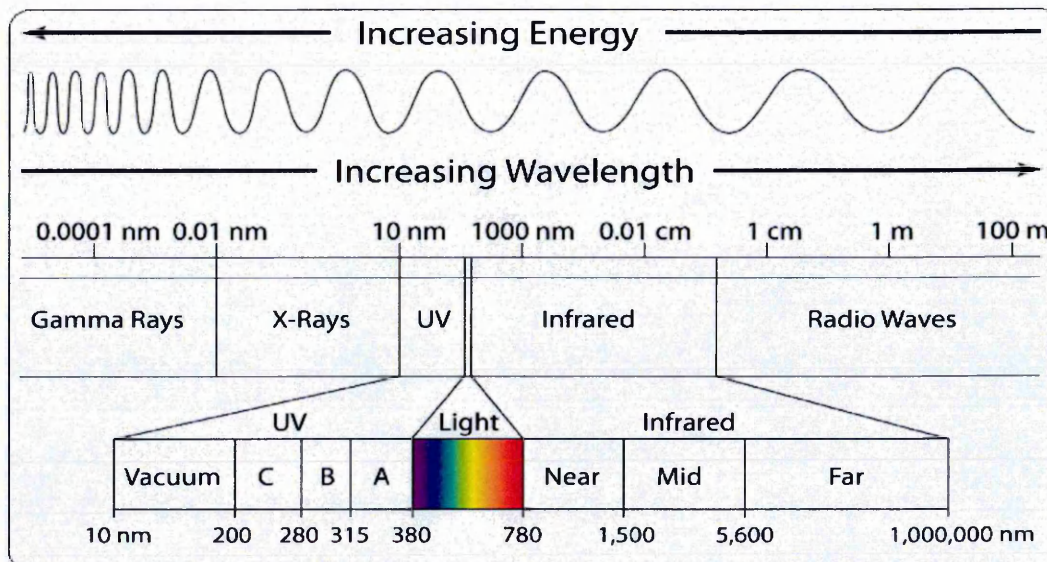


Figure 5.8. Electromagnetic spectrum (Wavelength Scale)

The molecules absorb differently because of differences in their structure. It is electronic arrangement of a molecule that is responsible for the absorption of light in the ultraviolet (UV) and visible parts of the electromagnetic spectrum. Absorption of light by electrons held in bonds can be viewed in terms of an energy diagram. Bonding between the carbon atoms in biological molecules is responsible for many of the light absorptions in the UV-visible region. The relationship between light absorption and concentration described by the Beer-Lambert law equation is as follows (5.3):

$$I = I_0 e^{-\alpha l}, \ln(I/I_0) = -\alpha l \quad (5.1)$$

$$A(\text{Abs.}) = \text{Log}_{10}(I_0/I) \quad (5.2)$$

where  $I$  is the light intensity after it passes through the sample,  $I_0$  is the initial light intensity,  $\alpha$  is the absorption coefficient.

In liquid samples, the light absorbance ( $A$ ) at a particular wavelength is proportional to the concentration of the molecule in solution ( $c$ ),  $l$  is the distance that the light has to pass through in the solution, and  $\epsilon$  is called the molar absorptivity or molar extinction coefficient.

$$A = \epsilon cl \quad (5.3)$$

The wavelength chosen for measurements is normally where the molecule of interest shows strong absorption characteristics as shown in Figure 5.9; in this way the sensitivity of measurements can be increased.

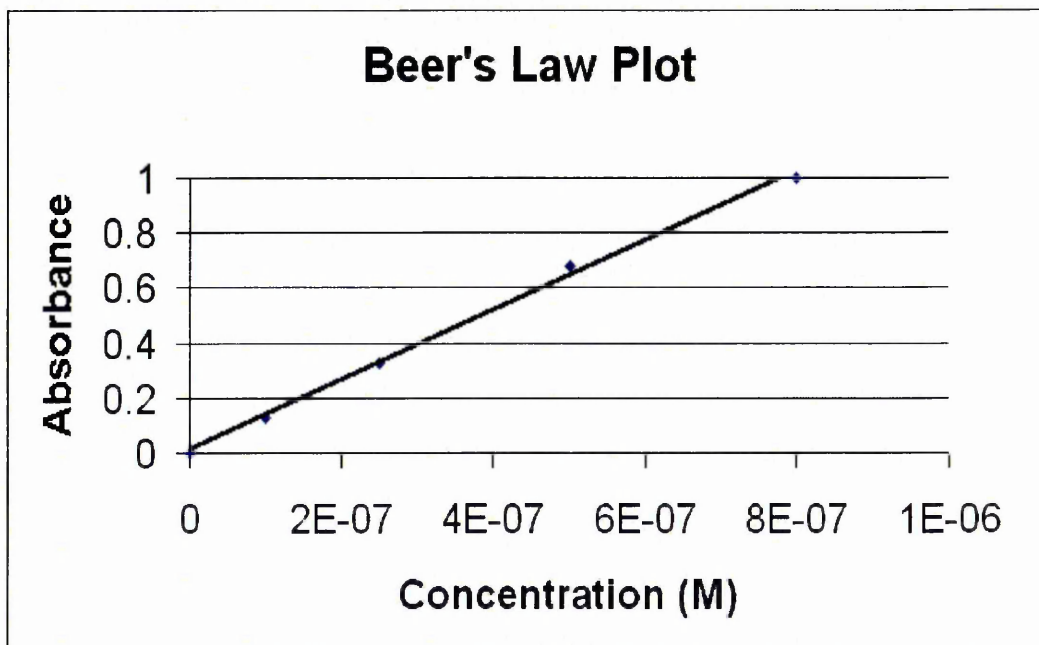


Figure 5.9. Relationship between light absorption and liquid concentration

The Beer-Lambert law is useful because many bio-molecules absorb in the UV-visible region and their concentration can be measured directly if the molar absorption is known. In addition, many molecules, such as proteins, do not absorb in the visible region [12]. The main idea of used UV-vis spectrophotometer is to selecting the best excitation wavelength during prevents the absorption and transparent wavelength region. The instrument used to measure light absorbance is called a spectrophotometer. A simplified diagram of a spectrophotometer is showing in Figure 5.10. The way the spectrophotometer works is simple: light from the light source, which are normally a tungsten lamp for visible light, and a deuterium lamp for UV light, falls onto a mirror.

The mirror can be rotated to reflect either UV or visible light on the instrument. Adjusting the angle of the mirror allows for the selection of the wavelength of light to be measured.

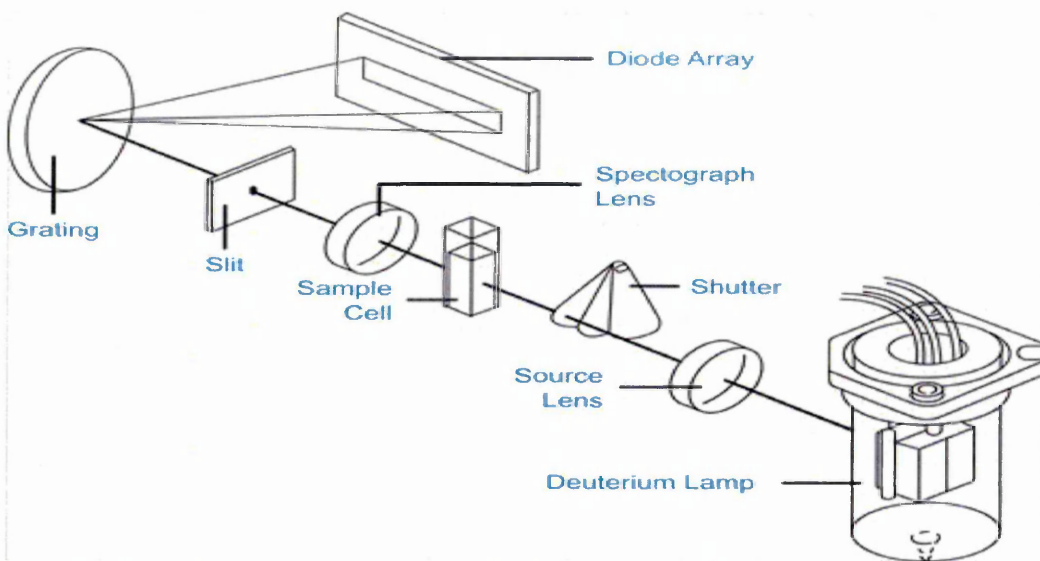


Figure 5.10. Schematic diagram of a UV-visible spectrophotometer

Modern instruments often use other light diffraction methods, such as holographic mirrors or diffraction gratings, to resolve light into its constituent wavelength. The light is then passing through the sample. Finally, the light falls onto a photo-detector, where its intensity is converted into an electrical signal. Photo-detector is interfaced to PC where the information recorded and processed further. Figure 5.11 the shows the spectrometer instrument used in this work.

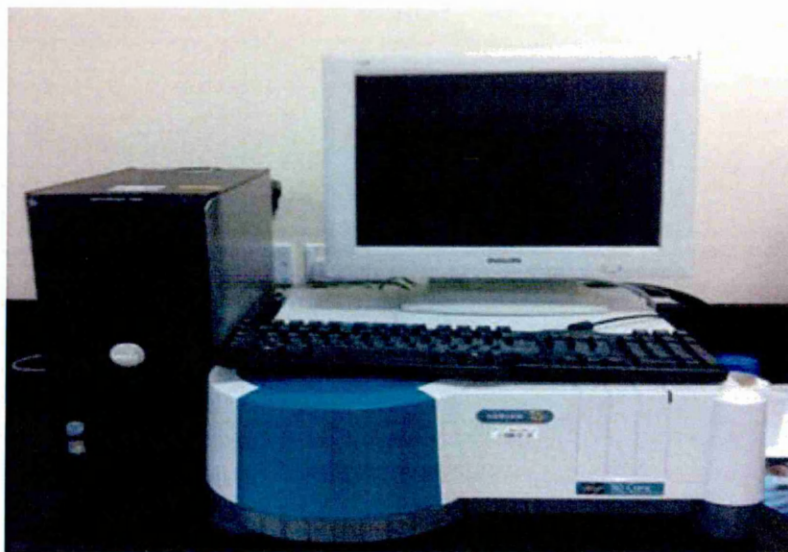


Figure 5.11. UV-visible spectrometer instrument Carry 50 (Varian)

## Reference:

1. Lemmer P. et al. (2008), SPDM: light microscopy with single-molecule resolution at the nanoscale, *Applied Physics, B* (93), pp. 1-12.
2. Spring K. R., Davidson M. W., (2008), *Introduction to Fluorescence Microscopy*, Nikon Microscopy-U, Retrieved.
3. Kaprelyants A. S, and Kell, D. B,(1992), Rapid assessment of bacterial viability and vitality by Rhodamine 123 and flow cytometry, *Journal of Applied Bacteriology*, Vol. (72), pp. 410-422,
4. Yu W, Dodds W. K, Banks M. K, Skalsky J, and Strauss E. A, (1991), Optimal Staining and Sample Storage Time for Direct Microscopic Enumeration of Total and Active Bacteria in Soil with Two Fluorescent Dyes, *Journal of Microbiology Methods*, Vol. (13), pp. 87-92.
5. Lecoeur H. (2002), Nuclear apoptosis detection by flow cytometry, influence of endogenous endonucleases, *Exp. Cell Res.* 277 (1), pp. 1-14.
6. Schwedt, Georg. (1997), *The Essential Guide to Analytical Chemistry*, (Brooks Haderlie, Trans), Chichester, NY: Wiley, pp. 16-17
7. Hsiu Li Lin, Chien Chung Lin, Yi Jen Lin, Hsiu Chen Lin, Chwen Ming Shih, Chi Rong Chen, Rong Nan Huang and Tai ChihKuo, (2010), Revisiting with a Relative-Density Calibration Approach the Determination of Growth Rates of Microorganisms by Use of Optical Density Data from Liquid Cultures, *Appl. Environ. Microbial*, vol. (76), no. 5, pp. 1683-1685.
8. Wang, C. H., and A. L. Koch. (1978), Constancy of growth on simple and complex media. *J. Bacteriol.* Vol. (136), pp. 969-975.
9. Guennadi Sezonov, Danièle Joseleau Petit, and Richard D' Ari, (2007), *Escherichia coli* Physiology in Luria-Bertani Broth, *J Bacteriol*, Issue 189, Vol. (23), pp. 8746-8749.
10. Joo, C., Balci, H., Ishitsuka, Y., Buranachai, C. and Ha, T., (2008), Advances in single-molecule fluorescence methods for molecular biology, *Annu Rev. Biochem*, Vol. (77), pp. 51-76.

11. Mathies, R. A., Peck, K. and Stryer, L., (1990), Optimization of high-sensitivity fluorescence detection, *Anal Chem.*, Vol. (62), pp. 1786-1791.
12. SuttonR, RockettB, SwindellsP, (2000), chemistry for the life sciences, *Lifelines*, by Tayloe& Francis, London, UK.

## CHAPTER 6

### Electrical Methodology

Many biological parameters and processes can be sensed and monitored using their electrical characteristics; this approach is not invasive and is relatively cheap. Cell growth, cell activity, changes in cell composition, numbers, shapes or cell locations are only some examples of processes that can be detected by microelectrode cell sensors. The electrical properties of a biological sample reflect actual physical properties of the cell membrane. Many biological parameters and metabolic activities can be studied and monitored using their electrical properties.

#### 6.1. Bio-Electrochemical Systems (BESs)

Electrical properties of bio-objects, such as cells and bacteria, were studied extensively in the past [1]. Recently, the subject of electrical characterisation of cells came back because of recent development in bio-cell sensors [2]. Electrochemical bio-cell sensor is a relatively young field, but is now achieving substantial successes in science, engineering, and technology. Some of the advantages of the electrochemical techniques, the measurements can be made quickly, which refer to the environment activities and can be easily transmitted, amplified and digitized; the measurements can be carried out in the laboratory, as a portable device (portable detector). Bio-electrochemical systems (BESs) take advantage of biological capacities (microbes, enzymes, plants) for the catalysis of electrochemical reactions [3]. Some examples of BES are: Microbial Fuel Cells, Plant-Microbial Fuel Cells, Enzymatic Fuel Cells, Microbial Electrolysis Cells, Microbial Electro-synthesis Cells and Microbial Desalination.

BESs have recently emerged as a promising technology for energy recovery and for providing valuable products, such as hydrogen, ethanol and other organic molecules. BES appears as a promising alternative for treating different types of wastewaters. BESs use whole cell biocatalysts to drive oxidation and reduction reactions at solid-state electrodes. Due to the separation between the two half-reactions, a whole range of processes is possible. The most widespread application is presently the microbial fuel cell, which aims to generate power or at least decrease the usage of power associated with wastewater treatment. In the slipstream of microbial fuel cells, microbial electrolysis cells have more recently emerged. The versatility of the latter has notably

expanded the range of applications of BESs. Key applications are wastewater treatment, sediment-based electrical power generation, value added product generation, bioremediation and detect the biomass (biological elements concentration). The electrical properties of biological material have been studied used suitable instrumentation. In addition, Impedance techniques have been used to study and monitoring the growth rate of organs in the life body, whole blood and erythrocytes, cultured cell suspensions [4], and bacterial growth [5]. The integration of impedance with biological recognition technology for detection of bacteria has led to the development of impedance biosensors that have come to be widely used in recent years. In addition, DC and AC properties of bacteria cell has been studied and monitored.

## **6.2. DC Elements**

The DC measurements are a very reliable technique for investigating the electrical properties of a liquid bacteria solution. If a DC potential applied across the electrodes, a current may flow under certain conditions. Thus, it is important to consider the addition of a resistive path in parallel with the capacitive in the electrical model of this surface. This resistor can be non-linear with the applied voltage. The flow of a current through this metal-electrolyte interface requires the net movement of a charge in response to an electric field (due to an applied voltage).

A **double layer** (DL, also called an electrical double layer, EDL) is a structure that appears on the surface of an electrode when it is exposed to a solution. The DL refers to two parallel layers, first layer, the surface charge (either positive or negative), comprises ions adsorbed onto the object due to chemical interactions. The second layer is composed of ions attracted to the surface charge via the Coulomb force, electrically monitoring the first layer. This second layer is insecurely connected with the item. It is made of free ions that move in the solution under the influence of electrical attraction and thermal motion rather than the organism being tightly anchored. It is thus called the "diffuse layer".

### **6.2.1. (I-V) Voltammetry**

Voltammetry is used in analytical chemistry and in a range of industrial processes [6,7]. Voltammetry experiments explore the half-cell reactivity of an analyte. Voltammetry is the study of current as a function of applied potential. These curves  $I = f(E)$  are called

voltammograms. The potential is swept through a bio-cell, then the form of the curves depends on the speed of potential variation and on the solution mass transfer. Experiments are mainly carried out by managing the potential (volts) of an electrode contact with the analyte even while measuring the current (amperes) [8].

At least two electrodes cells are needed to conduct such an experiment. The working electrode, which makes contact with the analyte, must relate the wanted potential in a controlled manner and enable the transport of charges to and from the analyte. A second electrode (counter electrode) acts as the other half of the cell. This second electrode must have a known potential which is used to estimate the potential of the working electrode. In addition, it must balance the charge added or removed by the working electrode. While this is a practical setup, it has a number of shortcomings. Most importantly, it is extremely tricky for an electrode to keep a stable potential while transitory current flows to counter redox action at the working electrode. To solve this difficulty, the role of supplying electrons and providing a reference potential are divided between two split electrodes. The reference electrode is a half-cell with a known decreased potential. Its only role is to take action as reference to measuring and controlling the working electrode's potential, and at no point does it pass any current. The supplementary electrode passes all the current required to balance the current observed at the working electrode. To reach this current, the auxiliary will often move backwards and forwards to extreme potentials at the borders of the solvent window, where it oxidizes or reduces the solvent or supporting electrolyte. These electrodes, the working, reference, and supplementary make up the recent three-electrode system.

In addition to thermodynamics method the data analysis requires a kinetic method, due to the sequential module of voltammetry. Idealized theoretical electrochemical thermodynamic correlations, such as the Nernst equation, are modelled without time dependence. These models are deficient to describe the active facets of voltammetry [9].

Cyclic voltammetry or CV is a kind of potentiodynamic electrochemical measurement. In a cyclic voltammetry test, the working electrode potential is ramped linearly against time similar to a linear sweep up voltammetry. Cyclic voltammetry takes the experiment a step further than linear sweep voltammetry that ends when it reaches a set potential. When cyclic voltammetry reaches active potential, the working electrode potential slope is upturned. This inversion can occur numerous times through a single experiment. The

current at the working electrode is plotted against the applied voltage to provide the cyclic voltammogram outline. Cyclic voltammetry is usually used to learn the electrochemical properties of an analyte in solution [8,9,10]. In cyclic voltammetry, the electrode potential changes linearly versus time. This ramping is known as the experiment's test rate (V/s). The voltage is applied between the electrodes and the current is measured between the working electrode and the counter-electrode. The data are most often plotted as current (I) against voltage (V). Cyclic voltammetry (CV) has become a significantly and broadly used electro analytical technique in many areas of chemistry. It is widely used to study a diversity of redox processes, to achieve stability of reaction products, the presence of in-betweens in oxidation-reduction reactions, reaction and electron transfer kinetics [8], and the reversibility of a reaction [11]. In addition, because concentration is proportional to current, the concentration of an unknown solution can be determined by generating a calibration curve of current versus concentration.

### **6.2.2. Electrochemical Cell Sensors**

Changes in the biological parameters, including the cells numbers, can be studied and monitored in the electrical properties of the bio-cells, i.e. with a bio-cell sensor. A typical bio-cell sensor consists of an anode and cathode, separated with an electrolyte solution, where the cathode electrode is coated with a cell-culture [12]. The current that easily passed through the aqueous electrolyte solutions can be affected by less conductive bacteria which contain the lipid bilayer of the bacteria cells' membrane acting as an insulator. These measurements can be performed on two or three electrode systems, with working electrodes coated with cell cultures. The applied external electrical field catalyses the live bacteria (that had a lipid layer) accumulating on the working electrode, creating an isolation layer coating the electrode, the conductivity decreasing as a result of this effect. Different artefacts, such as some chemical pollutants and radiation, may affect the functioning of cells (increasing or reducing the number of live bacteria) that appear as conductivity decreases or increases [13]. Therefore, comparing the results of electrochemical tests performed on a fresh cell culture and after exposure to the artefact can provide information on the concentration of pollutants or radiation dose. In the current project, this idea was explored using bacteria.

The three electrodes electrochemical set up is more stable than the two electrodes. Firstly, it contains an additional reference electrode having a stable electrochemical potential invariant of applied voltage and chemical composition of the solution; the potentials of other two electrodes are measured in respect to a reference electrode [14]. A typical three-electrode set-up for electrochemical measurements is showed in Figure 6.1.

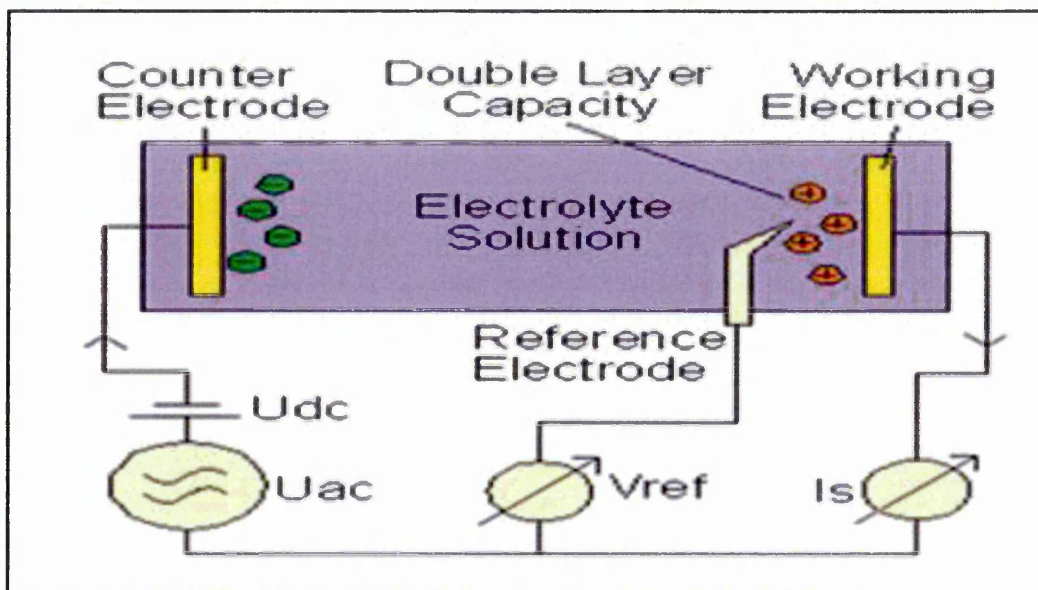


Figure 6.1. Three-electrode electrochemical cell set-up for impedance measurements [14]

Two parallel plate electrodes are indicated as Working and Counter electrodes, the third reference electrode was placed close to the working electrode. The electrical potentials of both working and counter electrodes are measured in respect to a reference electrode having a constant potential in electrolytes solutions. Typically Ag/AgCl reference electrodes are used in such measurements. Working and counter electrodes are typically made of metal. The working electrode is coated with the investigated substance, in this project cell-culture. Gold-coated glass slides seem to be the most common for working electrodes, since the chemistry of modification of gold is well established for coating gold with different biomaterials. Counter electrodes should be chemically inert; platinum is commonly used for this purpose. However, even chemically inert metals, such as Au and Pt, show instability of surface potential during electrochemical reactions, when a current flowing between electrodes is accompanied with chemical ion exchange electrode reactions. In this case, the role of reference electrodes is crucial for

performing accurate electrochemical measurements that are typically carried out using potentials stat. In some cases, however, when electrochemical reactions are not essential, simple measurements can be performed in a two-electrode system (without using reference electrode and potentiostat). These simple electrical (electrochemical) measurements are used in order to establish the correlation between electrical properties (conductivity, capacitance, current or resistance) of liquid bacteria samples and live bacteria counts, after that studying the effect of  $\gamma$ -radiation and heavy metal ions on bacteria. Electrochemical measurements were successfully used for studying electrical properties of cells deposited on metal electrodes and showed great prospects in using such cell-based sensors for detection of various analytic [15,16]. In the current study, the principles of cell-sensors were extended further to more complex objects, such as bacteria *E. coli*, and another type of bacteria, *D. radiodurans*, known by its high resistance to  $\gamma$ -radiation [17].

### **6.2.3. DC Electrometer (KEITHLEY)**

Keithley-digital Electrometer was used in this project in order to study DC electrical properties; this equipment offers accuracy and sensitivity specifications unmatched by any other meter of this type. It also offers a variety of features that simplify measuring high resistances and the resistivity of insulating materials. With reading rate of up to 425 readings/second, it is also significantly faster than competitive electrometers, so it offers a quick, easy way to measure low-level currents. The Keithley-digital Electrometer is an updated version, replacing the earlier digit electrometer, which was introduced in 1996. Software applications created for the digital electrometer using SCPI commands can run without modifications on the electrometer. However, the digital electrometer does offer some useful enhancements to the earlier design. Its internal battery-backed memory buffer can now store up to 50,000 readings, allowing users to log test results for longer periods and to store more data associated with those readings. The new model also provides faster reading rates to the internal buffer (up to 425 readings / second) and to external memory via the IEEE bus (up to 400 readings/second). Several connector modifications have been incorporated to address modern connectivity and safety requirements.

#### 6.2.4. Resistance Meter

Model 6517A uses the Force Voltage Measure Current (FVMI) configuration to measure resistance. From the known voltage and measured current, the resistance is calculated ( $R = V/I$ ) and displayed [18]. The resistance to be measured is connected to the central conductor of the INPUT triad connector and the V SOURCE OUT HI binding post. The Model 6517A can make resistance measurements up to  $10^{17}\Omega$  using the force voltage measure current (FVMI) technique. From this information, the Model 6517A calculates and displays the resultant resistance ( $R = V/I$ ). The Model 6517A can set the V-Source level automatically or the user can manually set it.

The V-Source can also be used with the Electrometer to form the Force Voltage Measure Current (FVMI) configuration. This configuration is used for resistance measurements and current measurements. For these measurements, V-Source LO and ammeter input LO can be connected internally via the METER-CONNECT option of the CONFIGURE VSOURCE menu.



Figure 6.2. High resistance meter model 6517a (electrometer high resistance) "Keithley"

### 6.3. AC Electrical Measurements

#### 6.3.1. Electrical Conductivity

Chemical composition of solutions can be studied by measuring AC conductivity which is the ratio of the current density to the electric field strength. The conductivity of an

electrolyte solution is a measure of its ability to conduct electricity [19]. An electrolyte solution was measured by determining the resistance of the solution between two flat or cylindrical electrodes separated by a fixed distance. An alternating voltage was chosen carefully to avoid electrolysis reaction. Typical frequencies used are in the range 1–3 kHz. The dependence on the frequency is usually small, but may become considerable at very high frequencies. Regarding non-conductivity, the bacteria membrane practically is a lipid bilayer (isolation material). Existing evidence indicates that the conductivities are highly dependent on the presence of the bacterial cell wall [20]. This is supported by two recent studies. The first has shown that the resistance of the bacterial membrane is too great to account for the high conductivities at low frequencies [21]. The second has shown that the conductivity of isolated bacterial cell walls is nearly high enough to explain the conductivities observed for intact cells [22].

Once studied, it was demonstrated with protoplasts of *Micrococcus Lysodeikticus* that the radio frequency dispersion of this organism arises from the presence of the cytoplasmic membrane rather than the cell wall. In the study, protoplasts were used to further confirm the importance of the bacterial cell wall in the low frequency, dielectric properties of bacteria [23]. It was shown here that the conductivity of the bacterial cell is very low if its cell wall is removed. Furthermore, removal of the cell wall from *M. Lysodeikticus* reduces its low frequency, effective, homogeneous dielectric constant by more than two orders of its magnitude. In this way, the use of protoplasts shows that the intact cell wall is responsible, not only for less conductivity, but also for the high dielectric constants of bacteria at low frequencies. Therefore, this study illustrates that the bacterial cell wall is responsible for the high dielectric constant and conductivity observed for *Micrococcus Lysodeikticus* at low frequencies. The effective, homogeneous conductivity of the protoplast is at least an order of magnitude lower than that of the intact cell.

### **6.3.2. Electrical Capacitance**

A common form of energy storage device is a parallel-plate capacitor. The capacitance is proportional to the area of overlap and inversely proportional to the separation between conducting, it's being proportional to the dielectric constant, is also related directly to the frequency behaviour. Electrolytic capacitors are used an aluminium or tantalum plates with an oxide dielectric layer. The second electrode is a liquid

electrolyte, connected to the circuit by another foil plate. Electrolytic capacitors offer very high capacitance but suffer from poor tolerances, high instability, gradual loss of capacitance especially when subjected to heat, and high leakage current. In this, project the bacteria working as insulator material in electrolyte solution, because the cell membrane is a phospholipid protein bilayer, which is a very good insulator which has a dielectric constant. The membrane separates the intracellular and extracellular fluids, which are conductors. The free charges in these conductors are ions. The interior of a cell is an equipotential volume and its potential is approximately (60 to 90 mV) below that of the extracellular fluids for human cells. Very high dielectric constants have been observed for bacteria at low frequencies. In addition, it has high dielectric constant [24].

### 6.3.3. Electrical Impedance

Impedance Spectroscopy is also called AC Impedance. The usefulness of impedance spectroscopy lies in the ability to distinguish the dielectric and electrical properties of individual contributions of components under investigation [25]. Impedance spectroscopy is a non-destructive technique and so can provide time dependent information about the electrical properties, also about ongoing processes such as bacteria density determination or distinguish between the live and dead bacteria etc. There are many advantages of electrical impedance techniques are: Useful on high resistance materials such as paints and coatings, Time dependent data is available, Non-destructive, Quantitative data available and Use service environments.

The reciprocal of impedance is admittance (i.e., admittance is the current-to-voltage ratio). Impedance is represented as a complex quantity  $Z$  and the term 'complex impedance' and real part is the resistance  $R$ , and the imaginary part is the reactance  $X$ . The reactance and impedance of a capacitor are respectively

$$X_c = -\frac{1}{\omega C} = -\frac{1}{2\pi f C} \quad (6.1)$$

$$Z_c = \frac{1}{j\omega C} = -\frac{j}{\omega C} = \frac{j}{2\pi f C} \quad (6.2)$$

where  $\omega$  is the angular frequency of the sinusoidal signal and  $j$  phase indicates.

Impedance decreases with increasing capacitance and increasing frequency. This implies that a higher-frequency signal or a larger capacitor results in lower voltage

amplitude per current amplitude and an AC "short circuit" or AC coupling. Conversely, for very low frequencies, the reactance will be high, so that a capacitor is nearly an open circuit; however, in AC analysis those frequencies have been "filtered out".

### 6.3.4. AC Electrometer

**4284A LCR Meter, 20 Hz to 1 MHz:** The 4284A LCR meter is a cost-effective technique for component and material electrical measurement. The wide 20 Hz to 1 MHz test frequency range and superior test-signal recital allows the 4284A to test components to the most commonly used test standards, such as IEC/MIL standards, and under conditions that simulate the intended application. Whether in research and development, the 4284A will meet all LCR meter test and measurement requirements. The HP 4284A is a general-purpose LCR meter for incoming inspection of components, quality control, and laboratory use. The HP 4284A is used for evaluating LCR components, materials, and semiconductor devices over a wide range of frequencies (20 Hz to 1 MHz) and test signal levels (5 mV to 2 V<sub>rms</sub>, 50 uA to 20 mA<sub>rms</sub>). With Option 001 the HP 4284A's tested signal level range spans 5 mV to 20 V<sub>rms</sub>, and 50 uA to 100 mA<sub>rms</sub>. The HP 4284A of measurements C-D measurements has a basic accuracy of  $\pm 0.05\%$  (C),  $\pm 0.0005$  (D) at all test frequencies with six digit resolution (the dissipation factor resolution is 0.000001) on every range [26].

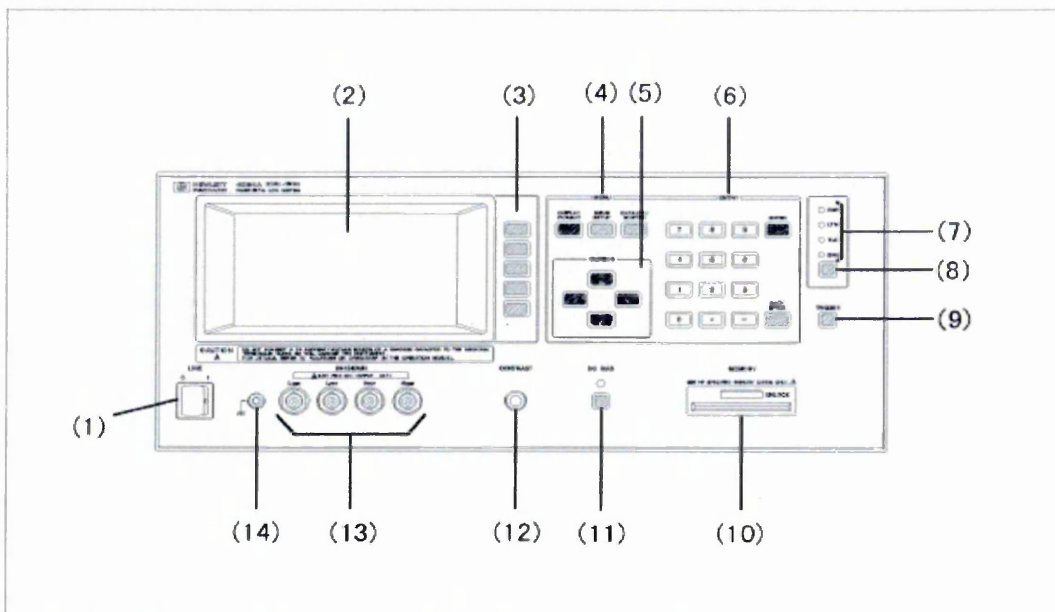


Figure 6.3. Brief description of each key on the HP 4284A's front panel

(1) LINE On/Off, (2) LCD, (3) SOFTKEYs, (4) MENU Keys, (5) CURSOR Keys, (6) ENTRY Keys, (7) HP-IB Status Indicators, (8) LCL Key, (9) TRIGGER Key, (10) MEMORY Card Slot and UNLOCK Button, (11) DC BIAS Key, (12) CONTRAST Control Knob, (13) UNKNOWN Terminals, (14) FRAME Terminal.

The 4284A has eight measurement ranges:  $10\Omega$ ,  $100\Omega$ ,  $300\Omega$ ,  $1k\Omega$ ,  $3k\Omega$ ,  $10k\Omega$ ,  $30k\Omega$ , and  $100k\Omega$ . When Option 001 is installed, the 4284A has nine measurement ranges:  $1\Omega$ ,  $10\Omega$ ,  $100\Omega$ ,  $300\Omega$ ,  $1k\Omega$ ,  $3k\Omega$ ,  $10k\Omega$ ,  $30k\Omega$ , and  $100k\Omega$ . The measurement range is selected according to the DUT's impedance, even if measurement parameter is capacitance or inductance. The measurement range is limited by the test frequency setting when the oscillator level is  $\leq 2V$ . When the measurement range and the test frequency are set under the above conditions, the test frequency must be set first, and then the measurement range. If you set the measurement range first and then the frequency, the resulting measurement range may not be the one you wanted to set. The 4284A can measure a device using a constant voltage or current level by using the automatic level control function.

The simple electrochemical sensor (bio-cell sensor) for detection of gamma radiation and heavy metals using bacteria was developed in this part of the study. The cell sensor design is shown in Figure 6.4. The cell body is built from PTFE (very cheap material), cells containing a gold plate (made from glass slides, a coated Chromium 0.4nm first layer and gold 40nm second layer) as a counter electrode (1), is sealed against the Platinum wire electrode (2) as a working electrode. The inlet (3) and outlet (4) tubes allow the injection of liquid samples into the cell.

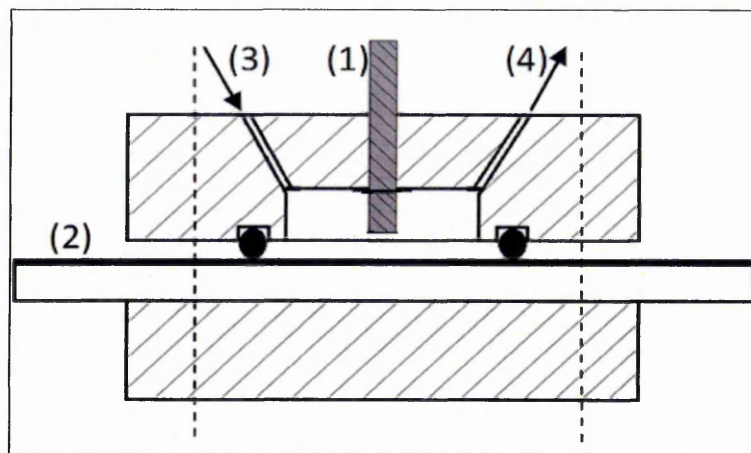


Figure 6.4. Two electrode cell design for DC/AC electrical measurements

A series of DC and AC electrical measurements were carried out on samples of two types of bacteria, namely (*E. coli* and *D. radiodurans*). The electrical characteristics of bacteria were explored using own cell sensors in order to study the effect of gamma radiation on bacteria samples (*E. coli* & *D. radiodurans*). For different radiation doses, the samples were exposed for different exposure times. In that time the effect of heavy metals ions on *E. coli* and *D. radiodurans* bacteria were studied by exposing these samples to different concentrations for different exposure times.

DC electrical measurements of liquid samples containing different concentrations of *E. coli* and *D. Radiodurans* bacteria, as a function of Gamma radiation and heavy metals ( $\text{CdCl}_2$  &  $\text{NiCl}_2$ ) concentration, as well as a clear broth (reference), were carried out at SHU using the two electrode cell and 6517A Keithley electrometer. In order to avoid electrochemical reaction (in oxidation and reduction region) the dc current-voltage characteristics recorded in a two-electrode cell and the correlation between the values of current at  $\pm 0.5\text{V}$  and bacteria concentration were studied. In addition, the DC I-V characteristics of *E. coli* and *D. radiodurans* samples of different concentrations (density measured in Abs units) were researched. AC electrical measurements were performed using (hp-4284A PRECISION LCR METER) in the frequency range from 20 Hz to 1 MHz, with the amplitude of AC voltage of 500mV, and no DC bias applied. The spectra of two parameters  $G_p$  and  $C_p$  corresponding to a parallel connection of conductance and capacitance were recorded. Typical spectra of AC conductance ( $G_p$ ) and capacitance ( $C_p$ ) for *E. coli* and *D. radiodurans* bacteria samples are showed and explored. The electrical characteristics for both bacteria samples (*E. coli* and *D. radiodurans*) were studied after being exposed to gamma radiation and heavy metals for a different time and in different concentrations. The effect of  $\gamma$ -radiation,  $\text{CdCl}_2$  and  $\text{NiCl}_2$  salt on  $G_p$  values at 900 kHz (high frequency) was selected and depended. The use of two types of bacteria may lead to pattern recognition of inhibition factors, in this case  $\gamma$ -radiation and ( $\text{Cd}^{2+}$ ,  $\text{Ni}^{2+}$ ) ions [27].

As mentioned above both DC and AC electrical measurements of liquid samples containing different concentration of *E. coli* and *D. radiodurans* bacteria, as well as clear broth (reference), were carried out at SHU using the two-electrode cell shown in Figure 6.4, and the 6517A Keithley electrometer. Also a series of electrical tests of the same *E. coli* samples were performed at IFS USP, Brazil: cyclic voltammograms (CV) using DropSens ( $\mu\text{STAT 200}$ ) potentiostat and three-electrode printed assemblies, comprising

gold working and counter electrodes and Ag/AgCl reference electrode. The effect of heavy metal ions on *E. coli* bacteria was studied by exposing the samples of *E. coli* overnight to NiCl<sub>2</sub> of different concentrations: 1mM, 10mM, and 0.5mM.

The three electrodes electrochemical set up is more stable than the two electrodes. Firstly, it contains an additional reference electrode having a stable electrochemical potential invariant of applied voltage and chemical composition of solution, the results of which will be explained in the next chapters.

#### 6.4. Equivalent Circuit

The main components describing the electrical performance of liquid bacteria samples are: the double layer capacitance  $C_s$  and resistance  $R_s$  connected in parallel and associated with bacteria adsorbed on the surface of metal electrodes and a series resistance, represented by spreading resistance  $R_b$  in the equivalent circuit. These three parameters depend on the cell geometry and the content of a liquid medium. The actual impedance of the system are shown in figure 6.5.

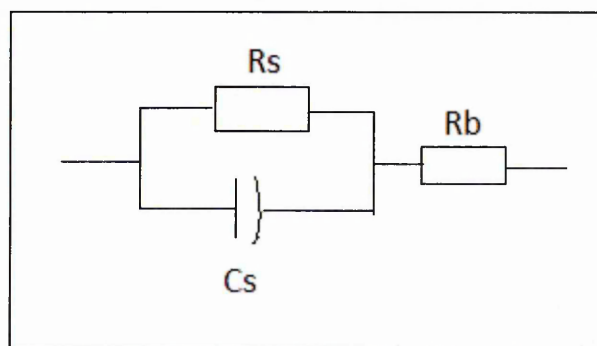


Figure 6.5. The equivalent circuit used for analysis of AC data

$$Z = Z' - jZ'' \quad (6.3)$$

$$Z' = \frac{R_s}{1 + \omega^2 R_s^2 C_s^2} + R_b, Z'' = \frac{\omega R_s^2 C_s}{1 + \omega^2 R_s^2 C_s^2}$$

Here  $R_s$  is the surface resistance,  $C_s$  is the surface capacitance, and  $R_b$  is the bulk resistance. Impedance measured:

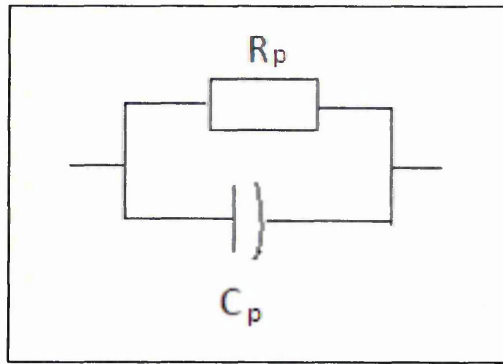


Figure 6.6. The measured circuit for AC measurements

From equation, 6.1 and the circuit in figure 6.6, the impedance can in terms of parallel resistance and parallel capacitance:

$$Z' = \frac{R_p}{1 + \omega^2 R_p^2 C_p^2}, Z'' = \frac{\omega R_p^2 C_p}{1 + \omega^2 R_p^2 C_p^2}$$

The above two cases present the same impedance so:

$$\frac{R_s}{1 + \omega^2 R_s^2 C_s^2} + R_b = \frac{R_p}{1 + \omega^2 R_p^2 C_p^2}$$

and

$$\frac{R_s^2 C_s}{1 + \omega^2 R_s^2 C_s^2} = \frac{R_p^2 C_p}{1 + \omega^2 R_p^2 C_p^2}$$

The conductive function of resistance for the above circuits takes the following forms:

$$G_s = \frac{1}{R_s}, G_b = \frac{1}{R_b}, G_p = \frac{1}{R_p}$$

Lets consider the above two cases

$$\omega = 0$$

$$R_s + R_b = R_p,$$

or

$$G_p = \frac{1}{R_s + R_b} \approx \frac{1}{R_s} \text{ because } R_b \ll R_s$$

$$R_s^2 C_s = R_p^2 C_p, C_p = C_s \frac{R_s^2}{R_p^2} = C_s \frac{R_s^2}{(R_s + R_b)^2} = C_s \frac{1}{\left(1 + \frac{R_b}{R_s}\right)^2}$$

$$C_p \approx C_s, \text{ If } R_b \ll R_s$$

Also at  $w = \infty$

$$\frac{R_s + R_b + \omega^2 R_b R_s^2 C_s^2}{1 + \omega^2 R_s^2 C_s^2} = \frac{R_p}{1 + \omega^2 R_p^2 C_p^2}$$

$$\frac{\omega^2 R_b R_s^2 C_s^2}{\omega^2 R_s^2 C_s^2} = \frac{R_p}{\omega^2 R_p^2 C_p^2}$$

$$R_b = \frac{1}{\omega^2 R_p C_p^2}$$

$$R_p = \frac{1}{\omega^2 R_b C_p^2}$$

So at  $w = \infty$  the  $R_p = 0$  or  $G_p = \infty$

$$\frac{C_s R_s^2}{\omega^2 R_s^2 C_s^2} = \frac{R_p^2 C_p}{\omega^2 R_p^2 C_p^2}$$

$$\frac{1}{C_s} = \frac{1}{C_p}, C_s = C_p$$

Overall, at;  $w = 0$

$$G_p = \frac{1}{R_s + R_b} \approx \frac{1}{R_s} \quad (6.4)$$

$$C_p = C_s \frac{1}{\left(1 + \frac{R_b}{R_s}\right)^2} \approx C_s \quad (6.5)$$

at  $w = \infty$

$$G_p = \infty \quad (6.6)$$

$$C_p = C_s \quad (6.7)$$

In this way, the parameters of the equivalent circuit can be evaluated from experimentally recorded spectra of parallel conductance  $G_p$  and capacitance  $C_p$ . The expected values (theoretical values) of conductance and capacitance for equivalent circuits matched to some extent the experimental values (see the experimental results in the next chapters).

#### References:

1. Carstensen E. L, Cox H.A, Mercer W. B, Natale L. A, (1995), Passive Electrical Properties of Microorganisms, *Biophysical Journal*, Vol. 5, Issue 3, pp. 289-300.
2. Kim R. Rogers, (1995), Biosensors for environmental applications, *Biosensors and Bioelectronics*, Vol. 10, Issues 6-7, pp. 533-541.
3. Hodgkin A. L, Huxley A. F, (1952), A quantitative description of membrane current and its application to conduction and excitation in nerve, *J. Physiol.* Vol. I 17, pp. 500-544.
4. Prodan C, Mayo A. F, Claycomb J. R, and Miller J. H, (2004), Low-frequency, low-field dielectric spectroscopy of living cell suspensions, *Journal of Applied Physics*, , Vol. 95, No 7.
5. Lawrence, L. Hause, Richard A. Komorowski, Francis Gayon, (1891), Electrode and Electrolyte Impedance in the Detection of Bacterial Growth, *IEEE Transaction on Biomedical Engineering*, Vol. BME-28, No. 5.
6. Kissinger, Peter; William R. Heineman. (1996), *Laboratory techniques in electroanalytical chemistry*, Second Edition, Revised and Expanded (2 ed.).
7. Zoski, Cynthia G. (2007), *Handbook of Electrochemistry*. Elsevier Science.
8. Bard, Allen J.; Larry R. Faulkner. (2000), *Electrochemical methods: Fundamentals and applications*, (2 ed.), Wiley.
9. Nicholson, R. S.; Irving. Shain, (1964), Theory of stationary electrode polarography. single Scan and cyclic methods applied to reversible, irreversible, and kinetic systems." *Analytical Chemistry*, 36 (4): pp. 706-723.

10. Heinze, Jurgen (1984). "Cyclic voltammetry" electrochemical spectroscopy", new analytical methods (25)". *Angew and Chemie International Edition in English* 23 (11): pp. 831-847.
11. Du Vall, Stacy DuVall; McCreery, Richard, (1999), Control of catechol and hydroquinone electron-transfer kinetics on native and modified glassy carbon electrodes", *Anal. Chem.* 71: pp. 4594-4602.
12. Allen, R.M.; Bennetto, H.P. (1993), Microbial fuel cells: Electricity production from carbohydrates". *Applied biochemistry and biotechnology*, Vol. 39, pp. 27-40.
13. Kim, B.H., Kim, H.J., Hyun, M.S., Park, D.H., (1999a), Direct electrode reaction of (Fe) reducing bacterium, *Shewanella Putrefaciens*, *J Microbiol. Biotechnol.* Vol. 9, pp. 127-131.
14. Aswin K. Manohar a, Orianna Bretschger a, Kenneth H. Neelson b, Florian Mansfeld, (2008), The use of electrochemical impedance spectroscopy (EIS) in the evaluation of the electrochemical properties of a microbial fuel cell, *Bioelectrochemistry*, Vol. 72, pp. 149-154.
15. Md. Abdul Kafi, Tae-Hyung Kim and Jeong-Woo Choi (2011), *SENSORDEVICES*, The international conference on sensor device technologies and application, pp. 147-150
16. Yufera A., Canete D., Daza P., (2011), Modeling microelectrode sensors for cell-culture monitoring, *Technologies and Application*, pp. 143-146.
17. Daly M J, Gaidamakova E. (2011), *SENSORDEVICES: The International Conference on Sensor Device*, *Science (AAAS)* 306. 5698: 1025-1028.
18. Model 6517A Electrometer User's Manual, (1996), Keithley Instruments, Inc. Cleveland, Ohio, U.S.A.
19. Marija Bešter-Rogač and Dušan Habe, (2006), Modern advances in electrical conductivity measurements of solutions", *Acta Chim.Slov.* Vol. 53, pp. 391-395.
20. Carstensen E. L, Cox H. A, Mercer W. B, and Natale L. A, (1965), Dielectric properties of protoplasm (Plasma Membrane), *Biophysical J.*, Vol. 5, pp. 289-295.

21. Denise T. B. De Salvi, Hernane S. Barud, Agnieszka Pawlicka, Ritamara I. Mattos, Ellen Raphael, Younés Messaddeq, Sidney J. L. Ribeiro, (2014), Bacterial cellulose/triethanolamine based ion-conducting membranes, *Cellulose* (Springer), Vol. 21, Issue 3, pp 1975-1985.
22. Carstensen E. L, and Marquis R. E, (1968), Dielectric Properties of Protoplasm (Plasma Membrane), *Biophysical J.*, 8, 536-542.
23. PAULY H. (1962), Electrical properties of the cytoplasmic membrane and the cytoplasm of bacteria and *Trans Biomed Electron. ;BME*. Vol. 9, pp. 93-95.
24. Charles W. Einolf Jr., Edwin L. Carstensen, (1973), Passive electrical properties of microorganisms: V. Low-Frequency dielectric dispersion of bacteria, *Biophysical Journal*, Vol. 13, pp. 8-13.
25. Alexander, Charles; Sadiku, Matthew (2006). *Fundamentals of electric circuits, revised (3ed.)*, McGraw-Hill. pp. 387-389.
26. Manual Identification (4284A) LCR Meter, Model Number: 4284A, (2000), Agilent Technologies, Date Printed: January Part Number: 04284-90040.
27. Al-Shanawa M, Nabok A, Hashim, Smith A. T, Forder S, (2013), Detection of  $\gamma$ -radiation and heavy metals using electrochemical bacterial-based sensor, IOP Publishing, *Journal of Physics: Conference Series* 450.

## CHAPTER 7

### Optical Study of the Effect of Gamma Radiation on Bacteria

#### 7.1. Sample Preparation

The paragraphs below covers in more detail the procedures of bacteria growth, exposure to Gamma-radiation and heavy metals ( $\text{CdCl}_2$  &  $\text{NiCl}_2$ ), then testing bacteria samples.

Two types of bacteria were selected in this study: (i) a non-pathogenic DH5 $\alpha$  strain of Escherichia coli (E. coli) and (ii) Anderson R1 strain of Deinococcus Radiodurans (D. radiodurans). LB (Luria-Bertani) broth and a Nutrient (OXOID CM3) broth were used, respectively, as a media for E. coli and D. radiodurans cell culture. The above bacteria strains and growing media were purchased from Sigma-Aldrich and OXOID LTD, respectively.

##### 7.1.1. E. coli Bacteria Growth

LB (Luria-Bertani) broth is the most commonly used medium in molecular biology for E.coli cell culture [1]. The advantages of using LB broth for growing E. coli are the fast growth rates of most strains, as well as its availability and simple composition. LB broth contains the enzymatic digestion product of casein, commonly known as peptone (some vendors term it as Tryptone, as with the sample that used), yeast extract, and sodium chloride. Peptone is rich in amino acids and peptides. In addition to these, yeast extract also contains nucleic acids, lipids, and other nutrients needed for bacterial growth. The following concentrations of materials were used to prepare the liquid broth medium:

1. Tryptone 5g/L
2. Yeast extracts 2.5g/L
3.  $\text{NaCl}$  5g/L

For solid broth medium, which is used to cultivate bacteria in Petri dishes, the Agar powder (15g/L) was added to the liquid broth medium.

Cultivation of E. coli was performed in several stages: (Stage 1) the cultivation of DH5 $\alpha$  strain of E. coli bacteria in a Petri dish containing solid broth agar in order to use it as a bacteria source in future; (Stage 2) when one colony of E. coli bacteria was added into a sterile flask containing 50ml of liquid broth; and finally (Stage 3), when the flask containing the bacterial culture was placed inside a shaking incubator operating at 150 rpm shaking speed and 37 C $^\circ$  incubation temperature. The bacteria start growing after 16 hours, and the growth reaches saturation after 20-22 hours.

### 7.1.2. D. radiodurans Bacteria Growth

Nutrient (OXOID CM3) broth media are basic culture media used for growing and maintaining D. radiodurans bacteria [2]. The liquid broth medium is prepared in order to cultivate D. radiodurans bacteria; the following concentrations of materials were used in the following units (gram/Liter):

1. Meat extracts 1g/L
2. Yeast extracts 2g/L
3. Peptone 5g/L
4. Sodium Chloride 5g/L

PH 7.4  $\pm$ 0.2 at 25°C

A similar sequence was used for cultivation of D. radiodurans: (Stage 1) the Anderson R1 strain of D. radiodurans was incubated in a Petri dish containing solid Nutrient Agar (OXOID CM3) for 24 hours 30 C°; (Stage 2) one colony was selected and added to a sterile flask containing 50 ml of liquid Nutrient broth; (Stage 3), the flask was placed inside a shaking incubator operating in 30°C for 24 hours, at a speed of 160 rpm, in order to achieve a maximal concentration of bacteria. The density of cultivated bacteria was measured with an optical density photometer (OD<sub>600</sub>) spectrophotometer. The method of detecting optical density of cell culture at 600 nm (OD<sub>600</sub>) is commonly used to determinate the density of cells [3]. There is a linear relationship between the cells density (concentration of cells) and the absorption ratio (Abs%) for OD<sub>600</sub> (see Chapter 5: optical methodology).

In this project, the intensity of scatter light (OD<sub>600</sub>) was investigated and plotted as a function of time exposed to pollutants.

### 7.2. Irradiation of Samples

A solid radioactive source (Co-57) with a half-life of 267 days was used for irradiation of bacteria samples. This source emits Gamma radiation in two energy lines with the equivalent dose of about 2000 mSv/h. The details of this source are shown in Table 7.1 below.

Primary Radiation Type	Secondary Radiation Type	Activity	Dose Equivalent at (0.1m)
Gamma ( $\gamma$ ) (0.136, 0.014) MeV	Beta ( $+\beta$ ) 0.00019 MeV	835 MBq	2000mSv/h

Table 7.1. Parameters of (Co<sup>57</sup>) radiation source used for exposure of bacteria samples.

The irradiation system shown in Figure 7.1 Bacteria samples were exposed to Gamma radiation for different periods of time (from 1 up to 720 hours). Each bacteria sample was tested using different techniques before and after exposure to gamma radiation.

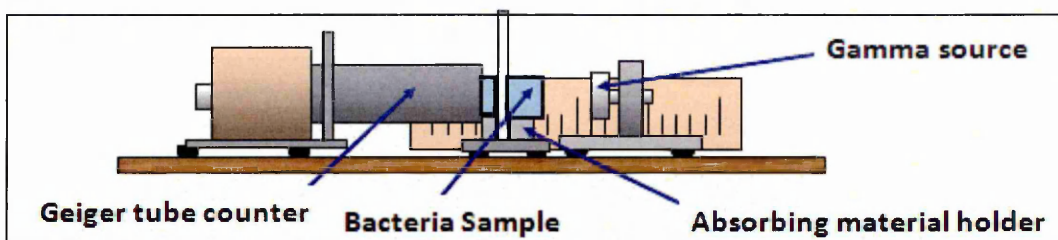


Figure 7.1. Irradiation system scheme used to irradiate bacteria sample

Figure 7.1 shows the schematic diagram of the experimental setup. A bacteria sample was placed directly at the front of the Gamma radiation source and isolated from the surroundings. The bacteria samples were exposed to the Gamma ray for different periods. The optimum equivalent dose was measured as a function of cross-sectional area and exposure time. In this study, the *E. coli* and *D. radiodurans* samples were exposed to the same equivalent dose of radiation. The bacteria container was placed perpendicularly to the radiation source at the same pre-determined distance, in order to obtain the same equivalent dose and to decrease the error as much as possible. For the sake of comparison, two identical samples of bacteria were used: one was inserted inside the Gamma irradiator system, while another was kept outside the irradiator system in the same environmental conditions.

### 7.3. Optical Study of Effect of Gamma Radiation on *E. coli*

Bacteria samples were exposed to gamma radiation for different time periods at a fixed distance (0.1m) between the radiation source and bacteria sample. Several experimental techniques were used to test and analyse the effect of gamma radiation doses on bacteria density.

The numbers of live and dead bacteria were determined with Fluorescence Microscopy(Olympus-BX61) by capturing images of (*E. coli* & *D. radiodurans*) samples. Bacteria samples were checked with this method after colouring bacteria samples with L7012 Live/Dead BacLight Bacterial Viability Kit. As mentioned in Chapter 5, the Live/Dead baclight bacterial viability kit is a mixture of (SYTO-9) green fluorescence nucleic acid stain and Propidium iodide red fluorescence nucleic acid stain. These stains differ in their spectral characteristics and in their ability to penetrate

healthy bacterial cells. The (SYTO-9) stain labels functional bacteria in the population, i.e. those with intact membranes. On the other hand, propidium iodide penetrates only bacteria with a damage membrane, causing a reduction in the (SYTO-9) stain fluorescence and converts their own colour to reddish.

The (LIVE/DEAD) bacLight, bacteria viability kits can easily, reliably, and quantitatively distinguish between live and dead bacteria in a short time. Thus, with an appropriate mixture of the (SYTO-9) and propidium iodide stains, living bacteria with intact cell membranes yield green fluorescence, whereas dead bacteria yield red fluorescence.

Bacteria samples were exposed to Gamma radiation for different periods of 1h, 3h, 5h, 15h, 24h, 48h, 75h, 92h, 120h, 240h, 360h, 480h, 600h and 720h. The equivalent dose of radiation was experimentally measured as 2000 mSv/h. Both bacteria samples of 4ml in volume were exposed to radiation and then stained in a mixture of 6 $\mu$ L/100 $\mu$ L of SYTO 9 and 6 $\mu$ L/100 $\mu$ L of propidium iodide. In order to separate the cells from each other, the solution was shaken. 10 $\mu$ L of that mixture was dropped on a glass slide and covered by glass slide cover. The samples were tested with a fluorescence microscope using a lens of 100 $\times$  magnification. A slide of stained bacteria was illuminated (excited) with blue light of 420nm in wavelength; the bacteria images were captured and analysed using (Q-Capture-Pro 6.0) software. Figure 7.2 shows examples of captured images of (*E. coli*) bacteria as a function of exposure time. Live bacteria stained green and dead bacteria stained red.

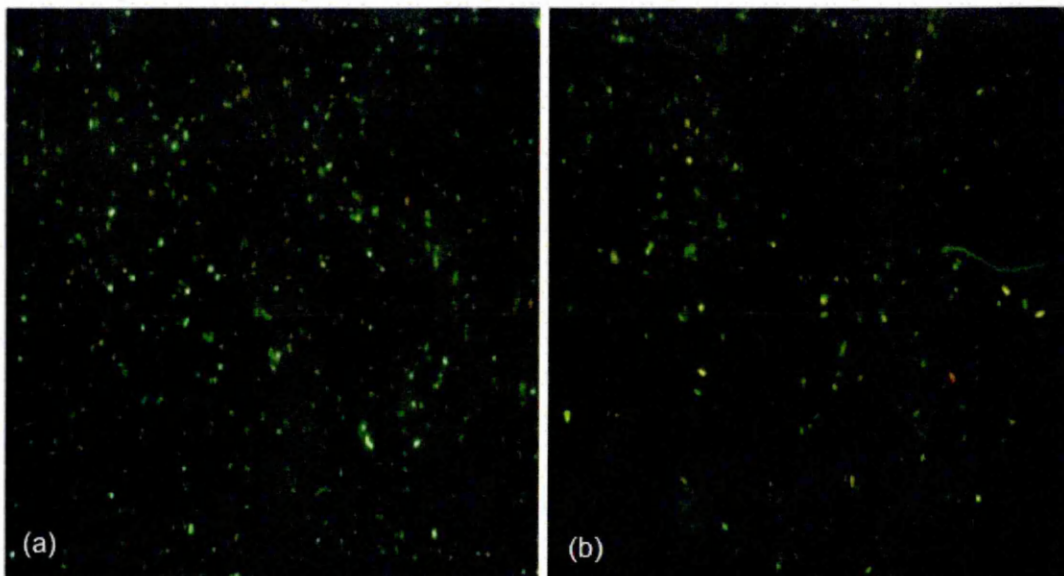


Figure 7.2. Fluorescence microscopy images of *E. coli* bacteria samples (a) before, and (b) after 1 hour exposure to gamma-radiation

Live bacteria emit green light and dead bacteria emit red fluorescence light. Obviously, the differences between the two images before and after exposure to radiation are not very clear because the samples were exposed for a short period of time, at just one hour. The difference is reasonably clear when the bacteria samples were exposed for longer time. That showed in appendix A.

Fluorescence microscopy images in Figures 7.3 show clearly the effect of radiation on live and dead bacteria count. After 480 hours of exposure, the number of green spots has dramatically dropped, which can be counted easily by the naked eye. At the same time, the cell membranes have been damaged by gamma radiation, creating an axis for the propidium iodide to penetrate inside the cell and emit bright red light.

There for a long time exposure to gamma radiation, the change in the ratio (Live/Dead) is very clear; also in the images were captured with fluorescence microscopy (see Figure 7.3) after 480 hours.

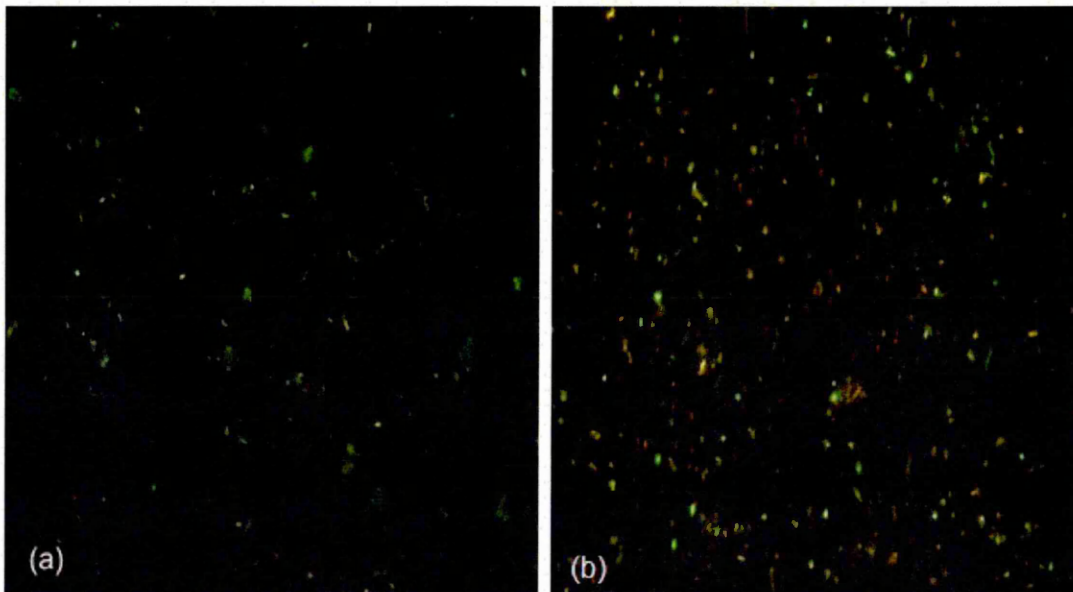


Figure 7.3. Fluorescence microscopy images of *E. coli* bacteria samples (a) before, and (b) after 480 hours exposure to gamma-radiation

The software provided good facilities for image analysis and allows us to estimate the numbers of green and red spots (live and dead bacteria cells), and thus the live/dead bacteria ratio.

Table 7.2 summarizes the data collected from the analysis of Fluorescence microscopy results. It can be easily seen that increasing the radiation dose causes a decrease in the live/dead *E. coli* bacteria ratio.

Time Expose (hours)	Dose Equivalent (mSv)	Ratio (Live/Dead) Bacteria After exposure to $\gamma$ -ray	Ratio (Live/Dead) Bacteria without exposure
0	0	1.51	1.51
1	2000	1.47	1.53
3	6000	1.38	1.5
5	10000	1.29	1.51
15	30000	1.15	1.47
24	48000	1.1	1.48
48	92000	0.915	1.45
96	1920000	0.824	1.46
120	2400000	0.78	1.38
240	4800000	0.54	0.93
360	720000	0.4	0.78
480	920000	0.345	0.69
600	1200000	0.284	0.55
720	1400000	0.22	0.41

Table 7.2. Summary of fluorescence microscopy measurements of effect of Gamma radiation on live/dead ratio of E. coli bacteria

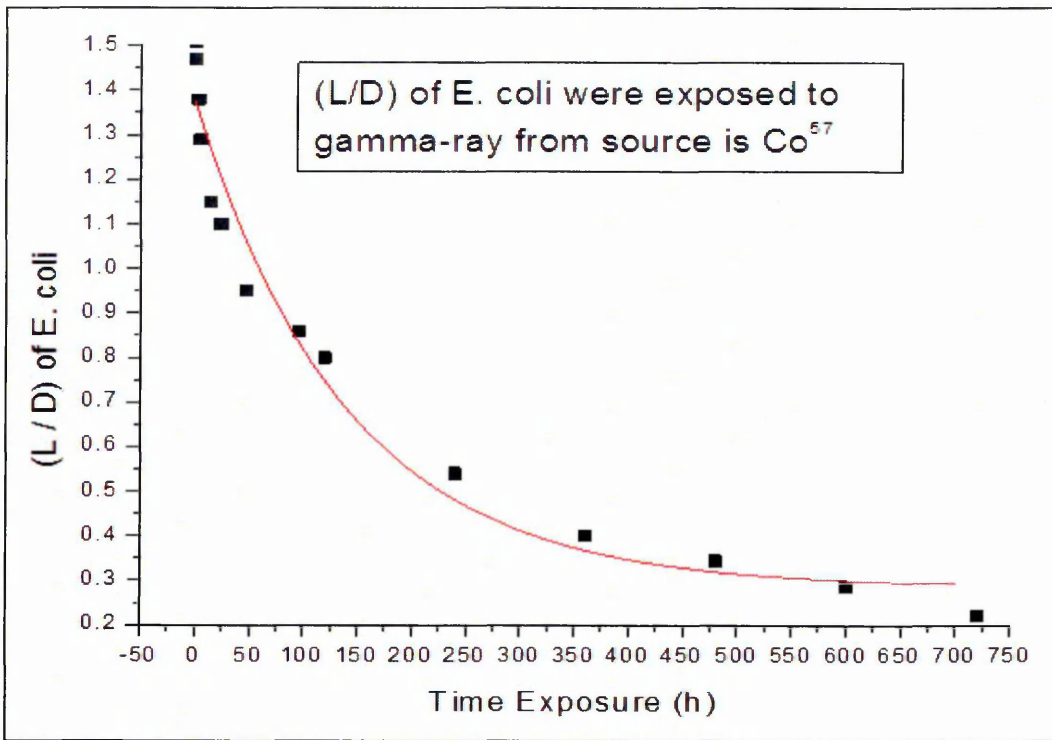


Figure 7.4. Relation between L/D (live/dead) bacteria ratio and exposure time to Gamma radiation (fluorescence microscopy results), with fitting curve showing as a solid line

Detailed analysis of the above dependence in Figure 7.4 shows an exponential correlation between the live/dead cells ratio of the exposed sample and the exposure time. Fitting the data in Fig. 7.6 to the exponential law yielded in (7.1) formula: origin programs provided perfect fitting formula.

$$L/D = 0.52 + 1.14e^{(-t/39.8)} \quad (7.1)$$

where  $t$  is the exposure time and the time constant,  $T = 39.8h$

On other hand, the samples that were kept outside the irradiator system were tested with fluorescence microscopy in order to estimate the ratio between live and dead bacteria; the results are presented in Table 7.2. The ratio was plotted as a function of time at room temperature (normal environment); see Figure 7.5.

The pattern recognition in Figure 7.6 showed the E. coli response in a normal environment, under gamma radiation conditions and without it, is considered very important and the graph is considered to be useful for estimating the radiation dose using the E. coli bacteria optical sensor. Figure 7.5 described the ratio between live and dead E. coli bacteria for different time exposure to gamma radiation which papered exponentially decay for time exposure increases.

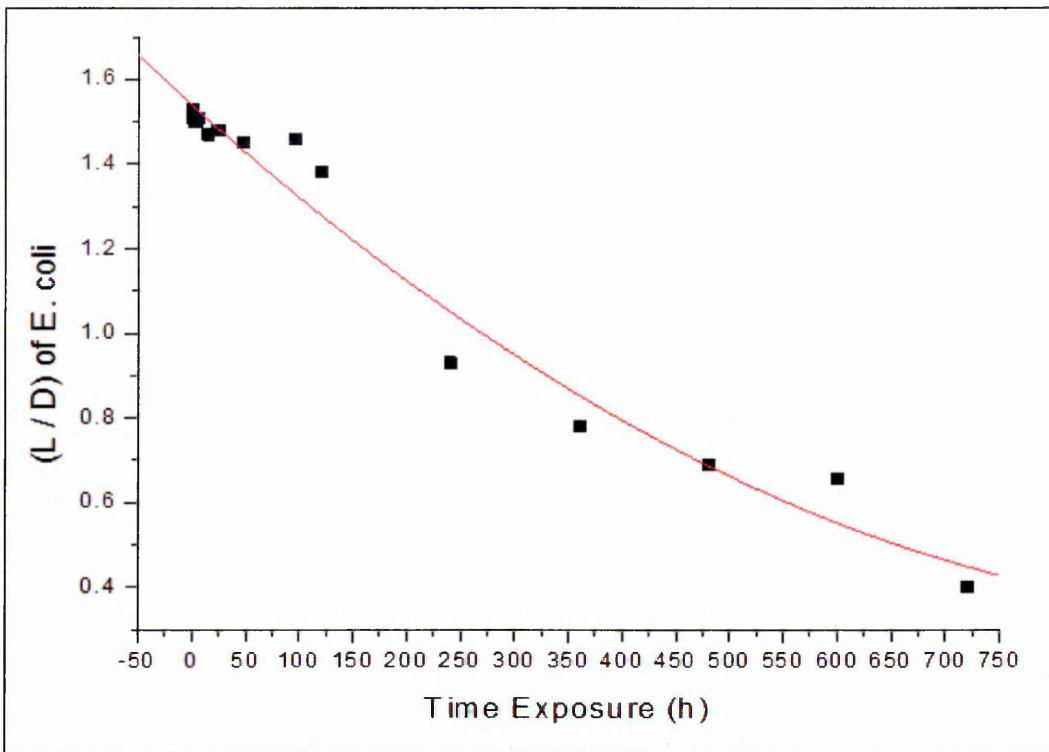


Figure 7.5. Relation between ratios L/D (live/dead) of E. coli bacteria not exposed to Gamma radiation and time (fluorescence microscopy results): Fitting curve showing as a solid line

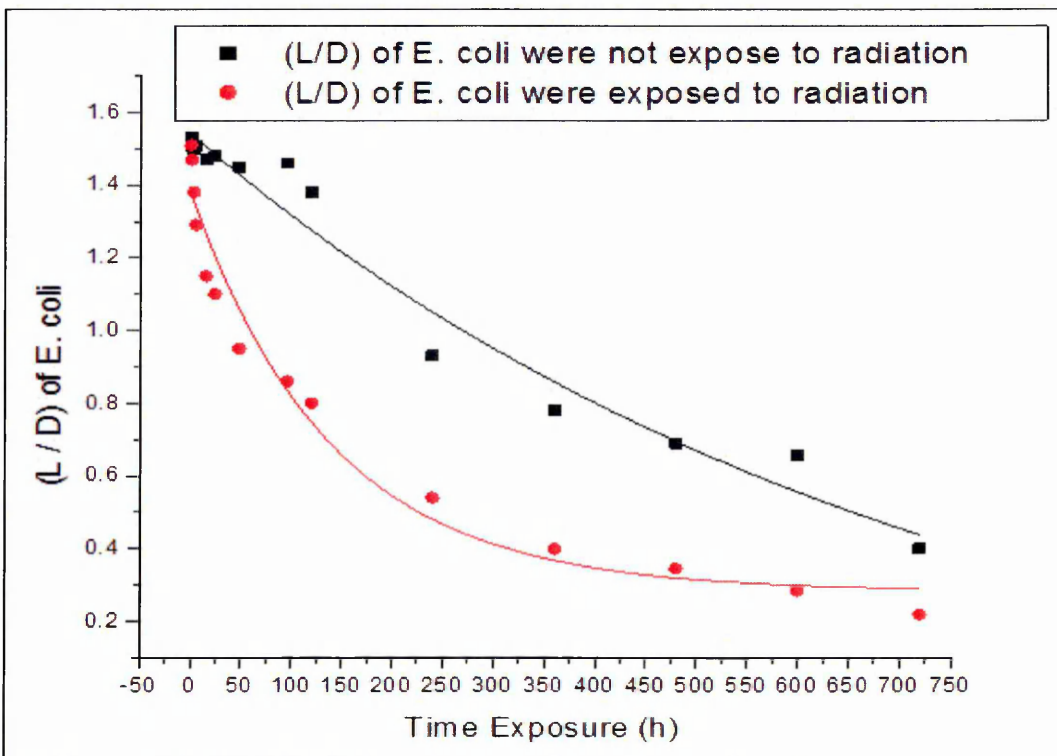


Figure 7.6. Pattern recognition of ratios (live/dead) of E. coli bacteria with and without Gamma Ray Vs. time (fluorescence microscopy results)

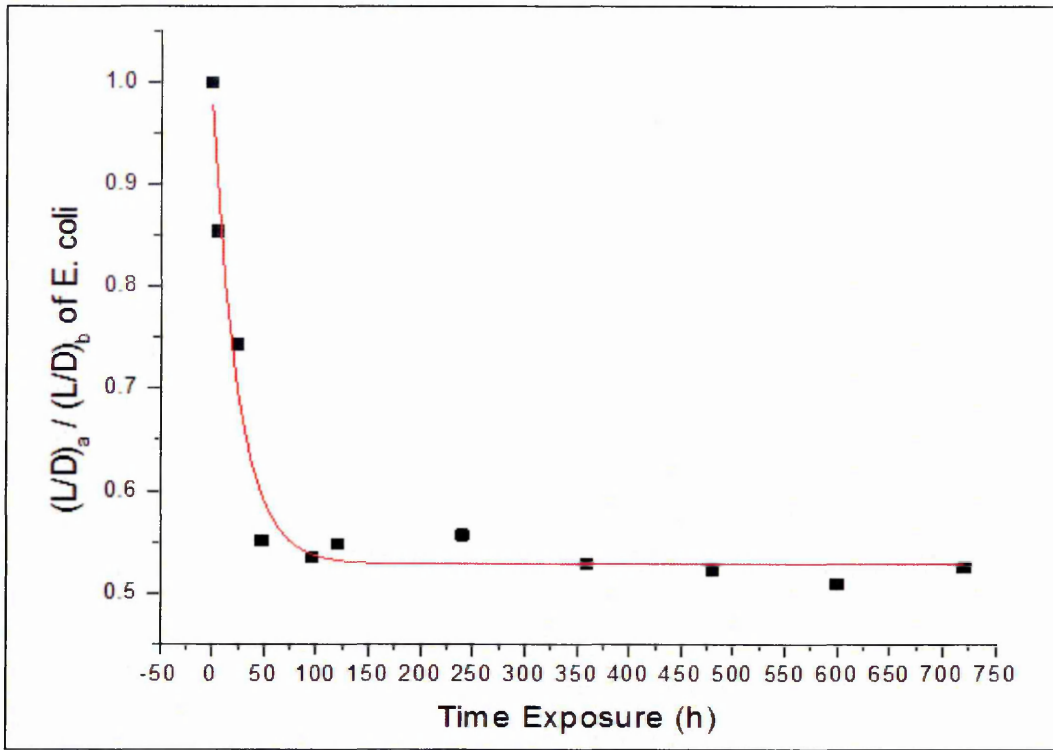


Figure 7.7. Relation between the  $((L/D)_a/(L/D)_b)$  ratio of live over dead bacteria after exposure to radiation and before exposure to radiation against time of exposure (fluorescence microscopy results): fitting curve showing as a solid line

$$\frac{(L/D)_a}{(L/D)_b} = 0.49 + 0.68 e^{(-t/35.5)} \quad (7.2)$$

Detailed analysis of the above dependence in Figure 7.7 shows an exponential correlation between the  $((L/D)_a/(L/D)_b)$  ratio of live over dead bacteria after exposure to radiation and before exposure to radiation, as a function of the time of exposure to radiation. The factors in formula (7.2) are very important for estimating the level of the radiation dose. The graph in Figure 7.7 is the reference standard graph to calculate the radiation dose by using the bacteria cell sensor, where  $t$  is the exposure time and the time constant,  $T=35.5h$

Control experiments showed that Gamma radiation does not affect the medium, i.e. the LB broth.

The optical density ( $OD_{600}$ ) technique was also used to estimate the bacteria cells' density, as a function of time exposed to radiation.  $OD_{600}$  recordings have been presented as either the absorption of light, which refers directly to bacteria cells density, or the transmittance of light. The effect of liquid broth has been neglected and considered as a blank.

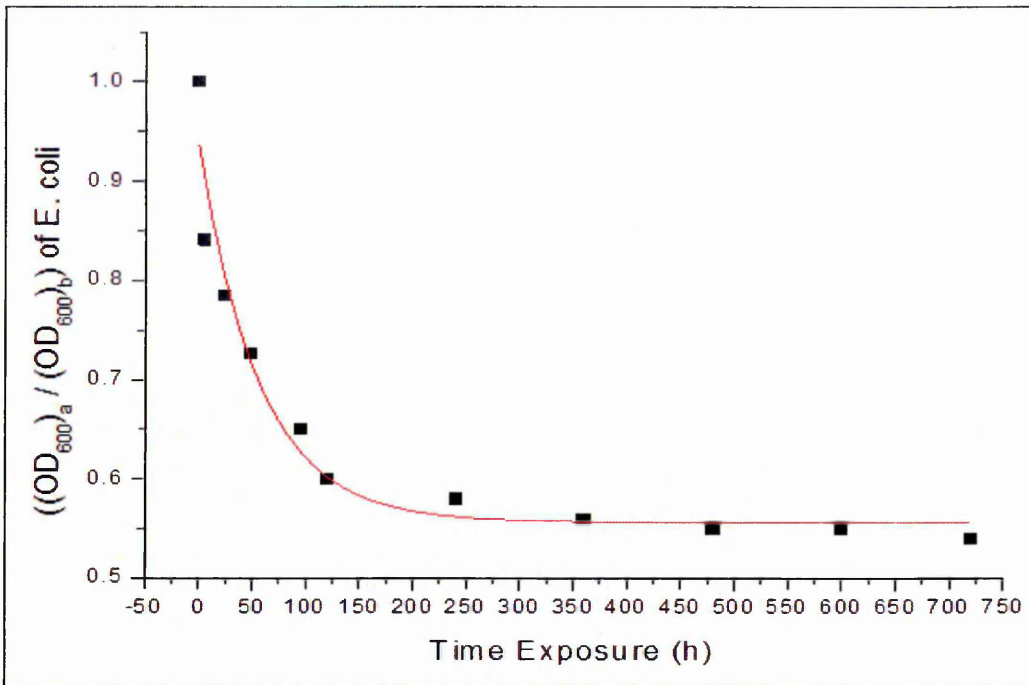


Figure 7.8. Optical density test: optical densities ratio  $((OD_{600})_a / (OD_{600})_b)$  for *E. coli* bacteria versus time exposure to gamma radiation dose where, the ratio  $ratio(OD_{600}) = ((OD)_a \text{ Abs. at } 600\text{nm (was Ex.)}) / ((OD)_b \text{ Abs. at } 600\text{nm (was'nt Ex.)})$

The bacteria samples were prepared as mentioned before and exposed to radiation for different periods, from 1 hour to 720 hours. In this test, the absorption level was recorded as an indication of cells density (cells concentration). The results obtained were shown in Figure 7.8. The data in Figure 7.8 are not obtained from the direct measurements of light intensity but are derived from the ratio between two tested samples. The original sample is divided in two halves: one exposed to radiation, and another one was non-exposed but kept in the same conditions near the radiation source. The results confirm previous observations in Figure 7.7.

The fitting of experimental data yields the following exponential decay function (7.3):

$$ratio OD_{600} = OD_a / OD_b = 0.44 + 0.58 * e^{(-t/39.9)} \quad (7.3)$$

Actually, it is a mixture of exponents: the faster one at short exposure times ( $t < 39.9$  h) and much slower decay at larger exposure times, at around 240 h and higher. Such behaviour implies two different physical-chemical processes.

Another optical technique of fluorescence spectroscopy was explored to confirm the above results on the effect of gamma radiation on bacteria count, as well as to study in

more detail the fluorescence spectra of *E. coli* bacteria. Fresh bacteria samples were prepared for this study in a purity of *E. coli* culture. The emission fluorescence spectra of bacteria samples were recorded using the excitation wavelength 315 nm, selected for the UV-visible absorption spectrum; therefore the samples were checked by UV-visible spectrophotometer in order to avoid the absorption peak and the full transmitted regions, the excitation wavelength selected in this region has low absorption intensity (shoulder rang), in terms of achieving sufficient energy to excite the bacteria samples, a short wavelength with high energy was identified as much as possible. Broth growth media (LB-broth) were used as a baseline (blank) to study the light absorbed from *E. coli* bacteria cells (see Figure 7.9).

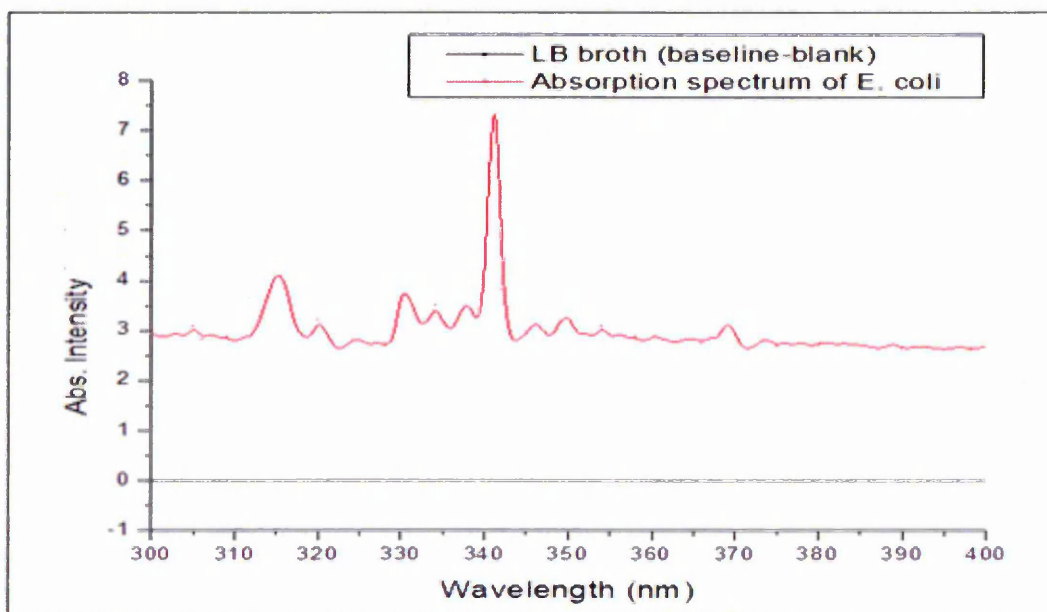


Figure 7.9. Absorption spectrum of *E. coli* bacteria sample (Red) and clear broth (LB-broth) as blank (black)

The spectra of clear LB broth were recorded and are presented in Figure 7.9; the relation between fluorescence intensity (a.u.) and bacteria concentration has been explored and the linearly correlation was confirmed. Maximum fluorescence intensity was seen to be cell concentration dependent. First of all, the fluorescence spectrum of the liquid broth medium used to grow the bacteria was plotted and analysed to determine the change after exposure to radiation (see Figure7.10).

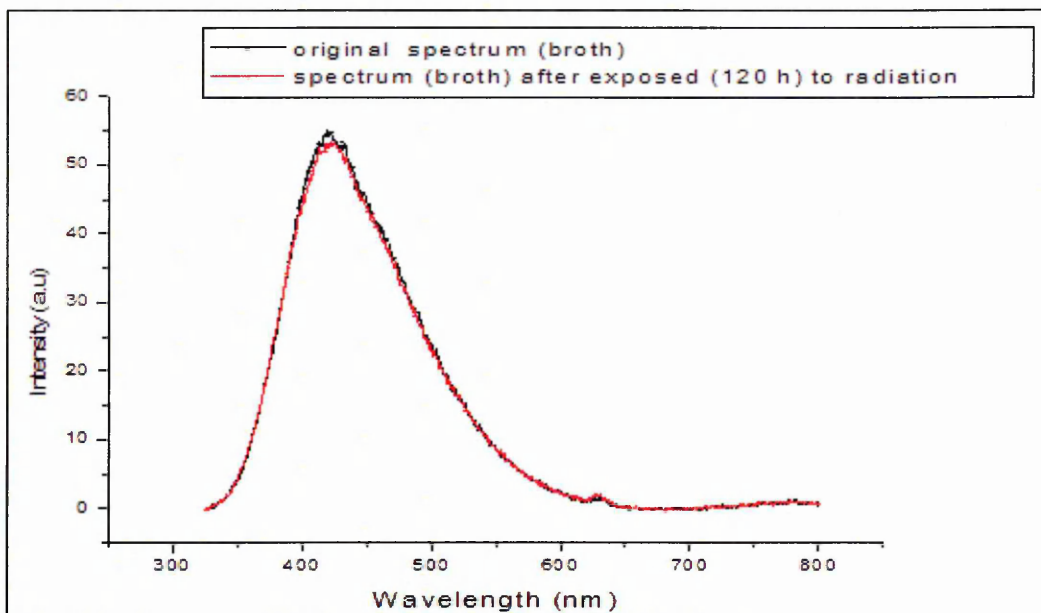


Figure 7.10. Fluorescence spectra of a liquid broth medium no-exposed (black curve) and exposed to gamma radiation for 120 hours

A broad peak with a maximum at about 420 nm appears in both spectra in Figure 7.10, indicating that the radiation exposure for 120 hours does not affect it, and this is true for longer exposure times as well.

Similar measurements were performed on *E. coli* bacteria samples and the results were shown in Figure 7.11 and 7.12. A broad spectral band with a maximum at 420nm is similar to that observed in clear broth samples. The radiation has little impact on this band, and thus it is of no interest to our study. However, another sharp peak appeared at about 630nm, and its intensity depends on radiation, i.e. it decreases with exposure time.

The observed peak, however, has nothing to do with fluorescence; it is simply a double excitation wavelength peak appearing as a second order of diffraction. Usually this peak is regarded as a parasitic one and ignored, but in our case it appeared to depend on radiation level.

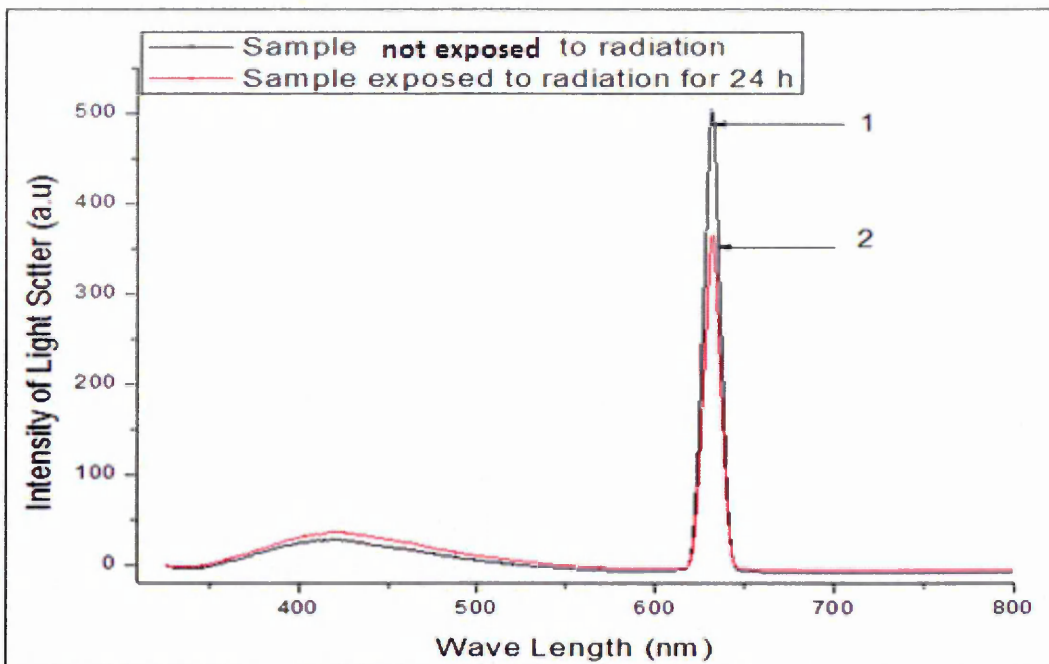


Figure 7.11. Fluorescence spectra (light scatter) of two *E. coli* bacteria samples: (1) not exposed to radiation (Black graph); and (2) exposed to Gamma radiation for 24h (48000 mSv) (Red graph)

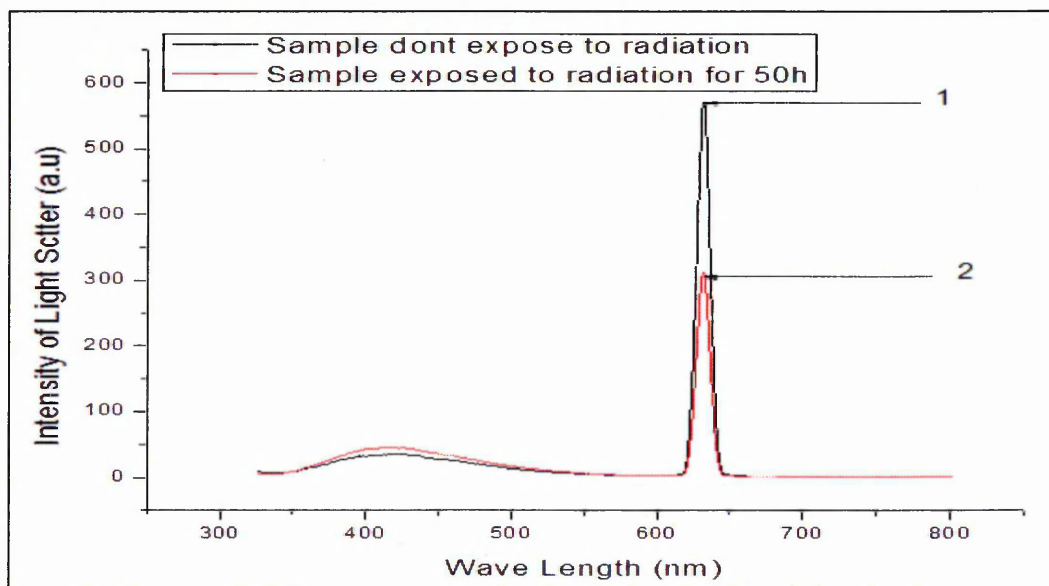


Figure 7.12. Fluorescence spectra (light scatter) of two *E. coli* bacteria samples: (1) not exposed to radiation (Black graph); and (2) exposed to Gamma radiation for 48h (96000 mSv) (Red graph)

The explanation of the above phenomenon is simple and lies in the enhancement of that 2-nd diffraction order peak due to light scattering on bacteria, which is why its intensity depends on the bacteria concentration. This peak does not appear on samples of clear broth. The same results were received, such as the change in the fluorescence peak's

intensity (double scatter intensity). Figure 7.13 shows the E. coli bacteria and LB-broth responses to gamma radiation.

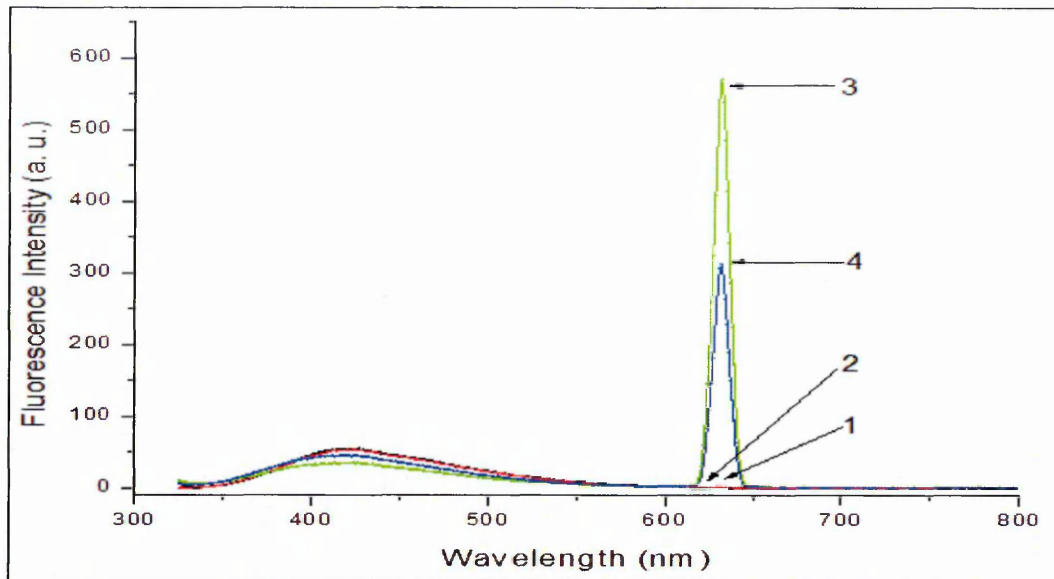


Figure 7.13. Fluorescence spectra of E. coli samples in LB broth non-exposed (3) and exposed to  $\gamma$ -radiation for 48 hours (4), (1) and (2) curves corresponds, respectively, to clear LB broth non-exposed and exposed to  $\gamma$ - radiation for 48 hours

However, in current experiments, the amplitudes were found to depend on the radiation dose and thus the decision to use this information in this study. The reason for such behaviour can be simply explained as the product of light scattering on living bacteria, which in turn causes the increase at the 2-nd diffraction order peak. As one can see, the peak at 630nm for E coli tends to decrease with the increase of radiation exposure time. Since the peak at 630 nm carries important information on bacteria counts, a series of experiments on bacteria samples exposed to different radiation doses were executed. The results have been presented in previous figures. The intensity of this peak goes recedes with exposure time, as is clearly seen from Figure 7.14. The decay is exponential (the fitting formula is given in Fig.7.14) with the characteristic decay time of 34.86 hours (see formula 7.3). Similarly, for results in Fig. 7.7 and Fig. 7.8, E. coli samples showed an exponential decrease in peak intensity. The best data fitting functions for graph (7.14) are shown below for E.coli.

$$P_{2-nd} = 0.48 + 0.53 e^{(-t/34.8)} \quad (7.4)$$

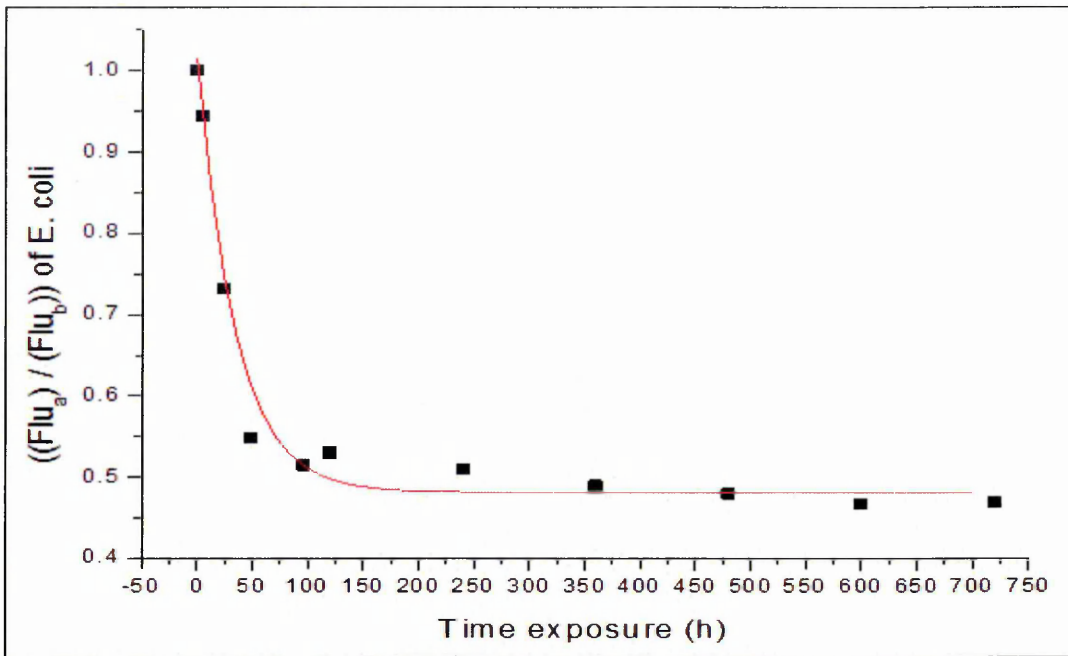


Figure 7.14. Effect of gamma radiation on 2nd order diffraction peak for E. coli,  $Flu_{(a)}$  for bacteria sample exposed to radiation and  $Flu_{(b)}$  for sample dose not exposed

The results showed a peak at 630nm, related to the concentration of bacteria, in order to prove that the control experiments were carried out on samples of E. coli bacteria grown for a different time but not exposed to radiation. The results are shown in Figure 5.15.

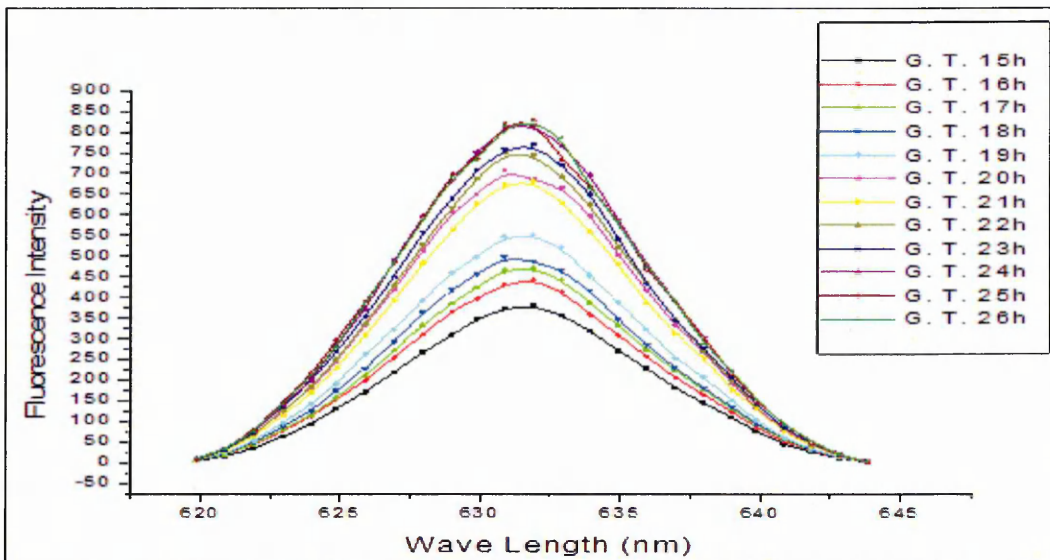


Figure 7.15. Intensity of 630nm peak for E. coli samples of different growth time (G. T)

The peak intensity clearly recedes, confirming the relation between bacteria growth time (cell density in samples) and the intensity of the 630nm peak, corresponding exactly to the bacteria growth kinetic [4]. Fluorescence spectrum peak at 630nm is assumed to be

related to the concentration of bacteria, as the intensity rises when the bacteria concentration increases.

Moreover, the above results correlate linearly to the results of the OD<sub>600</sub> method given earlier, as clearly seen in Figure 7.16.

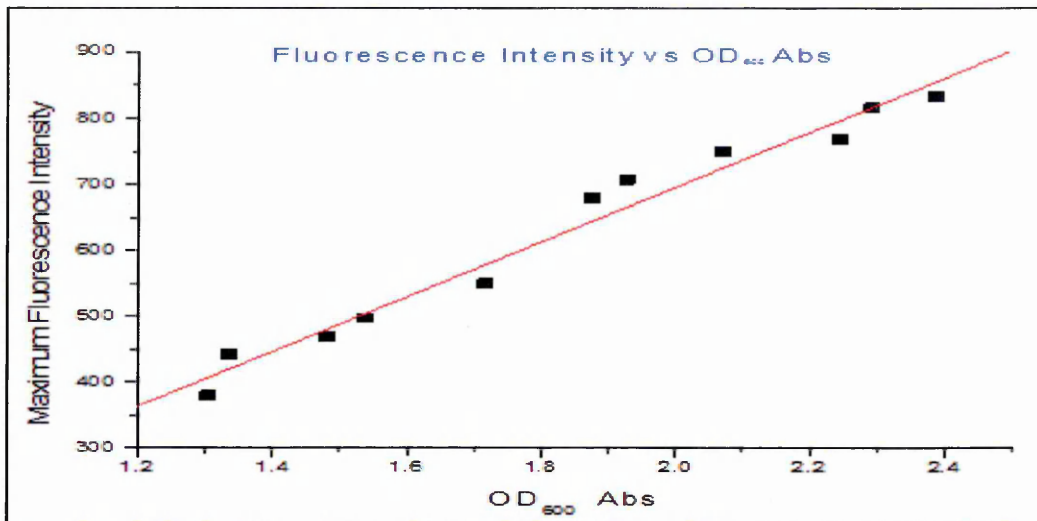


Figure 7.16. Correlation between peak intensity at 630 nm and absorption optical density at 600nm the E. coli bacteria growth time increases from left to right

All the above evidence supports the concept of a linear correlation between the 630nm peak intensity and the concentration of bacteria.

#### 7.4. Optical Study of Effect of Gamma Radiation on D. radiodurans

A similar sequence followed for the cultivation of D. radiodurans (Anderson R1 strain). The same irradiator system and radiation source, Co<sup>57</sup> was used to expose the D. radiodurans bacteria to the gamma radiation. The D. radiodurans bacteria seem less affected by radiation compared to the E coli. This type of bacteria shows resistance to ionized radiation, particularly for short exposure times (low radiation dose). The larger doses, however, cause damage to D. radiodurans. The samples were exposed to radiation for a different period, from 1 hour to 720 hours. The effect of gamma radiation on the bacteria density was examined and analysed using three previous different optical experimental techniques; fluorescence microscopy measurements were performed using an OLYMPUS-BX60 instrument. In this study, bacteria samples were stained using (L7012 Live/Dead) BacLight Bacterial Viability Kit, which is a mixture of the (SYTO-9) green fluorescence nucleic acid stain and Propidium iodide red fluorescence nucleic acid stain. A slide of stained bacteria was illuminated (excited) and the bacteria images

captured and then analysed. The numbers of live and dead bacteria were determined. Typical fluorescence microscopy images of samples of *D. radiodurans* bacteria are shown Figure 7.18. In these images, live bacteria emit green light while dead bacteria emit red light. The difference between images taken before and after exposure to radiation is not clearly obvious for a short and mid-period exposure; *D. radiodurans* bacteria having a characteristic “cocci” shape can be easily distinguished from *E. coli* that has a paisley shape; so for that, it is possible to distinguish between the fluorescence microscope images (see Figures 7.17, 7.18). More images are presented in appendix A.

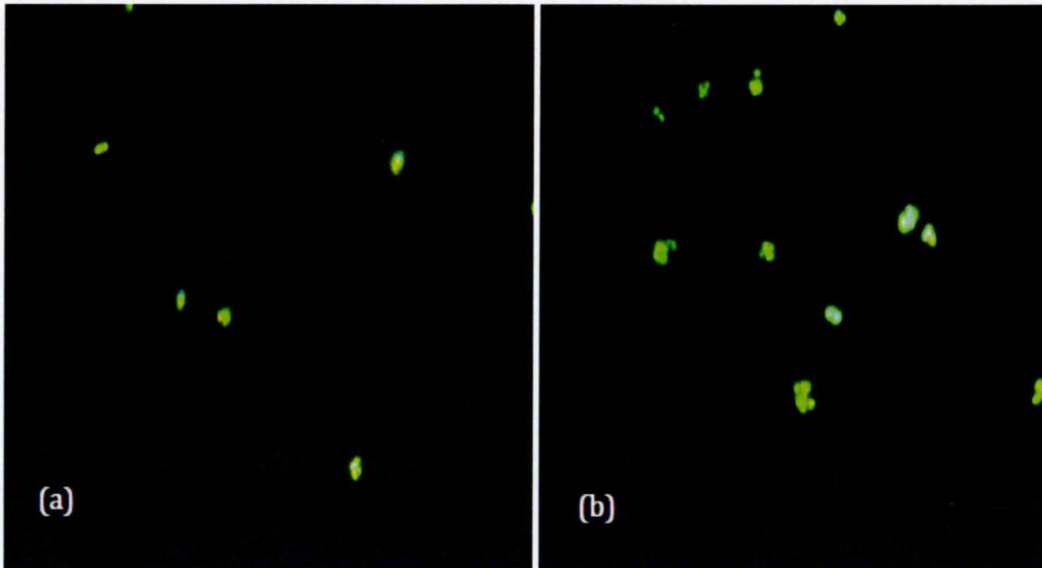


Figure 7.17. Fluorescence microscopy images for *D. Radiodurans* bacteria samples (a) before, and (b) after 24 hours exposure to gamma radiation

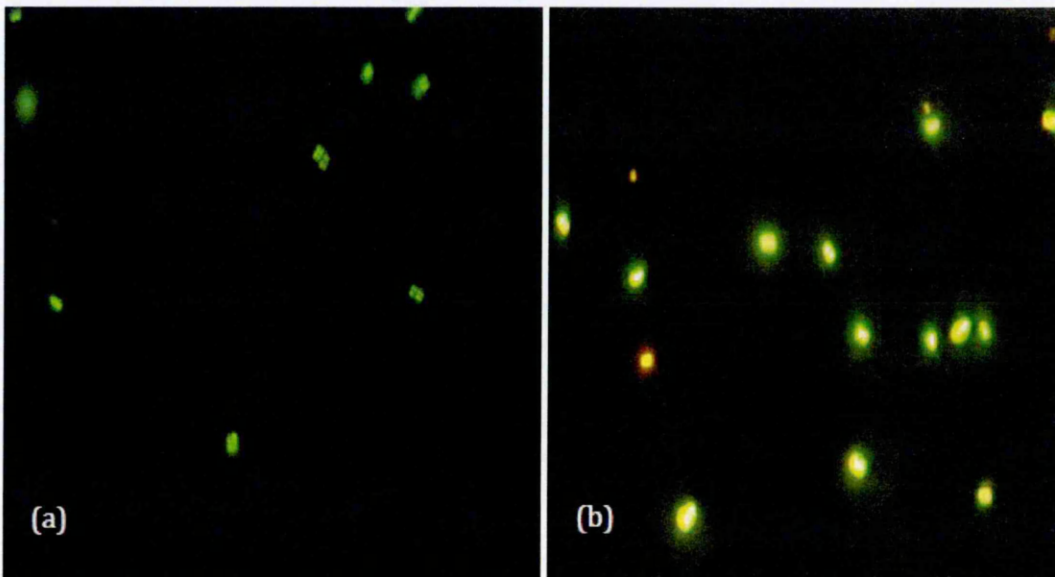


Figure 7.18. Fluorescence microscopy image for *D. Radiodurans* bacteria samples, (a) before, and (b) after 240 hours exposure to gamma radiation

The (Q-Capture-Pro 6.0) software has the ability to analyse images and allows for the estimation of the number of green and red spots (live and dead bacteria cells), and thus the live/dead bacteria ratio, as presented in Table 7.3.

Table 7.3 summarizes the data collected from the analysis of Fluorescence microscopy results of *D. radiodurans* bacteria. The live/dead ratio of *D. radiodurans* bacteria increases at low and intermediate levels of radiation doses; for a long exposure time to gamma radiation the change in the ratio (Live/Dead) is very clear and visible in the images captured by fluorescence microscopy.

Time Exposure (hours)	Dose Equivalent (mSv)	Ratio (Live/Dead) of <i>D. radiodurans</i> bacteria after exposure to $\gamma$ -ray	Ratio (Live/Dead) of <i>D. radiodurans</i> bacteria without exposure to $\gamma$ -ray
0	0	1.21	1.21
1	2000	1.261	1.26
3	6000	1.25	1.25
5	10000	1.271	1.27
15	30000	1.284	1.28
24	48000	1.3	1.28
48	92000	1.35	1.27
96	192000	1.352	1.26
120	240000	1.334	1.26
240	480000	1.355	1.29
360	720000	1.3	1.23
480	920000	1.11	1.21
600	1200000	0.95	1.18
720	1400000	0.81	1.19

Table 7.3. Summary of fluorescence microscopy measurements of effect of Gamma radiation on live/dead ratio of *D. radiodurans* bacteria

The pattern recognition in Figure 7.19 showed the *D. radiodurans* response in a normal environment, under gamma radiation conditions and without it, is considered very important and the graph is considered to be useful for estimating the radiation dose using the *D. radiodurans* bacteria optical sensor.

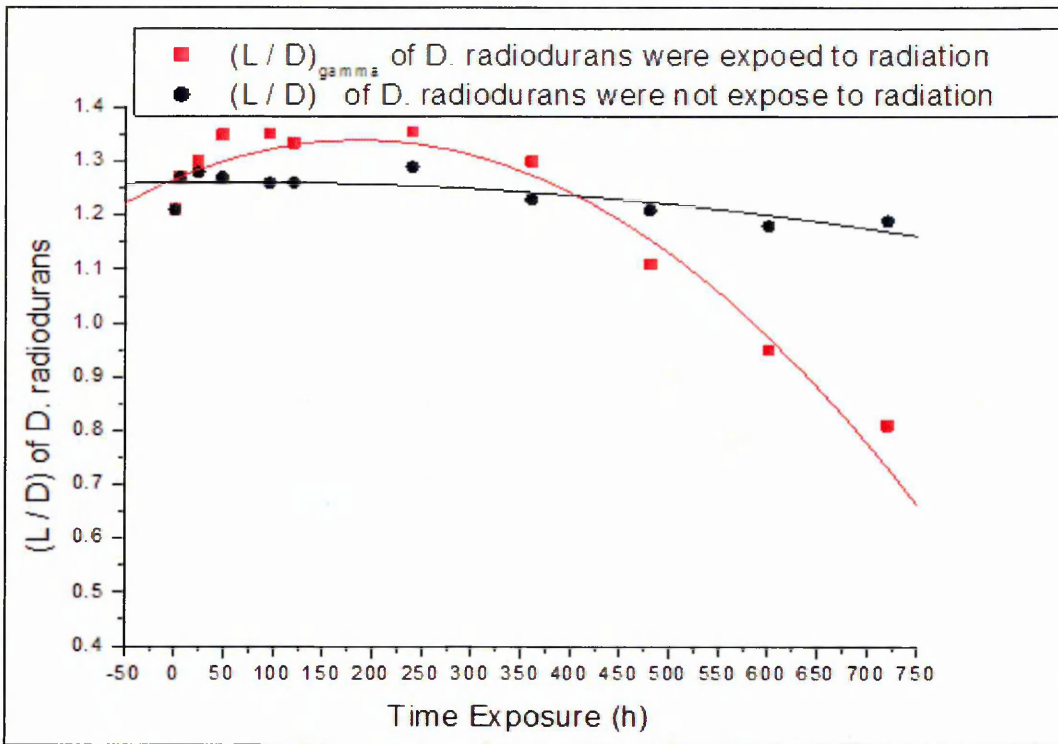


Figure 7.19. The pattern recognition of the ratios (live/dead) of *D. radiodurans* bacteria was exposed (red) and not exposed (black) to Gamma Ray vs. time (fluorescence microscopy results)

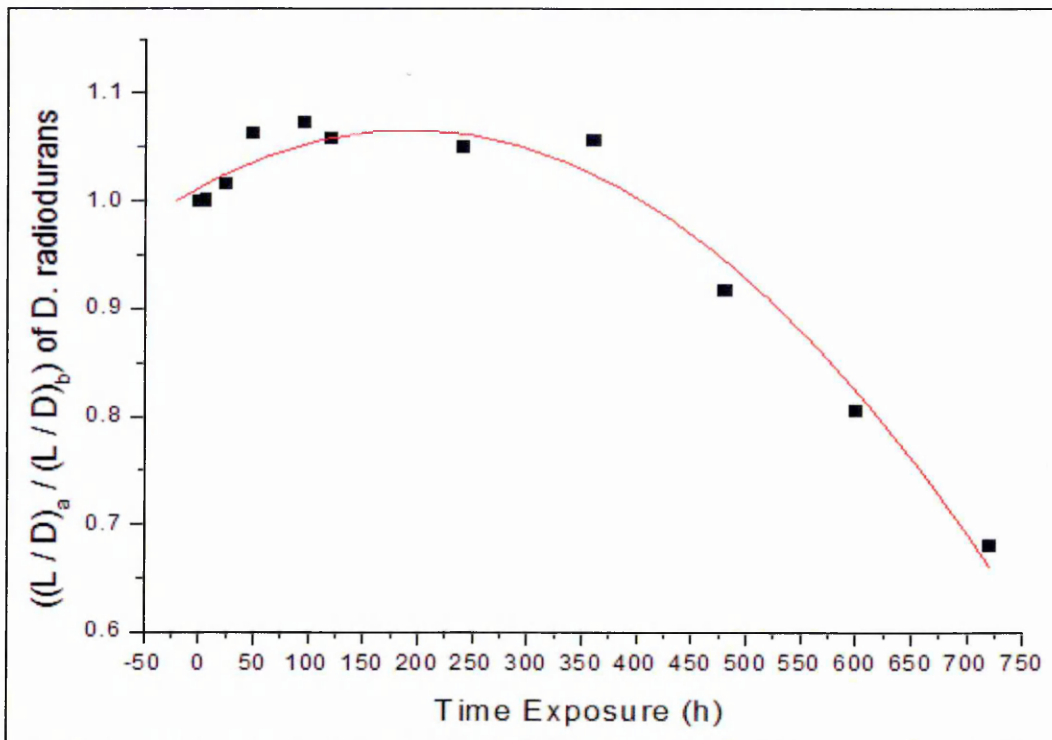


Figure 7.20. Relation between  $((L/D)_a / (L/D)_b)$  ratio of live/dead *D. radiodurans* bacteria after exposure to radiation and before exposure to radiation, against the time of exposure (fluorescence microscopy results), the fitting curve showing as a solid line

$$\left(\frac{(L/D)_a}{(L/D)_b}\right) = 1.01 + 5.5 * 10^{-4} * t - 1.44 * 10^{-6} * t^2 \quad (7.4)$$

From the fitting formula of Figure 7.20 the  $\max \left(\frac{(L/D)_a}{(L/D)_b}\right)_{t \sim 190h} = 1.06$

Optical density (OD<sub>600</sub>) technique was also used to estimate the *D. radiodurans* bacteria cells density as a function of the time of exposure to radiation. As has already been mentioned, in OD<sub>600</sub> experiments the absorbance values recorded do not represent the actual absorption of the light by the samples but rather losses of light intensity due to light scattering on live bacteria.

The data of OD<sub>600</sub> measurements of *D. radiodurans* bacteria are summarized in Figure 7.21. The values of absorbance presented were normalized (divided) by the values of absorbance of samples not exposed to radiation. The results confirmed previous observations of the polynomial decay of *D. radiodurans* bacteria counts as a function of exposure time. The dead bacteria did not contribute to light scattering, so that absorption intensity matches regarding the live bacteria density. The OD<sub>600</sub> results are presented in Figure 7.21.

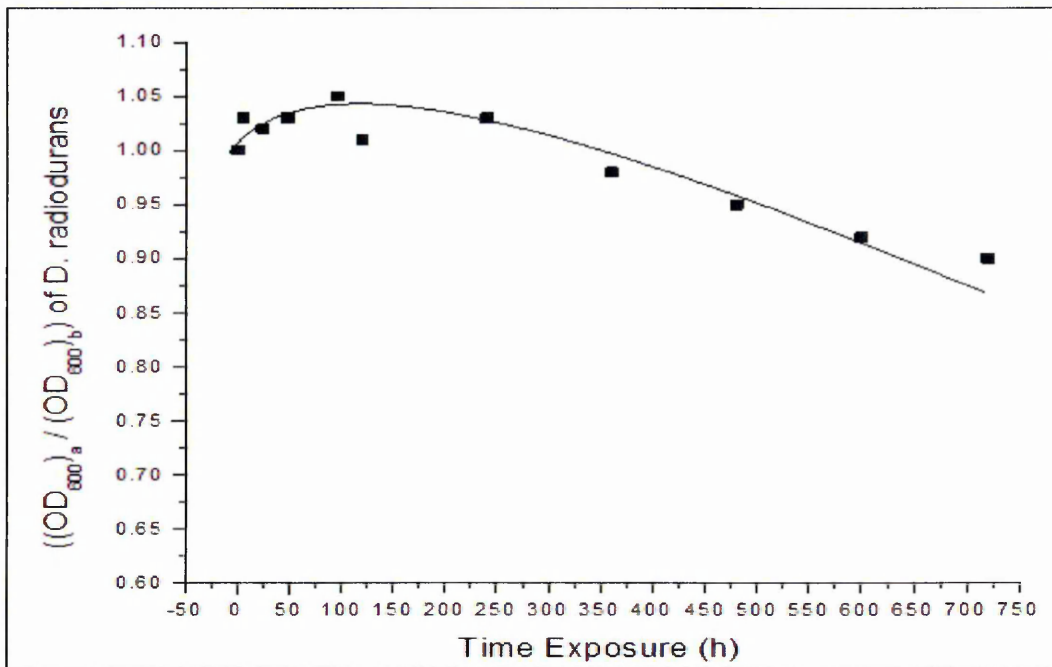


Figure 7.21. Optical Density test: Optical density ratio at 600nm for *D. radiodurans* bacteria versus time exposure to gamma radiation dose

The nutrient (OXOID CM3) broth media optical density used to estimate the bacteria cells density. OD<sub>600</sub> recordings have been presented as either absorption of light,

which refers directly to the bacteria cells density, or transmittance of light. The effect of liquid broth media has been neglected and considered as a blank. Figure 7.26 shows the polynomial correlation between live bacteria cells' density and exposure time.

Fluorescence spectroscopy was used to confirm the above results. The effect of gamma radiation on *D. radiodurans* bacteria count was estimated from the fluorescence spectra of bacteria. Fresh bacteria samples were prepared for this study. The excitation wavelength at 350 nm was not enough to record the emission fluorescence spectra of *D. radiodurans* bacteria at 700nm (double scatter wavelength). As mentioned, the excitation wavelength was selected regarding the UV-visible absorption spectrum; the excitation wavelength was selected in the region with a low absorption intensity peak. Broth growth media (OXOID-CM3 broth) was used as a baseline (blank) to study the light absorbed from *D. radiodurans* bacteria cells (see Figure 7.22).

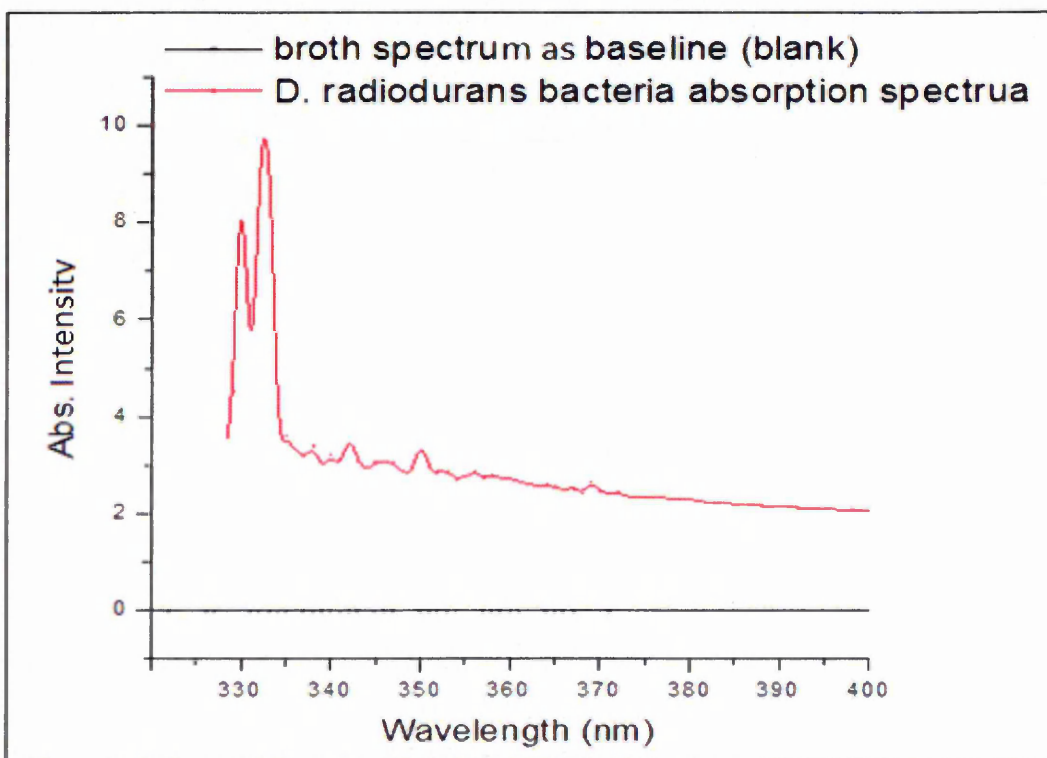


Figure 7.22. Absorption spectrum of *D. radiodurans* bacteria sample (Red) and clear broth (OXOID-CM3 broth) as blank

The relation between fluorescence intensity (a.u.) and bacteria concentration has been explored and linear correlation was confirmed. The maximum fluorescence intensity was indicated as cell concentration dependent. First of all the fluorescence spectrum of the liquid broth medium used to grow the bacteria was plotted and analysed to determine the change in spectrum after exposure to radiation (see Figure 7.23).

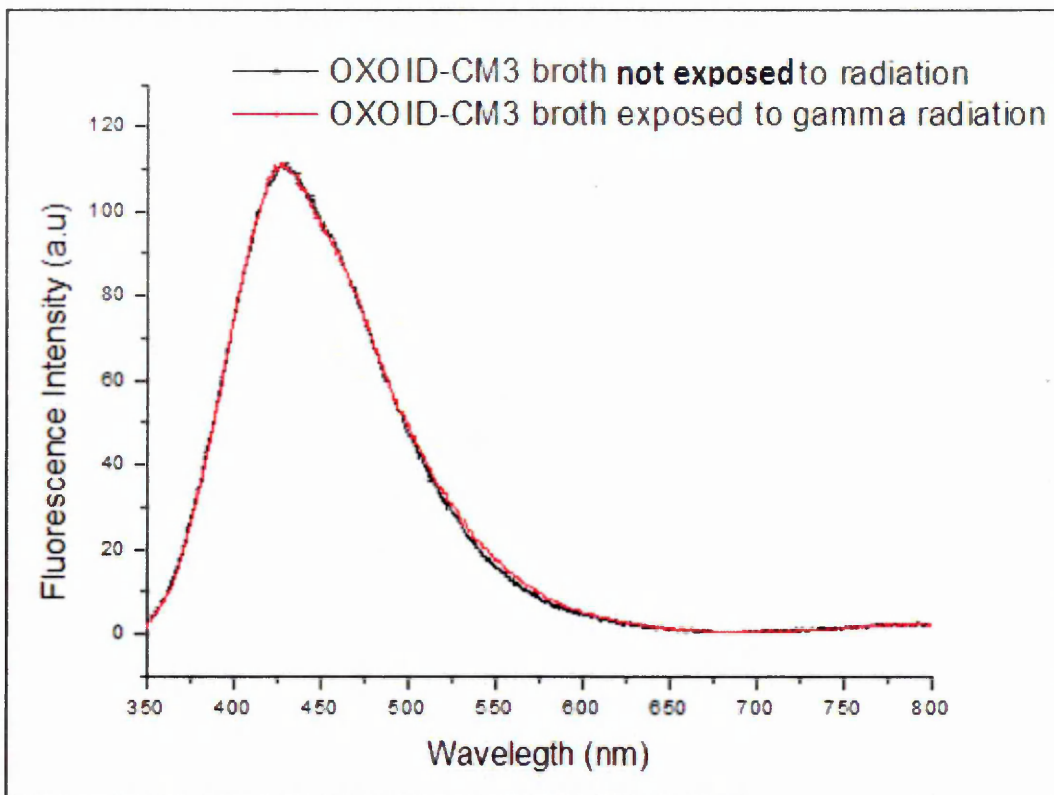


Figure 7.23. Fluorescence spectra of liquid broth medium not exposed (black curve) and exposed to gamma radiation for 120 hours

A broad peak with a maximum of about 425 nm appears in both spectra in Figure 7.23, indicating that radiation exposure for 120 hours did not affect the broth, and not did a longer exposure time.

A broad spectral band with a maximum at 425nm is similar to that observed in clear broth samples. There is no clear impact on this band, and thus it is of no interest. However, another sharp peak appeared at about 700nm, and its intensity does depend on radiation, i.e. increases or decreases related to exposure time.

However, as mentioned previously, the fluorescence peak has nothing to do with fluorescence; it is simply a double scattering wavelength peak.

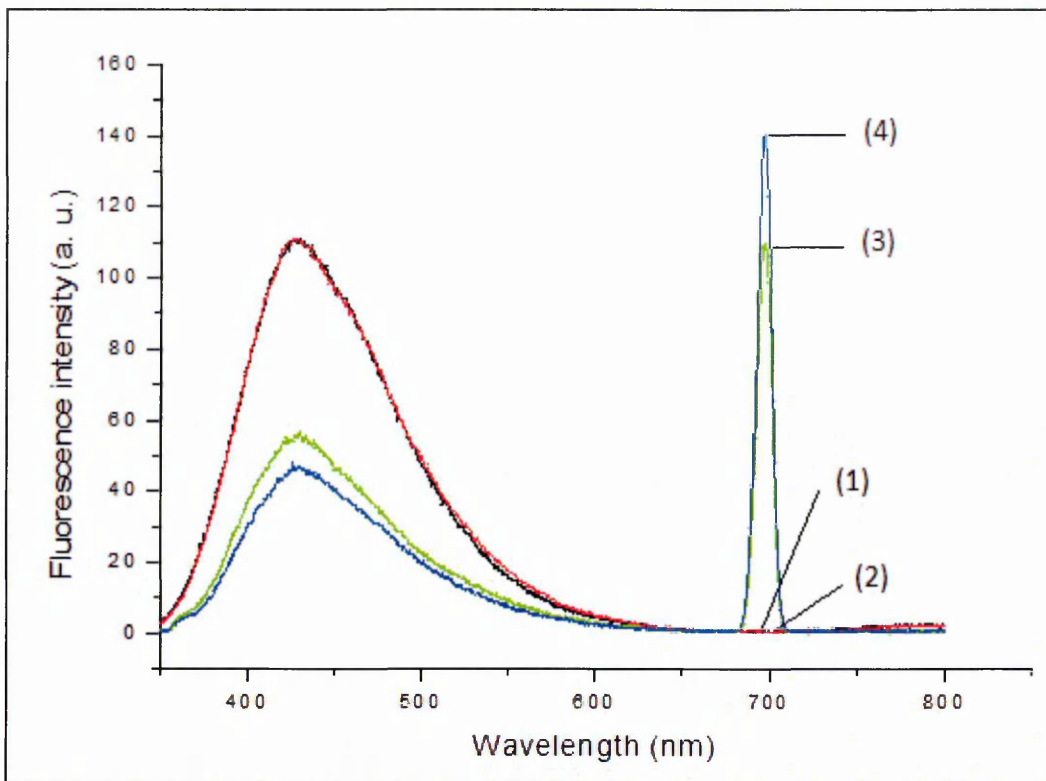


Figure 7.24. Fluorescence spectra of *D. radiodurans* samples in nutrient broth non-exposed (3) and exposed to gamma ray for 120 hours (4); (1) and (2) curves correspond, respectively, to clear nutrient broth non-exposed and exposed to gamma-ray for 120 hours. Source is  $\text{Co}^{57}$  (2000mSv/h)

Figure 7.24 is very interesting in terms of the change on the intensity of the fluorescence spectrum for nutrient the broth media of *D. radiodurans*, this change being related directly to the concentration of live bacteria, which changed, depending on the radiation dose level.

One the other hand, the reason for such behaviour as the light scattering on living *D. radiodurans* bacteria in turn causes an increase in the 2-nd diffraction order peak. As one can see, the peak at 700nm for *D. radiodurans* tends to increase with the increase of radiation exposure time (for short time exposure). Since the peak at 700nm carries important information on bacteria counts, a series of experiments on bacteria samples exposed to different radiation doses were undertaken. The results have been presented in previous Figures. The intensity of this peak fluctuates with exposure time, as is clearly seen from Figure 7.25.

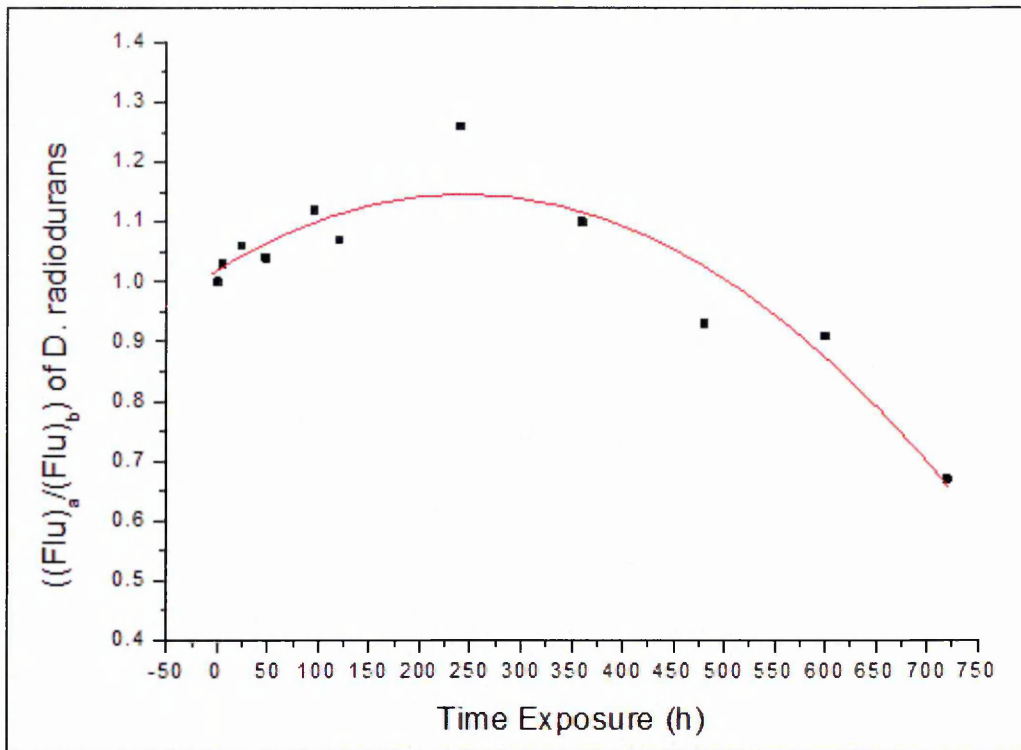


Figure 7.25. The effect of gamma radiation on 2nd order diffraction peak for D. radiodurans, (Flu)<sub>a</sub> for bacteria samples exposed to radiation and (Flu)<sub>b</sub> for samples not exposed

$$P_{2-nd} = 1.02 + 1.04 * 10^{-3} * t - 2.14 * 10^{-6} * t^2 \quad (7.7)$$

From the fitting formula of Figure 7.25 the max  $(P_{2-nd})_{t \sim 240h} = 1.12$ .

D. radiodurans samples showed polynomial change in the peak intensity. The best data fitting formula for the graph in Figure 7.25 are shown above in formula (7.7) for D. radiodurans.

### 7.5. Comparison of Optical Data for E. coli and D. radiodurans

The fluorescence microscopy data were summarized in Figure 7.26 for both E. coli and D. radiodurans bacteria. The two bacteria studied showed completely different behaviour. The L/D ratio for E. coli bacteria exhibited an exponential decay, while the ratio for D. radiodurans rose with small doses of radiation and began to fall noticeably at intermediate and high doses. This corresponds well with the reported earlier facts of radiation-stimulated growth of D. radiodurans bacteria [5].

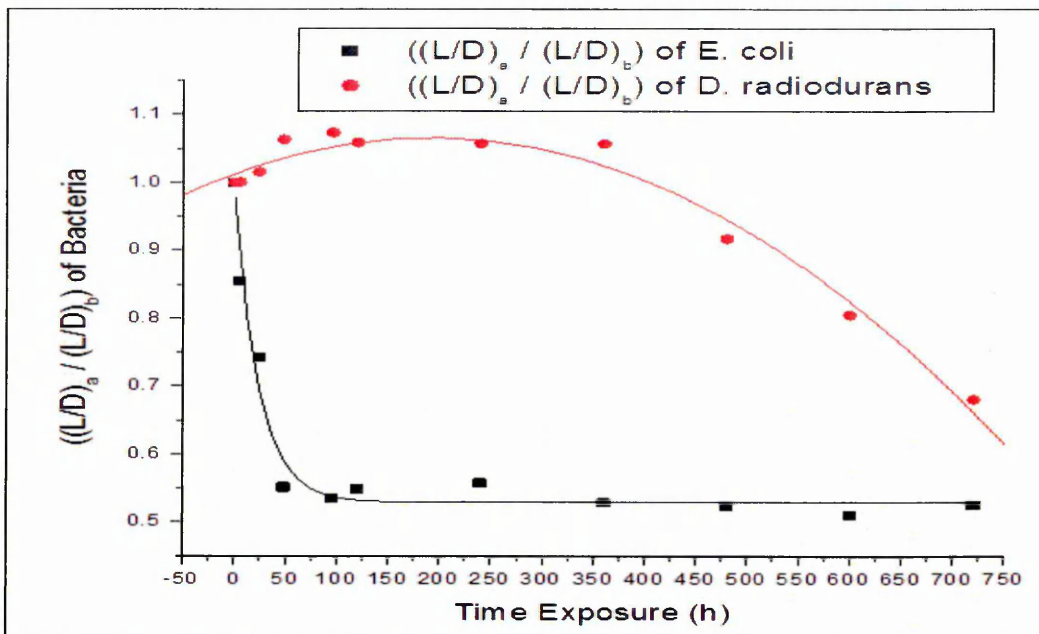


Figure 7.26. Dependence of L/D bacteria ratio for both *E. coli* and *D. radiodurans* bacteria on time of exposure to gamma rays, (fluorescence microscopy results) [6]

The data of  $OD_{600}$  measurements for both *E. coli* and *D. radiodurans* bacteria are summarized in Figure 7.27. The values of absorbance presented were normalized (divided) by the values of absorbance of samples not exposed to radiation. The results confirmed previous observations of the exponential decay of *E. coli* bacteria counts, as a function of exposure time. The data for *E. coli* are fitted to exponential decay (see Figure 7.27).

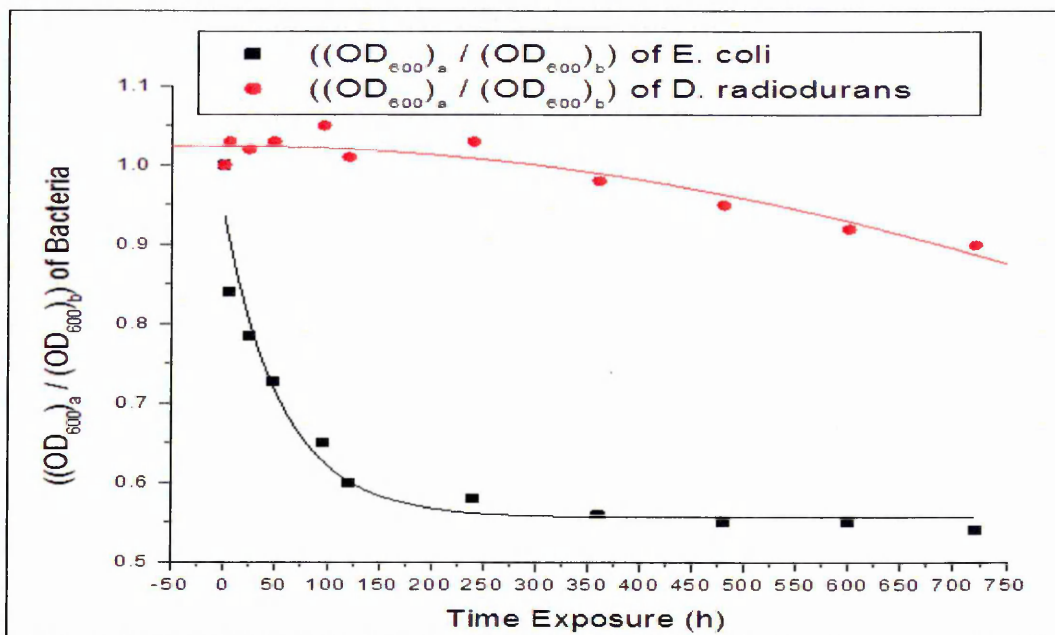


Figure 7.27. Dependence of normalized absorbance values for both *E. coli* and *D. radiodurans* bacteria on time of exposure to gamma ray ( $OD_{600}$  results) [6]

As mentioned in the  $OD_{600}$  experiments, the absorbance values recorded did not represent the actual absorption of the light by the samples but rather losses of light due to light scattering on live bacteria. The dead bacteria are sediment on the bottom of a spectroscopic cell and thus do not contribute to light scattering.

Finally, a series of experimental fluorescence spectral measurements were carried out on samples of both *E. coli* and *D. radiodurans* bacteria (see Figure 7.35), with the results presented in Figure 7.28. As has been mentioned in the above section, these peaks have nothing to do with fluorescence but correspond to a double excitation wavelength and appear as a second order of diffraction in the Carry Eclipse instrument. Typically, such peaks are regarded as parasitic in fluorescence spectroscopy, and are either eliminated using appropriate optical filters or ignored during discussion.

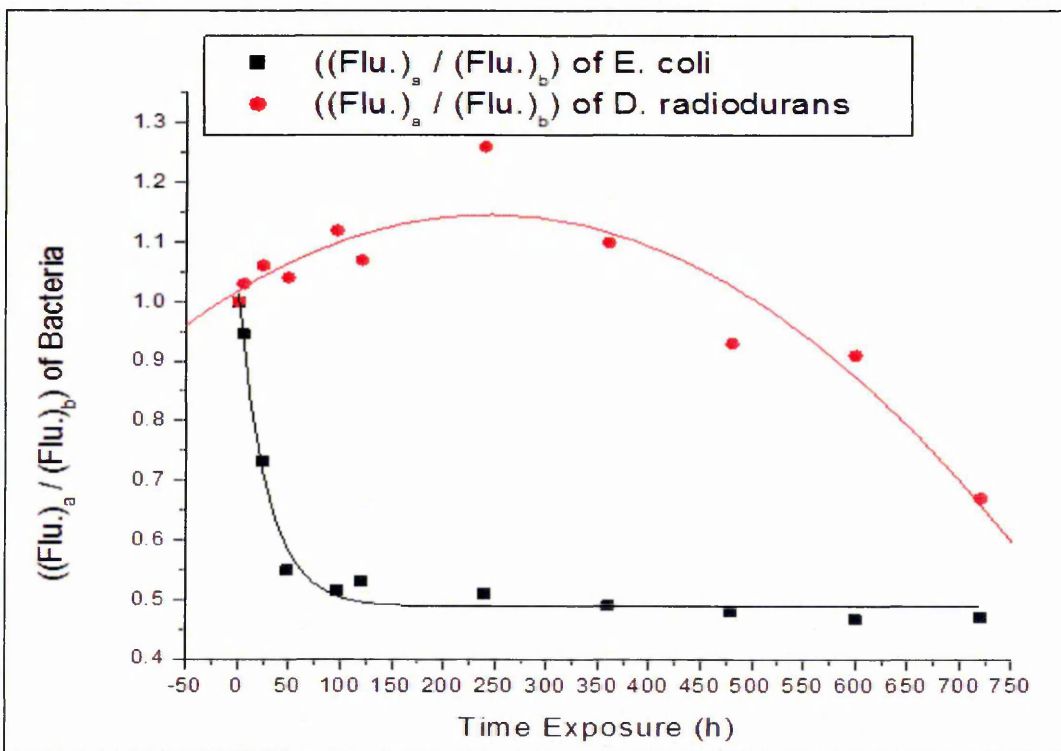


Figure 7.28. The effect of gamma rays on the 2nd order diffraction peak for *E. coli* and *D. radiodurans* bacteria [6]

However, in our experiments, the amplitudes were found to depend on the radiation dose and thus we decided to use this information in our study. The reason for such behaviour can be simply explained by light scattering on living bacteria, which in turn causes an increase in the 2nd diffraction order peak. As one can see, the peak at 630nm for *E. coli* tends to decrease with the increase in radiation exposure time, while for *D. Radiodurans* it rises at low exposure times and falls at high exposures to radiation. The

results of the effect of gamma radiation on the 2-nd order diffraction peaks for both types of bacteria are summarized in Figure 7.28, where the peaks were normalized by intensity levels before exposure to radiation. Similar to results in Figures 7.26 and 7.27, *E. coli* samples showed an exponential decrease in the peak intensity, while *D. radiodurans* showed an increase in peak intensity at low exposure times (up to 240 hours), followed by its gradual decrease at intermediate and higher exposure times (240-720 h).

It is important to highlight the different nature of the three methods used: fluorescence microscopy provides a direct means of recording live/dead bacteria ratios, though with limited accuracy, while the other two methods,  $OD_{600}$  and 2nd order of diffraction in fluorescence spectroscopy are both related to light scattering and give indirect but accurate accounts of live bacteria counts. All three optical methods complement each other and have shown exponential decay in response for *E. coli* with an increase in the radiation dose (characteristic decay time); while the response for *D. radiodurans* tends to increase a little at small radiation levels but then gradually decrease at higher doses.

It is interesting to compare the result of the optical study on the effect of gamma radiation on both *E. coli* and *D. radiodurans* bacteria. As has been mentioned, gamma radiation causes similar effects to all three optical characteristics in this study (L/D ratio, 2-nd order diffraction peak Fluorescence spectra, and optical density). In order to compare the above three characteristics, the relative response values (S) were calculated as ratios of parameters measured after and before exposure to gamma radiation:

$$S_1 = \frac{\text{Peak max. (after)}}{\text{Peak max. (before)}}, S_2 = \frac{OD_{600}(\text{after})}{OD_{600}(\text{before})}, S_3 = \frac{L/D(\text{after})}{L/D(\text{before})} \quad (7.6)$$

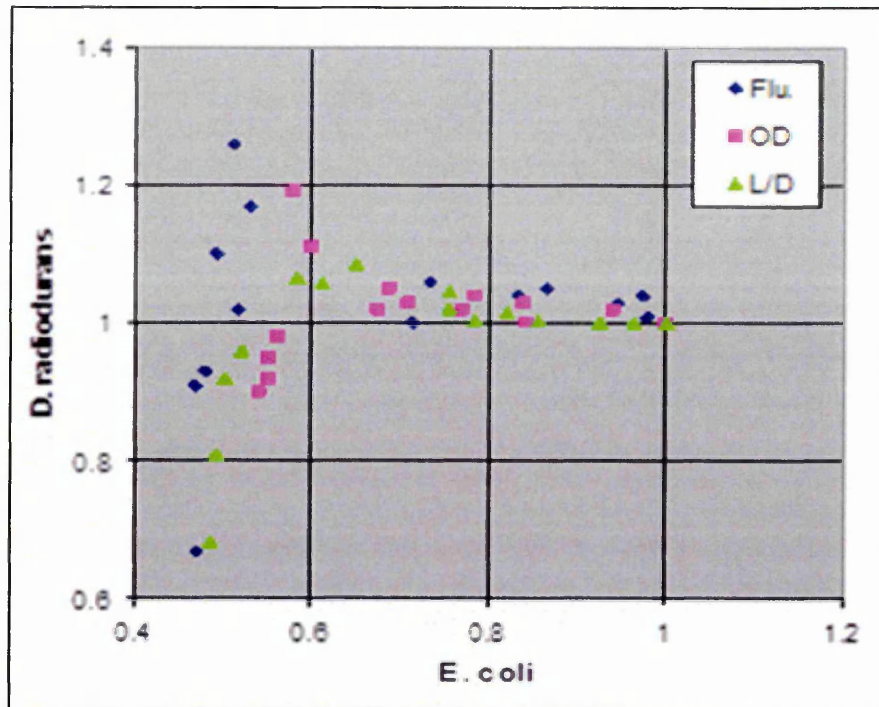


Figure 7.29. Comparison of relative responses of three optical methods to radiation for E.coli and D. radiodurans bacteria

The 2-D graph in Figure 7.29 shows relative responses (S1, S2 and S3; equation 7.9) of E. coli and D. radiodurans to gamma radiation, and proves that the results of all three optical methods are similarly affected by gamma radiation, since the data points appear to fall into the same area. From the experimental results, the fluorescence microscopy results are more reliable and confident in terms of identifying or counting exactly the live and dead bacteria. In addition, from Figure 7.29, the two optical techniques results appear to some extent to reflect the fluorescence microscopy results. The interpretation of these results involve both optical techniques (fluorescence spectroscopy and OD spectrophotometer) measuring the intensity of light scattered by particles (bacteria) that are suspended or swim in study samples. As mentioned, E. coli bacteria are motile, so the live bacteria are still swimming in the broth media and the dead bacteria are sedimented in a sample container, which does not contribute to the scattering of light. On the other side, the D. radiodurans bacteria are not motile, and then both the live and dead bacteria sediment in the sample container bottom. The dead bacteria, as a result of exposure to radiation, are sedimented faster than live bacteria, because the dead bacteria's membranes are cut or ruptured, which allows the broth liquid to penetrate inside the bacteria and become heavier, and also into the membrane pieces as well. Therefore the dead bacteria do not contribute to light scattering.

In the  $\gamma$ -radiation study, all three optical techniques revealed that *E. coli* bacteria (which belongs to a gram-negative bacteria type) are very sensitive to ionization radiation; the concentration of live *E. coli* bacteria appeared to decay exponentially with the increase of a  $\gamma$ -radiation dose with a characteristic time-frame, in the range of 35-38 h. *D. radiodurans* bacteria (which is a gram-positive bacteria) resists the radiation at low doses (the concentration of live bacteria increases slightly). However, they are damaged at high radiation doses (the bacteria concentration gradually decreases) [6].

**Reference:**

1. Bertani G, Studies on Lysogenesis I, (1952), The mode of phage liberation by lysogenic *Escherichia coli*, *Journal Bacteriology*, Vol. 62, pp. 293-300.
2. Lapage S., Shelton J. and Mitchell T., 'Methods in Microbiology', Norris J. and Ribbons D. (1970), Eds., Vol. 3, A., Academic Press, London.
3. Hsiu Li Lin, Chien Chung Lin, Yi Jen Lin, Hsiu Chen Lin, Chwen Ming Shih, Chi Rong Chen, Rong Nan Huang and Tai Chih Kuo, (2010), Revisiting with a Relative-Density Calibration Approach the Determination of Growth Rates of Microorganisms by Use of Optical Density Data from Liquid Cultures, *Appl. Environ. Microbial*, vol. 76, no. 5, pp. 1683-1685.
4. Guennadi Sezonov, Danièle Joseleau Petit, and Richard D Ari, (2007), *Escherichia coli* Physiology in Luria-Bertani Broth, *Journal of Bacteriol.* Vol. 189(23), pp. 8746-8749.
5. Venkateswaran A, (2000), Physiologic determinant of radiation resistance in *Deinococcus radiodurans*, *Applied and Environmental Microbiology*, pp. 2620-2626.
6. Al-Shanawa M, Nabok A, Hashim A, Smith T, Forder S, (2014), Optical Study of the Effect of Gamma Radiation and Heavy Metals on Microorganisms (Bacteria), *BioNanoSci*, Vol. 4, pp. 180-188.

## CHAPTER 8

### Electrical Study of Bacteria: the Effect of Gamma Radiation

As was presented in Chapter 7, bacteria samples were exposed to gamma radiation for different amounts of time. Several electrical experimental techniques (DC and AC characteristics) were used to test and analyse the same bacteria samples that were tested optically, showing the effect of gamma radiation doses on bacteria density.

#### 8.1. Samples Tested by Electrical Techniques

The effect of gamma radiation on bacteria samples were investigated during the study of the electrical properties of bacteria samples of both *E. coli* and *D. radiodurans*. The main aim of this part of the work is to develop a simple electrochemical sensor for the detection of  $\gamma$ -radiation and heavy metals using bacteria. A series of DC and AC electrical measurements were carried out on samples of two types of bacteria, namely *Escherichia coli* and *Deinococcus radiodurans*. A study of the effect of  $\gamma$ -radiation on DC and AC electrical characteristics of bacteria were carried out. As a first step, a correlation between DC and AC electrical (IV, conductivity, capacitance) and bacteria concentration has to be established.

The main target of this part of research is to utilise electrical properties of bacteria for the development of novel, simple, and cost effective methods for monitoring environmental pollutants, particularly radionuclide's and heavy metals being common contaminants of water resources [1,2]. Microorganisms such as bacteria are very sensitive to  $\gamma$ -radiation produced by radionuclide's [3, 4]. Identification of the types of pollutants in the environment and the evaluation of their concentration is a much more difficult task, which is impossible to solve using a single sensor. However, the sensor array approach utilising several types of bacteria being inhibited differently by different types of pollutants could solve the above problem [5]. Electrochemical measurements were successfully used for studying electrical properties of cells deposited on metal electrodes and showed great prospects of using such cell-based sensors for detection of various analytes [6,7]. Therefore, the principles of cell-sensors were extended further to using bacteria (*E. coli* and *D. radiodurans*).

#### 8.2. Samples Preparation and Measurements

The cultivated bacteria density and changes in the live bacteria counts after exposure to radiation were recorded with Optical Density Photometer (6715 UV-visible

Spectrophotometer JENWAY OD<sub>600</sub>). All electrical measurements were performed in a simple, sandwich-type form [8]. The cell schematically shown in Figure 6.4 has a PTFE body and contains a platinum counter electrode, and a gold-coated glass slide acting as working electrode sealed against the cell via rubber O-ring. The cell has inlet and outlet tubes, allowing the injection of liquid broth containing bacteria.

DC electrical tests were performed, using (6517A Keithley Electrometer) in a voltage range of  $\pm 0.5V$ , the measurements were done from  $-0.5$  to  $+0.5V$  voltage range in order to avoid oxidation and to reduce electrochemical reactions on metal electrodes, the IV relative (correlation) was studied.

AC electrical measurements were performed using (HP-4284A PRECISION LCR METER) in the frequency range 20 Hz to 1 MHz, with the amplitude of the AC voltage at 100mV and no DC bias applied. The spectra of two parameters,  $G_p$  and  $C_p$ , corresponding to a parallel connection of conductance and capacitance, were recorded.

### **8.3. DC Electrical Measurements of Bacteria**

First, in order to optimise conditions for DC characterisation of bacteria samples, the DC electrochemical measurements of LB liquid samples containing different concentration of E coli bacteria were performed in three-electrode cell. The cyclic voltammograms (CV) used DropSens ( $\mu$ STAT 200) potentiostat and three-electrode printed assemblies, comprising gold working and counter electrodes and an Ag/AgCl reference electrode. As mentioned before in Chapter 6, a three electrodes electrochemical set up is more stable than two electrodes, as it contains an additional reference electrode having a stable electrochemical potential invariant of applied voltage and the chemical composition of a solution; for this the CV characteristics of E coli bacteria samples measured in three-electrode system are given in Figure 8.1. As one can see, there is a “window” between  $-0.3V$  and  $+0.4V$  where the current is negligible, such a window was selected for further AC measurements. The cathodic current at  $V \geq -0.3V$  is most likely related to the reduction of Hydrogen. Both anodic and cathodic currents were not too high, thus the measurements performed in a two-electrode cell at a voltage between  $+0.5V$  and  $-0.5V$ . Figure 8.2 shows the correlation at  $I_c$  and  $I_a$  with bacteria concentration.

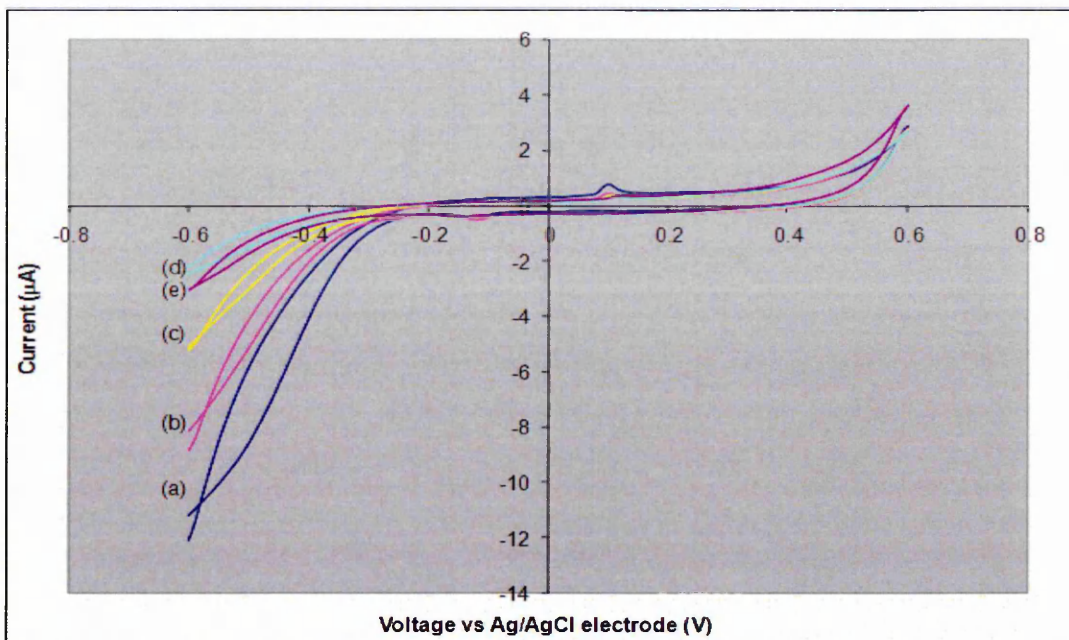


Figure 8.1. Current and Voltage characteristics recorded on LB broth (a) and *E. coli* samples of different dilutions: 1:10 (b), 1:5 (c), 1:2 (d), and stock solution ((e)~  $OD_{600}=2.1$  Abs)

From Figure 8.1, the three electrodes cell showed very useful results during studied the IV properties, especially at the cathodic current ( $I_c$ ), which is been sensitive to change of the bacteria density.

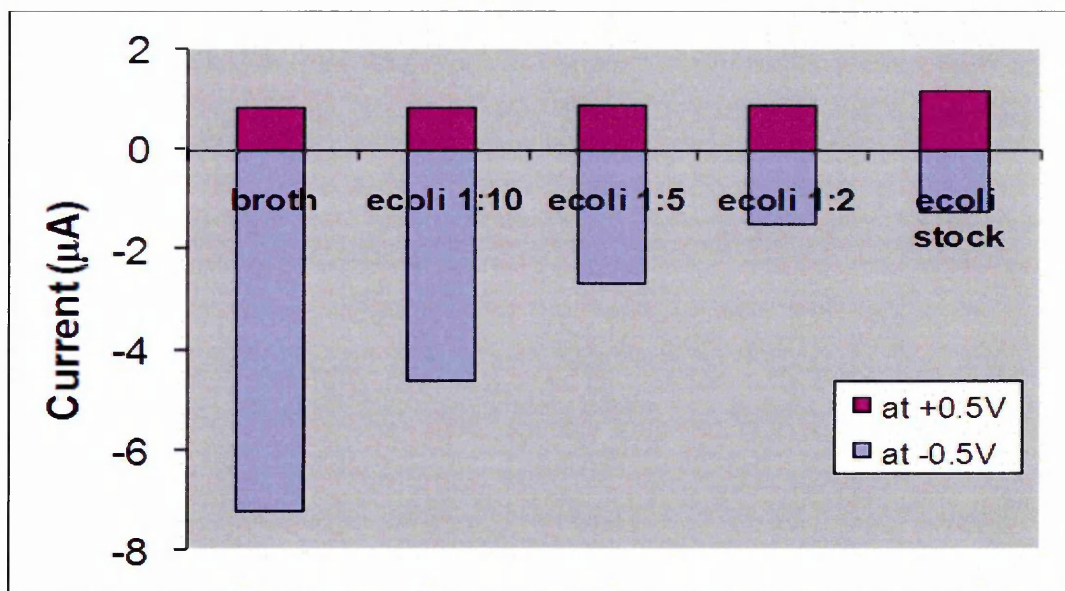


Figure 8.2. Values of anodic and cathodic current at ( $\pm 0.5V$ ) for different concentration of *E. coli* bacteria

Further study was therefore carried out and more analyses were performed, using electrochemical window of  $\pm 0.5V$ , and the resulting data are presented in Figure 8.3.

DC conductance correlates with E. coli concentration which was measured in optical density ( $OD_{600}$  in unit Abs.).

It is clear that the presence of E. coli bacteria reduces the DC conductance of solution and thus the current.

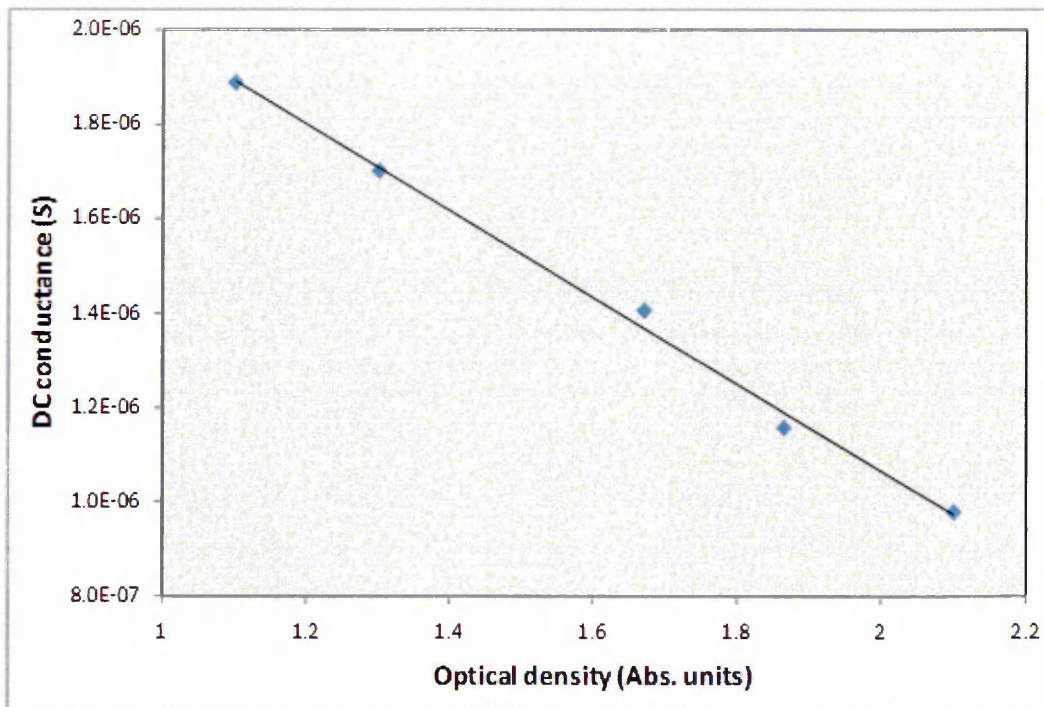


Figure 8.3. DC conductance from cathode current at -0.5V versus bacteria concentration of E. coli

The DC characteristics of bacteria samples using three electrodes system were studied, as presented in Figure 8.3, and the correlations with E. coli concentration was assessed, which justifies the use of a simple cell for further sensor development.

Typical I-V characteristics of E. coli samples having different concentrations of bacteria measured in two electrodes cell are shown in Figure 8.4. The results appeared to be similar to those recorded in three electrodes cell. The cathode current appeared to be much higher than anode current. The increase in bacteria concentration in the solution led to a decrease in the cathode current. This could be explained as a result of bacteria blocking the current by acting as an insulator [9]. Figure 8.4 shows typical DC I-V characteristics of E. coli samples of different concentrations measured in absorption (Abs.) units of optical density ( $OD_{600}$ ): (1) 0.375, (2) 0.734, (3) 1.57, (4) 1.87, (5) 2.08, (6) 2.33.

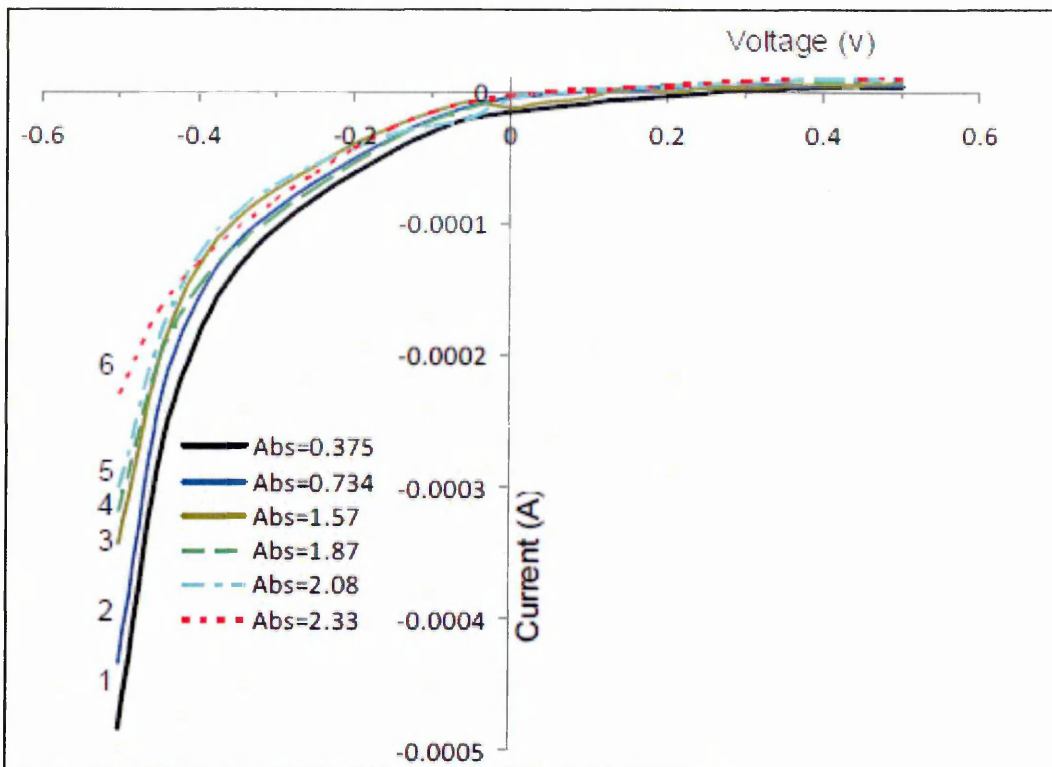


Figure 8.4. Typical DC I-V characteristics of *E. coli* samples of different concentrations measured in Abs units of optical density ( $OD_{600}$ )

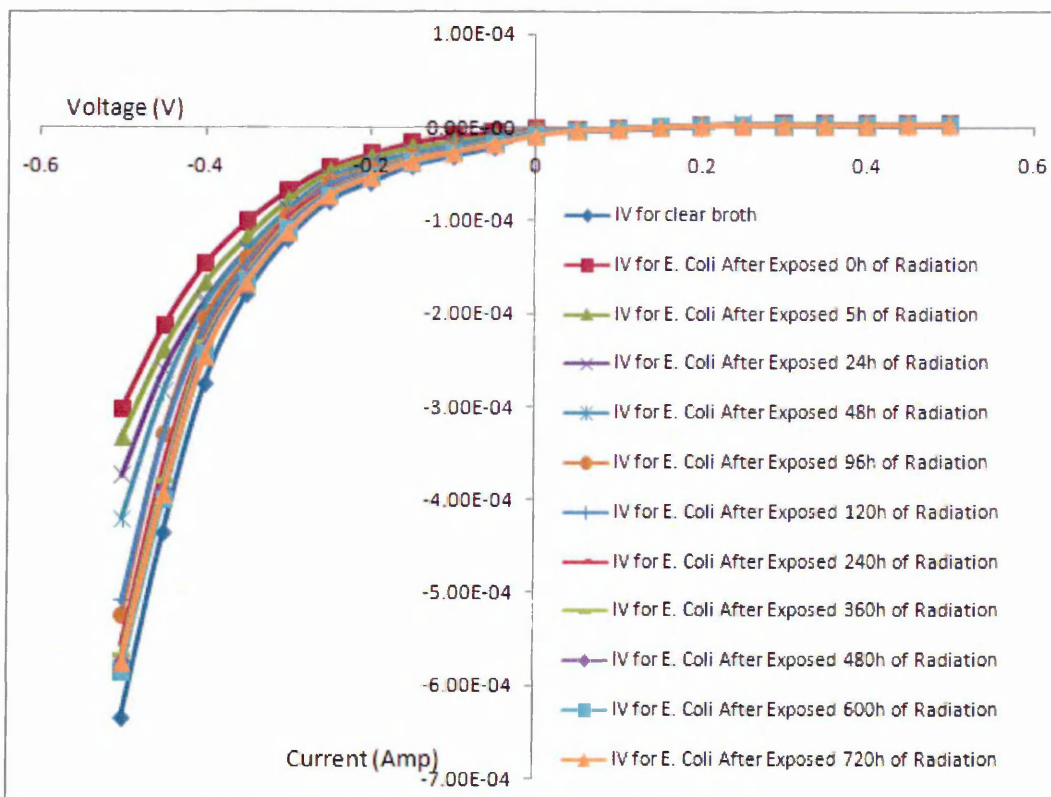


Figure 8.5. I-V characteristics of *E. coli* samples for different time exposure to gamma radiation

The effect of exposure for different periods (different doses) to gamma radiation on E. coli bacteria samples are plotted in Figure 8.5, which presents the I-V characteristic as a function of time exposure. As one can see, the cathode current showed clear sensitivity to radiation. This response of the cathode to the radiation (to the change in concentration of bacteria after being exposed to radiation) was utilised to evaluate the radiation level due to measuring the current in the cathode for (-0.5 V). On the other hand, the bacteria samples not exposed to radiation were also tested electrically in order to study the effect of environment on bacteria and normalised bacteria from the samples were exposed to radiation (see Figure 8.6).

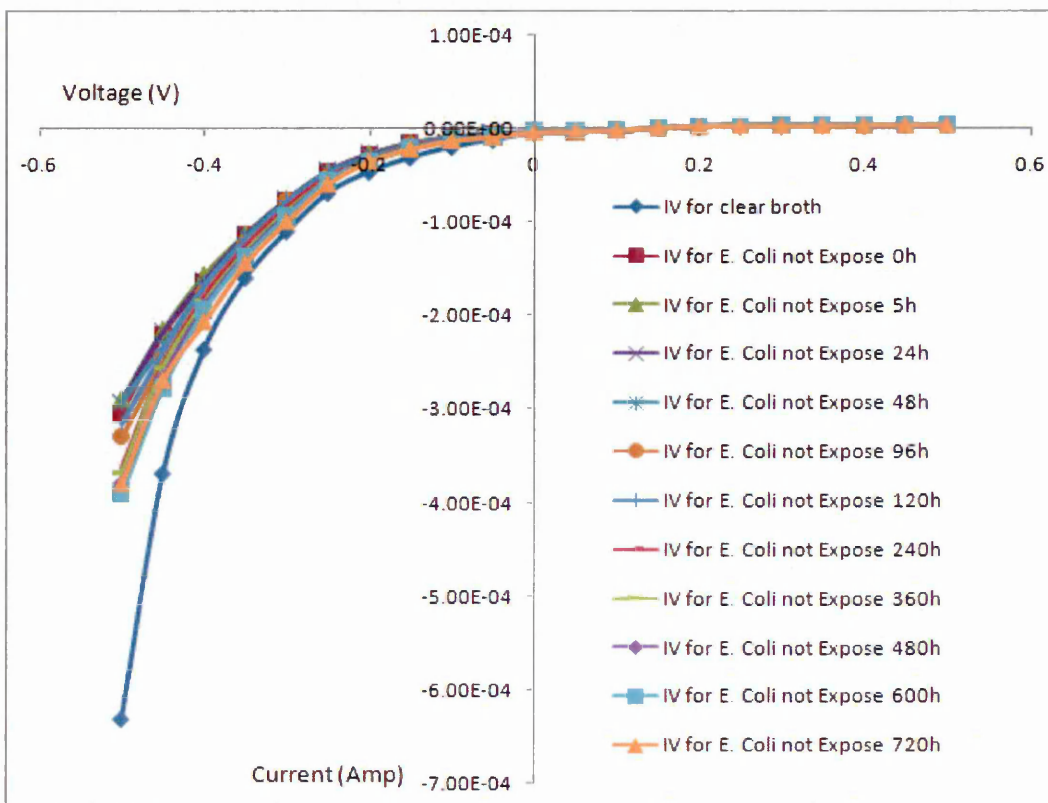


Figure 8.6. I-V characteristics of E. coli samples not exposed to gamma ray

The effect of  $\gamma$ -radiation on cathodic and anodic DC current is illustrated in Figure 8.7. As one can see, DC conductivity of E. coli bacteria samples increased as the radiation dose increased; the reason being that the increase in the gamma radiation dose affected the number of live bacteria, which decreases exponentially (see Figures; 7.6, 7.9, 7.10, and 7.16 in Chapter 7).

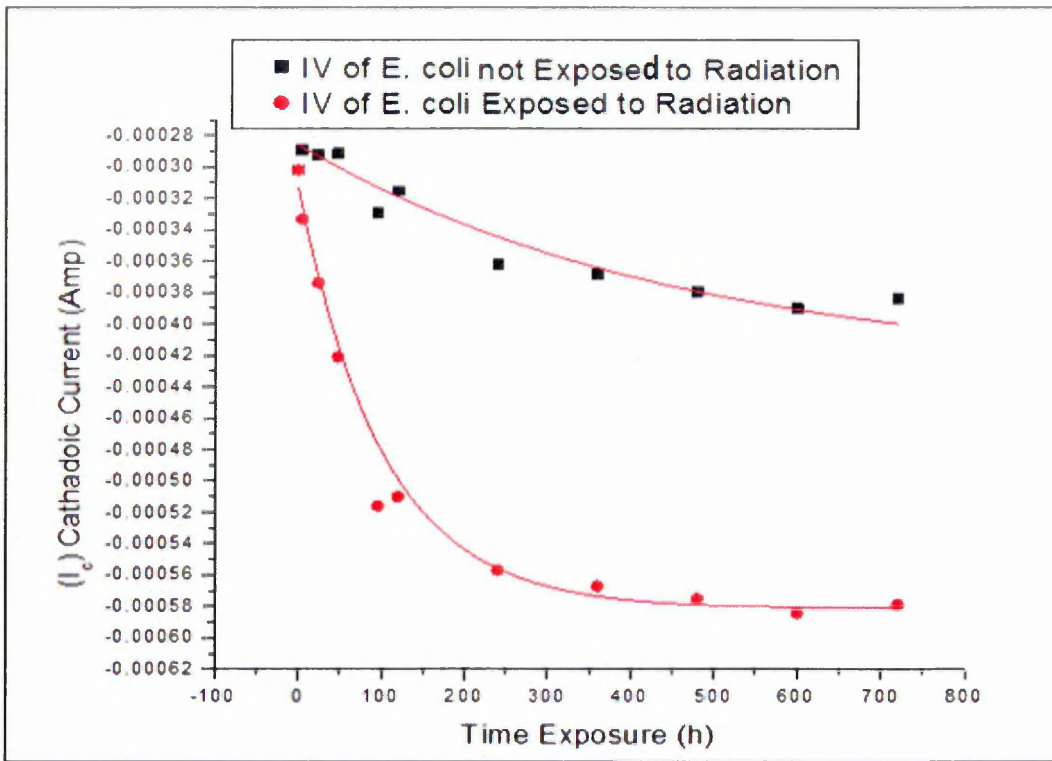
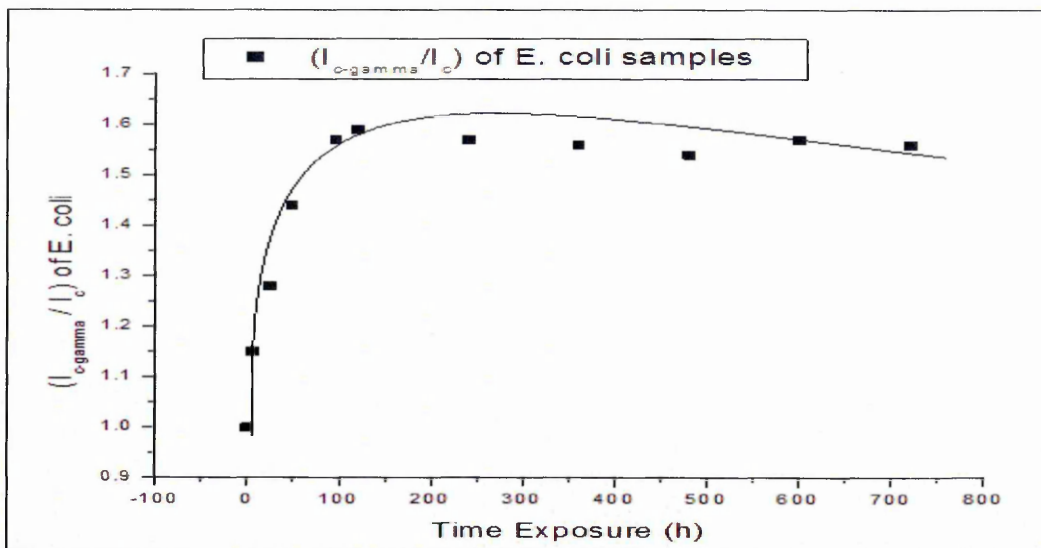


Figure 8.7.  $I_c$ (cathode current) at (-0.5 Volte);E. coli samples for different time exposure to gamma radiation dose, and other samples not exposed to radiation

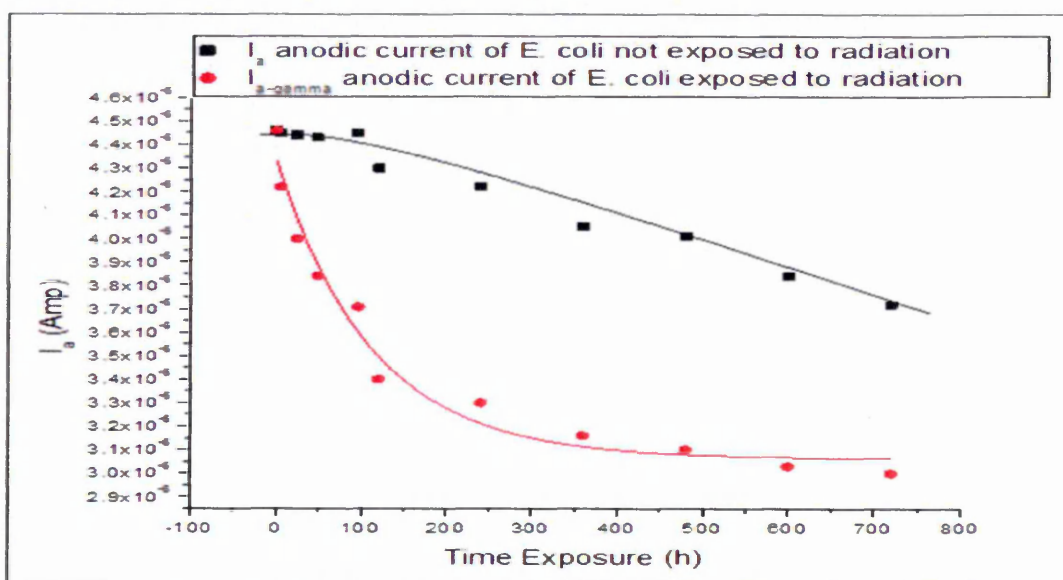
The behaviour of the cathode current of (E. coli) for the gamma dose is exponential. On the other hand, the E. coli samples not exposed to radiation were studied and analysed as well, and the DC measurement showed exponential decay in I-V characteristic against time out of the irradiator system. The effect of radiation on the E. coli bacteria sample was clearly dependent on the time variable.

The ratio between the two samples (the first one exposed to gamma radiation over the second one, not exposed) increased sharply at a low dose (short time exposure) because the radiation affected the bacteria; in the meantime, the bacteria samples not exposed remained alive. At intermediate and high doses the ratio decreased and eventually reaches a stationary phase, since bacteria in non-irradiator samples started to die under non-optimal environmental conditions, Figure 8.8 illustrates how the E. coli bacteria sensor was more reliable for use at low radiation doses, of up to (120h $\approx$ 240000mSv).



Figures 8.8.  $(I_{c-\text{gamma}} / I_c)$  cathode current ratio at (-0.5 Volte) E. coli samples for different time exposure to gamma radiation dose over current of samples not exposed to radiation

Figure 8.8 shows the relation between the current at the cathode for samples exposed, divided by the current at the cathode of samples not exposed to radiation for different time periods. As one can see the stationary ratio between the E. coli samples as a function of time exposure started at 120h, which means that the E. coli bacteria started to die at normal environment effects after 120h. At the anode current, the data for the samples exposed to radiation and the samples not exposed are presented in Figure 8.9. The effect of radiation on bacteria samples is clear here. Since  $I_a$  is much smaller than  $I_c$ , it was decided to use only  $I_c$  for DC analyses.



Figures 8.9.  $I_a$  anodic current at 0.5 V: E. coli samples for different time exposure to gamma radiation dose (red), and samples not exposed to radiation (black)

In order to build the sensor array for detecting gamma radiation the second type of bacteria, *D. radiodurans*, were also exposed to gamma radiation. To meet this goal, the typical I-V characteristics of *D. radiodurans* samples having different concentrations of bacteria are plotted in Figure 8.10. The cathode current appeared to be much larger than that at the anode, due to bacteria density. The increase in bacteria concentration in the solution led to a decrease in the cathode current and an increase in the current at the anode. The adsorption type of bacteria could explain this. Figure 8.10 gives typical DC I-V characteristics of *D. radiodurans* samples of different concentrations measured in Abs. units of optical density ( $OD_{600}$ ): (a) 0.23 Abs, (b) 0.53 Abs, (c) 0.86 Abs, (d) 1.1 Abs, (e) 1.35 Abs, (f) 1.51 Abs.

The *D. radiodurans* bacteria samples exposed to radiation were also tested electrically, in order to study the effect of gamma radiation on bacteria.

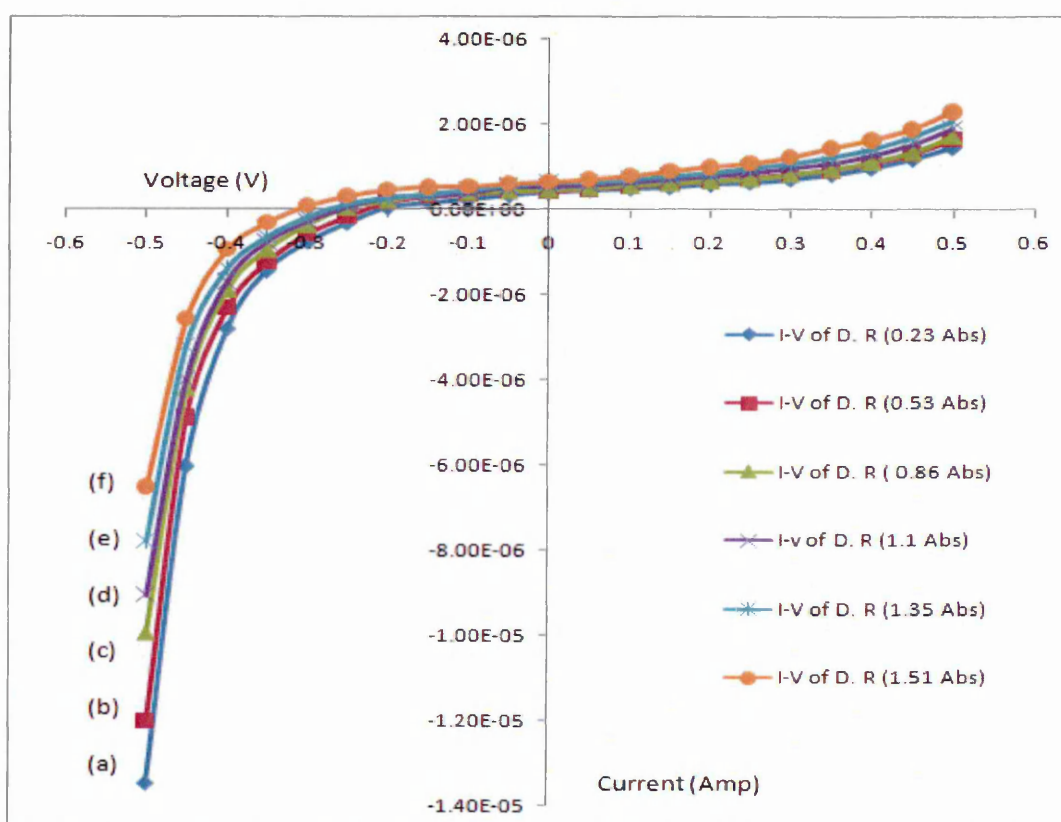


Figure 8.10. Typical DC I-V characteristics of *D. radiodurans* samples of different concentrations measured in Abs units of optical density ( $OD_{600}$ )

The *D. radiodurans* bacteria samples were exposed for different periods to gamma radiation from source  $Co^{57}$ . The effect of radiation, shown in Figure 8.11, as explained before, is to catalyse the bacteria to increase during short-term exposure, again

enhancing the bacteria immune system produced and increasing the different kinds of proteins and amino acids [10]. At intermediate and high radiation doses the bacteria started to die and the number of live bacteria decreased. Figure 8.11 shows the (I-V) characteristic of *D. radiodurans* after exposure to gamma radiation for different time exposures.

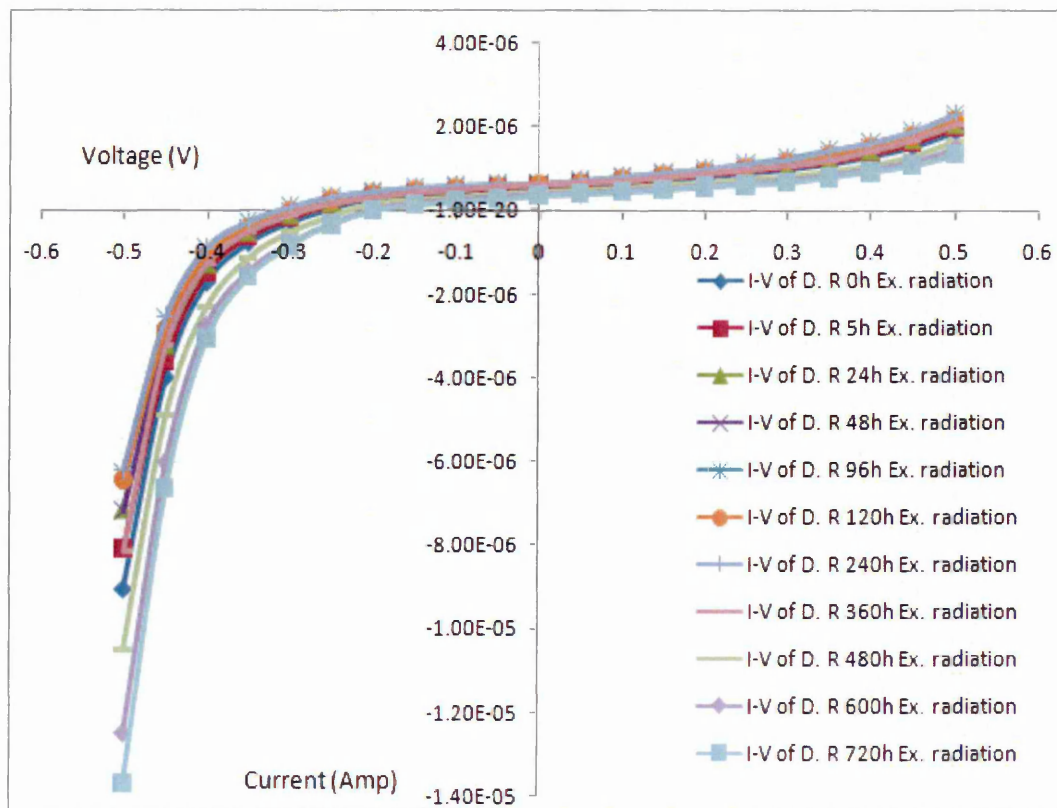


Figure 8.11. I-V characteristics of *D. radiodurans* samples with different time exposures to gamma rays

In order to study the effects of the environment on the *D. radiodurans* samples, the samples not exposed were tested electrically, the results of which are presented in Figure B1 (Appendix B). The results showing that there is little change in the current regarding to the time that samples remain in normal environment conditions, which is very clear when you observe the cathode and anode currents closely.

The current at the cathode was very sensitive to alterations in the number of live bacteria, which was already related to or changed directly during the period of exposure to gamma radiation. This response of the cathode current is shown in Figure 8.12, for both *D. radiodurans* bacteria samples, both exposed and not exposed to gamma radiation.

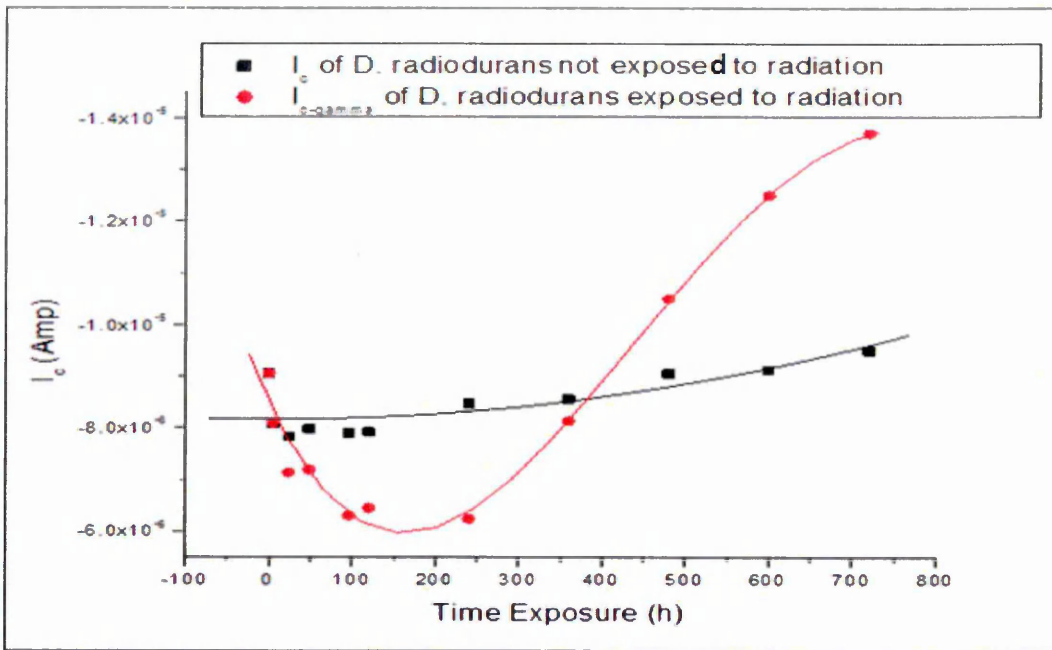


Figure 8.12. Change in current at cathode electrode of *D. radiodurans* in (-0.5V) for different exposure times

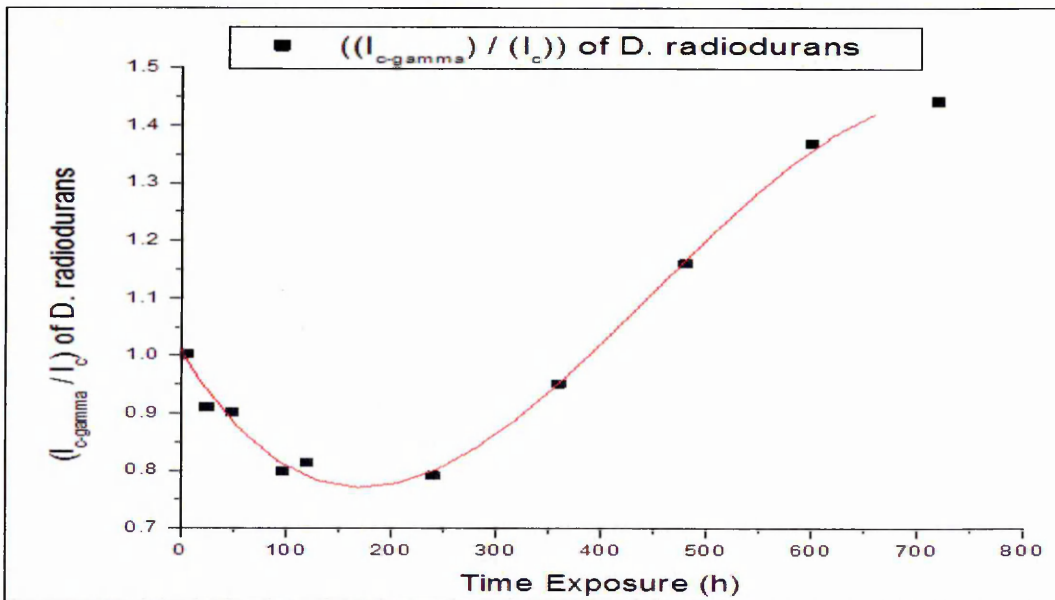


Figure 8.13. Current at cathode electrode ratio for bacteria exposed to radiation over cathode current for bacteria samples not exposed to radiation

Figure 8.13 shows the current at the cathode electrode for the *D. radiodurans* bacteria exposed to radiation after being normalised over the cathode current values for bacteria samples not exposed to radiation. Figure 8.14 presents a comparison between the relative responses of DC characteristic for the radiation of *E. coli* and *D. radiodurans* bacteria; this comparison being very important and useful for estimating the radiation dose level as a function of the current at the cathode. As one can see when obtaining the

value of the normalised cathode current for each bacteria sample, the radiation dose can be found from the curve of Figure 8.15; the time exposure referring to the radiation dose, which was 1 *heure*  $\approx 2000mSv$ .

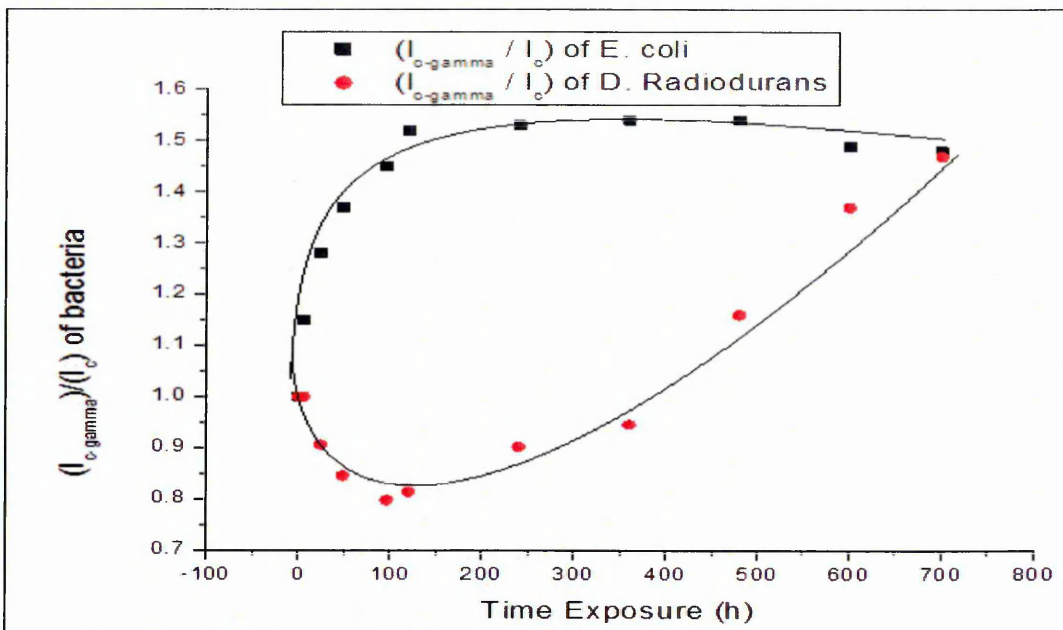
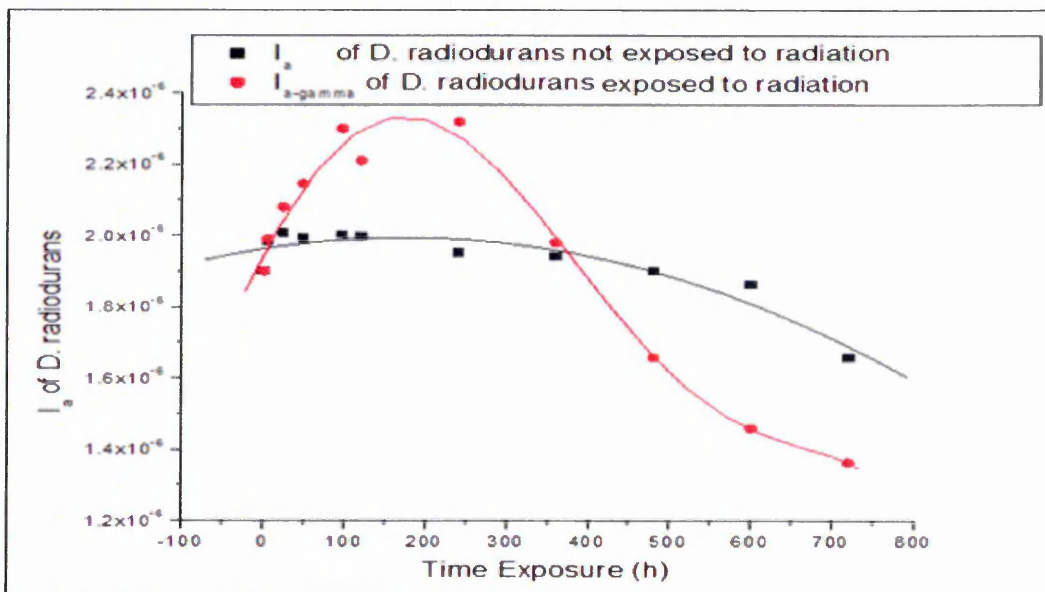


Figure 8.14. Comparison of relative responses of DC characteristic ( $I_c$  cathodic current) methods to radiation for E.coli and D. radiodurans bacteria



Figures 8.15.  $I_a$  anodic current at 0.5 V: D. radiodurans samples for different time exposures to gamma radiation dose (red), and samples not exposed to radiation (black)

The current at the anode is presented in Figure 8.15, where some samples were not exposed to radiation and some were. The analysis shows the data is similar to that of the

cathodic current. However, because the anodic current is much smaller than the cathodic current, it was decided to use only DC cathodic current.

#### 8.4. AC Electrical Measurements of Bacteria

The correlation between the AC electrical properties of liquid bacteria samples and live bacteria counts were established using the simple two electrodes cell sensor. Typical AC conductance (AC-Gp) graph of *E. coli* samples having different concentrations of bacteria are shown in Figure 8.16.

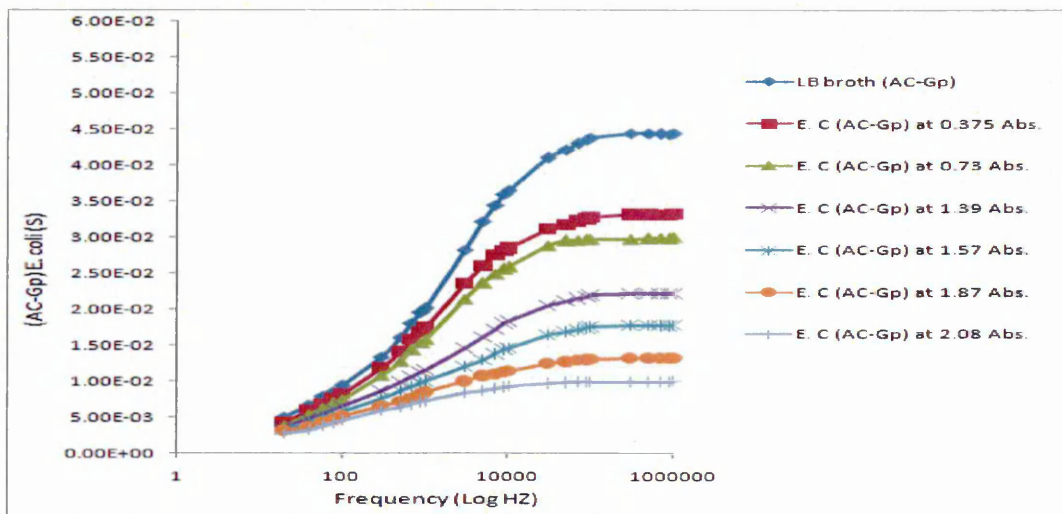


Figure 8.16. Typical AC-Gp characteristics of *E. coli* samples of different concentrations measured in Abs units of optical density ( $OD_{600}$ )

In addition, the changes in the capacitance of different concentrations of *E. coli* bacteria were studied. Figure 8.17 shows the capacitance exhibits maximum variation at low frequencies (20 Hz) and decreasing by 4-5 orders of magnitude at 1MHz. The increase in bacteria concentration leads to larger capacitance values, which can be interpreted to mean that the bacteria work as isolation materials. The increase in bacteria concentration leads to an increase in capacitance and a decrease in solution conductance.

Figure 8.17 shows the behaviour of the AC capacitance ( $C_p$ ) of *E. coli* bacteria, the capacitance is high at low frequency, but decreasing sharply at high frequency. In addition, the capacitance showed a clear and different response regarding the change in the bacteria density. These were found in the capacitance quantity and conductance at high frequency, especially at 900 KHZ. Figure 8.18 shows the capacitance trend as a function of bacteria density in a unit of Abs.

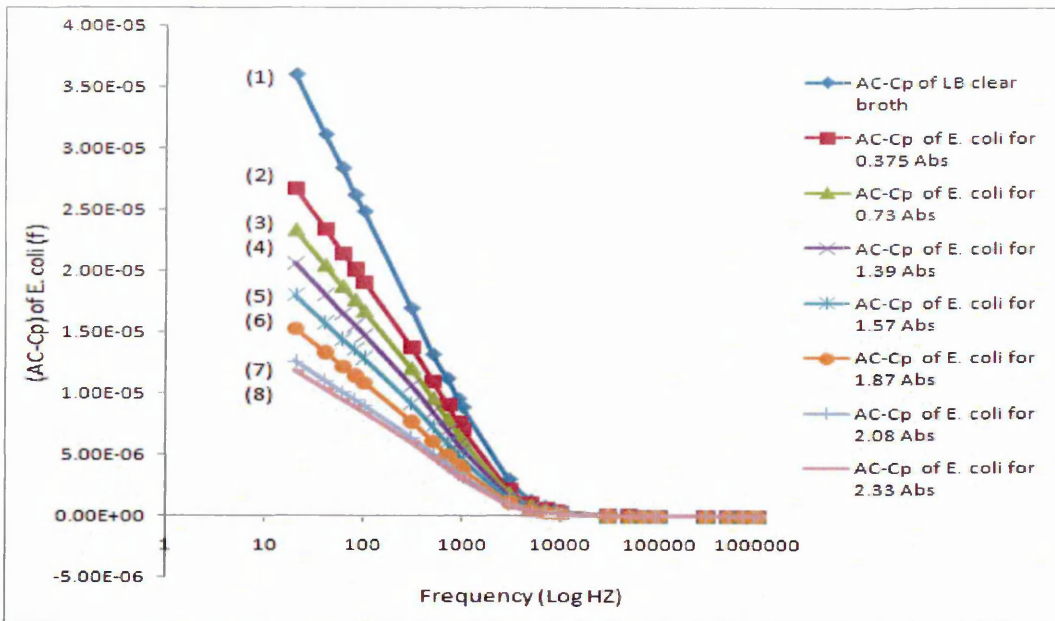


Figure 8.17. Spectra of Cp for E. coli bacteria samples of different concentrations in optical density Abs units: (1) clear broth, 0.0 Abs, (2) 0.375 Abs, (3) 0.73 Abs, (4) 1.39 Abs, (5) 1.57 Abs, (6) 1.87 Abs, (7) 2.08 Abs, and (8) 2.33 Abs

There was a peculiarity of Cp spectra observed at high frequency close to 1MHz (see Figure 8.18). The values of Cp are very low and do not affect over all shape of Cp spectra in Figure 8.19. This is most likely the instrumental error at the end of frequency range. However for further analysis we used the maximum values of Gp and Cp.

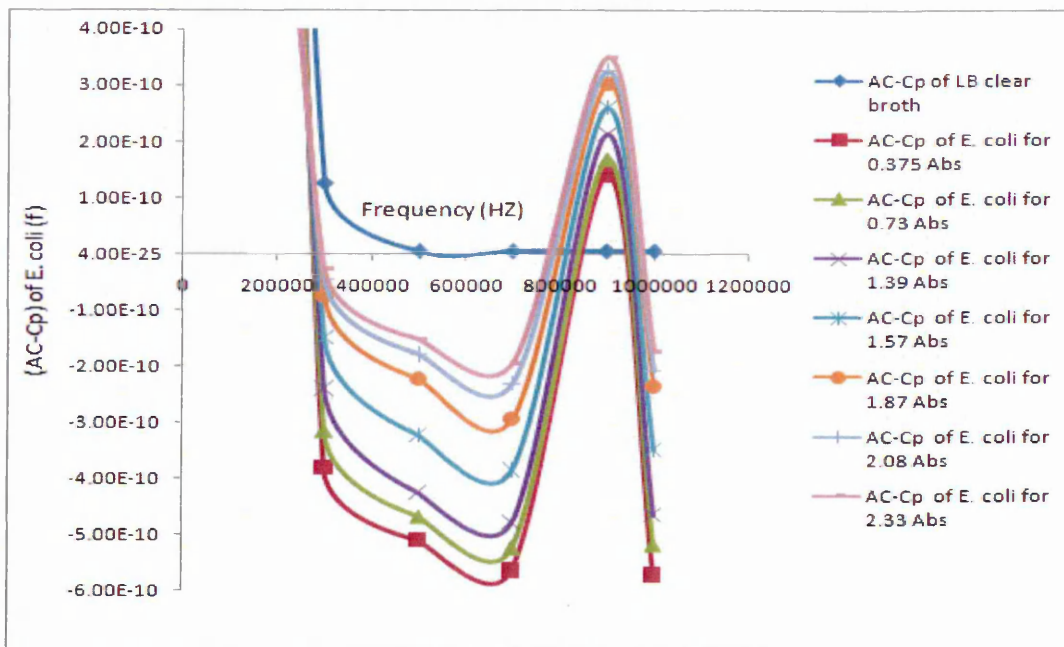


Figure 8.18. Spectra of Cp for E. coli bacteria samples of different concentrations presented in optical density Abs units: the negative capacitance maybe refer to the conductance (short current)

The *E. coli* bacteria were exposed to gamma radiation, in order to study the effect of radiation. The AC characteristics after and before exposure to radiation were also studied. The change in the conductance of Bacteria samples gave a good indicator (see appendix B Figures B2 and B3) for estimating the radiation level; the bacteria cell sensor was used for this task.

The *E. coli* bacteria which was not exposed to radiation were examined electrically (AC-conductance) in order to study the effect of non-optimum environment on bacteria. The data for exposed samples were normalised over the data for the samples not exposed to radiation, again in order to find out the effect of radiation. The changes in the AC conductance of *E. coli* bacteria as a function of time at 900kHz were plotted in Figure 8.19. A comparison curve of cell conductance was built, which is used to estimate gamma radiation levels. From the conductance data, at 900 kHz, the curve was plotted, see Figures 8.19, 8.20.

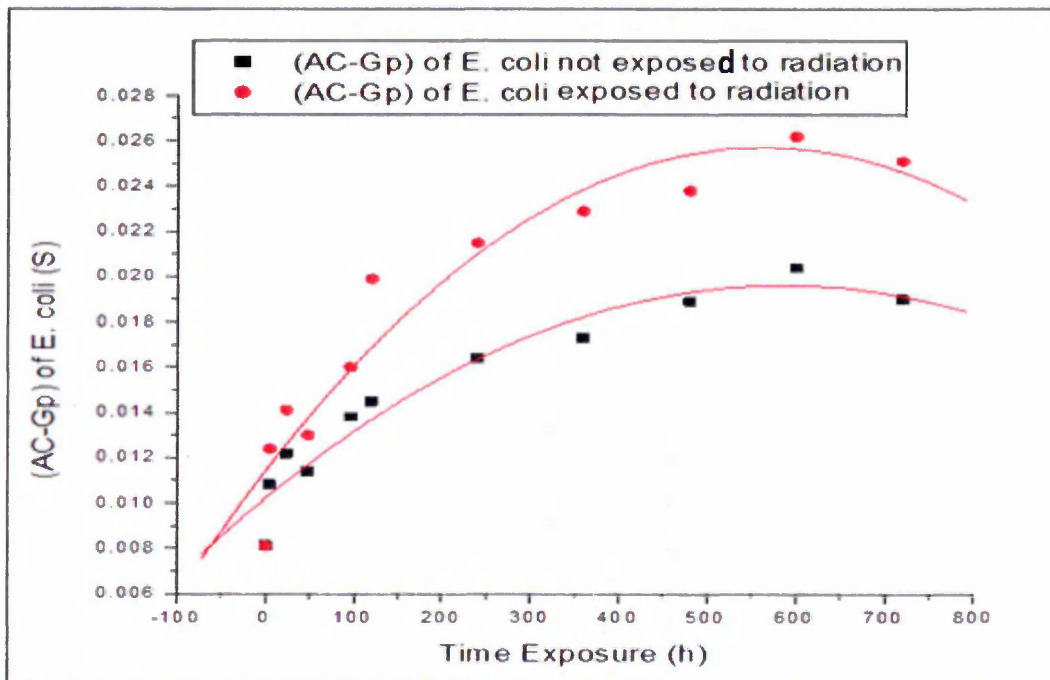


Figure 8.19. Change in the AC conductance of *E. coli* bacteria as a function of time at 900kHz

The ratio of the AC conductance of *E. coli* bacteria exposed to radiation over to the AC conductance of bacteria not exposed to radiation was calculated and plotted in Figure 8.20. The radiation dose can estimated due to measure the normalised conductance of *E. coli* bacteria samples.

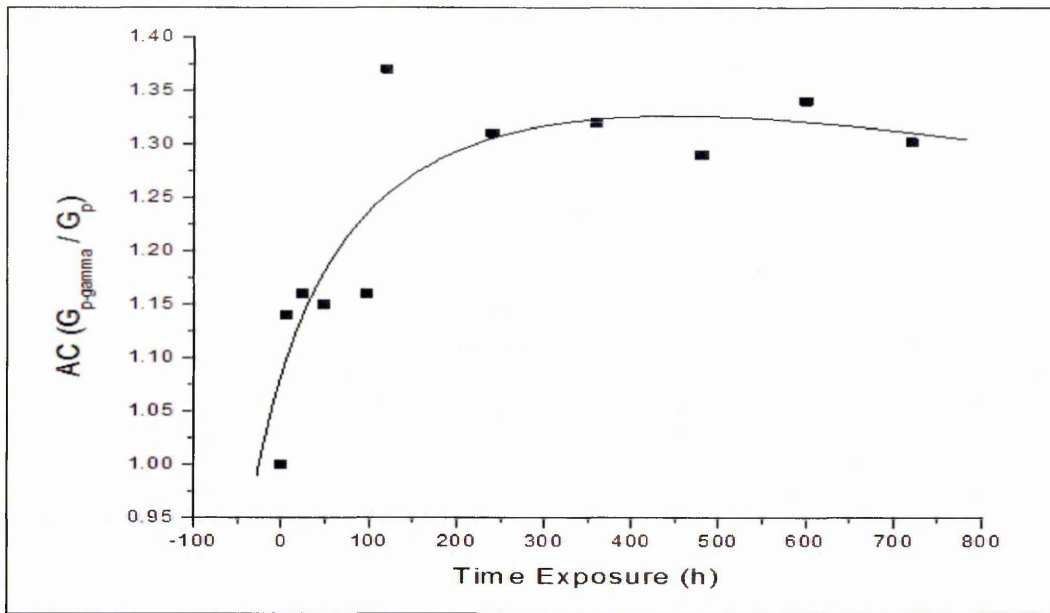


Figure 8.20. AC conductance ratio of E. coli bacteria after exposure to radiation to the conductance for samples not exposed at 900 KHz

Figure 8.21 shows the AC capacitance of bacteria sample exposed to the radiation, which can be easily evaluate the capacitance in relation to the time exposure period, which is equivalent to ( $1h \approx 2000mSv$ ). The effects of gamma radiation on E. coli bacteria were investigated through studying the relation between the AC capacitance for E. coli bacteria and the radiation dose, as Figures 8.21 and 8.22 illustrate.

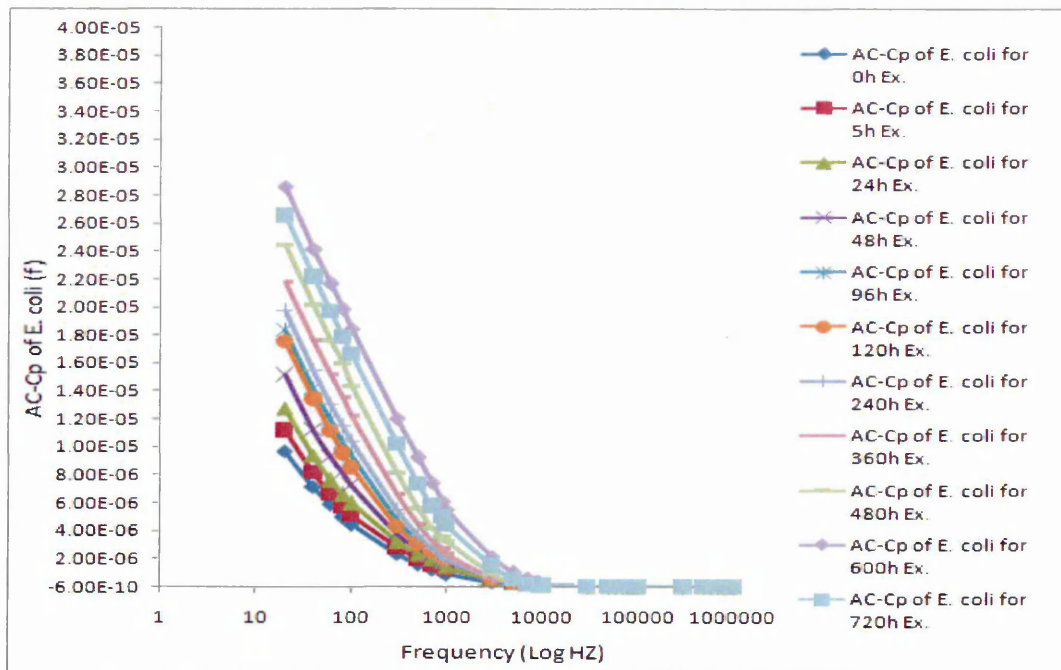


Figure 8.21. AC capacitance of E. coli samples by time exposure to gamma radiation

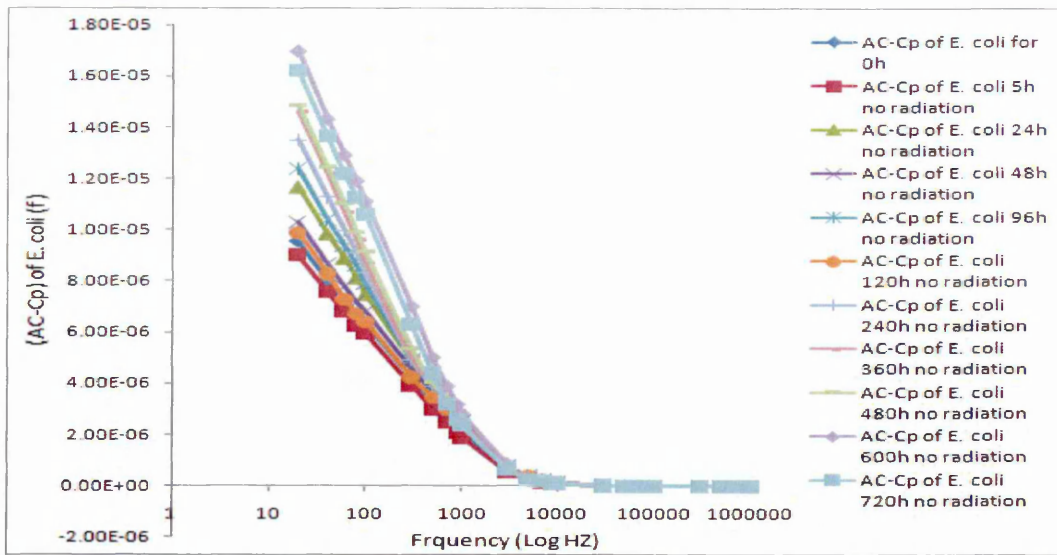


Figure 8.22. AC capacitance of E. coli samples not exposed to gamma radiation for different time periods, kept outside irradiator system

In order to study the effect of non-optimum environment on bacteria, the E. coli samples were located outside the irradiator system, the same environmental condition as the exposed samples. The data for exposed samples were normalised to the samples not exposed to radiation, in terms of the effects of radiation. Figure 8.25 illustrates the AC capacitance of E. coli bacteria not exposed to radiation. In order to find a reliable approach to estimating the gamma radiation level, the change in the AC capacitance of E. coli bacteria at high frequency were plotted as a function of time at 900kHz, as presented in Figure 8.22.

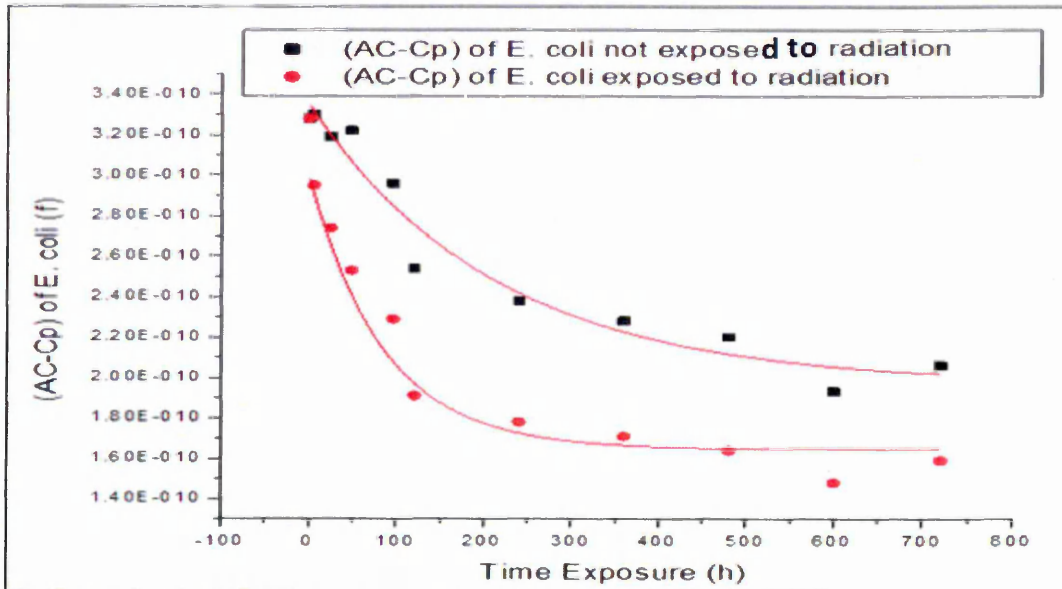


Figure 8.23. Change in the AC capacitance of E. coli bacteria as function of time for exposed bacteria samples and not exposed samples at 900kHz

The data in Figure 8.22 has been normalised; the ratio between AC capacitance of samples exposed to gamma radiation over the AC capacitance of samples not exposed is presented in Figure 8.23.

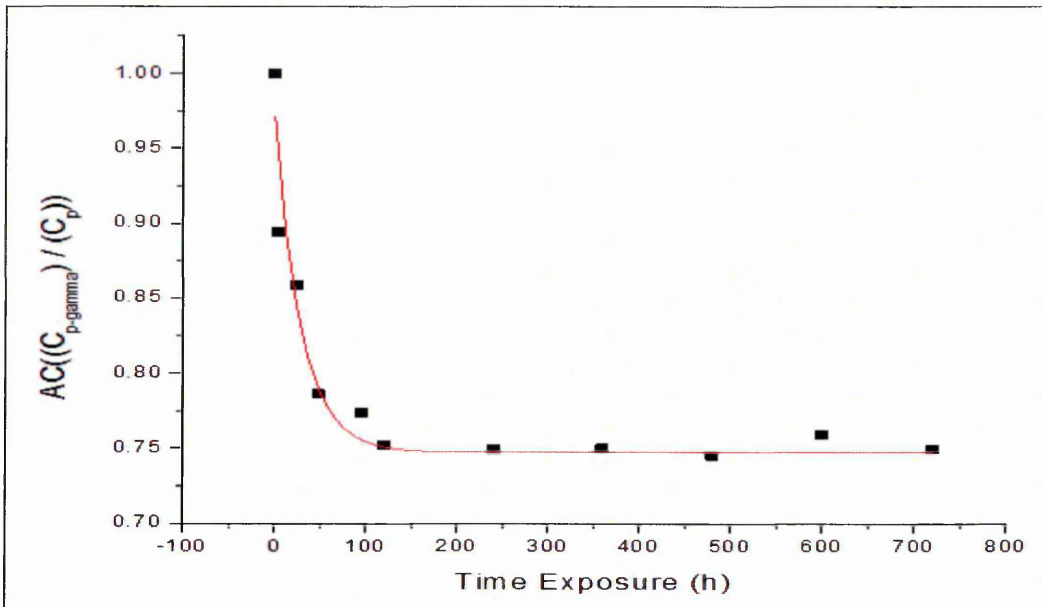


Figure 8.24. AC capacitance ratio of *E. coli* bacteria after exposure to radiation to capacitance for samples not exposed at 900kHz

The fitting equation (8.1) describes the behaviour of graph (8.23):

$$\left( \frac{C_{p-\gamma}}{C_p} \right)_{E.coli} = 0.75 + 0.22 * e^{(-t/29.6)} \quad (8.1)$$

As shown in equation (8.1), if the ratio of the capacitance is known, the radiation dose is easily calculated, and this is a very simple and reliable method (technique) for detecting radiation, which is one of the benefits of this sensor.

Meanwhile, the simple electrical (electrochemical) measurements for the *D. radiodurans* bacteria were checked. The correlation between the AC electrical conductivity of liquid bacteria samples and live bacteria counts were established. Typical AC conductance (AC-Gp) graph of *D. radiodurans* samples having different concentrations of bacteria are shown in Figures 8.25. In addition, the change in AC conductance of *D. radiodurans* bacteria regarding the change in time exposure was investigated and is presented in Figure 8.26.

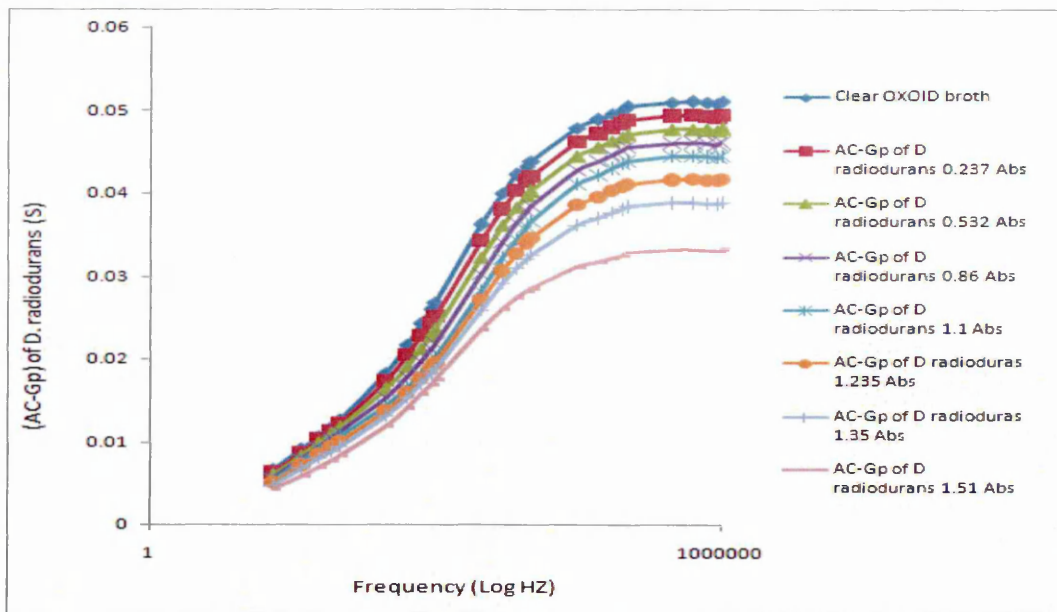


Figure 8.25. Typical AC-Gp characteristics of *D. radiodurans* samples of different concentrations measured in Abs units of optical density ( $OD_{600}$ )

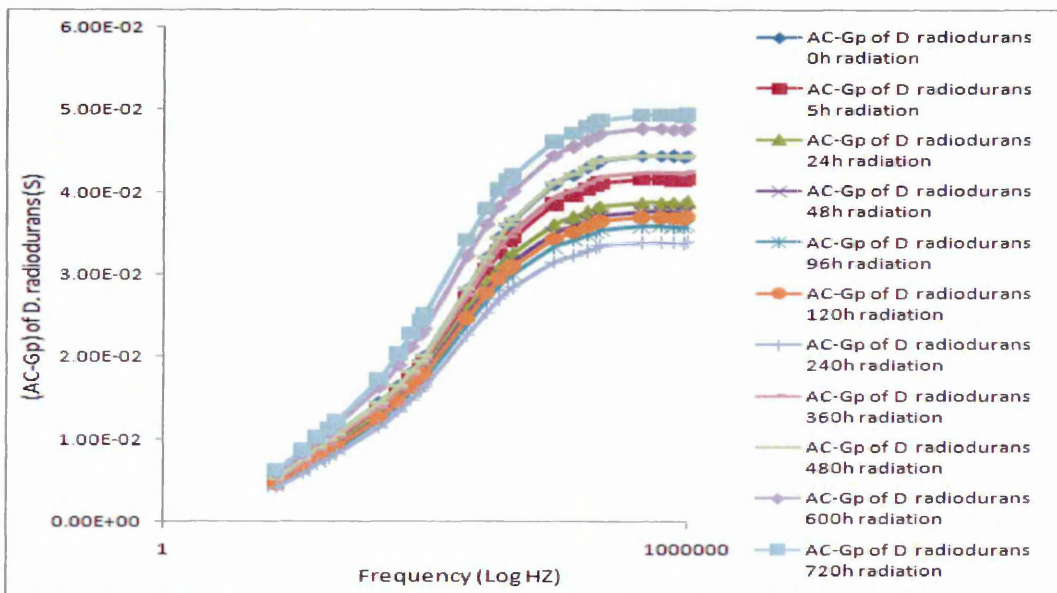


Figure 8.26. AC conductance of *D. radiodurans* samples for varied exposure to gamma radiation

As one can see the effect of gamma radiation on *D. radiodurans* bacteria is very clear, especially in the intermediate and high dose of radiation. The effect of environment on *D. radiodurans* bacteria were also investigated in order to study the effect of radiation on bacteria after ignoring the effect of the environment. For non-optimum environmental condition the bacteria response presented in Figure B4 at appendix B.

Figure 8.25 shows the AC characteristics for a range of frequencies as a function of time exposure to radiation or time exposure to the non-optimum environmental condition. For that, the response of bacteria to time exposure was selected at 900kHz because there is a very clear and sequential response at this frequency. Figure 8.26 describes the changes in the AC conductance of *D. radiodurans* bacteria for different time periods at 900kHz.

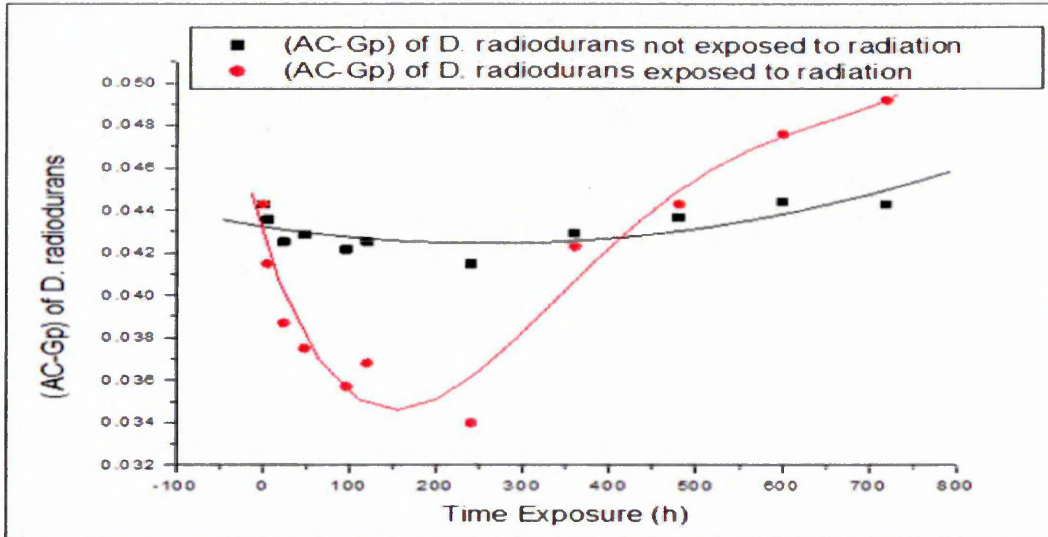


Figure 8.27. Change in AC conductance of *D. radiodurans* bacteria as function of time for exposed bacteria samples and not exposed samples at 900kHz

The data in graph 8.26 is normalised; the ratio between AC conductance of samples exposed to gamma radiation to the AC conductance of samples not exposed was calculated and is presented in Figure 8.27.

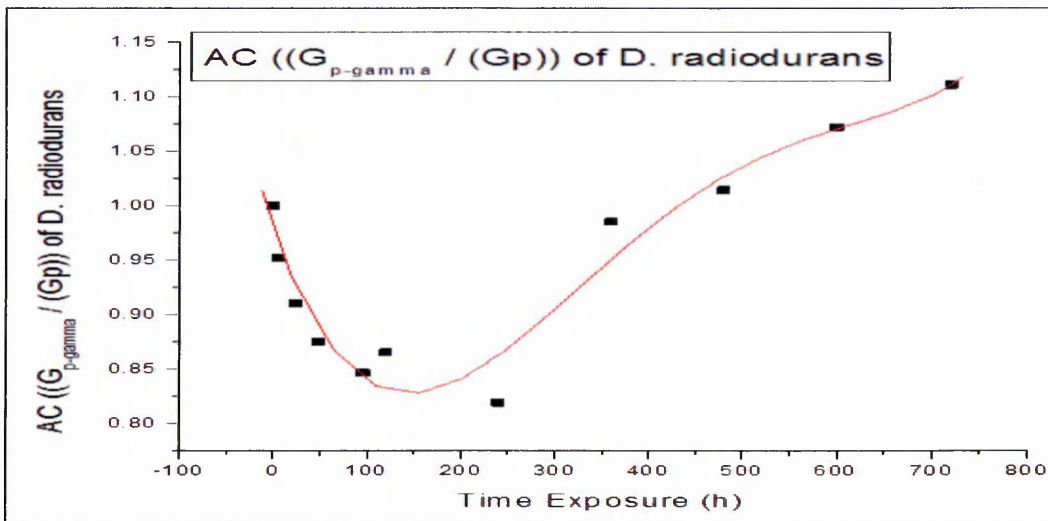


Figure 8.28. AC conductance ratio for *D. radiodurans* bacteria exposed to radiation to conductance of bacteria samples not exposed to radiation

The effects of gamma radiation on *D. radiodurans* bacteria were investigated through studying the relation between the AC Capacitance for *D. radiodurans* bacteria and the radiation dose are illustrated in Figures 8.28, 8.29. For more details, see appendix B.

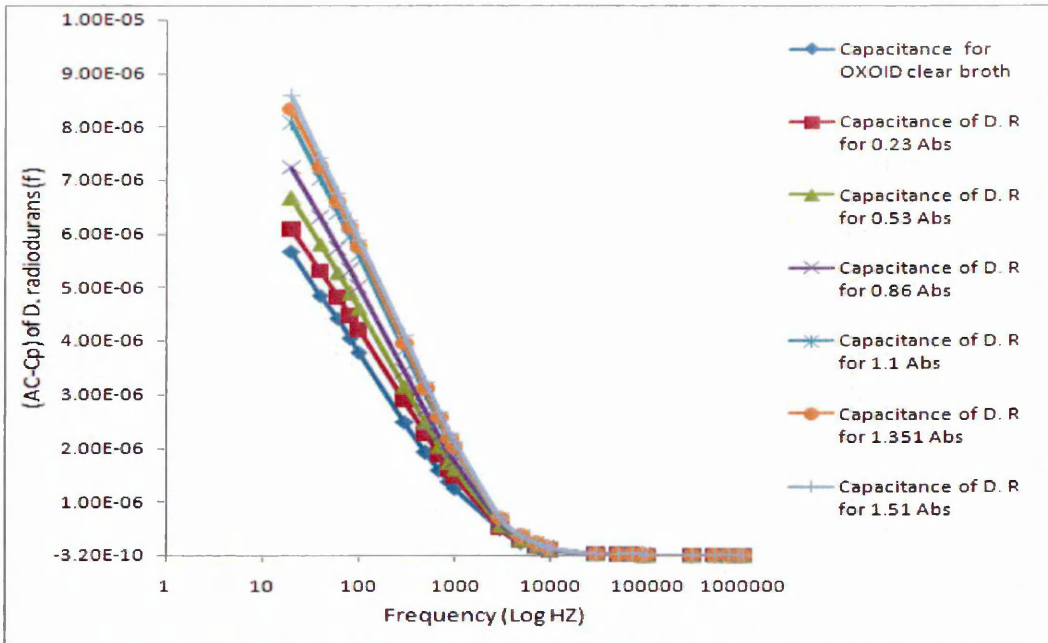


Figure 8.29. Typical AC capacitance characteristics of *D. radiodurans* samples of different concentrations measured in Abs units of optical density ( $OD_{600}$ ): frequency in log scale

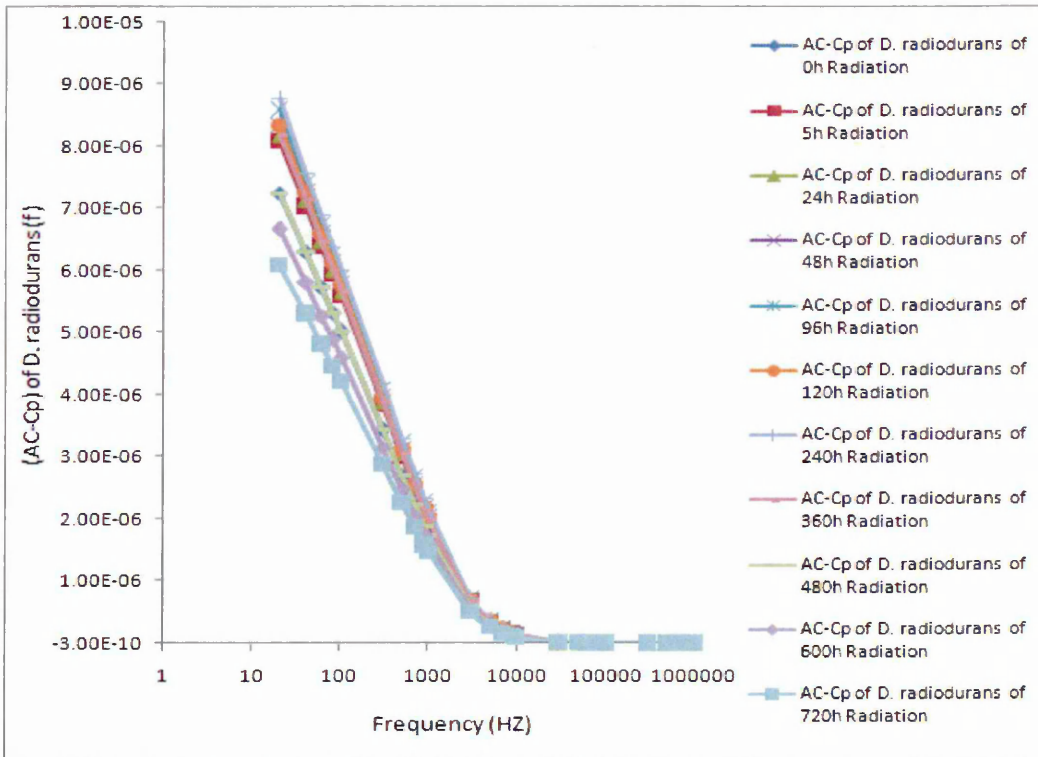


Figure 8.30. AC-Cp of *D. radiodurans* samples for varied exposure to gamma radiation

The changes in the AC capacitance of *D. radiodurans* bacteria for both cases, with radiation and without, for different times, at a high frequency of 900kHz are described in Figure 8.31.

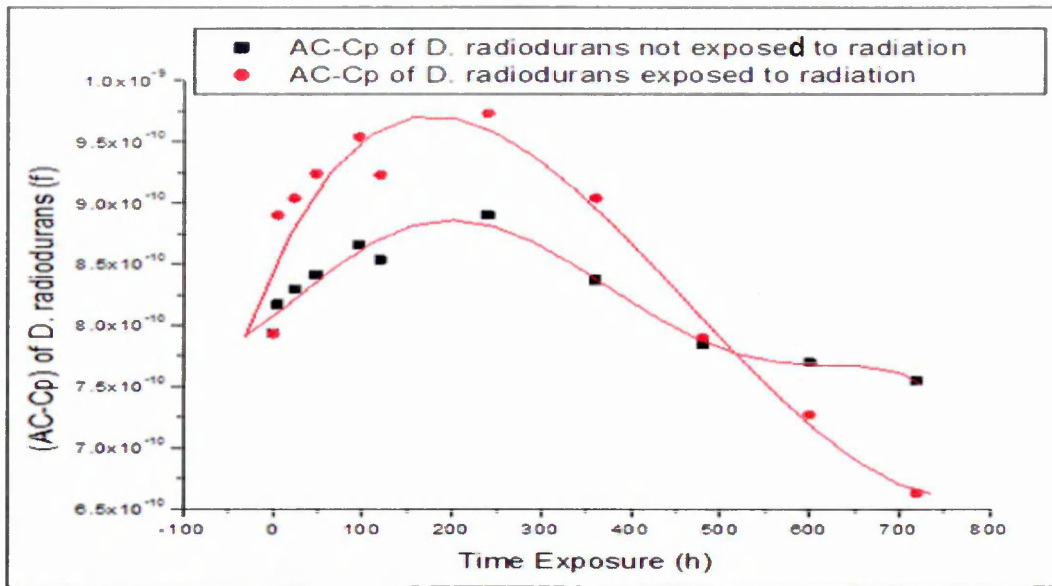


Figure 8.31. Change in AC capacitance of *D. radiodurans* bacteria as function of time for exposed and not exposed bacteria samples at 900kHz

The ratio of the AC capacitance of samples exposed to gamma radiation to the AC capacitance of samples not exposed was calculated and is presented in Figure 8.31.

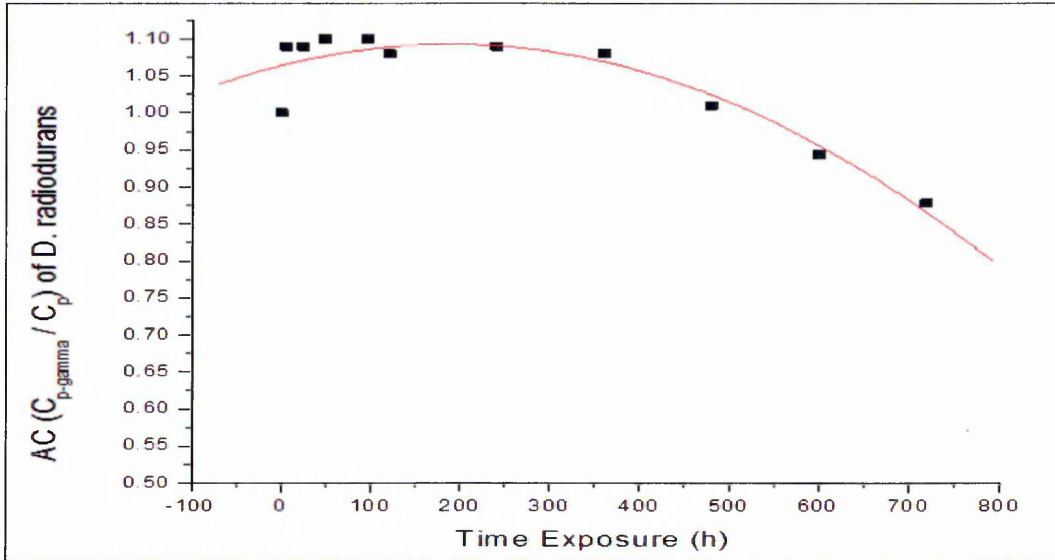


Figure 8.32. AC capacitance ratio for bacteria exposed to radiation to capacitance of bacteria samples not exposed to radiation at 900kHz

The best way to estimate the radiation dose level is through the comparison between curves that show relative responses of AC characteristics for *E. coli* and *D. radiodurans*

bacteria. This comparison is very important and useful too, as one can see when obtaining the results of normalised data for each bacteria sample; the radiation dose can be found directly from the curve (Figure 8.33) of AC conductance, the time exposure referring to radiation dose, is  $1 \text{ hour} \approx 2000 \text{ mSv}$ . Also, the AC capacitance comparison graph is presented in Figure 8.34.

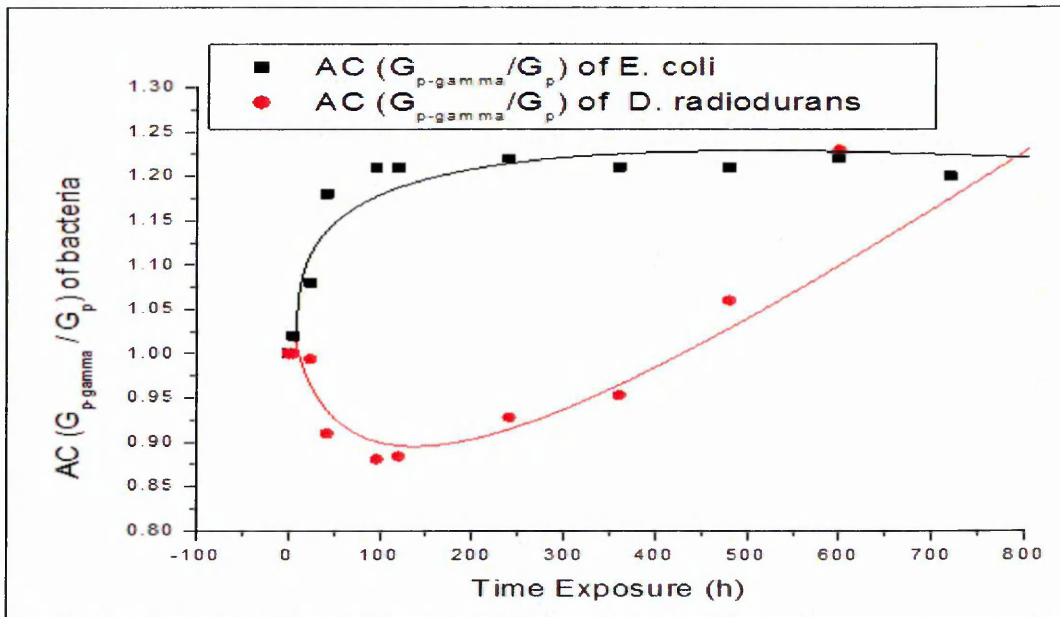


Figure 8.33. Comparison of relative responses of AC characteristic (conductance  $G_p$ ) methods to radiation for E.coli and D. radiodurans bacteria at 900kHz

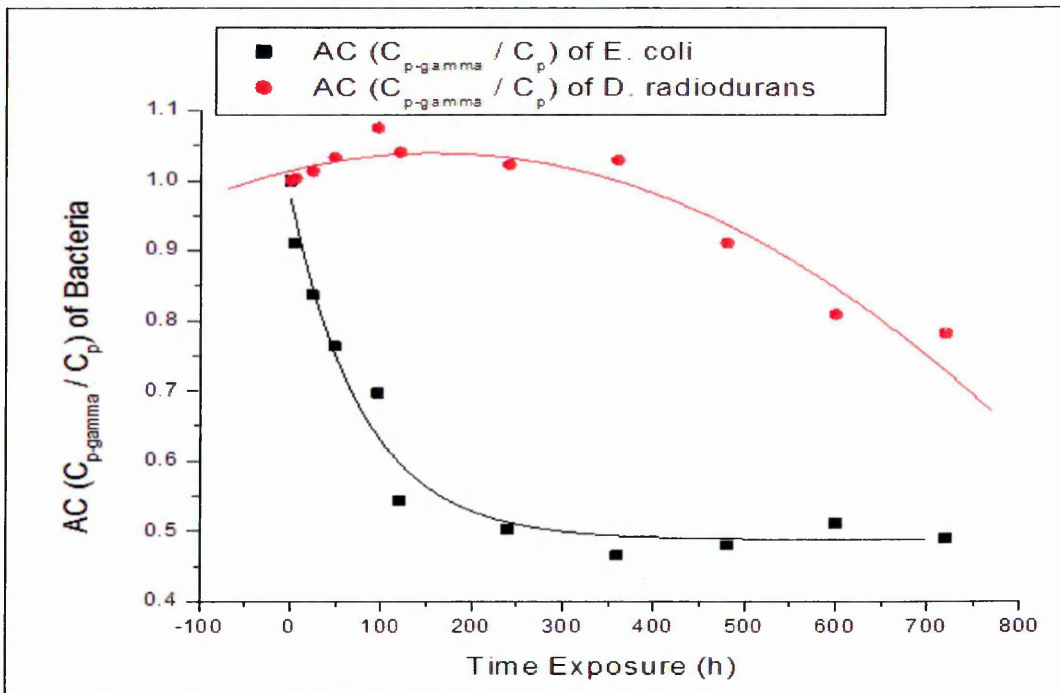


Figure 8.34. Comparison of relative responses of AC characteristic for capacitance  $C_p$  methods to radiation for E.coli and D. radiodurans bacteria at 900kHz

### 8.5. Data Analysis in Terms of Equivalent Circuit

As mentioned in Section 6.3, the assumed equivalent circuit included a surface (double layer) capacitance, and in parallel resistance and bulk resistance in series. The circuit items were calculated at low and high frequencies for different exposure periods. Firstly, the conductance at low frequency for *E. coli* bacteria samples for different exposure to radiation was estimated. The conductance at low frequency ( $\omega \sim 0$ ) is shown in equation (8.2).

$$G_{p(\omega \sim 0)} = \frac{1}{R_s + R_b} \approx \frac{1}{R_s} \quad (8.2)$$

From equation 8.2, the conductivity at low frequency includes the effect of surface and bulk resistances. The most of conductivity effect results from surface resistance, because the bulk resistance is much smaller than the surface resistance, which is considered to result from a thick layer of bacteria, as demonstrated by the resistance value. Secondly, the conductivity at low frequency for *E. coli* bacteria samples not exposed to radiation for different periods was calculated. The difference in the *E. coli* bacteria response to gamma radiation led to changes in the surface and bulk resistances. *E. coli* bacteria showed sensitivity to gamma radiation immediately but showed saturation at intermediate and high doses because the *E. coli* bacteria were dead in normal environmental conditions.

In order to study the changes that occurred in the surface resistance for *D. radiodurans* bacteria at low frequency, the same procedures were applied.

The equivalent circuit was also checked at high frequency for different exposure times. The conductivity for *E. coli* bacteria samples for different exposures is presented in Figure 8.34. The conductivity at high frequency ( $\omega \sim \infty$ ) is shown in equation (8.3).

$$G_{p(\omega \sim \infty)} = \frac{1}{R_b} \approx \infty \quad (8.3)$$

Equation 8.3 shows conductivity, including the effect of bulk resistance. As mentioned above, the bulk resistance is very small compared to surface resistance.

The conductance of *D. radiodurans* at high frequency for different exposures has been explored. Figure 8.34 shows the effect of gamma radiation on *D. radiodurans* as a change in resistance in the bio-cell sensors at high frequency. As one can see, bulk resistance is the smallest in terms of surface resistance, and less effect by radiation.

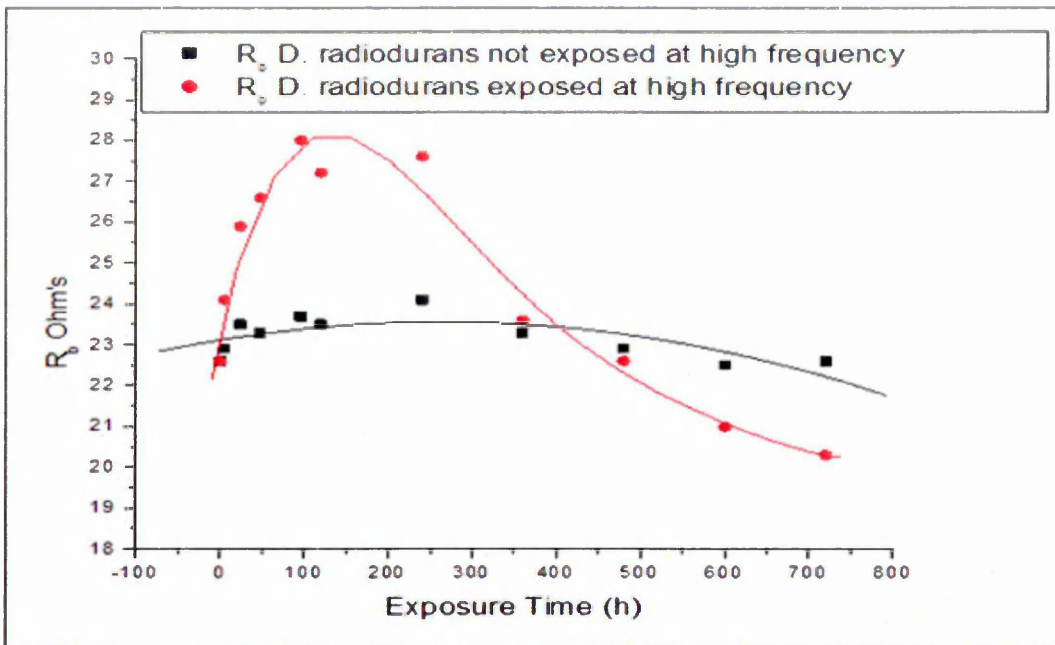


Figure 8.35. Changes in bulk ( $R_b$ ) resistance for *D. radiodurans* bacteria samples not exposed (black) and for samples exposed to gamma radiation (red) at high frequency

Bulk resistance at high frequencies of *D. radiodurans* bacteria exposed to gamma radiation was normalized to changes in resistance of *D. radiodurans* bacteria samples not exposed to gamma radiation. From the curve in Figure 8.35, the effect of gamma radiation on *D. radiodurans* bacteria can be seen.

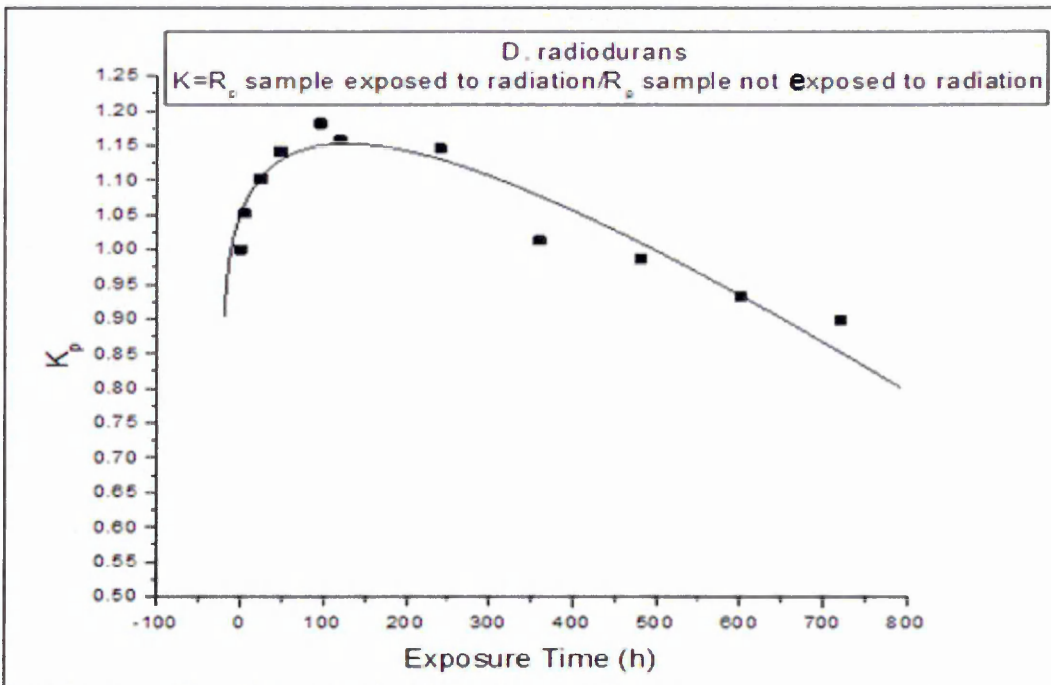


Figure 8.36. Normalised curve for bulk resistance of *D. radiodurans* bacteria exposed to gamma radiation against resistance of *D. radiodurans* bacteria samples not exposed to radiation at high frequency

As was discussed before, equations 8.2 and 8.3.

$$G_{p(\omega \sim 0)} = \frac{1}{R_s}, \quad G_{p(\omega \sim \infty)} = \frac{1}{R_b} \approx \infty$$

For that

$$R_s = \frac{1}{G_{p(\omega \sim 0)}} \quad (8.5)$$

As a result, the surface resistance for bacteria in their own cell sensor can be studied as bulk resistance was studied. The surface resistance ( $R_s$ ) of the *E. coli* bacteria is presented in Figure 8.36.

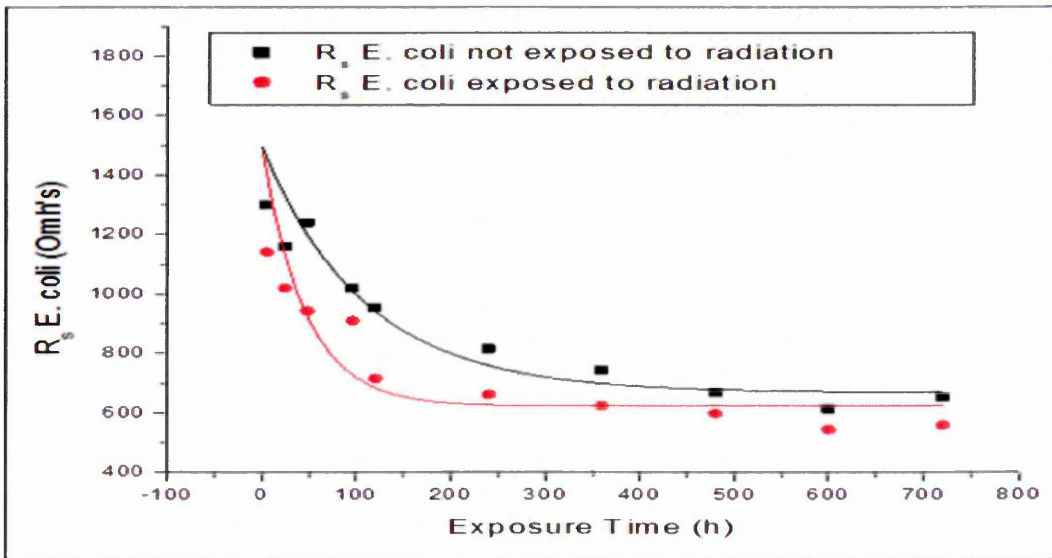


Figure 8.37. Changes in surface resistance ( $R_s$ ) of *E. coli* bacteria samples not exposed (black) and for samples exposed to gamma radiation (red)

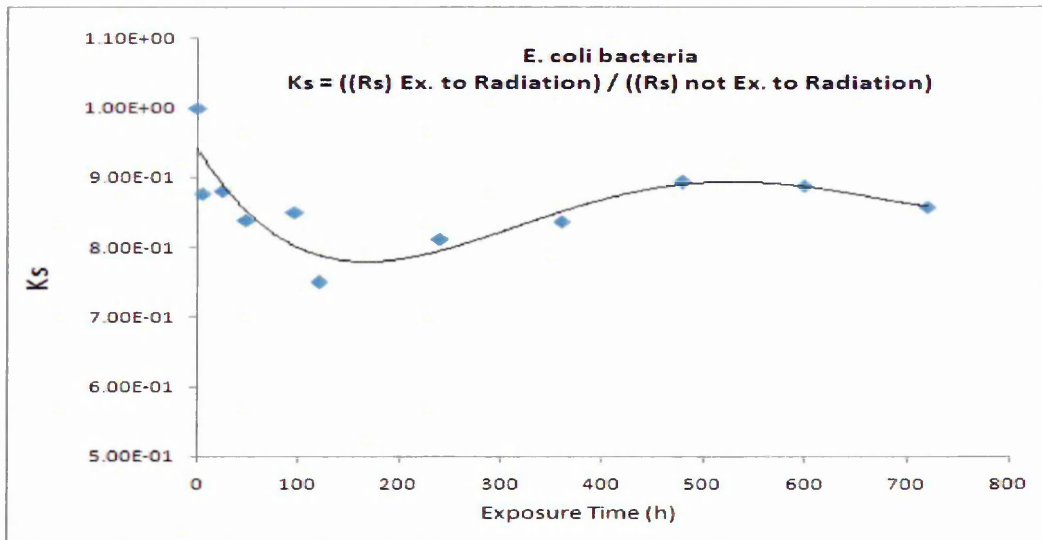


Figure 8.38. Curve for surface resistance of *E. coli* bacteria samples exposed to gamma radiation after being normalised against surface resistance of *E. coli* bacteria samples not exposed to radiation

In addition, equation 8.5 has been utilized to calculate the surface resistance ( $R_s$ ) for the bio-cell sensor, which is also easy to estimate from graphs that are presented in Figure 8.38.

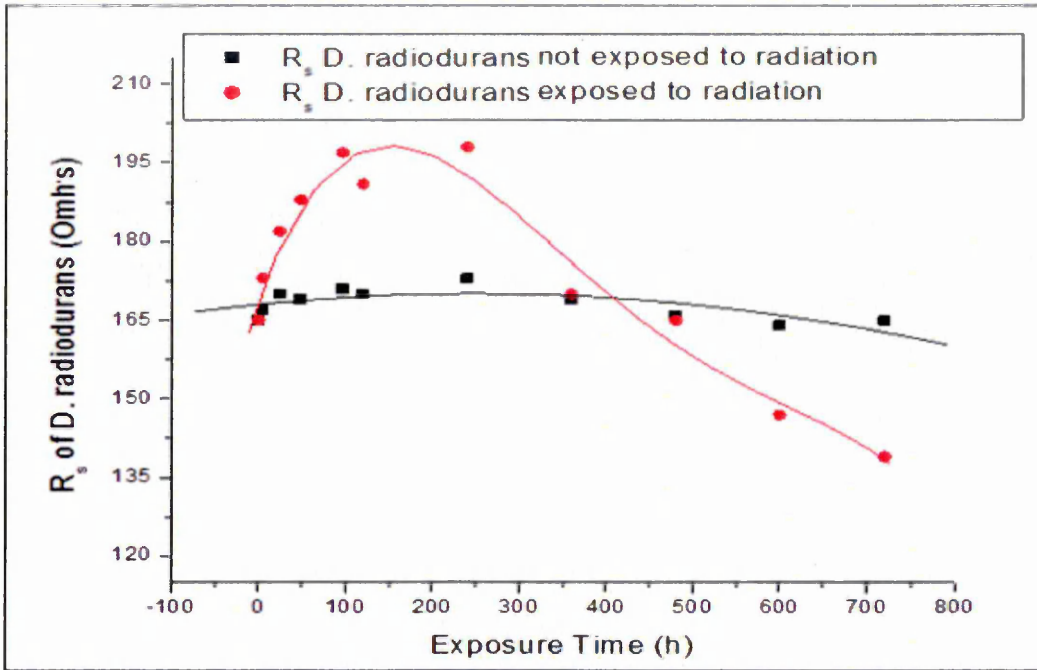


Figure 8.39. Changes in surface resistance ( $R_s$ ) of *D. radiodurans* bacteria samples not exposed (black curve) and for samples exposed to gamma radiation (red curve)

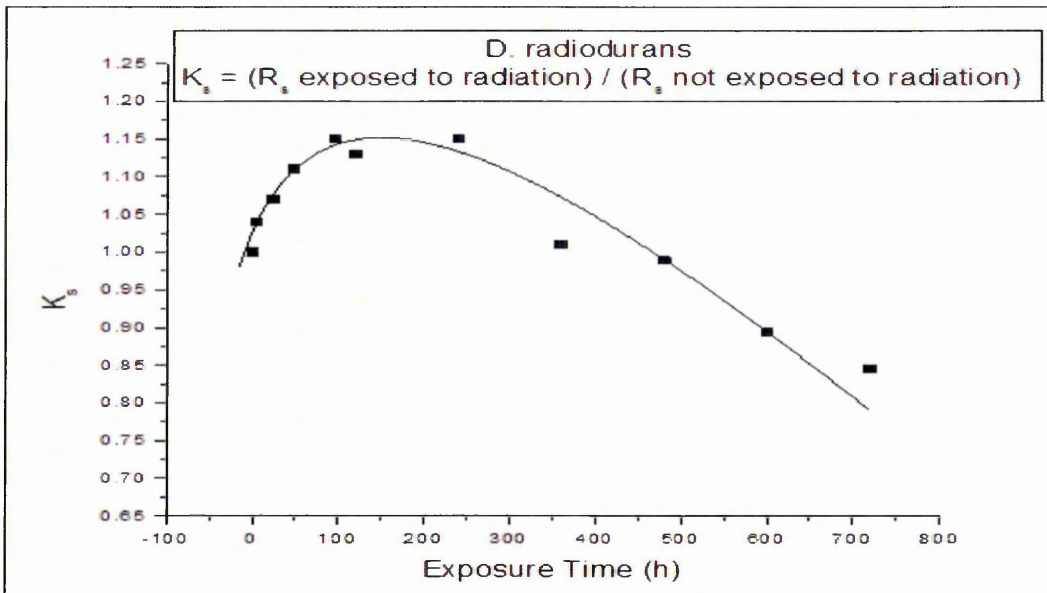


Figure 8.40. Curve for surface resistance of *D. radiodurans* bacteria samples exposed to gamma radiation after being normalised against surface resistance of *D. radiodurans* bacteria samples not exposed to radiation

Figures 8.39 and 8.40 show the effect of radiation exposure on surface resistance, which has affected the lives *D. radiodurans* bacteria.

Figure 8.41, shows a large difference in the surface resistance of *E. coli* and *D. radiodurans*, which are utilized to estimate the radiation level.

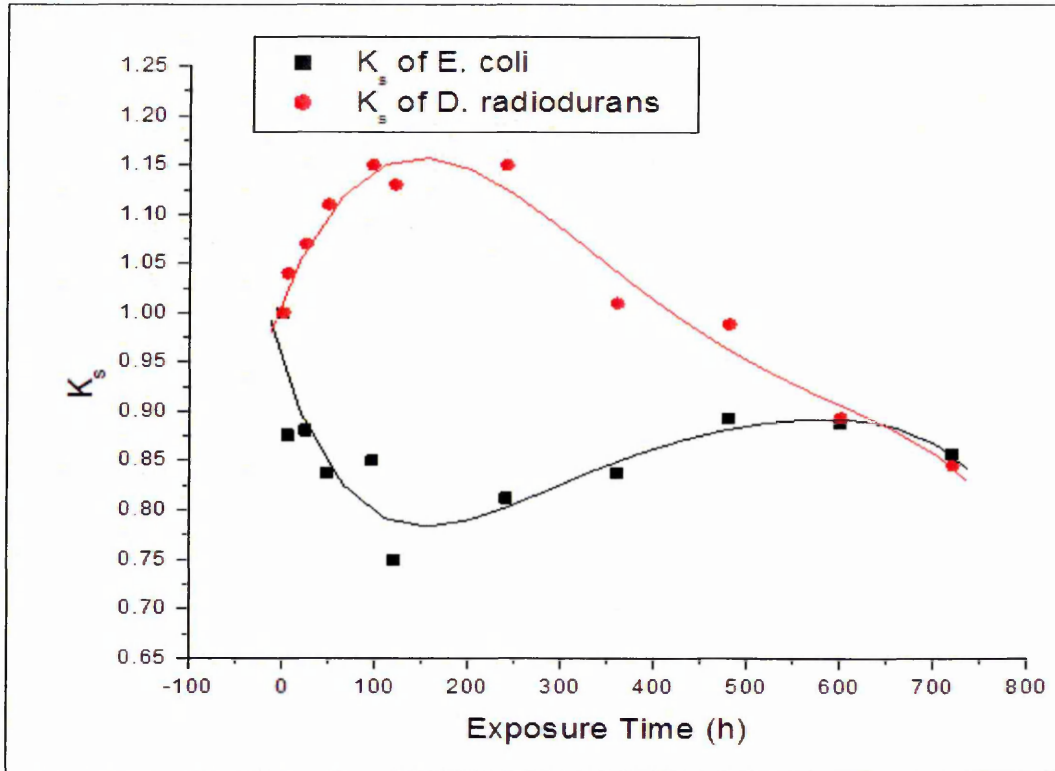


Figure 8.41. Comparison of curves of surface resistance ( $K_s$ ) for *E. coli* and *D. radiodurans* bacteria as function of exposure time

Double layer capacitance was created on the working electrode; this capacitance depends on the concentration of bacteria in the bio-cell sensor. From equation 6.4 the equivalent capacitance can be calculated thus:

First, at high frequency ( $\omega \sim \infty$ )

$$C_s = C_p \quad (8.6)$$

From equation 8.6, the equivalent capacitance at high frequency includes the effect of surface resistance and double layer capacitance on the working electrode. The capacitance at low frequency is calculated for *E. coli* bacteria and the results presented in Figure 8.41. Then,

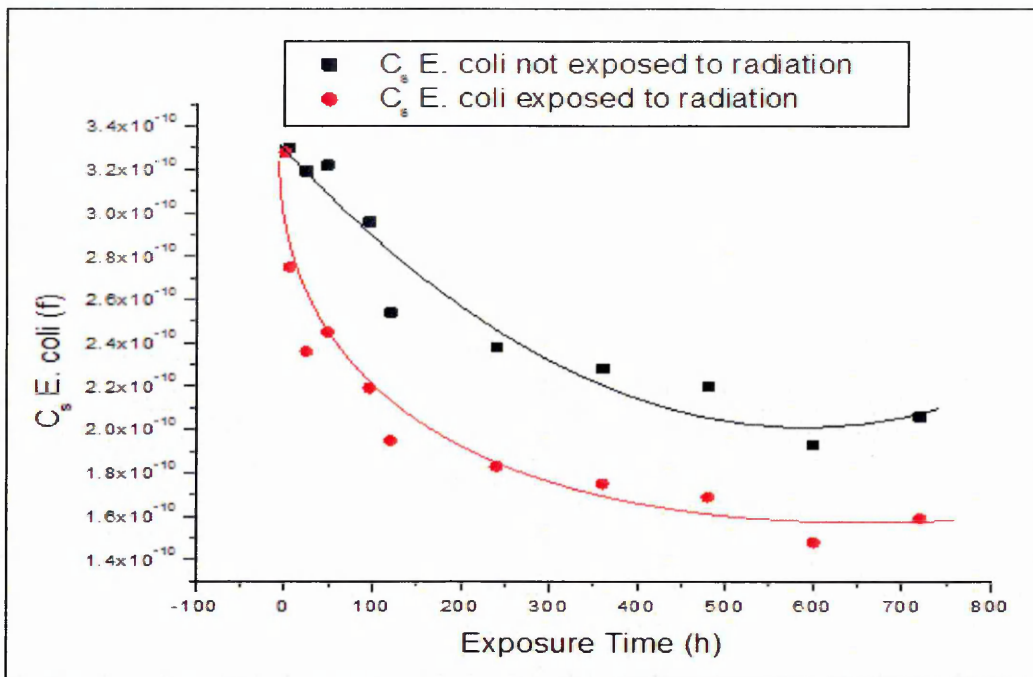


Figure 8.42. Changes of double layer capacitance ( $C_s$ ) of *E. coli* bacteria samples not exposed (black curve) and for samples exposed to gamma radiation (red curve)

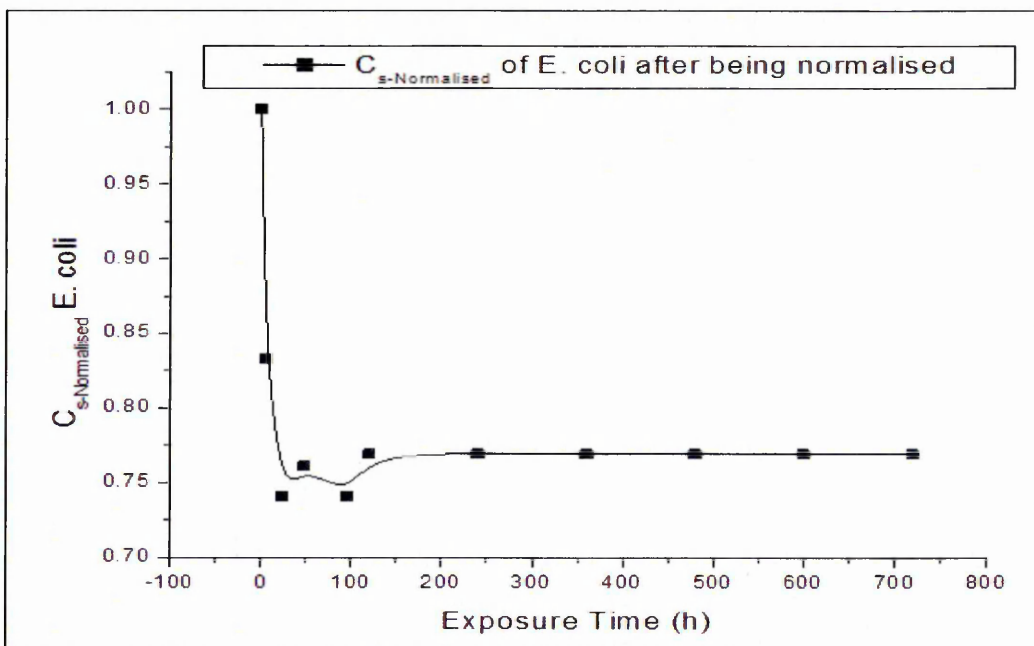


Figure 8.43. Curve for double layer capacitance ( $C_s$ ) of *E. coli* bacteria samples exposed to gamma radiation after being normalised

The equivalent double layer capacitance was studied for *D. radiodurans* bacteria. Bacteria accumulated on the working electrode that creates double layer capacitance. These capacitances  $C_s$  were calculated and are presented in Figure 8.43.

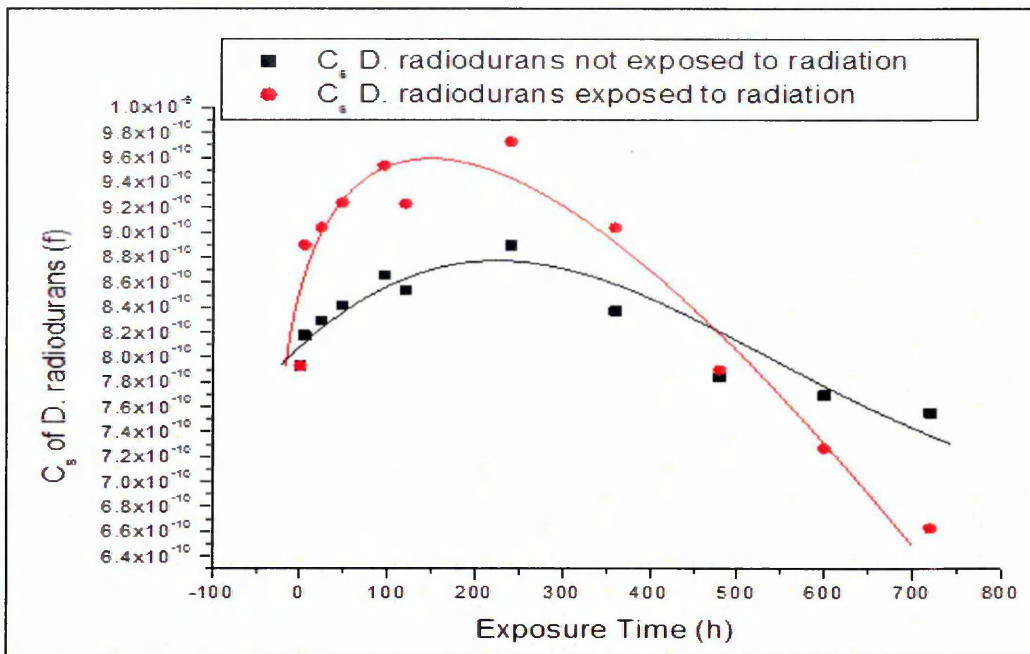


Figure 8.44. Changes of double layer capacitance ( $C_s$ ) of *D. radiodurans* bacteria samples not exposed (black curve) and for samples exposed to gamma radiation (red curve)

The  $C_s$  of *D. radiodurans* bacteria exposed to gamma radiation were normalised on  $C_s$  of *D. radiodurans* bacteria, which were not exposed to gamma radiation.

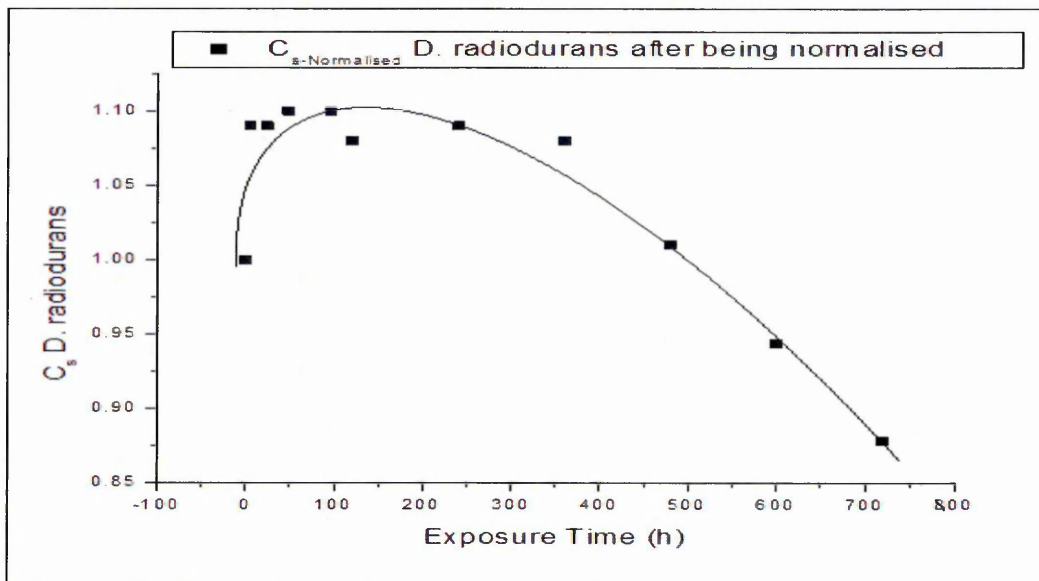


Figure 8.45. Curve for double layer capacitance ( $C_s$ ) of *D. radiodurans* bacteria samples exposed to gamma radiation after being normalised against double layer capacitance of *D. radiodurans* bacteria samples not exposed to radiation

Figure 8.46 compares the pattern for normalised  $C_s$  of *E. coli* bacteria, and normalised  $C_s$  of *D. radiodurans* and is useful for comparing the responses of the two bacteria to gamma radiation.

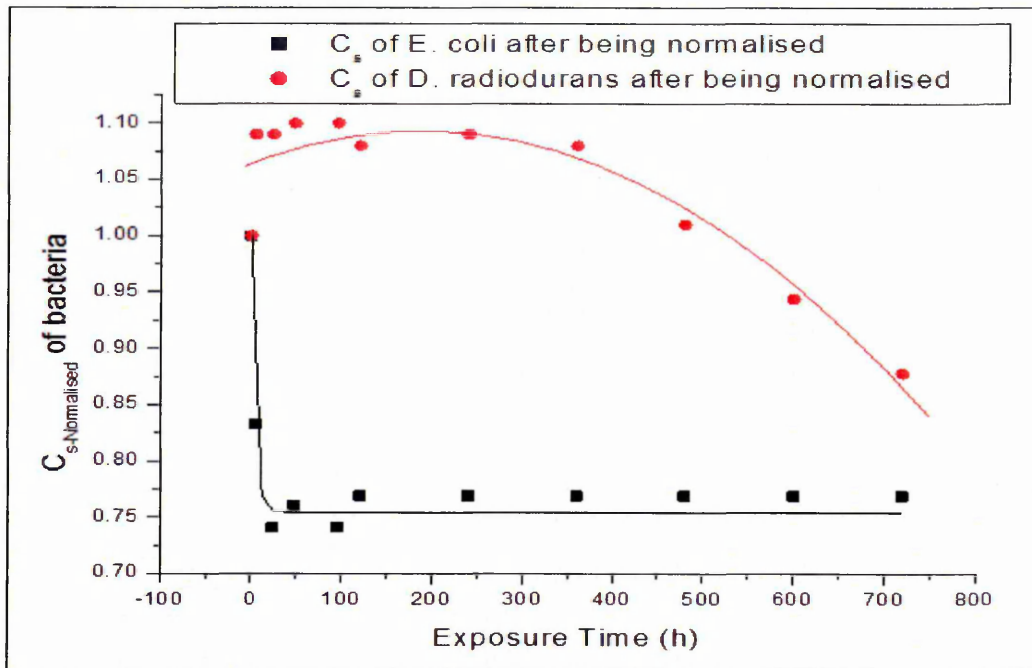


Figure 8.46. Comparison of curves of double layer capacitance ( $C_s$ ) for *E. coli* bacteria (black curve) and *D. radiodurans* bacteria (red curve) as a function of exposure time

Simple electrical DC and AC tests appeared to be suitable for evaluation of the gamma radiation effect on *E. coli* and *D. radiodurans* bacteria. Cathodic current is perhaps the most simple to measure giving clear distinction between two types of bacteria in regards to  $\gamma$ -ray effect. AC data are more complex to interpret through Gp and Cp spectra and are clearly dependent on bacteria concentration.

The equivalent circuit describes the AC behaviour widely and gives us logical outcome of the values of  $R_s$  and  $C_s$ , which are dependent of bacteria concentration and on gamma radiation dose. AC data can be also used for estimated of  $\gamma$ -ray.

#### Reference:

1. Jonesv D. G,(2001), Development and application of marine gamma-ray measurements, *Journal of Environmental Radioactivity*, Volume 53, Issue 3, pp. 313-333.
2. Adam Wanekava K, Wilfred Chen and Ashok Mulchandain, (2008),Recent biosensing developments in environmental security, *Journal of Environmental Monitoring*, Issue 6, pp. 703-712.

3. Kira Makarova S, Aravind L, Wolf Yuril, Roman Tatusoy L, Kenneth Minton W, Eugene Koonin V, and Michael Daly J, (2001), Genome of the Extremely Radiation-Resistant Bacterium *Deinococcus radiodurans* Viewed from the Perspective of Comparative Genomics, *Microbiol Mol Biol Rev*; 65(1): pp. 44-79.
4. Chua H, Yu P. H. F, Sin S. N, Cheung M. W. L, (1999), Microscale and Molecular Assessment of Impacts of Nickel, Nutrients, and Oxygen Level on Structure and Function of River Biofilm Communities, *Elsevier (Chemosphere)*. Vol 39, Issue 15, pp. 2681-2692.
5. Sensor array concept, any text book on sensors.
6. Abdul Kafi Md, Tae-Hyung Kim and Jeong-Woo Choi, (2001), Neural Cell Chip to Assess Toxicity Based on Spectroelectrochemical Technique, The international conference on sensor device technologies and application, *SENSORDEVICES*, pp. 147-150.
7. Yúfera A, Cañete D, Daza P, (2001), Cell Biometrics Based on Bioimpedance Measurements, *Technologies and Application*, pp. 143-146.
8. Daly M. J, Matrosova V. Y, Vasilenko A. K, Gaidamakova E, (2004), Accumulation of Mn(II) in *Deinococcus radiodurans* facilitates gamma-radiation resistance, The International Conference on Sensor Device, *Science (AAAS), SENSORDEVICES*, 306. 5698: pp. 1025-1028.
9. Al-Shanawa M, Nabok A, Hashim A, Smith T, Forder S, (2013), Detection of  $\gamma$ -radiation and heavy metals using electrochemical bacterial-based sensor, *Journal of Physics, Sensors & their Applications XVII conference*, IOP Publishing, Conference Series 450: 012025.
10. Venkateswaran A, (2000), Physiologic determinant of radiation resistance in *Deinococcus radiodurans*, *Applied and Environmental Microbiology*, pp. 2620-2626.

## CHAPTER 9

### Optical Study of the Effect of Heavy Metals on Bacteria

To study the effect of heavy metals,  $\text{CdCl}_2$  and  $\text{NiCl}_2$  salt were selected. Two types of bacteria were utilised (as was described in chapters 7, 8): (i) the non-pathogenic DH5 $\alpha$  strain of *Escherichia coli* (*E. coli*); and (ii) the Anderson R1 strain of *Deinococcus Radiodurans* (*D. radiodurans*) mixed with a solution including heavy metals. Solutions of different concentrations (0.1mM, 1mM, 10mM, 100mM, and 1M) of  $\text{CdCl}_2$  and  $\text{NiCl}_2$  were prepared using de-ionized water.

#### 9.1. Optical Study of the Effect of Cadmium Chloride ( $\text{CdCl}_2$ )

As mentioned in chapter 3, cadmium chloride is the most common compound of Cd salts. A hygroscopic solid is highly soluble in water and slightly soluble in alcohol, and forms hydrates [1]. Cadmium chloride dissolves well in water and other polar solvents. In water, its high solubility is due in part to the formation of complex ions, such as  $[\text{CdCl}_4]^{2-}$  [2]. In order to prepare one mole from  $\text{CdCl}_2 \cdot \text{H}_2\text{O}$ , 183.32g from  $\text{CdCl}_2$  was added to 1Liter of sterile deionized water, and the solvent was sterilized by a Physical filter, with the unit 0.22  $\mu\text{m}$  (MILLEX<sup>®</sup>GP). One mole concentration from  $\text{CdCl}_2$  was obtained, and the solution was diluted with water to obtain different concentrations (1M, 0.1M, 0.01M, 0.001M, 0.0001M). The salty solution was added to bacteria cultures, in the ratio 1:1. Finally the salty cultures were kept in a shaker under room temperature conditions for different periods of time.

The same three optical techniques, namely fluorescence microscopy, fluorescence spectroscopy, and optical density, were employed in order to study the effect of heavy metals on bacteria. Typical fluorescence microscopy images of samples of *E. coli* bacteria are shown Figure 9.1. In these images, live bacteria stained with SYTO-9 emit green light while dead bacteria stained with Propidium iodide emit red light. The difference between images taken without and with mixed or added  $\text{CdCl}_2$  is obvious. The (LIVE/DEAD) bacLight, bacteria viability kit is simple to use, reliable and quantitatively distinguishes between live and dead bacteria efficiently. In order to realise the effect of  $\text{CdCl}_2$  on bacteria samples, the same procedure sequence was employed to prepare the glass slides (see Chapter 7). The samples were tested with a fluorescence microscope using a lens of 100 $\times$  magnification. A slide of stained bacteria

was illuminated (excited) with blue light of 420nm wavelength; the bacteria images were captured using the (Q-Capture-Pro 6.0) program. Figure 9.1 shows the examples of captured images of (*E. coli*) bacteria as a function of heavy metal concentration and time exposure.

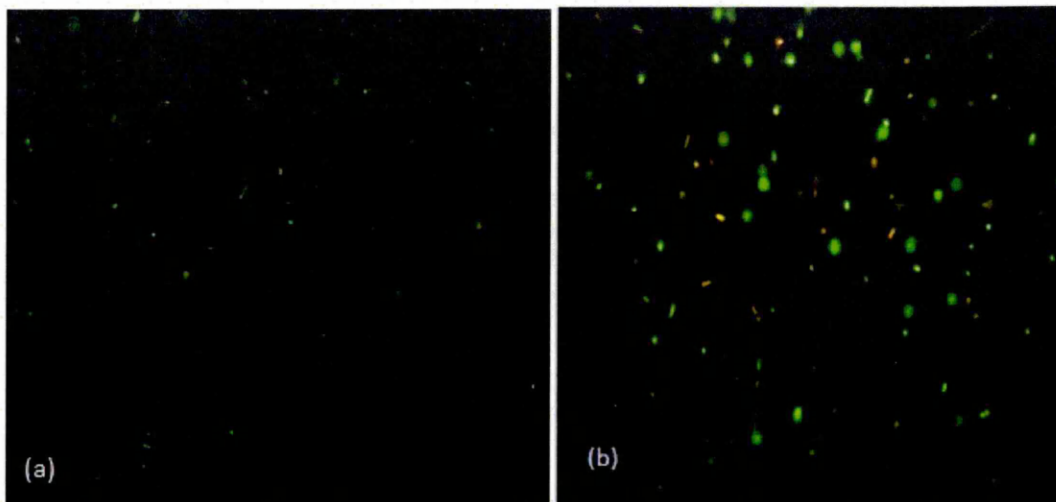


Figure 9.1. Fluorescence microscopy images of *E. coli* bacteria samples (a) without, and (b) with  $\text{CdCl}_2$  after 72 hours of added the metal

The Live/Dead ratio in Figure 9.2 for *E. coli* bacteria was obtained by analysing fluorescence microscopy images having bacteria which appeared as "green" spots while dead bacteria were stained "red". The reduction in the L/D ratio with the increase in  $\text{CdCl}_2$  concentration is apparent for *E. coli* (Figure 9.2). Exposure time has no significant effect on L/D ratio, mostlikely because 1 hour (the minimal exposure time used) is sufficiently enough time to cause damage to bacteria [3].

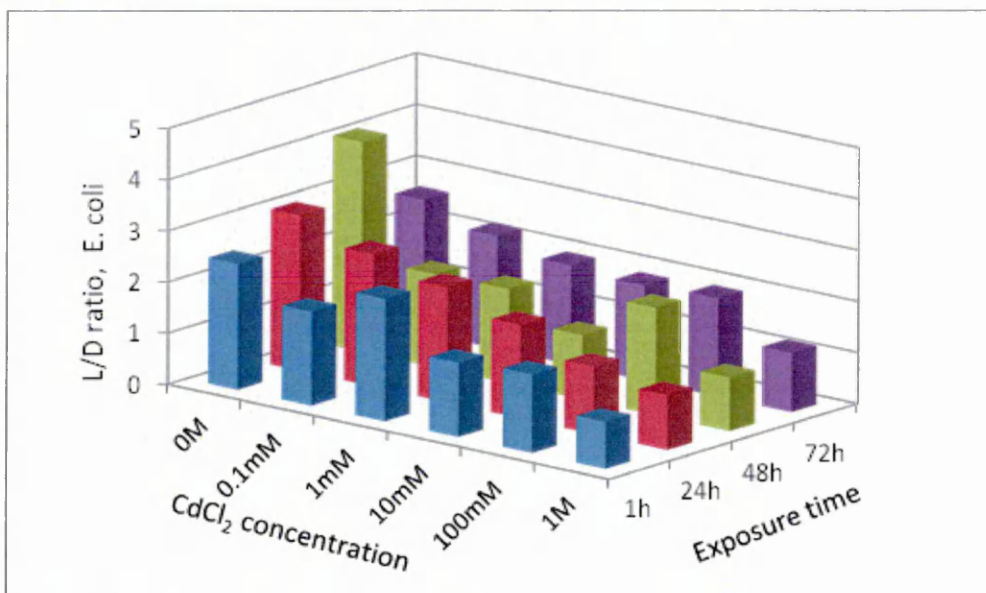


Figure 9.2. Effect of  $\text{CdCl}_2$  on the L/D ratio of *E. coli* for different time incubations

The method of fluorescence microscopy seems to give a reliable account of live bacteria concentration. The live/dead ratio in Figure 9.2 for *E. coli* bacteria was obtained by analyzing fluorescence microscopy images having living bacteria appearing as green cells while dead bacteria were stained red. As one can see, the live *E. coli* bacteria number decreases at short time after treated with salt because the bacteria had shocked when mixed with salt, then the bacteria seems to become used to the less affected of salt after this. Figure 9.3 shows the response of *E. coli*; it indicates that the concentration of  $\text{CdCl}_2$  can easily be estimated or evaluated, showing the ratio  $(L/D)_m$  after adding the salt against the ratio  $(L/D)_0$ .

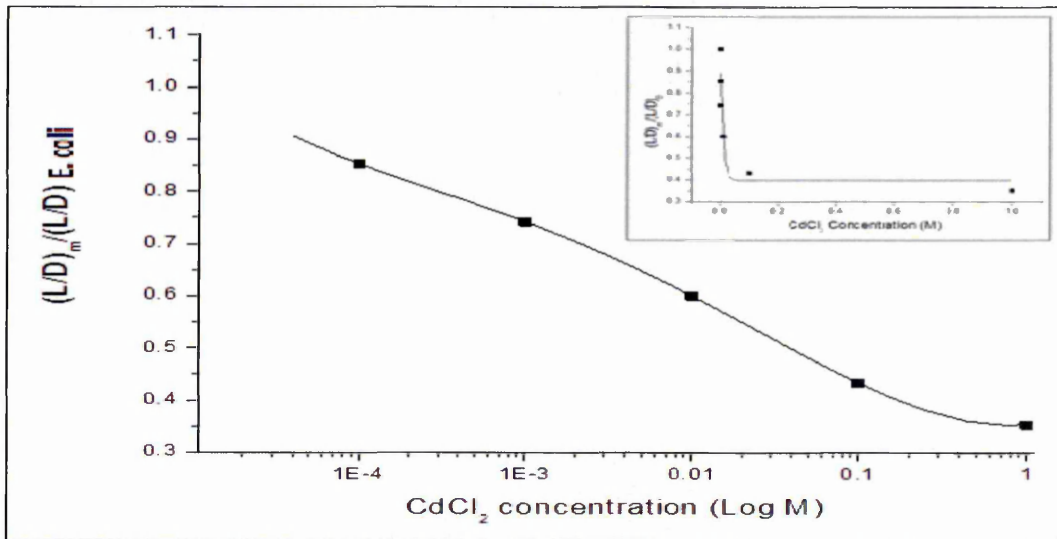


Figure 9.3. Ratio  $((L/D)_m / (L/D)_0)$  of *E. coli* after 72 hours exposure for different concentration of  $\text{CdCl}_2$ , inset described the  $(L/D)$  ratio for normal x-axis scale

The fitting formula for graph 9.3 is presented in equation 9.1.

$$\frac{(L/D)_m}{(L/D)_0} = 0.4 + 0.5 e^{(-C./0.01)} \quad (9.1)$$

where  $C.$  is the  $\text{CdCl}_2$  concentration.

A similar sequence was used for the cultivation of *D. radiodurans* (Anderson R1 strain). The *D. radiodurans* bacteria were exposed to  $\text{CdCl}_2$ . *D. radiodurans* bacteria seem to have been more sensitive compared to the *E. coli*. The bacteria samples were exposed to metal salts for a different period, from 1 hour up to 550 hours.

The effect of  $\text{CdCl}_2$  on the *D. radiodurans* bacteria density was examined and analysed using the three optical experimental techniques mentioned previously; fluorescence

microscopy measurements were performed using an OLYMPUS-BX60 instrument. The numbers of live and dead bacteria was determined. Typical fluorescence microscopy images of samples of *D. radiodurans* bacteria are shown Figures 9.4. Again, in these images, live bacteria emitted green light while dead bacteria emitted red light. The images are of bacteria taken with and without exposure to added  $\text{CdCl}_2$ .

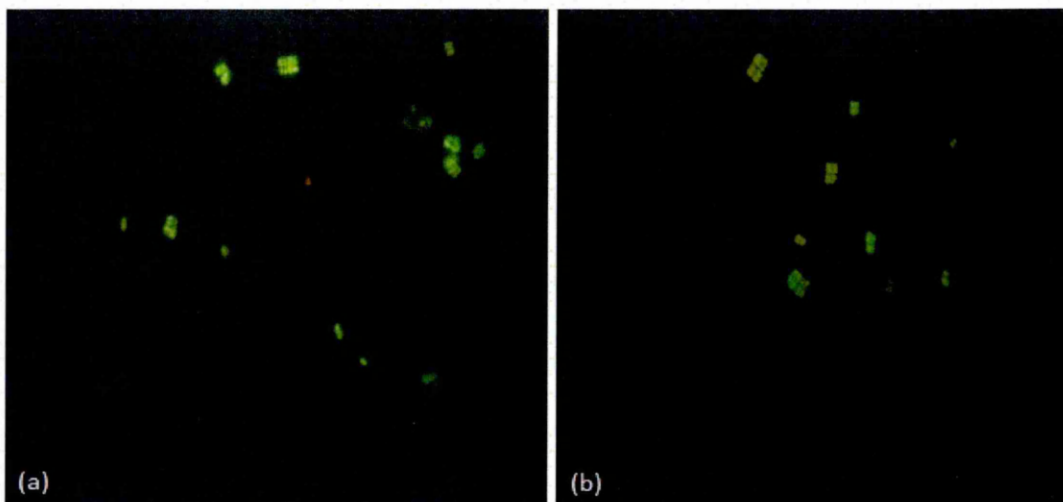


Figure 9.4. Fluorescence microscopy images of *D. radiodurans* bacteria sample (a) without salt and (b) with  $\text{CdCl}_2$  after 550 hours adding the metal

The same procedure was performed for *D. radiodurans*, and fluorescence microscope images were analysed and the ratio  $L/D$  was calculated and presented (see appendix C).

In order to estimate the  $\text{CdCl}_2$  concentration, the  $(L/D)$  of *D. radiodurans* bacteria response to the salt were utilised through being normalised on the  $(L/D)$  of bacteria at 0M of salt. Figure 9.5 shows the ratio  $(L/D)_m$  after adding the salt over the ratio  $(L/D)_0$ .

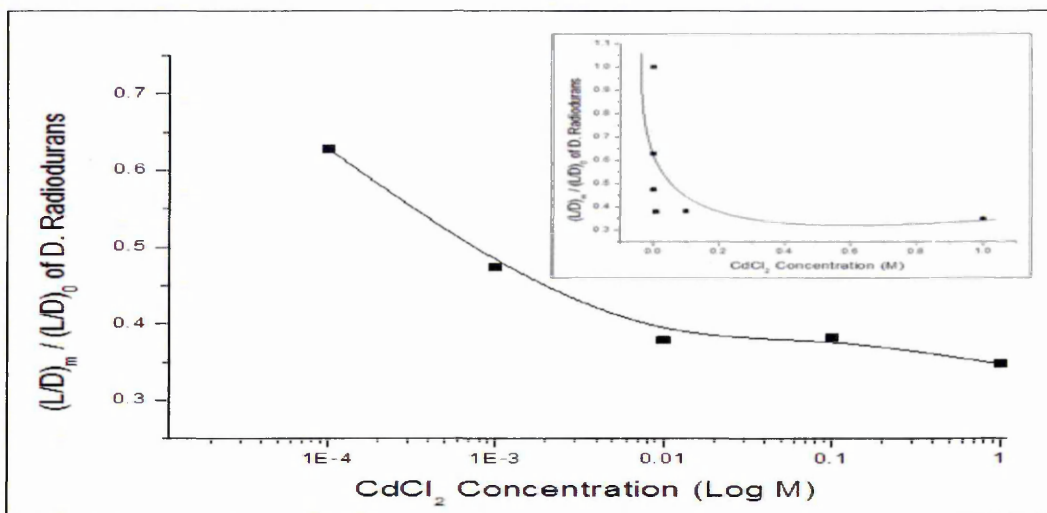


Figure 9.5. Ratio  $(L/D)_m$  of *D. radiodurans* after adding salt over ratio  $(L/D)_0$  of *D. radiodurans* without  $\text{CdCl}_2$ , after 72 hours exposure; for inset normal scale is used

Fitting the *D. radiodurans* data response to  $\text{CdCl}_2$  in Figure 9.5 shows exponential decay according to formula 9.2:

$$\frac{\left(\frac{L}{D}\right)_m}{\left(\frac{L}{D}\right)_0} = 0.39 + 0.6 * e^{(-C./0.0001)} \quad (9.2)$$

where C. is the  $\text{CdCl}_2$  concentration.

The fluorescence microscopy data for *E. coli* and *D. radiodurans* bacteria are compared in Figure 9.6. The two bacteria studied show nearly the same behaviour. The L/D ratio of *E. coli* bacteria exhibits an exponential decay; the ratio for *D. radiodurans* exhibits the same behaviour. The changes with time in the bacteria response for  $\text{CdCl}_2$  are shown in Figure 9.6.

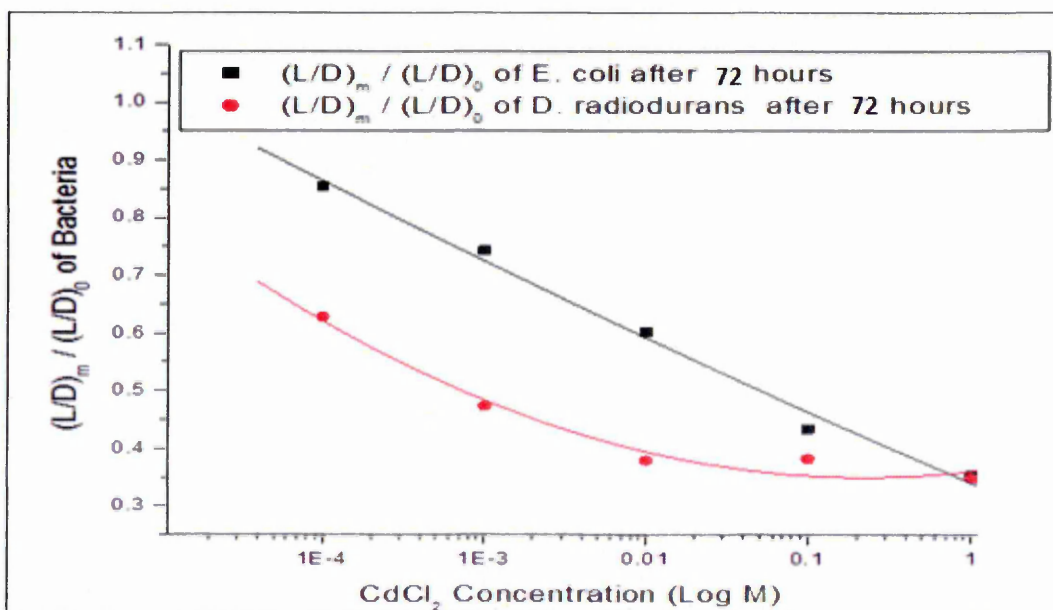


Figure 9.6. Dependence of  $\left(\frac{L}{D}\right)_m / \left(\frac{L}{D}\right)_0$  bacteria ratio for both *E. coli* and *D. radiodurans* bacteria on exposure time to  $\text{CdCl}_2$  (fluorescence microscopy results)

The optical density ( $\text{OD}_{600}$ ) technique was also used to estimate the bacteria cells density as a function of  $\text{CdCl}_2$  concentration and time of exposure to metals.  $\text{OD}_{600}$  recordings have been presented as either absorption of light, which refers directly to the bacteria cells density, or the size of bacteria being very effective on the density of scattered light, and related to their sensitivity to metals. The effect of liquid broth and  $\text{CdCl}_2$  has been neglected and considered as a blank. Figure 9.7 shows the  $\text{OD}_{600}$  of *E. coli* after adding the  $\text{CdCl}_2$  as a function of metal concentration and time of exposure to the metal.

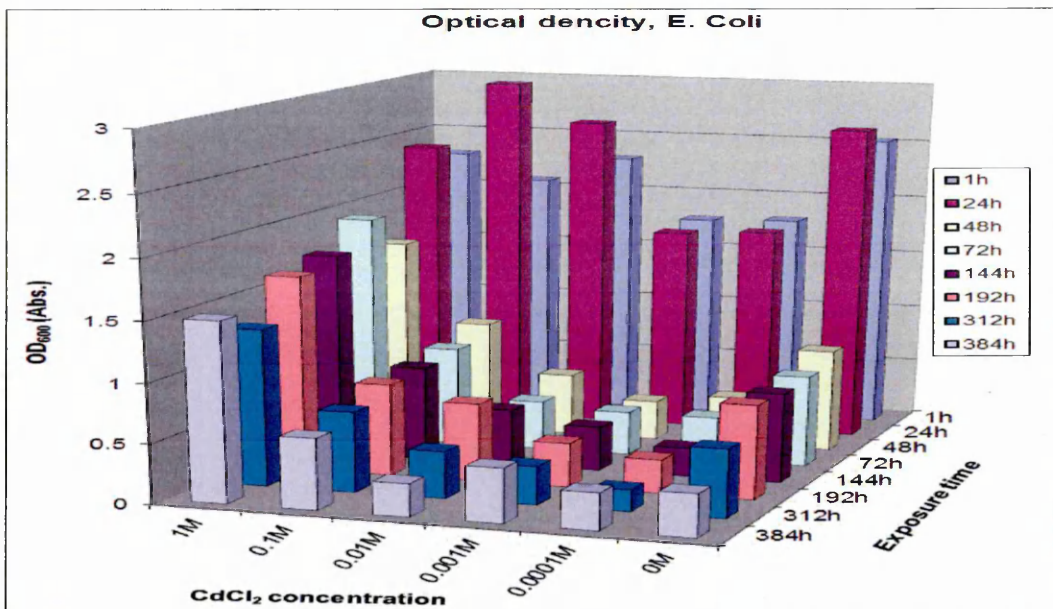


Figure 9.7. Optical Density test: optical densities OD<sub>600</sub> for E. coli bacteria versus CdCl<sub>2</sub> concentration and time exposure

Optical density (OD<sub>600</sub>) technique was also used to estimate the *D. radiodurans* bacteria cells density as a function of exposure time to different concentrations of CdCl<sub>2</sub>. Figure 9.8 shows the OD<sub>600</sub> of *D. radiodurans* after adding CdCl<sub>2</sub> as a function of metal concentration and exposure time to metal.

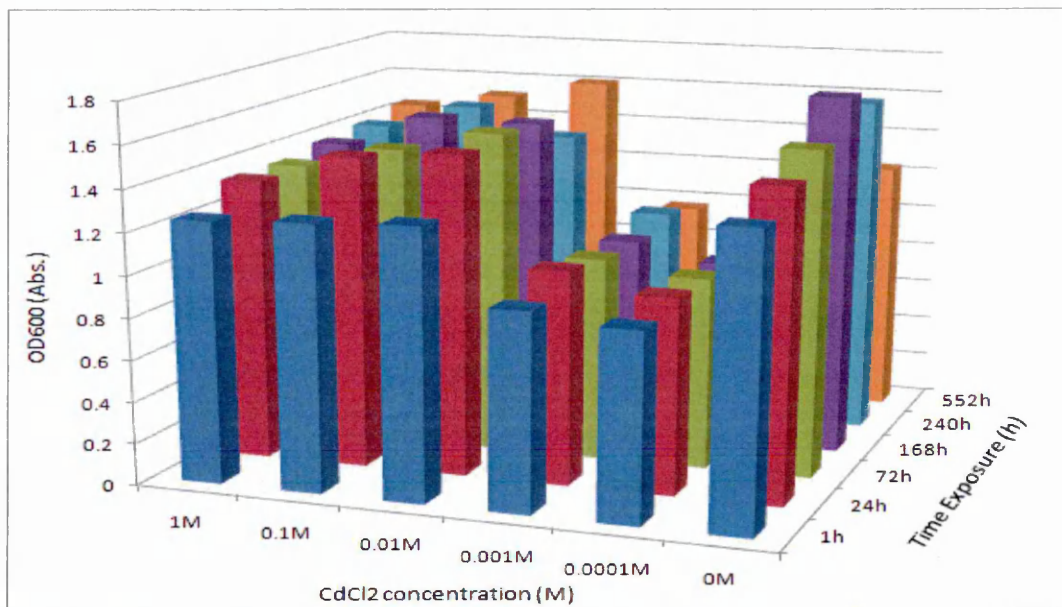


Figure 9.8. Optical Density test: optical densities at 600nm for *D. radiodurans* bacteria versus time exposure to CdCl<sub>2</sub> for different incubating times in the shaker

Another optical technique; fluorescence spectroscopy, has been employed, to confirm the above results on the effect of CdCl<sub>2</sub> on bacteria count, as well as to study in more

detail the fluorescence spectra of *E. coli* and *D. radiodurans* bacteria. The emission fluorescence spectra of bacteria samples were recorded using the excitation wavelength of 315 nm for *E. coli* and 350 nm for *D. radiodurans*. The fluorescence spectroscopy measurements were performed on *E. coli* and *D. radiodurans* bacteria samples and the spectra are shown in Figure 9.9 and 9.10. The maximum fluorescence intensity was indicated to be cell concentration dependent.

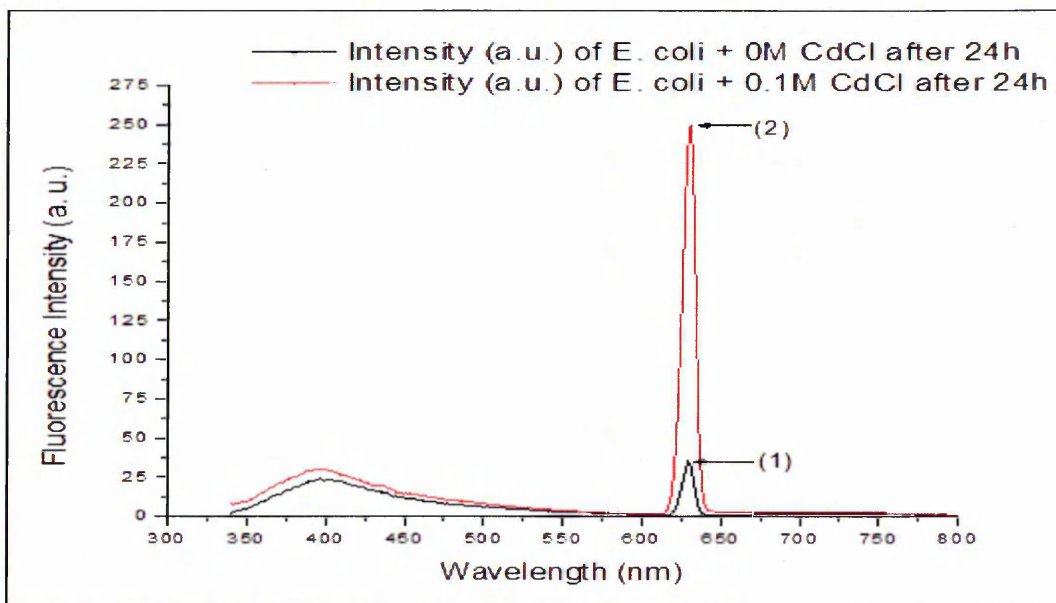


Figure 9.9. Fluorescence spectra (light scatter) of two *E. coli* bacteria samples: (1) not mixed with  $\text{CdCl}_2$ ; and (2) mixed with  $\text{CdCl}_2$  for 24h

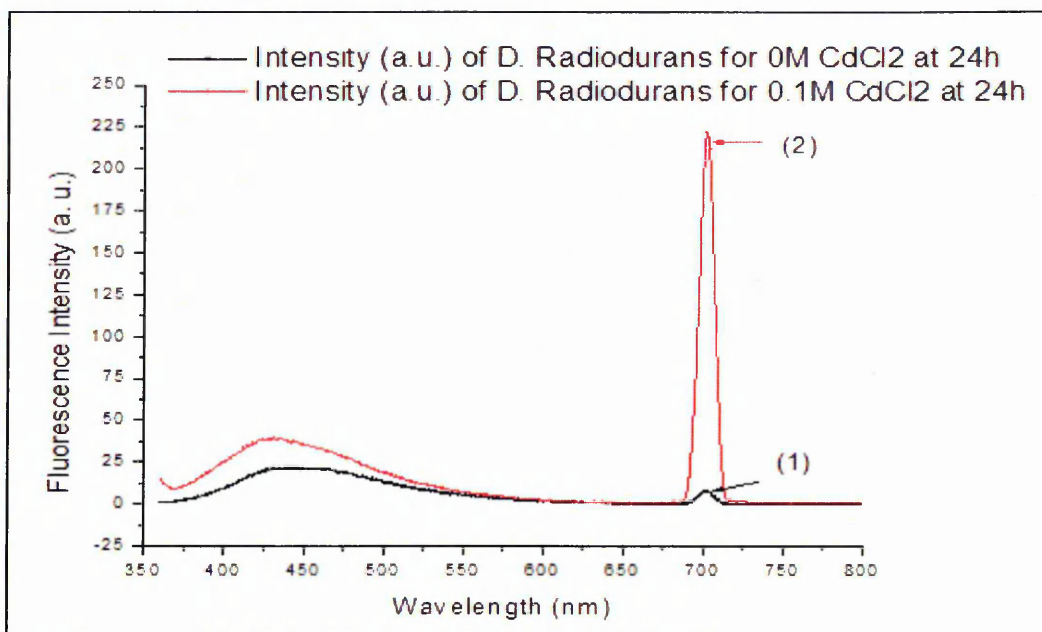


Figure 9.10. Fluorescence spectra (light scatter) of two *D. radiodurans* bacteria samples: (1) not mixed with  $\text{CdCl}_2$ ; and (2) mixed with  $\text{CdCl}_2$  for 24h

A peak appeared (Figures 9.9 and 9.10) at about 630nm for E. coli samples and at 700nm for D. radiodurans samples. The peak intensity is dependent on CdCl<sub>2</sub> concentration and changes with the exposure time. The rest results of fluorescence spectroscopy technique for D. radiodurans bacteria were presented in appendix C, Figures C3, C4. Then the data of fluorescence spectroscopy measurements for both E. coli and D. radiodurans bacteria are summarized in Figures 9.11. The intensity of the scattering of light for exposed samples were normalized on the intensity of scattered light of the bacteria samples not exposed to metal.

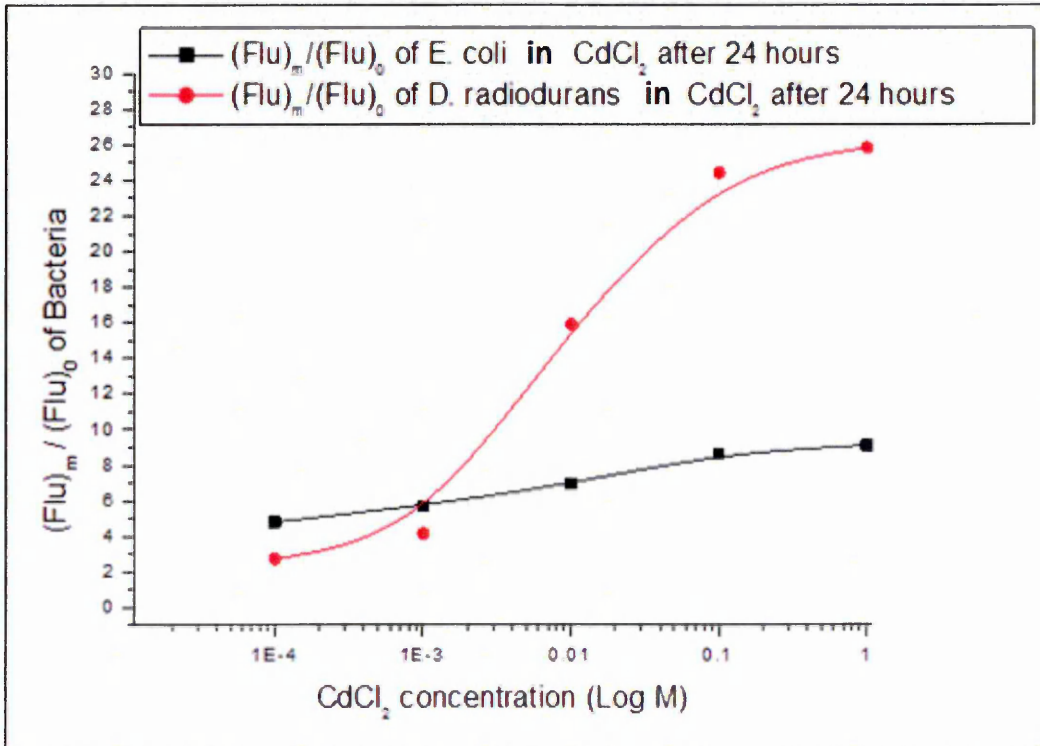


Figure 9.11. Effect of CdCl<sub>2</sub> on 2-nd order diffraction peak for E. coli and D. radiodurans bacteria

(Flu)<sub>m</sub> refers to the fluorescence spectroscopy results of the bacteria samples were exposed to CdCl<sub>2</sub>, and (Flu)<sub>0</sub> refers to the fluorescence spectroscopy results of bacteria samples that are not exposed to metal, and the CdCl<sub>2</sub> concentration is in unit of mol. Figure 9.11 illustrates how CdCl<sub>2</sub> metal concentration can be predicted. As one can see, when the CaCl<sub>2</sub> was added to the E. coli and D. radiodurans culture, the CdCl<sub>2</sub> salt can accumulate in the bacteria membrane and may be absorbed and stored in the channels that distribute in the bacteria membrane (lipid), then the size of the bacteria increases as a result, and the intensity of light scattered is increased, which is the reason why the fluorescence spectrum increased when the salt concentration increased [4].

## 9.2. Optical Study of the Effect of Nickel Chloride (NiCl<sub>2</sub>)

As mentioned in previous chapters, Nickel is a toxic element. Many plant species cannot grow on contaminated soils, although there are especially tolerant species, some of which can accumulate high concentrations. Nickel (II) chloride, is the chemical compound NiCl<sub>2</sub>, the anhydrous salt is yellow, but the more familiar hydrate NiCl<sub>2</sub>·6H<sub>2</sub>O is green. In addition, Nickel (II) chloride solutions are acidic, with a pH of around 4, due to the hydrolysis of the Ni<sup>2+</sup> ion.

The same procedure was followed to prepare one mole from of CdCl<sub>2</sub>·H<sub>2</sub>O, 129.6g from NiCl<sub>2</sub> was added to 1Liter of strile deionize water, the solvent was striled by physical filter (0.22 μm MILLEX<sup>®</sup>GP). One mole concentration from NiCl<sub>2</sub> was obtained, the solution was deliuted by water for different concentration (1M, 0.1M, 0.01M, 0.001M, 0.0001M). the salty solution were added to bacteria cultures ratio 1:1. Finally the salty cultures were kept in a shaker under room temperature conditions for different prieods.

The same previous three optical techniques, namely fluorescence microscopy, fluorescence spectroscopy, and spectrophotometer (optical density), were engaged, in order to study the effect of heavy metals (NiCl<sub>2</sub>) on bacteria. First of all, the (LIVE/DEAD) bacLight, bacteria viability kits is a reliable method for distinguishing between live and dead bacteria in a short time-frame, so this technique were used to studied the effect of NiCl<sub>2</sub> on bacteria samples. The same procedure sequence was used to prepare the glass slides. The samples were tested with fluorescence microscope using a lens of 100× magnification. Slides of stained bacteria were illuminated (excited) with blue light of 420nm in wavelength; the bacteria images were captured using the (Q-Capture-Pro 6.0) program. Figure 9.12 shows the examples of captured images of (E. coli) bacteria as a function of heavy metal concentration and exposure time.

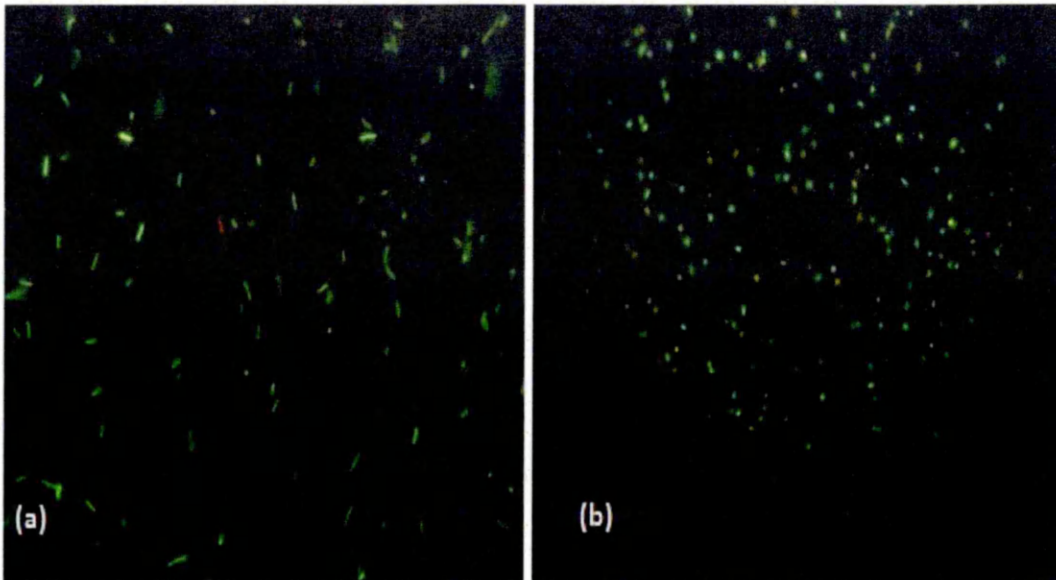


Figure 9.12. Fluorescence microscopy images of *E. coli* bacteria sample (a) without, and (b) with  $\text{NiCl}_2$  for 72 hours after adding the metal

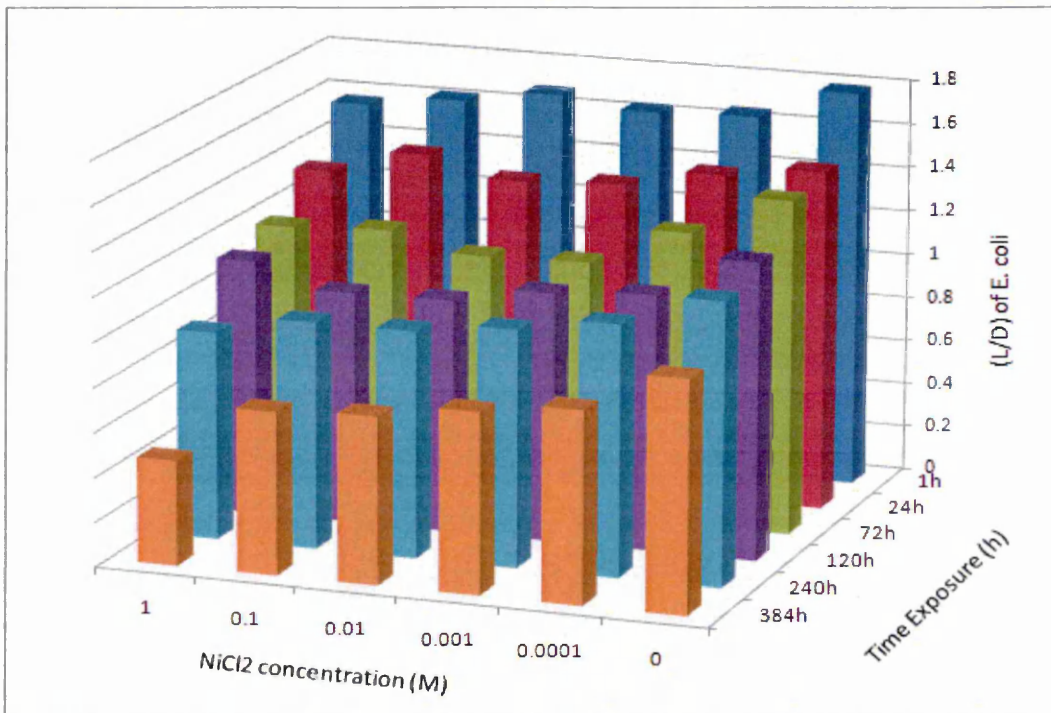


Figure 9.13. Effect of  $\text{NiCl}_2$  on (L/D) ratio of *E. coli* for different time incubations

Figure 9.13 shows how the fluorescence microscopy images giving the Live/Dead ratio for *E. coli* bacteria were obtained by having bacteria appearing as "green" spots while dead bacteria were stained "red". The reduction in the L/D ratio with the increase in  $\text{NiCl}_2$  concentration is apparent for *E. coli* (Fig. 9.13). Exposure time has a significant

effect on the L/D ratio and the metal concentration was effective in the live bacteria density as well. The results of L/D after 72h exposure gives a good indicator regarding the effect of NiCl<sub>2</sub> on E. coli bacteria samples. Figure 9.18 shows the response of E. coli. From Figure 9.14 the concentration of NiCl<sub>2</sub> can easily estimated or evaluated, which shows the ratio (L/D)<sub>m</sub> after adding salt against the ratio (L/D)<sub>0</sub>.

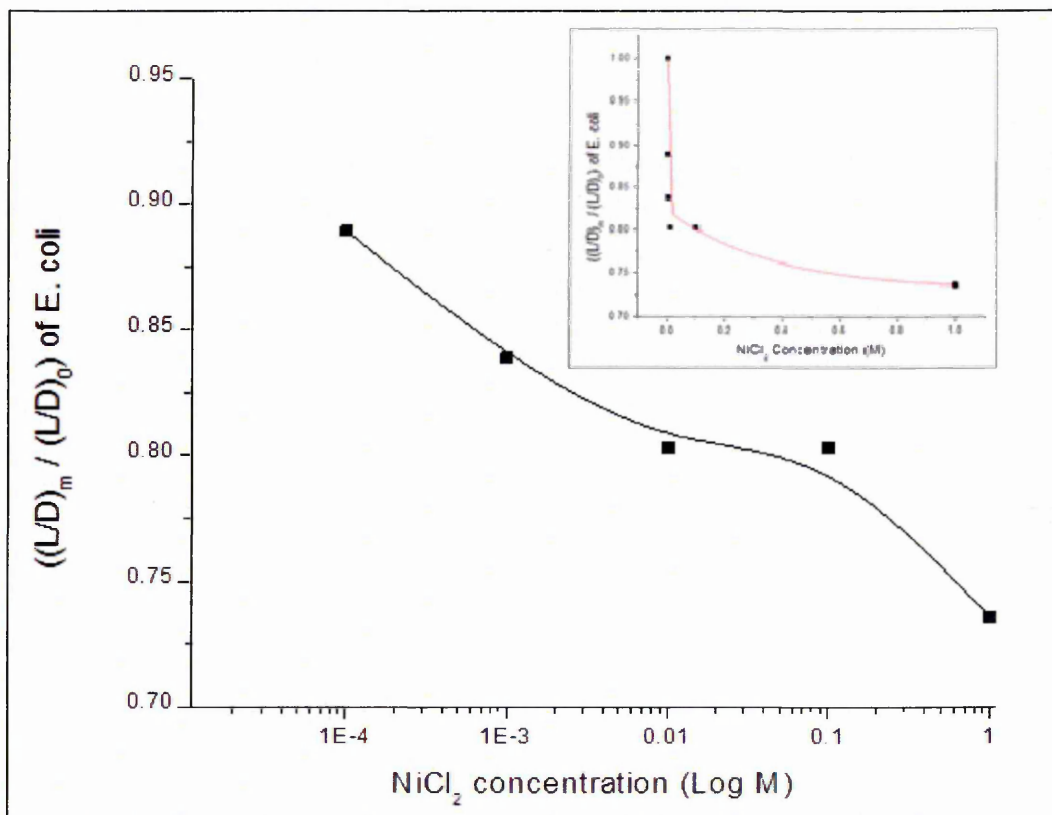


Figure 9.14. Ratio (L/D)<sub>m</sub> of E. coli after adding salt against ratio (L/D)<sub>0</sub> of E. coli without NiCl<sub>2</sub>, after 72 hours exposure

The fitting formula for graph 9.14 is presented in equation 9.3.

$$\frac{\left(\frac{L}{D}\right)_m}{\left(\frac{L}{D}\right)_0} = 0.79 + 0.2 * e^{(-C/0.00013)} \quad (9.3)$$

The D. radiodurans bacteria were also exposed to Nickel Chloride for different periods, from 1 hour up to 550 hour. The effect of NiCl<sub>2</sub> on the bacteria density was examined and analysed using three previous different optical experimental techniques. Fersit. fluorescence microscopy measurements were performed using the OLYMPUS-BX60 instrument. The numbers of live and dead bacteria were determined. Typical fluorescence microscopy images of samples of D. radiodurans bacteria are shown in Figure 9.15. Again, in these images, live bacteria emit green light while dead bacteria

emit red light. The difference are between images taken with and without exposure or added the  $\text{NiCl}_2$ .

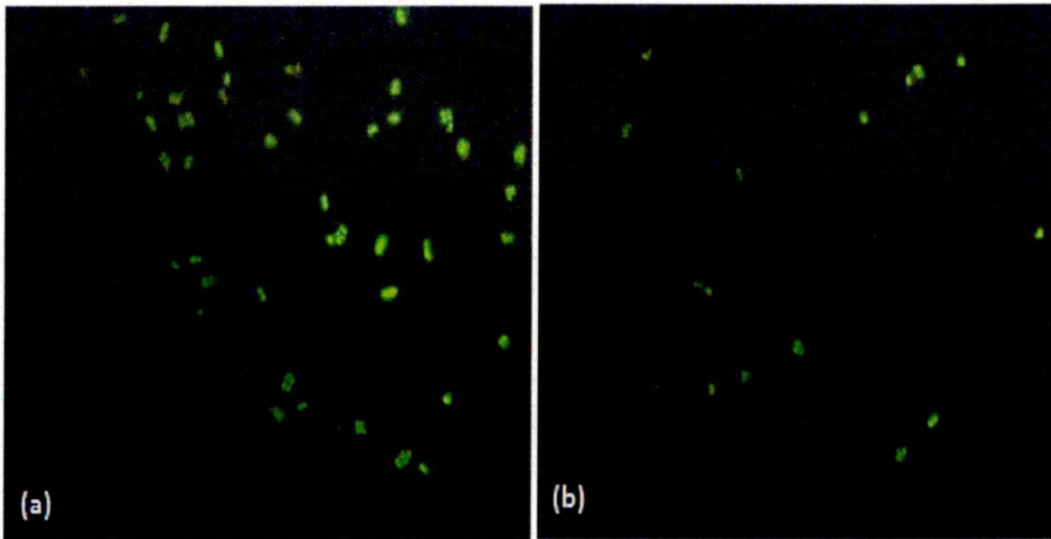


Figure 9.15. Fluorescence microscopy images of *D. radiodurans* bacteria sample (a) without and (b) with  $\text{NiCl}_2$  for 120 hours, after adding the metal

The data taken from fluorescence microscope images were analysed and calculated, and the ratio (L/D) of *D. radiodurans* plotted, as shown in Figure 9.16.

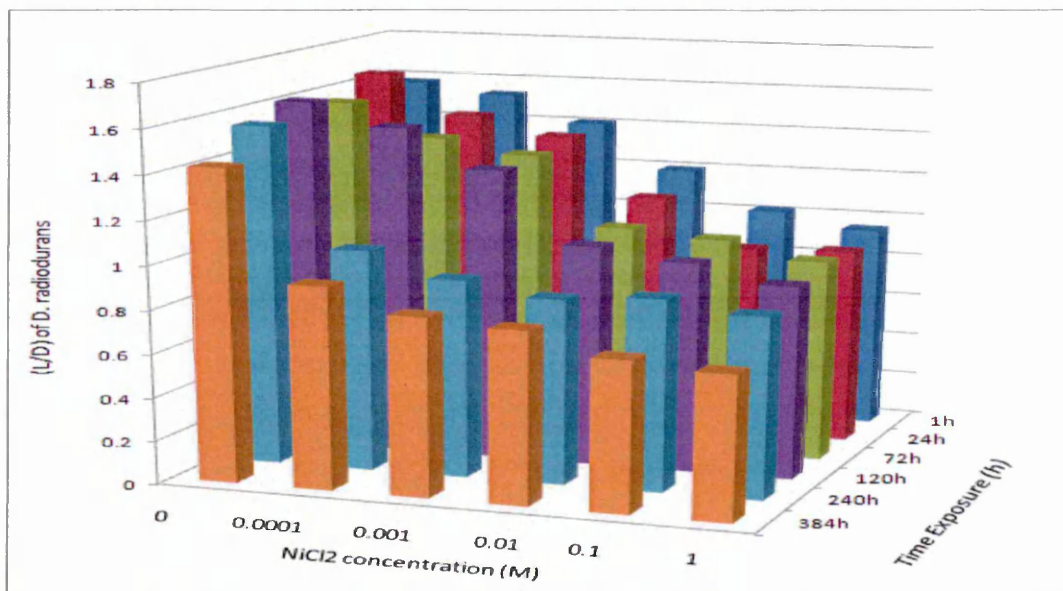


Figure 9.16. Effect of  $\text{NiCl}_2$  on L/D ratio of *D. radiodurans* for different time incubations

The concentration of  $\text{NiCl}_2$  can be estimated. The results of L/D after 72h exposure given a good indicator regarding the effect of  $\text{NiCl}_2$  on *D. radiodurans* bacteria samples. Figure 9.16 shows the response of *D. radiodurans* in the ratio  $(L/D)_m$  after adding the metal against the ratio  $(L/D)_0$  without metal.

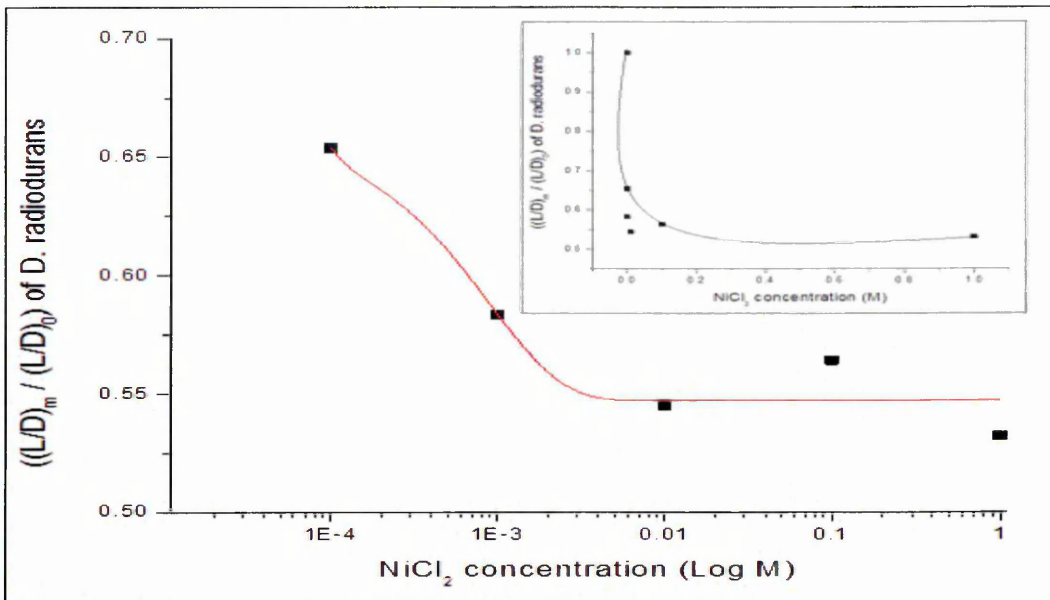


Figure 9.17. Ratio  $(L/D)_m$  of *D. radiodurans* after adding  $NiCl_2$  against ratio  $(L/D)_0$  of *D. radiodurans* without  $NiCl_2$ , after 72 hours exposure

The fitting formula for graph 9.17 is presented in equation 9.4.

$$\frac{\left(\frac{L}{D}\right)_m}{\left(\frac{L}{D}\right)_0} = 0.55 + 0.44 * e^{(-C./0.000066)} \quad (9.4)$$

The  $(L/D)$  ratio decreased very sharply, as is clear from Figure 9.17; and it is also clear in time constant value ( $6.6 * 10^{-5}$ ). The data of  $(L/D)$  measurements for both *E. coli* and *D. radiodurans* bacteria are summarized in Figures 9.18. The  $(L/D)$  ratio for exposed bacteria samples were normalized with non-exposed bacteria samples.

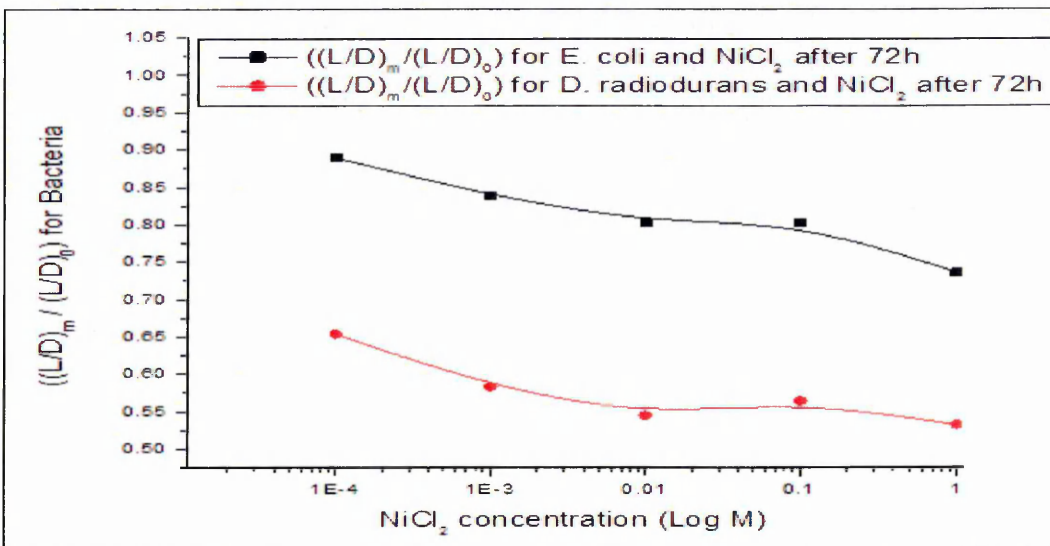


Figure 9.18. Dependence of  $(L/D)_m / (L/D)_0$  bacteria ratio for both *E. coli* and *D. radiodurans* bacteria through exposure time 72h to  $NiCl_2$

Optical density  $OD_{600}$  results were also recorded as a function of  $NiCl_2$  concentration and the time exposed to metals.  $OD_{600}$  recordings have been presented as either absorption of light, which refers directly to the bacteria cells density, or related to the size of bacteria which are very effective on the density of scattered light, which is sensitive to metals.  $OD_{600}$  results of *E. coli* after adding  $NiCl_2$  as a function of metal concentration and time of exposure to the metal were presented in Figure C5 (appendix C). An optical density  $OD_{600}$  technique was also used to estimate the *D. radiodurans* bacteria cells density as a function of exposure time to different concentrations of  $NiCl_2$ . It has to be mentioned that, in the  $OD_{600}$  experiments, the absorbance values recorded do not represent the actual absorption of the light by the samples but rather losses of light intensity due to light scattering on live bacteria. From the  $OD_{600}$  data, the metal may change the bacteria cell size, and the intensity of scattered light changed frequently.  $OD_{600}$  results of *D. radiodurans* after adding  $NiCl_2$  as a function of metal concentration and exposure time to the metal were presented in Figure C6 (appendix C). Another optical technique, fluorescence spectroscopy, was explored, in order to confirm the above results on the effect of  $NiCl_2$  on bacteria count, as well as to study the fluorescence spectra of *E. coli* and *D. radiodurans* bacteria in more detail. The emission fluorescence spectra of bacteria samples were recorded using the excitation wavelength of 315 nm for *E. coli*. The fluorescence spectroscopy measurements performed on *E. coli* and *D. radiodurans* bacteria samples and the spectrums shown in Figure 9.19.

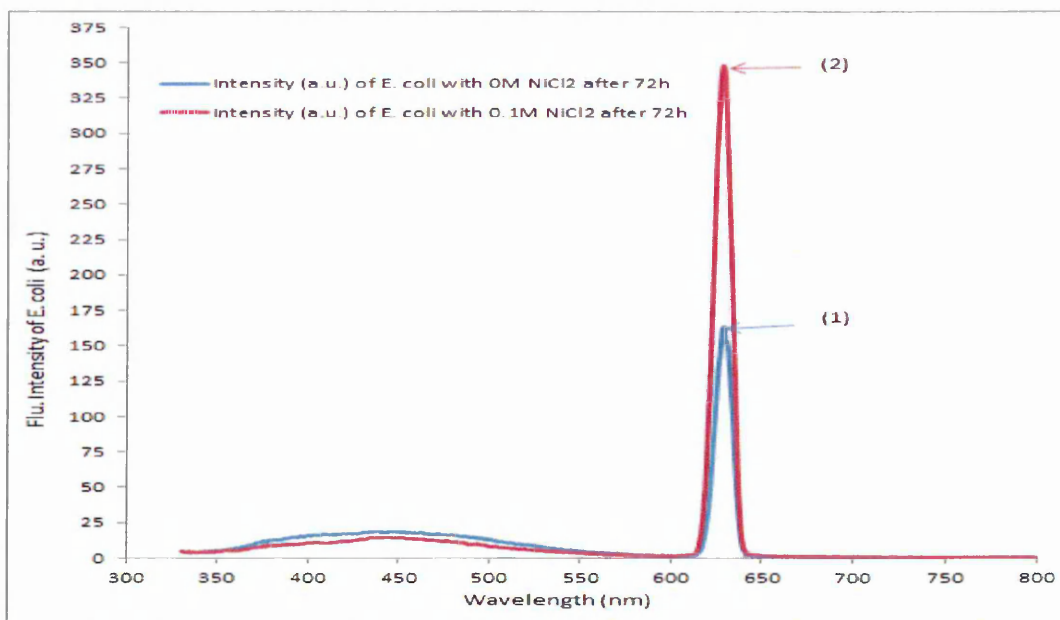


Figure 9.19. Fluorescence spectra (light scatter) of two *E. coli* bacteria samples: (1) not mixed with  $NiCl_2$ ; and (2) mixed with (0.1 mol) of  $NiCl_2$  after 72h

The emission fluorescence spectra of *D. radiodurans* samples were recorded using the excitation wavelength of 350 nm. The emission spectra presented in Figure 9.20. The maximum fluorescence intensity was indicated to be live cell concentration dependent.

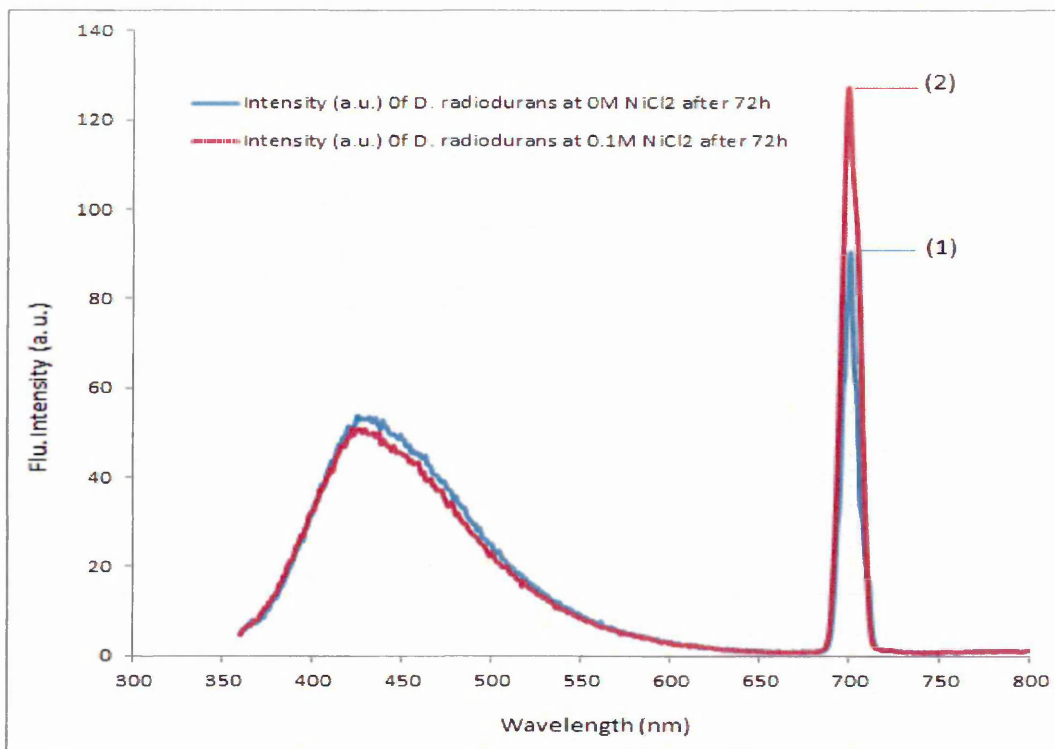


Figure 9.20. Fluorescence spectra (light scatter) of two *D. radiodurans* bacteria samples: (1) not mixed with NiCl<sub>2</sub>; and (2) mixed with (0.1 mol) of NiCl<sub>2</sub> after 72h

The peak appears in Figures 9.19 and 9.20 at about 630nm for *E. coli* samples and at 700nm for *D. radiodurans* samples. The intensity is depending on NiCl<sub>2</sub> concentration. Changes in exposure time are presented in Figures C7 and C8 (appendix C).

The data of fluorescence spectroscopy measurements for both *E. coli* and *D. radiodurans* bacteria are summarized and presented in Figures 9.21. The intensity of scattered light for exposed samples were normalized on the intensity of scattered light of the bacteria samples not exposed to metal.

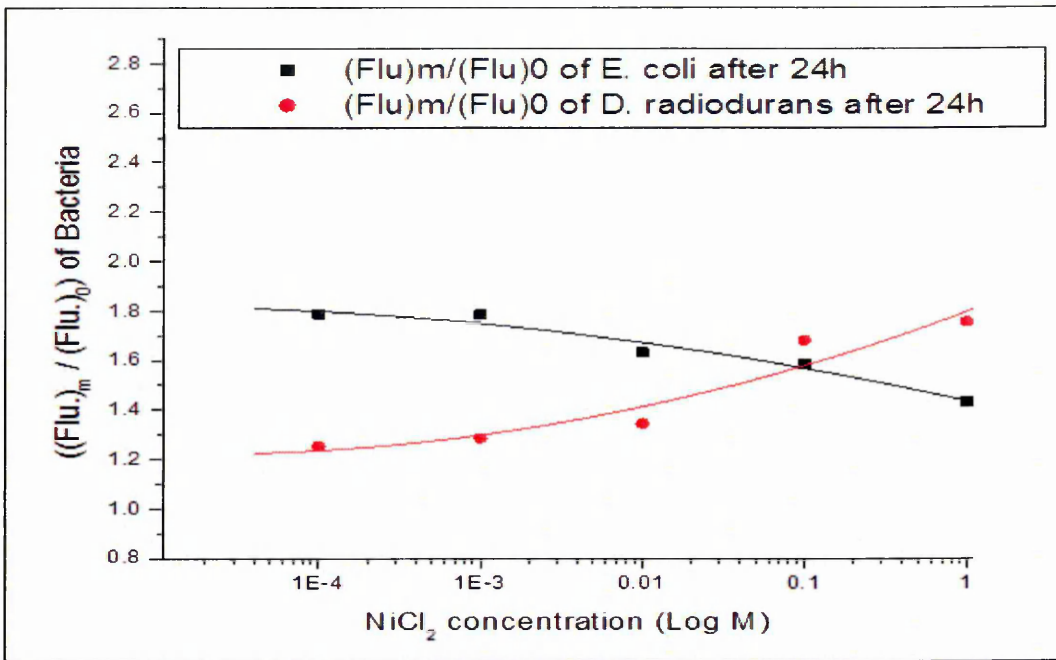


Figure 9.21. Effect of NiCl<sub>2</sub> on 2-nd order diffraction peak for E. coli and D. radiodurans bacteria

(Flu)<sub>m</sub> represents the fluorescence spectroscopy of bacteria samples exposed to NiCl<sub>2</sub>, (Flu)<sub>0</sub> represents the fluorescence spectroscopy of bacteria samples not exposed to metal, and the NiCl<sub>2</sub> concentration were measured in unit of mol.

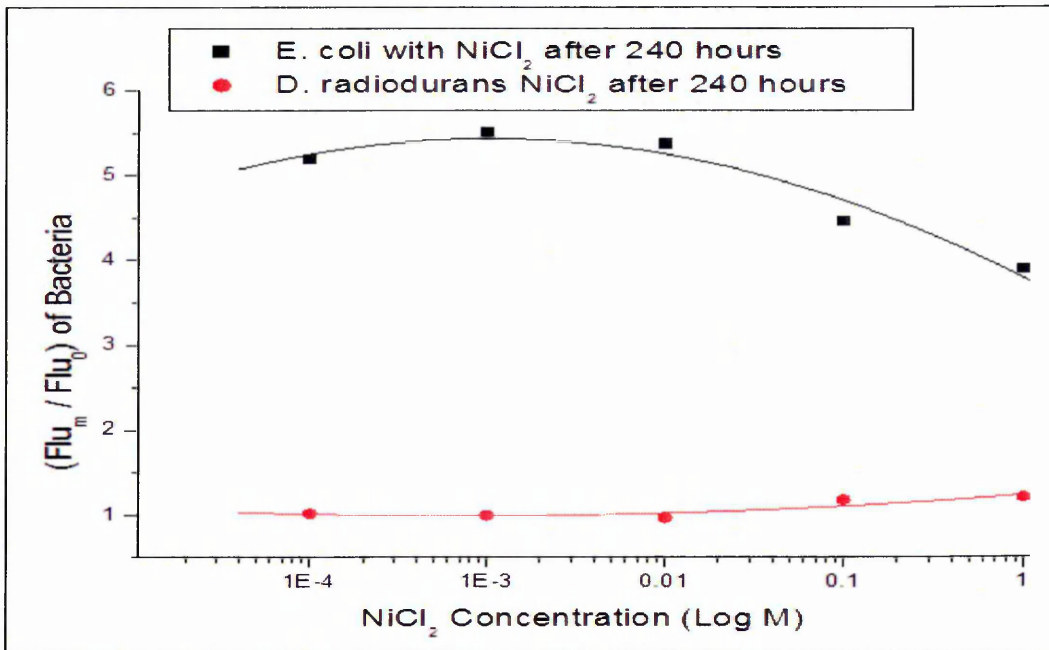


Figure 9.22. Effect of NiCl<sub>2</sub> on 2-nd order diffraction peak for E. coli and D. radiodurans bacteria after 240 hours

The comparison of the inhibition effects of gamma radiation, CdCl<sub>2</sub> and NiCl<sub>2</sub> on E. coli and D. radiodurans bacteria was carried out using true L/D ratio data of fluorescence

microscopy. It showed clearly a possibility of pattern recognition of the two inhibition factors, e.g. gamma radiation and heavy metals [6].

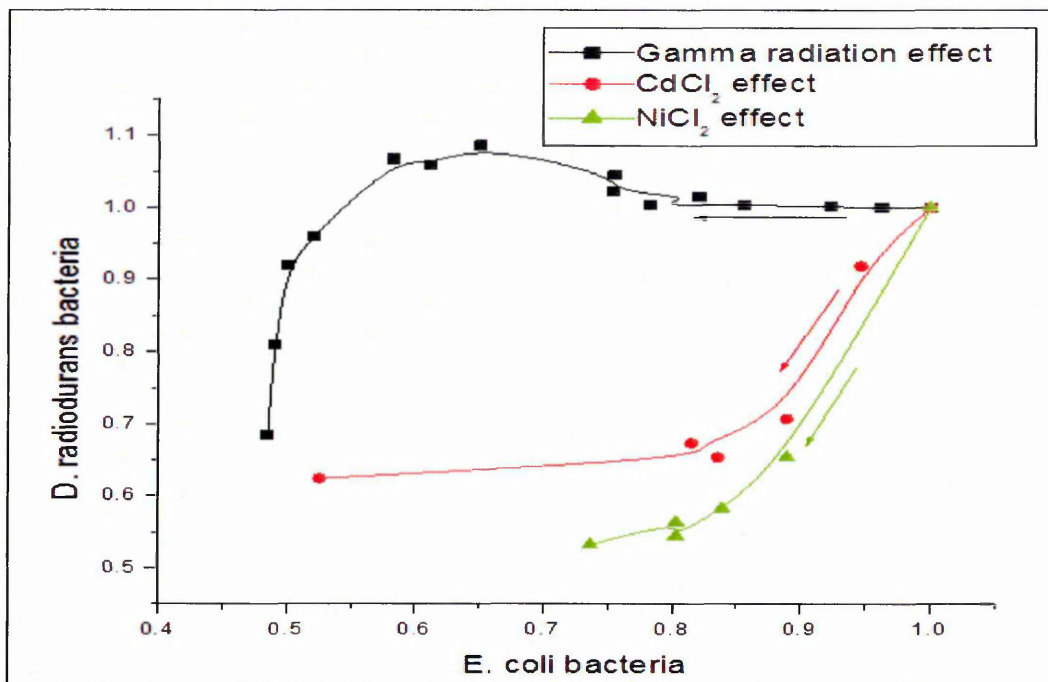


Figure 9.23. Comparisons of relative changes in (L/D) ratio, for *E. coli* and *D. radiodurans* bacteria in response to exposure to gamma radiation, CdCl<sub>2</sub> and NiCl<sub>2</sub>

From the pattern recognition in Figure 9.23, the big difference is in bacteria response for two kinds of pollutions (gamma radiation and heavy metal). Furthermore, the two types of bacteria also showed different reactions to each type of pollutant. The bacteria response is useful and can be employed to identify the type of pollutant present in water.

#### References:

1. Lide, David R., (1998), Handbook of Chemistry and Physics (87 ed.), Boca Raton, FL: CRC Press, pp. 4-67.
2. Greenwood N. N, A. Earnshaw, (1997), Chemistry of the Elements, 2nd ed., Butterworth-Heinemann, Oxford, UK.
3. Agranoff D., Krishna, S., (1998), Metal ion homeostasis and intracellular parasitism, Molecular Microbiology, Vol. 28. pp. 403-412.
4. Ken Gillera E, Ernst Witterb, Steve Mcgrathc P, (1998), Toxicity of heavy metals to microorganisms and microbial processes in agricultural soils: a review, Soil Biology and Biochemistry, Volume 30, Issues 10-11, pp. 1389-1414.

5. Pray, A. P, Tyree, S. Y, Martin Dean F, Cook James R,(1990),Anhydrous Metal Chlorides. *Inorganic Syntheses*, 28: pp. 321-322.
6. Al-Shanawa M, Nabok A, Hashim A, Smith T, Forder S,(2014), Optical study of the effect of gamma radiation and heavy metals on microorganisms (bacteria), *BioNanoScience Journal*, Elsevier, 4: pp. 180-188.

## CHAPTER 10

### Electrical Study of the Effect of Heavy Metals on Bacteria

As mentioned in Chapter 9, the bacteria samples were exposed (mixed) to CdCl<sub>2</sub> and NiCl<sub>2</sub> for different lengths of time. Several electrical experimental techniques (DC and AC characteristics) were used to test and analyse the bacteria samples: (i) the non-pathogenic DH5 $\alpha$  strain of Escherichia coli (E. coli); and (ii) the Anderson R1 strain of Deinococcus Radiodurans (D. radiodurans), that were tested optically (Chapter 8), and showed the effect of heavy metals on the bacteria density.

#### 10.1. Samples for Electrical Tests

Solutions of different concentrations (0.1mM, 1mM, 10mM, 100mM, and 1M) of CdCl<sub>2</sub> and NiCl<sub>2</sub> were prepared, using de-ionized water. Cadmium chloride and nickel chloride dissolves well in water and other polar solvents [1]. The salty solution was added to bacteria cultures in the ratio 1:1. After that the salty cultures were kept in a shaker under room temperature conditions for different periods. The aim of this part of work was to develop a simple electrochemical sensor for monitoring and studying the effect of heavy metals (CdCl<sub>2</sub> & NiCl<sub>2</sub>) using bacteria. A series of DC and AC electrical measurements were carried out on samples of two types of bacteria. As a first step, a correlation between DC and AC electrical currents (IV, conductivity, and capacitance) and bacteria concentration in a solution was established. The study of the effect of heavy metals on DC and AC electrical characteristics of bacteria revealed the inhibition factors. The analysis of DC and AC measurements is rather complicated. There are three major factors to consider:

1. The effect of CdCl<sub>2</sub> and NiCl<sub>2</sub> on E. coli and D. radiodurans bacteria.
2. Natural reduction of bacteria concentration without salt.
3. The effect of salt on broth medium.

The most logic way to deal with this is to use the conductivity of broth with salt as a reference for every curve, and construct relative changes of the bacteria sample conductivity.

$$\frac{I_c(\text{bacteria} + \text{broth} + \text{salt}) - I_c(\text{broth} + \text{salt})}{I_c(\text{bacteria} + \text{broth})}$$

or simply:  $I_{Net}(\text{metal}) = \frac{\Delta I_c}{I_{c0}}$  (10.1)

This method was applied for Gp and Rb, as well as for Rb, Rs and Cs.

## **10.2. Electrical Study of the Effect of Nickel Chloride( $\text{CdCl}_2$ ) on Bacteria**

In order to achieve this work simple electrical (electrochemical) measurements were used, i.e. firstly establishing the correlation between electrical properties (conductivity, capacitance and IV characteristic) of liquid bacteria samples and live bacteria counts. Series of DC and AC electrical measurements were carried out on samples of two types of bacteria. DC electrical tests were performed using the (6517A Keithley Electrometer), in the  $\pm 0.5\text{V}$  voltage range, which was selected in order to avoid electrochemical oxidation and reduction reactions on the metal electrodes while the relative IV (correlation) was studied.

AC electrical measurements were performed using (HP-4284A PRECISION LCR METER) in the frequency range 20 Hz to 1 MHz, with the amplitude of AC voltage of 100mV and no DC bias applied. The spectra of two parameters Gp and Cp corresponding to a parallel connection of conductance and capacitance were recorded.

### **10.2.1. DC Electrical Measurements of Bacteria and $\text{CdCl}_2$**

In this part of work, the simple electrical (electrochemical) measurements were achieved. Typical I-V characteristics of E. coli samples having different concentrations of bacteria are shown in Figure 8.1 (Chapter 8). The cathode current appeared to be much higher than the anode current. The increase in bacteria concentration in the solution leads to a decrease in the cathode current, which can be explained by insulation properties of bacteria. The use of two types of bacteria may lead to pattern recognition of inhibition factors ( $\text{CdCl}_2$  and  $\text{NiCl}_2$ ). The effect of exposure for different periods and different concentration of  $\text{CdCl}_2$  on E. coli bacteria samples were studied and plotted in Figure 10.1, which presents the I-V characteristics as a function of metal concentration. In addition, the (IV) characteristics for a different concentration, of mixed  $\text{CdCl}_2$  with an LB broth are presented in Figure 10.2.

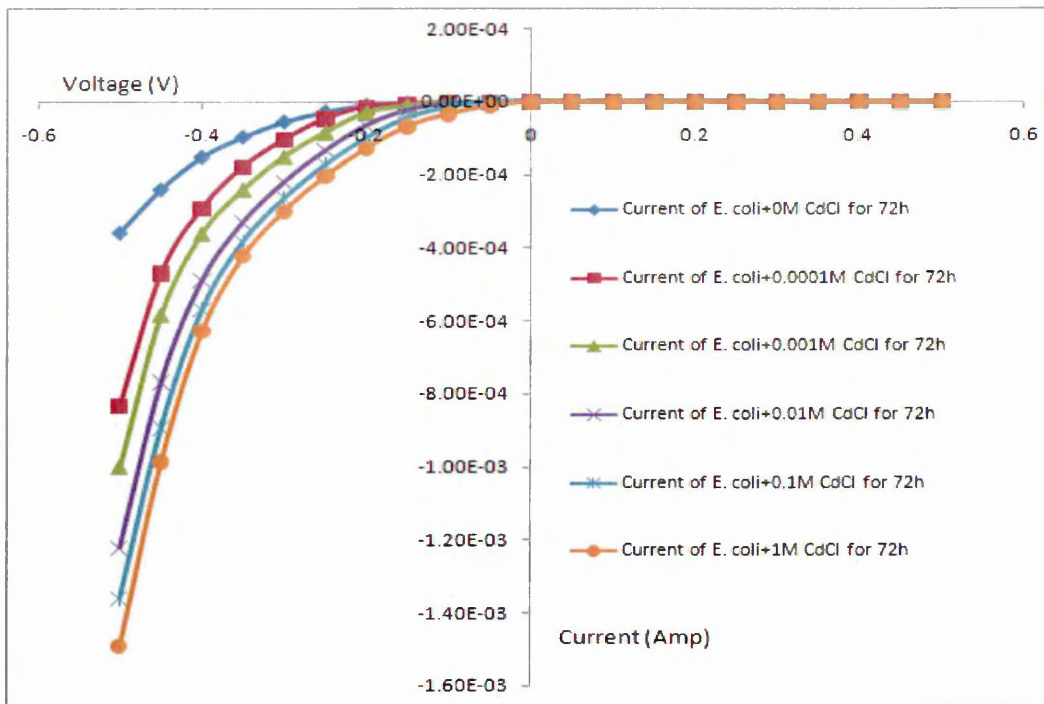


Figure 10.1.I-V characteristics of *E. coli* samples for different concentration of  $\text{CdCl}_2$  after 72 hours exposure time, in normal environmental conditions inside shaker

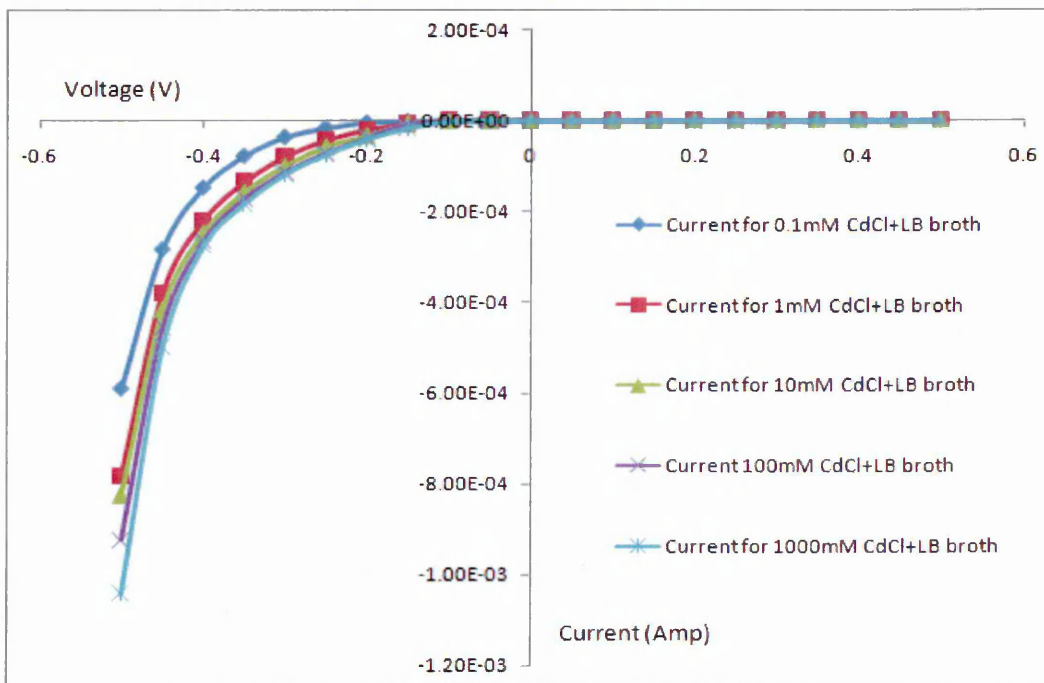


Figure 10.2.I-V characteristics for different concentrations of  $\text{CdCl}_2$  with LB broth

In order to study the effect of  $\text{CdCl}_2$  on *E. coli* bacteria, the cathodic current of *E. coli* bacteria after adding  $\text{CdCl}_2$  at  $-0.5\text{V}$  were measured and normalised to the cathodic current of  $\text{CdCl}_2$  with clear LB broth and the result are shown in Figure 10.3.

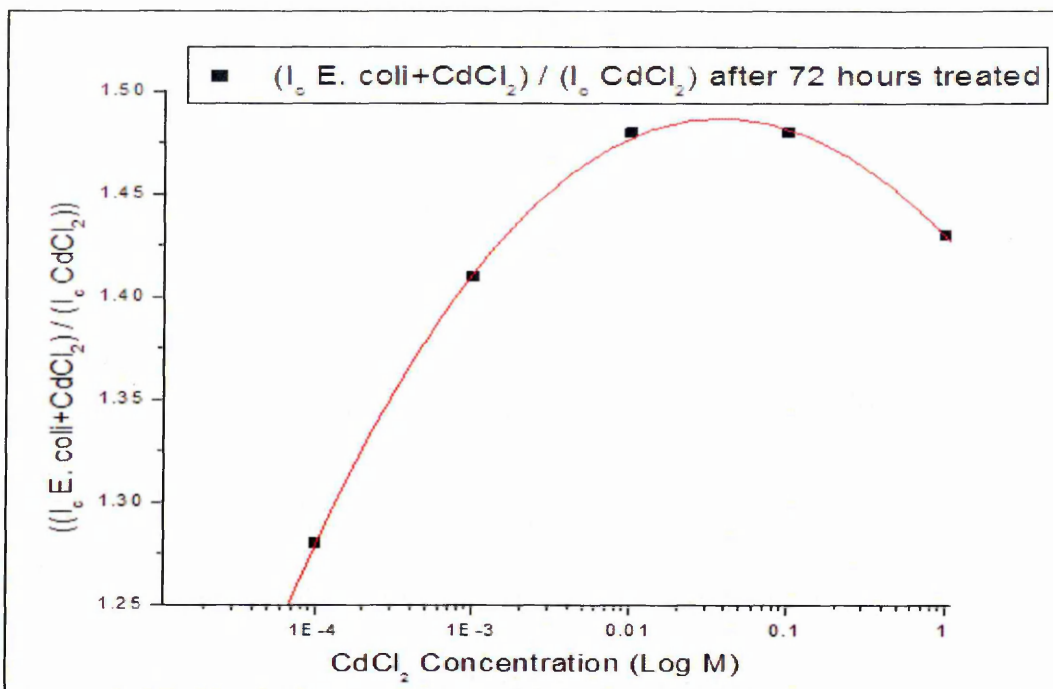


Figure 10.3.  $I_c$  E. coli in CdCl<sub>2</sub> /  $I_c$  cdc<sub>2</sub> characteristics for different concentrations of CdCl<sub>2</sub> with LB broth

The effect of CdCl<sub>2</sub> on E. coli bacteria was studied through normalising the cathodic current of E. coli bacteria after adding CdCl<sub>2</sub>, on the cathodic current of E. coli in (0M CdCl<sub>2</sub>) in LB broth, these interesting results are shown in Figure 10.4.

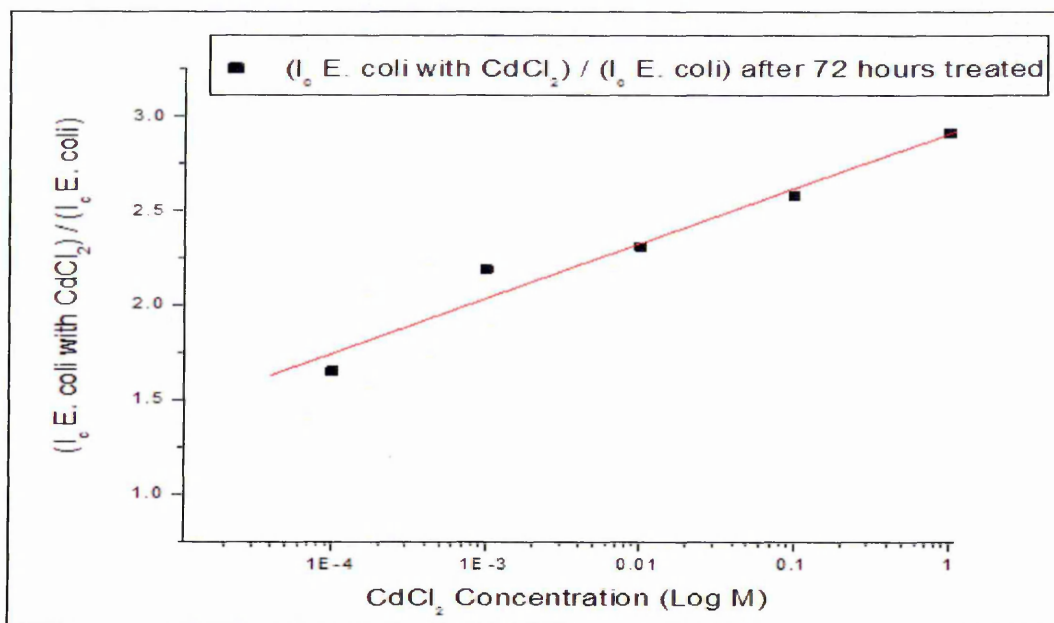


Figure 10.4.  $I_c$  E. coli in cdc<sub>2</sub> /  $I_c$  of E. coli characteristics for 0M CdCl<sub>2</sub> in LB broth at (-0.5V) after 72 hours

In order to study and analyse the effect of CdCl<sub>2</sub> on E. coli bacteria, the relative changes of cathode current at -0.5 Volt for bacteria samples after being treated with salt were

calculated with cathode current of salt over the cathode current of bacteria samples. See Figure 10.5.

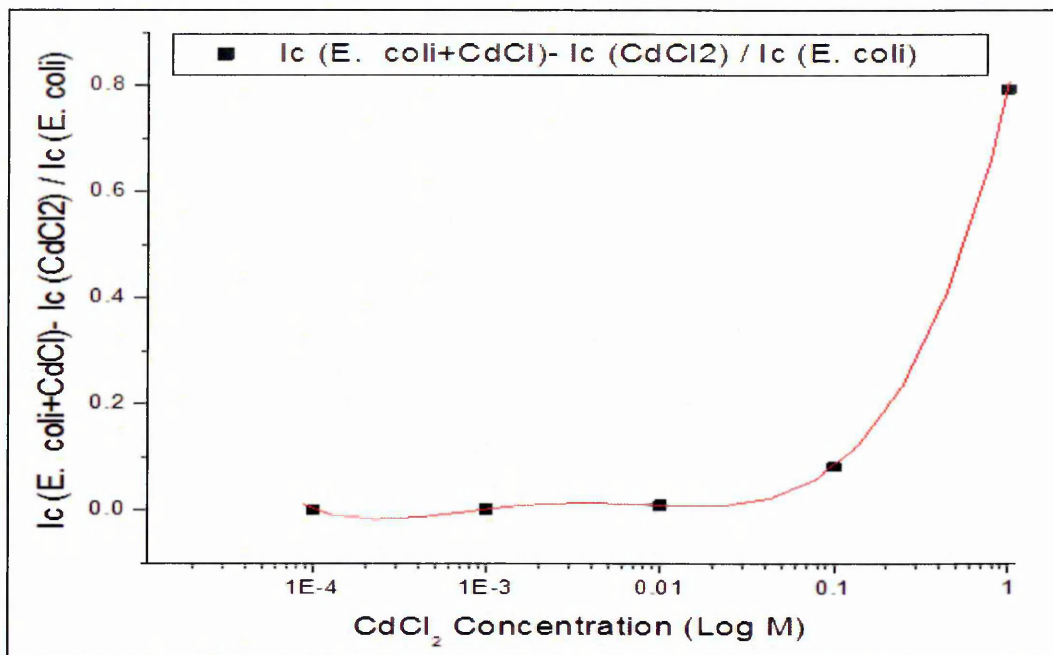


Figure 10.5. Relative changes of cathodic current  $I_c$  for *E. coli* indifferent concentrations of  $CdCl_2$  for  $I_c$  of  $CdCl_2$  in LB broth over  $I_c$  of *E. coli* sample after 72 hours

A similar sequence of measurements was followed for the cultivation of *D. radiodurans* (Anderson R1 strain). The *D. radiodurans* samples were mixed with different concentrations of  $CdCl_2$  and checked electrically for different periods, and the results are presented in appendix D, Figure D1.

Meanwhile, the OXOID CM3 nutrient broth was mixed with different concentration of  $CdCl_2$ . Further results are presented in appendix D.

The effect of *D. radiodurans* bacteria on  $CdCl_2$  was determined during measuring the change in the cathodic current. The cathodic current of *D. radiodurans* bacteria after adding  $CdCl_2$  at -0.5V were normalised the cathodic current of  $CdCl_2$  with OXOID broth, see Figure 10.6.

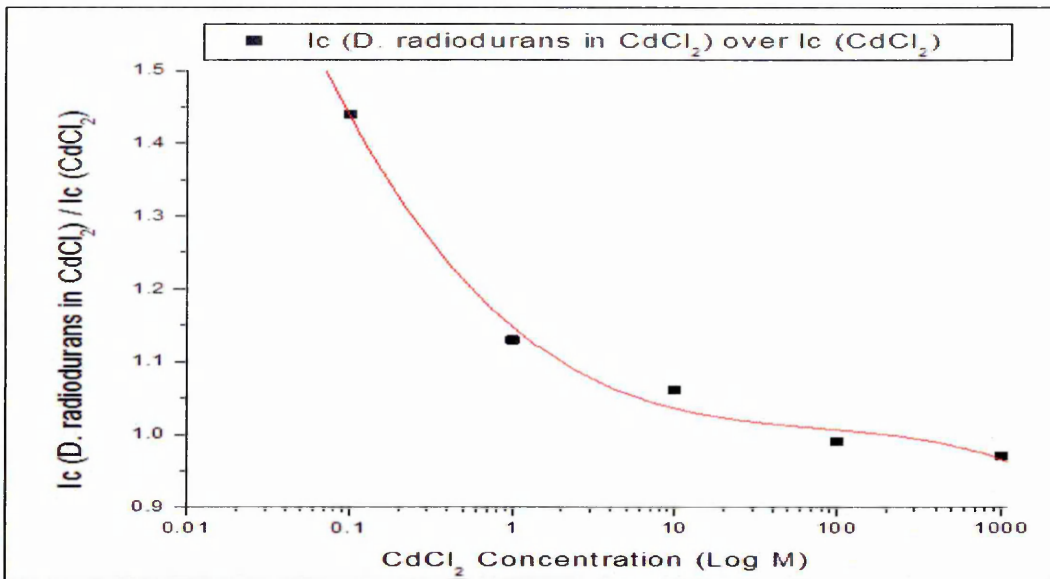


Figure 10.6.  $I_c$  of *D. radiodurans* in  $CdCl_2$  /  $I_c$  of  $CdCl_2$  characteristics for different concentrations of  $CdCl_2$  in OXOID broth

The effect of  $CdCl_2$  on *D. radiodurans* bacteria was determined through normalising the cathodic current of *D. radiodurans* bacteria after adding  $CdCl_2$  at (-0.5V) to the cathodic current of *D. radiodurans* with an LB broth, as shown in Figure 10.7.

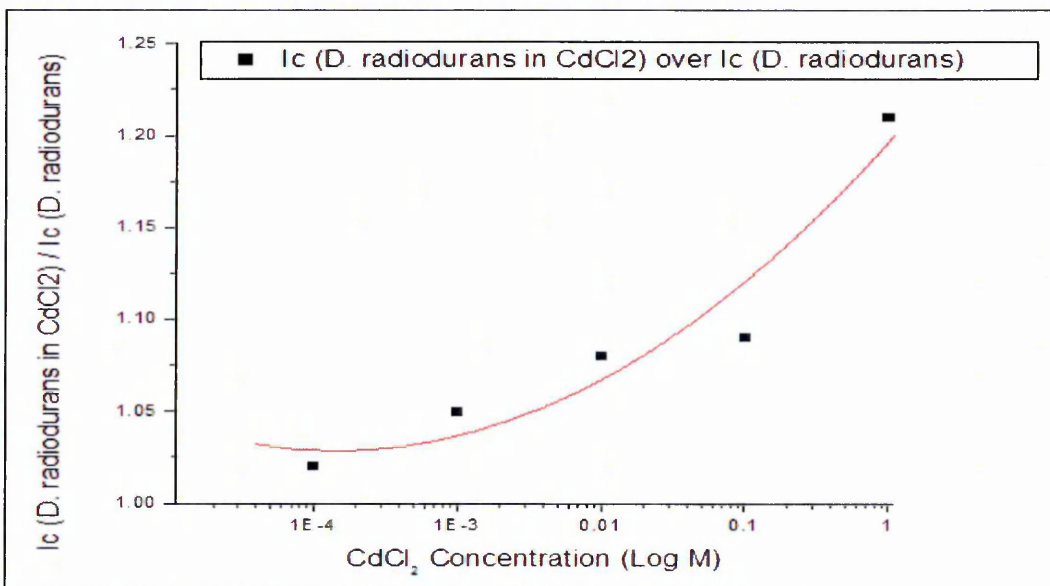


Figure 10.7.  $I_c$  *D. radiodurans* in  $CdCl_2$  /  $I_c$  of *D. radiodurans* characteristics for different concentrations of  $CdCl_2$  in OXOID broth at -0.5V after 72 hours

Again, in order to study and analyse the effect of  $CdCl_2$  on *D. radiodurans* bacteria, the relative change of cathode current at -0.5 Volt of bacteria samples after treated with salt calculated with cathode current of salt over the cathode current of bacteria samples. See Figure 10.8.

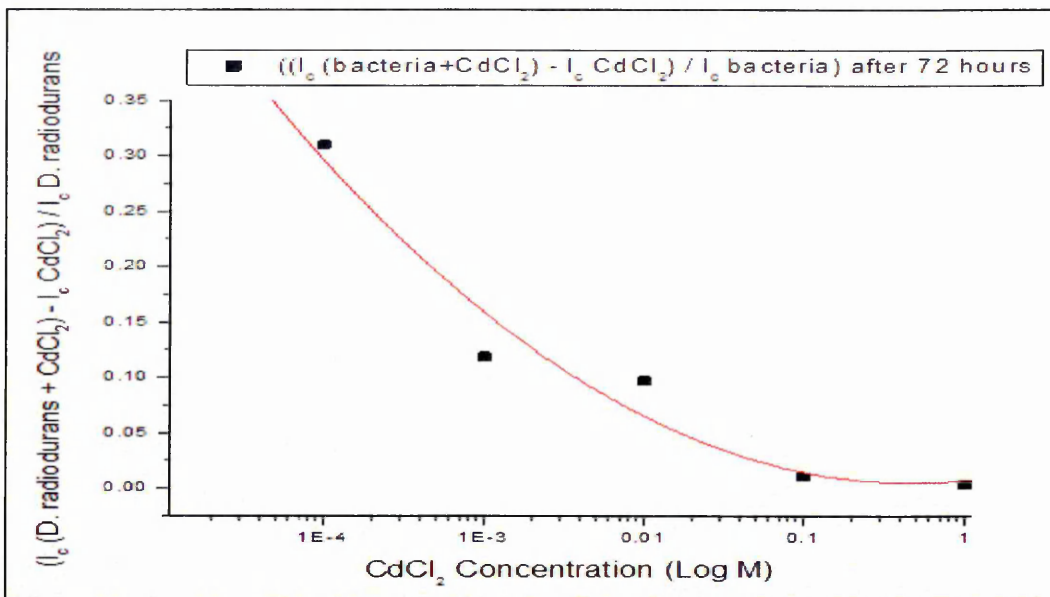


Figure 10.8. Relative change of cathodic current  $I_c$  for *D. radiodurans* in different concentration of  $CdCl_2$  for  $I_c$  of  $CdCl_2$  with LB broth over  $I_c$  of *D. radiodurans* sample after 72 hours

The best way to estimate the level (concentration) of  $CdCl_2$  is with pattern recognition, which can be achieved through a comparison of relative responses of  $I_c$  (cathodic current at -0.5V) for *E. coli* and *D. radiodurans* bacteria. This comparison is very important and useful, as one can see when obtaining the results of normalisation for each bacteria sample the metal concentration can be found directly from the curve of Figures (10.9, 10.10).

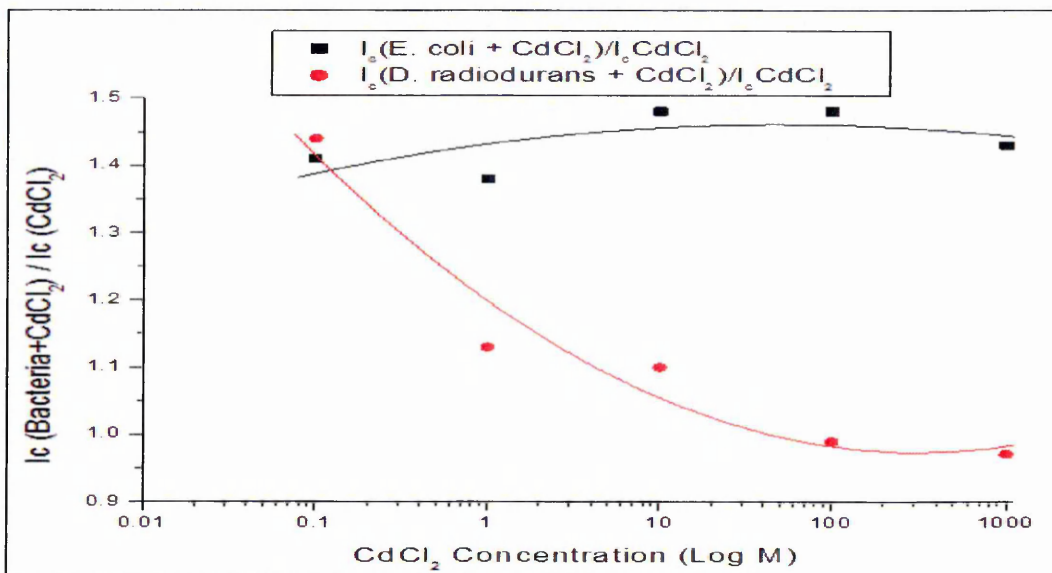


Figure 10.9. Comparison of relative responses of  $I_c$  (cathodic current) methods to  $CdCl_2$  for *E. coli* and *D. radiodurans* bacteria at (-0.5V)

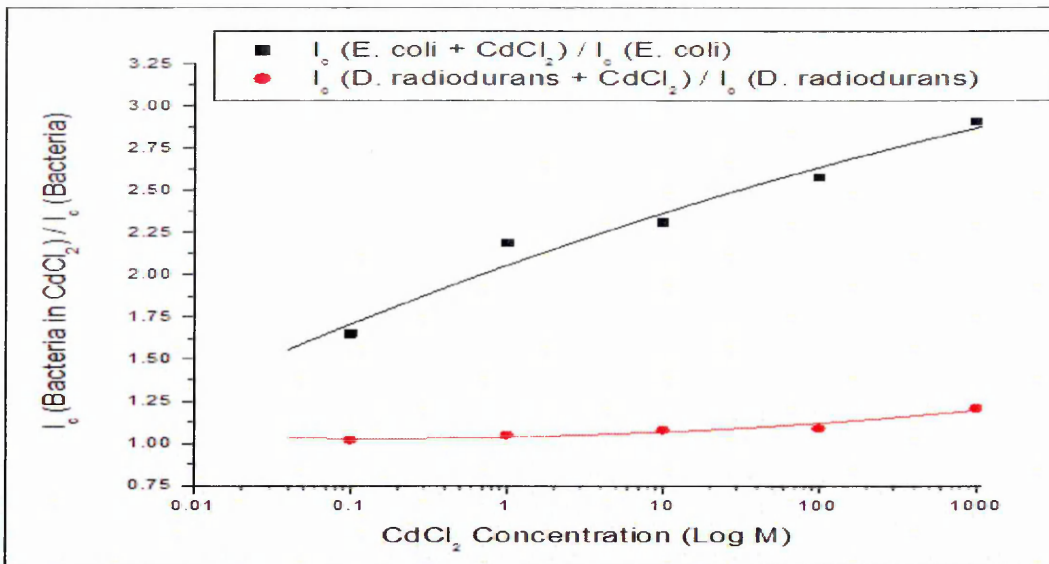


Figure 10.10. Comparison of relative responses of  $I_c$  (cathodic current) for E.coli and D. radiodurans bacteria with  $CdCl_2$  to  $I_c$  of bacteria without metal at (-0.5V)

As mentioned at the beginning of this chapter, the relative change of  $I_c$  was calculated for both bacteria types; this method gives clear vision of salt impact on bacteria, as shown in Figure 10.11.

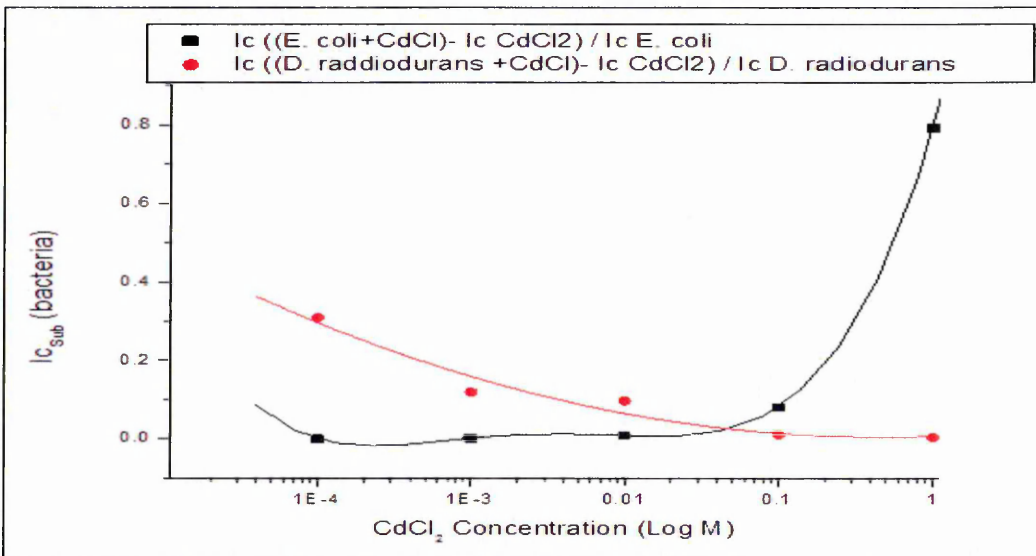


Figure 10.11. Comparison of relative changes of  $I_{c-sub}$  (cathodic current) methods to  $CdCl_2$  for both types of bacteria.

### 10.2.2. AC Electrical Measurements of Bacteria and $CdCl_2$

In this part, the simple electrical (electrochemical) AC measurements are carried out and discussed. A typical AC conductance (AC-Gp) graph of E. coli samples having different concentrations of  $CdCl_2$  are shown in Figure 10.12. The AC conduction of E.

coli increases with the increase in  $\text{CdCl}_2$  concentration, which correlates well with the decrease in live bacteria concentration.

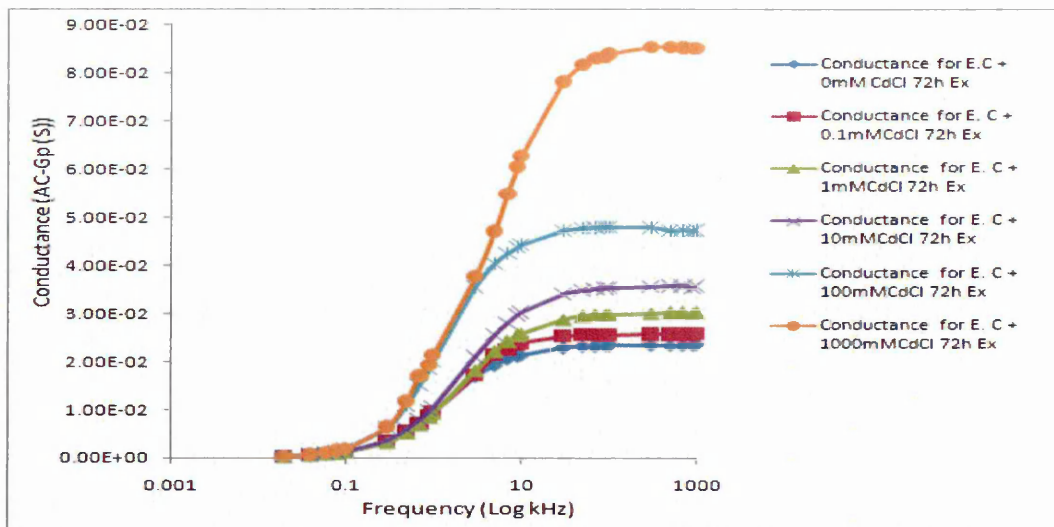


Figure 10.12. Typical AC-Gp characteristics of E. coli samples for different concentrations of  $\text{CdCl}_2$

In addition, the changes in the capacitance of E. coli for different concentrations of  $\text{CdCl}_2$  were studied. Figure 10.13 shows the capacitance change with the change in metal concentration. The increase in  $\text{CdCl}_2$  metal concentration leads to lower capacitance values, since the dead bacteria working as insulating materials. The increase in metal salt concentration leads to a decrease in capacitance and an increase in solution conductance.

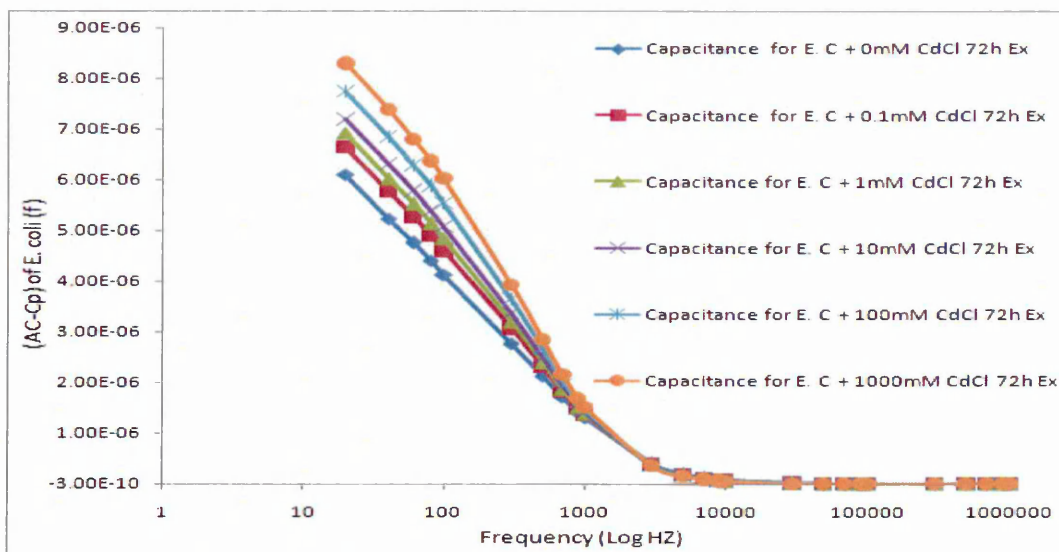


Figure 10.13. Typical AC-Cp characteristics of E. coli samples for different concentrations of  $\text{CdCl}_2$

In order to monitor the concentration of  $\text{CdCl}_2$  through studying the AC conductance of *E. coli* bacteria, the AC conductance of the LB broth with metal salt must be tested. The AC conductance of different concentrations of metal with LB broth was plotted in Figure 10.14.

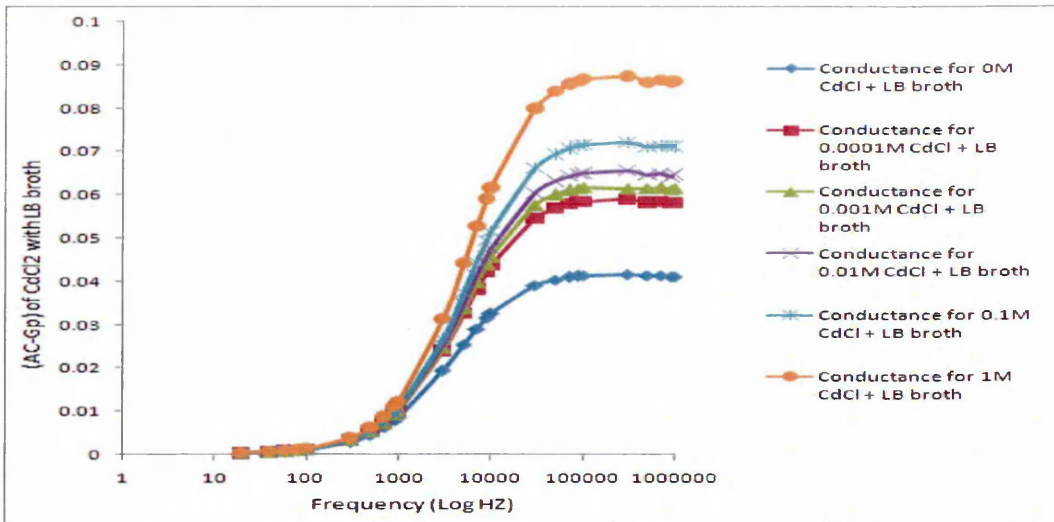


Figure 10.14. Typical AC-Gp characteristics of LB broth for different concentrations of  $\text{CdCl}_2$

In addition, the AC capacitances for different concentration of  $\text{CdCl}_2$  mixed with broth are plotted in Figure 10.15.

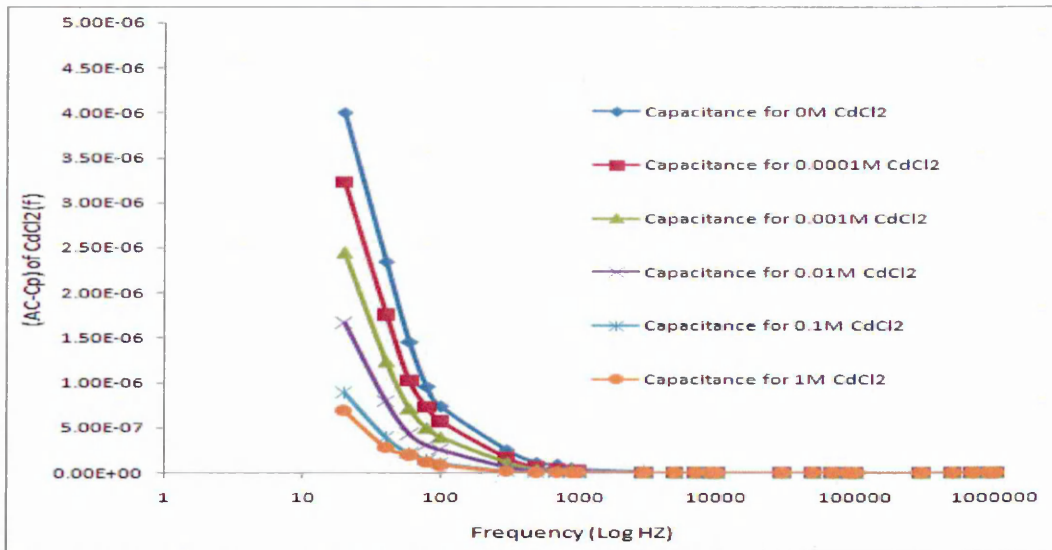


Figure 10.15. Typical AC-Cp characteristics of different concentrations of  $\text{CdCl}_2$  with LB broth

The data for exposed *E. coli* samples to  $\text{CdCl}_2$  were normalised over the data of the samples not exposed to find out the effect of metal. Figure 8.16 illustrates the AC conductance of normalised *E. coli* bacteria as a function of metal concentration after 72

hours. In addition, the AC capacitance data of exposed *E. coli* samples to  $\text{CdCl}_2$  were normalised to the AC capacitance data of the unexposed samples, in order to find the concentration of metal. Figure 8.17 illustrates the AC capacitance of normalised *E. coli* bacteria as a function of metal concentration after 72 hours.

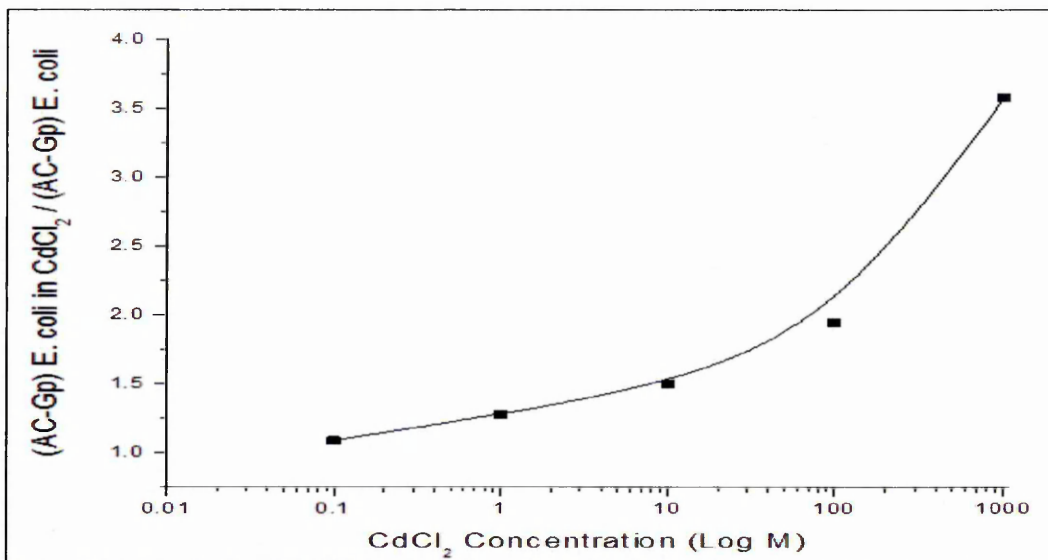


Figure 10.16. AC conductance ratio of *E. coli* bacteria exposed (mixed) to  $\text{CdCl}_2$  after 72 hours over AC conductance for bacteria samples not exposed against different concentration of  $\text{CdCl}_2$  at 900kHz

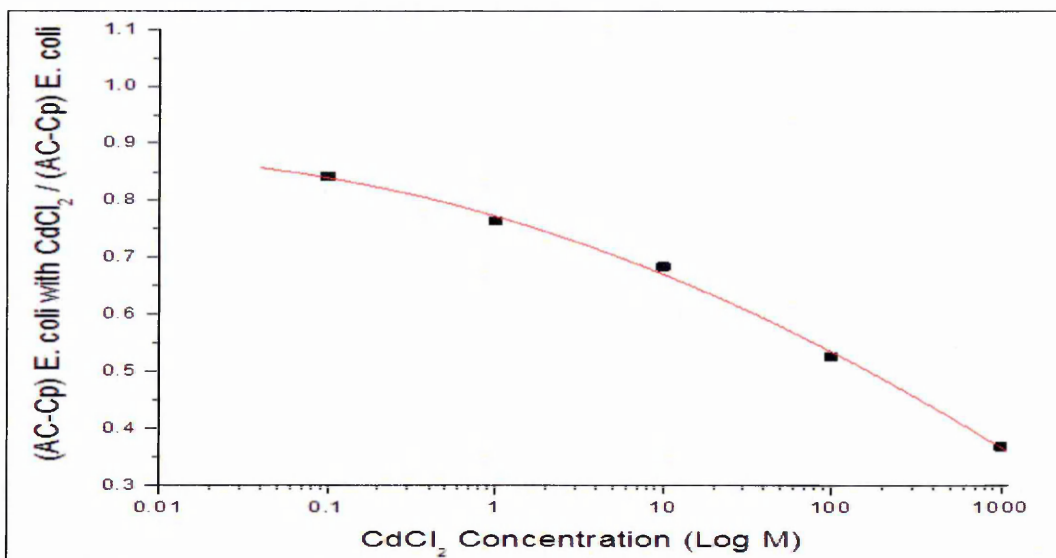


Figure 10.17. AC capacitance ratio of *E. coli* bacteria exposed (mixed) to  $\text{CdCl}_2$  after 72 hours over AC capacitance for samples not exposed at 900kHz

As shown in Figures 10.16, 10.17, the concentration of metal is easily calculated, which is a very simple and reliable method (technique) for detecting metal salt. In addition, the simple electrical measurements for *D. radiodurans* bacteria with  $\text{CdCl}_2$  were checked.

The AC-Gp of the liquid bacteria samples mixed with a CdCl<sub>2</sub> solution were studied. Typical AC conductance (AC-Gp) graph of D. radiodurans samples with different concentrations of metal are shown in Figure D3 (appendix D). In addition, the capacitance of the liquid bacteria samples mixed with CdCl<sub>2</sub> solution was studied. The typical AC capacitance (AC-Cp) graph of D. radiodurans samples with different concentrations of metal is plotted in Figure D4. In order to estimate the concentration of CdCl<sub>2</sub> on bacteria samples electrically using the conductivity and capacitance of D. radiodurans with different concentration of metal, the results were normalised for each bacteria sample on the results for bacteria not exposed to metal, therefore the metal concentration can be found directly. More details were shown in appendix D. The ratio change for the capacitance are studied, then the concentration of metal can easily be calculated. This is a very simple and reliable method (technique) to detect metal, as this is one of the benefits of the sensor studied in this work. In order to monitor the change of the concentration of CdCl<sub>2</sub> in bacteria samples through studying the AC conductance of D. radiodurans bacteria, the AC conductance and capacitance of CdCl<sub>2</sub> with OXOID broth must be studied. More details are presented in appendix D. Figures 10.18, 10.19 compare relative responses of the AC-Gp and AC-Cp characteristic methods to CdCl<sub>2</sub> for E.coli and D. radiodurans bacteria.

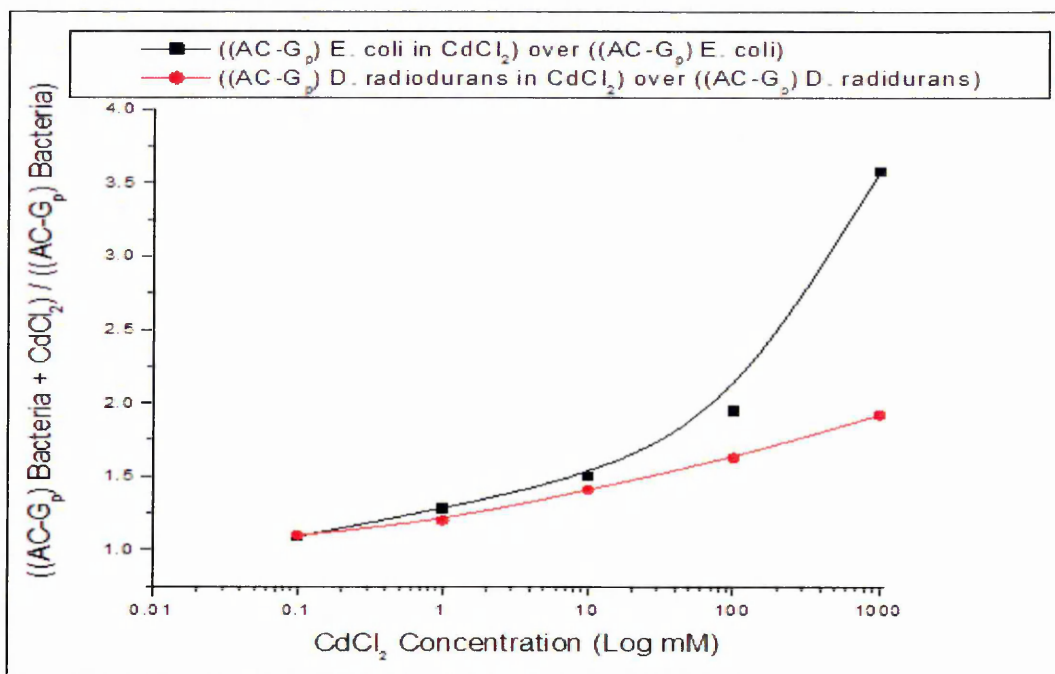


Figure 10.18. Comparison of relative responses of conductance (AC-G<sub>p</sub>) for E.coli and D. radiodurans bacteria with CdCl<sub>2</sub> to conductance (AC-G<sub>p</sub>) of bacteria at 72 hours

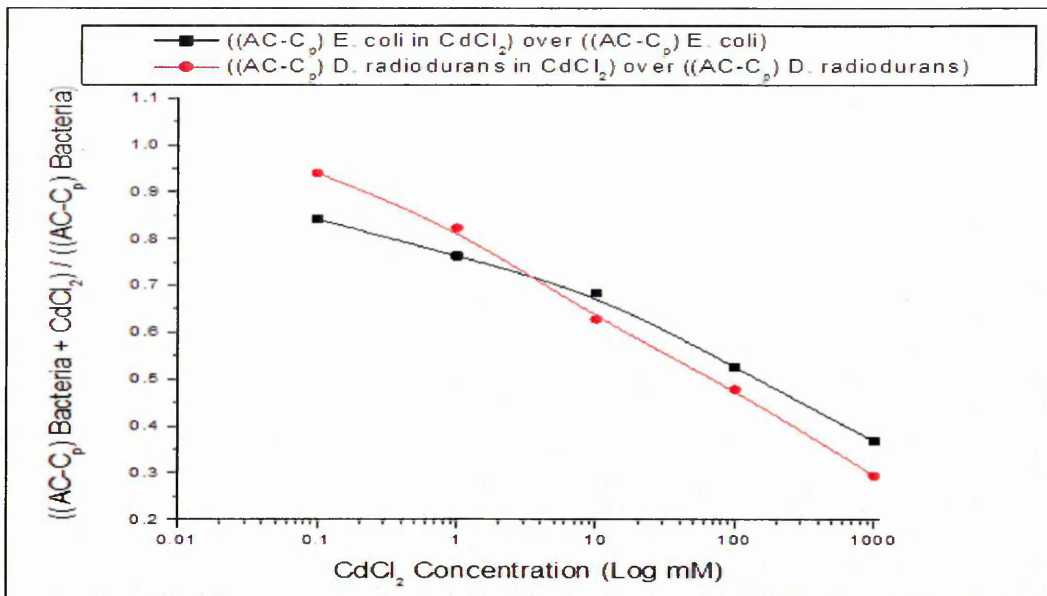


Figure 10.19. Comparison of relative responses of capacitance ( $AC-C_p$ ) for E.coli and D. radiodurans bacteria with  $CdCl_2$  to capacitance ( $AC-C_p$ ) of bacteria at 72 hours

This comparison being very important and useful for estimating the  $CdCl_2$  concentration as a function of normalised AC conductance and capacitance. As one can see when obtaining the value of normalised  $G_p$  or  $C_p$  for each bacteria sample, the  $CdCl_2$  can be found directly from the curve of Figures 10.18 and 10.19. Figure 10.20 compares the relative responses of E. coli conductance ( $AC-G_p$ ) characteristic with  $CdCl_2$  to  $CdCl_2$  with bacteria; this is very important and useful method to estimate the  $CdCl_2$  concentration as a function of normalised ac conductance.

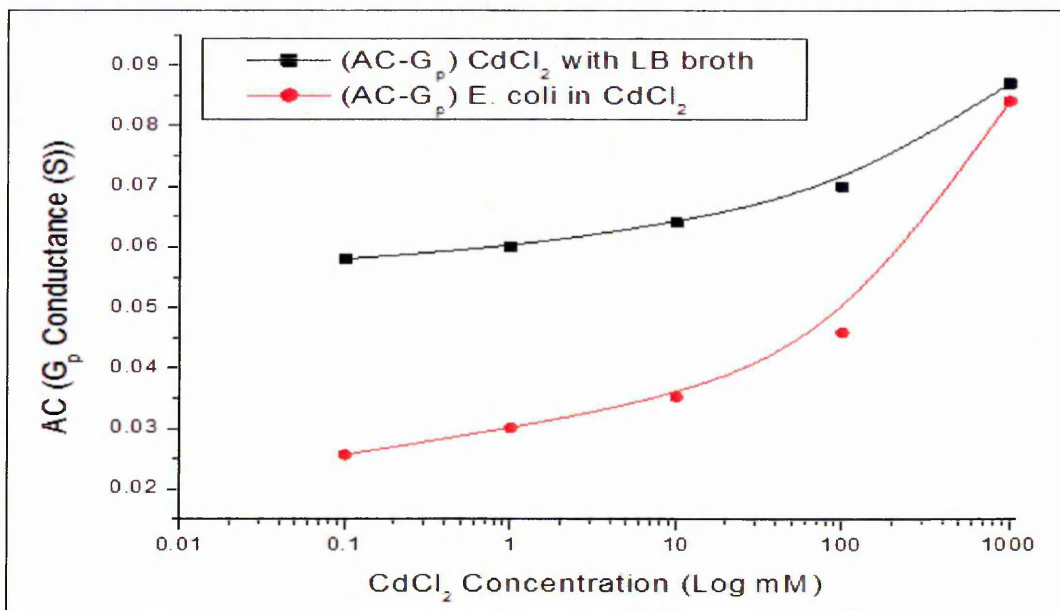


Figure 10.20. Comparison of relative responses of conductance ( $AC-G_p$ ) for E.coli bacteria in  $CdCl_2$  to conductance ( $AC-G_p$ ) of  $CdCl_2$  at 900kHz

As one can see, when obtaining the value of normalised G<sub>p</sub> for E. coli bacteria sample for CdCl<sub>2</sub> metal, the CdCl<sub>2</sub> can be found directly from the curve of Figure 10.21.

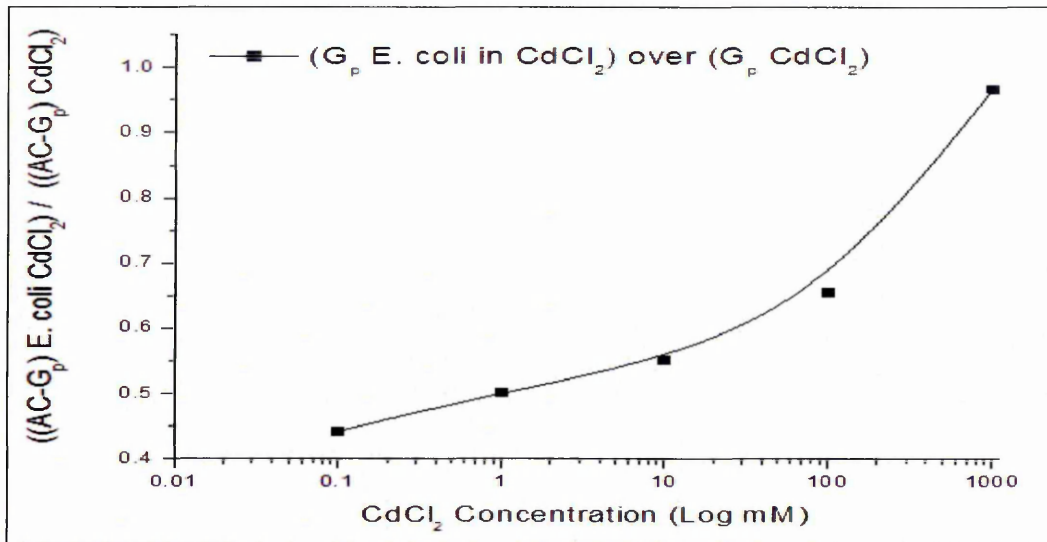


Figure 10.21. AC conductance ratio of E. coli bacteria in CdCl<sub>2</sub> after 72 hours over the conductance for CdCl<sub>2</sub> at 900kHz

The E. coli capacitance (AC-C<sub>p</sub>) characteristic methods for E. coli with CdCl<sub>2</sub> and for CdCl<sub>2</sub> are plotted in Figure 10.22; this comparison shows the different behaviour of bacteria and metal.

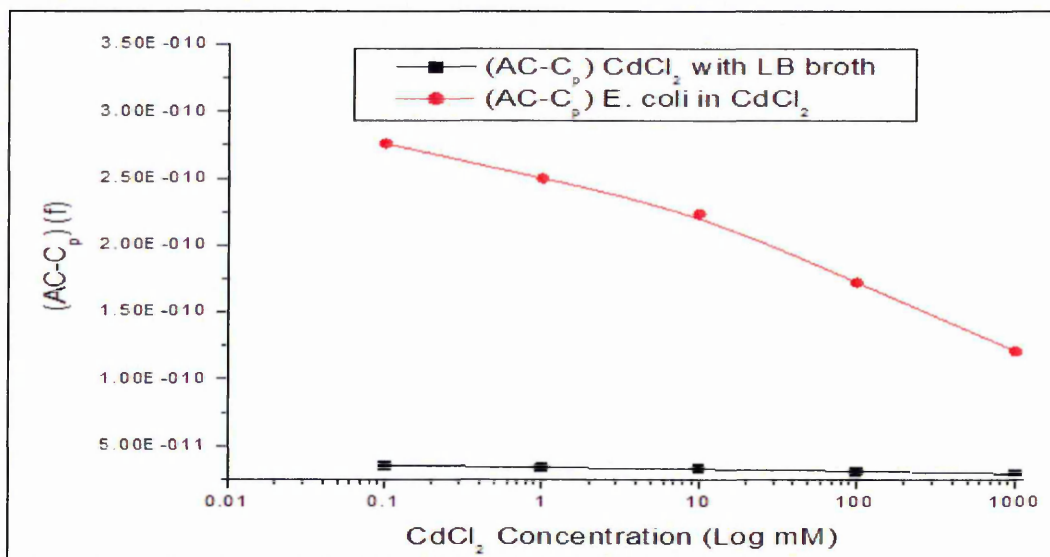


Figure 10.22. Comparison of relative responses of capacitance C<sub>p</sub> for E.coli bacteria with CdCl<sub>2</sub> and capacitance C<sub>p</sub> of CdCl<sub>2</sub> at 900kHz

As one can see, when obtaining the value of the normalised C<sub>p</sub> for E. coli bacteria sample with CdCl<sub>2</sub> to capacitance of CdCl<sub>2</sub>, the CdCl<sub>2</sub> concentration can be found directly from the curve of Figure 10.23.

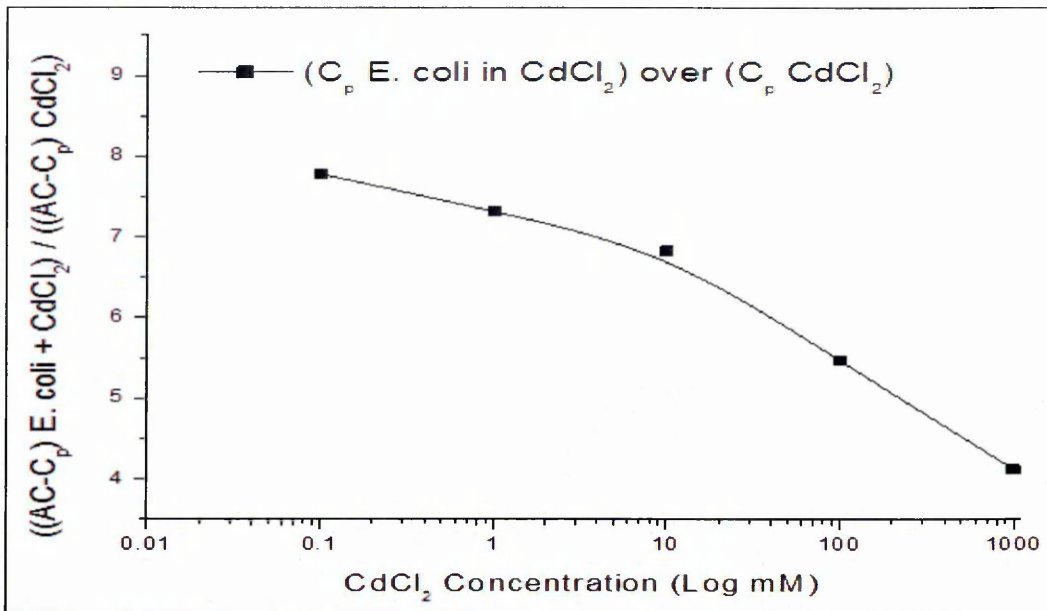


Figure 10.23.AC capacitance ratio of E. coli bacteria in CdCl<sub>2</sub> after 72 hours over the capacitance for CdCl<sub>2</sub>at 900kHz

Figure10.24 compares the AC conductance (AC-G<sub>p</sub>) characteristic of D. radiodurans with CdCl<sub>2</sub>to the AC conductance of CdCl<sub>2</sub> metal, which is very important and useful for monitoring and screening the effect and the change in electrical properties responses to CdCl<sub>2</sub> concentration. Also, when the conductance of D. radiodurans with different concentrations of CdCl<sub>2</sub>are normalised to the conductance for different concentrations of CdCl<sub>2</sub>, the concentration of CdCl<sub>2</sub>can easily be estimated using this method, see Figure 10.24.

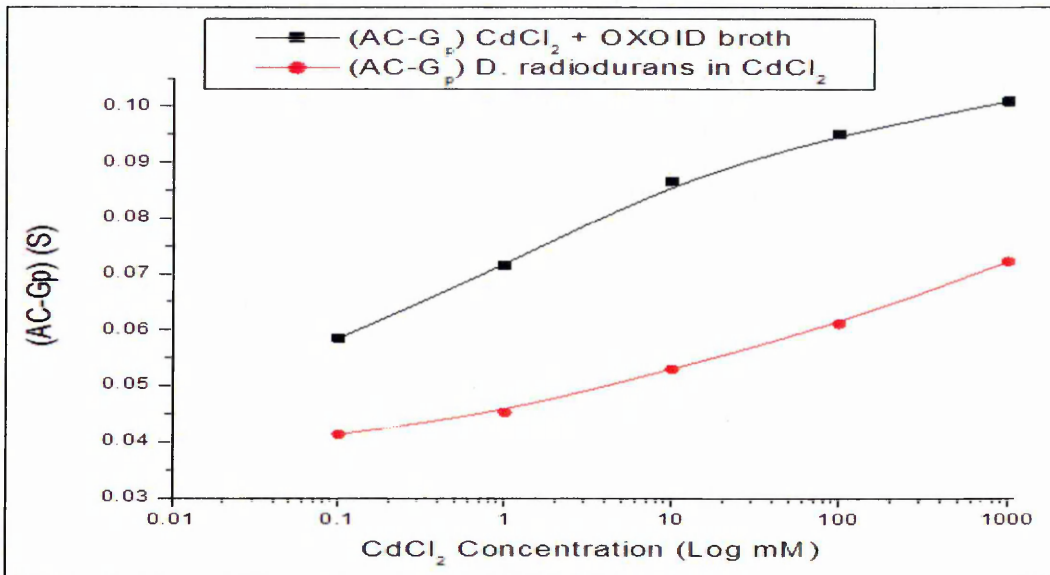


Figure 10.24.Comparison of relative responses of conductance (AC-G<sub>p</sub>) for D. radiodurans bacteria in CdCl<sub>2</sub> to conductance (AC-G<sub>p</sub>) of CdCl<sub>2</sub> at 900kHz

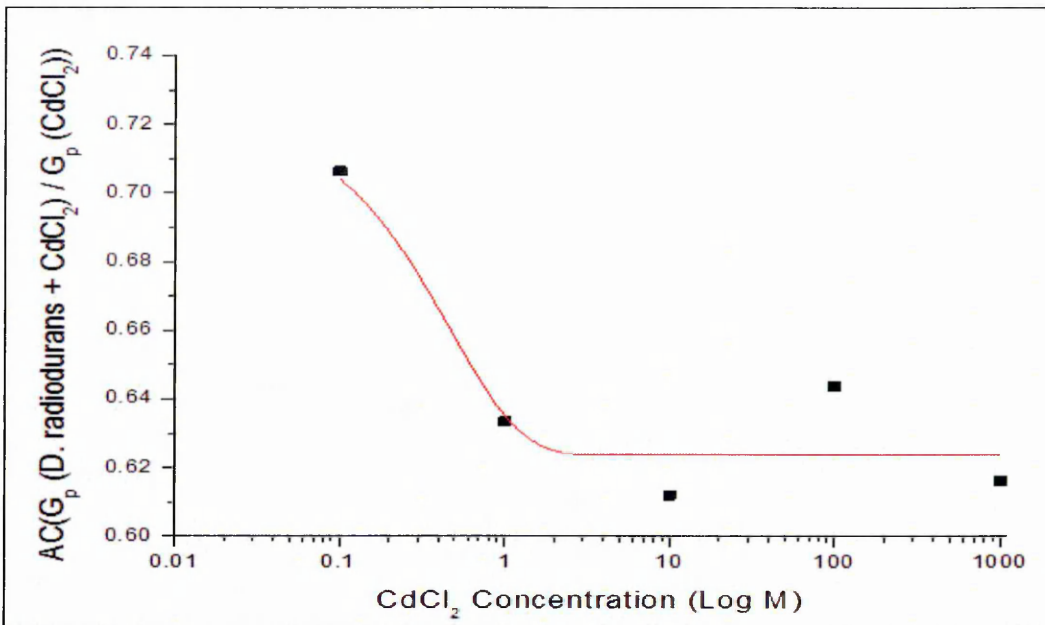


Figure 10.25. AC conductance ratios of *D. radiodurans* bacteria exposed (mixed) to CdCl<sub>2</sub> after 72 hours over conductance for CdCl<sub>2</sub> 900kHz

Also the AC capacitance of *D. radiodurans* with different concentrations of CdCl<sub>2</sub> and AC capacitance of different concentration of CdCl<sub>2</sub> with an OXOID broth are plotted in Figure 10.26, and the normalised Cp for *D. radiodurans* bacteria sample with CdCl<sub>2</sub> for different concentrations of CdCl<sub>2</sub> metal are presented in Figure 10.27.

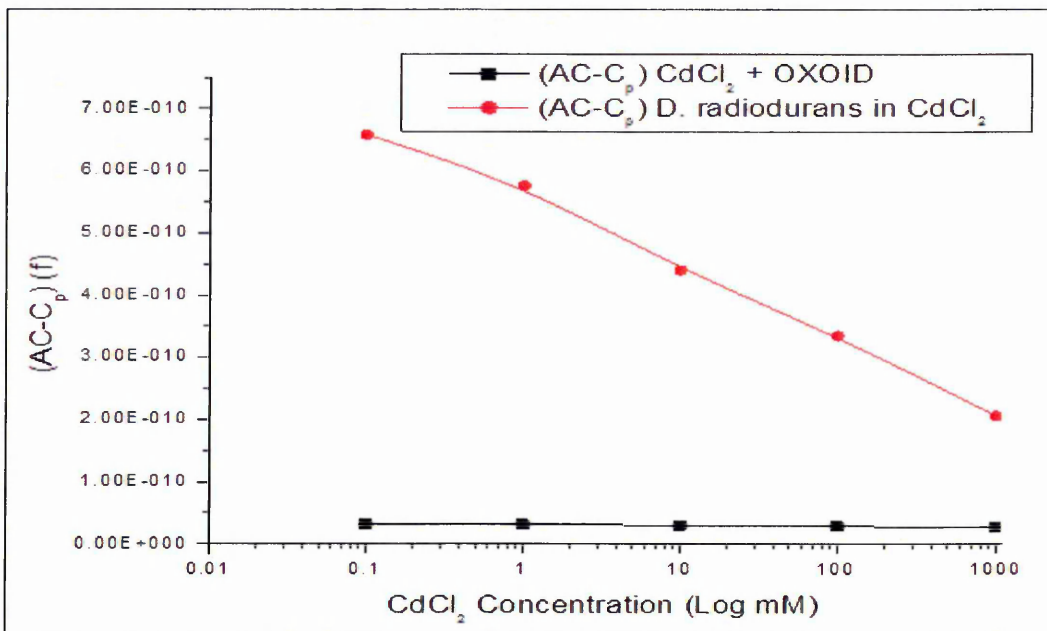


Figure 10.26. Comparison of relative responses of capacitance (AC-G<sub>p</sub>) for *D. radiodurans* bacteria in CdCl<sub>2</sub> to the capacitance (AC-G<sub>p</sub>) of CdCl<sub>2</sub> with OXOID broth at 900kHz

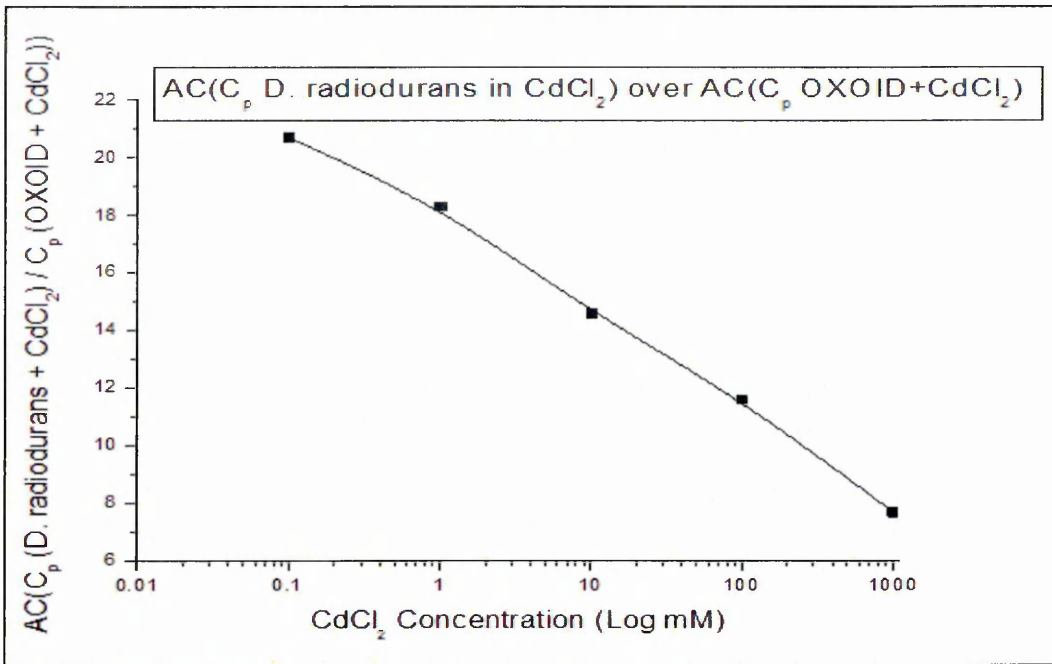


Figure 10.27.AC capacitance ratios of *D. radiodurans* bacteria in  $\text{CdCl}_2$  after 72 hours over capacitance for  $\text{CdCl}_2$  at 900kHz

A comparative graph of *E. coli* and *D. radiodurans* is plotted in Figure 10.28 and 10.29:

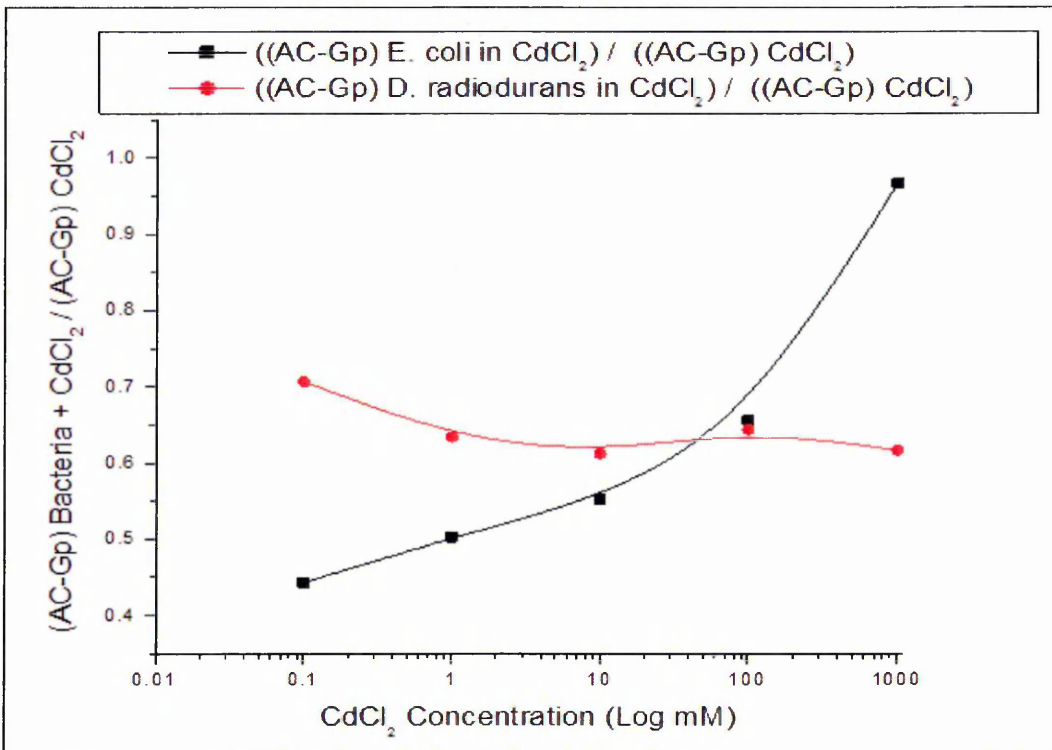


Figure 10.28.Comparison of relative responses of conductance (AC-G<sub>p</sub>) for *E.coli* and *D. radiodurans* bacteria in  $\text{CdCl}_2$  to conductance (AC-G<sub>p</sub>) of  $\text{CdCl}_2$  after 72 hours

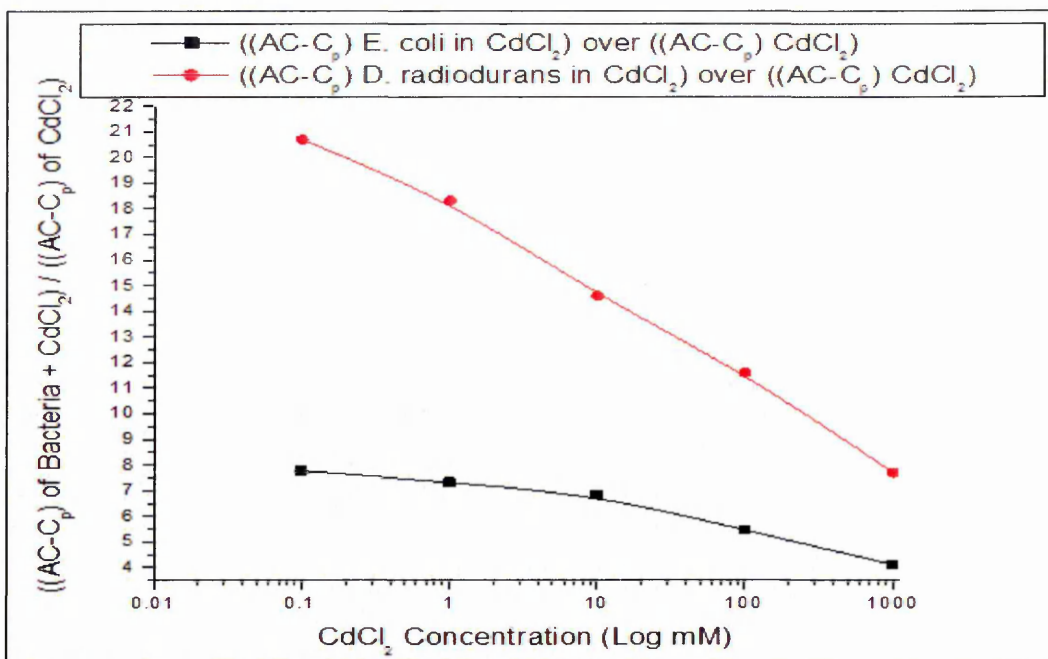


Figure 10.29. Comparison of relative responses of capacitance  $(AC-C_p)$  for E.coli and D. radiodurans bacteria in  $CdCl_2$  to capacitance  $(AC-C_p)$  of  $CdCl_2$  after 72 hours

### 10.3. Electrical Study of the Effect of Nickel Chloride ( $NiCl_2$ ) on Bacteria

Nickel (II) chloride ( $NiCl_2$ ) is a yellow anhydrous salt, but the more familiar hydrate  $NiCl_2 \cdot 6H_2O$  is green. Normal environmental concentrations of nickel are low, but large amounts can be found in some naturally derived serpentine soils, and surrounding mining and smelting area.

Nickel is a toxic element. Many plant species cannot grow on contaminated soils, although there are especially tolerant species, some of which can accumulate high concentrations. The main aim of this part is to build electrical sensor for detecting  $NiCl_2$ . One mole concentration from  $NiCl_2$  was obtained and then the solution was deliuted by water for different concentration (1M, 0.1M, 0.01M, 0.001M, 0.0001M). The salty solution were added to bacteria cultures in the ratio 1:1. Finally the salty cultures were kept in shaker under room temprature condition for different priedods. In order to achieve this work; simple electrical (electrochemical) measurements were used, i.e. first, the correlation between electrical properties (conductivity, capacitance and IV characteristics) of liquid bacteria samples with different concentration of  $NiCl_2$  were established [2]. Again, the DC electrical tests were performed using 6517A Keithley Electrometer in the voltage range  $\pm 0.5V$ ; the measurements were carried out with a bio-

cell sensor in the  $\pm 0.5\text{V}$  voltage range, which is selected in order to avoid oxidation and reduction electrochemical reactions on metal electrodes, and the IV relative (correlation) was studied.

AC electrical measurements were performed using an HP-4284A PRECISION LCR METER in the frequency range 20 Hz to 1 MHz, with the amplitude of AC voltage of 100mV and with no DC bias applied. The spectra of two parameters,  $G_p$  and  $C_p$ , corresponding to a parallel connection of conductance and capacitance were recorded.

### 10.3.1. DC Electrical Measurements of Bacteria and $\text{NiCl}_2$

In this part of the work, simple electrical measurements were achieved. Typical current-voltage (I-V) characteristics at room temperature for both *E. coli* and *D. radiodurans* bacteria before and after exposure (mixed) for different periods and at different concentrations to heavy metals were studied. I-V properties of the mixed solution of *E. coli* and  $\text{NiCl}_2$  are plotted in Figure 10.30. In contrast, the I-V characteristics for different concentrations of  $\text{NiCl}_2$  with an LB broth were explored and are shown in Figure 10.31.

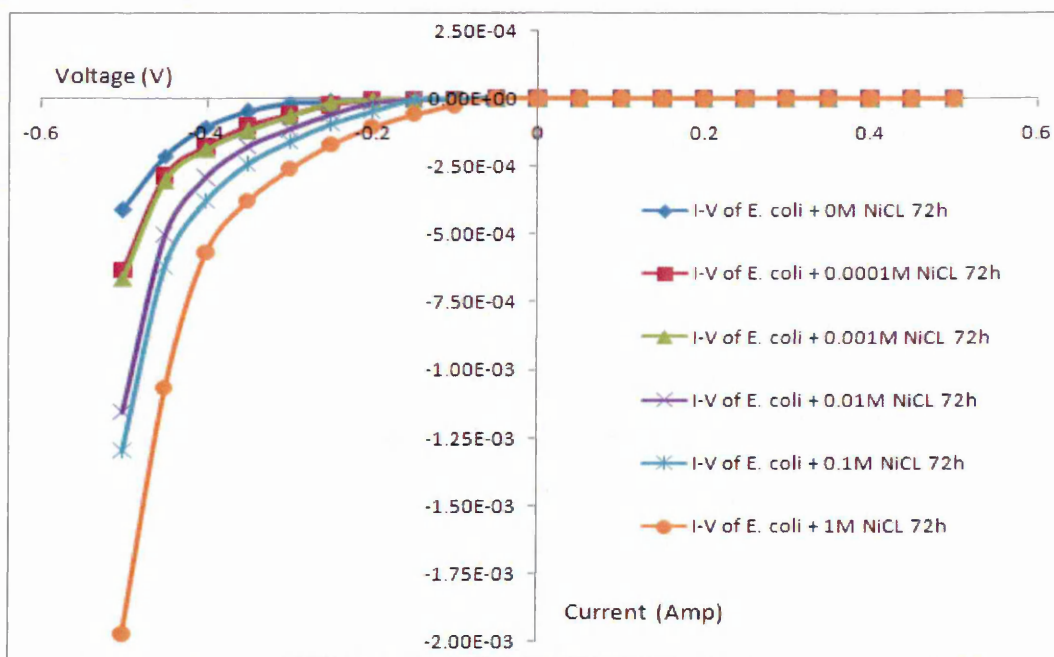


Figure 10.30. I-V characteristics of *E. coli* samples for different concentrations of  $\text{NiCl}_2$ , after 72 hours exposure time in normal environmental conditions

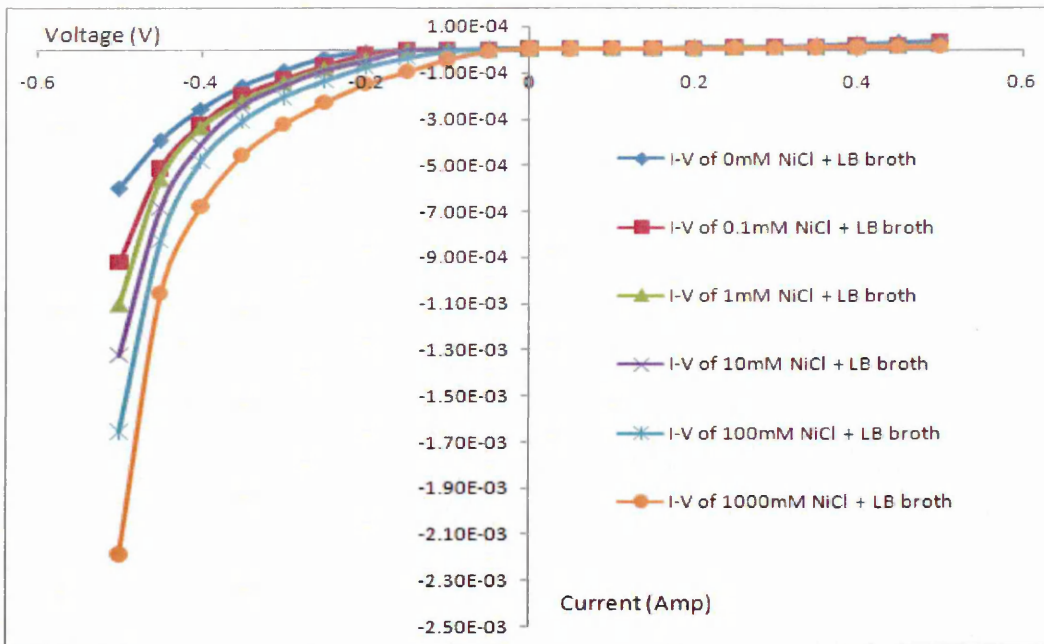


Figure 10.31. I-V characteristics for different concentration of NiCl<sub>2</sub> with LB broth

In order to study the effect of NiCl<sub>2</sub> on *E. coli* bacteria the cathode current of *E. coli* bacteria after adding NiCl<sub>2</sub> at (-0.5V) were explored and normalised on the cathode current of NiCl<sub>2</sub> with an LB broth, see Figures 10.32, 10.33, 10.34.

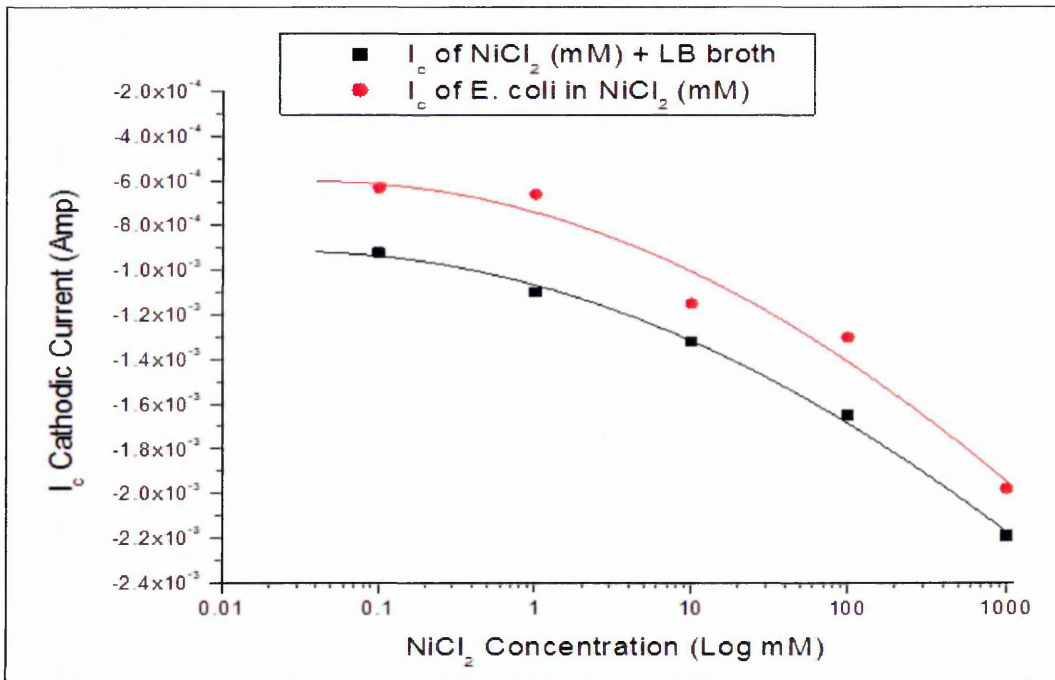


Figure 10.32. I<sub>c</sub> of *E. coli* and NiCl<sub>2</sub> characteristics for different concentrations of NiCl<sub>2</sub> in LB broth

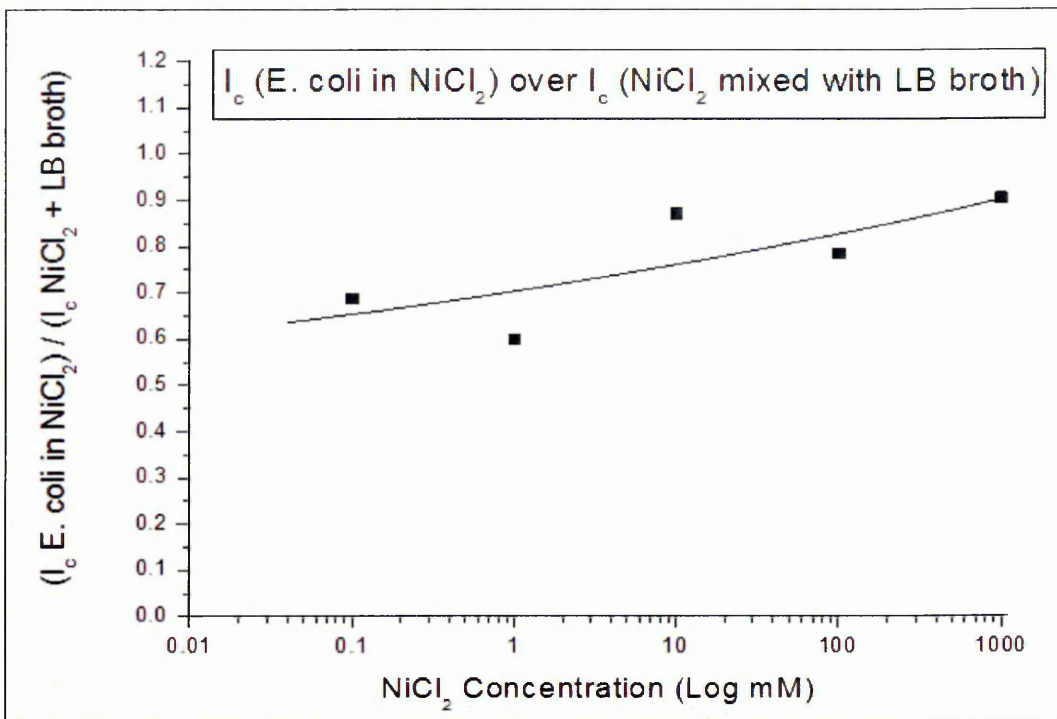


Figure 10.33.  $I_c$  of *E. coli* in  $NiCl_2$  over  $I_c$   $NiCl_2$  mixed with LB broth characteristics for different concentrations of  $NiCl_2$

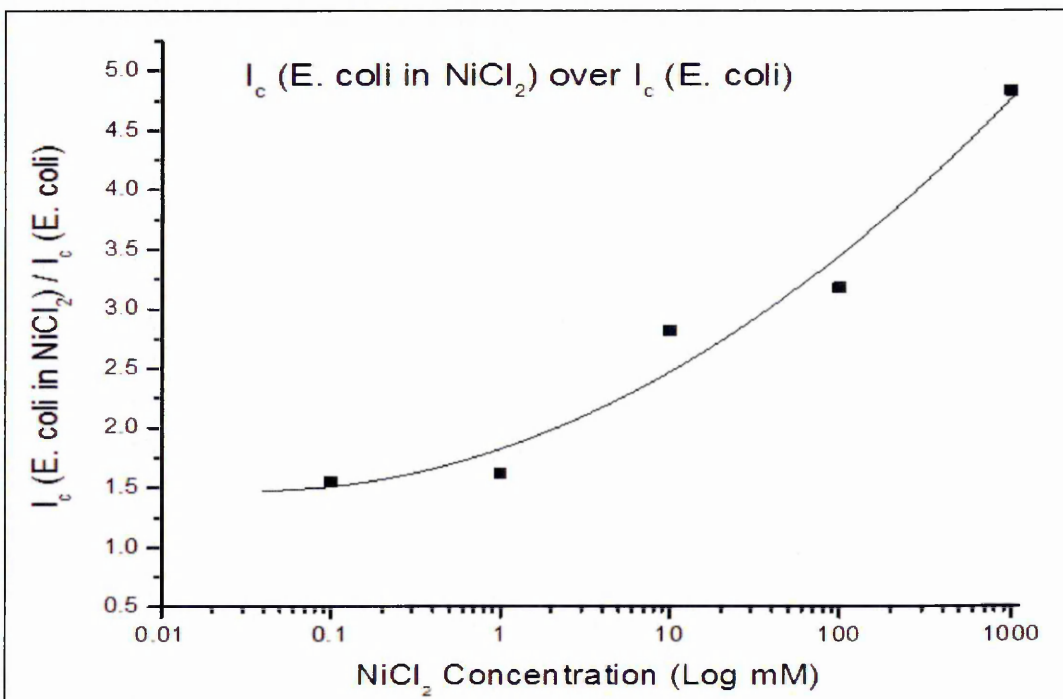


Figure 10.34.  $I_c$  of *E. coli* in  $NiCl_2$  over  $I_c$  of *E. coli* characteristics for different concentration of  $NiCl_2$  after 72 hours

Figures 10.32, 10.33 provide good information about the effect of  $NiCl_2$  on *E. coli* bacteria, where the concentration of  $NiCl_2$  can easily be estimated. In order to study and analyse the effect of  $NiCl_2$  on *E. coli* bacteria, the cathode current at (-0.5) Volt of

bacteria samples was studied after being treated with salt then subtract it from cathode current of salt over the cathode current of bacteria samples as shown in Figure 10.35.

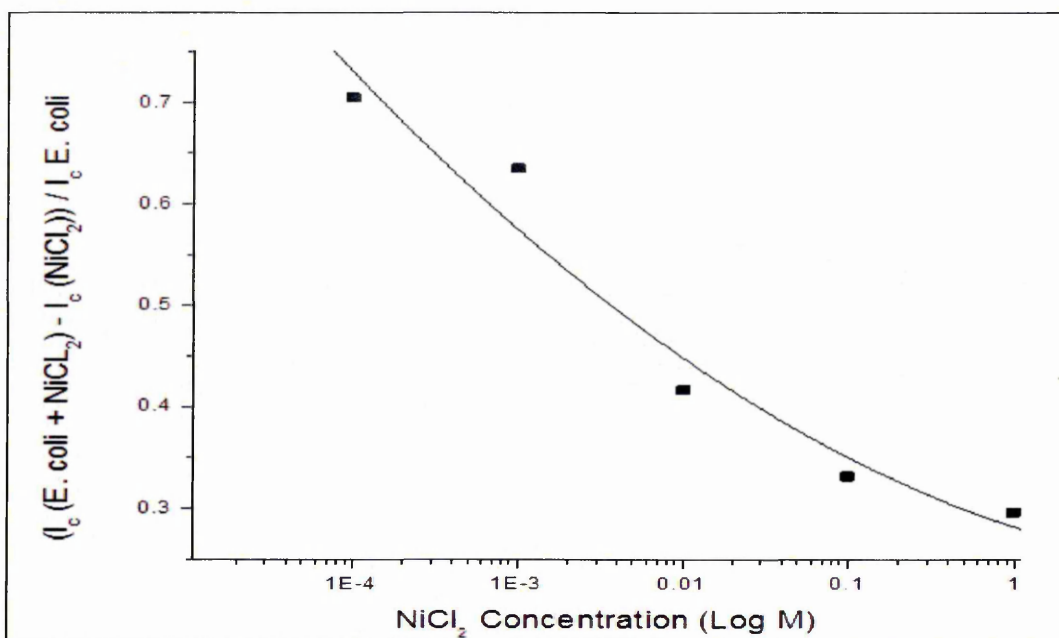


Figure 10.35. Relative changes of cathodic current  $I_c$  for *E. coli* in different concentrations of  $NiCl_2$  for  $I_c$  of  $NiCl_2$  with LB broth over  $I_c$  of *E. coli* sample after 72 hours

Again, in order to create a novel method for detecting the  $NiCl_2$  concentration, especially in an aqueous environment, a similar sequence was followed for cultivation of *D. radiodurans* (Anderson R1 strain). The *D. radiodurans* samples were mixed (1:1) with different concentrations of  $NiCl_2$ . The solution was checked electrically after exposure for different periods. More results are presented appendix D.

The effect of  $NiCl_2$  metal on *D. radiodurans* bacteria was studied during the monitoring of changes in the cathode current. The cathode current of *D. radiodurans* bacteria after adding  $NiCl_2$  at (-0.5V) was normalised on the cathode current of  $NiCl_2$  with an OXOID broth and on the cathode current of *D. radiodurans* bacteria without metal, as is clear in Figures 10.36. For more details, see appendix D.

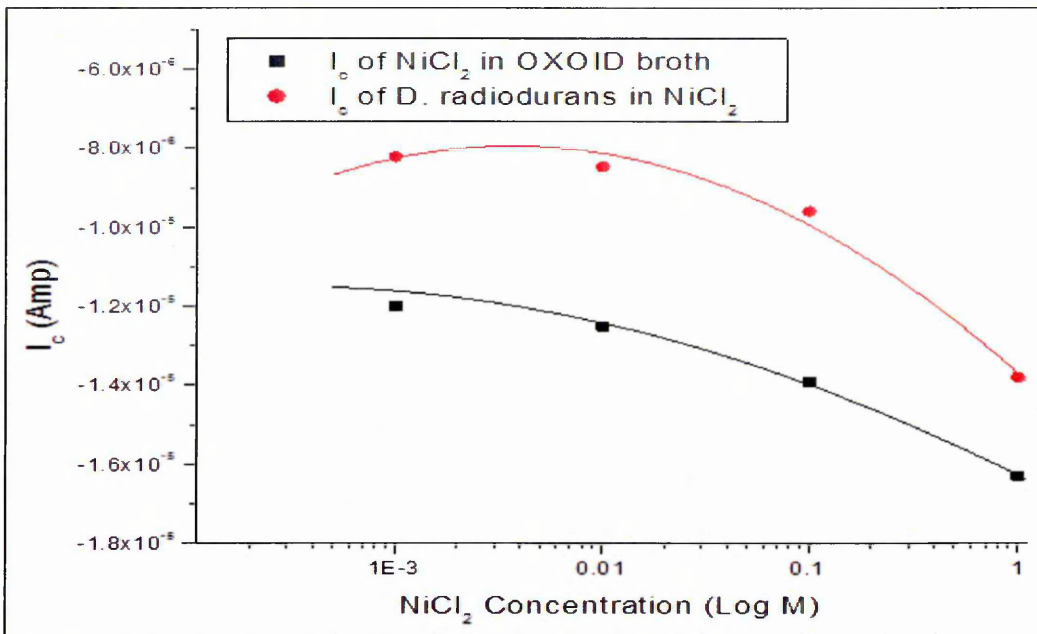


Figure 10.36.  $I_c$  (cathode current) of *D. radiodurans* with  $NiCl_2$  and  $I_c$  for different concentration of  $NiCl_2$  with OXOID broth

Figures 10.37 and 10.38 compare  $I_c$  cathode current ratio of *D. radiodurans* with  $NiCl_2$  and  $I_c$  of *E. coli*  $NiCl_2$  metal, which is very important and useful to monitoring and screening changes in the DC electrical property's responses to  $NiCl_2$  concentration, and The graphs 10.37 and 10.38 give good and clear information about how the bacteria deals with  $NiCl_2$ , and about the influence of metal on bacteria. In addition, the above graphs provide a method of evaluating  $NiCl_2$  concentration.

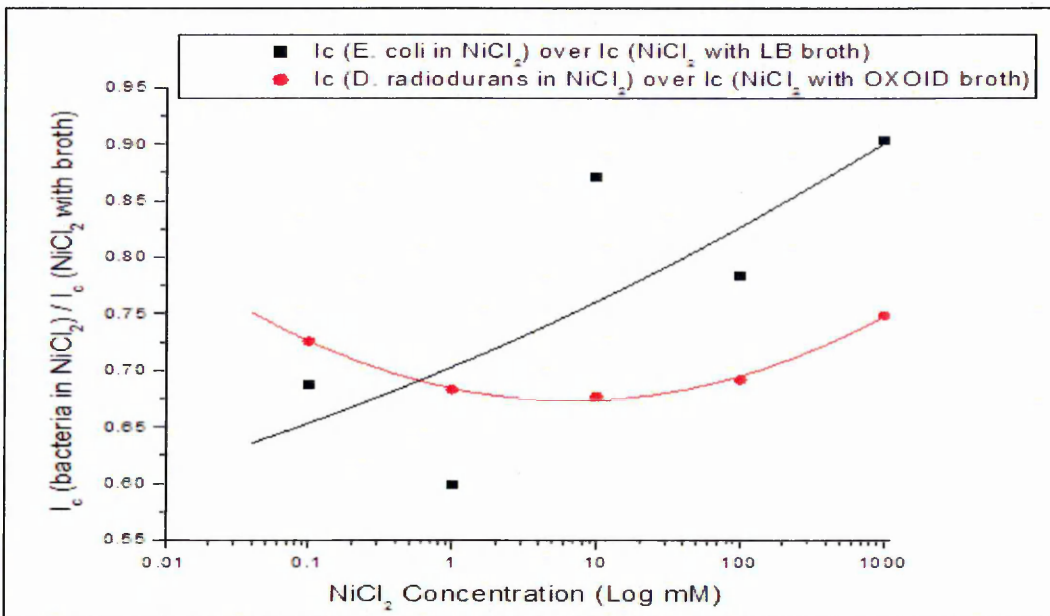


Figure 10.37. Ratios of  $I_c$  (cathode current) for *D. radiodurans*, with  $NiCl_2$  and  $I_c$  for *E. coli* with  $NiCl_2$  as a function of different concentrations of  $NiCl_2$

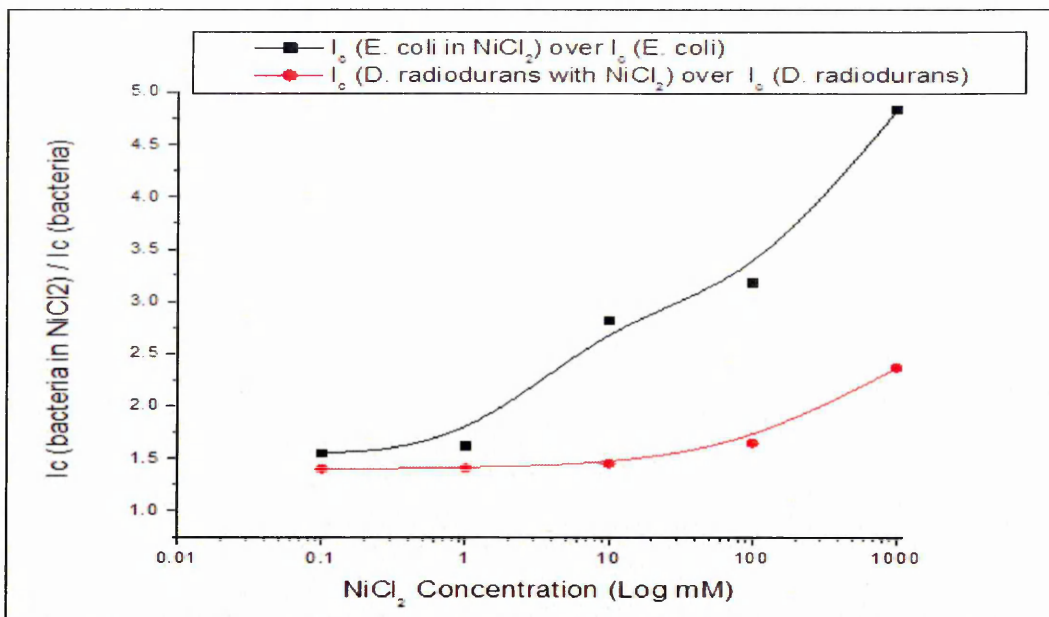


Figure 10.38. Ratios of  $I_c$  (cathode current) for *D. radiodurans* with  $NiCl_2$  over  $I_c$  for *D. radiodurans* and  $I_c$  for *E. coli* with  $NiCl_2$  over  $I_c$  for *E. coli* as a function of different concentration of  $NiCl_2$

Finally, the effect of  $NiCl_2$  on *D. radiodurans* bacteria was studied, this was achieved through mortaring the cathode current change at -0.5 Volt of bacteria samples after treated with salt and then subtracted it on the cathode current of salt over the cathode current of bacteria samples. See Figure 10.39.

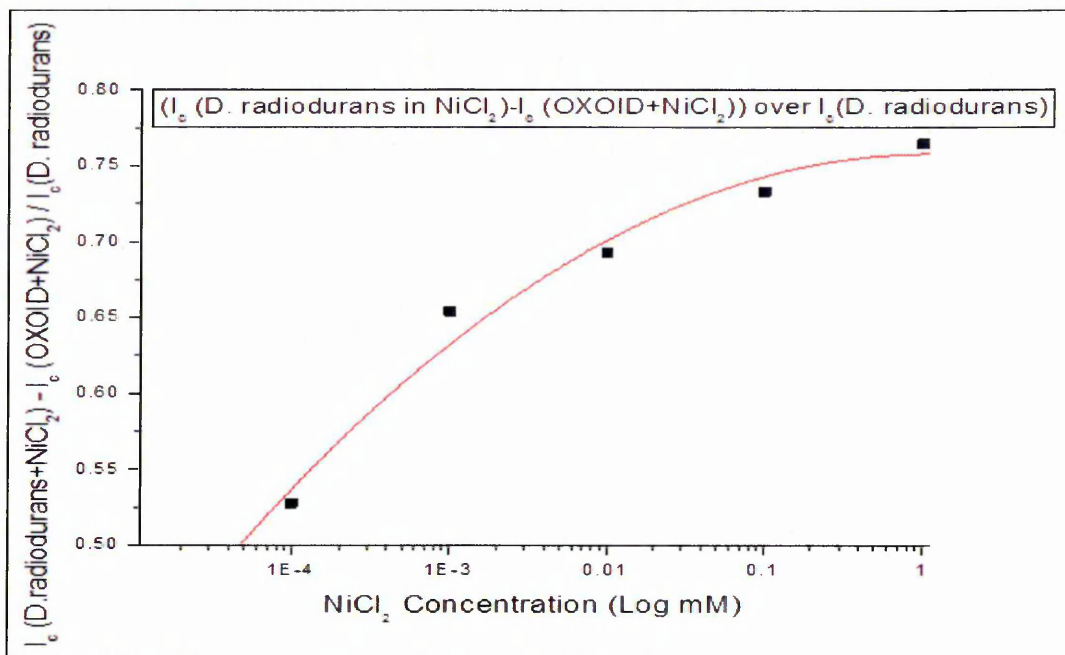


Figure 10.39. Relative changes of  $I_c$  for *D. radiodurans* in different concentrations of  $NiCl_2$  for  $I_c$  of  $NiCl_2$  in OXOID broth over  $I_c$  of *D. radiodurans* sample after 72 hours

Also the substantial graph of *D. radiodurans* bacteria was compressed with substantial graph of *E. coli* bacteria, this pattern was showed differ response of both types of bacteria for  $\text{NiCl}_2$ , see Figure 10.40.

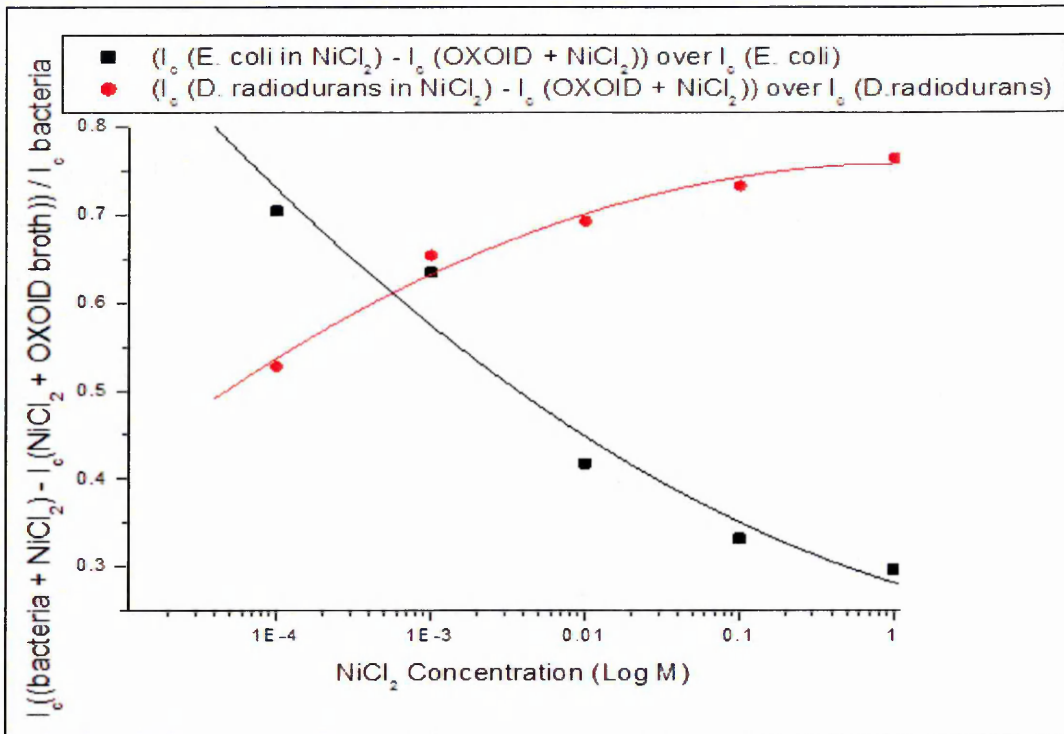


Figure 10.40. Comparison of relative responses of  $I_c$  (cathodic current) methods to  $\text{NiCl}_2$  for both types of bacteria after subtraction

### 10.3.2. AC Electrical Measurements of Bacteria and $\text{NiCl}_2$

Simple electrical (electrochemical) AC measurements were achieved. A typical AC conductance (AC-Gp) graph of *E. coli* samples having different concentrations of  $\text{NiCl}_2$  are shown in Figure 10.41. AC conduction of *E. coli* increased with an increase in  $\text{NiCl}_2$  concentration that correlates well with the decrease in bacteria concentration.

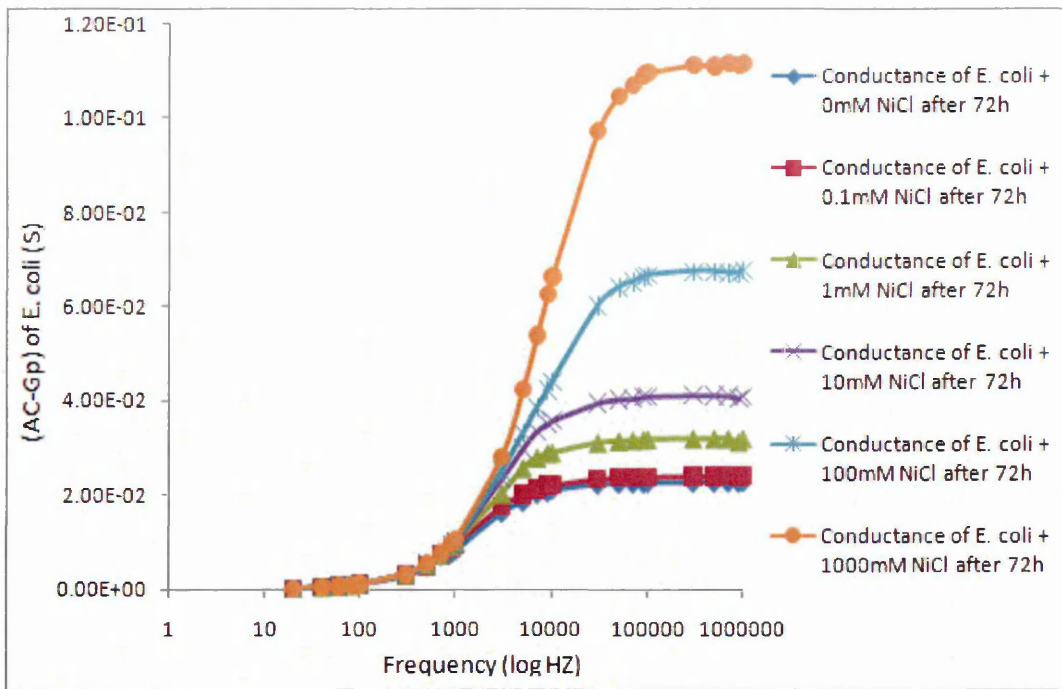


Figure 10.41. Typical AC-Gp characteristics of E. coli samples for different concentrations of  $\text{NiCl}_2$

In order to identify the change in bacteria density after being mixed with  $\text{NiCl}_2$ , the variation of the metal AC conductivity mixed with LB broth was studied and results are shown in Figure 10.42.

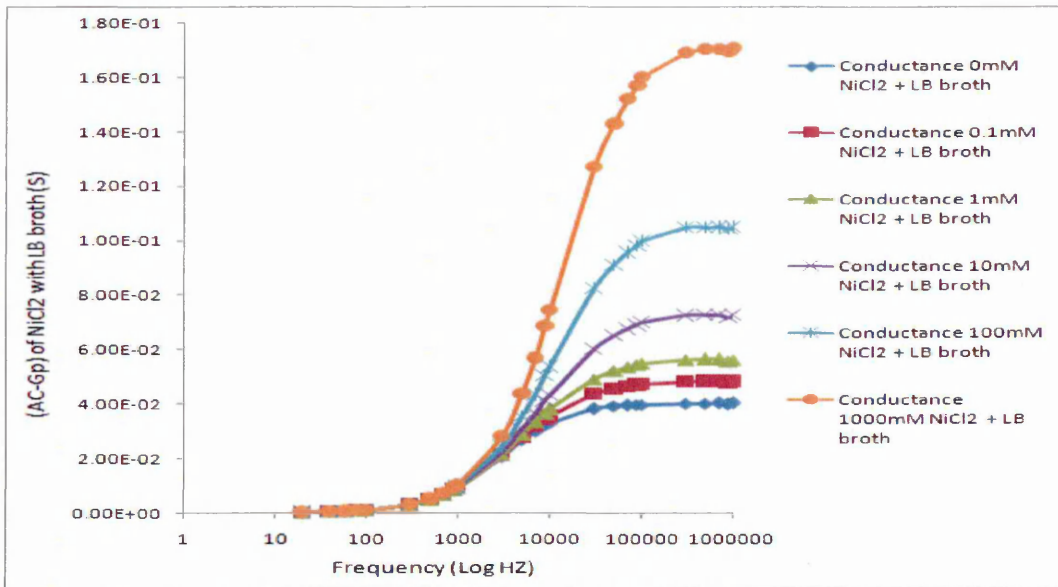


Figure 10.42. Typical (AC-Gp) conductance characteristics of LB broth mixed (1:1) with different concentrations of  $\text{NiCl}_2$

Figure 10.43, Comparison of relative responses of (AC-Gp) characteristic methods to  $\text{NiCl}_2$  for E.coli bacteria, which is very important and useful for studying effect of  $\text{NiCl}_2$  on E. coli.

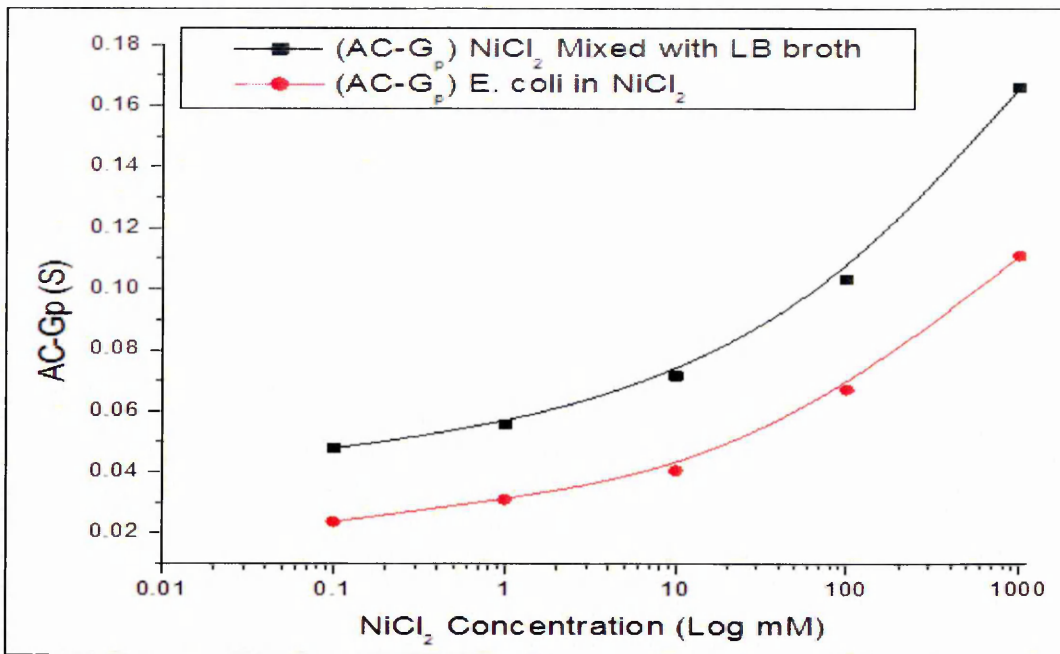


Figure 10.43. Comparison of relative responses of conductance (AC-G<sub>p</sub>) for E.coli bacteria in NiCl<sub>2</sub> and conductance (AC-G<sub>p</sub>) of NiCl<sub>2</sub> after 72 hours

The data for exposed E. coli samples to NiCl<sub>2</sub> were normalised over the data belonging to the samples not exposed in order to find out the effect of the metal. Figures 10.44, 10.45 illustrate the ac conductance of normalised E. coli bacteria as a function of metal concentration after 72 hours.

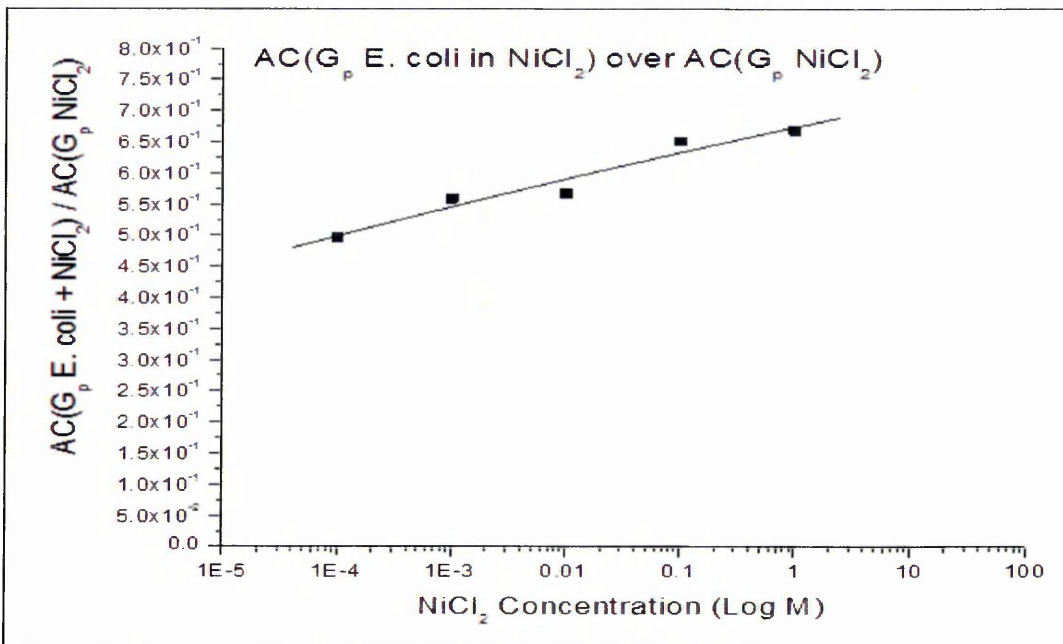


Figure 10.44. AC conductance ratios of E. coli bacteria exposed (mixed) to NiCl<sub>2</sub> after 72 hours against AC conductance for NiCl<sub>2</sub> at 900kHz

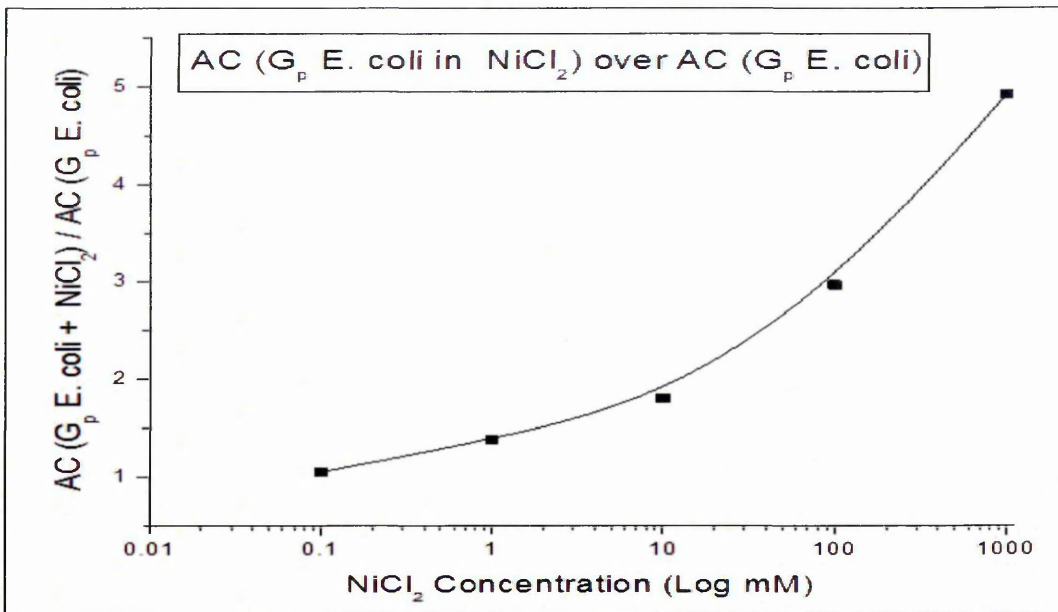


Figure 10.45. AC conductance ratios of *E. coli* bacteria exposed (mixed) to NiCl<sub>2</sub> after 72 hours against AC conductance for *E. coli* bacteria at 900kHz

In addition, as discussed for *E. coli* bacteria the AC conductance characteristics of *D. radiodurans* for different concentrations of NiCl<sub>2</sub> were studied. Meanwhile, the AC conductance of NiCl<sub>2</sub> with OXOID were also investigated and results are presented in appendix D. Figure 10.46, compares relative responses of AC conductance (G<sub>p</sub>) characteristics to NiCl<sub>2</sub> for *D. radiodurans* bacteria, which is very important and useful for studying the effect of NiCl<sub>2</sub> on *D. radiodurans*.

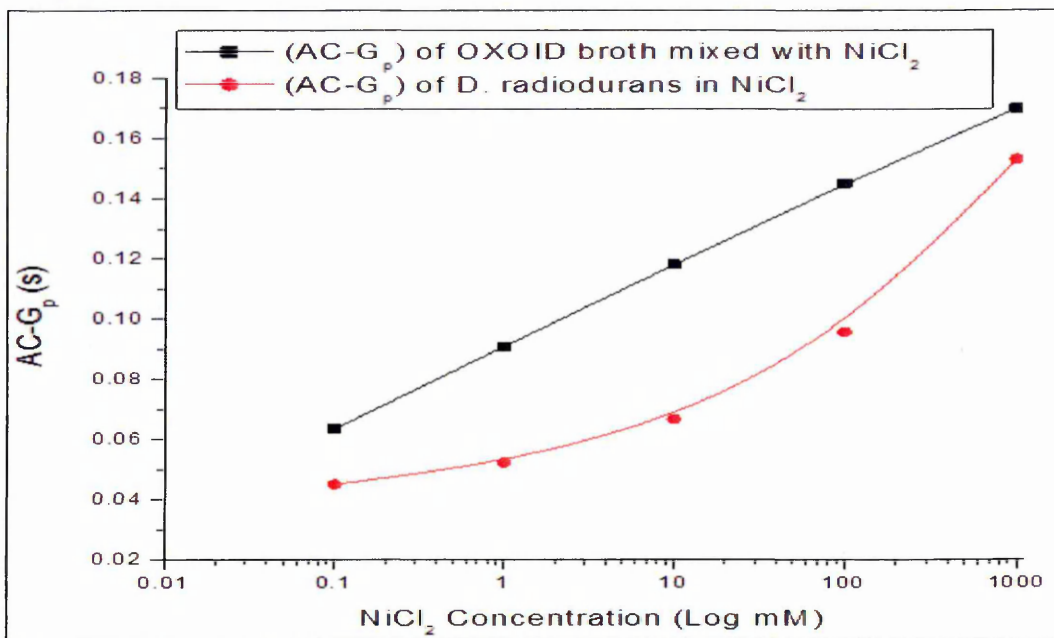


Figure 10.46. Comparison of relative responses of conductance (AC-G<sub>p</sub>) for *D. radiodurans* bacteria in NiCl<sub>2</sub> and conductance (AC-G<sub>p</sub>) of NiCl<sub>2</sub> after 72 hours

The AC conductance of *D. radiodurans* bacteria mixed with  $\text{NiCl}_2$  were normalised to the conductance for  $\text{NiCl}_2$  and to the AC conductance for *D. radiodurans* with broth. Comparison curves between the *E. coli* and *D. radiodurans* bacteria responses for  $\text{NiCl}_2$  metal are presented in Figures 10.47 and 10.48.

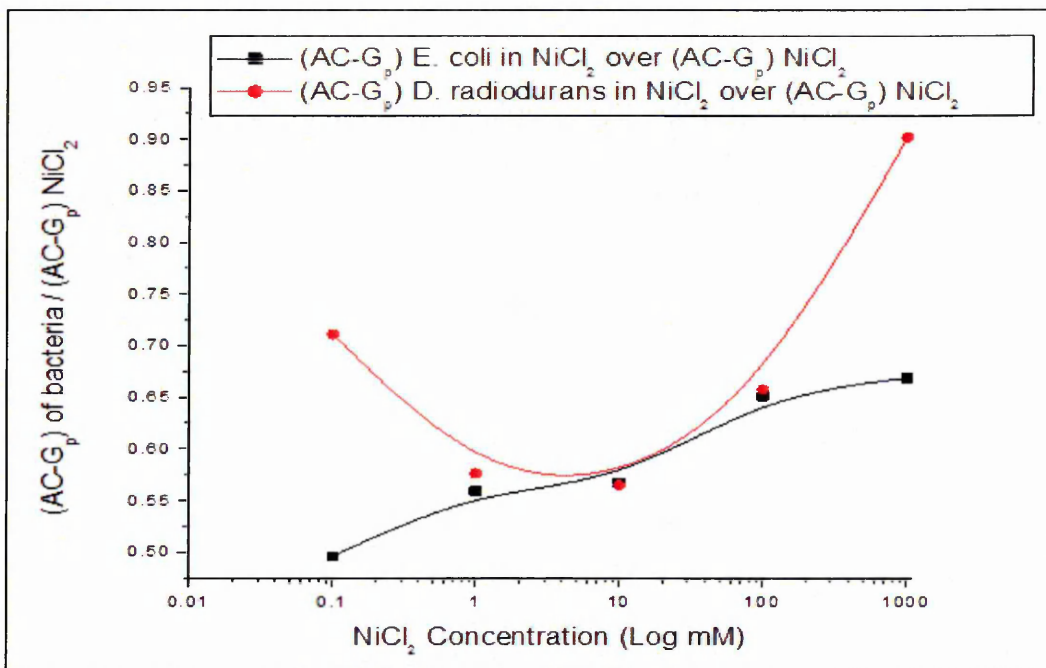


Figure 10.47. Comparison of relative response of conductance (AC-G<sub>p</sub>) for *E. coli* and *D. radiodurans* bacteria in  $\text{NiCl}_2$  over (AC-G<sub>p</sub>) conductance of  $\text{NiCl}_2$  after 72 hours

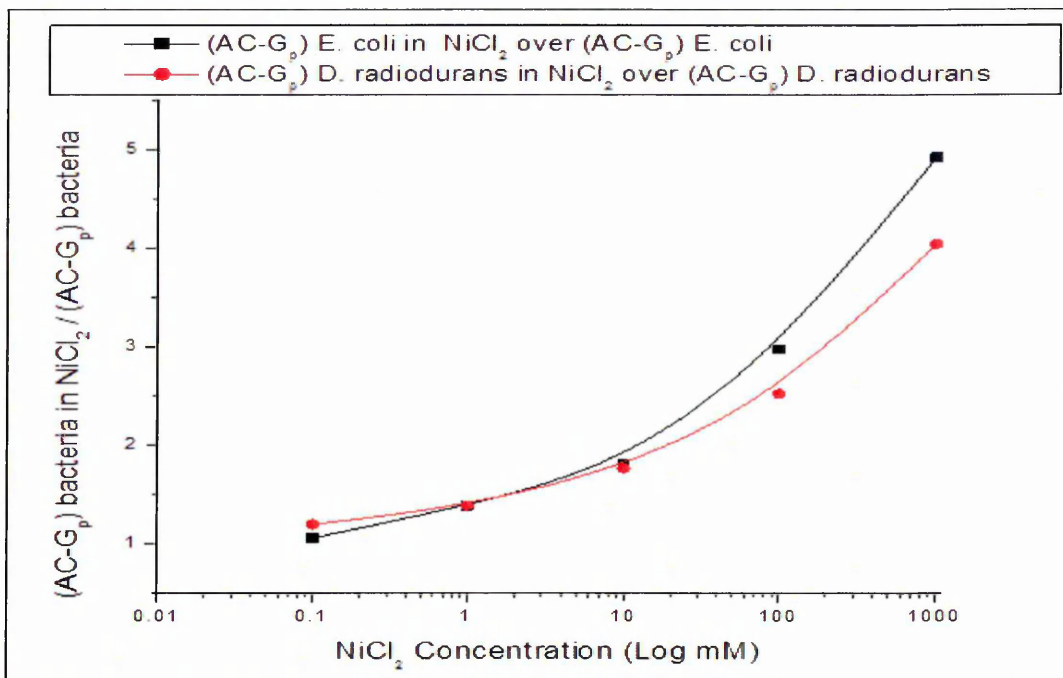


Figure 10.48. Comparison of relative response of conductance (AC-G<sub>p</sub>) for *E. coli* and *D. radiodurans* bacteria in  $\text{NiCl}_2$  over (AC-G<sub>p</sub>) conductance of bacteria after 72 hours

The change in AC capacitance of bacteria (*E. coli* and *D. radiodurans*) as a function of  $\text{NiCl}_2$  were explored in order to study the effect of metal on bacteria and the bacteria response to the metal, in order to estimate the  $\text{NiCl}_2$  concentration in the samples. Figure 10.49 show the AC capacitance for different concentrations of  $\text{NiCl}_2$  metal mixed with an LB broth (1:1), as a function of frequency

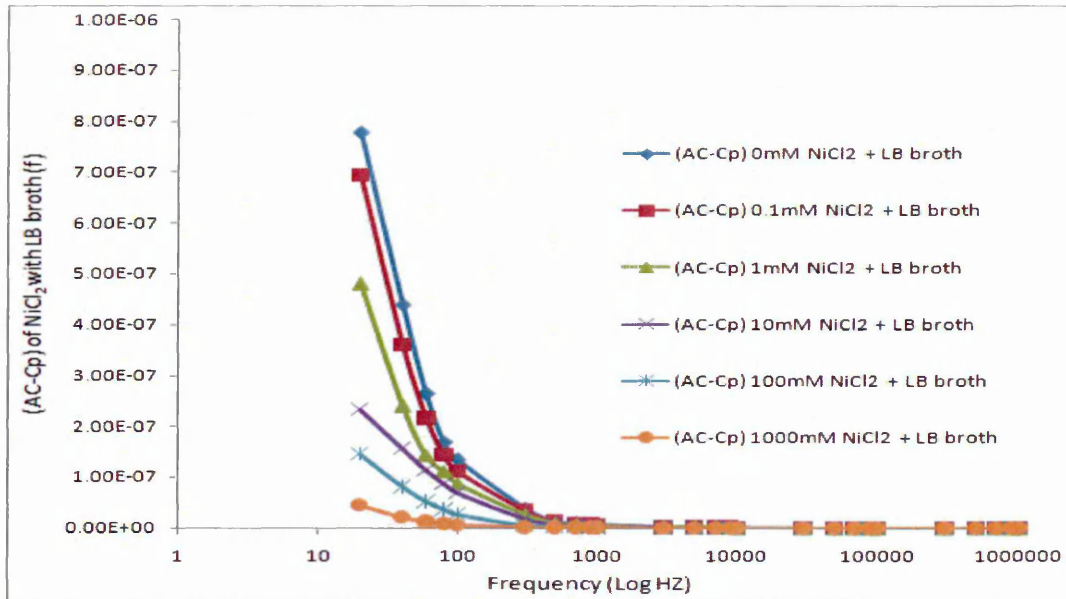


Figure 10.49. AC capacitance of  $\text{NiCl}_2$  metal mixed with LB broth

The AC capacitance of *E. coli* bacteria mixed with different concentrations of  $\text{NiCl}_2$  were explored for multi incubation periods, see Figure 10.50.

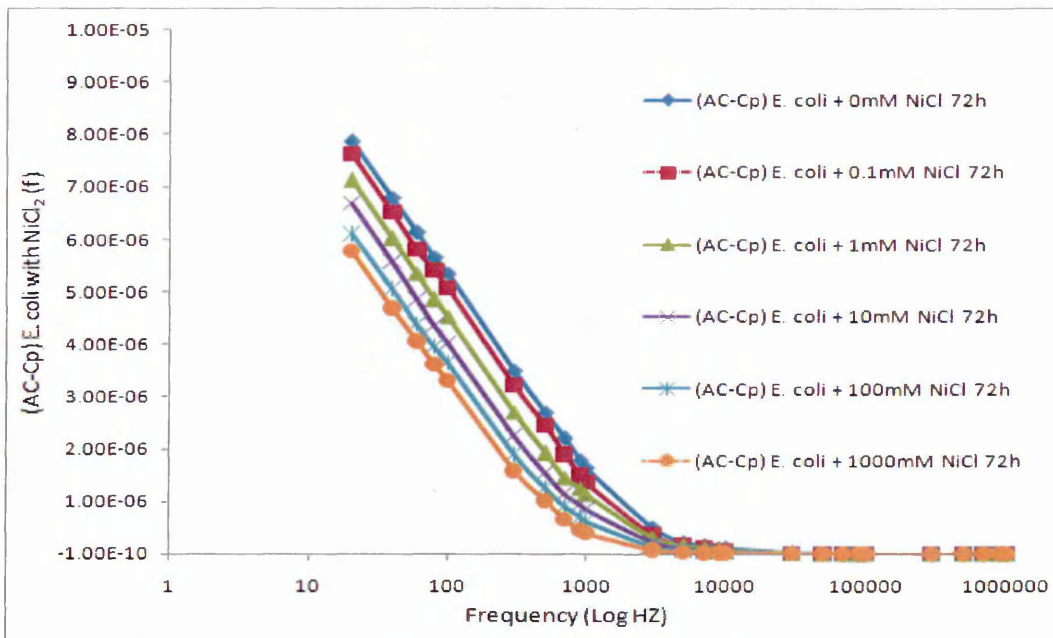


Figure 10.50. AC capacitance of *E. coli* bacteria mixed with  $\text{NiCl}_2$  metal after 72 hours

The normalisation methods are useful for estimating NiCl<sub>2</sub> concentration. Firstly, the AC capacitance of E. coli with different concentrations of NiCl<sub>2</sub> was normalised for capacitance of NiCl<sub>2</sub>, and secondly was normalised on capacitance of E. coli without metal.

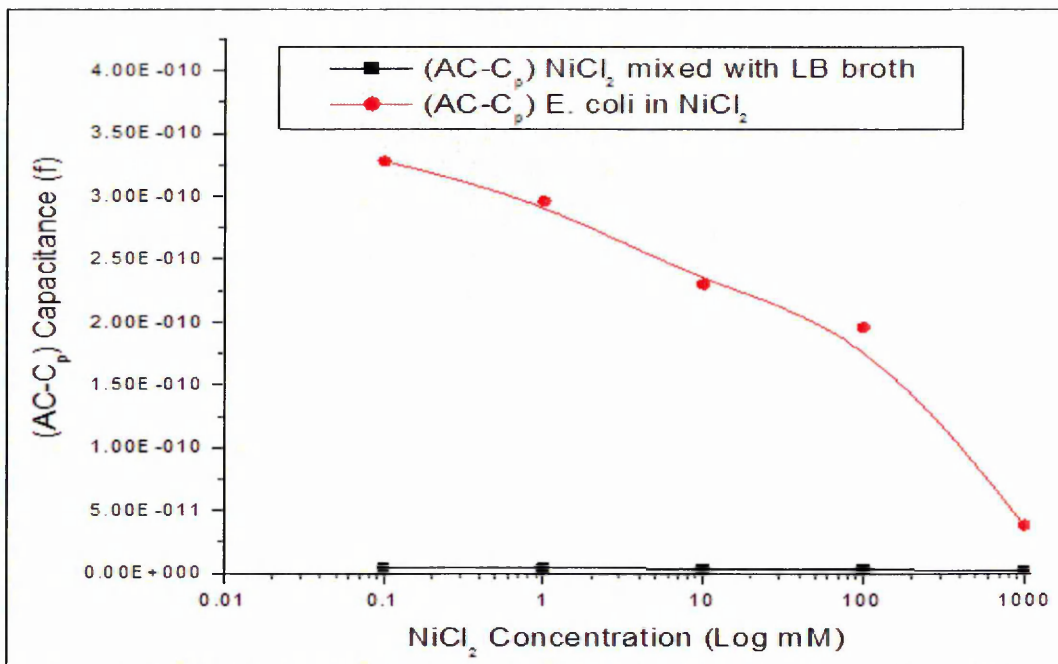


Figure 10.51. AC capacitance of E. coli bacteria mixed with NiCl<sub>2</sub> and capacitance of NiCl<sub>2</sub> after 72 hour's exposure at 900kHz

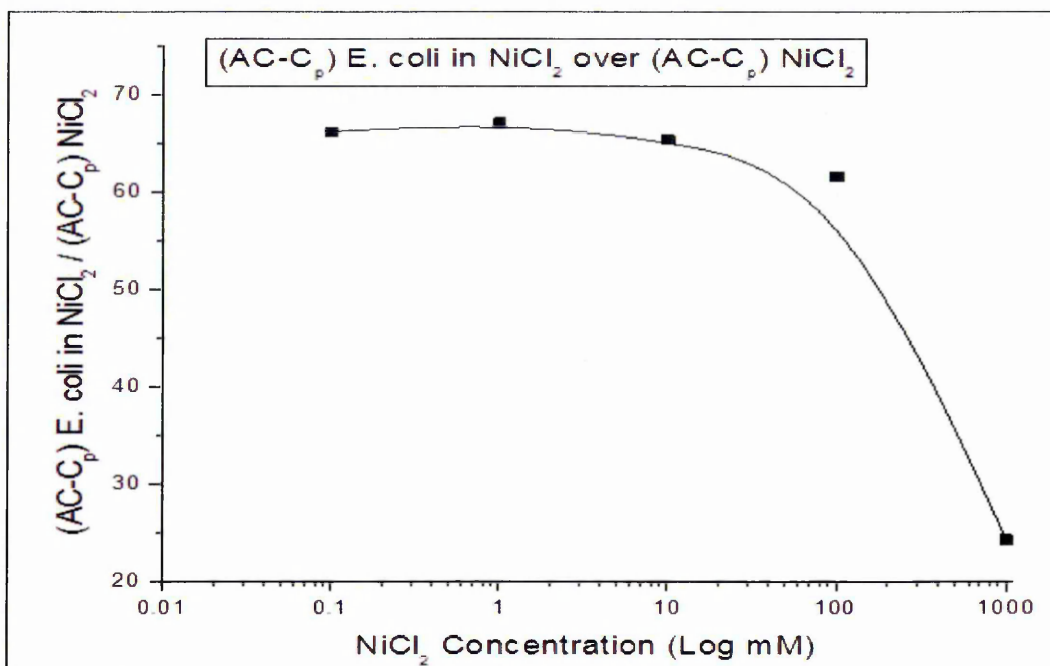


Figure 10.52. AC capacitance ratios of E. coli bacteria exposed (mixed) to NiCl<sub>2</sub> after 72 hours over the AC capacitance for NiCl<sub>2</sub> at 900kHz

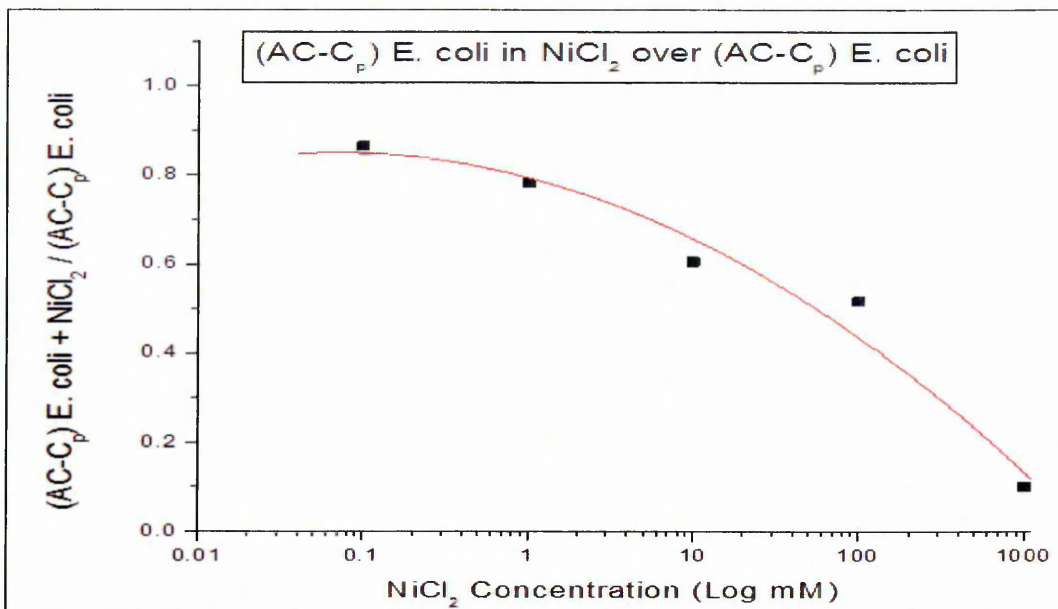


Figure 10.53. AC capacitance ratios of *E. coli* bacteria exposed (mixed) to  $\text{NiCl}_2$  after 72 hours over the AC capacitance for *E. coli* at 900kHz

As one can see, the capacitance of *E. coli*, after being mixed with  $\text{NiCl}_2$ , decreases exponentially as  $\text{NiCl}_2$  concentration increases. The capacitance of *E. coli* with the  $\text{NiCl}_2$  metal is ten times larger than the capacitance of  $\text{NiCl}_2$  mixed with an LB broth.

The AC capacitances of *D. radiodurans* bacteria after being mixed with different concentrations of  $\text{NiCl}_2$  were investigated. The results are employed to predict the metal concentration. As mentioned before the same techniques were followed to find out the effect of  $\text{NiCl}_2$  on *D. radiodurans* bacteria, see appendix D. The AC capacitances of different concentrations of  $\text{NiCl}_2$  with OXOID broth (1:1) were also presented.

The study has shown that the capacitance decreases gradually with increasing frequency. The AC capacitances of different concentrations of  $\text{NiCl}_2$  with OXOID broth (1:1) are studied; for more details see appendix D.

The results has also shown that the AC capacitance of *D. radiodurans* bacteria changes as a result of adding different concentrations of  $\text{NiCl}_2$ ; similar changes are observed for  $\text{NiCl}_2$  itself after being mixed with OXOID broth.

Normalisation method is used to estimate  $\text{NiCl}_2$  concentration. Firstly, the AC capacitance of *D. radiodurans* with different concentrations of  $\text{NiCl}_2$  was normalised for capacitance of  $\text{NiCl}_2$ , and secondly was normalised to the capacitance of *D. radiodurans*.

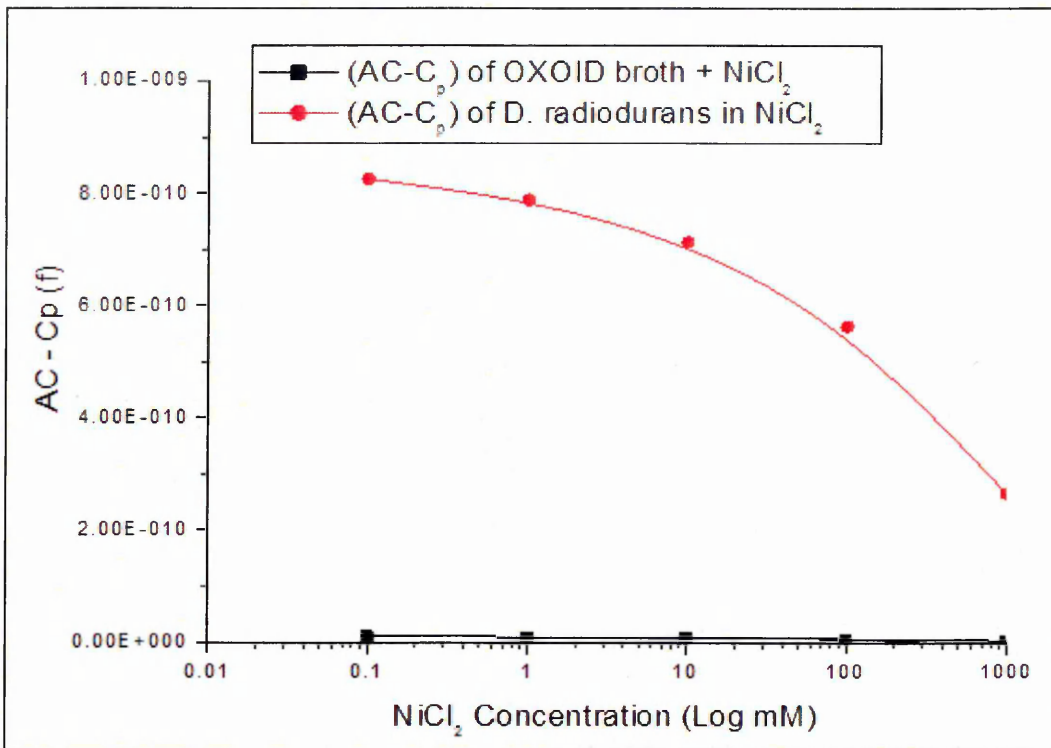


Figure 10.54. AC capacitance of *D. radiodurans* bacteria mixed with NiCl<sub>2</sub> after 72 hours and for NiCl<sub>2</sub> mixed with OXOID broth at 900kHz

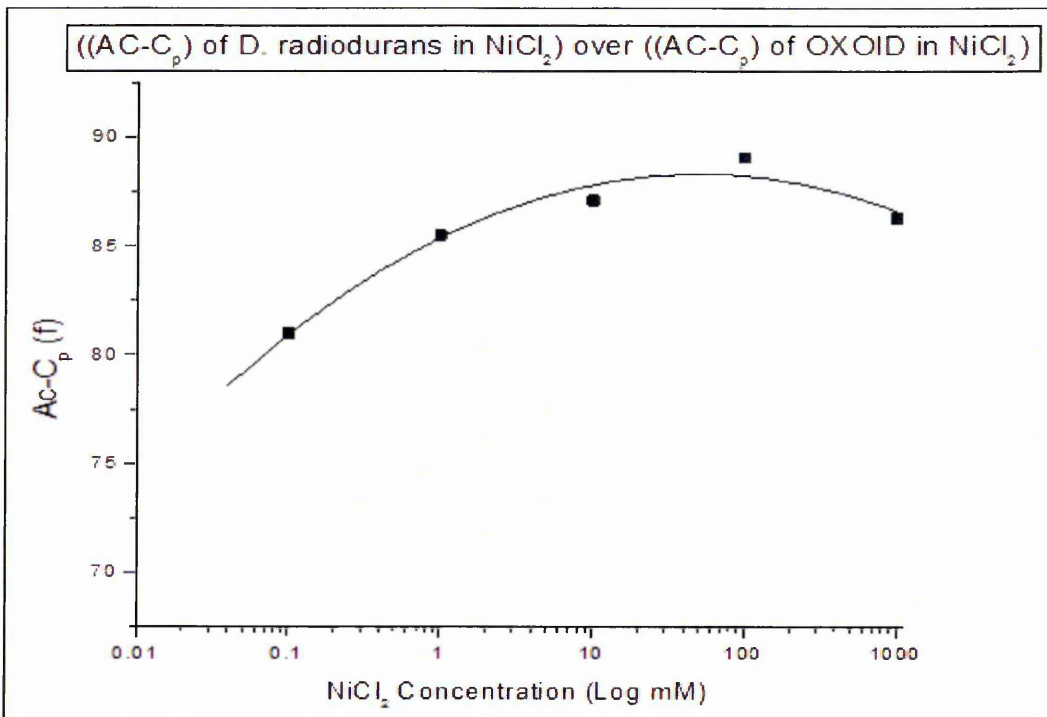


Figure 10.55. AC capacitance ratios of *D. radiodurans* bacteria exposed (mixed) to NiCl<sub>2</sub> over AC capacitance of OXOID broth in NiCl<sub>2</sub> for 900kHz frequency

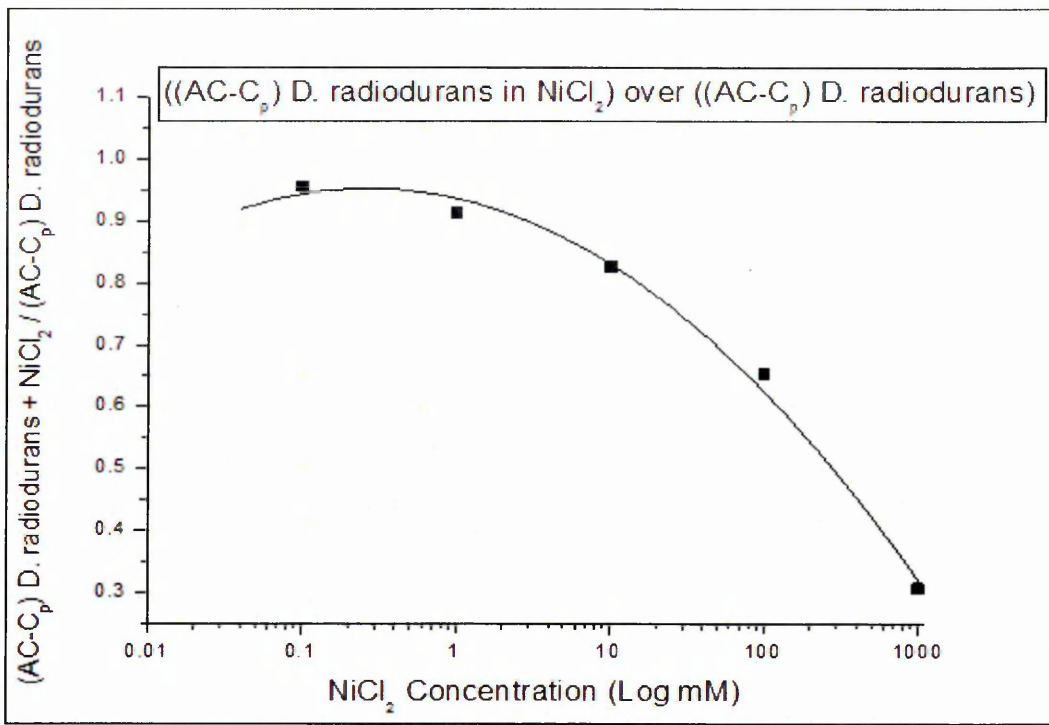


Figure 10.56. AC capacitance ratios of *D. radiodurans* bacteria mixed with  $\text{NiCl}_2$  after 72 hours over the AC capacitance for *D. radiodurans* at 900kHz

The comparison curves between *E. coli* capacitance and that of *D. radiodurans* bacteria responses to  $\text{NiCl}_2$  metal are presented in Figures 10.57 and 10.58.

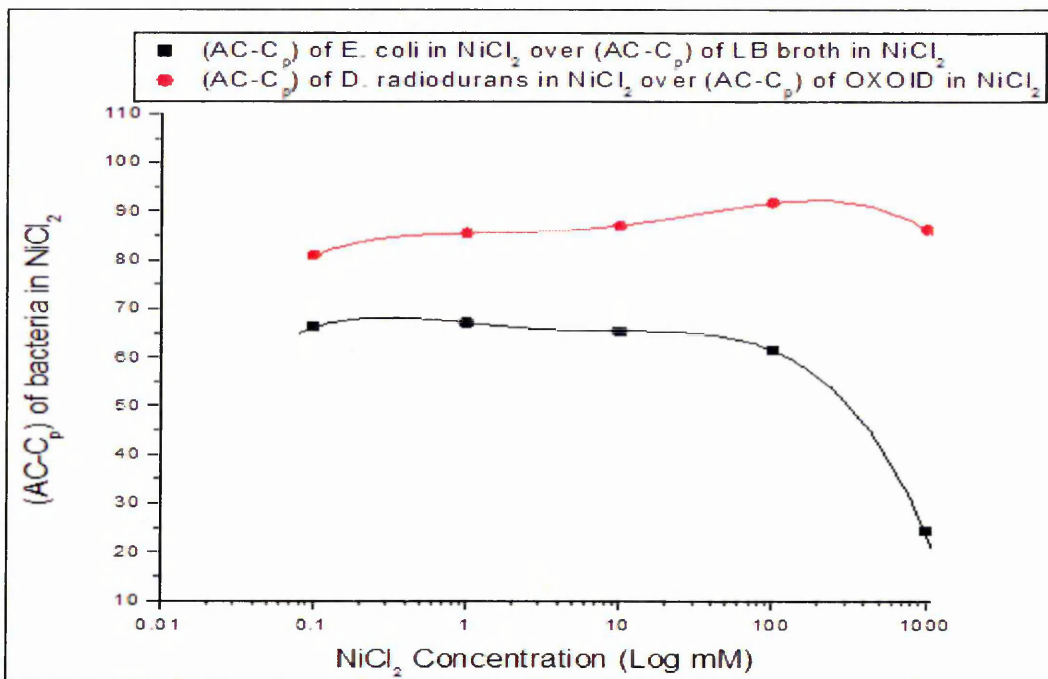


Figure 10.57. Comparison of relative response of capacitance ( $\text{AC-C}_p$ ) for *E. coli* and *D. radiodurans* bacteriamixed with  $\text{NiCl}_2$  over ( $\text{AC-C}_p$ ) capacitance of  $\text{NiCl}_2$  for 72 hours

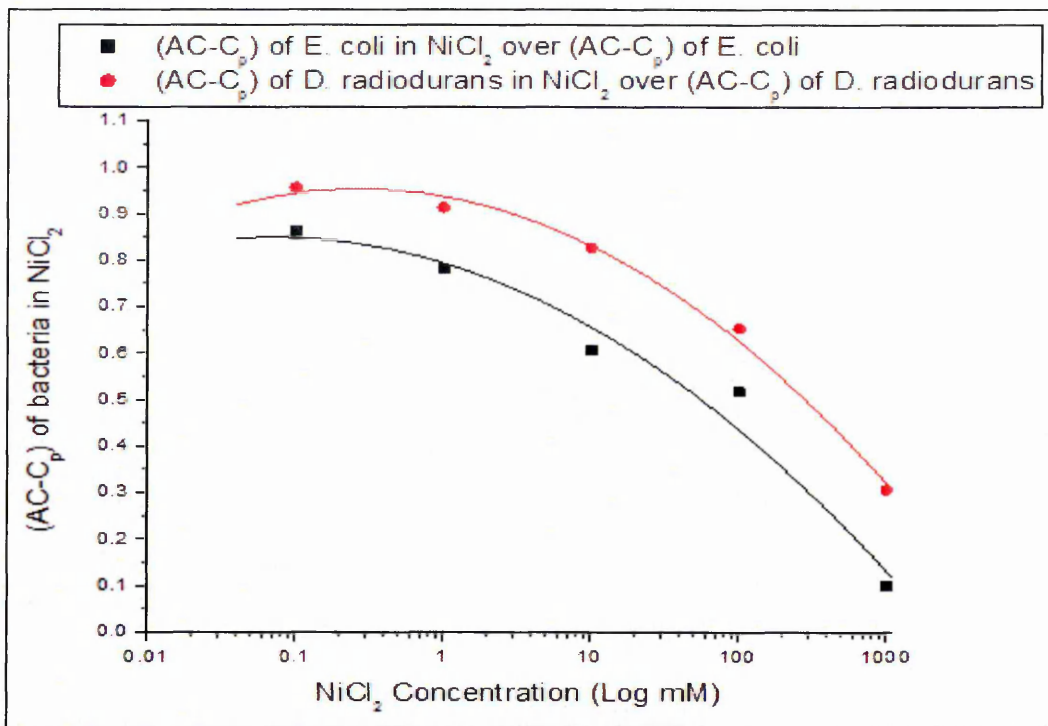


Figure 10.58. Comparison of relative response of capacitance ( $AC-C_p$ ) for E.coli and D. radiodurans bacteriamixed with  $NiCl_2$  over ( $AC-C_p$ ) of E. coli D. radiodurans after 72 hours at 900kHz

Figures 10.57, 10.58 are very interesting in terms of understanding the bacteria's response to  $NiCl_2$ , as one can see the there is a big difference between the E. coli and D. radiodurans response, as a function of metal concentration. This response can be utilised to detect the metal.

#### 10.4. Equivalent Circuit Results

As mentioned in Section 6.3, and also analysed and discussed in Section 8.5, the assumed equivalent circuit was calculated at low and high frequencies for both types of bacteria for different concentrations of salt  $CdCl_2$ ,  $NiCl_2$ . Firstly, the conductivity at low frequency for E. coli and D. radiodurans bacteria samples was estimated. The conductivity at low frequency ( $\omega \sim 0$ ) is shown in equation (10.2).

$$G_{p(\omega \sim 0)} = \frac{1}{R_s} \quad (10.2)$$

The equivalent circuit was also depicted at high frequency. The conductivity at high frequency ( $\omega \sim \infty$ ) is shown in equation (10.3).

$$G_{p(\omega \sim \infty)} = \infty \quad (10.3)$$

Figure 10.59 shows surface resistance at high frequency of E. coli bacteria after  $CdCl_2$  being added. As a result, the surface resistance for bacteria in their own sensor

cell can be calculated from (10.1). The surface resistances ( $R_s$ ) of *E. coli* bacteria and  $\text{CdCl}_2$  are presented in Figures 10.59, 10.60.

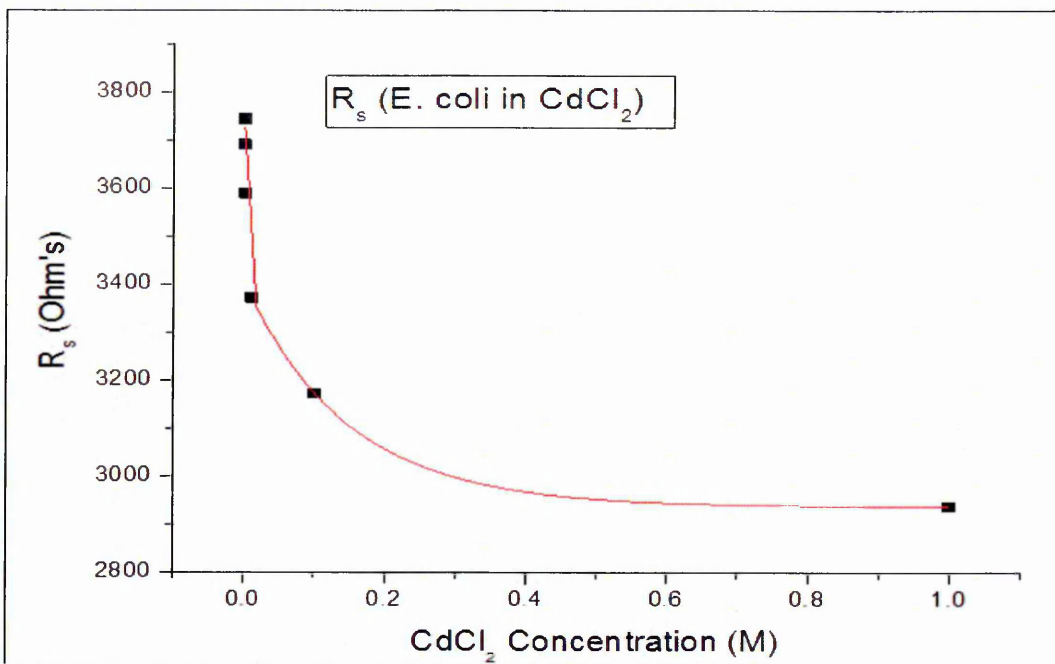


Figure 10.59. Changes in surface resistance ( $R_s$ ) of *E. coli* bacteria samples after being added  $\text{CdCl}_2$  after 72 hours exposure

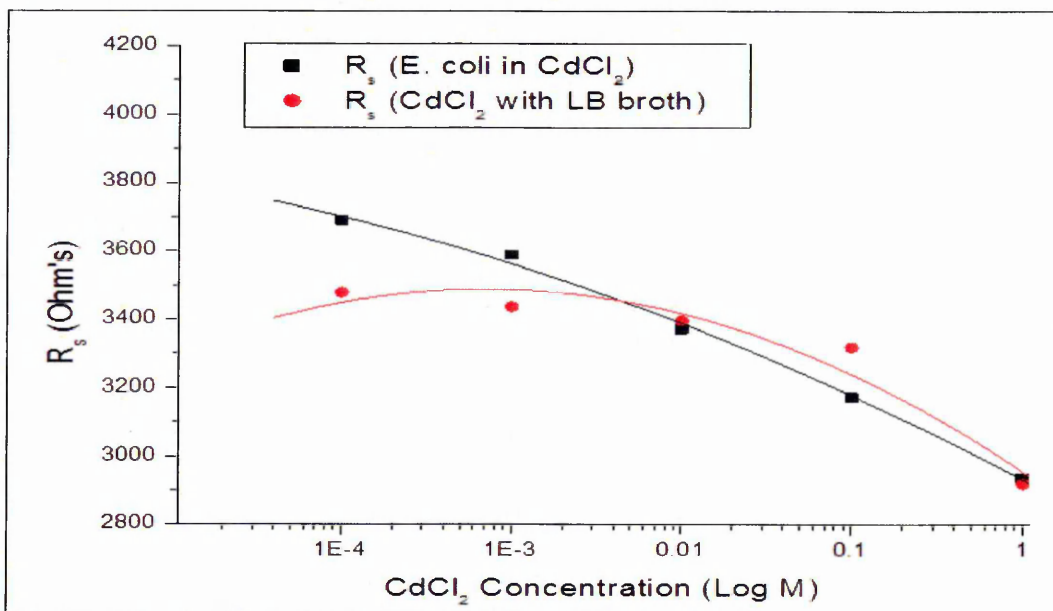


Figure 10.60. Changes in surface resistance ( $R_s$ ) of *E. coli* bacteria samples after being added  $\text{CdCl}_2$  and for  $\text{CdCl}_2$  with LB broth after 72 hours exposure

It can be seen that most of bacteria cell resistance appeared as surface resistance, as clearly depicted from the  $R_s$  results, (see figures 10.59 and 10.60), which are correlated exponentially with the salt concentration.

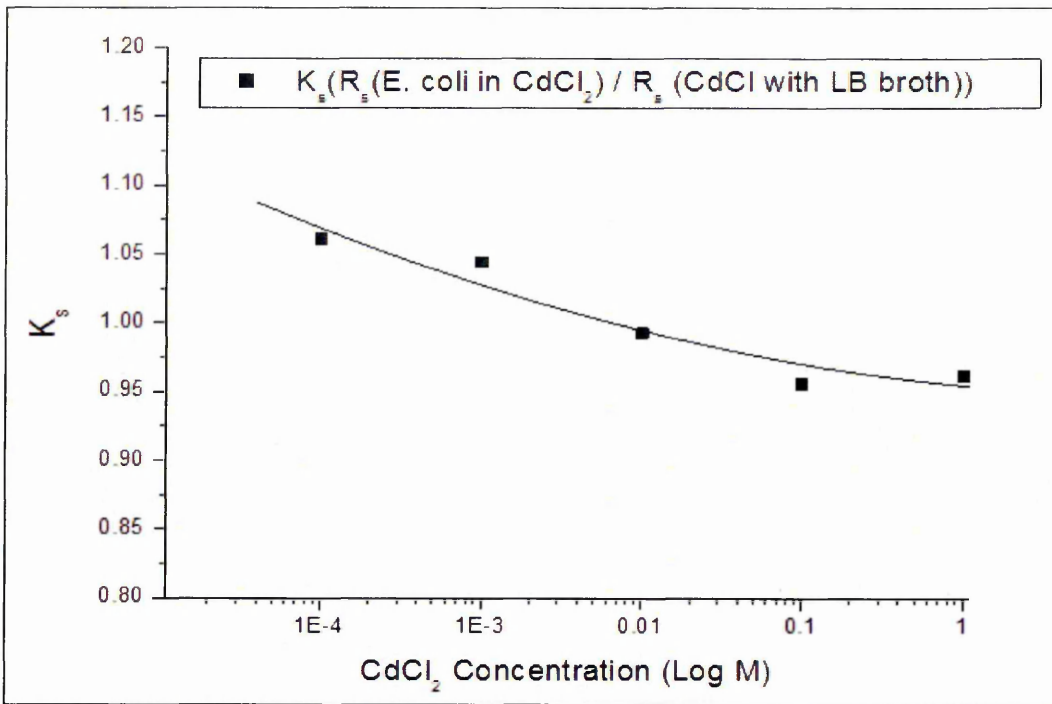


Figure 10.61. Normalised curve for ratio of surface resistance of *E. coli* bacteria in CdCl<sub>2</sub> to surface resistance of CdCl<sub>2</sub> with LB broth after 72 hours

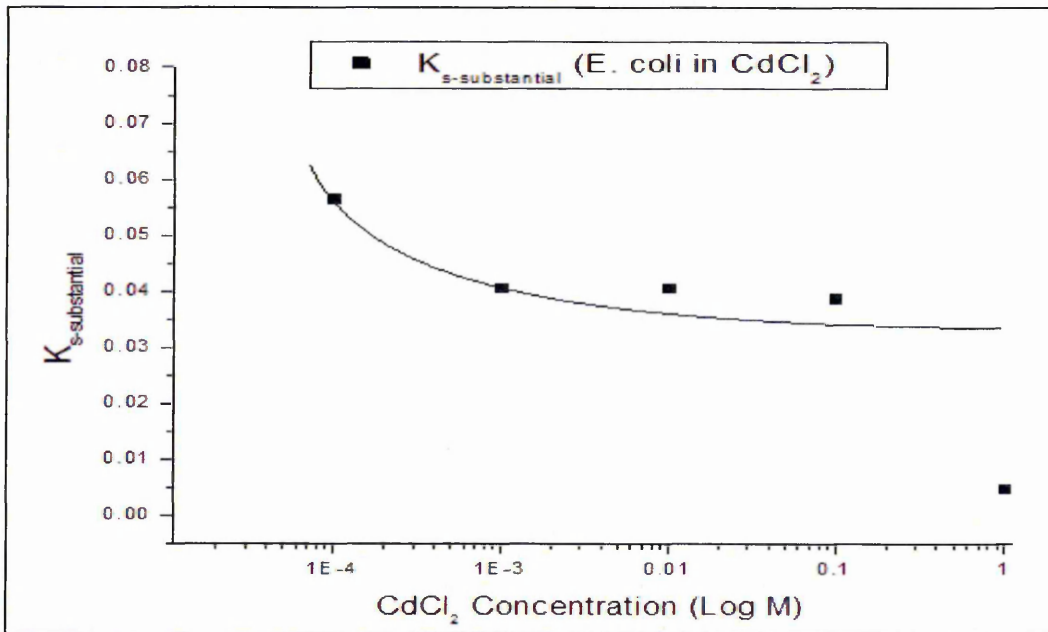


Figure 10.62. Relative changes curve for ratio of surface resistance of *E. coli* bacteria in CdCl<sub>2</sub> to surface resistance of CdCl<sub>2</sub> with LB broth over surface resistance of *E. coli* at 0M CdCl<sub>2</sub> after 72 hours

The surface resistance of *D. radiodurans* for different concentrations of CdCl<sub>2</sub> has been calculated. Figure 10.63 shows surface resistance changes for *D. radiodurans* bacteria and CdCl<sub>2</sub>.

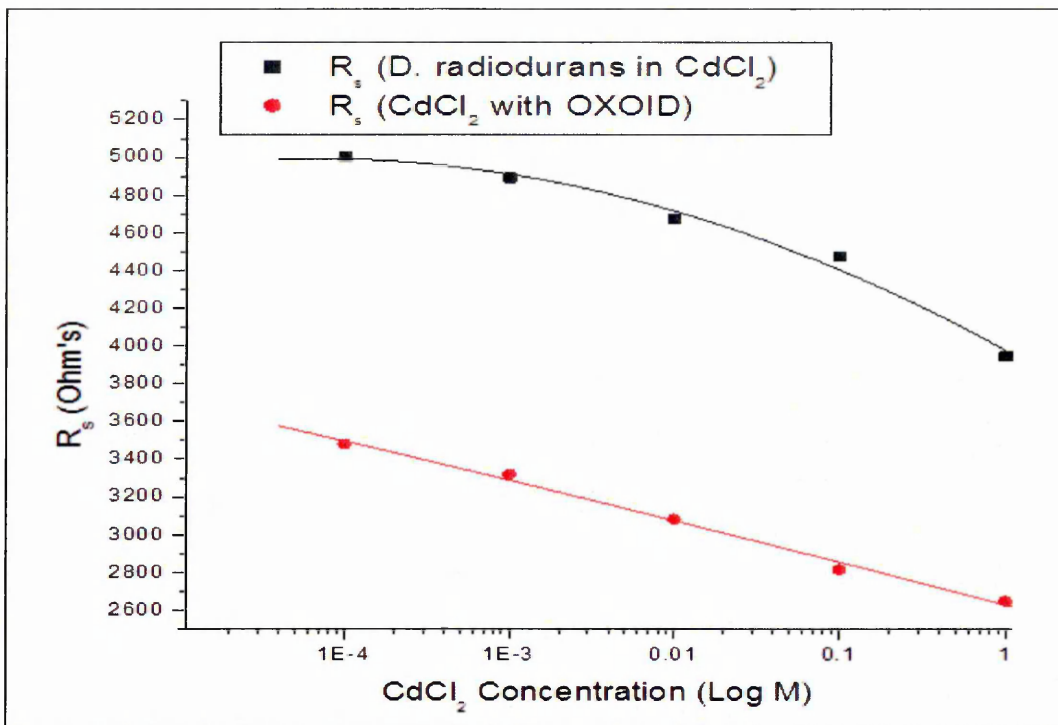


Figure 10.63. Changes in surface resistance ( $R_s$ ) of *D. radiodurans* bacteria after being added  $CdCl_2$  and for  $CdCl_2$  with OXOID broth after 72 hours exposure

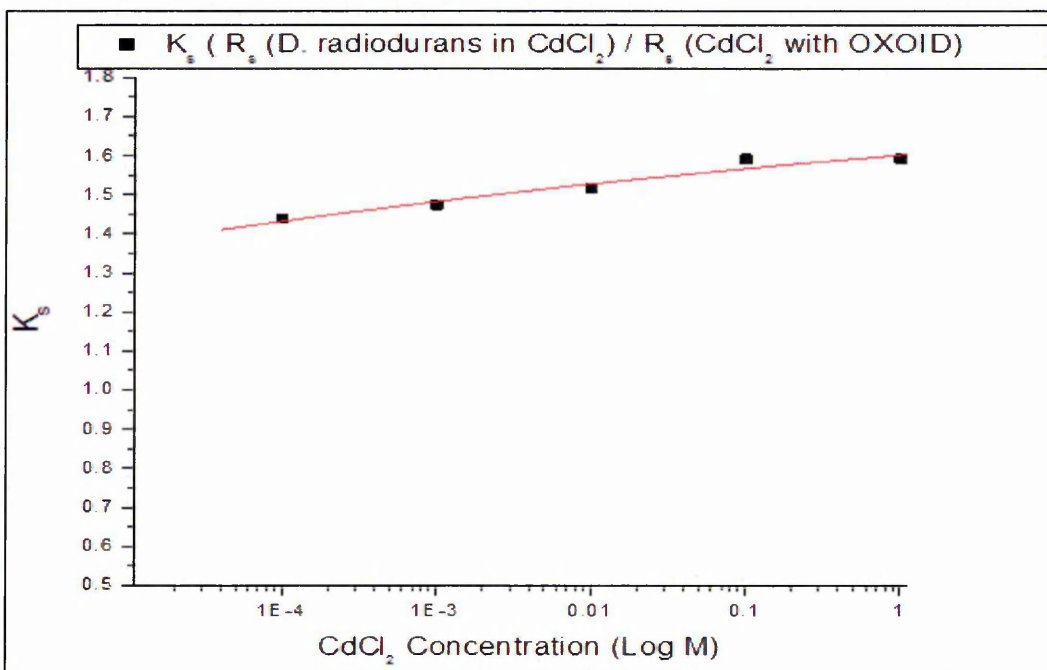


Figure 10.64. Normalised curve for ratio of surface resistance of *D. radiodurans* bacteria in  $CdCl_2$  to surface resistance of  $CdCl_2$  with OXOID broth after 72 hours

In order to estimate the salt concentration in the studied samples, the surface resistance of bacteria cell was calculated using the equivalent circuit design of the cell including

the *D. radiodurans* bacteria after meal salt being added and subtracted to evaluate the salt concentration and to eliminate the salt effect, see figure 65.

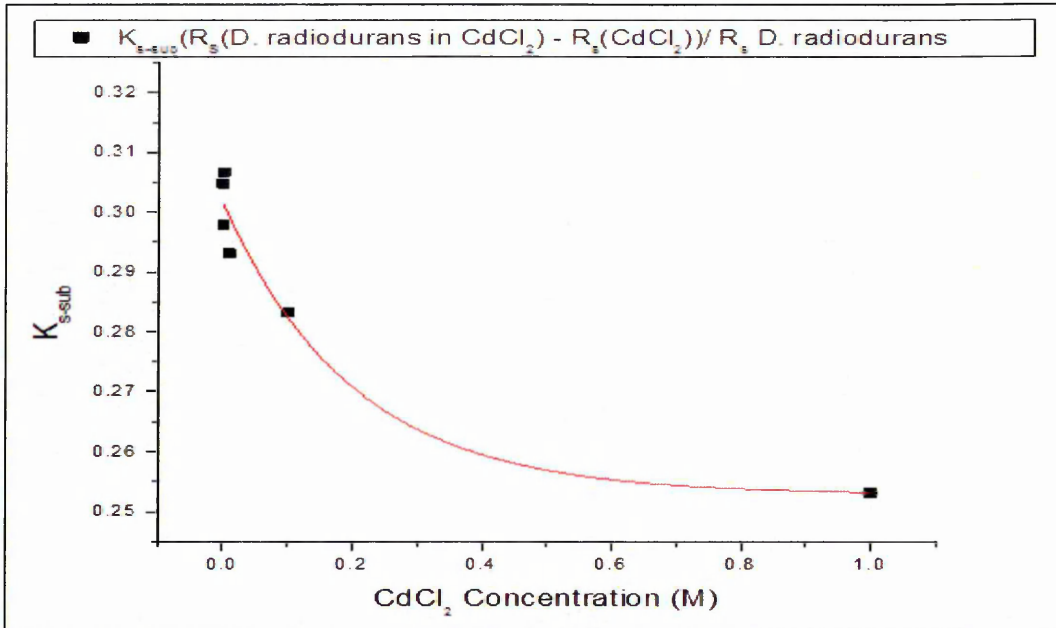


Figure 10.65. Relative changes curve for ratio of surface resistance of *D. radiodurans* bacteria in CdCl<sub>2</sub> to surface resistance of CdCl<sub>2</sub> with OXOID broth over surface resistance of *D. radiodurans* at 0M CdCl<sub>2</sub> after 72 hours

For further information and comparison between the bacteria response for CdCl<sub>2</sub>, the subtracted results of surface resistances for both bacteria types are plotted in figure 10.66 for different concentrations of salt.

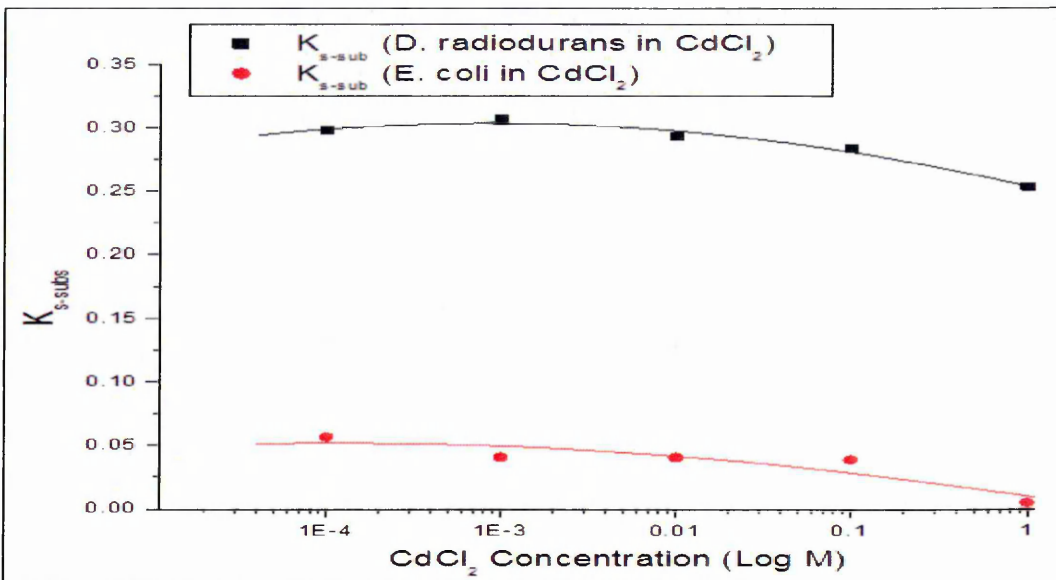


Figure 10.66. Comparison curves for surface resistance substantial (K<sub>b-Sub</sub>) between *E. coli* and *D. radiodurans* bacteria response to CdCl<sub>2</sub>

Double layer capacitance was created on the working electrode; this capacitance depends on the concentration of bacteria in the bio-cell sensor. From equation 6.5, the surface capacitance from the equivalent circuit identify the parallel capacitance that is measured experimentally, then the surface capacitance calculated at high frequency ( $\omega \sim \infty$ ) and presented in figure 10.67.

$$C_p(\omega \sim \infty) = C_s \quad (10.4)$$

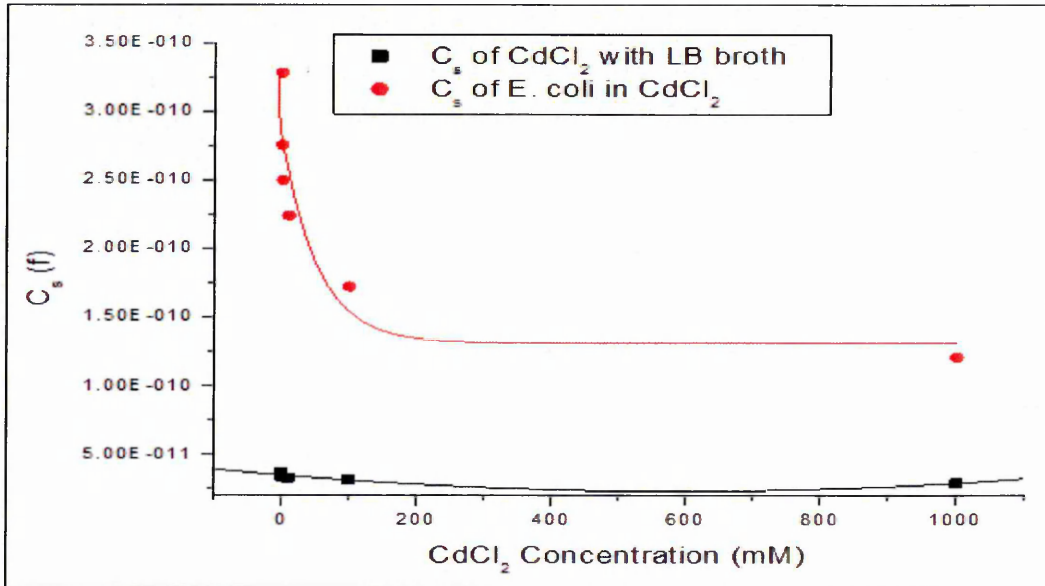


Figure 10.67. Changes in surface capacitance ( $C_s$ ) of E. coli bacteria samples after being added CdCl<sub>2</sub> and for CdCl<sub>2</sub> with LB broth after 72 hours exposure

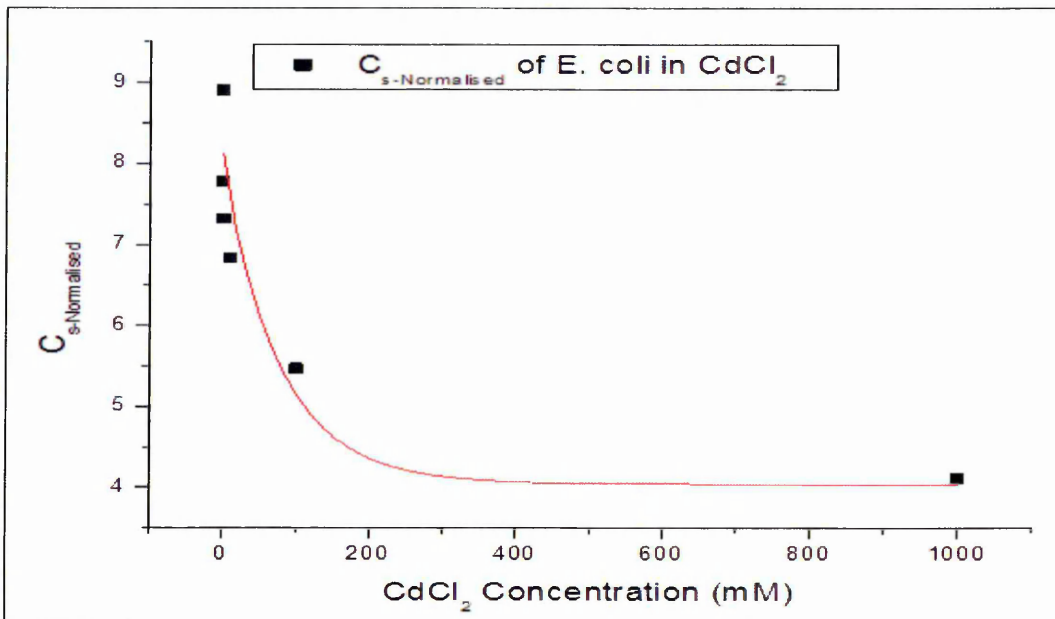


Figure 10.68. Normalised curve for ratio of surface capacitance of E. coli bacteria in CdCl<sub>2</sub> to surface capacitance of CdCl<sub>2</sub> with LB broth after 72 hours

The subtraction of salt contribution from surface capacitance data of *E. coli* bacteria in  $\text{CdCl}_2$  is a useful method to estimate the salt concentration in bacteria samples, see figure 10.69.

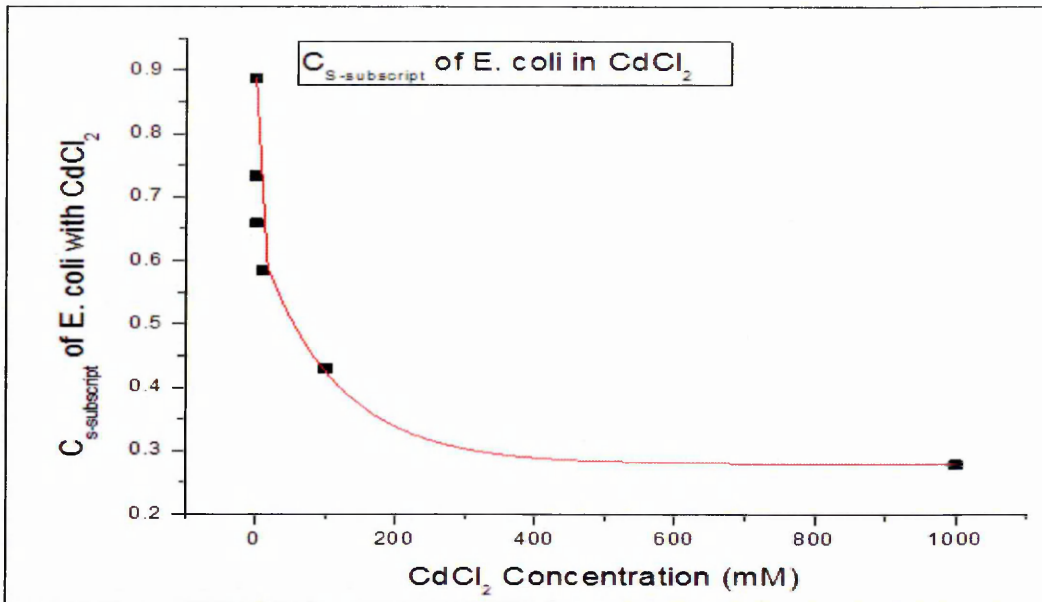


Figure 10.69. Relative changes curve for ratio of surface capacitance of *E. coli* bacteria in  $\text{CdCl}_2$  to surface capacitance of  $\text{CdCl}_2$  with LB broth over surface capacitance of *E. coli* at 0M  $\text{CdCl}_2$  after 72 hours

The double layers capacitance of *D. radiodurans* for different concentrations of  $\text{CdCl}_2$  has been calculated. Figure 10.71 shows the surface capacitance change for *D. radiodurans* bacteria and  $\text{CdCl}_2$ .

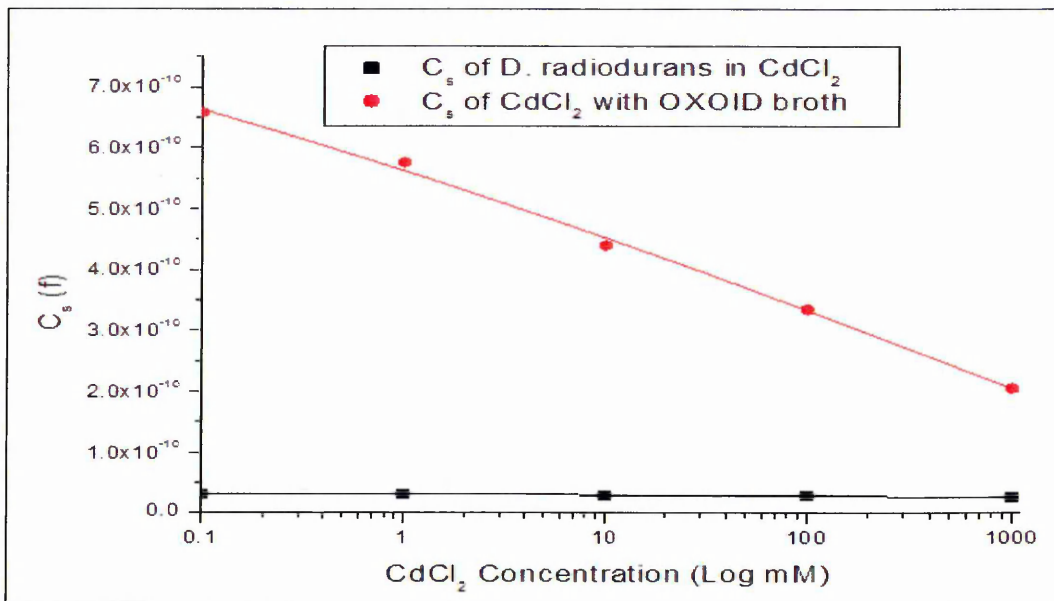


Figure 10.70. Changes in surface capacitance ( $C_s$ ) of *D. radiodurans* bacteria samples after being added  $\text{CdCl}_2$  and for  $\text{CdCl}_2$  with OXOID broth after 72 hours exposure

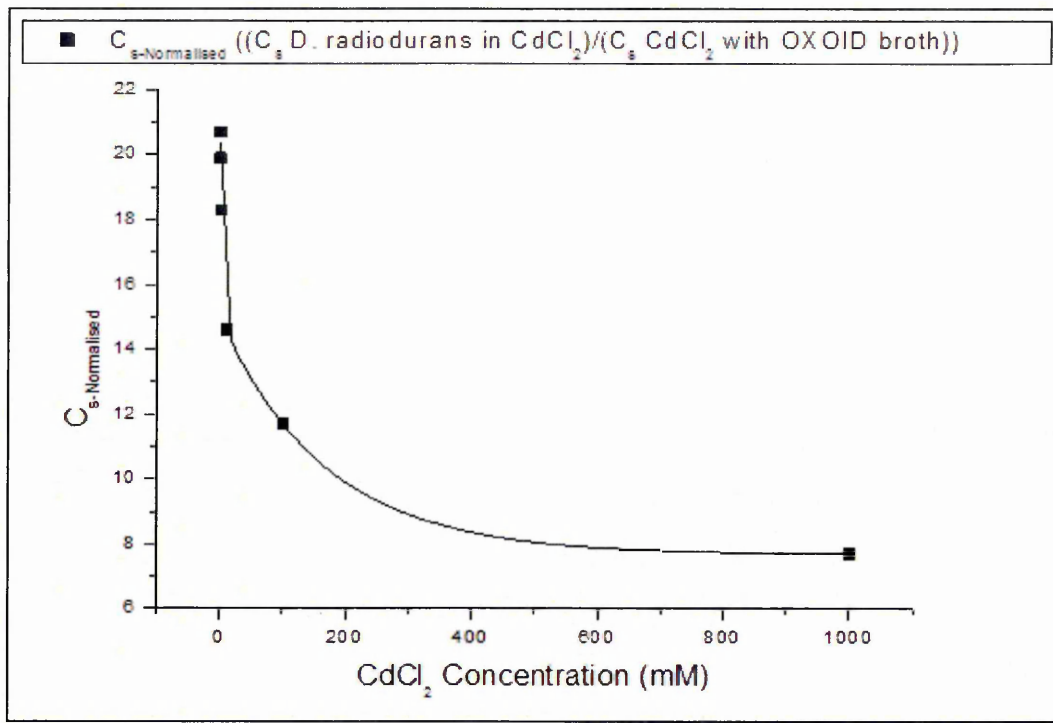


Figure 10.71. Normalised curve for ratio of surface capacitance of *D. radiodurans* bacteria in  $\text{CdCl}_2$  to surface capacitance of  $\text{CdCl}_2$  with LB broth after 72 hours

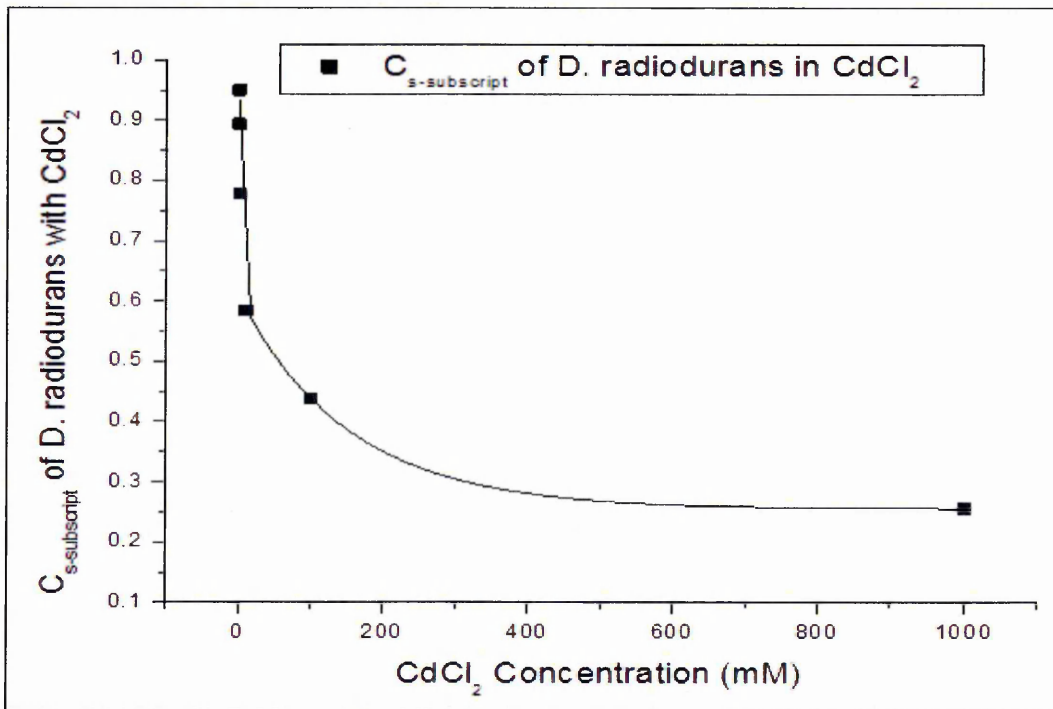


Figure 10.72. Relative changes curve for ratio of surface capacitance of *D. radiodurans* bacteria in  $\text{CdCl}_2$  to surface capacitance of  $\text{CdCl}_2$  with OXOID broth over surface capacitance of *D. radiodurans* at 0M  $\text{CdCl}_2$  after 72 hours

Figure 10.74. Shows results derived from the equivalent circuit for both types of bacteria (*E. coli* and *D. radiodurans*).

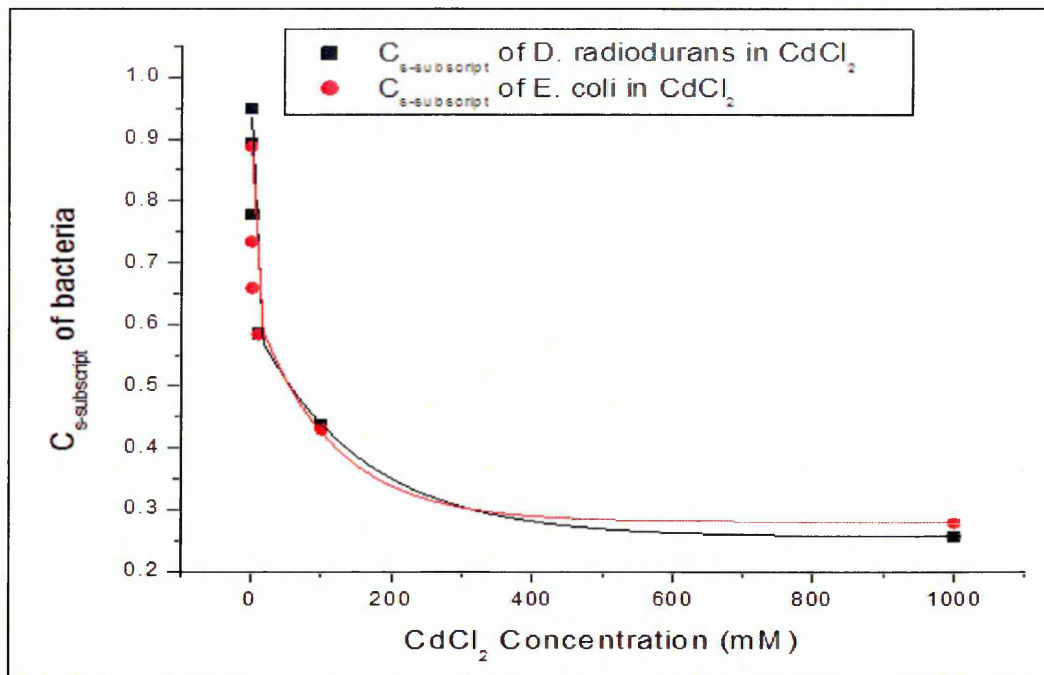


Figure 10.73. Relative changes curve comparison for surface capacitance of E. coli and D. radiodurans bacteria in CdCl<sub>2</sub> after 72 hours

An equivalent circuit was also used to estimate the surface resistance ( $R_s$ ) and double layer capacitance ( $C_s$ ) of E. coli and D. radiodurans bacteria cells density as a function of exposure time to different concentrations of NiCl<sub>2</sub>. It has to be mentioned that equations (10.2) and (10.3) were used for calculate the surface resistance at high frequency.

Surface resistance ( $R_s$ ) was estimated for both E. coli and D. radiodurans bacteria, as a function of exposure time to different concentrations of NiCl<sub>2</sub>. Equations (10.2) and (10.3) were used for this task in high and low frequency.

First, the surface resistance for E. coli bacteria and NiCl<sub>2</sub> salt in their own cell sensor were calculated and presented in Figure 10.74.

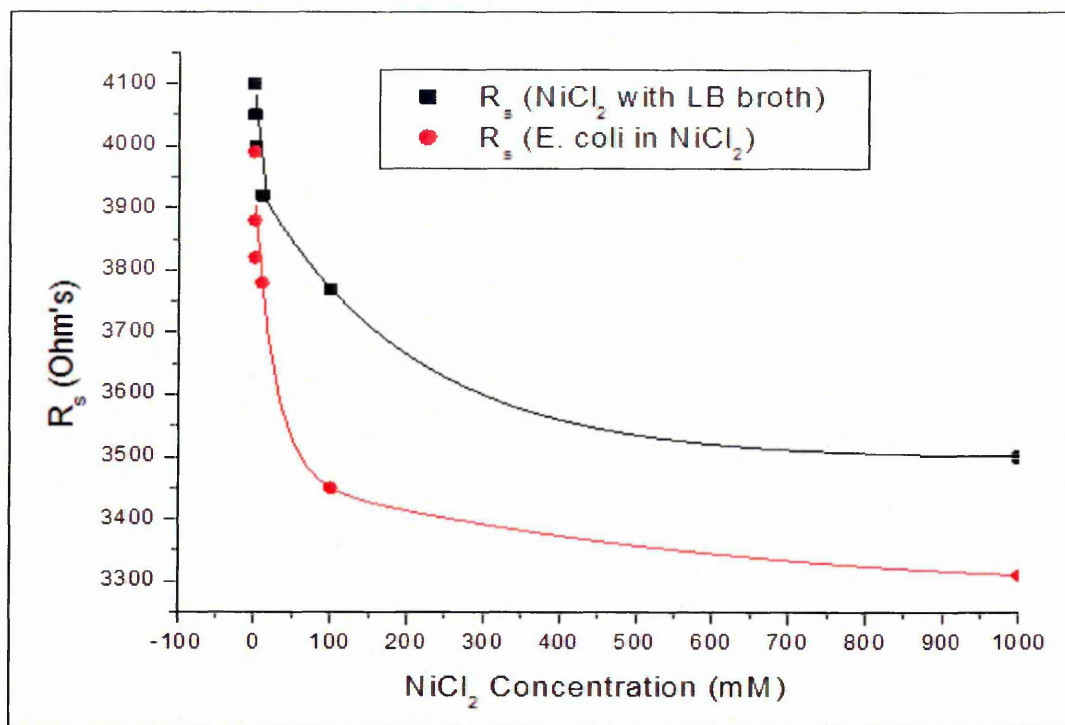


Figure 10.74. Changes in surface resistance ( $R_s$ ) of *E. coli* bacteria after adding  $NiCl_2$  and for  $NiCl_2$  with LB broth after 72 hours exposure

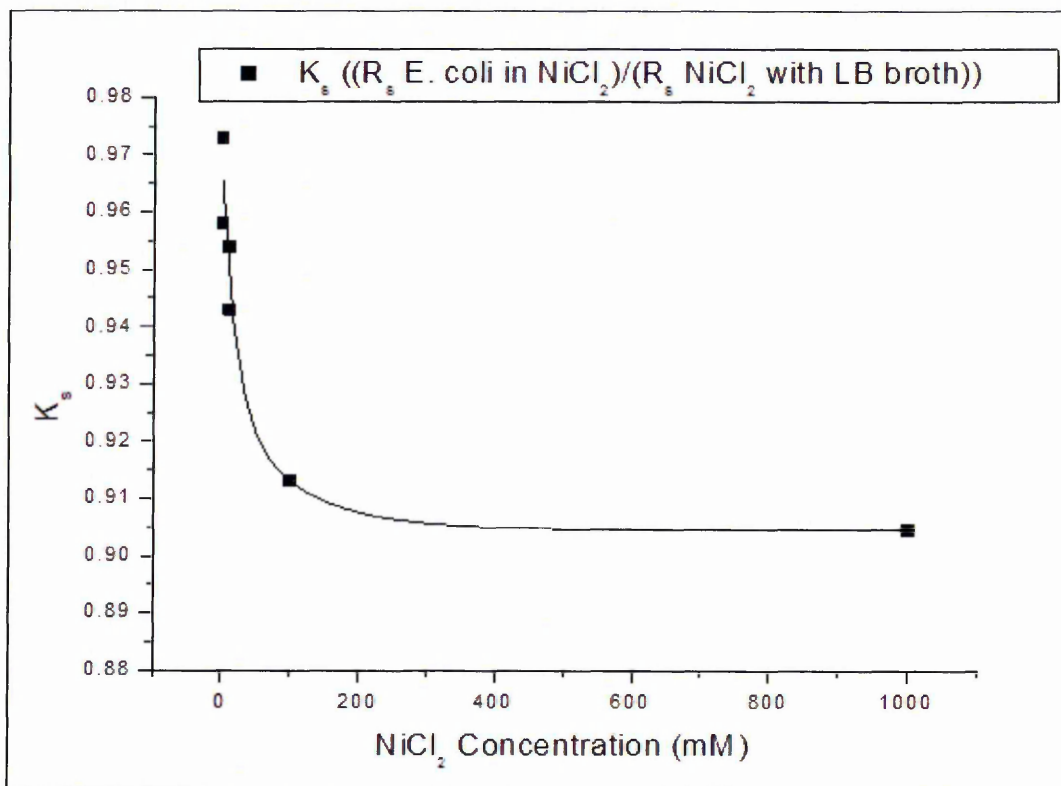


Figure 10.75. Normalised curve for ratio of surface resistance of *E. coli* bacteria in  $NiCl_2$  to surface resistance of  $NiCl_2$  with LB broth after 72 hours

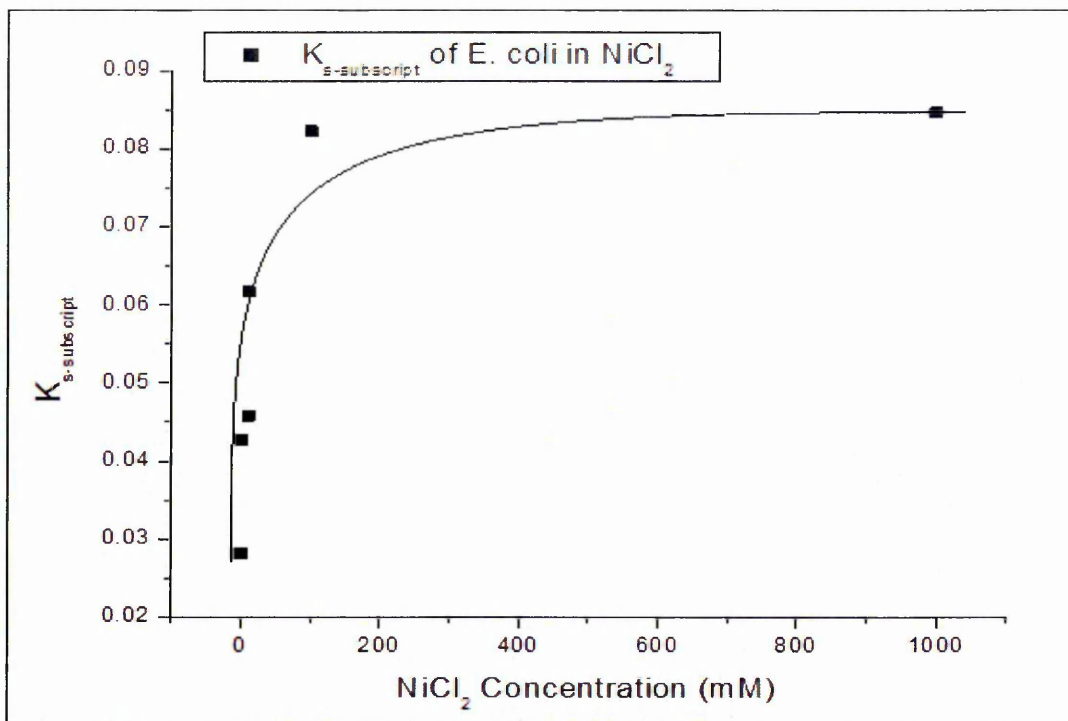


Figure 10.76. Relative changes curve for ratio of surface resistance of *E. coli* bacteria in  $\text{NiCl}_2$  to surface resistance of  $\text{NiCl}_2$  with LB broth over surface resistance of *E. coli* at 0M  $\text{NiCl}_2$  after 72 hours

Surface resistance for *D. coli* bacteria and  $\text{NiCl}_2$  salt in their own cell sensor were calculated and presented in Figure 10.78.

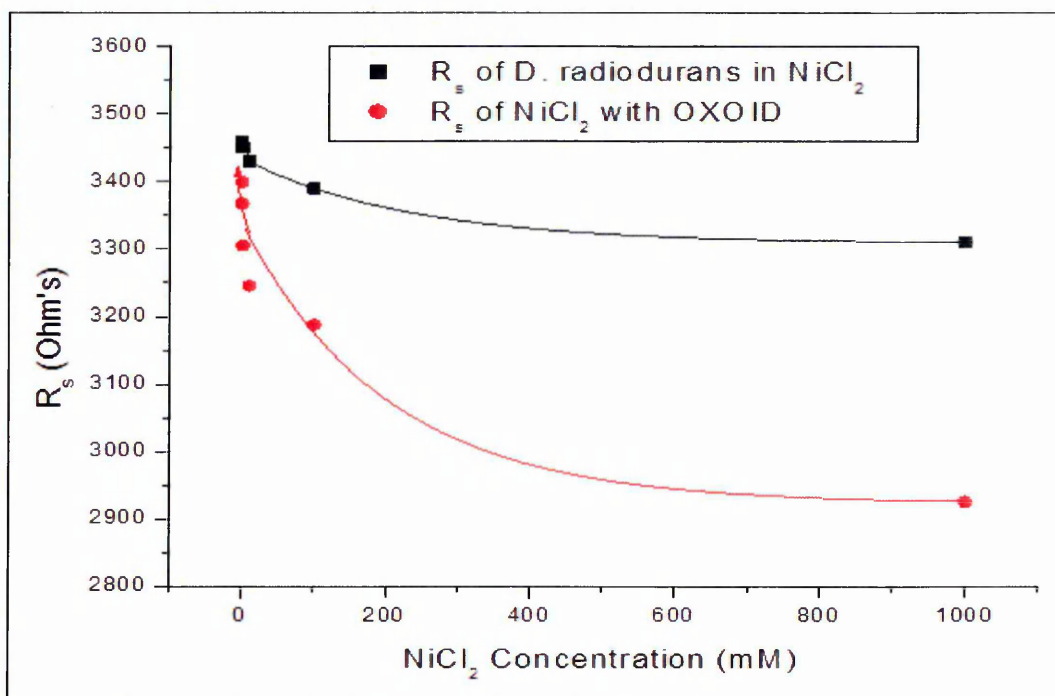


Figure 10.77. Changes in surface resistance ( $R_s$ ) of *D. radiodurans* bacteria after adding  $\text{NiCl}_2$  and for  $\text{NiCl}_2$  with OXOID broth after 72 hours exposure

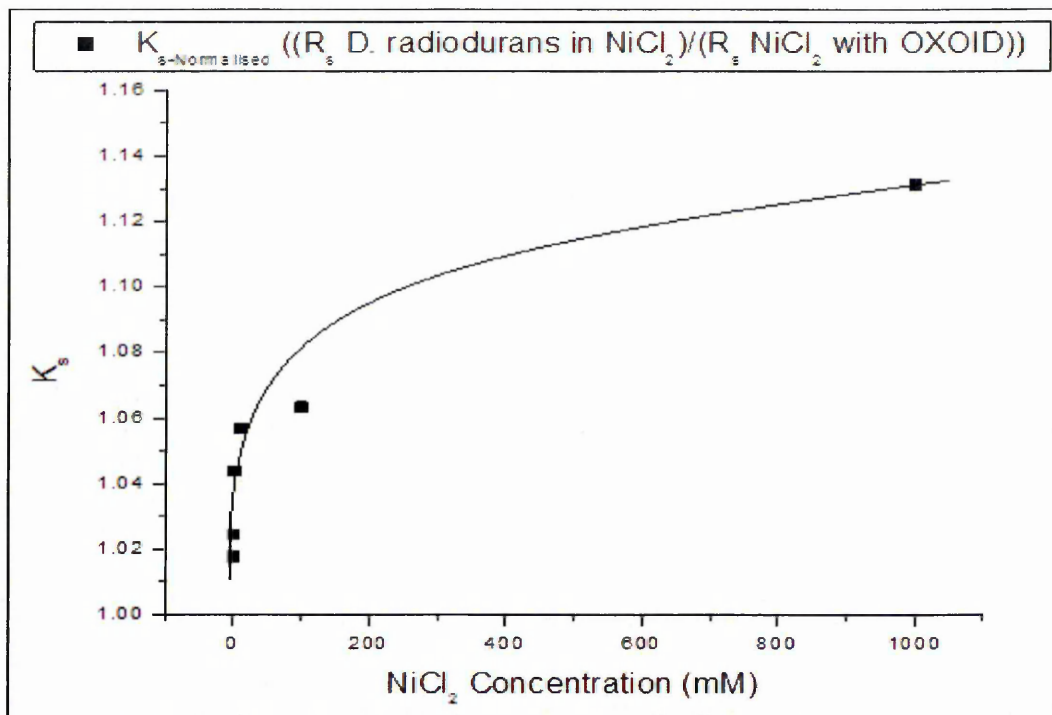


Figure 10.78. Normalised curve for ratio of surface resistance of *D. radiodurans* bacteria in  $NiCl_2$  to surface resistance of  $NiCl_2$  with OXOID broth after 72 hours

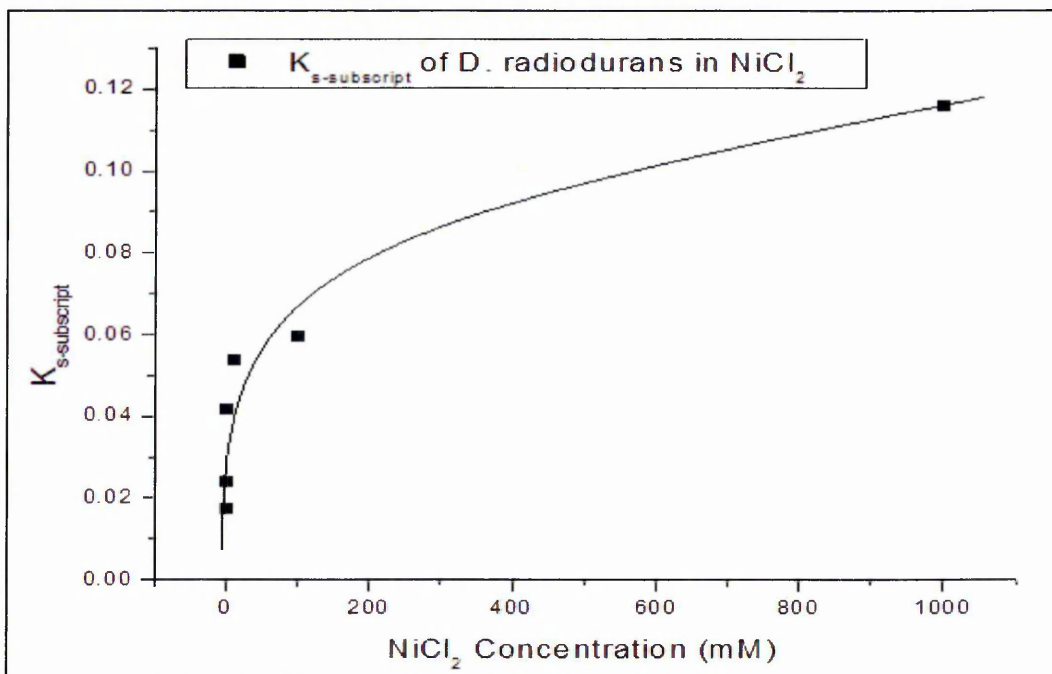


Figure 10.79. Relative changes curve for ratio of surface resistance of *D. radiodurans* bacteria in  $NiCl_2$  to surface resistance of  $NiCl_2$  with OXOID broth over surface resistance of *D. radiodurans* at 0M  $NiCl_2$  after 72 hours

Comparison between the relative changes in the surface resistance after being normalised or subtracted for equivalent circuit are very useful way to estimate the salt concentration on studied samples; these are shown in Figures 10.81 and 10.82.

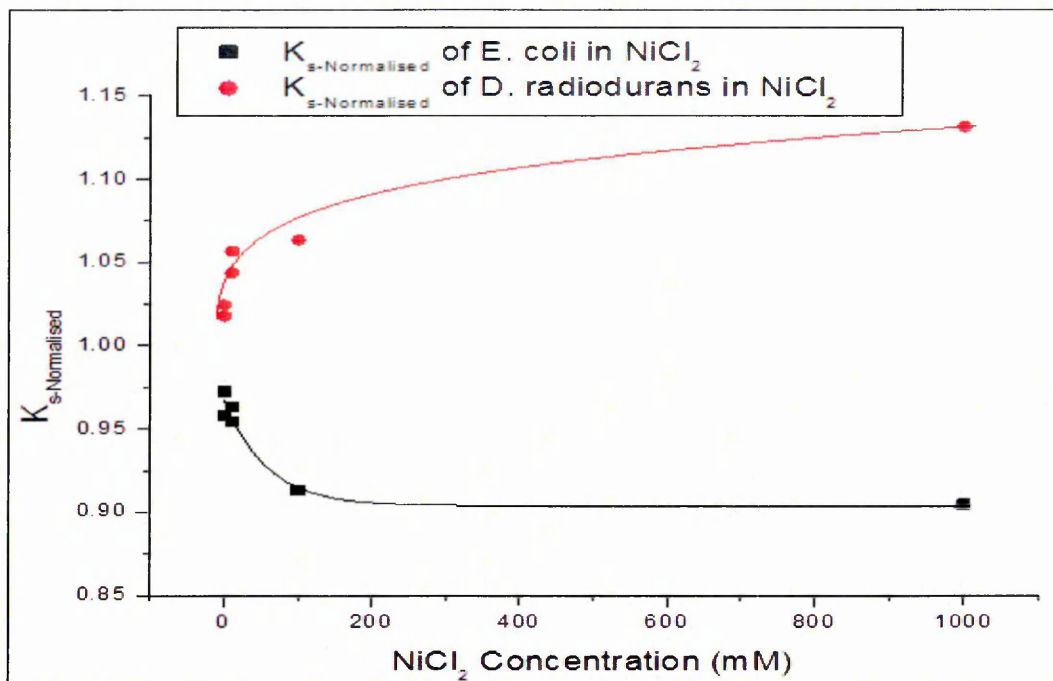


Figure 10.80. Comparison curves of normalised surface resistance ( $K_s$ ) for *E. coli* (black) and *D. radiodurans* (blue) in  $NiCl_2$  after 72 hours

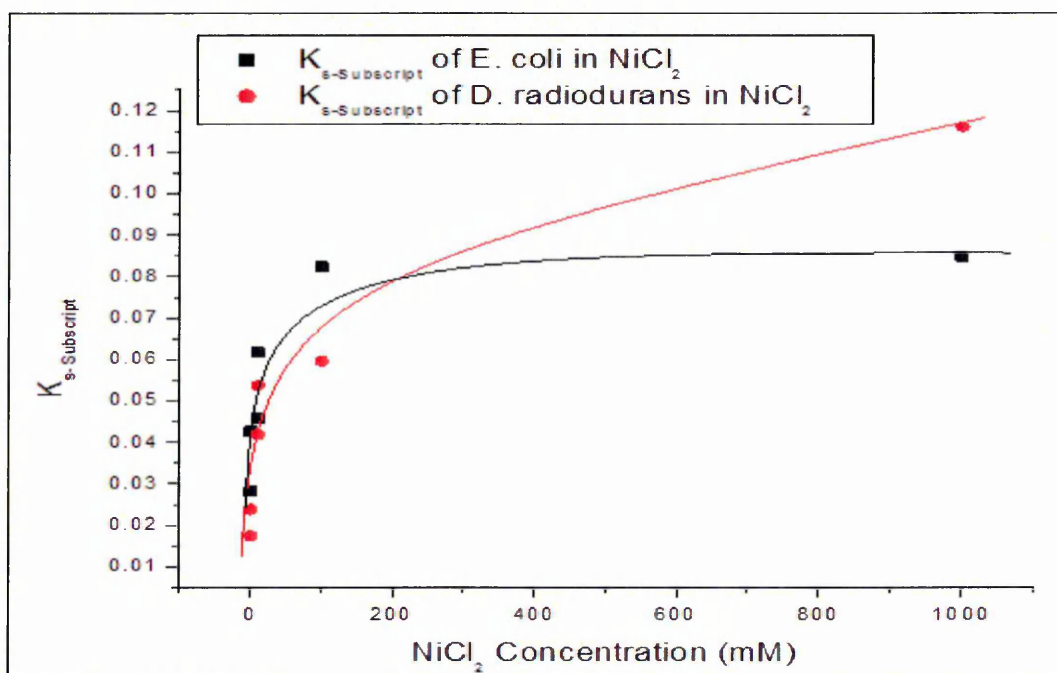


Figure 10.81. Comparison curves of relative changes for surface resistance ( $K_{s-sub}$ ) for *E. coli* (black) and *D. radiodurans* (blue) in  $NiCl_2$  after 72 hours

Double layer capacitance was created on the working electrode; this capacitance depends on the concentration of bacteria in the bio-cell sensor. Equation 6.4 has been used to calculate the equivalent capacitance can thus: At high frequency ( $\omega \sim \infty$ ), from

equation 10.4, the equivalent capacitance at low frequency includes the effect of surface resistance and double layer capacitance on the working electrode. The capacitance at high frequency is calculated and presented in figures 10.82 and 10.83.

$$C_s = C_p$$

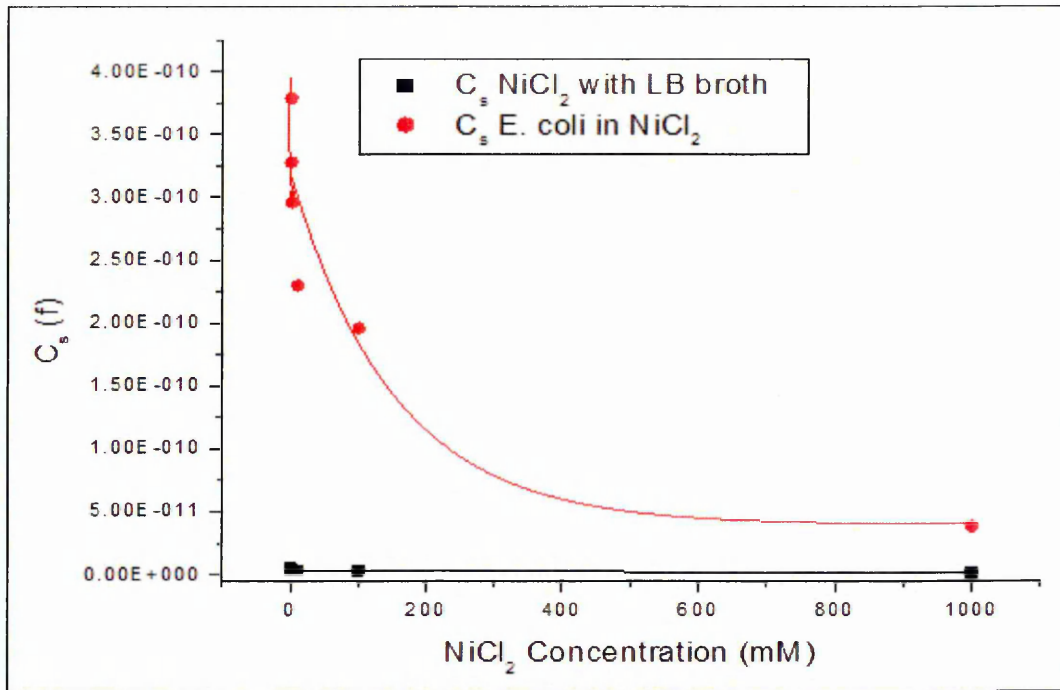


Figure 10.82. Changes in surface capacitance ( $C_s$ ) of *E. coli* bacteria samples after being added  $\text{NiCl}_2$  and for  $\text{NiCl}_2$  with LB broth after 72 hours exposure

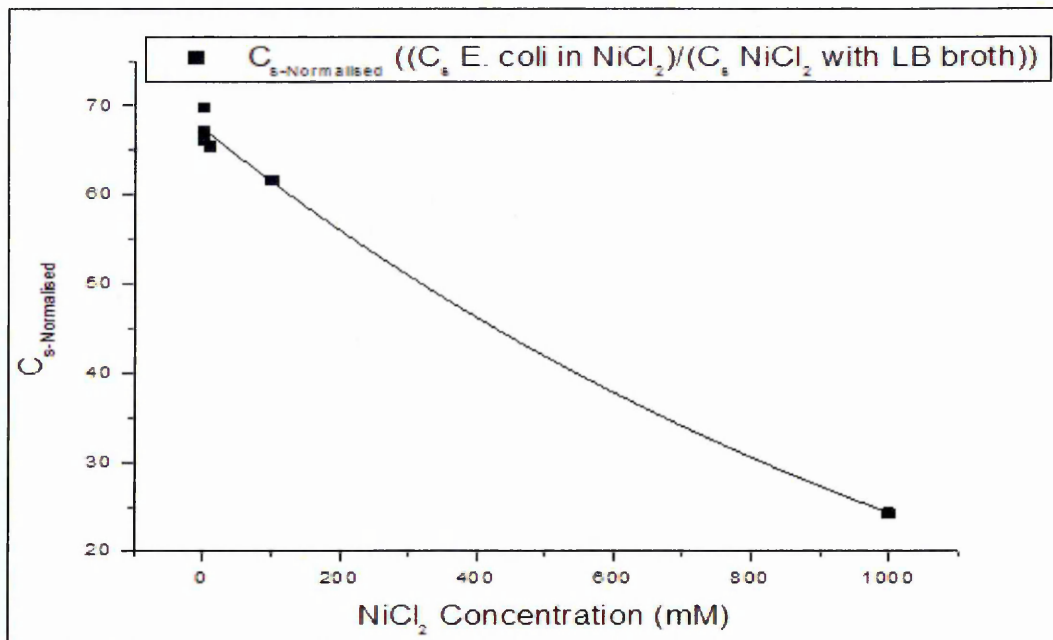


Figure 10.83. Normalised curve for ratio of surface capacitance of *E. coli* bacteria in  $\text{NiCl}_2$  to surface capacitance of  $\text{NiCl}_2$  with LB broth after 72 hours

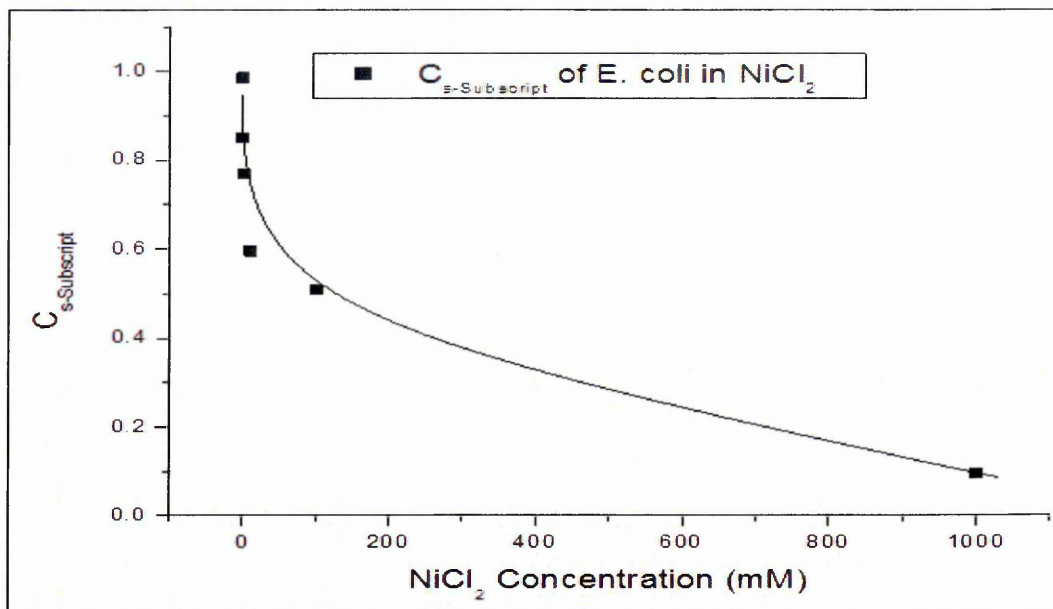


Figure 10.84. Relative changes curve for ratio of surface capacitance of *E. coli* bacteria in  $\text{NiCl}_2$  to surface capacitance of  $\text{NiCl}_2$  with LB broth over surface capacitance of *E. coli* at 0M  $\text{NiCl}_2$  after 72 hours

The equivalent double layers capacitance of *D. radiodurans* for different concentrations of  $\text{NiCl}_2$  has been calculated. Then the results were normalised and subtracted for samples unexposed to the salt, see figures 10.85 and 10.86. More details are presented in appendix D.

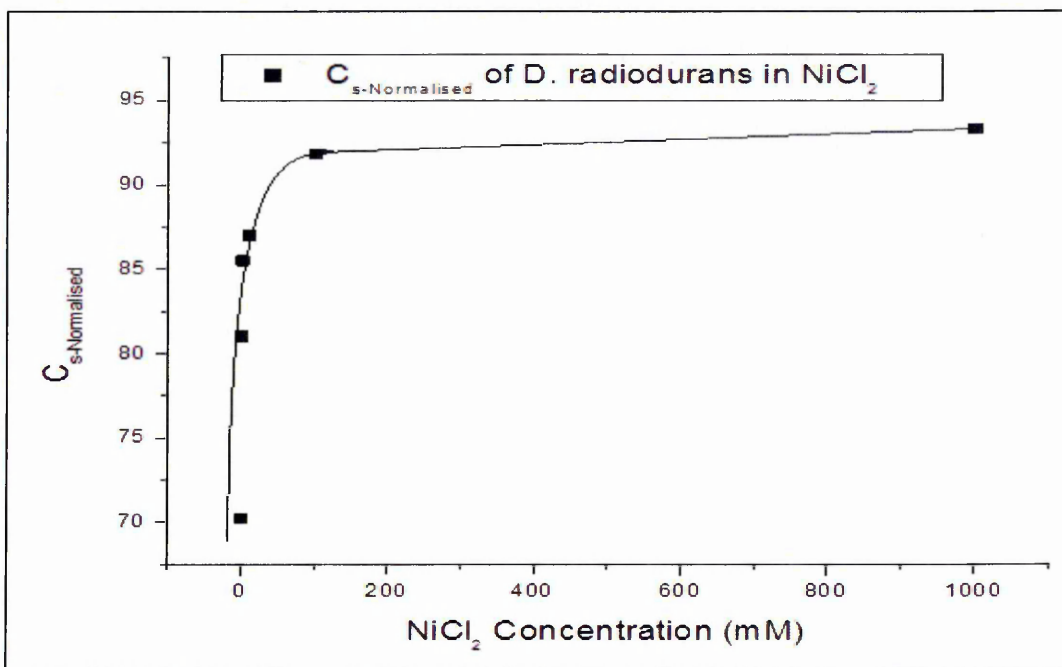


Figure 10.85. Normalised curve for ratio of surface capacitance of *D. radiodurans* bacteria in  $\text{NiCl}_2$  to surface capacitance of  $\text{NiCl}_2$  with OXOID broth after 72 hours

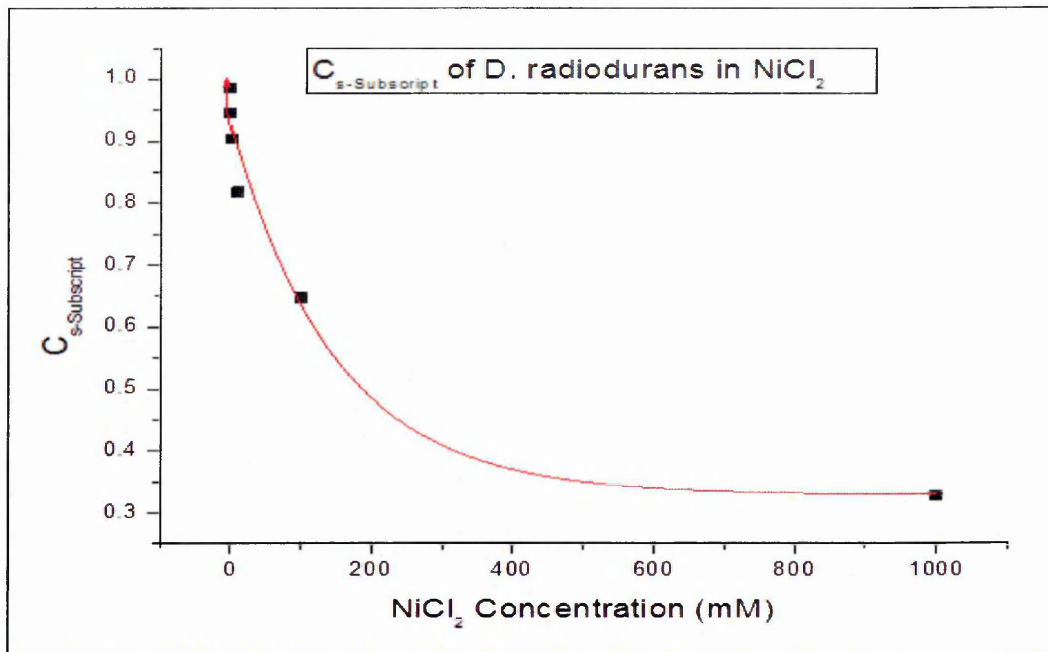


Figure 10.86. Relative changes curve for ratio of surface capacitance of *D. radiodurans* bacteria in NiCl<sub>2</sub> to surface capacitance of NiCl<sub>2</sub> with OXOID broth over surface capacitance of *D. radiodurans* at 0M NiCl<sub>2</sub> after 72 hours

Comparison between the relative changes in the equivalent surface resistance after NiCl<sub>2</sub> being added, using the normalisation and subtraction method to estimate the salt concentration in studied samples.

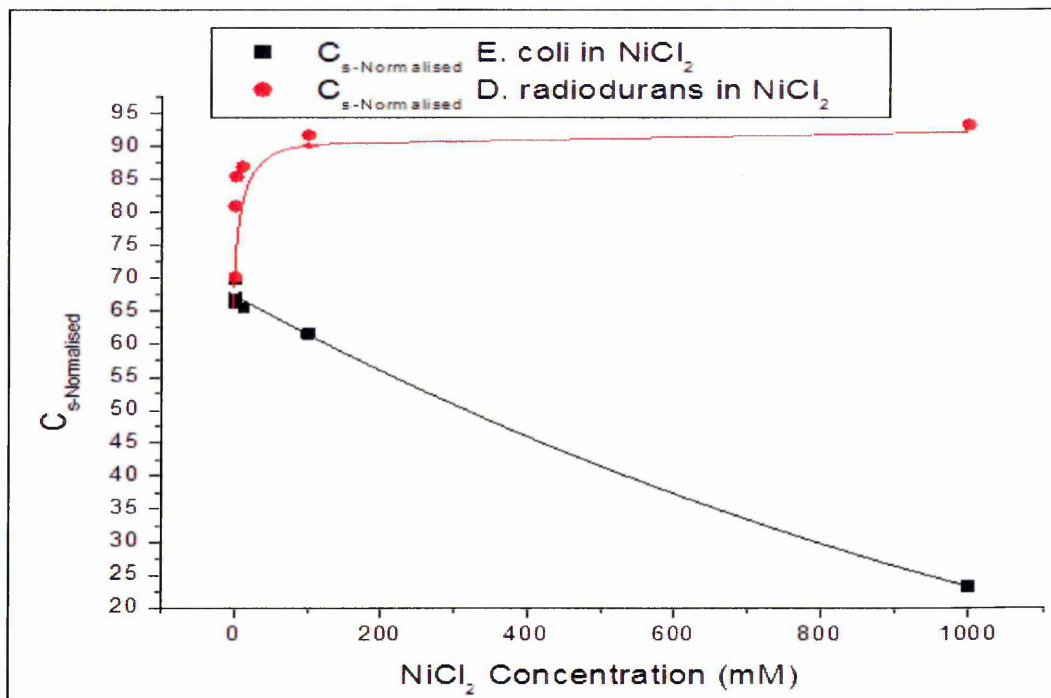


Figure 10.87. Comparison curves of normalised surface capacitance (C<sub>s-Normalised</sub>) for *E. coli* (blue) and *D. radiodurans* (black) in NiCl<sub>2</sub> after 72 hours

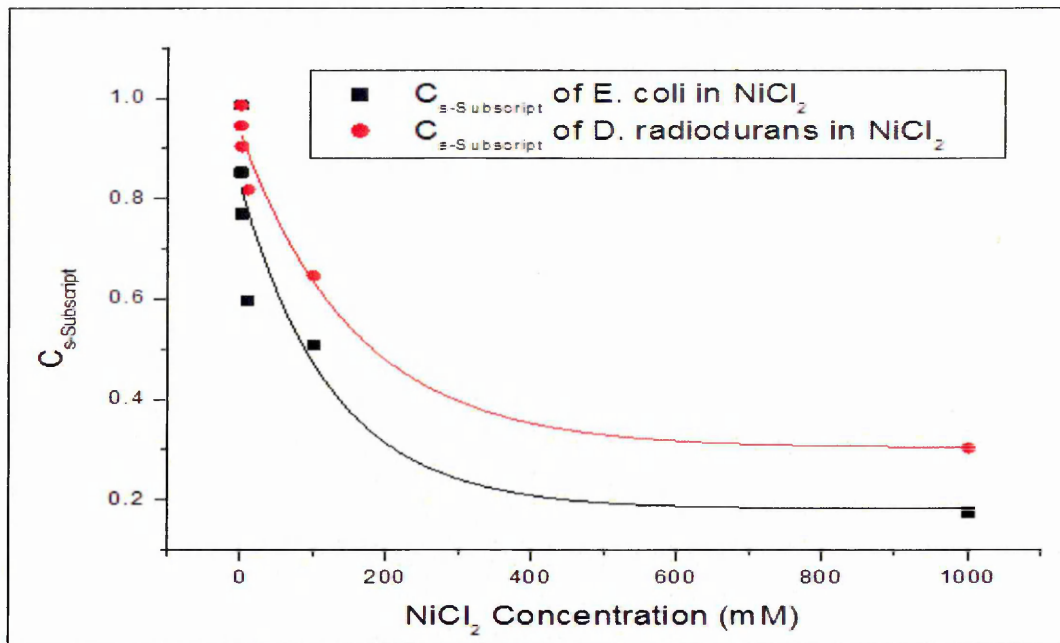


Figure 10.88. Comparison curves of relative changes in surface capacitance ( $C_{s-sub}$ ) for *E. coli* (red) and *D. radiodurans* (black) in  $NiCl_2$  after 72 hours

It is important and necessary to build or draw a calibration curve (standard curve) that includes the bacteria responses for  $CdCl_2$  and  $NiCl_2$ , in order to find or detect the heavy metals pollution and their concentrations. To meet this goal the normalisation and subtraction of obtained results of bacteria were plotted and reported in figures 10.89 and 10.90.

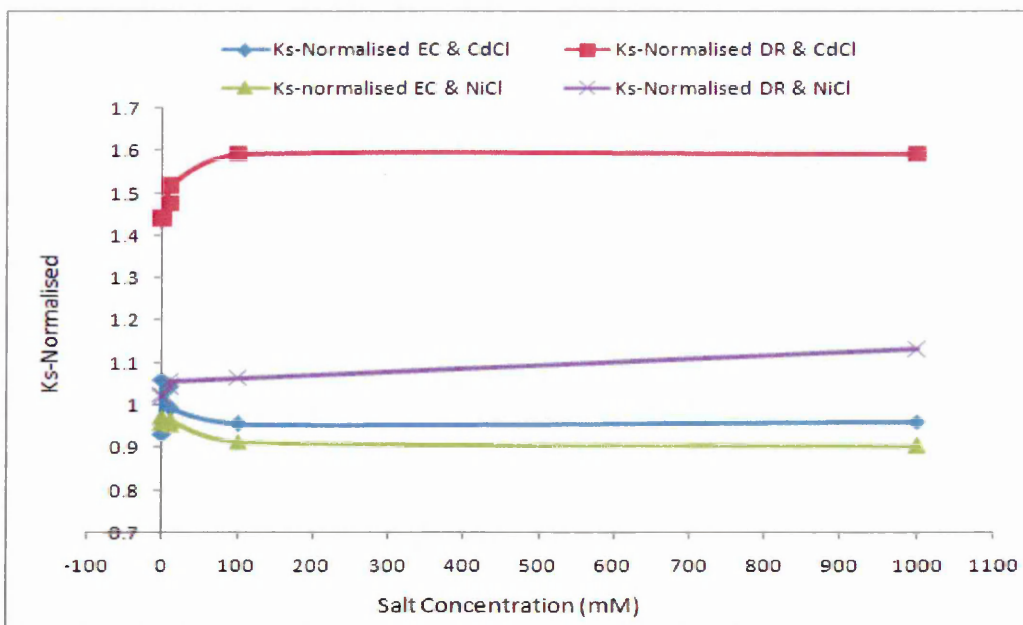


Figure 10.89. Comparison curves of normalised surface resistances ( $K_{s-Normalised}$ ) for *E. coli* and *D. radiodurans* bacteria in ( $NiCl_2$  &  $CdCl_2$ ) after 72 hours

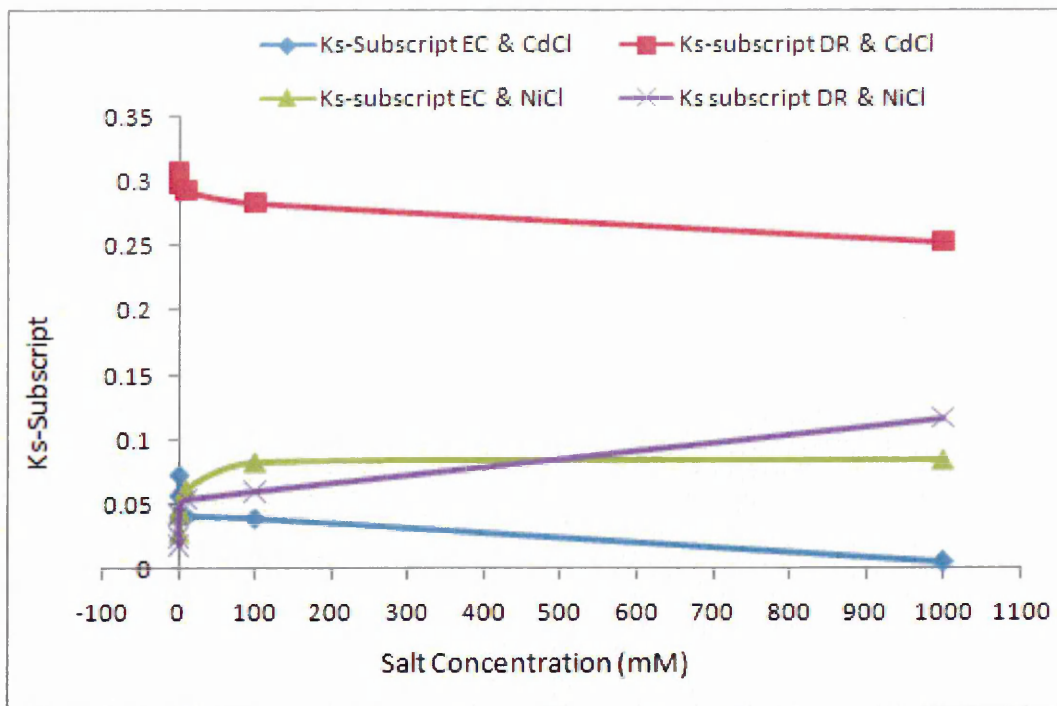


Figure 10.90. Comparison curves of relative changes surface resistances  $K_{s-Sub}$  for *E. coli* and *D. radiodurans* bacteria in ( $NiCl_2$  &  $CdCl_2$ ) after 72 hours

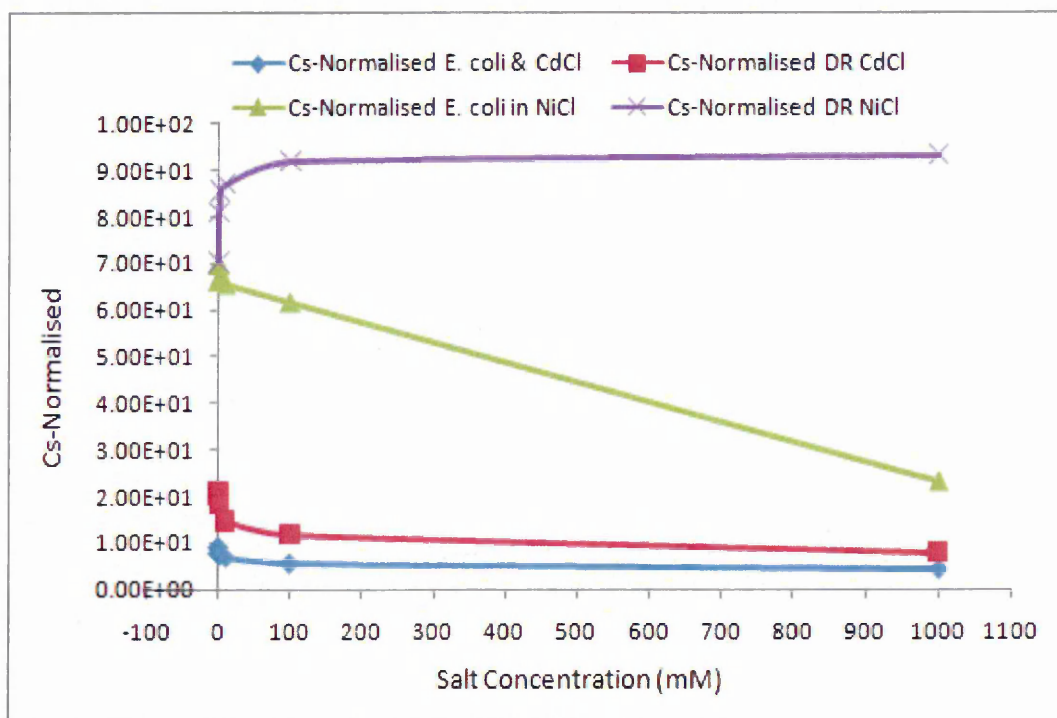


Figure 10.91. Comparison curves of normalised surface capacitance ( $F_s$ ) for *E. coli* and *D. radiodurans* bacteria in ( $NiCl_2$  &  $CdCl_2$ ) after 72 hours

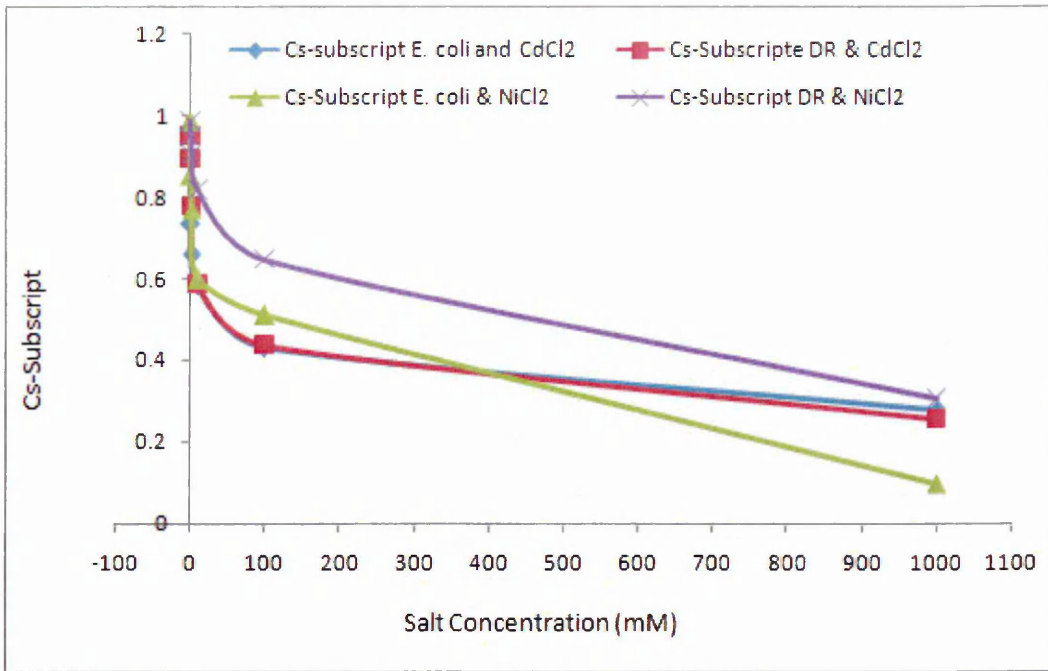


Figure 10.92. Comparison curves of relative changes in surface capacitance ( $F_s$ ) for *E. coli* and *D. radiodurans* bacteria in ( $NiCl_2$  &  $CdCl_2$ ) after 72 hours

The comparison of the inhibition effects of gamma radiation,  $CdCl_2$  and  $NiCl_2$  on bacteria was carried out using electrical measurements ( $I_c$  cathodic current and conductivity). It was clearly shown that there is a possibility of developing pattern recognition of the two inhibiting factors, e.g. gamma radiation and heavy metals.

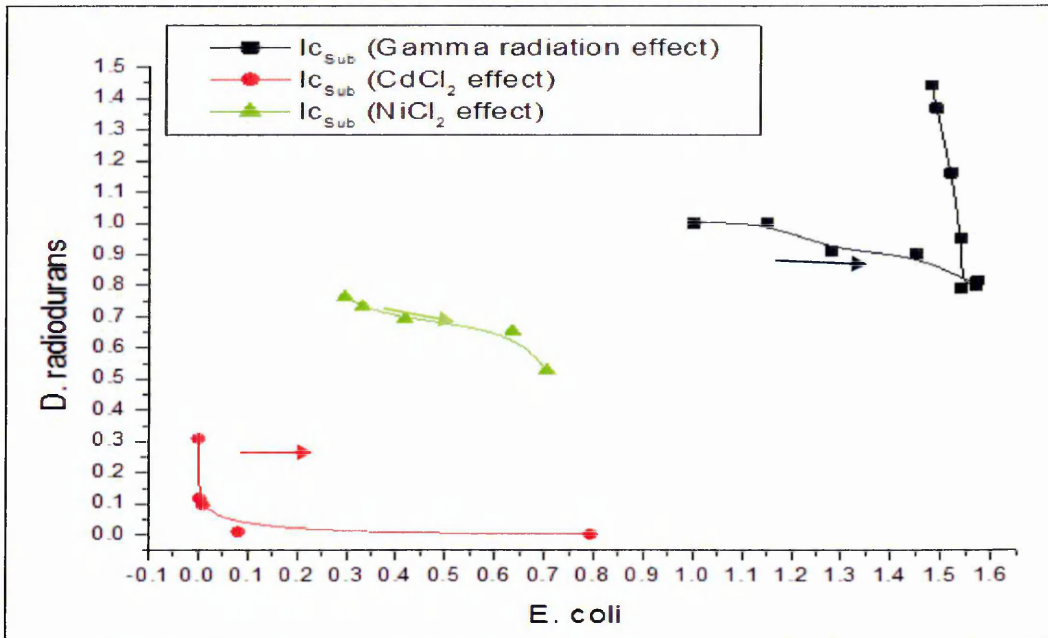


Figure 10.93. Comparisons of relative changes in  $I_{c-Subscript}$  for *E. coli* and *D. radiodurans* bacteria in response to exposure to gamma radiation,  $CdCl_2$  or  $NiCl_2$

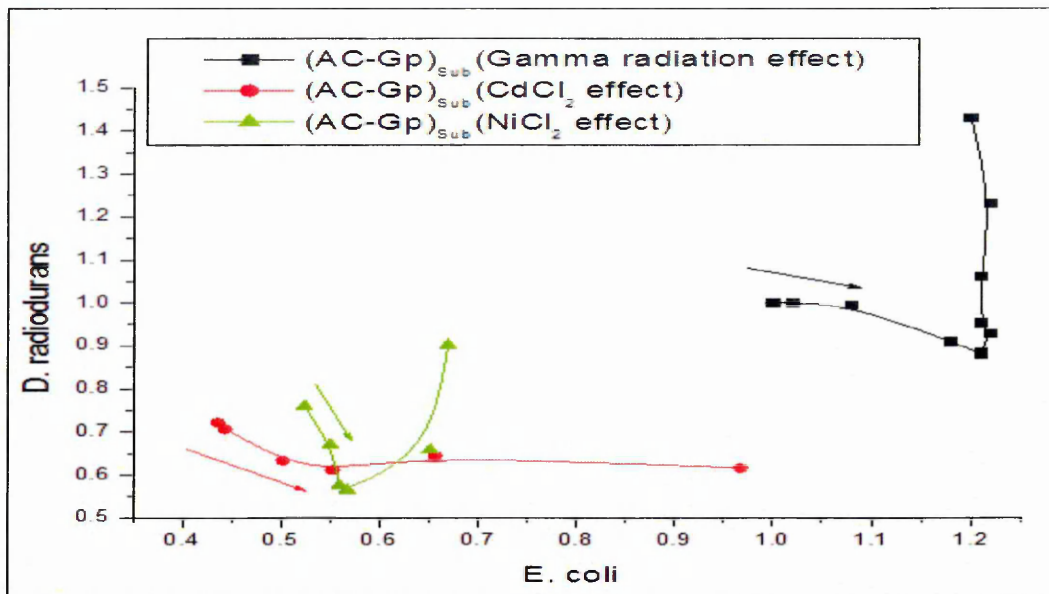


Figure 10.94. Comparisons of relative changes in  $(AC-Gp)_{Sub}$ , for *E. coli* and *D. radiodurans* bacteria in response to exposure to gamma radiation,  $CdCl_2$  or  $NiCl_2$

**Reference:**

1. Lide, David R. (1998), Handbook of Chemistry and Physics (87 ed.), Boca Raton, FL: CRC Press, pp. 4-67.
2. Mond L, Langer, C, Quincke F, (1890), Action of Carbon Monoxide on Nickel, Journal of the Chemical Society, Transactions 57: pp. 749-753.

## CHAPTER 11

### Conclusion and Future Work

#### 11.1. Thesis Conclusion

The optical and electrical characteristics of bacteria and the effect of environmental pollution on these is the subject of this thesis. This research concentrated on studying the effects of gamma radiation and heavy metal salts ( $\text{CdCl}_2$ ,  $\text{NiCl}_2$ ) on living bacteria. It was shown that many types of bacteria have the ability to survive at high levels of environmental contamination. The types of bacteria that can resist gamma radiation are in general classified as gram positive, a typical example of which is *D. Radiodurans*, known for having the highest resistance to ionization radiation. On the other hand, the highly sensitive types of bacteria, called gram-negative, such as *E. coli*, are sensitive to radiation. In this study  $\text{Co}^{57}$  an ionization-radiation source was used to study the effects of radiation doses on bacteria samples.

Characterisation of samples were carried out using a variety of experimental techniques, i.e. optical methods including optical density measurements, UV-vis spectrophotometer, fluorescent microscopy and spectroscopy for studying light scattering in bacteria samples, and electrical methods both DC and AC.

To study the effect of gamma radiation, fluorescence microscopy measurements were carried out on samples of *E. coli* and *D. radiodurans* bacteria stained with two organic dyes: green and red, associated respectively with living and dead bacteria. The results showed a significant difference in images of bacteria before and after exposure to the radiation. The numbers of live *E. coli* bacteria decreased exponentially with the increase in exposure time. On other hand, *D. radiodurans* (which is gram-positive bacteria) resisted the radiation at low doses, and the concentration of live bacteria increase slightly. However, they were damaged at high radiation doses (the bacteria concentration gradually decreased). The method of fluorescence was very illustrative, allowing direct observation of live and dead bacteria. However, this method did not provide correct bacteria counts because of the limited resolution of the analysis of microscopy images. An improved analysis was based on the calculation of total intensities of green and red fluorescence.

Optical density ( $\text{OD}_{600}$ ) techniques have been used to estimate the bacteria cell's density as a function of exposure time to radiation. In addition, the fluorescence spectroscopy

study revealed that a parasitic peak corresponding to a second order of diffraction was utilised. Both methods of  $OD_{600}$  and the 2<sup>nd</sup> order diffraction peak (at 630 nm for *E. coli* and at 700nm for *D. radiodurans* bacteria) in fluorescence spectra, which are both related to light scattering on live bacteria, have yielded similar values of the time characteristic constant of about 40 hours for *E. coli* bacteria. To our knowledge, the use of a 2<sup>nd</sup> order diffraction peak at a double excitation wavelength (usually regarded as parasitic peak) in fluorescence spectra for the analysis of bacteria count is reported for the first time.

The same three optical techniques, namely fluorescence microscopy, fluorescence spectroscopy, and optical density, were employed to study the effect of heavy metals on bacteria. Exposure time has no significant effect on L/D ratios, most likely because 1 hour (the minimum exposure time used) is sufficiently large to cause damage to bacteria. The results of the other two optical methods (Fluorescence Spectroscopy and Optical Density  $OD_{600}$ ) appeared to be completely different and did not correlate with the L/D bacteria ratio, which are due to the effect of ( $Cd^{2+}$ ,  $Ni^{2+}$ ) ions on light scattering. The effect of  $CdCl_2$  and  $NiCl_2$  salt appeared to be quite similar on both *E. coli* and *D. radiodurans* bacteria. Fluorescence microscopy seems to give the most reliable count of live bacteria concentrations. Therefore, the comparison of the inhibition effects of gamma radiation and heavy metals on *E. coli* and *D. radiodurans* bacteria was carried out using true L/D ratio data of fluorescence microscopy. It showed clearly the possibility of pattern recognition of the two inhibition factors, e.g. gamma radiation and salt.

A simpler way of detecting pollutants was developed using the electrical properties of bacteria. The effect of radiation and the heavy metal salts' ( $NiCl_2$  and  $CdCl_2$ ) on electrical characteristics of microorganisms was studied.

The obtained data for DC and AC electrical study of two types of bacteria *E. coli* and *D. radiodurans* correlated, as did both with the data of the optical study. The measurements of DC current, as well as  $G_p$ , and  $C_p$  spectra, were used for quantification of live bacteria concentrations, and thus the effect of  $\gamma$ -radiation and metals ions on bacteria.

The DC I-V characteristics of the bacteria showed the exponential behaviour of the current at the cathode for *E. coli* after being exposed to gamma radiation, which was similar to the optical result. On the other hand, the DC I-V characteristics of *D. radiodurans* showed polynomial behaviour of the cathode current when the samples

were exposed to gamma radiation. In addition, the AC characteristics, that included conductance and capacitance, were depicted as a function of radiation exposure time. The AC capacitance increases when the bacteria concentration increases; in contrast AC conductance decreases. The capacitance and conductance were scanned for a wide range of frequencies; the big difference in the results of the two types of bacteria was very clearly related to the electrical properties change, which is related to the change in bacteria density or their concentration. The results at high frequency were very interesting, which encouraged us to utilise it to evaluate radiation levels.

The electrical technique was used to study the effect of heavy metals ( $\text{CaCl}_2$  and  $\text{CaCl}_2$ ) on bacteria. The effect of metal salt appeared to be comparable on both *E. coli* and *D. radiodurans* bacteria. AC and DC properties of electrochemical solutions that contained *E. coli* and *D. radiodurans* bacteria were studied, and the results were compared to and normalised to the results of samples not mixed with metals. Comparative Figures can be used to estimate metal concentration and the effect of metal on bacteria.

Moreover, the difference in the responses of *E. coli* and *D. radiodurans* bacteria to  $\gamma$ -radiation and heavy metal ions allows the application of the principle of pattern recognition for identification and quantification of pollutants. This work has proved the concept of a simple and cost effective electrical bacteria-based sensor and sensor array for preliminary assessment of the presence of toxins in water. This part of work has been achieved, through calculation and plotting of the pattern recognition of (L/D) ratio for *E. coli* and *D. radiodurans* bacteria. Furthermore the cathodic current ( $I_{c\text{-Sub}}$ ) and AC conductance ( $(AC\text{-}Gp)_{\text{Sub}}$ ) were evaluated for gamma radiation effect,  $\text{CdCl}_2$  effect and  $\text{NiCl}_2$  effect.

Meanwhile, the electrical equivalent circuit of the bacteria cell sensor was estimated. The simplest idea for this circuit consists of surface resistance in parallel with surface capacitance, both in series with block resistance. The capacitance and conductance of equivalent circuits were calculated at low frequency ( $\omega \sim 0$ ) and at high frequency ( $\omega \sim \infty$ ). For some tests, the theoretical results showed a clear identification with practical results. This identification in results confirms the validity of results obtained, whether practical or theoretical.

## 11.2. Suggestion for Future Work

This project was focused on the fundamental research of environmental pollution detection using microorganism (bacteria). Understanding the effect of the environmental pollution on microorganisms (bacteria) is very important step to towards the development of bio-cell sensor utilizing bacteria. In order to achieve these goals, further measurements need to be one and more techniques must be used.

1. In order to identify the effective radiation dose and the working domain of each type of bacteria responsible for radiation detection. The effect of gamma radiation on bacteria cell membrane and cellular components must be studied further using and another technique for example confocal microscopy.
2. To improve pattern recognition, another (third) type of bacteria must be used, to work at the intermediate level of radiation dose (between the *E. coli* and *D. radiodurans* working region).
3. More detailed study of light scattering on bacteria treated with metals must be done to understand the interaction between bacteria and metals.
4. A more stable and longer half-life radiation source is to be used, in order to estimate the radiation dose that depends on the amount of change in the optical and electrical properties for bacteria in a bio-cell sensor.
5. Other techniques, such as Chromatography or Inductively coupled Plasma Mass Spectrometry (ICP-MS), can be used in order to study the ability of bacteria to reduce the concentration of heavy metals in study samples.
6. Remediation of environmental contamination has become a very interesting subject, which needs to develop its methods further.

## APPENDIX A

Figures A1 and A2 showed the *E. coli* bacteria samples after exposed to gamma radiation for different time exposure.

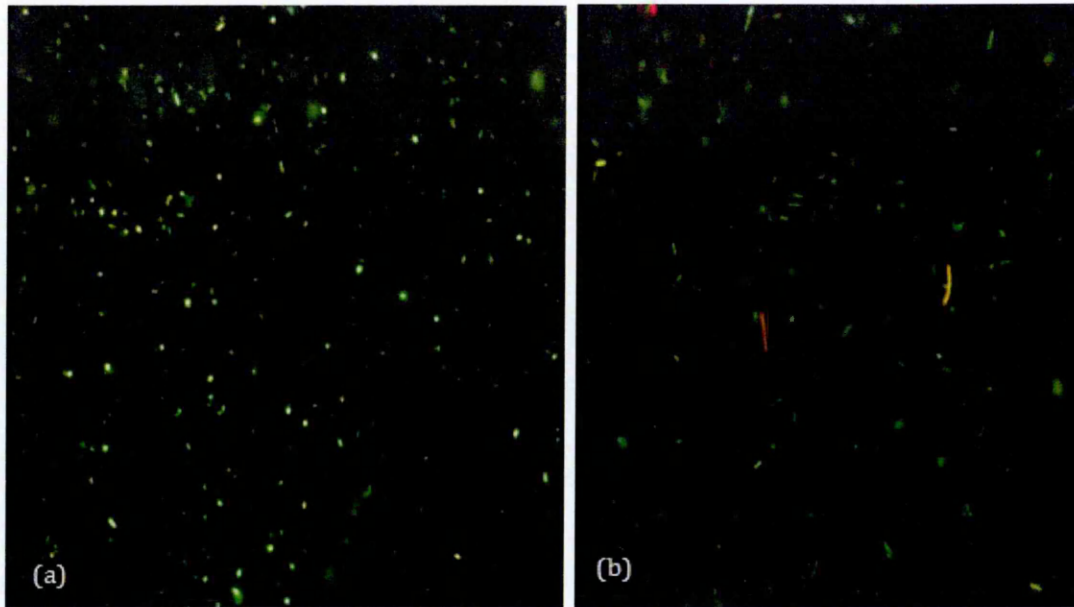


Figure A1. Fluorescence microscopy images of *E. coli* bacteria samples before (a) and after (b) 2 hours exposure to gamma-radiation

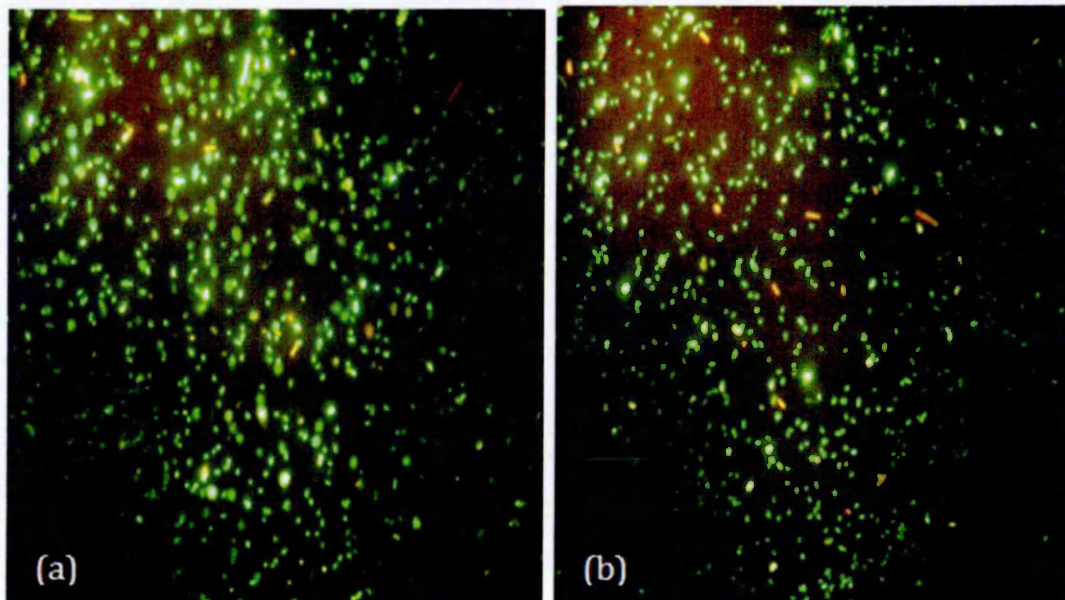


Figure A2. Fluorescence microscopy images of *E. coli* bacteria samples (a) before, and (b) after 48 hours exposure to gamma-radiation

The difference between images taken (a) before and (b) after exposure to radiation of *D. radiodurans* bacteria is clear for 360 hours of exposure (see Figure A3).

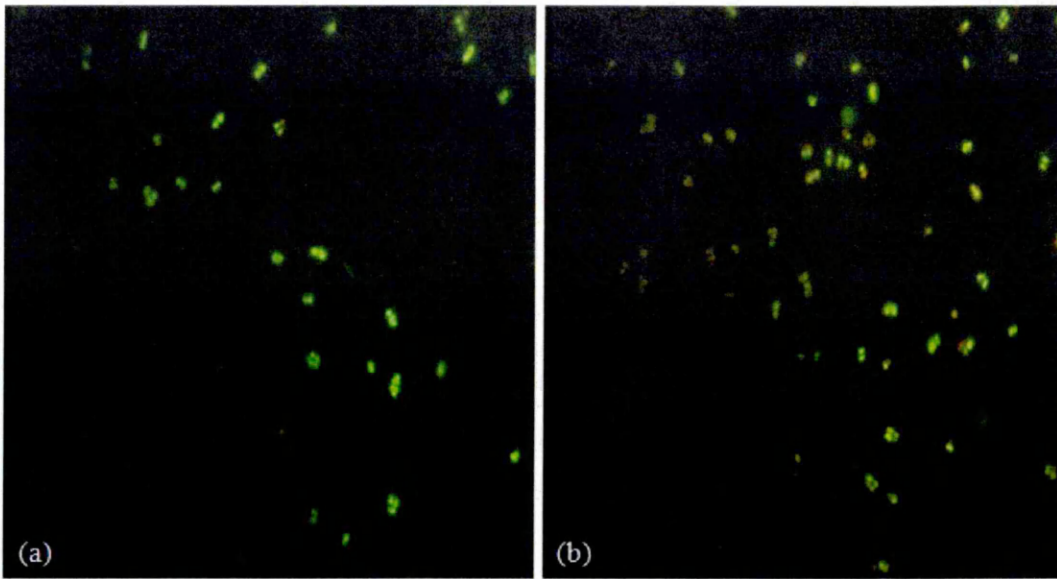


Figure A3. Fluorescence microscopy image for *D. Radiodurans* bacteria samples, (a) before, and (b) after 360 hours exposure to gamma radiation

Detailed analysis of the below dependence in Figure A4, shows a polynomial regression for data of (live/dead) cell ratios against the exposure time for normal environmental conditions.

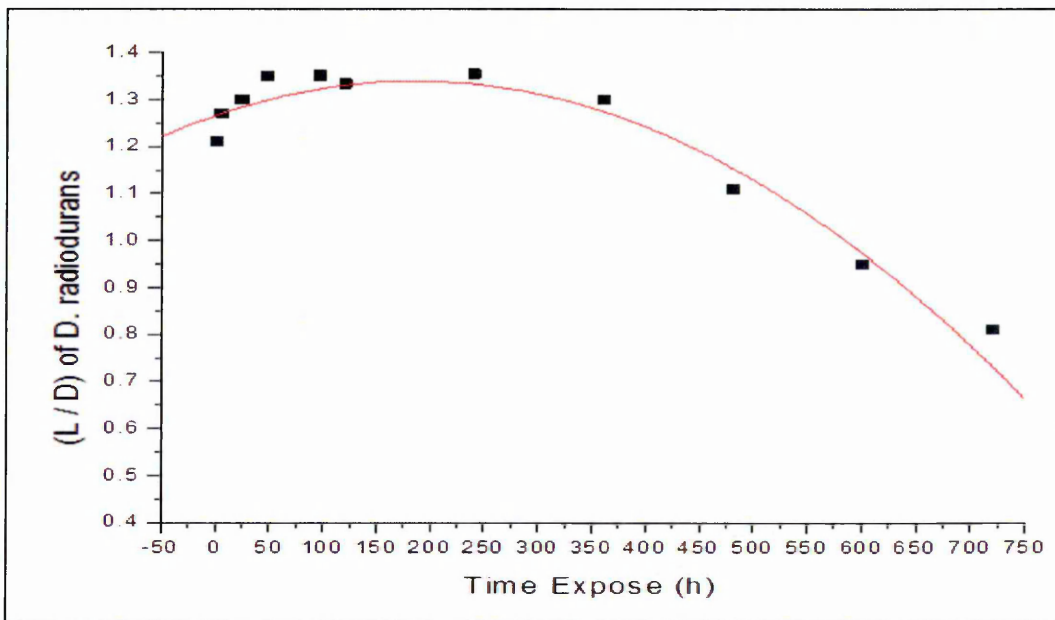


Figure A4. Relation between (live/dead) *D. radiodurans* bacteria ratio and exposure time to Gamma radiation (fluorescence microscopy results), the fitting curve showing as a solid line

On the other hand, the samples that were kept outside the irradiator system (non-irradiated) were checked with fluorescence microscopy in order to estimate the ratio

between live and dead bacteria; the results are presented in Table 7.3. The ratio was plotted as a function of time (normal environment) in Figure A5.

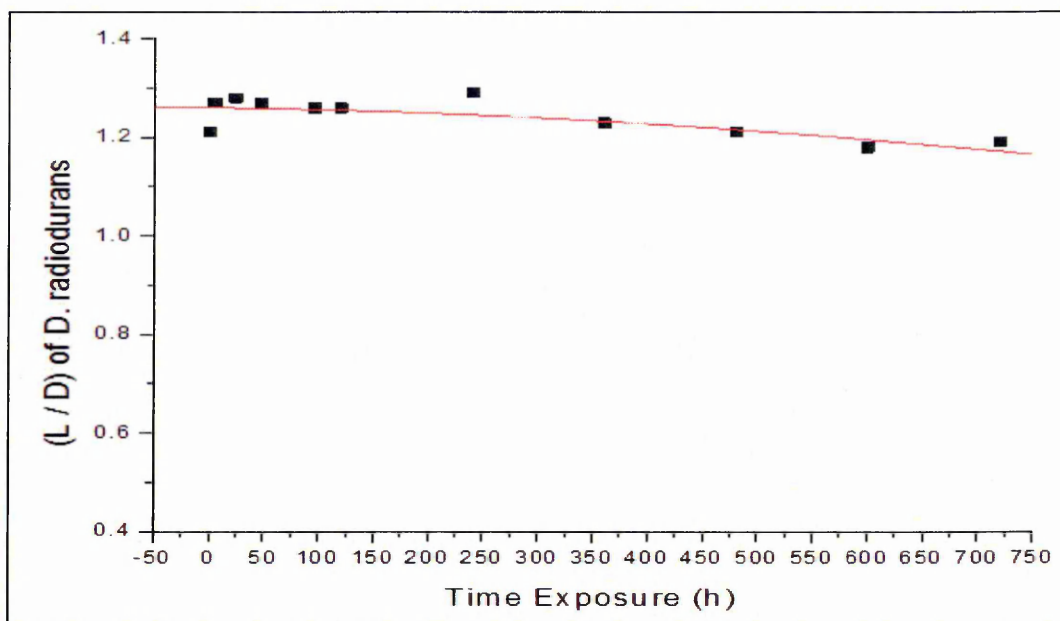


Figure A5. Relation between ratios (live/dead) of *D. radiodurans* bacteria not exposed to Gamma Ray and time (fluorescence microscopy results), the fitting curve showing as a solid line

The fluorescence spectrum of *D. radiodurans* bacteria samples results are shown in Figure A6 and A7.

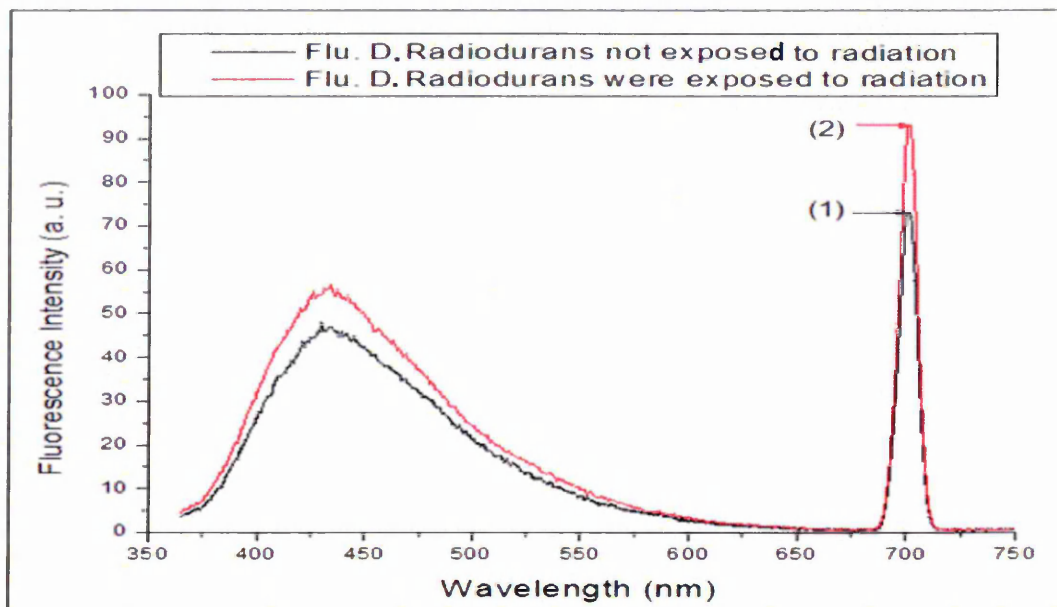


Figure A6. Fluorescence spectra (light scatter) of two *D. radiodurans* bacteria samples: (1) not exposed to radiation (black graph), and (2) exposed to gamma radiation for 120h (240000 mSv) (red graph)

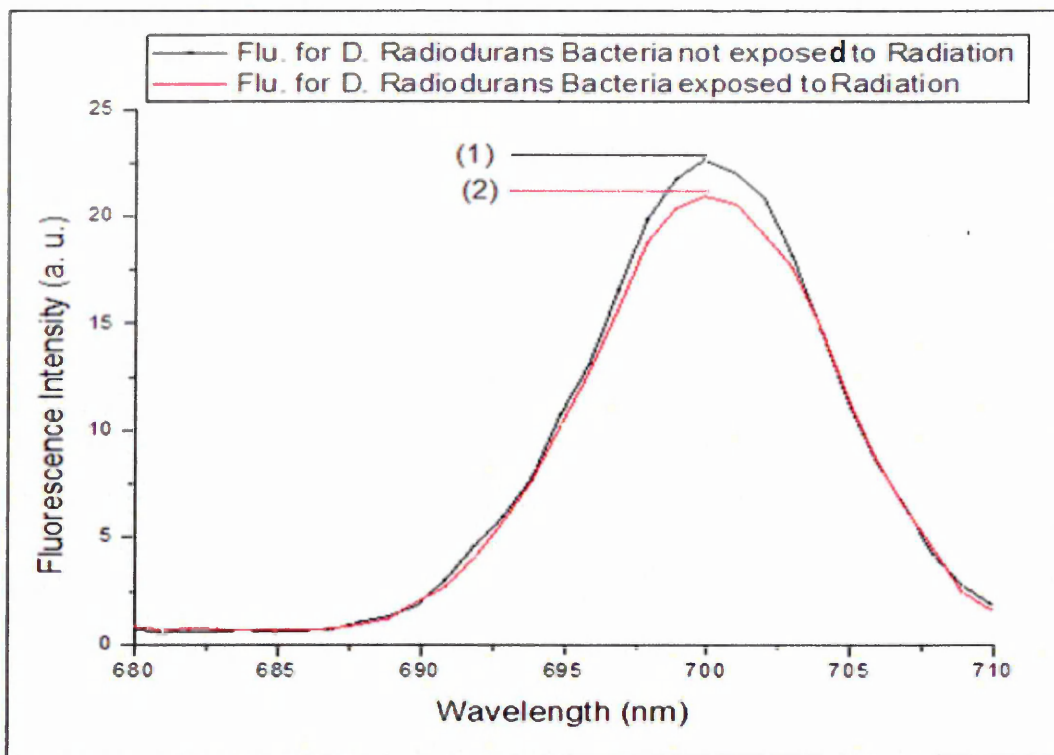


Figure 7. Fluorescence spectra (light scatter) of two *D. radiodurans* bacteria samples: (1) not exposed to radiation (black graph), and (2) exposed to gamma radiation for 600h 1200000 mSv, (red graph)

## APPENDIX B

In order to study the effects of the environment on the *D. radiodurans* samples, the samples not exposed were tested electrically, the results of which are presented in Figure B1.

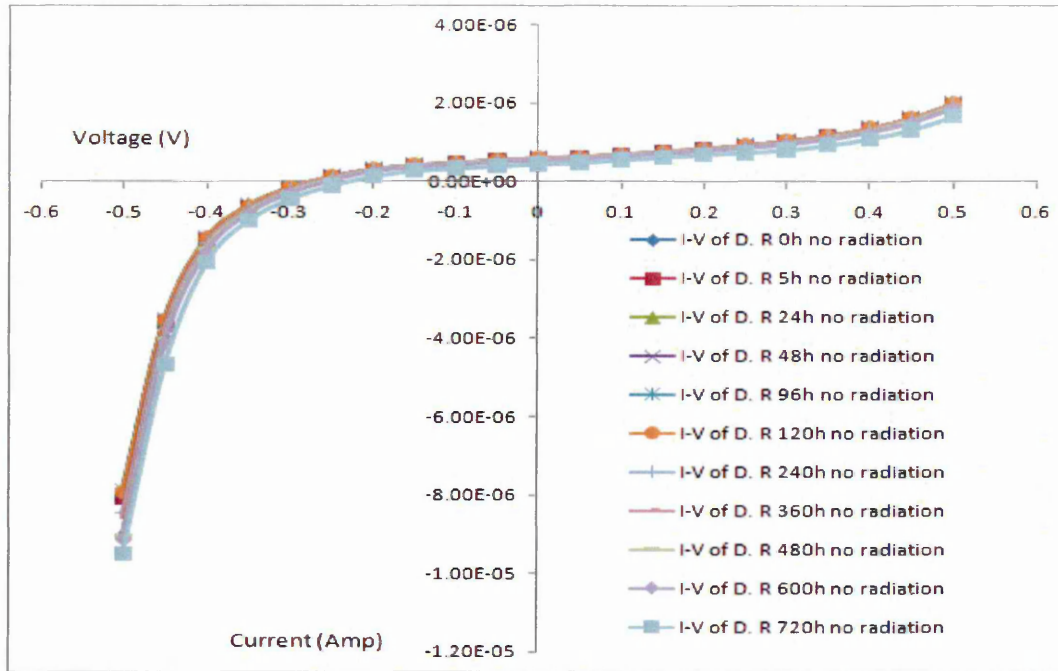


Figure B1. I-V characteristics of *D. radiodurans* samples not exposed to gamma radiation

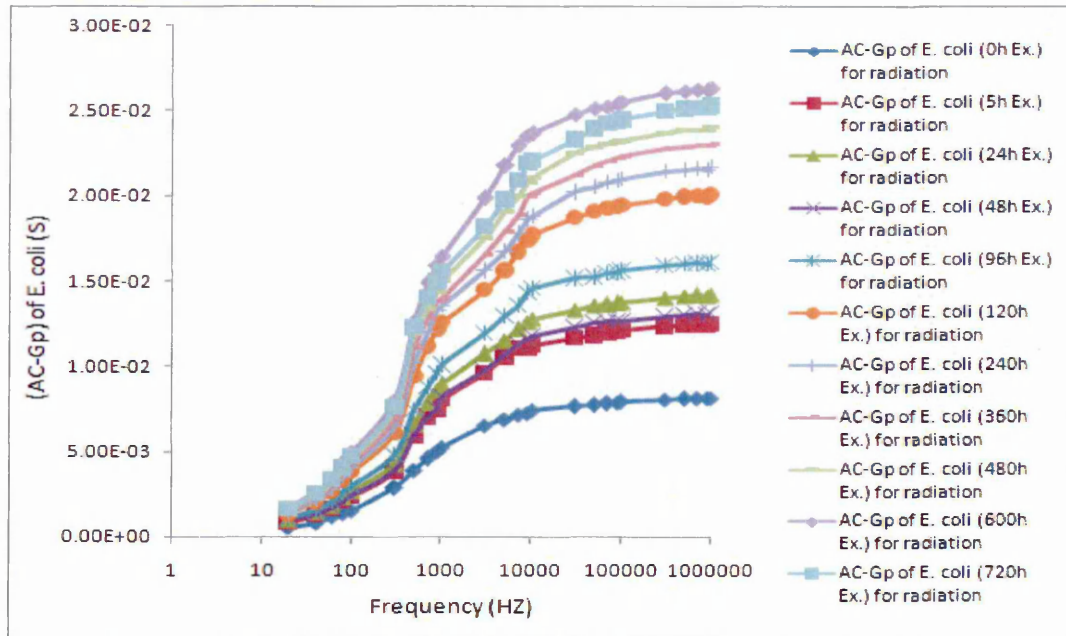


Figure B2. Conductance  $G_p$  of *E. coli* samples for different time exposure to gamma radiation

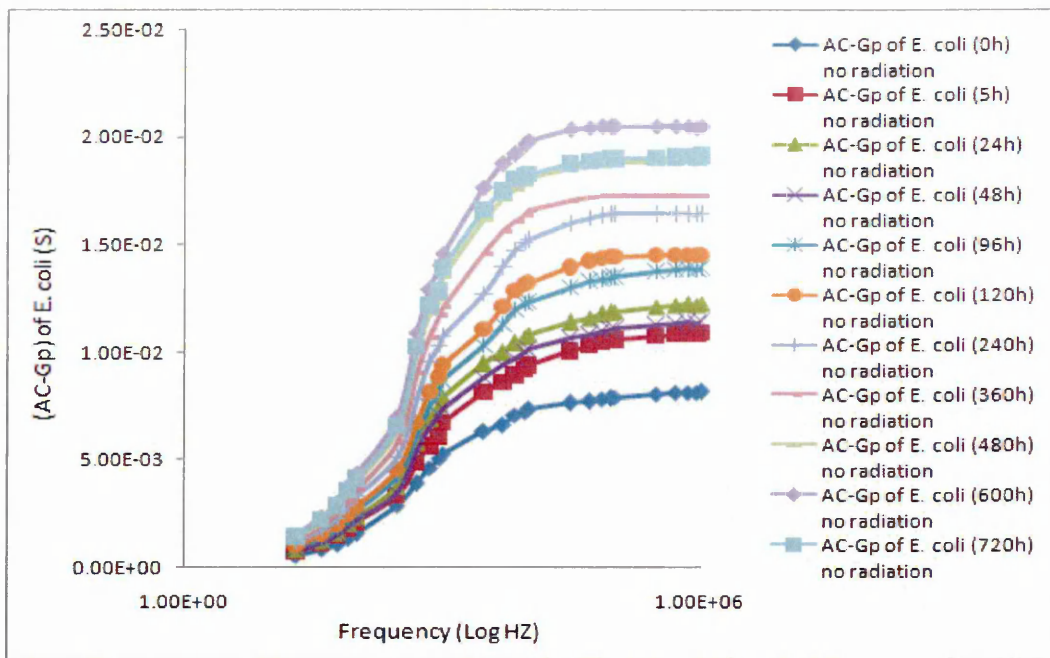


Figure B3. Conductance  $G_p$  of *E. coli* samples not exposed to gamma radiation for different time periods outside irradiator system

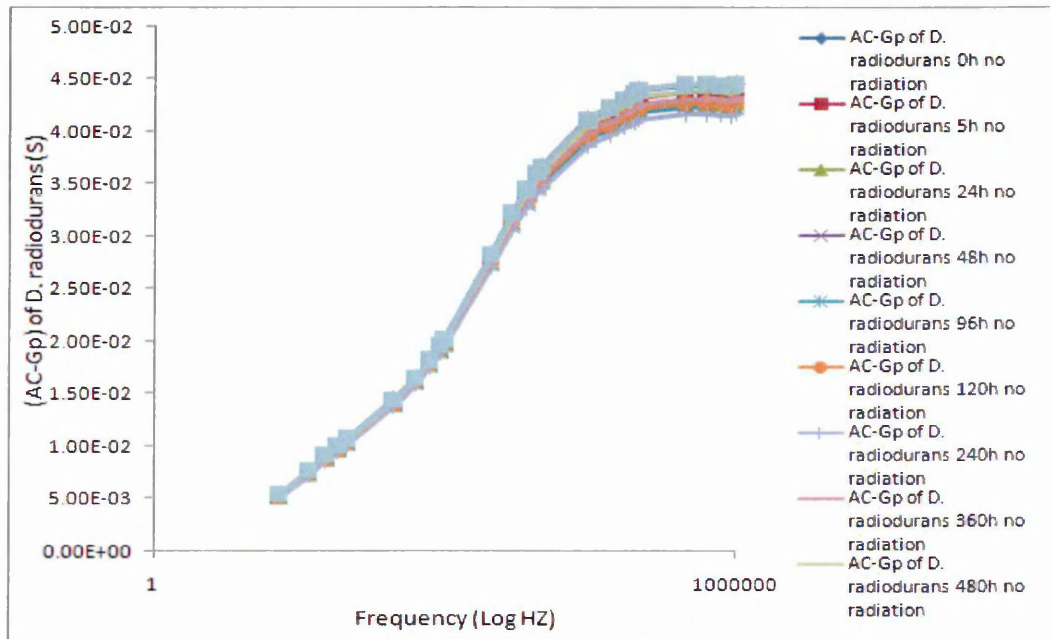


Figure B4. AC conductance of *D. radiodurans* samples not exposed to gamma radiation for different periods of time, kept outside irradiator system

When zoomed at high frequency, the capacitances of *D. radiodurans* bacteria showed clear sequences were dependent on bacteria concentration, as shown in Figure B5.

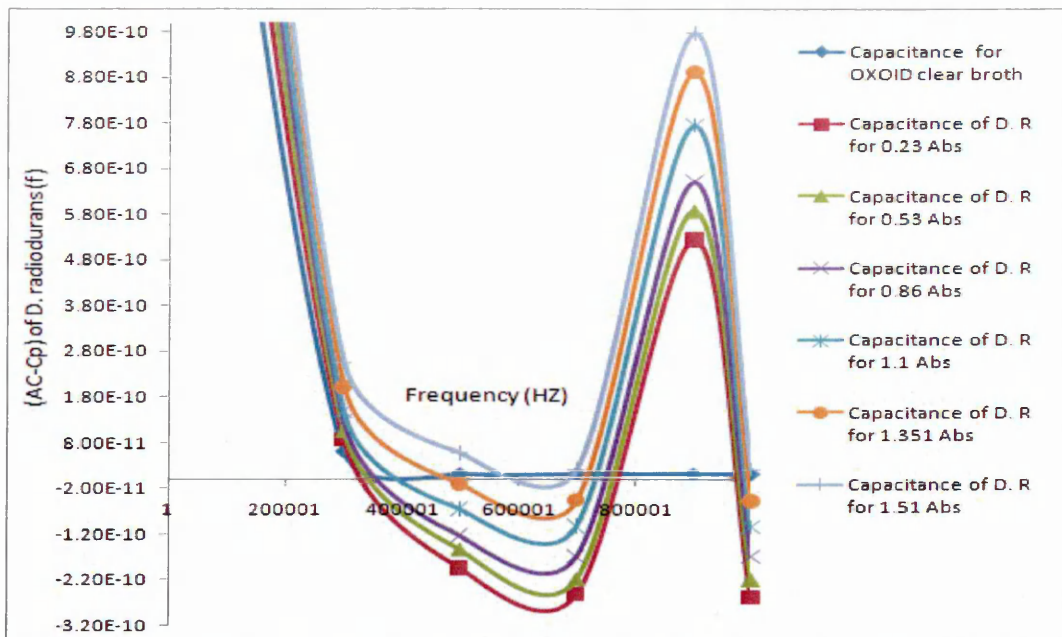


Figure B5. Typical AC-Cp characteristics of *D. radiodurans* samples of different concentrations measured in Abs units of optical density ( $OD_{600}$ ), at high frequency 900kHz

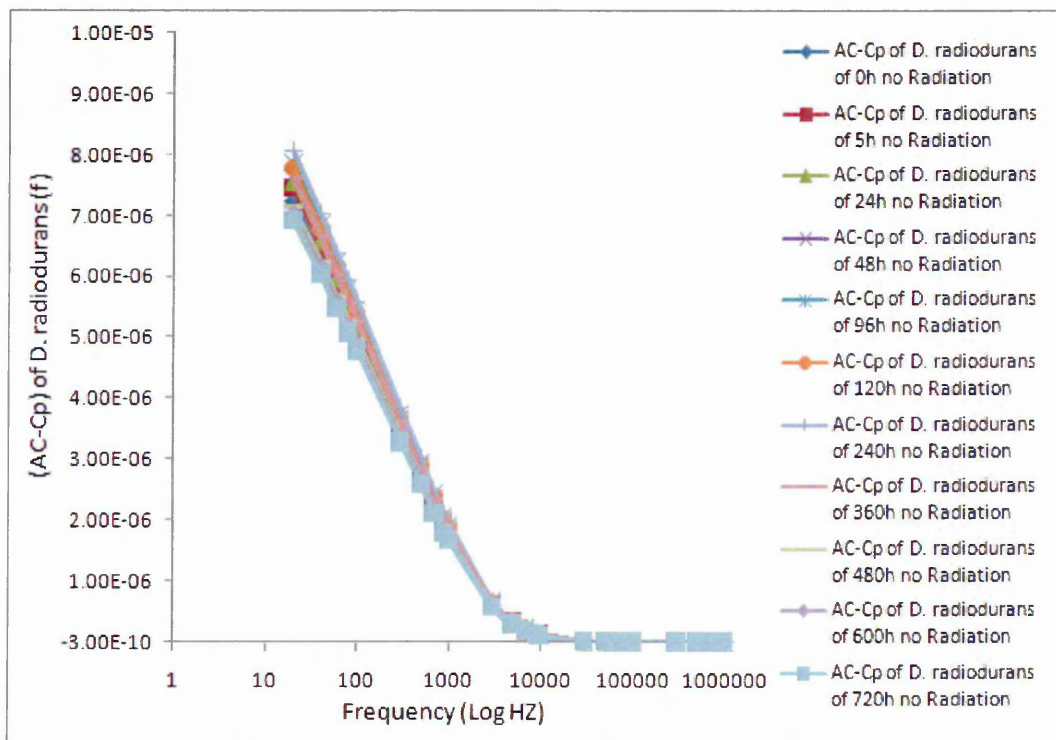


Figure B6. AC capacitance of *D. radiodurans* samples not exposed to gamma radiation in different periods, where samples were placed outside the irradiator system

## APPENDIX C

Fluorescence microscope results (images) were analysed and the ratio (L/D) was calculated then presented in figure C1 and C2.

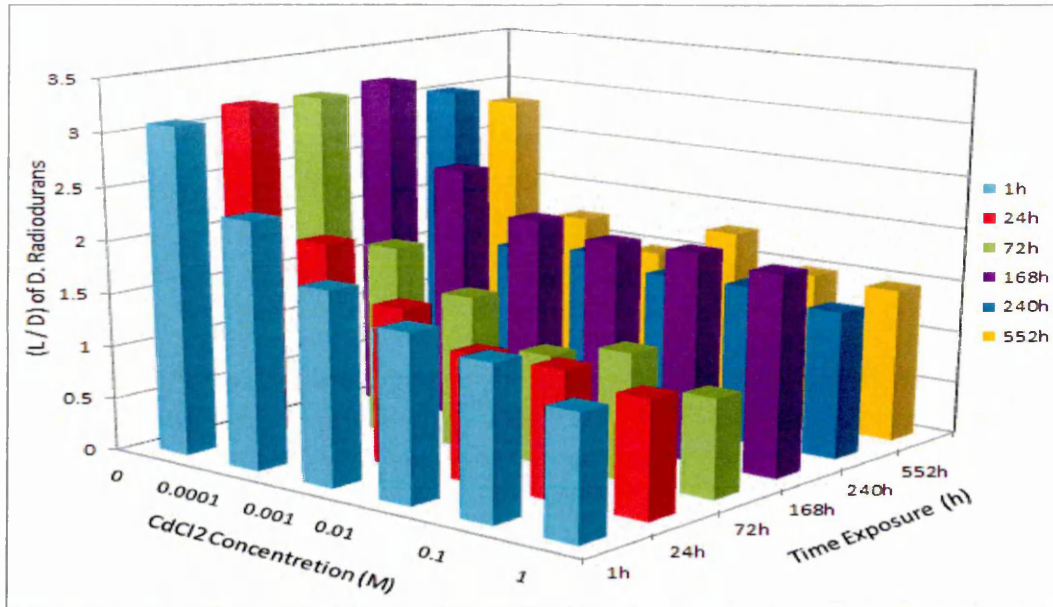


Figure C1. Effect of different concentrations of CdCl<sub>2</sub> on L/D ratio of D. radiodurans for different incubation times

D. radiodurans response are clearly shown in Figure C2, and the correlation between (L/D) and CdCl<sub>2</sub> concentrations are plotted as well.

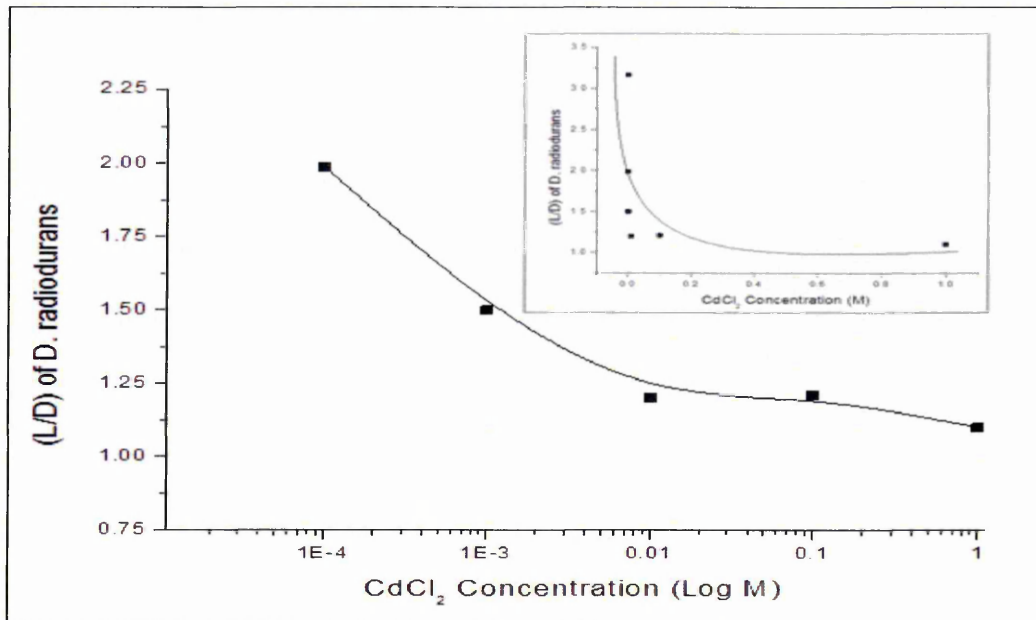


Figure C2. Ratio (L/D)<sub>m</sub> of D. radiodurans after adding salt for 72 hours exposure, inset the (L/D) ratio of D. radiodurans with salts at normal scale

The rest results of fluorescence spectroscopy technique for *D. radiodurans* bacteria were presented in appendix c, Figures C3, C4.

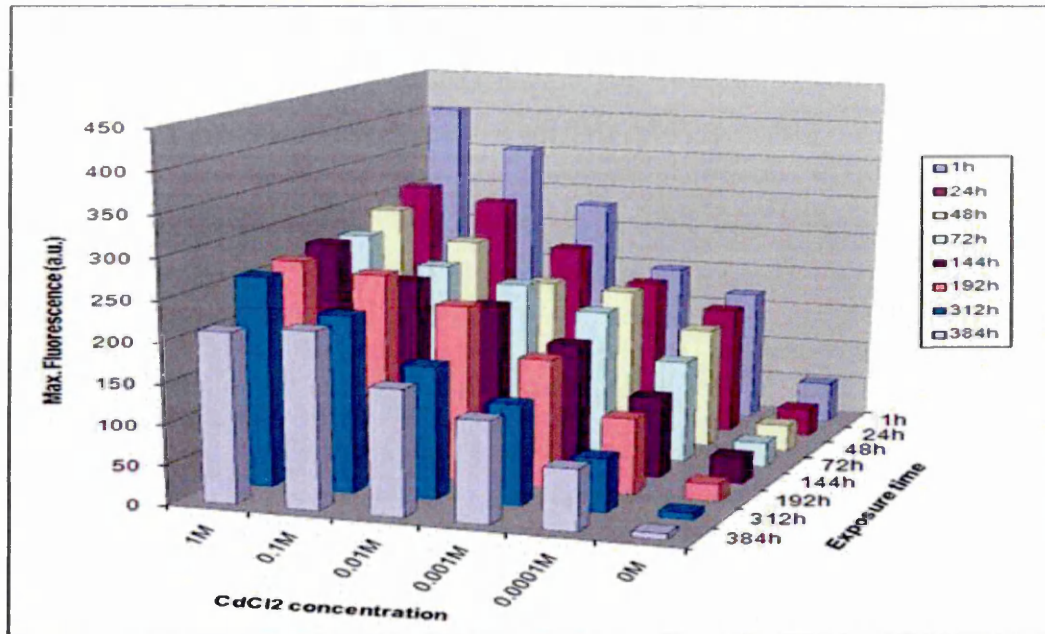


Figure C3. Effect of CdCl<sub>2</sub> on second order diffraction peak for *E. coli*, fluorescence for bacteria sample exposed to CdCl<sub>2</sub>

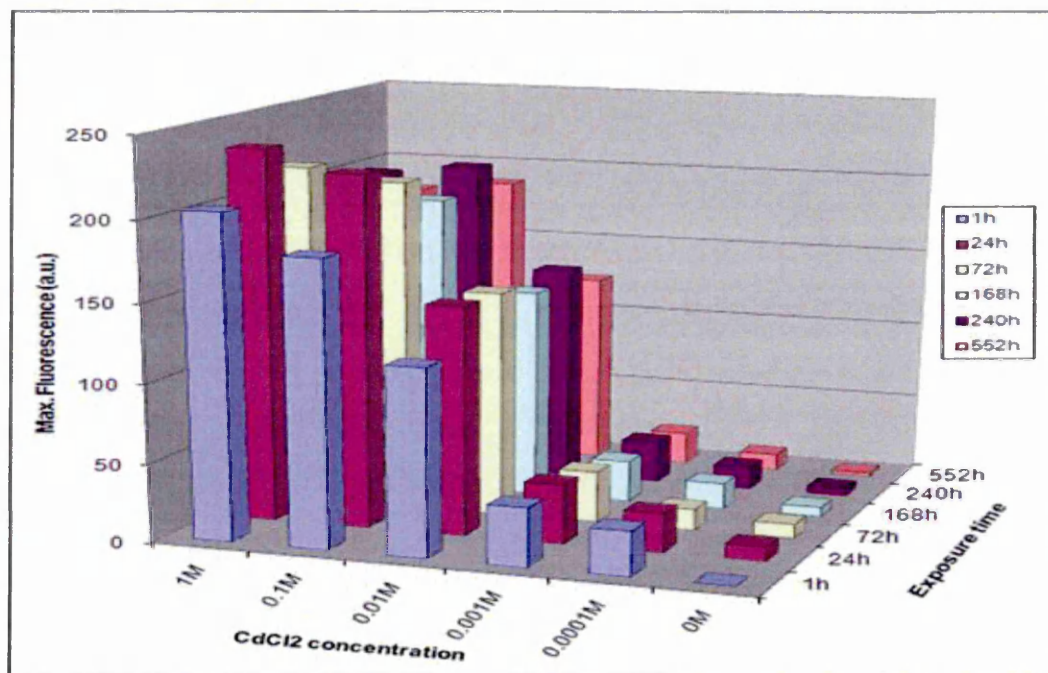


Figure C4. Effect of CdCl<sub>2</sub> on 2-nd order diffraction peak for *D. radiodurans*, fluorescence for bacteria sample exposed to CdCl<sub>2</sub>

Figure C5 and C6 shows the OD<sub>600</sub> results of *E. coli* and *D. radiodurans* bacteria after adding NiCl<sub>2</sub> as a function of metal concentration and time of exposure.

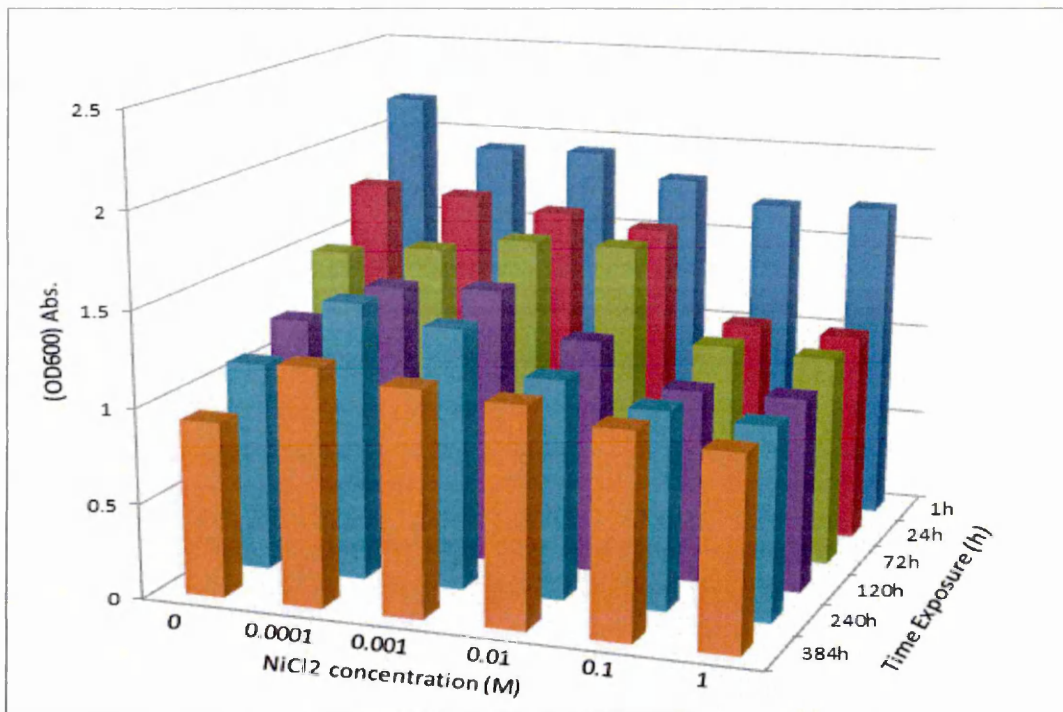


Figure C5. Optical Density test: Optical densities OD<sub>600</sub> for *E. coli* bacteria versus NiCl<sub>2</sub> concentration and time exposure

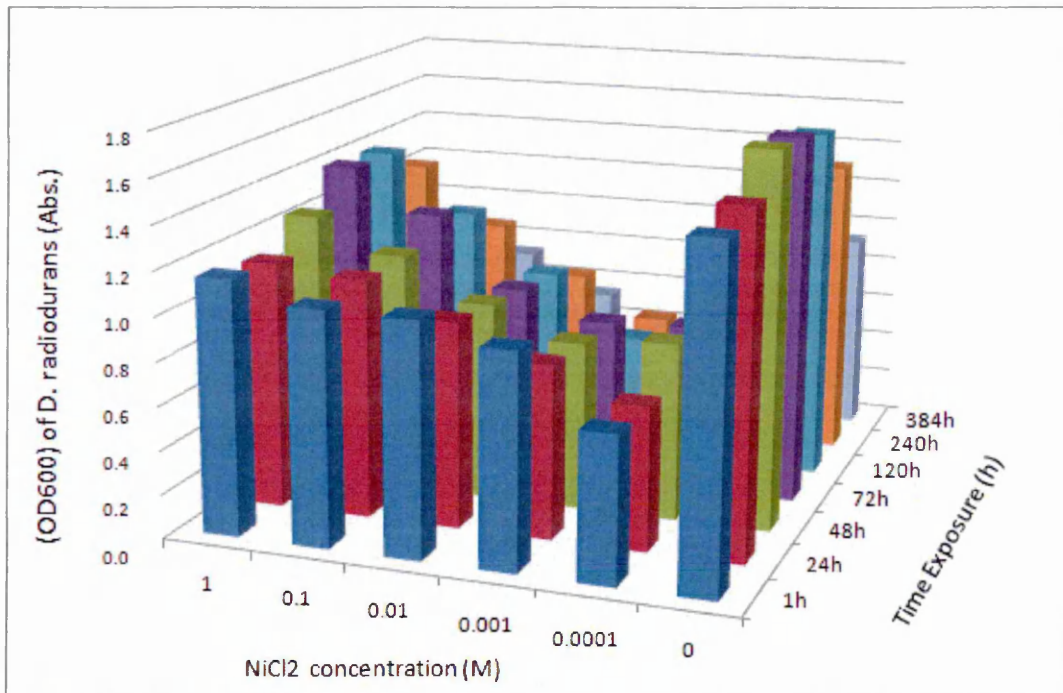


Figure C6. Optical Density test: optical densities OD<sub>600</sub> for *D. radiodurans* bacteria versus the NiCl<sub>2</sub> concentration and time exposure

The intensity is depend on NiCl<sub>2</sub> concentration. Changes in exposure time are presented in Figures C7 and C8 (appendix C).

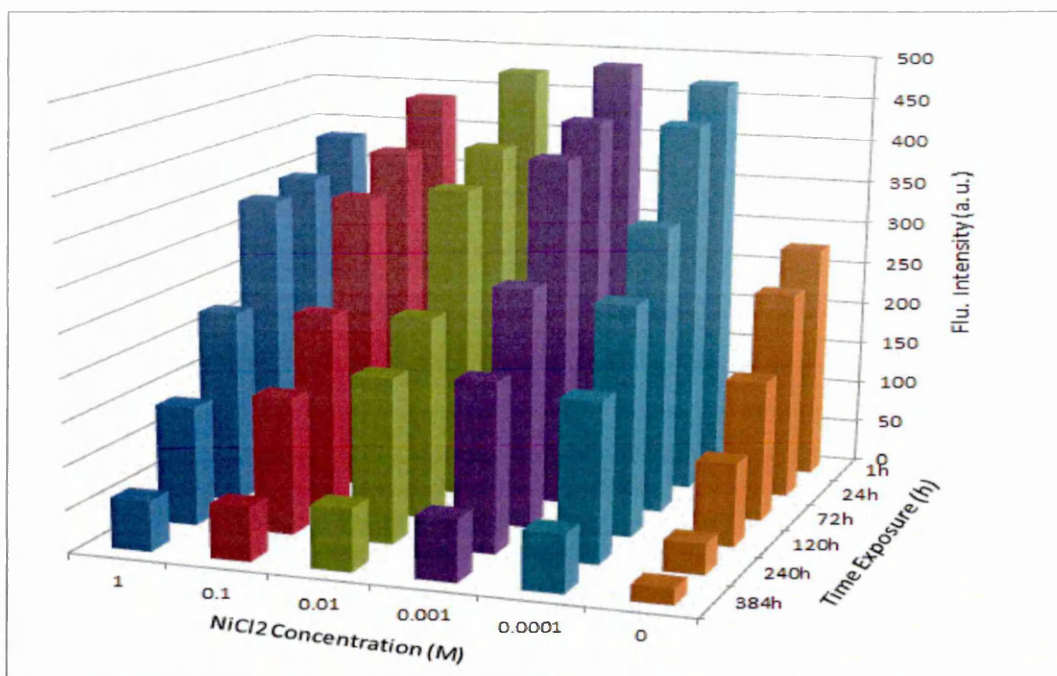


Figure C7. Effect of NiCl<sub>2</sub> on second order diffraction peak for E. coli, fluorescence for bacteria sample exposed to NiCl<sub>2</sub>

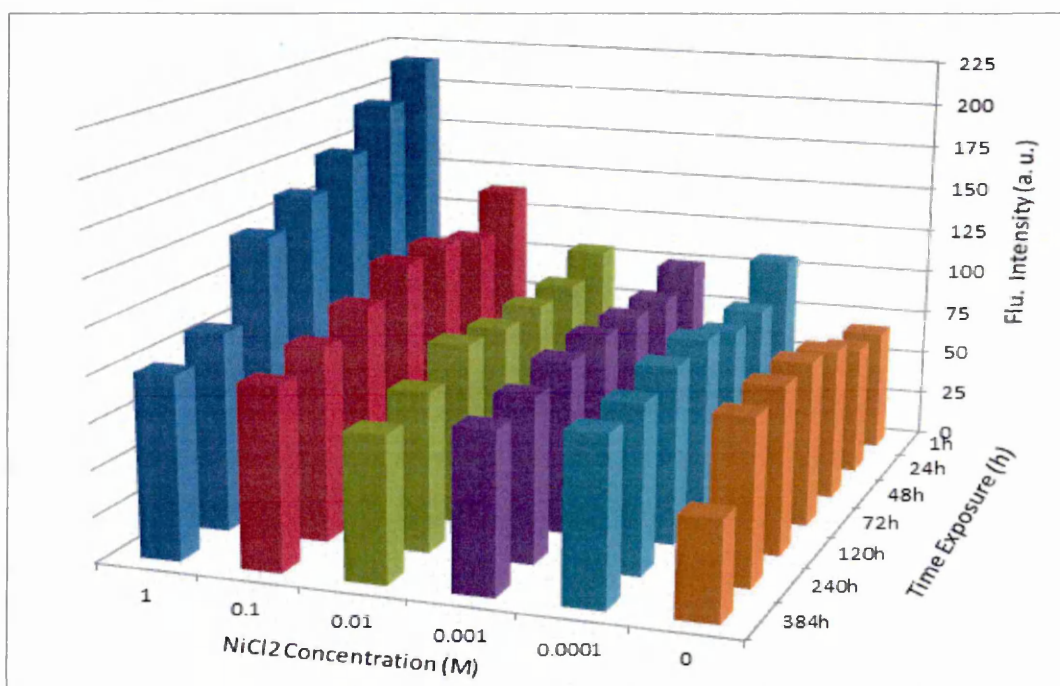


Figure C8. Effect of NiCl<sub>2</sub> on second order diffraction peak for D. radiodurans, fluorescence for bacteria sample exposed to NiCl<sub>2</sub>

## APPENDIX D

The *D. radiodurans* samples were mixed with different concentrations of  $\text{CdCl}_2$  and checked electrically for different periods

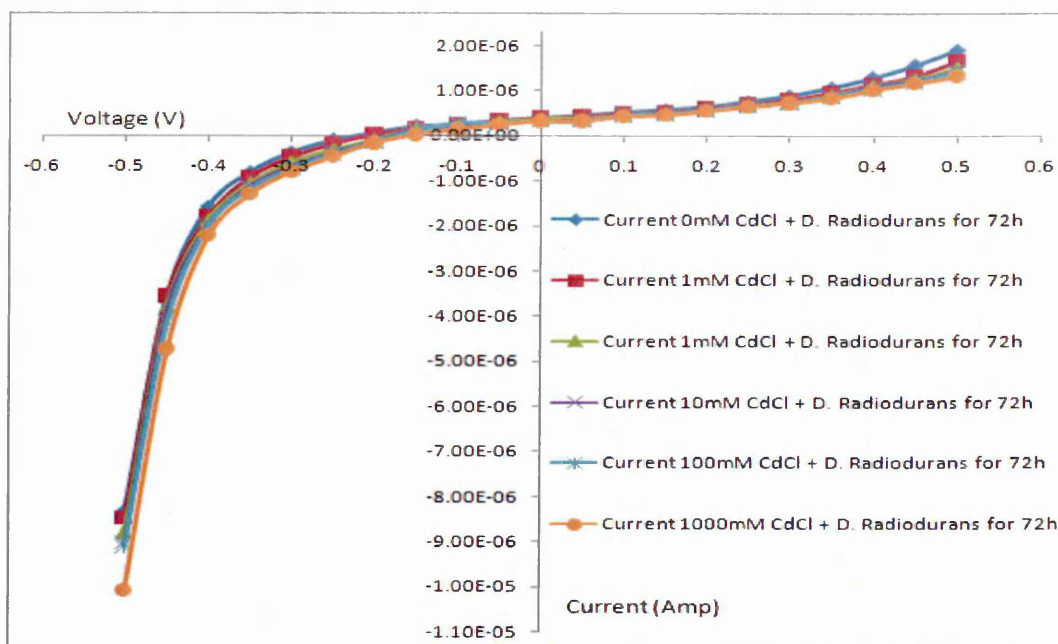


Figure D1. I-V characteristics of *D. radiodurans* samples for different concentrations of  $\text{CdCl}_2$ , after 72 hours exposure time, at normal environment

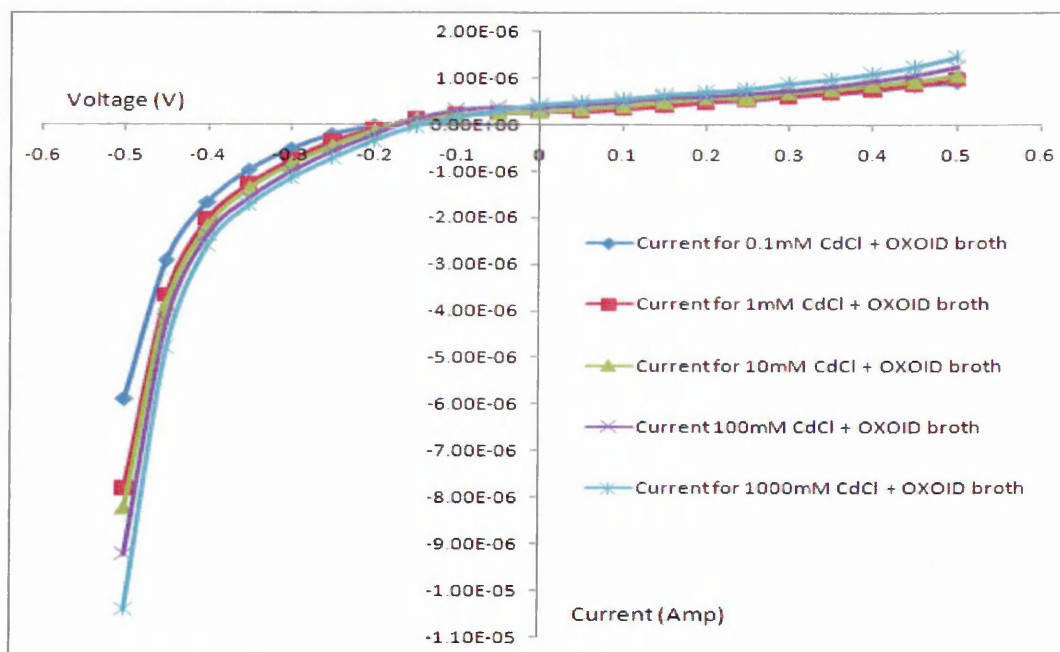


Figure D2. I-V characteristics for different concentrations of  $\text{CdCl}_2$  with OXOID broth

Typical AC conductance (AC-Gp) graph of *D. radiodurans* samples with different concentrations of metal are shown in Figure D3 (appendix D).

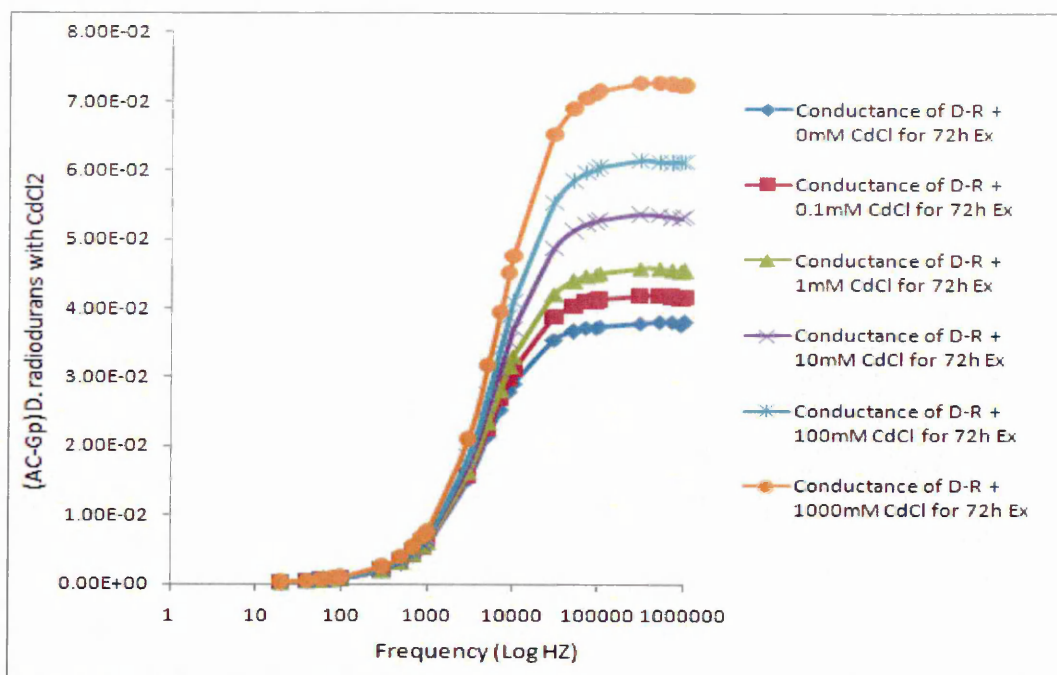


Figure D3. Typical AC-Gp characteristics of *D. radiodurans* samples for different concentrations of  $\text{CdCl}_2$

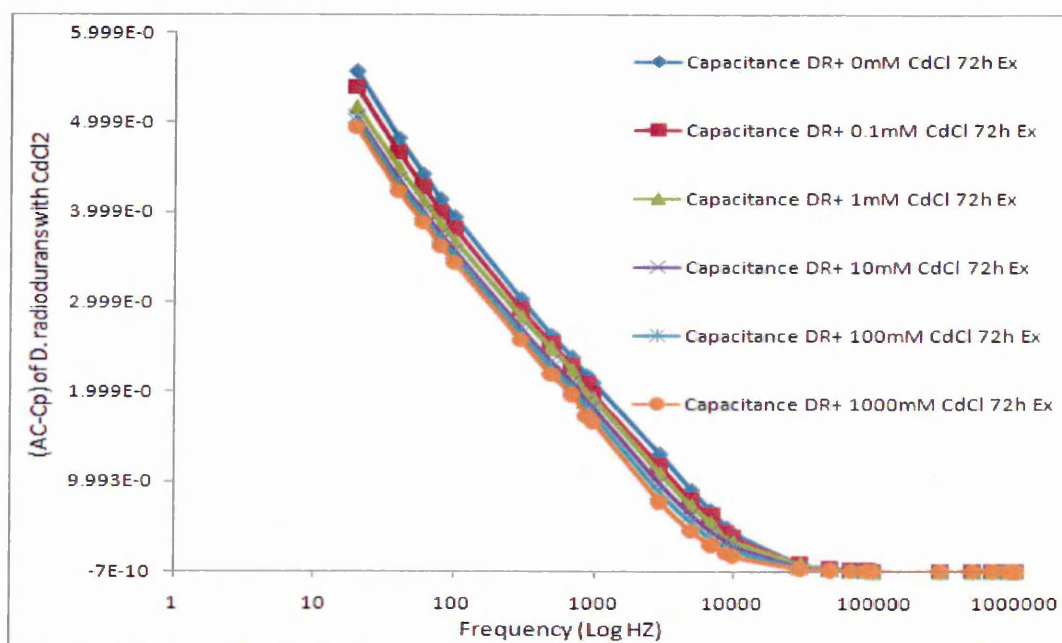


Figure D4. Typical AC-Cp characteristics of *D. radiodurans* samples for different concentrations of  $\text{CdCl}_2$

The AC conductance and capacitance for different concentrations of metal with OXOID broth are plotted in Figures D5 & D6.

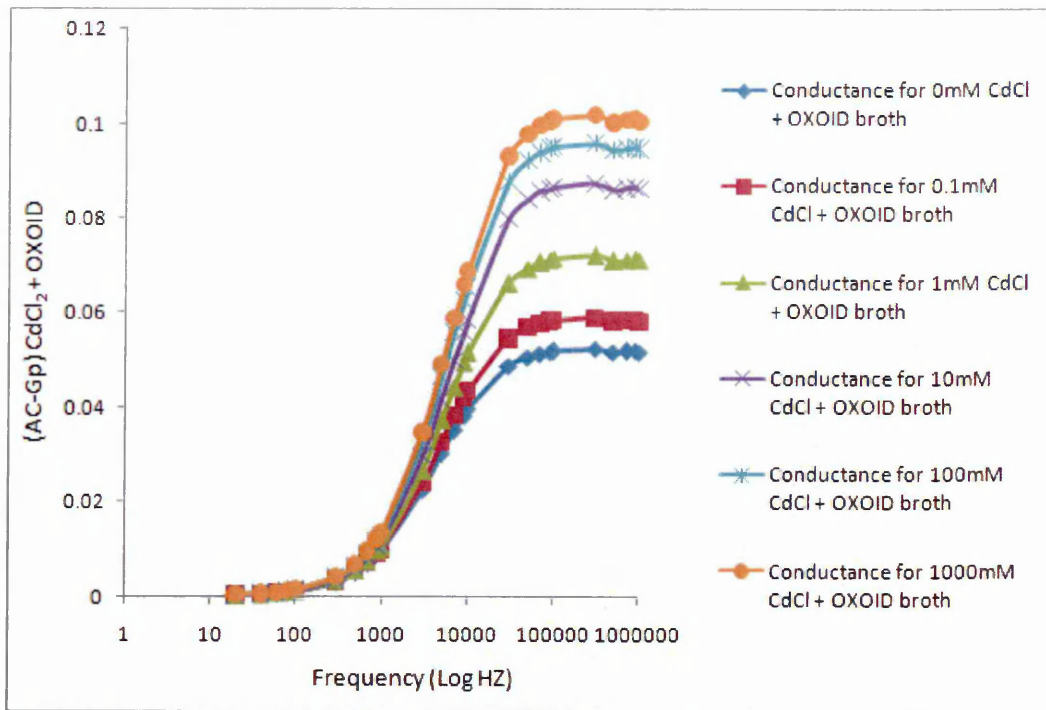


Figure D5. Typical AC-Gp characteristics of OXOID broth for different concentrations of CdCl<sub>2</sub>

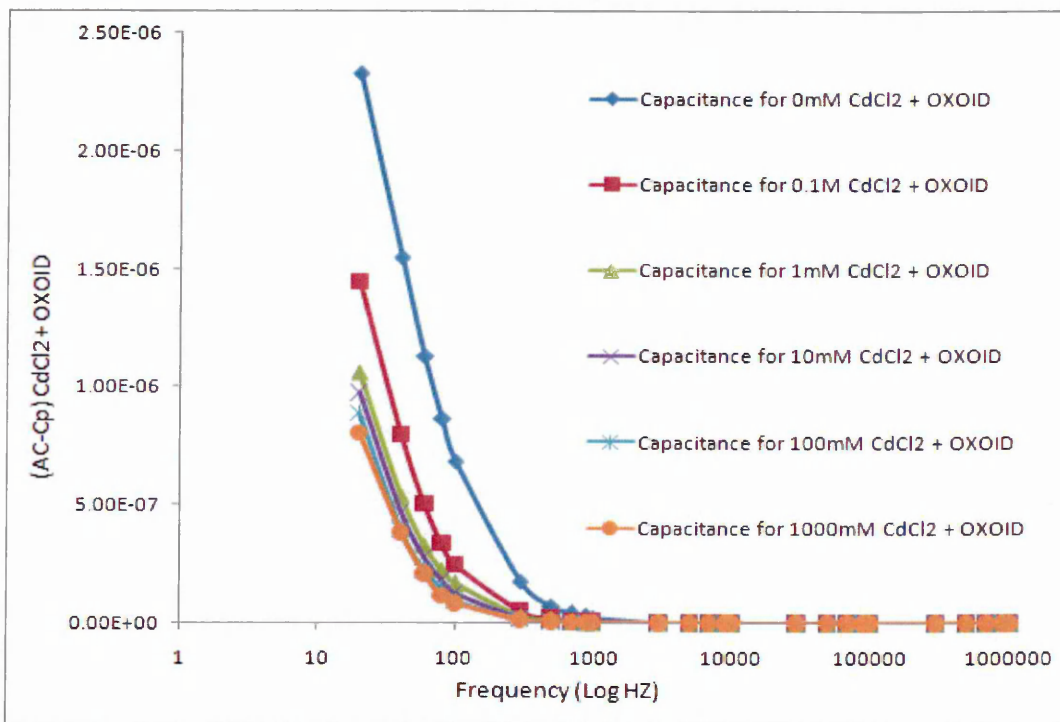


Figure D6. Typical AC-Gp characteristics of different concentrations of CdCl<sub>2</sub> with OXOID broth

the metal concentration can be found directly. More details were shown in this appendix.

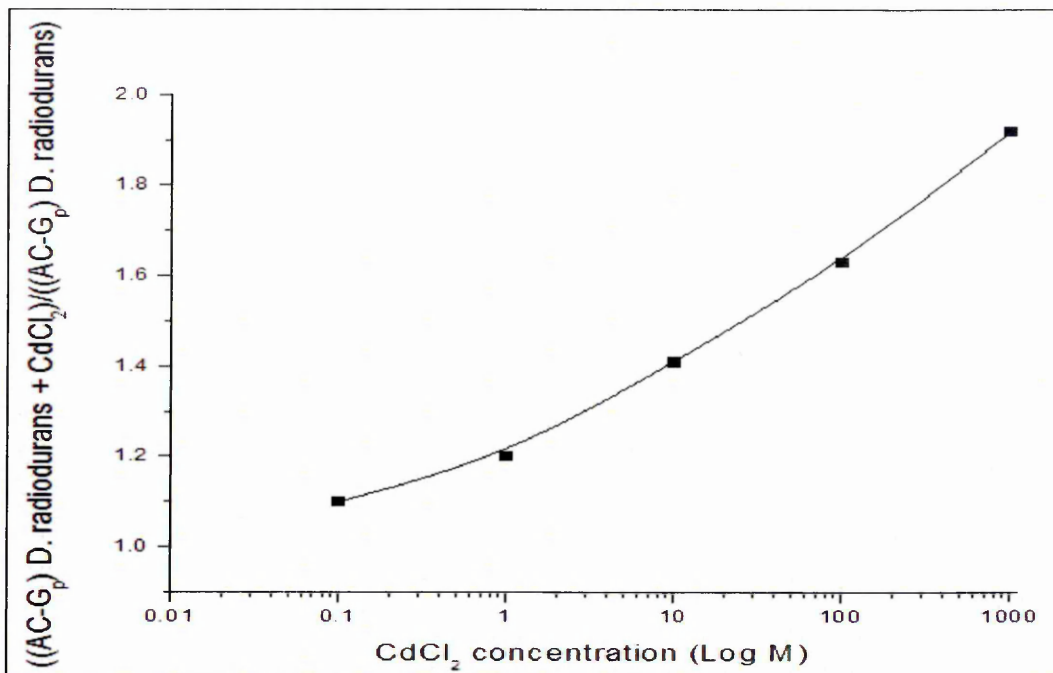


Figure D7. AC conductance ratio of *D. radiodurans* bacteria exposed (mixed) with  $\text{CdCl}_2$  after 72 hours over conductance for samples not exposed at 900kHz

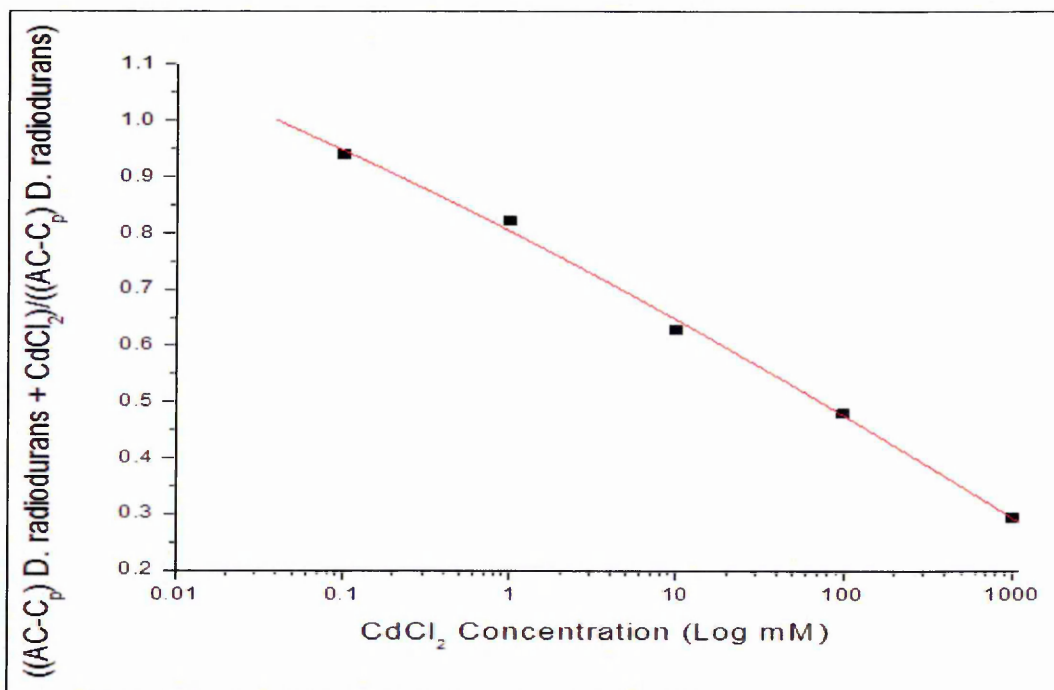


Figure D8. AC capacitance ratios of *D. radiodurans* bacteria exposed (mixed) to  $\text{CdCl}_2$  after 72 hours over the AC capacitance for samples not exposed at 900kHz

The *D. radiodurans* samples were mixed (1:1) with different concentrations of  $\text{NiCl}_2$ . The more results are presented Figures D9 and D10.

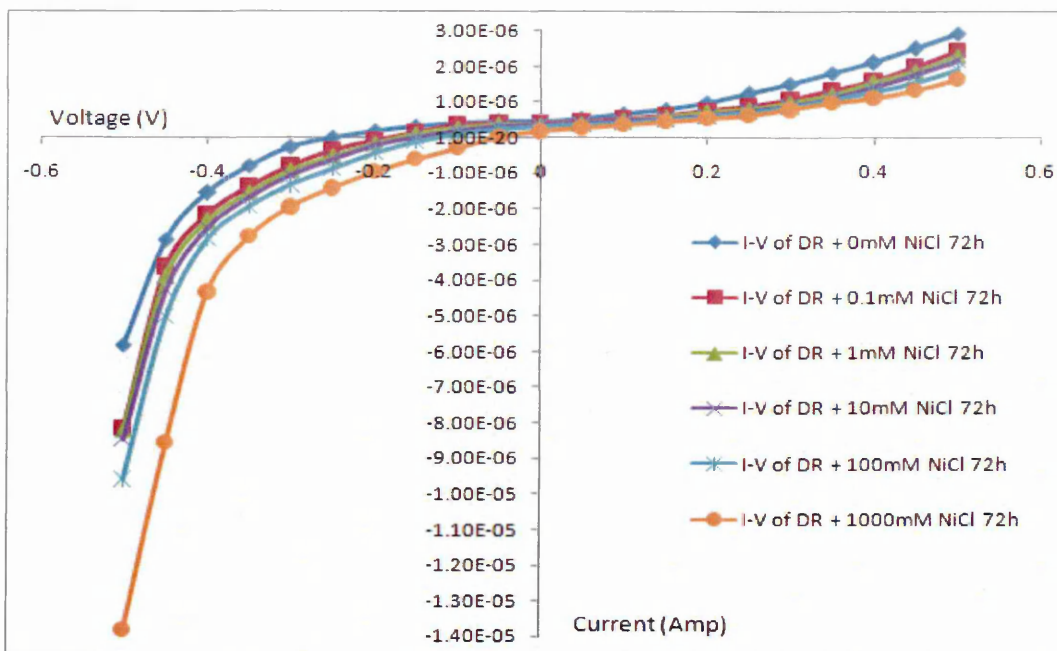


Figure D9. I-V characteristics of *D. radiodurans* samples for different concentrations of  $\text{NiCl}_2$ , after 72 hours exposure time in normal environmental conditions inside shaker

The I-V characteristic for different concentration of  $\text{NiCl}_2$  mixed with OXOID broth was examined and is presented in Figure D10.

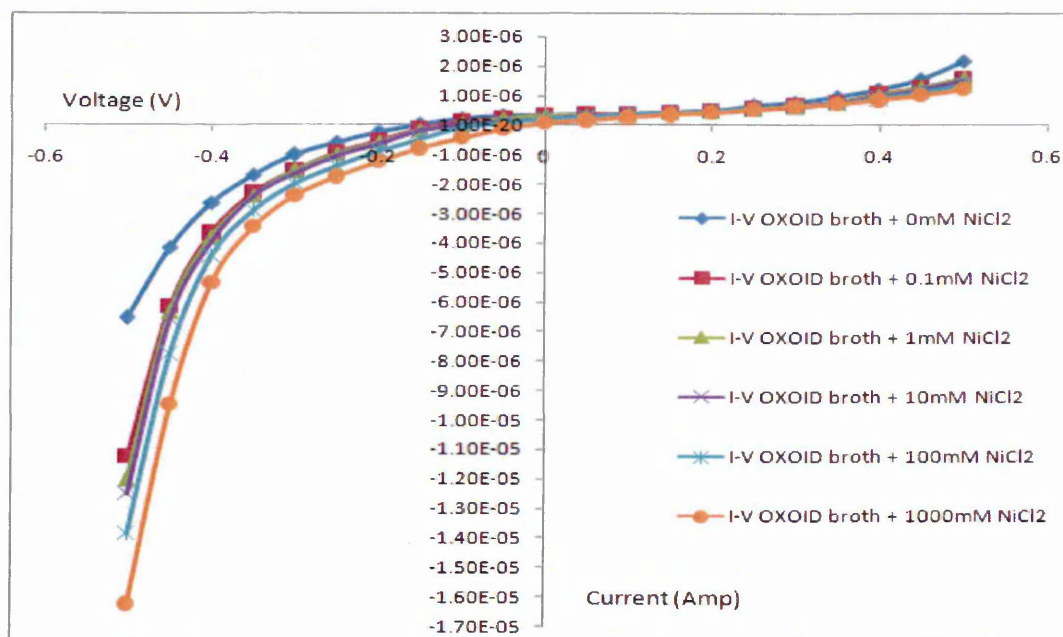


Figure D10. I-V characteristics for different concentrations of  $\text{NiCl}_2$  in OXOID broth

The cathode current of *D. radiodurans* bacteria after adding  $\text{NiCl}_2$  at (-0.5V) was normalised on the cathode current of  $\text{NiCl}_2$  with an OXOID broth and on the cathode current of *D. radiodurans* bacteria without metal, as is clear in Figures D11 and D12.

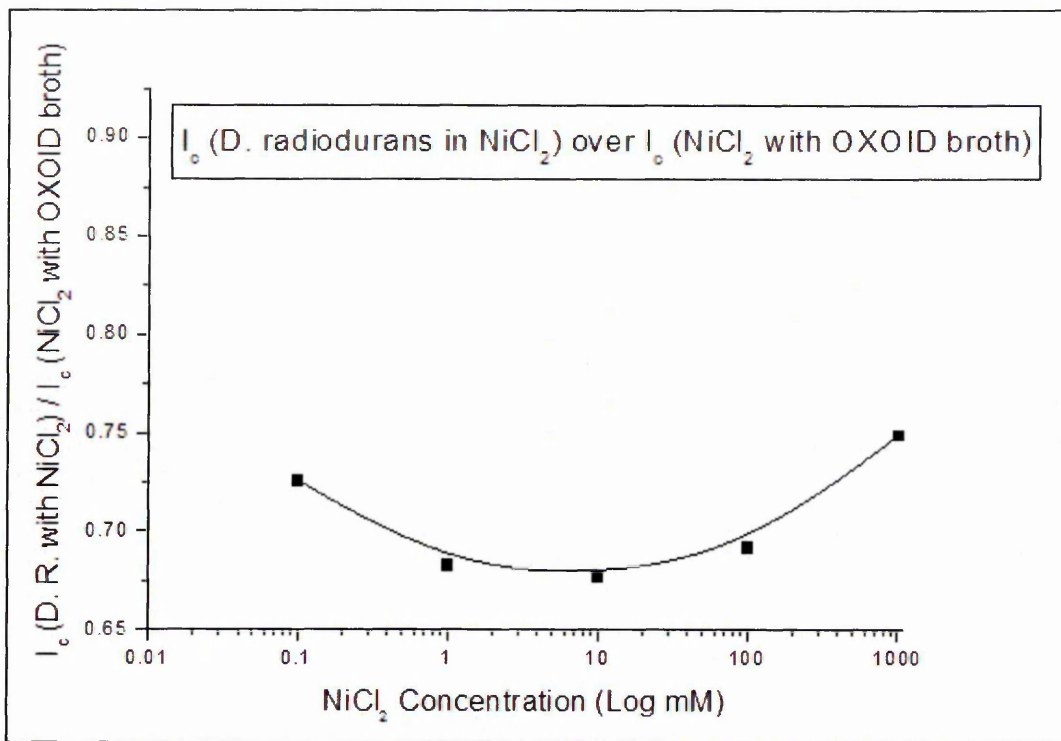


Figure D11.  $I_c$  D. radiodurans with NiCl<sub>2</sub> /  $I_c$  NiCl<sub>2</sub> with LB broth characteristics for different concentration of NiCl<sub>2</sub>

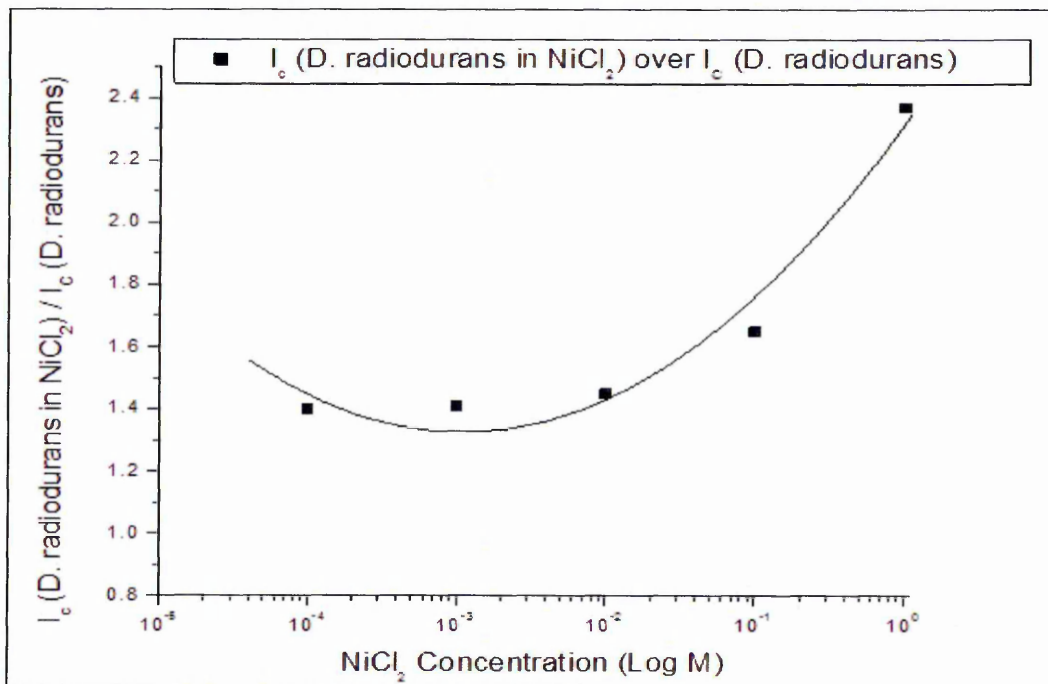


Figure D12.  $I_c$  D. radiodurans with NiCl<sub>2</sub> /  $I_c$  D. radiodurans characteristics for different concentration of NiCl<sub>2</sub>

Figure D13 shows the AC conductance (AC-Gp) of D. radiodurans with NiCl<sub>2</sub>. Also the AC conductance of NiCl<sub>2</sub> with OXOID were studied, see figure D14.

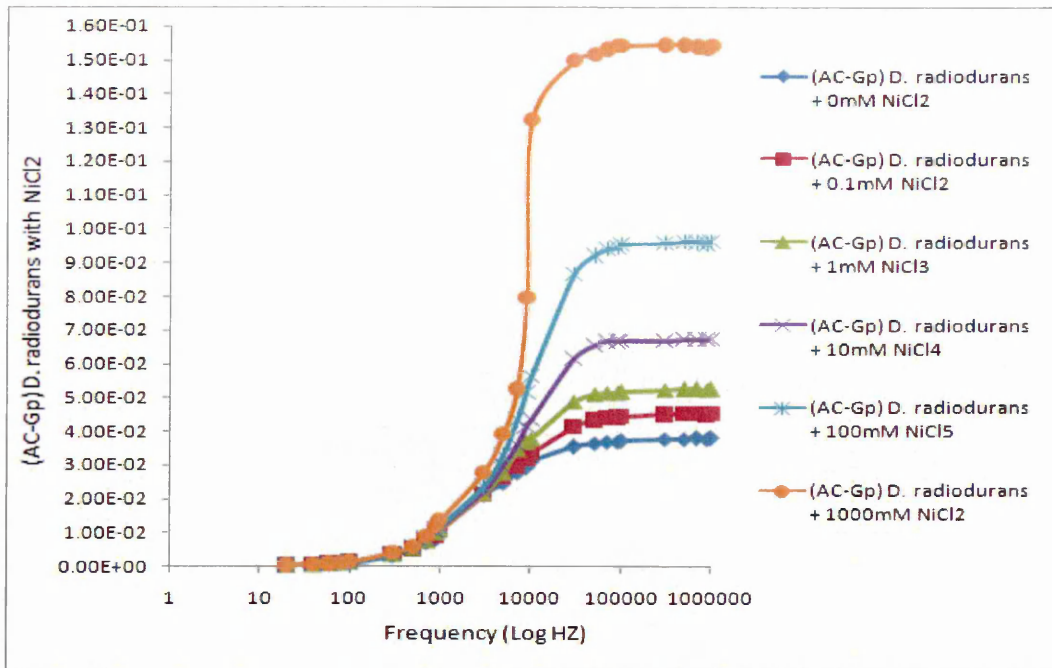


Figure D13. Typical AC-Gp characteristics of *D. radiodurans* samples for different concentrations of  $\text{NiCl}_2$  after 72 hours exposure

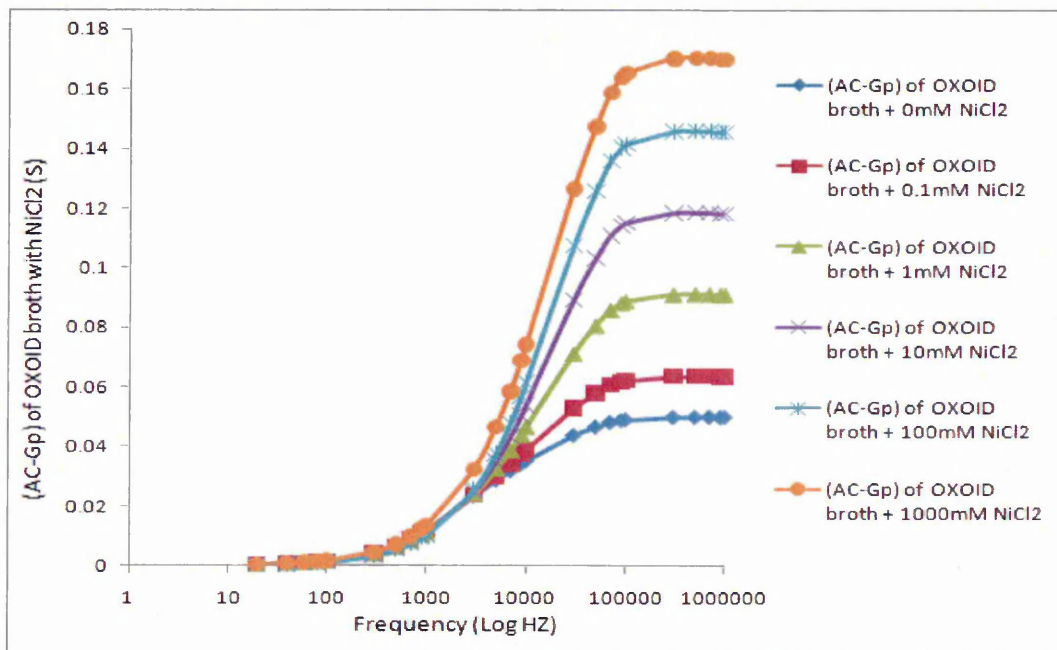


Figure D14. Typical (AC-Gp) conductance characteristics of OXOID broth mixed with different concentrations of  $\text{NiCl}_2$

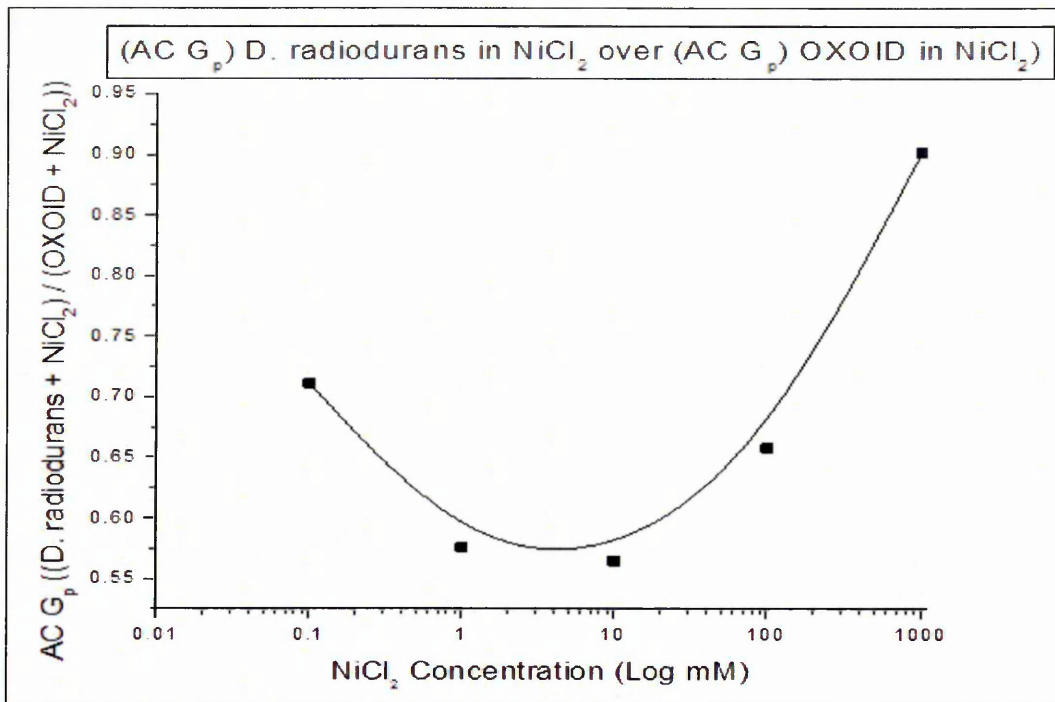


Figure D15. AC conductance ratios of *D. radiodurans* bacteria mixed with NiCl<sub>2</sub> after 72 hours over the AC conductance for NiCl<sub>2</sub> at 900kHz

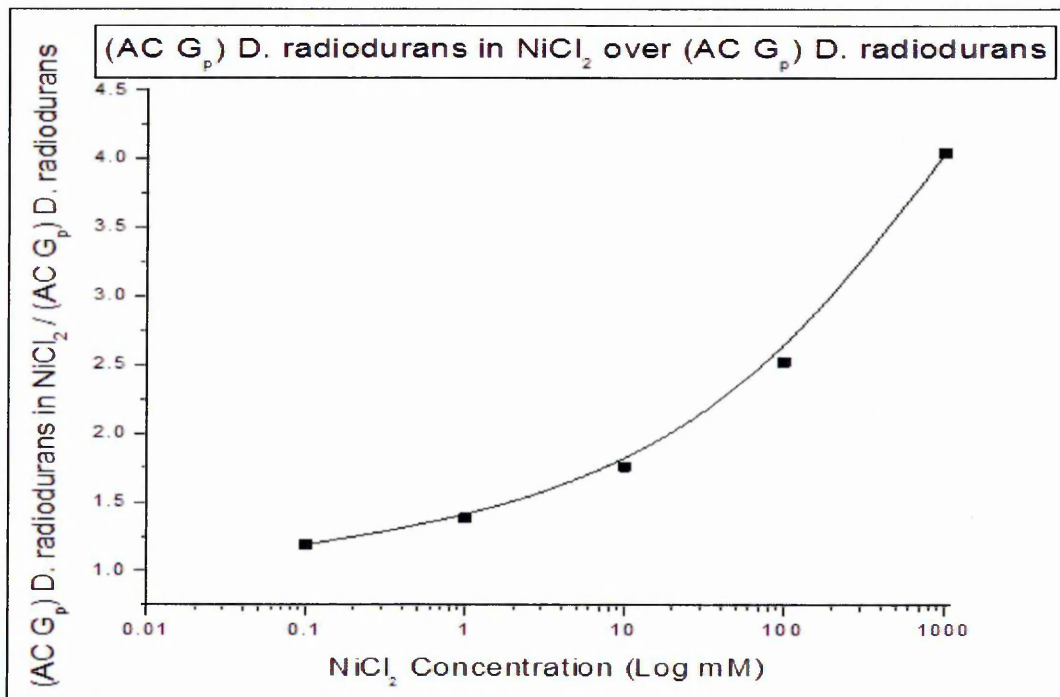


Figure D16. AC conductance ratios of *D. radiodurans* bacteria exposed (mixed) with NiCl<sub>2</sub> after 72 hours over the AC conductance for *D. radiodurans* 900kHz

The AC capacitances of *D. radiodurans* bacteria after being mixed with different concentrations of NiCl<sub>2</sub> were investigated.

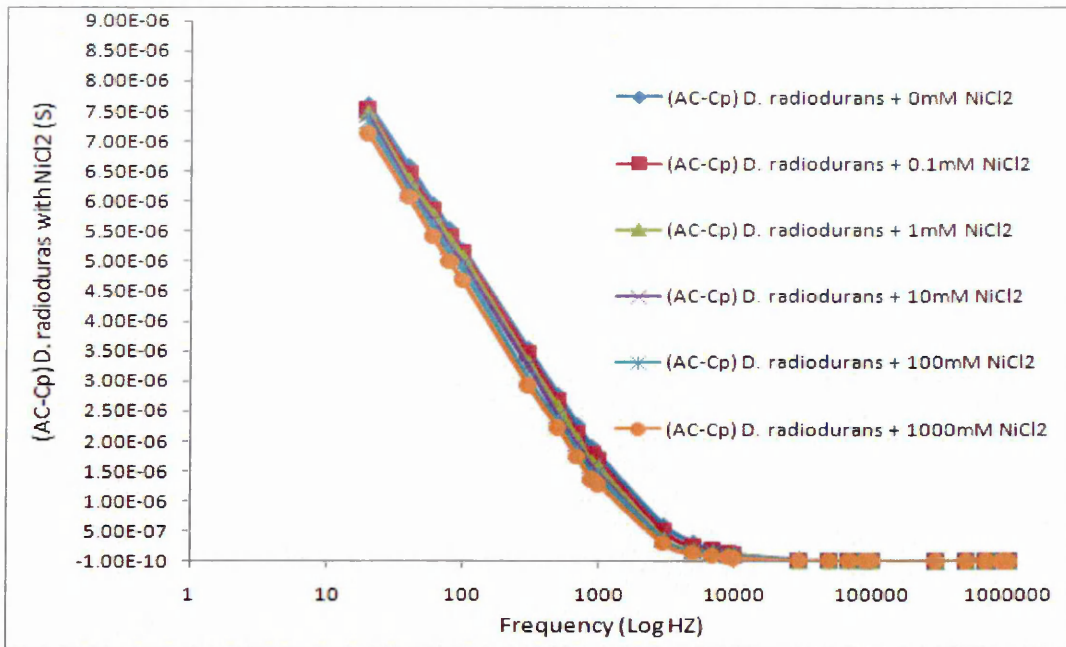


Figure D17. AC capacitance of *D. radiodurans* mixed with  $\text{NiCl}_2$  metal after 72 hours of mixed; at 900kHz

Figure D17 shows the AC capacitance behaviour of *D. radiodurans* bacteria mixed with different concentrations of  $\text{NiCl}_2$ .

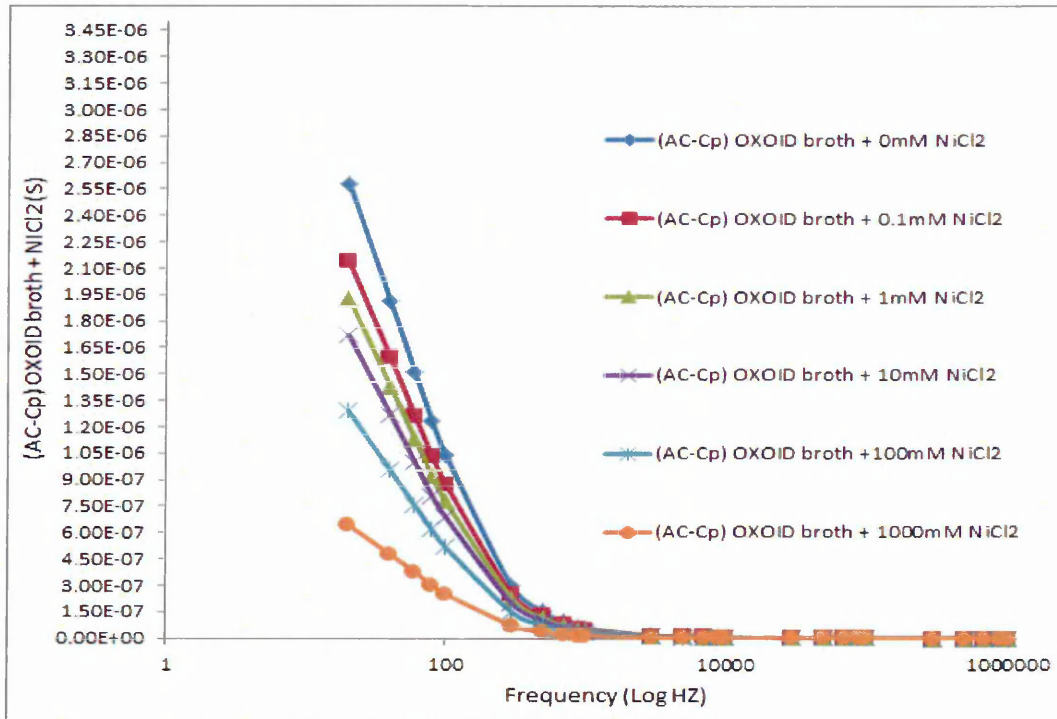


Figure D18. AC capacitance of  $\text{NiCl}_2$  metal were mixed with OXOID broth after 72 hours

The equivalent double layers capacitance of *D. radiodurans* for different concentrations of  $\text{NiCl}_2$  has been calculated. Then the results were normalised and subscripted for samples were not exposed to the salt. See figure D19.

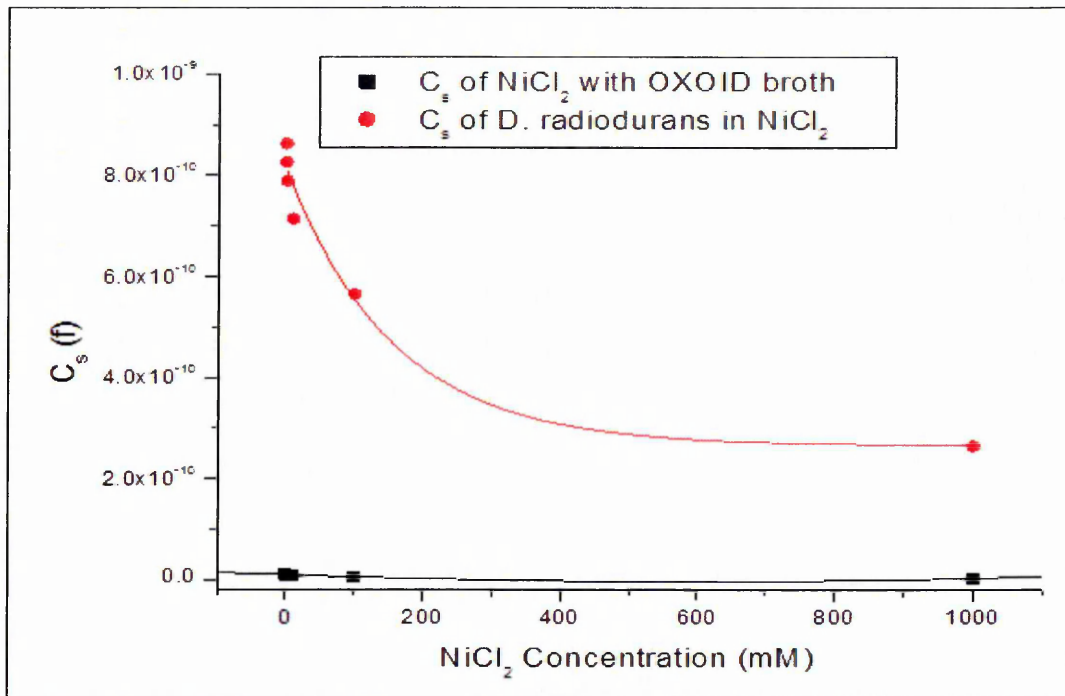


Figure D19. Changes in surface capacitance ( $C_s$ ) of *D. radiodurans* bacteria after being added  $\text{NiCl}_2$  and for  $\text{NiCl}_2$  with OXOID broth after 72 hours exposure